US006610746B2

(12) **United States Patent**
Fryburg et al.

(10) **Patent No.: US 6,610,746 B2**
(45) **Date of Patent: Aug. 26, 2003**

(54) **SYNERGISTIC EFFECT OF A SULFONYLUREA AND/OR NON-SULFONYLUREA K+ATP CHANNEL BLOCKER, AND A PHOSPHODIESTERASE 3 TYPE INHIBITOR**

(75) Inventors: **David A. Fryburg**, East Lyme, CT (US); **Janice C. Parker**, Ledyard, CT (US)

(73) Assignee: **Pfizer Inc.**, New York, NY (US)

(*) Notice: Subject to any disclaimer, the term of this patent is extended or adjusted under 35 U.S.C. 154(b) by 0 days.

(21) Appl. No.: **09/829,874**

(22) Filed: **Apr. 10, 2001**

(65) **Prior Publication Data**

US 2002/0013268 A1 Jan. 31, 2002

Related U.S. Application Data

(60) Provisional application No. 60/196,728, filed on Apr. 13, 2000.

(51) **Int. Cl.**[7] **A61K 31/64**; A61K 38/28

(52) **U.S. Cl.** **514/592**; 514/3; 514/350; 514/352; 514/356; 514/396; 514/592

(58) **Field of Search** 514/3, 350, 352, 514/396, 357, 592, 600

(56) **References Cited**

FOREIGN PATENT DOCUMENTS

WO WO9836755 8/1998 ..... A61K/31/64

OTHER PUBLICATIONS

Fujimoto, S., et al., The Novel Insulinotropic Mechanism of Pimobendan: Direct Enhancement of the Exocytotic Process of Insulin Secretory Granules by Increased Ca^2 Sensitivity in β–Cells, *Endocrinology*, vol. 139, No. 3, pp. 1133–1140.

Hohn, H., et al., Potential Antidiabetic Agents. Pyrazolo[3, 4–b]pyridines, *Journal of Medicinal Chemistry*, vol. 16, No. 12, pp. 1340–1346, (1973).

Grill, V., et al., Interacting Effects of Sylfonylureas and Glucose on Cyclic AMP Metabolism and Insulin Release in Pancreatic Isle of the Rat, *J. Clin. Invest.*, vol. 61, No. 5, pp. 1346–1354, (1978).

Parker, J. C., et al., Effects of Cyclic AMP Phosphodiesterase Inhibitors on Insulin Secretion and Glycemia, *Diabetologia*, vol. 39, Suppl. 1, p. A225, Sep. 1, 1996.

J. C. Parker, et al. Cycluc AMP Phosphodiesterases of Human and Rat Islets of Langerhans: Contributions of Types III and IV to the Modulation of Insulin Secretion, *Biochemical and Biophysical Research Communictions*. Dec. 26, 1995. vol. 217, No. 3. pp. 816–923.

M. El–Metwally, et al. The Effect of selective phosphodiesterase inhibitors on plasma insulin concentration and insulin secretion in vitro in the rat. *European Journal of Pharmacology*. 1997. vol. 324. pp. 227–232.

J. C. Parker, et al. Modulation of Insulin Secretion and Glycemia by Selective Inhibition of Cyclic AMP Phosphodiesterase III. *Biochemical and Biophysical Research Communications*. 1997. vol. 236. Article No. RC977034. pp. 665–669.

M.D. Leibowitz, et al. A Novel Insulin Secretagogue Is a Phosphodiesterase Inhibitor. *Diabetes*. Jan. 1995. vol. 44. pp. 67–74.

Primary Examiner—Christopher S. F. Low
Assistant Examiner—Chih-Min Kam
(74) *Attorney, Agent, or Firm*—Peter C. Richardson; Gregg C. Benson; Carl J. Goddard

(57) **ABSTRACT**

The present invention provides methods of treating non-insulin dependent diabetes mellitus, insulin resistance, Syndrome X, diabetic neuropathy, diabetic nephropathy, diabetic retinopathy, diabetic cardiomyopathy, polycystic ovary syndrome, cataracts, hyperglycemia, or impaired glucose tolerance, the methods comprising the step of administering to a patient having or at risk of having non-insulin dependent diabetes mellitus, insulin resistance, Syndrome X, diabetic neuropathy, diabetic nephropathy, diabetic retinopathy, diabetic cardiomyopathy, polycystic ovary syndrome, cataracts, hyperglycemia, or impaired glucose tolerance a synergistic amount of:1) a sulfonylurea, a non-sulfonylurea K^+ ATP channel blocker, or a sulfonylurea and a non-sulfonylurea K^+ ATP channel blocker; and 2) a cAMP phosphodiesterase type 3 inhibitor. The present invention also provides kits and pharmaceutical compositions that comprise: 1) a sulfonylurea, a non-sulfonylurea K^+ ATP channel blocker, or a sulfonylurea and a non-sulfonylurea K^+ ATP channel blocker; and 2) a cAMP phosphodiesterase type 3 inhibitor. The present invention also relates to kits and pharmaceutical compositions that comprise 1) a sulfonylurea, a non-sulfonylurea K^+ ATP channel blocker, or a sulfonylurea and a non-sulfonylurea K^+ ATP channel blocker; 2) a cAMP phosphodiesterase type 3 inhibitor; and 3) an additional compound useful for the treatment of non-insulin dependent diabetes mellitus, insulin resistance, Syndrome X, diabetic neuropathy, diabetic nephropathy, diabetic retinopathy, diabetic cardiomyopathy, polycystic ovary syndrome, cataracts, hyperglycemia, or impaired glucose tolerance.

8 Claims, 1 Drawing Sheet

US 20030216294A1

(19) United States

(12) Patent Application Publication (10) Pub. No.: US 2003/0216294 A1

Fryburg et al. (43) Pub. Date: Nov. 20, 2003

(54) SYNERGISTIC EFFECT OF A SULFONYLUREA AND/OR NON-SULFONYLUREA K+ATP CHANNEL BLOCKER, AND A PHOSPHODIESTERASE 3 TYPE INHIBITOR

(75) Inventors: **David A. Fryburg**, East Lyme, CT (US); **Janice C. Parker**, Ledyard, CT (US)

Correspondence Address:
PFIZER INC.
PATENT DEPARTMENT, MS8260-1611
EASTERN POINT ROAD
GROTON, CT 06340 (US)

(73) Assignee: **Pfizer Inc.**

(21) Appl. No.: **10/456,371**

(22) Filed: **Jun. 5, 2003**

Related U.S. Application Data

(62) Division of application No. 09/829,874, filed on Apr. 10, 2001, now Pat. No. 6,610,746.

(60) Provisional application No. 60/196,728, filed on Apr. 13, 2000.

Publication Classification

(51) **Int. Cl.**[7] **A61K 38/28**; A61K 31/4439; A61K 31/426; A61K 31/175

(52) **U.S. Cl.** **514/3**; 514/365; 514/342; 514/592

(57) **ABSTRACT**

The present invention provides methods of treating non-insulin dependent diabetes mellitus, insulin resistance, Syndrome X, diabetic neuropathy, diabetic nephropathy, diabetic retinopathy, diabetic cardiomyopathy, polycystic ovary syndrome, cataracts, hyperglycemia, or impaired glucose tolerance, the methods comprising the step of administering to a patient having or at risk of having non-insulin dependent diabetes mellitus, insulin resistance, Syndrome X, diabetic neuropathy, diabetic nephropathy, diabetic retinopathy, diabetic cardiomyopathy, polycystic ovary syndrome, cataracts, hyperglycemia, or impaired glucose tolerance a synergistic amount of: 1) a sulfonylurea, a non-sulfonylurea K^+ ATP channel blocker, or a sulfonylurea and a non-sulfonylurea K^+ ATP channel blocker; and 2) a cAMP phosphodiesterase type 3 inhibitor. The present invention also provides kits and pharmaceutical compositions that comprise: 1) a sulfonylurea, a non-sulfonylurea K^+ ATP channel blocker, or a sulfonylurea and a non-sulfonylurea K^+ ATP channel blocker; and 2) a cAMP phosphodiesterase type 3 inhibitor. The present invention also relates to kits and pharmaceutical compositions that comprise 1) a sulfonylurea, a non-sulfonylurea K^+ ATP channel blocker, or a sulfonylurea and a non-sulfonylurea K^+ ATP channel blocker; 2) a cAMP phosphodiesterase type 3 inhibitor; and 3) an additional compound useful for the treatment of non-insulin dependent diabetes mellitus, insulin resistance, Syndrome X, diabetic neuropathy, diabetic nephropathy, diabetic retinopathy, diabetic cardiomyopathy, polycystic ovary syndrome, cataracts, hyperglycemia, or impaired glucose tolerance.

US005977154A

United States Patent [19]

Bell et al.

[11] Patent Number: 5,977,154

[45] Date of Patent: *Nov. 2, 1999

[54] SELECTIVE β3 ADRENERGIC AGONIST

[75] Inventors: **Michael Gregory Bell**; **Christine Ann Droste**; **Cynthia Darshini Jesudason**, all of Indianapolis; **Christopher John Rito**, Mooresville; **Anthony John Shuker**, Indianapolis; **Mark Alan Winter**, Indianapolis, all of Ind.

[73] Assignee: **Eli Lilly and Company**, Indianapolis, Ind.

[*] Notice: This patent issued on a continued prosecution application filed under 37 CFR 1.53(d), and is subject to the twenty year patent term provisions of 35 U.S.C. 154(a)(2).

[21] Appl. No.: **08/882,931**

[22] Filed: **Jun. 26, 1997**

Related U.S. Application Data

[63] Continuation of application No. 08/708,621, Sep. 5, 1996, abandoned

[60] Provisional application No. 60/004,082, Sep. 21, 1995.

[51] **Int. Cl.**[6] **C07D 413/10**; A61K 31/40

[52] **U.S. Cl.** **514/394**; 514/359; 514/406; 514/414; 514/415; 514/234.5; 514/253; 514/318; 514/322; 544/124; 544/132; 544/139; 544/140; 544/144; 544/364; 544/366; 544/370; 544/371; 544/373; 546/194; 546/199; 546/268.4; 546/273.4; 546/275.7; 546/277.4

[58] **Field of Search** 514/394, 359, 514/406, 414, 415, 234.5, 253; 548/259, 309.7, 362.5, 503, 306.1, 465

[56] **References Cited**

U.S. PATENT DOCUMENTS

4,032,575	6/1977	Ikezaki et al.	260/570.6
4,288,452	9/1981	Sombroek et al.	424/304
4,309,443	1/1982	Smith et al.	424/319
4,338,333	7/1982	Ainsworth et al.	424/309
4,367,235	1/1983	Ross et al.	424/273 B
4,385,066	5/1983	Ainsworth et al.	424/309
4,391,826	7/1983	Mills et al.	424/324
4,396,627	8/1983	Ainsworth et al.	424/309
4,432,993	2/1984	Ferris	424/285
4,478,849	10/1984	Ainsworth et al.	424/285
4,497,813	2/1985	Ostermayer et al.	514/166
4,503,067	3/1985	Wiedemann et al.	514/411
4,636,511	1/1987	Ostermayer et al.	514/311
4,652,679	3/1987	Alig et al.	564/86
4,697,022	9/1987	Leinert	548/444
4,727,067	2/1988	Ostermayer et al.	514/162
4,751,246	6/1988	Philion	514/649
4,772,631	9/1988	Holloway et al.	514/539
4,940,800	7/1990	Bertolini et al.	548/327
4,977,148	12/1990	Holloway et al.	514/183
5,013,761	5/1991	Beedle et al.	514/650
5,321,036	6/1994	Sher	514/365
5,393,772	2/1995	Yue et al.	514/410
5,420,294	5/1995	Beedle et al.	548/507
5,453,436	9/1995	Ohlstein	514/411
5,534,640	7/1996	Tegeler et al.	549/80
5,541,197	7/1996	Fisher et al.	514/311
5,541,204	7/1996	Sher et al.	514/359
5,561,142	10/1996	Fisher et al.	514/312

FOREIGN PATENT DOCUMENTS

0 015 505 A1	9/1980	European Pat. Off. .
0 040 000	11/1981	European Pat. Off. .
0 052 963	6/1982	European Pat. Off. .
0 061 907	10/1982	European Pat. Off. .
0 063 004	10/1982	European Pat. Off. .
0 066 351	12/1982	European Pat. Off. .
0 068 669	1/1983	European Pat. Off. .
0 070 134	1/1983	European Pat. Off. .
0 082 665	6/1983	European Pat. Off. .
0 089 154	9/1983	European Pat. Off. .
0 091 749	10/1983	European Pat. Off. .
0 095 827	12/1983	European Pat. Off. .
0 099 707	2/1984	European Pat. Off. .
0 102 213	3/1984	European Pat. Off. .
0 171 702	2/1986	European Pat. Off. .
0 196 849	10/1986	European Pat. Off. .
0 211 721	2/1987	European Pat. Off. .
0 236 624	9/1987	European Pat. Off. .
0 345 056 A2	12/1989	European Pat. Off. .
0 386 920	9/1990	European Pat. Off. .
0 436 435 A1	7/1991	European Pat. Off. .
0 455 006 A2	11/1991	European Pat. Off. .
0 500 443 A1	8/1992	European Pat. Off. .
0 565 317 A1	10/1993	European Pat. Off. .
0 642 787 A2	3/1995	European Pat. Off. .
0 687 472 A2	12/1995	European Pat. Off. .
0 714 663 A2	6/1996	European Pat. Off. .
WO 92/18461	10/1992	WIPO .
WO 93/22277	11/1993	WIPO .
WO 94/03425	2/1994	WIPO .
WO 94/29290	12/1994	WIPO .
WO 95/01170	1/1995	WIPO .
WO 95/04047	2/1995	WIPO .

Primary Examiner—Fiona T. Powers
Attorney, Agent, or Firm—Steven G. Davis

[57] **ABSTRACT**

The present invention is in the field of medicine, particularly in the treatment of Type II diabetes and obesity. More specifically, the present invention relates to selective β3 adrenergic receptor agonists useful in the treatment of Type II diabetes and obesity. The invention provides compounds and method of treating type II diabetes, comprising administering to a mammal in need thereof compounds of the Formulas I and II:

(I), (II)

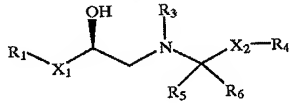

46 Claims, No Drawings

引用非特許文献

特許出願の番号	特願２００７－５０８６７９
作成日	平成２３年　５月３０日
作成者	川嵜　洋祐　　４７６５　４Ｃ００
発明の名称	心筋の病気を治療するための方法および組成物

付 1

1144-132 L-Type Calcium Channel Inhibitor Diltiazem Prevents Diastolic Dysfunction and Stress-induced Cardiac Decompensation and Death in a Mouse Model of Familial Hypertrophic Cardiomyopathy

Dirk Westermann, Björn Kaolmann, Heinz-Peter Schultheiss, Paul Steendijk, Carsten Tschoepe, Charité University Medical Center, Berlin, Germany, Georgetown University Medical Center, Georgetown, WA

The cardiac troponin T (TnT) I79N mutation has been linked to familial hypertrophic cardiomyopathy (FHC) and a high incidence of sudden death. To investigate the effect of this mutation on left ventricular (LV) function, we determined LV pressure-volume (PV) relationships in transgenic mice expressing human wild type (Wt) and human mutant TnT (I79N). A micro-conductance catheter was introduced in the LV (n =8/group). Load-independent end-diastolic PV relationships were obtained (EDPVR) under basal and stress conditions (0.25 mg/kg isoproterenol i.p.). After treatment with the calcium channel inhibitor diltiazem we investigated the LV function in another set of I79N mice.
Basal conditions: I79N mice showed increased systolic function compared to Wt: EF:63.3±4.3* vs. 51.1±5.0%; SV:35±2.2* vs. 27.1±1.8µl; CO: 16663±1300* vs. 12119±1027µl/min; * p<0.05 without differences in HR and LVP. Load dependent diastolic pressure indices as LVEDP were unchanged, but the load independent EDPVR was increased (0.5±0.1* vs. 0.2±0.03; * p<0.05), showing increased LV stiffness leading to a diastolic dysfunction.
Stress conditions: HR (654±21 vs. 626±35 bpm) and LVP (159.8±8.8 vs. 160.5±11.8mmHg; p<0.05) response was similar in all groups, but systolic function of I79N mice decreased compared to Wt (EF: 28.1±5.5* vs. 51.7±8.4%; SV: 14.0±2.3* vs. 22.17±4.4µl; CO: 8916±1842* vs. 13615±1598µl/min; Ves: 42.2±2.5* vs. 35.8±3.8µl *p<0.05). Diastolic indices demonstrate diastolic dysfunction in I79N compared to Wt: (LVEDP: 17.1±2.2* vs. 8.4±2.2mmHg; *p<0.05). This cardiac decompensation due to stress conditions leads to death in all I79N, but in none of the Wt animals.
Diltiazem prevented the reduction in SV, EF, CO and the rise in LVEDP without affecting HR significantly compared to non treated I79N and decreased mortality due to stress to 25 %.
I79N mice show an increased cardiac stiffness under basal conditions, and a diastolic dysfunction leading to decompensation and death under stress. Diltiazem prevents cardiac decompensation and death. These data gain an inside into hemodynamic pathology of the I79N mutation leading to FHC and why sudden death is common in FHC.

1144-133 β3-adrenergic Receptor Activation Decreases Peripheral Vascular Resistance in Heart Failure by Restoring Endothelial Dependent Vasorelaxation via Endothelial Nitric Oxide Synthase Upregulation

Hoang M. Thai, Bao Do, Raymond Hoang, Peter Spooner, Julie Indyk, Steve Goldman, Mohamed Gaballa, Southern Arizona VA Health Care System, Tucson, AZ, Sarver Heart Center at The University of Arizona, Tucson, AZ

Background: Peripheral vascular resistance (PVR) is increased in heart failure (HF). Therapy designed to decrease PVR by restoring nitric oxide (NO) mediated endothelial dependent (ED) vasorelaxation may prove to be vital in improving survival. Recent data suggests that beta-3 adrenoreceptor (β3-AR) activation may increase NO bioavailability. This study was performed to evaluate whether β3-AR activation with BRL, a β3-AR agonist, decreases PVR via NO mediated ED vasorelaxation in HF.
Methods: Sprague-Dawley rats with HF after coronary artery ligation were randomized into untreated controls and BRL treatment. After four weeks of therapy, hemodynamics was obtained and aortic vasorelaxation in response to isoproterenol with and without L-NMMA were performed. Additionally, bovine pulmonary artery endothelial cells in culture were incubated for 24 hours with BRL at 10 µM and 20 µM concentrations. Western blots for endothelial NO synthase (eNOS) protein concentration was performed.
Results: In HF rats treated with BRL, heart rate, systolic blood pressure, and left ventricular (LV) dP/dt was decreased (P<0.05) compared to untreated HF rats. LV end diastolic pressure (LVEDP) was unchanged. BRL significantly improved endothelial dependent vasorelaxation (37.1 ± 15.3 versus 17.2 ± 8.8 %, P<0.05) compared to untreated HF rats at peak isoproterenol dose. Addition of L-NMMA completely blunted all vasorelaxation responses. Bovine cell cultures incubated with BRL resulted in greater (P<0.05) than two fold increases of eNOS compared to untreated cell cultures.
Conclusions: β3-AR activation decreases peripheral vascular resistance in heart failure by restoring endothelial dependent vasorelaxation via endothelial nitric oxide synthase upregulation.

1144-134 Direct Comparison of Bone Marrow Stromal Versus Mononuclear Cells in Murine Cardiac Function After Cellular Cardiomyoplasty

Yoshihiro Morimoto, Igor Klem, Emilee Velasquez, Brad S. Sullen, Bryce H. Davis, Robert M. Judd, Doris A. Taylor, Duke University Medical Center, Durham, NC

Background: Cellular cardiomyoplasty, transplantation of bone marrow cells into injured myocardium, has been reported to improve cardiac function but the mechanism is unknown. Thus, in a mouse cryoinjury model, we compared the functional effects of potentially myogenic bone marrow stromal cells (BM), potentially angiogenic bone marrow mononuclear cells (MNC), or media alone (sham) with historical myoblast (Mb) controls where myogenesis is clear. Methods: C57BL/6 mice (n=6, each group) were subjected to LV cryoinfarction. Animals received myocardial injections of 10^7 BM, MNC or media 7 days after injury. Contiguous short-axis (2mm) ECG-gated segmental FLASH images were acquired on a 1.5T clinical scanner (eyecoil) immediately before, and again 4 wks after injection. Result: After infarction, all animals showed poor ejection fraction (EF, %) (57±11 in BM, 58±8 in MNC and 60±16 in sham) and all infarction areas were detectable. At 4 wks EF was improved in BM (61±20) and MNC (62±14) similar to Mb, yet deteriorated in the sham group (56±8). Conclusions: Although both MNC and BM cells stabilize cardiac function to a similar degree as myoblasts, histological evidence suggests differing mechanisms of angiogenesis versus myogenesis, respectively.

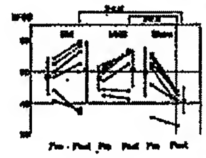

POSTER SESSION

1145 Heart Failure: Miscellaneous Topics

Tuesday, March 09, 2004, Noon-2:00 p.m.
Morial Convention Center, Hall G
Presentation Hour: 1:00 p.m.-2:00 p.m.

1145-115 Congestive Heart Failure in Rheumatoid Arthritis Patients: Rates, Predictors, and the Effect of Antitumor Necrosis Factor Therapy

Frederick Wolfe, Kaleb Michaud, Alan Mandelstein, Arthritis Research Center Foundation, Wichita, KS, Centocor, Inc., Malvern, PA

Background: Cardiovascular morbidity (e.g. pericarditis, diastolic dysfunction) is increased in rheumatoid arthritis (RA) patients though data on rates of congestive heart failure (CHF) in RA patients is unknown. Elevated tumor necrosis factor (TNF-alpha) levels have been identified as potential factors in CHF development. However, clinical studies have demonstrated limited value of anti-TNF blockade in patients with CHF. This study examined background CHF risk factors in RA and osteoarthritis (OA) patients, CHF prevalence and incidence rates in RA patients, and evaluated the relationship of anti-TNF agents and rates of CHF. Methods: Cohorts of RA patients (n = 13,171) and OA patients (n=2,568) in a longitudinal outcome study of the National Data Bank for Rheumatic Diseases were assessed via questionnaire and medical record review for CHF during a two-year period ending in 6/2002. Propensity scores were used to adjust for the risk of anti-TNF prescription. Results: Adjusted prevalence of CHF in RA patients was increased over that in OA patients (3.9% vs. 2.2%). CHF risk factors (e.g., hypertension, prior MI, diabetes, advanced age) were similar between RA and OA patients though measures of RA severity (HAQ, education, weight) were contributory to CHF rates. Adjusted rates of CHF were lower in anti-TNF treated RA patients (n = 5,632) than in non anti-TNF RA treated patients (2.8% vs. 3.9%, average treatment effect −1.2%[-1.9 to -0.5]). The rate of new-onset incident cases was low (0.2%) and unrelated to anti-TNF therapy. Conclusions: In 13,171 RA patients, rates of CHF were increased compared to concordant OA patients. Non-RA factors predicting CHF are the same in RA patients as in patients from general population studies, but RA activity/severity measures also predicted heart failure. Patients receiving anti-TNF therapy had lower rates of prevalent CHF compared to non anti-TNF treated patients. Incidence rates of CHF were low and unrelated to treatment.

1145-116 Prevalence and Mechanism of Functional Mitral Regurgitation in Dilated Cardiomyopathy: Baseline Data From the Acorn Trials

Seung Woo Park, Spencer Kubo, Mariell Jessup, Steven Bolling, Michael Acker, Jae K. Oh, Mayo Clinic, Rochester, MN, Acorn Cardiovascular Inc., St. Paul, MN

Background: Functional mitral regurgitation (MR) in dilated cardiomyopathy has significant prognostic implication, but its mechanism needs to be elucidated. The aim of the study was to determine the prevalence and the main echocardiographic factors determining the severity of MR in theses patients. Method: From the baseline echocardiographic results of Acorn cardiac support device trials, 154 patients with dilated cardiomyopathy without organic mitral valve disease were identified. Echocardiographic parameters were correlated with the severity of MR assessed by color flow imaging. Results: There were 94 males and the mean age was 55 ± 13 years. Mitral regurgitation was detected in 111 patients (72%); 29 in grade I (26%), 32 in grade II (29%), 29 in grade III (26%), and 21 in grade IV (20%). In univariate analysis, systolic and diastolic left ventricular dimensions (p<0.01), systolic and diastolic spherical indices of left ventricle (p<0.0005), systolic and diastolic mitral annulus size and area (p<0.0001), left atrial area and volume (p<0.0001), tethering distance from papillary muscle to annulus fibrosa (p<0.0001), tenting height (p<0.0001) and tenting area (p<0.0001) of mitral valve, and stroke volume (p<0.005) showed significant correlation with the severity of MR. Left ventricular volume or ejection fraction did not show significant correlation. In multivariate analysis, only tenting area showed significant correlation with severity of MR (p<0.0001). Conclusion: Functional MR was found in more than two thirds of patients with dilated cardiomyopathy, and severity of MR was mainly related with the tenting area of the mitral valve. Therefore, treatment interventions for functional MR may have to be directed to reduce the tenting area of regurgitant valve in addition to reducing the size of the mitral annulus.

PubMed Horinouchi 2002 fundus smooth muscle

Display Settings: Abstract

Nihon Yakurigaku Zasshi. 2002 Nov;120(1):109P-111P.

[Beta 3-adrenoceptor-mediated relaxation of guinea-pig gastric funds smooth muscle: cAMP-independent characteristics and a primary role of 4-aminopyridine-sensitive voltage-dependent K+ (Kv) channels].

[Article in Japanese]

Horinouchi T, Tanaka Y, Koike K.

Department of Chemical Pharmacology, Toho University School of Pharmaceutical Sciences, 2-2-1 Miyama, Funabashi-City, Chiba 274-8510, Japan.

Abstract

beta-Adrenoceptor subtypes which mediate relaxation of guinea-pig gastrointestinal **smooth** muscles in response to catecholamines ((-)-isoprenaline, (-)-noradrenaline and (-)-adrenaline) and beta 3-adrenoceptor agonists (BRL37344 and (+/-)-CGP12177A) are predominantly beta 3-adrenoceptors. Although cAMP-PKA system is thought to play a substantial role in the **smooth muscle** relaxation mediated via beta 1- and beta 2-adrenoceptors, there is little information on the role of cAMP in beta 3-adrenoceptor-meidated relaxation. The present study was carried out to elucidate the role of cAMP in beta 3-adrenoceptor-meidated relaxation of guinea-pig **gastric fundus smooth muscle**. Furthermore, possible contribution of two types of K+ (voltage-dependent and Ca(2+)-activated K+, BKCa; voltage-dependent, Kv) channels was also examined pharmaco-mechanically. In **gastric fundus smooth muscle**, catecholamines and beta 3-adrenoceptor agonists elicited potent relaxations in the presence of beta 1- and beta 2-adrenoceptor antagonists. All of these relaxations were not diminished by an adenylate cyclase inhibitor, SQ-22,536 (100 microM), which indicates their characteristic of cAMP-independency. SQ-22,536-resistant, beta 3-adrenoceptor-mediated relaxations were strongly attenuated by a Kv channel blocker, 4-aminopyridine (3 mM), but not by iberiotoxin (100 nM), a selective blocker of BKCa channel. The present results indicate that 4-aminopyridine-sensitive Kv channels play a primary role in cAMP-independent relaxation of guinea-pig **gastric fundus smooth muscle** in response to the stimulations of beta 3-adrenoceptors.

PMID:12491798[PubMed - indexed for MEDLINE]

Publication Types, MeSH Terms, Substances

LinkOut - more resources

引用非特許文献

特許出願の番号	特願２００７－５０８６７９
作成日	平成２３年　５月３０日
作成者	川嵜　洋祐　　４７６５　４Ｃ００
発明の名称	心筋の病気を治療するための方法および組成物

Journal of Autonomic Pharmacology 20, 253–258

Functional identification of β_3-adrenoceptors in the guinea-pig ileum using the non-selective β-adrenoceptor antagonist (±)-bupranolol

T. Horinouchi & K. Koike

Department of Chemical Pharmacology, Toho University School of Pharmaceutical Sciences, 2-2-1 Miyama, Funabashi, Chiba 274-8510, Japan

Correspondence:
K. Koike

Summary

1 To clarify whether there is a species difference or a tissue difference in β_3-adrenoceptors, the β_3-adrenoceptors mediating relaxations to catecholamines ((–)-isoprenaline, (–)-noradrenaline and (–)-adrenaline), a selective β_3-adrenoceptor agonist BRL37344 and a non-conventional partial β_3-adrenoceptor agonist (±)-CGP12177A (a potent β_1- and β_2-adrenoceptor antagonist with a partial β_3-adrenoceptor agonist property) were investigated in the guinea-pig ileum.

2 Catecholamines and β_3-adrenoceptor agonists induced concentration-dependent relaxations of pre-contracted strips of the guinea-pig ileum. The rank order for their relaxing potency was (–)-isoprenaline (pD_2: 7.60) > BRL37344 (7.05) > (–)-noradrenaline (6.38) > (±)-CGP12177A (6.25) > (–)-adrenaline (6.07).

3 In the presence of the non-selective β_1- and β_2-adrenoceptor antagonist (±)-propranolol (1 μM), only small rightward shifts of the concentration–response curves (CRCs) to these agonists were observed and the rank order of potency of agonists was BRL37344 (pD_2: 7.00) > (±)-CGP12177A (6.17) > (–)-isoprenaline (6.01) > (–)-noradrenaline (5.69) > (–)-adrenaline (5.41).

4 In the presence of (±)-propranolol (1 μM), the additional presence of (±)-bupranolol (3–30 μM), a non-selective β_1-, β_2- and β_3-adrenoceptor antagonist, caused a concentration-dependent rightward shift of the CRCs to catecholamines and β_3-adrenoceptor agonists. Schild plot analyses of (±)-bupranolol against these agonists gave pA_2 values of 6.02 ((–)-isoprenaline), 6.03 ((–)-noradrenaline), 6.01 ((–)-adrenaline), 6.56 (BRL37344) and 5.74 ((±)-CGP12177A), respectively. All Schild plot slopes were not significantly different from unity. The pA_2 values of (±)-bupranolol obtained for the guinea-pig β_3-adrenoceptors were about one log unit less than the values obtained for the rat β_3-adrenoceptors and about two log units less than the values obtained for dog β_3-adrenoceptors.

5 These results confirm that functional β_3-adrenoceptors are present in the guinea-pig ileum and that the relaxations of these agonists are mainly mediated via β_3-adrenoceptors in this tissue. The differential antagonistic potency of (±)-bupranolol may suggest that there is a species difference between the three species (guinea-pig, dog and rat) in their β_3-adrenoceptors.

Introduction

β-Adrenoceptors were initially subclassified by Lands, Arnold, McAuliff, Luduena & Brown Jun (1967a) and Lands, Luduena & Buzzo (1967b) into β_1- and β_2-adrenoceptor subtypes. In the guinea-pig ileum, the β-adrenoceptor-mediated relaxation was suggested to be mediated via a homogeneous population of β_1-adrenoceptor subtype (Grassby & Broadley, 1984), however, Bond & Clark (1987) reported the presence of both propranolol-sensitive (β_1- and/or β_2-adrenoceptor-mediated) and insensitive responses. Recently, several studies showed β-adrenoceptors in the ileum with characteristics distinct from β_1- and β_2-adrenoceptor subtypes and referred to as β_3-adrenoceptors or atypical β-adrenoceptors (for review, see Manara, Croci & Landi, 1995).

We have reported that β_3-adrenoceptors or atypical β-adrenoceptors are involved in mediating the relaxant response of the guinea-pig duodenum and the guinea-pig gastric fundus (Horinouchi &

Journal of Autonomic Pharmacology 20, 253–258

Koike, 1999a, b). Furthermore, Horinouchi & Koike (1999a, b) showed that the pA_2 value of (±)-bupranolol against (−)-isoprenaline and β_3-adrenoceptor agonist (±)-CGP12177A was 6.02–6.08 and 5.70–5.80, respectively. However, several pA_2 values for (±)-bupranolol have been reported: the value against (−)-isoprenaline is 8.19 at β_3-adrenoceptors in the dog detrusor (Yamazaki *et al.*, 1998) and the value against (±)-CGP12177A is 6.70 at β_3-adrenoceptors in the rat fat cell (Galitzky *et al.*, 1997). It remains possible that there is a species difference or a tissue difference in the distribution of β_3-adrenoceptors.

The aim of the present study was to characterize the β_3-adrenoceptors involved in relaxant responses in the guinea-pig ileum using functional experiments with catecholamines ((−)-isoprenaline, (−)-noradrenaline and (−)-adrenaline), β_3-adrenoceptor agonists (BRL37344 and (±)-CGP12177A) and a non-selective β_1-, β_2- and β_3-adrenoceptor antagonist (±)-bupranolol. To clarify whether there is a species difference or a tissue difference in β_3-adrenoceptors, we compared pA_2 values for antagonism by (±)-bupranolol of the β_3-adrenoceptors of the guinea-pig ileum with published values for the β_3-adrenoceptors obtained from the guinea-pig duodenum, the guinea-pig gastric fundus, the dog detrusor and the rat fat cell.

Methods

Mechanical responses

Male Hartley guinea-pigs weighing 300–500 g were killed by cervical dislocation and the distal ileum was removed. After washing out the luminal contents, longitudinal smooth muscle from the ileum was isolated by rubbing the ileum with a cotton swab. Each segment 2–3 cm in length was set up in a 20-ml organ bath under an initial resting tension of 500 mg in oxygenated (a mixture of 95% O_2 and 5% CO_2) Ringer–Locke solution maintained at 32 °C with desmethylimipramine (1 μM; to block neuronal uptake of catecholamines), normetanephrine (10 μM; to block extraneuronal uptake of catecholamines) and phentolamine (10 μM; to block α-adrenoceptors). The composition (mM) of Ringer–Locke solution was as follows: NaCl, 154; KCl, 5.6; $CaCl_2$, 2.2; $MgCl_2$, 2.1; $NaHCO_3$, 5.9 and glucose, 2.8. Changes in tension of strips were recorded isometrically. Strips were allowed to equilibrate for at least 30 min before experimental procedures were begun.

The relaxant action of β-adrenoceptor agonists was determined by measuring relaxation of histamine-induced contraction evoked by addition of the agonists. Initially, two concentration-response curves (CRCs) to histamine were constructed for each tissue, to determine a concentration of histamine which gave submaximal contraction. A submaximal concentration of histamine was used.

CRCs to β-adrenoceptor agonists were constructed by cumulative addition to histamine-contracted strips until a maximal relaxant response was observed and the relaxation induced by agonists was expressed as a percentage of the maximal agonist (3 μM (−)-isoprenaline) response. CRCs were constructed at 30 min interval, allowing 30 min equilibration time for antagonists, which were added at the end of each CRC.

In experiment testing the effect of antagonists on the relaxation induced by BRL37344 or (±)-CGP12177A, only one CRC to the agonist (BRL37344 or (±)-CGP12177A) was constructed in any one tissue. In these cases paired experiments were carried out. If CRCs to (−)-isoprenaline were not significantly different in the paired tissues then one tissue was subsequently treated with BRL37344 in the absence of antagonist. The antagonist was present for 30 min before the construction of CRCs to BRL37344.

Data analysis

The data were presented as mean ± SEM of 6–8 experiments. Agonistic potency was expressed as the pD_2 value (Van Rossum, 1963). The intrinsic activity (IA) of an agonist was measured relative to the maximal relaxation induced by the full agonist (−)-isoprenaline (3 μM). A ligand in which an IA was significantly lower than 1 was defined as a partial agonist. The pA_2 values for antagonists, as defined by Arunlakshana & Schild (1959), were calculated according to the method of Tallarida, Cowan & Adler (1979). Statistical analyses were performed with the Newman–Keuls test when appropriate. A *P*-value of less than 0.05 was considered statistically significant.

Drugs

(−)-Isoprenaline hydrochloride, (−)-noradrenaline bitartrate, (−)-adrenaline bitartrate, (±)-propranolol hydrochloride, histamine dihydrochloride, desmethylimipramine hydrochloride and normetanephrine hydrochloride were purchased from Sigma Chemical Co. (St Louis, MO, USA). BRL37344 [(R*, R*)-(±)-4-[2-[(2-(3-chlorophenyl)-2-hydroxyethyl)amino]propyl]phenoxyacetic acid] was obtained from Nacalaitesque (Kyoto, Japan). (±)-CGP12177A ([4-[3-[(1,1-dimethylethyl)amino]-2-hydroxypropoxy]-1,3-dihydro-2H-benzimidazol-2-one] hydrochloride) was from Research Biochemicals (Natick, MA, USA). Phentolamine mesylate was provided by Novartis (Basal, Switzerland). (±)-Bupranolol hydrochloride was a gift from Kaken Pharmaceutical Co., Ltd (Tokyo, Japan). All the drugs were dissolved in

Journal of Autonomic Pharmacology, 20, 253–258

distilled water. All other chemicals used were of analytical reagent grade.

Results

Effects of catecholamines

In the absence of (±)-propranolol (1 μM), the three catecholamines relaxed histamine-induced tone in the guinea-pig ileum (Fig. 1a). The pD_2 values and intrinsic activities are shown in Table 1. (−)-Noradrenaline and (−)-adrenaline were partial agonists as their intrinsic activities (0.90 ± 0.02 and 0.92 ± 0.02, respectively) were significantly lower than 1 ($P < 0.05$). The relative rank order of potency was (−)-isoprenaline > (−)-noradrenaline > (−)-adrenaline.

(±)-Propranolol (1 μM) weakly antagonized the relaxant responses to catecholamines without reducing the maximum relaxation and caused only 39-, 5- and 3-fold rightward shifts of CRCs to (−)-isoprenaline, (−)-noradrenaline and (−)-adrenaline, respectively (Fig. 1b). In the presence of (±)-propranolol (1 μM), the rank order of agonist potency was (−)-isoprenaline > (−)-noradrenaline > (−)-adrenaline (Fig. 1b; Table 1).

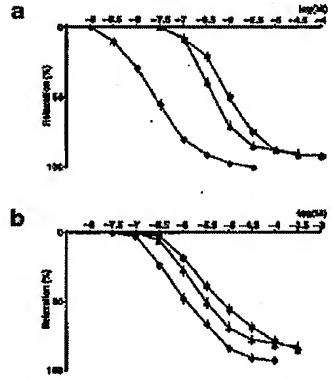

Figure 1 Concentration–response curves for (−)-isoprenaline (●), (−)-noradrenaline (▲) and (−)-adrenaline (■) in the absence of (±)-propranolol and (b) in the presence of (±)-propranolol (1 μM). Ordinate: relaxation (%), expressed as a percentage relative to the maximum relaxation induced by (−)-isoprenaline (3 μM); abscissa: concentration (M) of the test drugs. Each point represents the mean ± SEM of 6 to 8 experiments.

Effects of β3-adrenoceptor agonists

In the absence of (±)-propranolol (1 μM), BRL37344 and (±)-CGP12177A caused relaxation of the guinea-pig ileum concentration-dependently (Fig. 2a, b). BRL37344 was similar in potency to (−)-isoprenaline and (±)-CGP12177A was somewhat less potent than (−)-isoprenaline (Table 1). However, the maximum responses obtained with BRL37344 and (±)-CGP12177A were significantly lower than that achieved with (−)-isoprenaline (Fig. 2a, b), indicating that the two β_3-adrenoceptor agonists acted as a partial agonist in this tissue. The CRCs to BRL37344 and (±)-CGP12177A were not affected by (±)-propranolol (1 μM, Fig. 2a, b).

Effects of (±)-bupranolol on relaxation induced by catecholamines and β3-adrenoceptor agonists

The effects of (±)-bupranolol on agonists-induced relaxation, in the presence of (±)-propranolol (1 μM), were shown in Figs 3–5 and 6a, b. With concentrations of (±)-bupranolol, ranging from 3 to 30 μM, clear rightward shifts of the concentration–response curves to these agonists were consistently observed. The Arunlakshana–Schild plot of the data revealed the pA_2 values for (±)-bupranolol against catecholamines and β_3-adrenoceptor agonists to be 6.02 ± 0.05 ((−)-isoprenaline, slope: 1.02 ± 0.02, $n = 6$), 6.03 ± 0.05 ((−)-noradrenaline, 1.03 ± 0.03, $n = 7$), 6.01 ± 0.03 ((−)-adrenaline, 1.04 ± 0.04, $n = 8$), 6.56 ± 0.02 (BRL37344,

Table 1 Potencies of catecholamines and β_3-adrenoceptor agonists and effect of (±)-propranolol (1 μM) on the guinea-pig ileum

	Absence of (±)-propranolol		Presence of (±)-propranolol	
Agonist	pD_2 value	IA	pD_2 value	IA
(−)-Isoprenaline	7.60 ± 0.04	1	6.01 ± 0.06	0.59 ± 0.03
(−)-Noradrenaline	6.38 ± 0.05	0.90 ± 0.02	5.69 ± 0.05	0.82 ± 0.02
(−)-Adrenaline	6.07 ± 0.04	0.92 ± 0.02	5.41 ± 0.02	0.84 ± 0.03
BRL37344	7.05 ± 0.04	0.73 ± 0.03	7.00 ± 0.02	0.70 ± 0.02
(±)-CGP12177A	6.25 ± 0.04	0.81 ± 0.02	6.17 ± 0.03	0.85 ± 0.03

Values are mean ± SEM from 6 to 8 experiments. pD_2 value = − log EC_{50} (EC_{50}: concentration of agonist producing half-maximum response). IA is calculated for each agonist in the absence or presence of (±)-propranolol (1 μM) relative to the maximum relaxation induced by (−)-isoprenaline (3 μM) in the absence of (±)-propranolol.

Journal of
Autonomic Pharmacology
20, 253–258

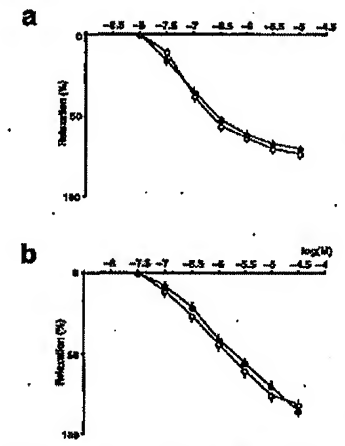

Figure 2 Effect of (±)-propranolol (1 μM) on concentration–response curves for BRL37344 and (±)-CGP12177A: (a) BRL37344 only (○), BRL37344 plus (±)-propranolol (1 μM) (●); (b) (±)-CGP12177A only (○), (±)-CGP12177A plus (±)-propranolol (1 μM) (●). Ordinate: relaxation (%), expressed as a percentage relative to the maximum relaxation induced by (−)-isoprenaline (3 μM); abscissa: concentration (M) of the test drugs. Each point represents the mean ± SEM of 6 to 8 experiments.

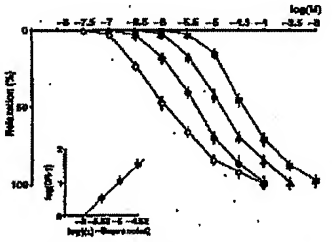

Figure 3 Effect of (±)-bupranolol on concentration–response curves for (−)-isoprenaline in the presence of (±)-propranolol (1 μM). Control, no (±)-bupranolol (○); (±)-bupranolol 3 μM (●); (±)-bupranolol 10 μM (▲); (±)-bupranolol 30 μM (■). Ordinate: relaxation (%), expressed as a percentage relative to the maximum relaxation induced by (−)-isoprenaline (3 μM); abscissa: concentration (M) of the test drugs. Each point represents the mean ± SEM of six experiments. The inset shows the corresponding Schild plot calculated from the individual experiments.

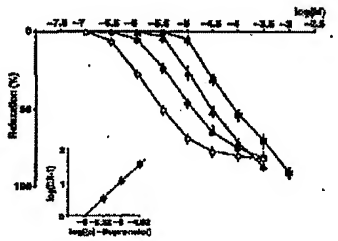

Figure 4 Effect of (±)-bupranolol on concentration–response curves for (−)-noradrenaline in the presence of (±)-propranolol (1 μM). Control, no (±)-bupranolol (○); (±)-bupranolol 3 μM (●); (±)-bupranolol 10 μM (▲); (±)-bupranolol 30 μM (■). Ordinate: relaxation (%), expressed as a percentage relative to the maximum relaxation induced by (−)-isoprenaline (3 μM); abscissa: concentration (M) of the test drugs. Each point represents the mean ± SEM of seven experiments. The inset shows the corresponding Schild plot calculated from the individual experiments.

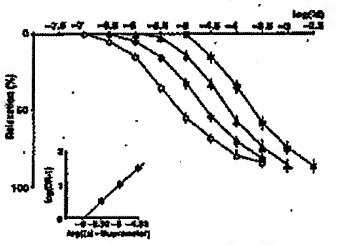

Figure 5 Effect of (±)-bepranolol on concentration–response curves for (−)-adrenaline in the presence of (±)-propranolol (1 μM). Control, no (±)-bupranolol (○); (±)-bupranolol 3 μM (●); (±)-bupranolol 10 μM (▲); (±)-bupranolol 30 μM (■). Ordinate: relaxation (%), expressed as a percentage relative to the maximum relaxation induced by (−)-isoprenaline (3 μM); abscissa: concentration (M) of the test drugs. Each point represents the mean ± SEM of eight experiments. The inset shows the corresponding Schild plot calculated from the individual experiments.

1.01 ± 0.01, $n = 8$) and 5.74 ± 0.03 ((±)-CGP12177A, 1.00 ± 0.06, $n = 8$). The slope of each regression line was not significantly different from unity (Figs 3–5 and 6a, b; Table 2).

Discussion

The presence of β_3-adrenoceptors or the atypical β-adrenoceptor has now been generally accepted. The high potency of a novel class of β-adrenoceptor agonists (Arch *et al.*, 1984) has provided strong

Journal of Autonomic Pharmacology, 20, 253–258

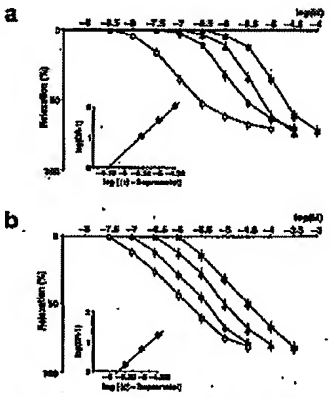

Figure 4 Effect of (±)-bupranolol on concentration–response curves for BRL37344 (a) and (±)-CGP12177A (b) in the presence of (±)-propranolol (1 μM). Control, no (±)-bupranolol (○); (±)-bupranolol 3 μM (●); (±)-bupranolol 10 μM (▲); (±)-bupranolol 30 μM (■). Ordinate: relaxation (%), expressed as a percentage relative to the maximum relaxation induced by (−)-isoprenaline (3 μM); abscissa: concentration (M) of the test drugs. Each point represents the mean ± SEM of eight experiments. The inset shows the corresponding Schild plot calculated from the individual experiments.

support for the existence of β_3-adrenoceptors. These receptors were reported to be abundantly present in adipose and gastrointestinal tissue (for review see Arch & Kaumann, 1993).

The present study was designed to characterize the β_3-adrenoceptors mediating relaxation of the guinea-pig ileum to catecholamines and selective β_3-adrenoceptor agonists. The potency of catecholamines and selective β_3-adrenoceptor agonists was very similar to values reported for the guinea-pig duodenum (Horinouchi & Koike, 1999a) and the guinea-pig gastric fundus (Horinouchi & Koike, 1999b), indicating the involvement of similar β_3-adrenoceptor populations in the three tissues. Propranolol (1 μM) shifted CRCs to the catecholamines to a variable extent, which indicated variable contribution of β_1- and β_2-adrenoceptors to relaxations induced by these agonists. The relaxant responses induced by β_3-adrenoceptor agonists were not antagonized by (±)-propranolol (1 μM). As (±)-propranolol is a very potent and non-selective classical β-adrenoceptor antagonist, it can be concluded that β_3-adrenoceptor agonists-induced relaxations of the guinea-pig ileum were not mediated by classical β-adrenoceptors but solely by β_3-adrenoceptors, whereas catecholamines-induced relaxations were shown to involve both classical β_1- and/or β_2-adrenoceptors and, predominantly, β_3-adrenoceptors. The order of potency of the catecholamines was of the same rank order as in the rat jejunum in which β_3-adrenoceptor responses are observed (MacDonald, Forbes, Gallacher, Heeps & McLaughlin, 1994). This was not affected by (±)-propranolol (1 μM) and provides strong support for the view that β_3-adrenoceptors were quantitatively more abundant than classical β_1- and/or β_2-adrenoceptors.

The non-selective β-adrenoceptor antagonist (±)-bupranolol, at a dose much higher than that antagonizing β_1- and β_2-adrenoceptor-mediated effects (Kaumann & Molenaar, 1996), also antagonized the β_3-adrenoceptor-mediated effects (Arch & Kaumann, 1993). In order to assay the β_3-adrenoceptors, we included (±)-propranolol (1 μM) in functional competition experiments to block coexisting β_1- and β_2-adrenoceptors. (±)-Bupranolol antagonized the relaxant responses to catecholamines and selective β_3-adrenoceptor agonists in a concentration-dependent manner. pA_2 values for (±)-bupranolol against catecholamines and β_3-adrenoceptor agonists were not significantly different from the pA_2 values obtained in the guinea-pig duodenum and the guinea-pig gastric fundus (Horinouchi & Koike, 1999a, b), suggesting there is no tissue difference between the three tissues

Table 2 Comparison of pA_2 values and Schild slopes for bupranolol against catecholamines and β_3-adrenoceptor agonists on the guinea-pig, dog and rat tissues

	Guinea-pig ileum		Dog detrusor pA_2 value	Rat fat cell pA_2 value
	pA_2 value	Slope		
(−)-Isoprenaline	6.02 ± 0.05	1.02 ± 0.02	8.19*	
(−)-Noradrenaline	6.03 ± 0.05	1.03 ± 0.03		
(−)-Adrenaline	6.01 ± 0.03	1.04 ± 0.04		
BRL37344	6.56 ± 0.02	1.01 ± 0.01		
(±)-CGP12177	5.74 ± 0.03	1.00 ± 0.06		6.70†

Values are mean ± SEM from 6 to 8 experiments.
*Value from Yamazaki *et al.* (1998).
†Value from Galitsky *et al.* (1997).
Significant (*$P < 0.05$, †$P < 0.01$) against corresponding value obtained in guinea-pig ileum.

Journal of Autonomic Pharmacology, 20, 253–258

with respect to in β_3-adrenoceptor-mediated responses. However, the pA_2 value for (±)-bupranolol of 6.02 against (−)-isoprenaline in the guinea-pig ileum was lower than the value of 8.19 in the dog detrusor reported by Yamazaki *et al.* (1998). Furthermore, the value of 5.74 against (±)-CGP12177A in the guinea-pig ileum was also lower than the value of 6.70 in the rat fat cell reported by Galitzky *et al.* (1997). Thus, the pA_2 values of β_3-adrenoceptor antagonists obtained in guinea-pig tissues were about one or two log units lower than the values obtained in the dog and rat tissues, indicating that there is a species difference between β-adrenoceptors stimulated by (−)-isoprenaline and (±)-CGP12177A. The reasons for these differences in potency for β_3-adrenoceptor antagonists are not apparent, but have been suggested to result from β_3-adrenoceptor heterogeneity and/or species differences because of variations in the β_3-adrenoceptor amino acid sequence (Blin, Nahmias, Drumare & Strosberg, 1994; De Ponti, Gibelli, Crema & Lecchini, 1995).

In conclusion, the present study suggests that in the guinea-pig ileum, relaxation responses induced by catecholamines and selective β_3-agonists were mediated predominantly by β_3-adrenoceptors, whereas β_1- and/or β_2-adrenoceptors play a subordinate role. In addition, our present results taken together with our previous studies (Horinouchi & Koike, 1999a, b) on β_3-adrenoceptors in the guinea-pig duodenum and gastric fundus, suggest that there is no tissue difference in β_3-adrenoceptor profile in these tissues. However, as (±)-bupranolol was more potent at both the dog and rat β_3-adrenoceptors than in the guinea-pig, it is possible that there is a species difference in the pharmacological profile of β_3-adrenoceptor between these species.

Acknowledgements

Kaken Pharmaceutical Co., Ltd (Tokyo, Japan) are thanked for the gift of (±)-bupranolol hydrochloride.

References

ARCH, J.R.S., AINSWORTH, A.T., CAWTHORN, M.A., PIERCY, V., SENNITT, M.V., THODY, V.E., WILSON, C. & WILSON, S. (1984). Atypical β-adrenoceptor on brown adipocytes as target for antiobesity drugs. *Nature*, 309, 163–165.

ARCH, J.R.S. & KAUMANN, A.J. (1993). β_3- and atypical β-adrenoceptors. *Med. Res. Rev.*, 13, 663–729.

ARUNLAKSHANA, O. & SCHILD, H.O. (1959). Some quantitative uses of drug antagonists. *Br. J. Pharmacol. Chemother.*, 14, 48–58.

BLIN, N., NAHMIAS, C., DRUMARE, M.F. & STROSBERG, A.D. (1994). Mediation of most atypical effects by species homologues of the β_3-adrenoceptor. *Br. J. Pharmacol.*, 112, 911–919.

BOND, R.A. & CLARKE, D.E. (1987). A response to isoprenaline unrelated to α- and β-adrenoceptor agonism. *Br. J. Pharmacol.*, 91, 683–686.

DE PONTI, F., GIBELLI, G., CREMA, F. & LECCHINI, S. (1995). Functional evidence for the presence of β_3-adrenoceptors in the guinea-pig common bile duct and colon. *Pharmacology*, 51, 288–297.

GALITZKY, J., LANGIN, D., VERWAERDE, P., MONTASTRUC, J.L., LAFONTAN, M. & BERLAN, M. (1997). Lipolytic effects of conventional β_1-adrenoceptor agonists and of CGP 12,177 in rat and human fat cells: preliminary pharmacological evidence for a putative β_4-adrenoceptor. *Br. J. Pharmacol.*, 122, 1244–1250.

GRASSBY, P.F. & BROADLEY, K.J. (1984). Characterization of β-adrenoceptors mediating relaxation of the guinea-pig ileum. *J. Pharm. Pharmacol.*, 36, 602–607.

HORINOUCHI, T. & KOIKE, K. (1999a). Characterization of atypical β-adrenoceptors in the guinea pig duodenum. *Eur. J. Pharmacol.*, 376, 61–66.

HORINOUCHI, T. & KOIKE, K. (1999b). Pharmacological analysis of atypical β-adrenoceptors in the guinea pig gastric fundus using the β_3-adrenoceptor antagonist bupranolol. *Pharmacology*, 59, 290–297.

KAUMANN, A.J. & MOLENAAR, P. (1996). Differences between the third cardiac β-adrenoceptor and the colonic β_3-adrenoceptor in the rat. *Br. J. Pharmacol.*, 118, 2085–2098.

LANDS, A.M., ARNOLD, A., MCAULIFF, J.P., LUDUENA, F.P. & BROWN JUN, T.G. (1967a). Differentiation of receptor systems activated by sympathomimetic amines. *Nature*, 214, 597–598.

LANDS, A.M., LUDUENA, F.P. & BUZZO, H.J. (1967b). Differentiation of receptors responsive to isoproterenol. *Life Sci.*, 6, 2241–2249.

MACDONALD, A., PORSES, I.J., GALLACHER, D., HEEPS, G. & MCLAUGHLIN, D.P. (1994). Adrenoceptor mediating relaxation to catecholamines in rat isolated jejunum. *Br. J. Pharmacol.*, 112, 576–578.

MANARA, L., CROCI, T. & LANDI, M. (1995). β_3-adrenoceptors and intestinal motility. *Fund. Clin. Pharmacol.*, 9, 332–342.

TALLARIDA, R.J., COWAN, A. & ADLER, M.W. (1979). pA_2 and receptor differentiation: a statistical analysis of competitive antagonism. *Life Sci.*, 25, 637–654.

VAN ROSSUM, J.M. (1963). Cumulative dose-response curves, II. Technique for the making of dose-response curves in isolated organs and the evaluation of drug parameters. *Arch. Int. Pharmacodyn. Ther.*, 143, 299–330.

YAMAZAKI, Y., TAKEDA, H., AKAHANE, M., IGAWA, Y., NISHIZAWA, O. & AJISAWA, Y. (1998). Species differences in the distribution of β-adrenoceptor subtypes in bladder smooth muscle. *Br. J. Pharmacol.*, 124, 593–599.

(Received 29 February 2000
Revised 30 August 2000
Accepted 2 October 2000)

FOREIGN LANGUAGE EDITIONS
of The Merck Manual

Arabic—Larike Publications Services, Cyprus
Chinese—People's Medical Publishing House, Beijing
Czech—Egem, Prague
French—Editions d'Apres, Paris
German—Urban & Fisher Verlag, GmbH, Munich
Greek—Medical & Scientific Publishing, Athens
Hungarian—Melania, Budapest
Italian—Medicom Italia Srl, Milan
Japanese—Nikkei BP, Tokyo
Polish—Urban & Partner, Wroclaw
Portuguese—Editora Roca, Ltda, São Paulo
Russian—MIR Publishers, Moscow
Spanish—Harcourt, Madrid
Turkish—Yüce, Istanbul

OTHER MERCK BOOKS

THE MERCK INDEX
First Edition, 1889

THE MERCK VETERINARY MANUAL
First Edition, 1955

THE MERCK MANUAL OF GERIATRICS
First Edition, 1990

THE MERCK MANUAL OF MEDICAL INFORMATION—HOME EDITION
First Edition, 1997

Merck books are published on a nonprofit basis as a service to the scientific community and the public.

SEVENTEENTH EDITION

THE MERCK MANUAL

OF DIAGNOSIS AND THERAPY

Editors
MARK H. BEERS, M.D., and ROBERT BERKOW, M.D.

Senior Assistant Editors
ROBERT M. BOGIN, M.D., and
ANDREW J. FLETCHER, M.B., B.Chir.

Editorial Board
Philip K. Bondy, M.D.
Preston V. Dilts, Jr., M.D.
Douglas A. Drossman, M.D.
L. Jack Faling, M.D.
Eugene P. Frenkel, M.D.
Glen O. Gabbard, M.D.
Robert A. Hoekelman, M.D.
Gerald L. Mandell, M.D.
Fred Plum, M.D.
G. Victor Rossi, Ph.D.
Paul H. Tanser, M.D., F.R.C.P.(C)

Published by MERCK RESEARCH LABORATORIES
Division of MERCK & CO., INC.
Whitehouse Station, N.J. 1999

203 / HEART FAILURE

(Congestive Heart Failure)

Symptomatic myocardial dysfunction resulting in a characteristic pattern of hemodynamic, renal, and neurohormonal responses.

(For heart failure in children, see Ch. 261.)

No definition of heart failure (HF) is entirely satisfactory. Congestive heart failure (CHF) develops when plasma volume increases and fluid accumulates in the lungs, abdominal organs (especially the liver), and peripheral tissues.

Physiology

At rest and during exercise, cardiac output (CO), venous return, and distribution of blood flow with O_2 delivery to the tissues are balanced by neurohumoral and intrinsic cardiac factors. Preload, the contractile state, afterload, the rate of contraction, substrate availability, and the extent of myocardial damage determine left ventricular (LV) performance and myocardial O_2 requirements. The Frank-Starling principle, cardiac reserve, and the oxyhemoglobin dissociation curve play a role.

Preload (the degree of end-diastolic fiber stretch) reflects the end-diastolic volume, which is influenced by diastolic pressure and the composition of the myocardial wall. For clinical purposes, the end-diastolic pressure, especially if above normal, is a reasonable measure of preload in many conditions. LV dilatation, hypertrophy, and changes in myocardial distensibility or compliance modify preload.

The **contractile state** in isolated cardiac muscle is characterized by the force and velocity of contraction, which are difficult to measure in the intact heart. Clinically, the contractile state is often expressed as the ejection fraction (LV stroke volume/end-diastolic volume).

Afterload (the force resisting myocardial fiber shortening after stimulation from the relaxed state) is determined by the chamber pressure, volume, and wall thickness at the time of aortic valve opening. Clinically, afterload approximates systemic BP at or shortly after aortic valve opening and represents peak systolic wall stress. The **heart rate and rhythm** also influence cardiac performance.

Reduced substrate availability (eg, of fatty acid or glucose), particularly if O_2 availability is reduced, can impair the vigor of cardiac contraction and myocardial performance.

Tissue damage (acute with MI or chronic with fibrosis due to various diseases) impairs local myocardial performance and imposes an additional burden on viable myocardium.

The **Frank-Starling principle** states that the degree of end-diastolic fiber stretch (preload) within a physiologic range is proportional to the systolic performance of the ensuing ventricular contraction (FIG. 203–1). This mechanism operates in HF, but, because ventricular function is abnormal, the response is inadequate. If the Frank-Starling curve is depressed, fluid retention, vasoconstriction, and a cascade of neurohumoral responses lead to the syndrome of CHF. Over time, LV remodeling (change from the normal ovoid shape) with dilatation and hypertrophy further compromises cardiac performance, especially during physical stress. Dilatation and hypertrophy may be accompanied by increased diastolic stiffness.

Cardiac reserve (unused ability of the resting heart to deliver O_2 to the tissues) is an important component of cardiac function during emotional or physical stress. Its mechanisms include increases in heart rate, systolic and diastolic volume, stroke volume, and tissue extraction of O_2. For example, in well-trained young adults during maximal exercise, heart rate may increase from 55 to 70 at rest to 180 beats/min; CO (stroke volume × heart rate) may increase from its normal resting value of 6 to ≥ 25 L/min; and O_2 consumption can increase from 250 to ≥ 1500 mL/min. In the normal young adult at rest, arterial blood contains about 18 mL O_2/dL of blood, and mixed venous or pulmonary artery blood contains about 14 mL/dL. The arteriovenous O_2 difference ($A-Vo_2$) is thus about 4.0 ± 0.4 mL/dL. Even maximal CO during exercise is insufficient to meet tissue metabolic needs; hence, the tissues extract more O_2, and mixed venous blood O_2 content falls considerably. $A-Vo_2$ may increase to about 12 to 14 mL/dL. Increased $A-Vo_2$ due to lower venous O_2 content is a common adaptive mechanism in HF.

The **oxyhemoglobin dissociation curve** (see FIG. 203–2) influences O_2 availability to the tissues and can provide another reserve mechanism in HF. The position of this curve is frequently expressed as P_{50} (the partial pressure of O_2 in blood at 50% oxyhemoglobin saturation). An increase in the normal P_{50} (27 ± 2 mm Hg) indicates a rightward shift of the oxyhemoglobin dissociation curve (decreased affinity of Hb for O_2). For a given Po_2, less O_2 is combined with Hb, and the saturation is lower; thus, at the capillary level, more O_2 is released and available to the tissues. Increased hydrogen ion concentration (reduced pH) shifts the curve to the right (Bohr effect); as does increased concentration of 2,3-diphosphoglycerate in RBCs, which alters the spatial relationships within the Hb molecule.

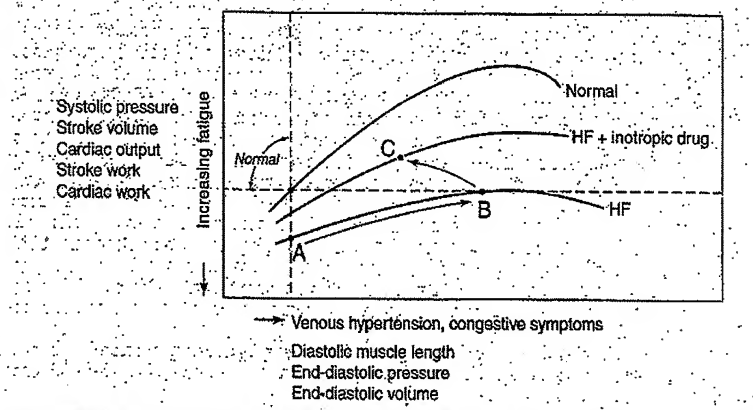

FIG. 203–1. Frank-Starling relationship. The ordinate (systolic pressure, stroke volume, cardiac output, stroke work, cardiac work) represents the ability of the ventricle to function as a pump. The abscissa (diastolic muscle length, end-diastolic pressure, end-diastolic volume) depicts the direct or indirect measurements of length or stretch of myocardial fiber. *Dotted lines* depict resting normal values; the normal curve includes point of intersection. Under normal conditions, left ventricular systolic pressure, stroke volume, and work increase rapidly as the myocardial fiber is lengthened at end-diastole. There is a family of ventricular function curves depicting cardiac performance under normal and abnormal conditions. During heart failure (HF) consequent to reduced contractility, ventricular performance falls sharply (*point A*). Reduced stroke volume causes increased end-diastolic volume with consequent stretching of diastolic muscle length. Ventricular function moves to the right on a relatively flat ventricular function curve to achieve relatively normal resting cardiac performance (*point B*). Thus, adequate resting cardiac performance results from increased ventricular diastolic volume and pressure. Treatment of the failing ventricle with an inotropic drug improves the ventricular function curve (*point C*), which, however, remains abnormal. Afterload reduction may have similar effects. This diagram assumes a direct relationship between diastolic muscle length, end-diastolic pressure, and end-diastolic volume, a relationship that is generally true when ventricular contractility is reduced. This relationship does not apply to HF due to increased myocardial diastolic stiffness; cardiac output is usually normal, end-diastolic pressure is high, yet diastolic muscle length may be normal. The problem in disease causing increased diastolic stiffness is a markedly reduced myocardial compliance, hence abnormally high ventricular filling pressure and congestion with adequate ventricular emptying. (Adapted from Spann JF, Mason DT, Zelis R: "Recent advances in the understanding of congestive heart failure (II)." *Modern Concepts of Cardiovascular Disease* 39:79–84, 1970; used with permission of the American Heart Association, Inc.)

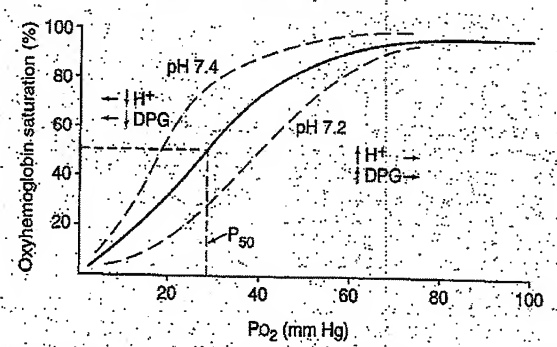

FIG. 203–2. Oxyhemoglobin dissociation curve. Arterial oxyhemoglobin saturation (ordinate) is related to partial pressure of O_2 (abscissa). P_{50} (P_{O_2} at 50% saturation) is normally 27 mm Hg. The dissociation curve is shifted to the right by increased hydrogen ion (H^+) concentration and increased RBC diphosphoglycerate (DPG). The curve is shifted to the left by decreased H^+ and lower RBC diphosphoglycerate. Hb characterized by rightward shifting of the curve has a decreased affinity for O_2; Hb characterized by a leftward shifting of the curve has an increased affinity for O_2.

Classification and Etiology

In many forms of heart disease, the clinical manifestations of HF may reflect impairment of the left or right ventricle.

Left ventricular (LV) failure characteristically develops in coronary artery disease, hypertension, and most forms of cardiomyopathy and with congenital defects (eg, ventricular septal defect, patent ductus arteriosus with large shunts).

Right ventricular (RV) failure is most commonly caused by prior LV failure (which increases pulmonary venous pressure and leads to pulmonary arterial hypertension) and tricuspid regurgitation. Mitral stenosis, primary pulmonary hypertension, multiple pulmonary emboli, pulmonary artery or valve stenosis, and RV infarction are also causes. Volume overload and increased systemic venous pressure may also occur in polycythemia or overtransfusion; acute renal failure with overhydration, and obstruction of either vena cava simulating HF. In these conditions, myocardial function may be normal.

HF is manifest by **systolic or diastolic dysfunction**, or both. Combined systolic and diastolic abnormalities are common.

In systolic dysfunction (primarily a problem of ventricular contractile dysfunction), the heart fails to provide tissues with adequate circulatory output. A wide variety of defects in energy utilization, energy supply, electrophysiologic functions, and contractile element interaction occur, which appear to reflect abnormalities in intracellular Ca^{++} modulation and cyclic adenosine monophosphate (cAMP) production. Systolic dysfunction has numerous causes; the most common are coronary artery disease, hypertension, and dilated congestive cardiomyopathy. There are many known and probably many unidentified causes for dilated myocardiopathy. More than 20 viruses have been identified as causal. Toxic substances damaging the heart include alcohol, a variety of organic solvents, certain chemotherapeutic drugs (eg, doxorubicin), β-blockers, Ca blockers, and antiarrhythmic drugs.

Diastolic dysfunction (resistance to ventricular filling not readily measurable at the bedside) accounts for 20 to 40% of cases of HF. It is generally associated with prolonged ventricular relaxation time, as measured during isovolumic relaxation (the time between aortic valve closure and mitral valve opening when ventricular pressure falls rapidly). Resistance to filling (ventricular stiffness) directly relates to ventricular diastolic pressure; this resistance increases with age, probably reflecting myocyte loss and increased interstitial collagen deposition. Diastolic dysfunction is presumed to be dominant in hypertrophic cardiomyopathy, circumstances with marked ventricular hypertrophy (eg, hypertension, advanced aortic stenosis), and amyloid infiltration of the myocardium.

High output failure is HF associated with a persistent high CO that eventually results in ventricular dysfunction. Conditions associated with high CO include anemia, beriberi, thyrotoxicosis, pregnancy, advanced Paget's disease, and arteriovenous fistula. CHF may develop in high-output states but is often reversible by treating the underlying cause. CO is elevated in various forms of cirrhosis, but the onset of congestion reflects cardiac and hepatic mechanisms of fluid retention.

Pathophysiology

In LV failure, CO declines and pulmonary venous pressure increases. Elevated pulmonary capillary pressure to levels that exceed the oncotic pressure of the plasma proteins (about 24 mm Hg) leads to increased lung water, reduced pulmonary compliance, and a rise in the O_2 cost of the work of breathing. Pulmonary venous hypertension and edema resulting from LV failure significantly alter pulmonary mechanics and, thereby, ventilation/perfusion relationships. Dyspnea correlates with elevated pulmonary venous pressure and the resultant increased work of breathing, although the precise cause is debatable. When pulmonary venous hydrostatic pressure exceeds plasma protein oncotic pressure, fluid extravasates into the capillaries, the interstitial space, and the alveoli. Pleural effusions characteristically accumulate in the right hemithorax and later bilaterally. Lymphatic drainage is greatly enhanced but cannot overcome the increase in lung water. Unoxygenated pulmonary arterial blood is shunted past nonaerated alveoli, decreasing mixed pulmonary capillary P_{O_2}. A combination of alveolar hyperventilation due to increased lung stiffness and reduced $P_{A_{O_2}}$ is characteristic of LV failure. Thus, arterial blood gas analysis reveals an increased pH and a reduced Pa_{O_2} (respiratory alkalosis) with decreased saturation reflecting increased intrapulmonary shunting. Typically, Pa_{CO_2} is reduced also. A Pa_{CO_2} above normal signifies alveolar hypoventilation possibly due to respiratory muscle failure and requires urgent ventilatory support.

In RV failure, systemic venous congestive symptoms develop. Moderate hepatic dysfunction commonly occurs in CHF secondary to RV failure, with usually modest increases in conjugated and unconjugated bilirubin, prothrombin time, and hepatic enzymes (eg, alkaline phosphatase, AST, ALT). However, in severely compromised circulatory states with markedly reduced splanchnic blood flow and hypotension, increases due to central necrosis around the hepatic veins may be severe enough to suggest hepatitis with acute liver failure. Reduced aldosterone breakdown by the impaired liver further contributes to fluid retention.

In systolic dysfunction, inadequate ventricular emptying leads to increased preload, diastolic volume, and pressure. Sudden (as in MI) and progressive (as in dilated cardiomyopathy) myocyte loss induces ventricular remodeling, resulting in increased wall stress accompanied by apoptosis (accelerated myocardial cell death) and inappropriate ventricular hypertrophy. Later, the ejection fraction falls, resulting in progressive pump failure. Systolic HF may primarily affect the LV or the RV (see above), although failure of one ventricle tends to lead to failure of the other.

In diastolic dysfunction, increased resistance to LV filling as a consequence of reduced ventricular compliance (increased stiffness) results in prolonged ventricular relaxation (an active state following contraction) and alters the pattern of ventricular filling. Ejection fraction may be normal or increased. Normally, about 80% of the stroke volume enters the ventricle passively in early diastole, reflected in a large e wave and smaller a wave on pulsed-wave Doppler echocardiography. Generally, in diastolic LV dysfunction the pattern is reversed, accompanied by increased ventricular filling pressure and a-wave amplitude.

Whether the failure is primarily systolic or diastolic and regardless of which ventricle is affected, various hemodynamic, renal, and neurohumoral responses may occur.

Hemodynamic responses: With reduced CO, tissue O_2 delivery is maintained by increasing $A-V_{O_2}$. Measurement of $A-V_{O_2}$ with systemic arterial and pulmonary artery blood samples is a sensitive index of cardiac performance and reflects, via the Fick equation ($V_{O_2} = CO \times A-V_{O_2}$), CO (inversely related) and the body's O_2 consumption (V_{O_2}—directly related).

Increased heart rate and myocardial contractility, arteriolar constriction in selected vascular beds, venoconstriction, and Na and

water retention compensate in the early stages for reduced ventricular performance. Adverse effects of these compensatory efforts include increased cardiac work, reduced coronary perfusion, increased cardiac preload and afterload, fluid retention resulting in congestion, myocyte loss, increased K excretion, and cardiac arrhythmia.

Renal responses: The mechanism by which an asymptomatic patient with cardiac dysfunction develops overt CHF is unknown, but it begins with renal retention of Na and water, secondary to decreased renal perfusion. Thus, as cardiac function deteriorates, renal blood flow decreases in proportion to the reduced CO, the GFR falls, and blood flow within the kidney is redistributed. The filtration fraction and filtered Na decrease, but tubular resorption increases.

Neurohumoral responses: Increased activity of the renin-angiotensin-aldosterone system influences renal and peripheral vascular response in HF. The intense sympathetic activation accompanying HF stimulates the release of renin from the juxtaglomerular apparatus near the descending loop of Henle in the kidney. Probably, decreased arterial systolic stretch secondary to declining ventricular function also stimulates renin secretion. Reflex and adrenergic stimulation of the renin-angiotensin-aldosterone system produces a cascade of potentially deleterious effects: Increased aldosterone levels enhance Na reabsorption in the distal nephron, contributing to fluid retention. Renin produced by the kidney interacts with angiotensinogen, producing angiotensin I from which is cleaved the octapeptide angiotensin II by ACE. Angiotensin II has various effects believed to enhance the syndrome of CHF, including stimulation of the release of arginine vasopressin (AVP), which is antidiuretic hormone (ADH); vasoconstriction; enhanced aldosterone output; efferent renal vasoconstriction; renal Na retention; and increased norepinephrine release. Angiotensin II is also believed to be involved in vascular and myocardial hypertrophy, thus contributing to the remodeling of the heart and peripheral vasculature, which contributes to HF in various myocardial and other heart diseases.

Plasma norepinephrine levels are markedly increased, largely reflecting intense sympathetic nerve stimulation, because plasma epinephrine levels are not increased. High plasma norepinephrine levels in patients with CHF are associated with a poor prognosis.

The heart contains many neurohormonal receptors (α_1, β_1, β_2, β_3, adrenergic, muscarinic, endothelin, serotonin, adenosine, angiotensin II). In patients with HF, β_1 receptors (which constitute 70% of cardiac β receptors), but not the other adrenergic receptors, are down-regulated, potentially adversely affecting myocardial function. This down-regulation, which is probably a response to intense sympathetic overdrive, has been detected even in asymptomatic patients with the early stages of HF. Altered myocardial stimulator or receptor functions for various other neurohormonal factors may adversely influence myocyte performance in HF.

Serum levels of atrial natriuretic peptide (released in response to increased atrial volume and pressure load) and brain natriuretic peptide (released from the ventricle in response to ventricular stretch) are markedly increased in patients with CHF. These peptides enhance renal excretion of Na, but, in patients with CHF, the effect is blunted by decreased renal perfusion pressure, receptor down-regulation, and perhaps enhanced enzymatic degradation. Serum atrial natriuretic peptide appears to be important for diagnosis and prognosis in CHF and correlates well with functional impairment.

AVP is released in response to a fall in BP or ECF volume and by the effects of various neurohormonal stimuli. An increase in plasma AVP diminishes excretion of free water by the kidney and may contribute to the hyponatremia of HF. AVP levels in CHF vary, but experimental AVP blockers have increased water excretion and serum Na levels.

Other sequelae: Protein-losing enteropathy characterized by marked hypoalbuminemia, ischemic bowel infarction, acute and chronic GI hemorrhage, and malabsorption may result from severe chronic venous hypertension. Peripheral gangrene in the absence of large vessel occlusion or chronic irritability and decreased mental performance may result from chronic markedly reduced Po_2, reflecting severely reduced cerebral blood flow and hypoxemia.

Cardiac cachexia (loss of lean tissue ≥ 10%) may accompany severely symptomatic HF. The failing heart produces tumor necrosis factor-α, which is a key cytokine in the development of catabolism and possibly of cardiac cachexia. Marked anorexia is characteristic of the syndrome. Restoring cardiac function to normal can reverse cardiac cachexia.

Symptoms and Signs

HF may be predominantly right-sided or left-sided and may develop gradually or suddenly (as with acute pulmonary edema).

Cyanosis may occur with any form of HF. The cause may be central and may reflect hypoxemia. A peripheral component due to capillary stasis with increased $A-Vo_2$ and resultant marked venous oxyhemoglobin unsaturation may also be present. Improved color of the nail bed with vigorous massage suggests peripheral cyanosis. Central cyanosis cannot be altered by increasing local blood flow.

LV failure: Pulmonary venous hypertension may become apparent with tachycardia, fatigue on exertion, dyspnea on mild exercise, and intolerance to cold. Paroxysmal nocturnal dyspnea and nocturnal cough reflect the redistribution of excess fluid into the lung with the recumbent position. Occasionally, pulmonary venous hypertension and increased pulmonary fluid manifest as bronchospasm and wheezing. Cough may be prominent, and pink-tinged or brownish sputum due to blood and the presence of HF cells is common. Frank hemoptysis due to ruptured pulmonary varices with massive blood loss is uncommon but may occur. Signs of chronic LV failure include diffuse and laterally displaced apical impulse, palpable and audible ventricular (S_3) and atrial gallops (S_4), accentuated pulmonic second sound, and inspiratory basilar rales. Right-sided pleural effusion is common.

Acute pulmonary edema is a life-threatening manifestation of acute LV failure secondary to sudden onset of pulmonary venous hypertension. A sudden rise in LV filling pressure results in rapid movement of plasma fluid through pulmonary capillaries into the interstitial spaces and alveoli. The patient presents with extreme dyspnea, deep cyanosis, tachypnea, hyperpnea, restlessness, and anxiety with a sense of suffocation. Pallor and diaphoresis are common. The pulse may be thready, and BP may be difficult to obtain. Respirations are labored, and rales are widely dispersed over both lung fields anteriorly and posteriorly. Some patients manifest marked bronchospasm or wheezing (cardiac asthma). Noisy respiratory efforts often render cardiac auscultation difficult, but a summation gallop, merger of S_3 and S_4, may be heard. Hypoxemia is severe. CO_2 retention is a late, ominous manifestation of secondary hypoventilation and requires immediate attention.

RV failure: The principal symptoms include fatigue; awareness of fullness in the neck; fullness in the abdomen, with occasional tenderness in the right upper quadrant (over the liver); ankle swelling; and, in advanced stages, abdominal swelling due to ascites. Edema over the sacrum is likely in supine patients. Signs include evidence of systemic venous hypertension, abnormally large a or v waves in the external jugular pulse, an enlarged and tender liver, a murmur of tricuspid regurgitation along the left sternal border, RV S_3 and S_4, and pitting edema of the lowest parts of the body.

Diagnosis

Although symptoms and signs (eg, exertional dyspnea, orthopnea, edema, tachycardia, pulmonary rales, a third heart sound, jugular venous distention) have a diagnostic specificity of 70 to 90%, the sensitivity and predictive accuracy are low.

Recommended laboratory tests include CBC, blood creatinine, BUN, electrolytes (eg, Mg, Ca), glucose, albumin, and liver function tests. Thyroid function test results should be assessed in patients with atrial fibrillation and in selected, especially older, persons. In patients with suspected coronary artery disease, stress testing with radionuclide or ultrasound imaging or coronary angiography may be indicated. Endocardial biopsy is of limited usefulness.

ECG should be performed in all patients with HF, although findings are not specific; ambulatory ECG is not generally useful. Various abnormalities (eg, of ventricular hypertrophy, MI, or bundle branch block) may provide etiologic clues. Recent onset of rapid atrial fibrillation may precipitate acute LV or RV failure. Frequent premature ventricular contractions may be secondary and may subside when the HF is treated.

Chest x-ray should be performed in all patients. Pulmonary venous congestion and interstitial or alveolar edema are characteristics of pulmonary edema. Kerley B lines

reflect chronic elevation of left atrial pressure and chronic thickening of the intralobular septa from edema. Microvascular volume increases, most strikingly in dependent areas, ie, the bases in upright posture. Careful examination of the cardiac silhouette, evaluation of chamber enlargement, and a search for cardiac calcifications may reveal important etiologic clues.

Echocardiography can help evaluate chamber dimensions, valve function, ejection fraction, wall motion abnormalities, and LV hypertrophy. Doppler or color Doppler echocardiography accurately detects pericardial effusion, intracardiac thrombi, and tumors and recognizes calcifications within the cardiac valves, mitral annulus, and the wall of the aorta. Underlying coronary artery disease is strongly suggested by localized or segmental wall motion abnormalities. Doppler studies of mitral and pulmonary venous inflow are often useful in identifying and quantitating LV diastolic dysfunction.

Treatment

Even in the most urgent situation, the cause of HF must be determined. Correctable conditions require immediate treatment, which usually begins before the etiologic evaluation is completed. For patients requiring hospitalization, initial nonspecific treatment includes bed rest with the head elevated or chair rest with the feet dependent, nasal O_2 (often at 3 L/min for 24 to 36 hr), and sedation as needed.

Drug treatment of systolic dysfunction: Drug treatment of systolic dysfunction primarily involves diuretics, ACE inhibitors, digitalis, and β-blockers; most patients are treated with at least two of these classes.

Diuretics (see TABLE 203–1) may improve ventricular function even in asymptomatic patients. Loop diuretics are preferred; the most commonly used is IV or po furosemide. IV doses (usually 20 to 40 mg, increased to 320 mg if needed) are often used initially because of quick onset and peak action in about 30 minutes. In resistant cases, chlorothiazide 250 mg IV, bumetanide 0.5 to 2 mg po, 0.5 to 1.0 mg IV, or metolazone po (dosage varies with formulation) may have an additive effect. Overdosage of loop diuretics may cause hypovolemia, hyponatremia, hypomagnesemia and profound hypokalemia,

TABLE 203–1. THE PHARMACOKINETICS OF DIURETICS

Drug	Dosage* and Route	Onset	Peak	Duration
Loop diuretics				
Furosemide	20–120 mg IV	5 min	30 min	2 h
	20–60 mg po daily or bid	30 min	1–2 h	6–8 h
Bumetanide	0.5–1 mg IV	5 min	30–45 min	2 h
	0.5–2 mg/day po	0.5–1 h	1–2 h	4–6 h
Torsemide	20–100 mg IV	5 min	15–30 min	12–16 h
	20–100 mg/day po	30 min	1 h	12–16 h
Thiazides				
Chlorothiazide	250–500 mg IV q 12 h	15 min	30 min	2 h
	250–500 mg po bid	1–2 h	4 h	6–12 h
Chlorthalidone	50–100 mg/day po	2 h	2–6 h	24–72 h
Hydrochlorothiazide	25–50 mg/day po	2 h	4–6 h	6–12 h
Indapamide	2.5–5 mg/day po	1–2 h	2 h	36 h
Metolazone	5–10 mg/day po	1 h	2 h	12–24 h
K-sparing drugs				
Spironolactone	25–200 mg/day po	3 days†	1–2 h	2–3 days
Triamterene	100 mg po bid	2–4 days	2–4 h	7–9 h
Amiloride	5–10 mg/day po	2 h	3–4 h	24 h

*Clinically accepted dosages and intervals in heart failure are not strictly determined by pharmacokinetics.
†Although plasma levels are detected in 2 h, the maximum diuretic effect occurs in ≤ 3 days.
Adapted from Cody RJ: "Diuretic therapy," in *Heart Failure*, edited by Poole-Wilson PA, Colucci WS, Massie BM, et al. New York, Churchill Livingston, 1997.

so close electrolyte monitoring is essential. Diuretics may also induce renal failure and enhance the intense sympathetic stimulation characteristic of HF. K-sparing drugs may be used to offset the K-losing effects of loop diuretics, but hyperkalemia may complicate their use. Thiazide diuretics are not usually effective in patients with advanced symptoms of CHF.

The clinical efficacy of diuretics depends on dietary Na restriction using a stepped approach: eliminating salt at the table and avoiding heavily salted foods; eliminating salt from cooking and consuming about 1.2 to 1.8 g/day of Na^+; and, in the most severely ill, consuming < 1 g/day of Na through restriction to low-Na foods. A log of daily weight should be maintained by the patient to enhance ambulatory care of HF and to help prevent recurrent hospitalizations by detecting early evidence of Na^+ and water accumulation.

ACE inhibitors cause peripheral arterial and venous vasodilatation, sustained decreases in LV filling pressure at rest and on exercise due to venodilation, decreased systemic vascular resistance, favorable effects on remodeling, possible improved diastolic function, probable reduced loss of myocardial cells, and a negative inotropic effect on the failing heart. Various ACE inhibitors enhance survival in HF and reduce the incidence of recurrent angina and MI in coronary artery disease. Volume expansion and renal failure reduce their usual benefit. Side effects include a decrease in BP (sometimes severe) in almost all patients, especially those with hyponatremia. Moderate renal insufficiency may result from vasodilation of the efferent glomerular arteriole. K retention may occur due to reduced aldosterone effect, especially in patients receiving K supplements. Cough occurs in 5 to 20% of patients, probably due to accumulation of bradykinin as a result of reduced breakdown to inactive metabolites. Occasionally, rash or dysgeusia occurs. Angioneurotic edema is rare but can be life threatening.

ACE inhibitors are started in small doses, which are gradually increased, then continued indefinitely; doses should be adjusted upward as tolerated. Usual doses are captopril 25 to 50 mg/day, enalapril and lisinopril 2.5 to 5 mg/day, and quinapril 10 mg/day. Although an early effect may be observed, the full drug effect is usually not seen for 2 to 4 wk or considerably longer. Large doses produce a similar frequency of side effects as lower doses but are more effective (studies showing survival and other benefits have generally used large doses).

The dose of a coadministered diuretic may frequently be reduced, especially if ACE inhibitor–induced renal insufficiency occurs. Aspirin may reduce the effect of ACE inhibitors in HF, possibly because it inhibits the effects of kinins.

The **angiotensin II receptor blocker** losartan 25 to 50 mg/day has effects similar to those of ACE inhibitors, although comparative trials have not been reported. Theoretically, cough should not occur because losartan does not influence kinins.

Digitalis preparations have many actions, including weak inotropism; blockade of the atrioventricular node, thus slowing the ventricular rate in atrial fibrillation or prolonging PR time in sinus rhythm; weak vasoconstriction; and improved renal blood flow. The drug is widely prescribed in the USA, although its role continues to be debated and its usefulness in HF in the absence of atrial fibrillation is controversial.

Digoxin is the most commonly prescribed digitalis preparation. It is excreted by the kidney with an elimination half-life of 36 to 48 h in patients with normal renal function. Patients with reduced renal function require lower doses. Oral bioavailability of digoxin tablets is around 65 to 75%. Digitoxin, an alternative in patients with known or suspected renal disease, is largely excreted in the bile and is thus not influenced by abnormal renal function.

Digoxin modestly improves LV function, allows reduced diuretic dosage, and reduces the need for hospitalization. Unlike ACE inhibitors, digoxin does not improve exercise tolerance. When digoxin is withdrawn in HF, the hospitalization rate and symptoms increase, although digoxin does not appear to influence mortality. Thus, digoxin is useful in symptomatic HF when used with diuretics and an ACE inhibitor. Digoxin is most effective in patients with large LV end-diastolic volumes and a third heart sound.

Digoxin (0.25 to 0.50 mg/day depending on body size) in patients with normal renal function will achieve full digitalization in about 1 wk (5 half-lives). Digoxin 1 mg IV administered as 0.5 mg initially, then 0.25 mg at 8 and 16 h (or 1.25 mg po administered as 0.5 mg

initially, then 0.25 mg at 8, 16, and 24 h), should achieve adequate levels in tissue and plasma in the absence of toxicity. These doses are followed by 0.125 to 0.375 mg/day depending on body size; the elderly rarely need > 0.125 mg/day. Patients with reduced renal function require lower doses.

Digoxin (and all digitalis glycosides) has a narrow therapeutic-toxic threshold. About 80% of the therapeutic effect can be achieved with serum levels of 1.0 to 1.5 ng/mL, generally well below the toxic threshold of ≥ 2 ng/mL. In the management of atrial fibrillation, moderately low doses of digoxin may be combined with β-blockers or Ca blockers (eg, verapamil, diltiazem), which have a significant atrioventricular blocking effect, to control ventricular rate at rest or during exercise.

Digoxin prolongs conduction in the atrioventricular node. First-degree heart block is common and, if not progressive, digoxin dosage need not be adjusted. Wenckebach phenomenon may occur. The most important toxic effects of digitalis are life-threatening arrhythmias due to complete heart block or ventricular arrhythmia. Digitalis increases the automaticity of Purkinje's fibers and may enhance reentry, resulting in coupled extrasystoles, ventricular fibrillation, or ventricular tachycardia. Bidirectional ventricular tachycardia is pathognomonic of digitalis toxicity. Nonparoxysmal junctional tachycardia in the presence of atrial fibrillation is a serious sign of digitalis toxicity but is frequently overlooked.

Hypokalemia and hypomagnesemia (often caused by diuretics) potentiate the capacity of digoxin to induce malignant ventricular arrhythmia or heart block. Recognition and treatment of electrolyte depletion are mandatory in patients taking diuretics and digoxin, except in the presence of atrioventricular block, in which a temporary pacemaker must be functioning prior to correcting the electrolyte abnormality.

Other manifestations of digitalis toxicity include nausea, vomiting, anorexia, diarrhea, confusion, amblyopia, and rarely xerophthalmia.

The first step in treating digitalis toxicity is to discontinue the drug. The ECG should be closely monitored, and if serum K is low, 80 mEq of potassium chloride IV should be given in 1 L 5% D/W at 6 mL/min (0.5 mEq/min). Low serum Mg is treated with magnesium sulfate 1 g q 6 h for four doses IM or IV if mild or 5 g/h in 5% D/W over 3 h (28 mg/min). Administration of digoxin immune Fab (if available) is better than administration of another antiarrhythmic drug. Ventricular arrhythmias are treated with lidocaine or phenytoin. Heart block with slow ventricular rate is best treated with a temporary perivenous pacemaker. Isoproterenol is contraindicated because of the increased tendency to ventricular arrhythmia.

Several **inotropic drugs** have been evaluated in the treatment of HF, but, except for digoxin, preparations have shown increased mortality.

With careful administration of **β-blockers**, some patients, especially those with dilated cardiomyopathy, will improve clinically and may have reduced mortality. Therapy must be initiated with caution using 1/4 to 1/10 of the standard daily dose, with a very gradual increase to the standard dose, if tolerated, over several weeks.

After initial treatment of HF by β-blockers, heart rate falls, stroke volume and filling pressure are unchanged, and myocardial O_2 consumption falls. With the slower heart rate, diastolic function improves. Ventricular filling returns to a more normal pattern (increasing in early diastole) that appears less restrictive. Improved myocardial function is measurable after 6 to 12 mo, with an increase in ejection fraction, a fall in LV filling pressure, and an increase in CO. Functionally, exercise capacity appears to improve.

Carvedilol, a 3rd-generation nonselective β-blocker, is also a vasodilator with α blockade and an antioxidant. Randomized controlled trials have shown significant reduction in all-cause mortality and cardiac events in patients with mildly symptomatic CHF and ejection fraction ≤ 0.35. Ventricular function is significantly improved. In a patient taking stable doses of diuretics, ACE inhibitors, and digoxin, the recommended starting dose of carvedilol is 3.125 mg bid for 2 wk with cautious upward titration by doubling the dose every 2 wk to the highest level tolerated to a maximum of 25 mg bid for those weighing < 85 kg and 50 mg bid for those weighing ≥ 85 kg.

Vasodilators improve ventricular function by reducing systolic ventricular wall stress, aortic impedance, ventricular chamber size, and valvular regurgitation. An improved balance between myocardial O_2 supply and demand results. Acutely ill patients with severe pulmonary congestion and deteriorating ventricular function may respond to IV nitroglycerin or nitroprusside.

Addition of hydralazine and isosorbide dinitrate to standard triple therapy of HF may improve hemodynamics and exercise tolerance and reduce mortality in refractory patients. Hydralazine is initiated at 25 mg 4 times/day and increased every 3rd day to a maximum of 300 mg/day, although most patients with refractory HF cannot tolerate dosages > 200 mg/day without developing hypotension. Isosorbide dinitrate is administered at 20 mg 3 or 4 times/day and increased to a maximum of 160 mg/day. Patients must be carefully monitored for hypotension as the dosage is increased; hospitalization may be required. Benefit may not be evident for several weeks. Except in acutely ill or refractory cases of HF, vasodilators have been replaced by ACE inhibitors, which are easier to use and usually better tolerated.

The use of **Ca blockers** in patients with reduced LV function causing HF has been disappointing. Several Ca blockers have shown a deleterious effect (nifedipine, diltiazem, verapamil) or lack of evidence of clinical or hemodynamic improvement (nisoldipine, nicardipine, felodipine).

Amlodipine is well tolerated in CHF. It significantly reduces mortality in patients with idiopathic dilated cardiomyopathy. Amlodipine (or another long-acting vasoselective Ca blocker such as felodipine) may be useful in patients with cardiomyopathy whose HF is insufficiently controlled by diuretics, ACE inhibitors, digitalis, and β-blockers. Amlodipine may also be useful in treating associated angina or hypertension.

Drug treatment of diastolic dysfunction: Patients with diastolic dysfunction cannot tolerate reduced BP or plasma volume. Thus, diuretics, ACE inhibitors, and vasodilators are usually contraindicated. Treatment of HF in hypertrophic cardiomyopathy (see below) with a β-blocker, verapamil, or disopyramide aims to reduce cardiac contractility; thus, digoxin is also contraindicated. Successful treatment of hypertension or valve replacement for aortic stenosis will decrease LV hypertrophy and reduce ventricular stiffness. Generally, treatment of dominant systolic dysfunction will improve diastolic dysfunction. Management of patients with extensive ventricular infiltration (eg, in amyloid) remains unsatisfactory. Slowing the heart rate with a β-blocker prolongs diastole, possibly improving ventricular relaxation and allowing a more normal ventricular filling pattern.

Drug treatment of arrhythmia: Sinus tachycardia is common in HF but generally subsides with effective treatment of the HF. If tachycardia is persistent, associated causes should be sought (eg, overactive thyroid, pulmonary emboli, fever, anemia), and cautious treatment with a β-blocker may be considered. Uncontrolled atrial fibrillation may contribute importantly to LV dysfunction. Some patients have well-controlled ventricular rates at rest that become very rapid during minimal emotional or physical stress. Judicious treatment with digoxin, β-blockers, or Ca blockers (eg, verapamil, diltiazem) alone or in combination is often effective. Occasionally, dosages that control the tachycardia induce periods of asystole. Insertion of a pacemaker with maintenance on large doses of drugs that block atrioventricular conduction or complete or partial ablation of the atrioventricular node may be required. Ventricular extrasystoles are common in HF. They are generally ignored in the absence of sustained ventricular tachycardia because most subside with successful treatment of HF.

Amiodarone, a vasodilator, has antiarrhythmic effects and direct negative inotropic action and is anti-ischemic. However, in HF, amiodarone 200 to 300 mg/day po improves LV function, possibly because its vasodilating effect overcomes its negative inotropic action. Some studies suggest improved survival in cardiomyopathy, especially hypertrophic obstructive cardiomyopathy or when of ischemic origin. Paradoxically, treatment of ventricular arrhythmia with other antiarrhythmics except β-blockers in HF has not reduced mortality.

Treatment of arrhythmia in HF may be difficult because antiarrhythmic drugs other than amiodarone and β-blockers have adverse proarrhythmic effects in the presence of LV dysfunction. If rapid atrial fibrillation does not respond to therapy with digoxin, β-blockers, or Ca blockers, nonpharmacologic treatment with permanent pacemaker insertion and complete or partial atrioventricular node ablation should be considered.

Treatment of **acute pulmonary edema** includes administration of O_2 by mask, the upright position if tolerated, morphine IV 1 to 5 mg once or twice, and IV furosemide 0.5 to 1.0 mg/kg. If hypoxia is severe (pulse oximeter) or CO_2 retention is evident (arterial blood gas), tracheal intubation and assisted ventilation may be required. Rapid evaluation of the cause of HF by history, physical examination, ECG, and, if indicated, echocardiogram should be undertaken. Specific treatment depends on etiology: a vasodilator for severe hypertension; an IV antiarrhythmic or cardioversion for supraventricular or ventricular tachycardia; and an IV Ca blocker, IV β-blocker, IV digoxin, or cardioversion to slow the ventricular rate in paroxysmal atrial fibrillation.

Acute MI is the commonest cause of acute LV failure. If BP is maintained, treatment is as above; adding sublingual nitroglycerin 0.4 mg, repeated in 5 min, followed by IV nitroglycerin 10 to 100 μg/min. A thrombolytic drug should be administered, if indicated. Because fluid status before onset of acute HF is usually normal in MI patients, diuretics are less useful and may precipitate hypotension. If BP falls or shock develops, IV dobutamine and intra-aortic balloon pump (counterpulsation) may be required. Emergency coronary angiography and evaluation for PTCA or bypass surgery may be undertaken in patients who fail to improve.

Treatment of refractory HF: Various factors may cause a failure to respond to appropriate treatment or a gradual loss of effective response after an initial favorable result. Causes include suboptimal quadruple therapy, deteriorating renal function, occult thyroid disease, anemia, treatment-induced hypotension, supervening arrhythmia (eg, atrial fibrillation with rapid ventricular response, intermittent ventricular tachycardia), alcohol consumption, and the adverse effects of concomitant drug administration (especially NSAIDs). If treatable causes are not found, additional medical therapy or referral for surgery can be considered.

Surgery: Heart transplantation is the only treatment that potentially alters the natural history of HF long-term. Currently, 1- and 3-yr survival are about 82 and 75%; however, mortality while waiting for a donor is 12 to 15%. Dynamic cardiomyoplasty has been used experimentally to boost LV function by wrapping the latissimus dorsi muscle around the heart and stimulating this skeletal muscle repetitively. Functional status has been reported to improve in about 80% of patients. Another experimental procedure attempts to relieve wall tension by removing ventricular strips and reducing LV volume, but outcome data are limited. Several implantable ventricular assist devices are being evaluated. Ventricular assist with an external power source has been successful in supporting selected patients with refractory HF before heart transplantation. Newer devices in which the power source is inserted wholly within the body, thus reducing the major complication of infection, are also being evaluated.

End-of-life care: Death is inevitable in patients with progressive disease who are not transplant candidates and in whom severe symptoms cannot be controlled. Care must focus on relief of pain and suffering (see Ch. 294).

CARDIOMYOPATHY

Any structural or functional abnormality of the ventricular myocardium, except congenital developmental defects; valvular disease; systemic or pulmonary vascular disease; isolated pericardial, nodal, or conduction system disease; or epicardial coronary artery disease, unless chronic diffuse myocardial dysfunction is present.

Cardiomyopathy has many causes (see TABLE 203–2). Pathophysiologic classification (dilated congestive, hypertrophic, or restrictive cardiomyopathy) by means of history, physical examination, and invasive or noninvasive testing is most useful initially (see TABLE 203–3). If no cause can be found, cardiomyopathy is considered primary or idiopathic.

DILATED CONGESTIVE CARDIOMYOPATHY

Disorders of myocardial function with heart failure in which ventricular dilation and systolic dysfunction predominate.

Etiology and Pathophysiology

The most common identifiable cause in temperate zones is diffuse coronary artery disease with diffuse ischemic myopathy; for other causes, see TABLE 203–2.

Most commonly, at presentation there is chronic myocardial fibrosis with diffuse loss of myocytes. In some patients, the underlying pathologic process is believed to start with an acute myocarditic phase (probably viral in most cases), followed by a variable latent phase, then a phase of chronic fibrosis and diffuse loss of myocardial myocytes due to an autoimmune reaction to virus-altered myocytes. Regardless of the cause, the result is dilation, thinning, and compensatory hypertrophy of the remaining myocardium (see FIG. 203–3) interspersed with fibrosis. Altered ventricular geometry often leads to secondary functional mitral or tricuspid regurgitation and atrial dilation. The primary result is impaired ventricular systolic function reflected by a low ejection fraction (EF). Cardiac output is maintained through tachycardia and an increased end-diastolic volume, which increases wall tension and myocardial O_2 demand. Diastolic compliance and pressure become abnormal only late in the disease.

Symptoms and Signs

The disorder is usually chronic, presenting with effort dyspnea and fatigue due to elevated left ventricular diastolic pressure and low cardiac output. Because both ventricles may be affected, symptoms and signs of right ventricular failure are also often prominent.

Less often, when an infective agent is responsible, the disorder begins as acute myocarditis associated with fever. Infection with coxsackievirus B is most common in temperate zones (see VIRAL INFECTIONS in Ch. 265), whereas Chagas' disease due to *Trypanosoma cruzi* is most prevalent in

TABLE 203–2. ETIOLOGY AND PATHOPHYSIOLOGIC CLASSIFICATION OF CARDIOMYOPATHY

Etiology	Pathophysiology
Dilated congestive cardiomyopathy (acute or chronic)	Diffuse (all chambers involved)
Chronic diffuse myocardial ischemia (coronary artery disease)	Nondiffuse (one or more chambers spared)
Infections (acute or chronic): bacteria, spirochetes, rickettsia, viruses (including HIV), fungi, protozoa, helminths	
Granulomatous diseases: sarcoidosis, granulomatous or giant cell myocarditis, Wegener's granulomatosis	
Metabolic disorders: nutritional disorders (beriberi, selenium deficiency, carnitine deficiency, kwashiorkor), familial storage disorders, uremia, hypokalemia and hypomagnesemia, hypophosphatemia; endocrinopathy (diabetes mellitus, hyperthyroidism or hypothyroidism, pheochromocytoma, acromegaly), morbid obesity	
Drugs and toxins: ethanol, cocaine, anthracyclines, cobalt, psychotherapeutic drugs (tricyclic, quadricyclic, phenothiazine), catecholamines, cyclophosphamide, radiation	
Neoplasms	
Connective tissue disorders	
Heredofamilial neuromuscular and neurologic disorders (Friedreich's ataxia)	
Pregnancy (peripartum period)	
Hypertrophic cardiomyopathy	Asymmetric (obstructive [subaortic or midventricular], nonobstructive, and apical)
Hereditary autosomal dominant, pheochromocytoma, acromegaly, neurofibromatosis	Symmetric
Restrictive cardiomyopathy	Diffuse (obliterative and nonobliterative)
Amyloidosis; diffuse systemic sclerosis; hemochromatosis; endocardial fibrosis, fibroelastosis, and Löffler's disease; neoplasms; Gaucher's disease	Nondiffuse

TABLE 203–3. DIAGNOSIS AND MANAGEMENT OF CARDIOMYOPATHIES

	Dilated Congestive	Hypertrophic	Restrictive
Clinical examination	Left and right heart failure Cardiomegaly Functional AV valve regurgitation S_3 and S_4	Angina, effort dyspnea, syncope, sudden death Ejection ± mitral regurgitation murmurs S_4, bifid carotid Rapid carotid upstroke	Effort dyspnea and fatigue Left ± right heart failure Functional AV valve regurgitation
ECG	Nonspecific ST- and T-wave abnormalities Q waves	Left ventricular hypertrophy Deep septal Q waves	Left ventricular hypertrophy or low voltage
X-ray	Cardiomegaly Pulmonary venous congestion	No cardiomegaly	No or mild cardiomegaly
Echocardiography	Dilated hypokinetic ventricles ± mural thrombus	Hypertrophied ventricle ± mitral systolic anterior motion ± asymmetric hypertrophy	Increased wall thickness ± cavity obliteration
Hemodynamics	Normal or high EDP, low EF, diffusely dilated hypokinetic ventricles ± AV valve regurgitation Low CO	High EDP, high EF ± outflow subvalvular gradient ± mitral regurgitation Normal or low CO	High EDP, dip and plateau diastolic left ventricular pressure curve Normal or low CO
Pathophysiology	Systolic dysfunction	Diastolic dysfunction ± outflow obstruction	Diastolic dysfunction
Therapy	Preload and afterload reduction, β-blockers, inotropic drugs, anticoagulants	Reduced contractility with β-blocker or Ca blockers ± septal myotomy or myectomy, AV pacing	Endocardial resection Phlebotomy for hemochromatosis
Prognosis	70% 5-yr mortality	4%/yr mortality	70% 5-yr mortality

AV = atrioventricular; ± = with or without; EDP = end-diastolic pressure; EF = ejection fraction; CO = cardiac output; S_3 = third heart sound; S_4 = fourth heart sound.

Central and South America (see EXTRAINTESTINAL PROTOZOA in Ch. 161). Dilated congestive cardiomyopathy is increasingly common in patients with AIDS (see Ch. 163).

Physical examination reveals a normal or low BP, sinus tachycardia, basal rales, neck vein distention with prominent a and v waves (see FIG. 197–1) and hepatojugular reflux, and peripheral pitting edema. In severe cases, hepatomegaly, ascites, and skeletal muscle wasting occur. The precordium often has a diffuse parasternal lift, and a diastolic impulse coincides with a third heart sound (S_3) gallop and a murmur of mitral regurgitation at the apex. The murmur of tricuspid regurgitation at the lower left sternal border may be heard, increasing with inspiration and associated with regurgitant waves in the neck veins and systolic pulsation of the liver.

In a few patients, the pathologic process is isolated to one ventricle (usually the left), thus altering the clinical picture. A rare form involving only the right ventricle is characterized by atrial arrhythmias and sudden death due to malignant ventricular tachyarrhythmias.

Mural thrombus formation in any chamber is frequent once chamber dilation is significant. Cardiac arrhythmias often complicate the acute myocarditic phase and late chronic dilated phase.

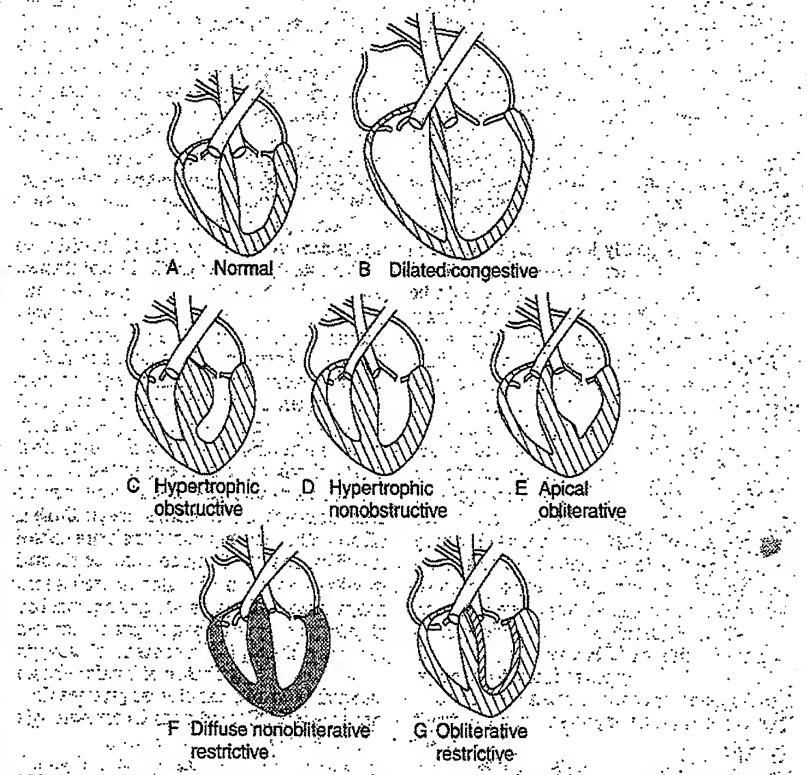

FIG. 203–3. Cardiomyopathies according to pathophysiologic type. (A) Normal; (B) systolic dysfunction; (C–G) diastolic dysfunction.

Diagnosis

Diagnosis depends on the characteristic history and physical examination and exclusion of other causes of ventricular failure (eg, systemic hypertension, primary valvular disease, MI). The ECG may show sinus tachycardia, low-voltage QRS, and nonspecific ST segment depression with low-voltage or inverted T waves. Sometimes pathologic Q waves are present in the precordial leads, simulating remote MI. Left bundle branch block is common. In about 25% of cases, differentiation from previous MI may be further complicated by chest pain, which may mimic angina pectoris but most often is atypical in character and position and not clearly related to exertion.

Chest x-ray reveals cardiomegaly that usually involves all chambers. Pleural effusion, particularly on the right, often accompanies raised pulmonary venous pressure and interstitial edema. M-mode and two-dimensional echocardiography shows dilated, hypokinetic cardiac chambers with reduced fractional shortening and rules out primary valvular disease or segmental wall motion abnormalities, as seen in discrete MI. Echocardiography also may reveal a mural thrombus, which frequently complicates dilated congestive cardiomyopathy. Radionuclide studies show diffusely dilated, hypokinetic cardiac chambers. In acute myocarditis, gallium scanning may identify an acute inflammatory phase (see RADIONUCLIDE IMAGING in Ch. 198), whereas MRI reveals abnormal myocardial tissue texture.

Cardiac catheterization is reserved for patients in whom the diagnosis is in doubt after

noninvasive investigation, particularly when chest pain is a symptom. Cardiac output can be normal or low, but EF is depressed and diffuse hypokinesis is seen on angiography. Valvular gradients and calcification are absent, and the coronary arteries are normal. Left ventricular end-diastolic pressure is elevated late in disease. Myocardial biopsy of either ventricle can be performed during catheterization. When special studies show a disproportionately low cardiac output in other forms of heart disease, the possibility of a coexisting cardiomyopathy should be considered.

Prognosis

The prognosis generally is poor: 70% of patients die in ≤ 5 yr. Fifty percent of deaths are sudden, suggesting malignant arrhythmia. Unless a treatable primary cause can be found and eliminated (eg, alcohol, an infective agent), no specific therapy can prolong life. Prognosis is better if reactive hypertrophy is adequate to preserve ventricular wall thickness and is worse if thinning of ventricular walls is marked. Poor prognosis is related to poor ventricular function or frequent ventricular arrhythmia on 24-h ECG monitoring. Males survive half as long as females. Blacks survive half as long as whites.

Treatment

Treatment is specific for any underlying cause (eg, toxoplasmosis, thyrotoxicosis, beriberi) and may include elimination of potential toxins or myocardial depressants, therapy for low cardiac output and heart failure, and treatment of complications. However, most often, no cause is found. If possible, alcohol, some psychotherapeutic drugs, and electrolyte disorders should be eliminated. Therapy for heart failure and low cardiac output depends on the appropriate balance of afterload reduction, inotropic drugs, and preload reduction to optimize cardiac output and relieve systemic and pulmonary venous congestion.

Combined afterload and preload reduction with ACE inhibitors (eg, captopril, enalapril, lisinopril) or hydralazine plus nitrate (eg, isosorbide dinitrate) is the mainstay of therapy. These drugs favorably alter prognosis. Carvedilol and possibly other β-blockers prolong life and reduce morbidity. Digitalis glycosides, which reduce morbidity, are of value as weak inotropic drugs and for controlling the ventricular rate in patients with atrial fibrillation. Diuretics can lower left and right ventricular filling pressures so that pulmonary edema or significant hepatic congestion is avoided. Use of a phosphodiesterase inhibitor (eg, amrinone, milrinone [unavailable in USA]) or intermittent short-term (48- to 72-h) catecholamine infusion with dopamine or dobutamine is undergoing trials and temporarily helps some patients. These therapies have not been shown to prolong life. Corticosteroids with or without azathioprine and equine antithymocyte globulin may shorten the acute phase of certain inflammatory myocarditic myopathies proved by biopsy (eg, acute postviral or sarcoid myocarditis) but do not alter the course of chronic myopathy and are no longer used. Therefore, proof of active myocarditis on biopsy is recommended before starting corticosteroids or azathioprine.

Because of the risk of mural thrombus formation, prophylactic oral anticoagulant therapy helps prevent systemic or pulmonary emboli (see Ch. 72). Cardiac arrhythmias, which often complicate acute myocarditic phase myopathy and late chronic dilated phase, are treated with antiarrhythmic drugs as required (see Ch. 205). CAUTION: *Most antiarrhythmics have a depressant effect on myocardial contractility; thus, potent negative inotropic drugs (eg, disopyramide, procainamide) are best avoided.* The proarrhythmic effect of class I antiarrhythmic drugs (eg, encainide, flecainide) is greater the worse the ventricular function. Permanent pacemakers may be required if heart block complicates the chronic dilated phase; however, atrioventricular block during acute myocarditis often resolves, and permanent pacing usually is not needed.

In patients with underlying diffuse coronary artery disease with diffuse ischemic myopathy, therapy for angina pectoris with nitrates, β-blockers, and Ca blockers may be indicated (see Ch. 202). However, the benefit of Ca blockers in controlling angina must be weighed against the negative inotropic effects; Ca blockers, except for amlodipine or felodipine, are best avoided. Some studies suggest that low-dose β-blockers may be of benefit for some patients in whom a significant compensatory adrenergic response is causing chronic down-regulation of cardiac myocyte β-adrenoceptors. Therapy must be started with very low doses (eg, carvedilol 6.25 mg or metoprolol 5 mg bid), and thorough evaluation for worsening of heart failure is essential. If tolerated, the dose is increased to 25 mg bid and 50 mg bid, respectively. Greatest benefit occurs with younger patients with dilated congestive cardiomyopathy of short duration. Females benefit more than males. Short-acting nifedipine normally acts as a vasodilator and afterload reducer; however, in the presence of cardiac decompensation, the reflex sympathetic response to arteriolar vasodilation may already be maximal, and the direct negative inotropic effect of the drug may manifest with a worsening of heart failure.

Appropriate rest, sleep, and stress avoidance are important, but prolonged bed rest should be prescribed only as symptoms dictate. Physical exercise within the limits imposed by symptoms improves overall well-being and may slightly prolong life.

Because of the grim prognosis, these patients represent the greatest proportion of heart transplantation recipients. Patients selected should be without associated systemic disease, psychologic disorders, or high, irreversible pulmonary vascular resistance, and they should generally be < 60 yr old because younger patients are the preferred recipients of these scarce organ resources.

A surgical procedure involving removal of strips of myocardium to remodel the dilated ventricle has shown promise in uncontrolled trials. Controlled trials comparing this procedure with optimal medical therapy are underway. A procedure whereby the latissimus dorsi muscle is wrapped around the failing ventricle and stimulated by a skeletal muscle pacemaker has been shown to be of no value.

Several ventricular assist devices having an internal power source with or without an external power source are being used to keep the patient alive pending heart transplantation or as long-term therapy instead of transplantation.

HYPERTROPHIC CARDIOMYOPATHY

Congenital or acquired disorders characterized by marked ventricular hypertrophy with diastolic dysfunction in the absence of an afterload demand (eg, valvular aortic stenosis, coarctation of the aorta, systemic hypertension).

Identifiable causes are listed in TABLE 203-2.

Pathology and Pathophysiology

The cardiac muscle is abnormal with cellular and myofibrillar disarray, although this finding is not specific to hypertrophic cardiomyopathy. Usually, the interventricular septum is hypertrophied more than the left ventricular posterior wall (asymmetric septal hypertrophy). In the most common asymmetric form of hypertrophic cardiomyopathy, there is marked hypertrophy and thickening of the upper interventricular septum below the aortic valve. During systole, the septum thickens and the anterior leaflet of the mitral valve, already abnormally oriented due to the abnormal shape of the ventricle, is sucked toward the septum, producing outflow tract obstruction. This is termed hypertrophic obstructive cardiomyopathy or asymmetric hypertrophic septal stenosis. It further reduces cardiac output, which is already abnormally low because of diastolic dysfunction caused by the noncompliant, hypertrophied ventricle.

Congenital hypertrophy is autosomally dominant in cases of asymmetric septal hypertrophy but not in other varieties. The most common abnormality is a missense point mutation in exon 13 of the β cardiac myosin heavy chain gene on the DNA locus of chromosome 14. Less often, an abnormal α/β cardiac myosin heavy chain hybrid gene is present. Other gene defects can also cause the disorder.

The major consequence of hypertrophy is that the stiff, noncompliant chamber (usually the left ventricle) resists diastolic filling, leading to elevated end-diastolic pressure, which raises pulmonary venous pressure. Angina pectoris results from an imbalance between O_2 demand by the hypertrophied myocardium and O_2 supply via the coronary arteries, which may be compromised by the noncompliant myocardium. Inadequate capillary density relative to myocyte size as well as hyperplasia and hypertrophy of the intima and media of intramyocardial coronary arteries, which compromise lumen diameter, also produces ischemia in hypertrophic cardiomyopathy in the absence of epicardial coronary artery disease.

Effort-induced light-headedness and syncope are caused by inadequate cardiac output, sometimes worsened by an outflow tract

gradient in those with asymmetric septal hypertrophy. The fall in cardiac output results from the decreased diastolic filling period related to effort-induced sinus tachycardia. Shortening of the diastolic filling period in the noncompliant, hypertrophied ventricle reduces preload and leads to increased apposition of the anterior leaflet of the mitral valve against the hypertrophied ventricular septum. Exercise also lowers peripheral vascular resistance and hence aortic root diastolic pressure. This may induce ischemia, which may lead to nonsustained ventricular or atrial arrhythmia, causing syncope. Syncope in hypertrophic cardiomyopathy is a clinical marker of increased probability of sudden death, which is believed to result from ventricular tachycardia or fibrillation.

Infective endocarditis can complicate hypertrophic cardiomyopathy because of mitral valve abnormality that appears to result from the altered ventricular geometry with anterior positioning of the papillary muscles and mitral apparatus and the Venturi effect produced by the rapid early systolic flow through the outflow tract. Heart block is sometimes a late complication. Midventricular hypertrophy leads to an intracavitary gradient at the papillary muscle level. The distal left ventricle may ultimately thin and dilate in an aneurysmal manner.

Symptoms, Signs, and Diagnosis

Clinical manifestations may occur alone or in any combination: Chest pain is usually typical angina related to exertion. Syncope is usually exertional and due to a combination of ischemia, arrhythmia, outflow tract obstruction, and poor diastolic filling of the ventricle. Dyspnea on exertion results from poor diastolic compliance of the left ventricle, which leads to a rapid rise in left ventricular end-diastolic pressure as flow increases. Outflow tract obstruction, by lowering cardiac output, may contribute to the dyspnea. Systolic function is preserved, and fatigability is seldom a complaint. Palpitations are produced by ventricular or atrial arrhythmias. Thus, symptoms of hypertrophic cardiomyopathy may simulate those of aortic stenosis or coronary artery disease.

Physical examination usually clarifies the differential diagnosis. Signs of raised venous pressure (eg, jugular venous distention, ascites, ankle edema, pleural effusion) are rare until the terminal phase. BP and heart rate are usually normal. The carotid pulse in cases with asymmetric septal hypertrophy and outflow tract obstruction has a brisk upstroke, a bifid peak due to dynamic obstruction in the latter part of systole, and a rapid downstroke. Precordial palpation reveals the apex beat in its normal position with a sustained thrust due to left ventricular hypertrophy. Sometimes a biphasic apical thrust can be appreciated in cases with severe outflow obstruction.

Systolic murmurs are usually present, but patients with apical and symmetric hypertrophic cardiomyopathy may have no murmur. Most common is a crescendo-diminuendo ejection-type murmur that does not radiate to the neck; it is best heard at the left sternal edge in the 3rd or 4th intercostal space. This murmur is caused by obstruction of left ventricular ejection (produced in systole when the hypertrophied interventricular septum and the anterior leaflet of the mitral valve approach each other). A mitral regurgitation murmur due to distortion of the mitral apparatus is heard in some patients. It has a characteristic blowing quality and is best heard at the apex, radiating toward the left axilla. Rarely, early or midsystolic clicks are heard. In some patients with right ventricular outflow tract narrowing, a systolic ejection murmur is heard in the second interspace at the left sternal border. An S_4, almost always present, indicates a forceful atrial contraction against a poorly compliant left ventricle in late diastole.

The ejection murmur of hypertrophic cardiomyopathy can be altered by maneuvers to decrease venous return, reducing left ventricular diastolic volume and increasing apposition of the anterior mitral valve leaflet with the hypertrophied interventricular septum. Thus, Valsalva maneuver increases the intensity of the murmur, as will maneuvers to lower aortic pressure (eg, amyl nitrite inhalation) or a postextrasystolic contraction, by increasing the outflow tract pressure gradient. Handgrip raises aortic pressure, thereby reducing the murmur's intensity.

Laboratory Findings

Noninvasive tests to confirm the diagnosis have generally replaced heart catheterization. The ECG usually shows voltage criteria for left ventricular hypertrophy. Asymmetric septal hypertrophy is often suggested by very deep septal Q waves in leads I, aVL, V_5, and V_6, a QS complex sometimes occurs in V_1 and V_2, simulating previous septal infarction. The T waves are abnormal in most cases; the most common finding is deep symmetric T-wave inversion in leads I, aVL, V_5, and V_6. ST segment depression in the same leads is common. The P wave is often broad and notched in leads II, III, and aVF, with a biphasic P wave in V_1 and V_2, indicative of left atrial hypertrophy. Preexcitation phenomenon of the Wolff-Parkinson-White syndrome type occurs more often than by chance alone and is one of the mechanisms of arrhythmia-induced palpitations.

The chest x-ray is often deceptively normal looking because hypertrophy occurs at the expense of the ventricular cavities; a globular left ventricular contour within a normal-sized cardiac silhouette may be the only abnormality. Cardiac fluoroscopy will rule out aortic valve calcification.

M-mode and two-dimensional echocardiography with Doppler study is the best noninvasive diagnostic technique. Thickened ventricular walls can be measured, allowing forms of hypertrophic cardiomyopathy to be differentiated (see FIG. 203–3). Anterior positioning of the papillary muscles and mitral apparatus is usual. Outflow tract obstruction can often be quantitated by observing the degree of systolic anterior movement of the anterior leaflet of the mitral valve and its degree and duration of apposition to the hypertrophied interventricular septum. Doppler velocity analysis of flow across the ventricular outflow tract can quantitate the gradient and area of the stenotic segment and is particularly useful for monitoring the effect of medical or surgical treatment. Doppler analysis of mitral inflow velocity in diastole usually shows evidence of diastolic dysfunction of the left ventricle; left ventricular fractional shortening and ejection fraction (EF) are normal or increased. Midsystolic closure of the aortic valve sometimes occurs in patients with severe outflow tract obstruction. Radionuclide angiography shows a small ventricular cavity with a normal or high EF.

Cardiac catheterization is usually performed only when surgical therapy is considered. Intraventricular pressure gradients may be found in the left and, less commonly, the right ventricle. The gradient rises in a postextrasystolic beat, during Valsalva maneuver, and after amyl nitrite inhalation.

End-diastolic pressure is often high because of poor ventricular compliance. EF is normal or high. Ventriculography shows characteristic chamber deformity depending on the form of hypertrophic cardiomyopathy and sometimes confirms mitral valve regurgitation. The coronary arteries are usually widely patent with torrential flow, although sophisticated metabolic studies may reveal myocardial ischemia due to intramyocardial artery lumen reduction, capillary/myocyte imbalance, and abnormal ventricular wall stress. In older patients, coronary artery disease may coexist.

A few cases gradually lose myocytes, probably from chronic diffuse ischemia as a result of capillary/myocyte imbalance. As myocytes die, they are replaced by diffuse fibrosis, and the hypertrophied ventricle with diastolic dysfunction gradually becomes dilated with systolic dysfunction and becomes an end-stage congestive cardiomyopathy.

Prognosis

Prognosis is guarded; the annual mortality rate is 4%. (The mortality rate is inversely proportional to the age at which symptoms appear and greatest in those with frequent nonsustained ventricular tachycardia, syncope, or resuscitated sudden death.) Family history of sudden death in young patients and angina or effort dyspnea in patients > 45 yr denote a worse prognosis. Sudden death is most common, with chronic heart failure occurring less often. Genetic counseling is appropriate for patients with asymmetric septal hypertrophy, which appears to accelerate during puberty.

Treatment

Therapy is directed primarily at abnormal diastolic compliance. β-Adrenoceptor blockers and Ca blockers alone or in combination are the mainstays of treatment. Both decrease myocardial contractility, which dilates the heart and decreases outflow obstruction, improving diastolic ventricular function. β-Blockers and rate-limiting Ca blockers also slow the heart rate, prolonging the diastolic filling period and thus decreasing outflow obstruction. β-Blockers with intrinsic sympathomimetic action (eg, pindolol, oxprenolol, acebutolol) are best avoided. Ca blockers vary in their negative inotropic effect and arterial vaso-

dilator capacity. It is important to choose a weak vasodilator that has a significant depressant effect on contractility. Verapamil is the Ca blocker of choice for hypertrophic cardiomyopathy.

Drugs that reduce preload (eg, nitrates, diuretics, ACE inhibitors, angiotensin blockers) decrease chamber size and make the signs and symptoms worse. Inotropic drugs (eg, digitalis glycosides, catecholamines) worsen outflow tract obstruction, do not relieve the high end-diastolic pressure, and may induce arrhythmias. Vasodilators increase the outflow tract gradient and produce a reflex tachycardia that further decreases ventricular diastolic function. Although antiarrhythmic therapy can be prescribed for arrhythmias proved by ECG or 24-h ambulatory monitoring, there is no evidence that it alters the risk of sudden death. However, uncontrolled retrospective studies of amiodarone suggest it may reduce mortality in patients with nonsustained ventricular tachyarrhythmias or syncope. The antifibrillatory action of β-blockers may help to prevent sudden death, but this has not been proved. Disopyramide has a negative inotropic effect and has been used as an antiarrhythmic and as a negative inotropic drug.

Defibrillators have been implanted in persons who have been resuscitated from sudden death. Although this treatment is reasonable, it has not been proven to reduce overall mortality in hypertrophic cardiomyopathy. Antibiotic prophylaxis for infective endocarditis should be recommended (see Ch. 208). Competitive sports should be avoided because many sudden deaths occur with increased exertion.

Patients who progress to the dilated congestive phase of the disease are managed in the same manner as those with dilated cardiomyopathy with predominant systolic dysfunction.

Septal myotomy or myomectomy is reserved for patients with incapacitating symptoms despite medical therapy, in whom outflow tract obstruction has been shown by echocardiography and catheterization studies. It lessens symptoms in most carefully selected cases but does not alter mortality. Selective septal infarction using absolute ethanol injection through steerable catheters inserted in septal perforator branches of the anterior descending artery has shown promise and may be an alternative to septal myectomy. In a few cases, mitral valve tailoring or replacement has been done for severe mitral dysfunction; this coincidentally eliminates the outflow tract gradient. Dual chamber pacemakers have been used to alter the sequence of ventricular depolarization in some patients with outflow tract obstruction. In most cases, the severity of obstruction was reduced and symptoms lessened. The long-term effect of this treatment and the effect on mortality require further study.

RESTRICTIVE CARDIOMYOPATHY

Myocardial disorders characterized by rigid, noncompliant ventricular walls that resist diastolic filling of one or both ventricles, most commonly the left.

This form of cardiomyopathy is the least prevalent.

Etiology and Pathology

The cause is usually unknown (for identified causes, see TABLE 203–2). Amyloidosis involving the myocardium is usually systemic, as is iron infiltration in hemochromatosis. Sarcoidosis and Fabry's disease involve the myocardium, and nodal conduction tissue can be involved. Löffler's disease (a subcategory of hypereosinophilic syndrome with primary cardiac involvement) is a cause of restrictive cardiomyopathy. It occurs in the tropics. It begins as an acute arteritis with eosinophilia, with subsequent thrombus formation on the endocardium, chordae, and atrioventricular valves, progressing to fibrosis. Endocardial fibrosis occurs in temperate zones and involves only the left ventricle.

Restrictive cardiomyopathy is divided into a diffuse nonobliterative variety in which the myocardium is infiltrated by abnormal substance (eg, amyloidosis) and an obliterative variety in which the endocardium and subendocardium are fibrosed (eg, endomyocardial fibrosis). Either may be nondiffuse if the disease affects only one chamber or part of one chamber unevenly.

Pathophysiology

The pathophysiologic consequences include endocardial thickening or myocardial infiltration with loss of myocytes, compensatory hypertrophy, and fibrosis. Any of these may lead to atrioventricular valve malfunction resulting in mitral or tricuspid regurgitation. Involvement of nodal and conduction tissue results in sinoatrial node dysfunction and, in some cases, various grades of heart block. Amyloidosis can involve the coronary arteries.

The main hemodynamic consequence of these pathologic states is diastolic dysfunction with a rigid, noncompliant chamber with a high filling pressure. Systolic function may deteriorate if compensatory hypertrophy is inadequate in cases of infiltrated or fibrosed chambers. Mural thrombosis and systemic emboli can complicate the restrictive or obliterative variety.

Symptoms, Signs, and Diagnosis

Similar to hypertrophic cardiomyopathy, the main dysfunction is abnormal compliance and diastolic filling of one or both ventricles, most commonly the left. Symptoms are due to high diastolic pressure, giving rise to pulmonary venous hypertension with effort dyspnea and orthopnea and peripheral edema when the right ventricle is involved. Limited effort is a consequence of a fixed cardiac output due to resistance to ventricular filling. Angina and syncope are uncommon, but atrial and ventricular arrhythmias and heart block are common.

Physical examination reveals a quiet precordium, a low volume and rapid carotid pulse, pulmonary rales, and pronounced neck vein distention with a rapid y descent (see FIG. 197–1). An S_4 is heard in virtually all cases, and an S_3 may occur and must be differentiated from a precordial knock, but often no murmur is present. In some cases, a murmur of functional mitral or tricuspid regurgitation results from changes in chordae or ventricular geometry as a result of infiltration or fibrosis of myocardium and endocardium. Symptoms and signs thus closely mimic constrictive pericarditis; noninvasive tests—including CT, which demonstrates a normal pericardium—may help make this differentiation, but occasionally even heart catheterization is not diagnostic, and thoracotomy is required to explore the pericardium.

The ECG is usually nonspecifically abnormal, showing ST segment and T-wave abnormalities and sometimes low voltage. Pathologic Q waves sometimes occur without previous MI. Left ventricular hypertrophy due to compensatory hypertrophy of the myocardium sometimes occurs. On chest x-ray, the heart size is often normal or small but can be enlarged in late-stage amyloidosis or hemochromatosis.

Echocardiography shows normal systolic function. The atria are often dilated. Disease due to amyloidosis shows an unusually bright echo pattern from the myocardium. Echocardiography helps differentiate constrictive pericarditis with its thickened pericardium, but paradoxical septal motion can occur in either disorder. Myocardial hypertrophy often occurs in restrictive myopathy. MRI reveals abnormal myocardial texture in diseases with myocardial infiltration (eg, of amyloid or iron).

Cardiac catheterization and myocardial biopsy are often necessary. High atrial pressure with a prominent y descent and an early diastolic dip followed by a high diastolic plateau in the ventricular pressure curve are found. Unlike in constrictive pericarditis, diastolic pressure usually is a few millimeters of mercury higher in the left ventricle than in the right. Angiography reveals normal-sized ventricular cavities with normal or decreased systolic shortening. Functional atrioventricular valve regurgitation may result from infiltration of myocardium and papillary muscles or endocardial thickening. Biopsy can demonstrate endocardial fibrosis and thickening, myocardial infiltration with iron or amyloid, or chronic myocardial fibrosis. Coronary angiography is normal, except in rare cases of amyloidosis involving the epicardial coronary arteries.

Primary causes of restrictive cardiomyopathy should be sought (eg, rectal biopsy for amyloidosis, iron studies or biopsy for hemochromatosis).

Prognosis and Treatment

Prognosis is poor (see TABLE 203–3), similar to that of dilated congestive cardiomyopathy (see above).

No therapy is available for most patients. Diuretics must be used with caution because they can lower preload, on which the noncompliant ventricles depend to maintain cardiac output. Digitalis does little to alter the hemodynamic abnormality and may be dangerous in amyloidosis cardiomyopathy, in which extreme digitalis sensitivity is common. Afterload reducers may induce profound hypotension and usually are not of value.

Hemochromatosis may improve with regular phlebotomy to reduce the body's iron stores, and patients with active biopsy-proven sarcoidosis will respond to corticosteroids. Patients in the acute phase of the hypereosinophilic syndrome may respond to corticosteroids and cytotoxic drugs (eg, hydroxyurea). Rarely, in the chronic phase, patients with endocardial fibroelastosis or Löffler's disease improve after surgical debridement of the endocardial fibrotic and thrombotic thickening and freeing up of chordae and valve tissue. Sometimes atrioventricular valve replacement has helped severe functional atrioventricular valve regurgitation. In some cases of significant compensatory hypertrophy, Ca blockers might be of value. Hemodynamic monitoring during initiation of such therapy to confirm its efficacy is prudent.

COR PULMONALE

Right ventricular enlargement secondary to a lung disorder that produces pulmonary artery hypertension (eg, intrinsic pulmonary disease, abnormal chest bellows, depressed ventilatory drive).

Cor pulmonale does not refer to right ventricular (RV) enlargement secondary to left ventricular (LV) failure, congenital heart disease, or acquired valvular heart disease. It is usually chronic but may be acute and reversible.

Etiology

Acute cor pulmonale usually results from massive pulmonary embolization but often occurs as acute reversible exacerbations of chronic cor pulmonale in patients with COPD, usually during acute respiratory infection. **Chronic cor pulmonale** is usually caused by COPD (chronic bronchitis, emphysema) and less often by extensive loss of lung tissue from surgery or trauma, chronic unresolved pulmonary emboli, primary pulmonary hypertension (see below), pulmonary veno-occlusive disease, scleroderma, diseases leading to diffuse interstitial fibrosis, kyphoscoliosis, obesity with alveolar hypoventilation, neuromuscular diseases involving respiratory muscles, and idiopathic alveolar hypoventilation.

Pathogenesis

Cor pulmonale is directly caused by alterations in pulmonary circulation that lead to pulmonary arterial hypertension, thereby increasing the mechanical load on RV emptying (afterload). **Pulmonary hypertension** (see also PRIMARY PULMONARY HYPERTENSION, below) can be caused by irreversible reduction in the size of the vascular bed, as in diseases primarily affecting pulmonary blood vessels (eg, embolization [see Ch. 72], scleroderma) or in massive loss of lung tissue (eg, from emphysema or surgery).

However, the most important mechanism leading to pulmonary hypertension is alveolar hypoxia, which results from localized inadequate ventilation of well-perfused alveoli or from a generalized decrease in alveolar ventilation. Alveolar hypoxia, whether acute or chronic, is a potent stimulus of pulmonary vasoconstriction, and chronic alveolar hypoxia also promotes hypertrophy of smooth muscle in the pulmonary arterioles. These hypertrophied vessels respond to subsequent acute hypoxia. Hypercapnic acidosis augments the pulmonary vasoconstriction. During chronic hypoxia, pulmonary hypertension may be intensified by increased blood viscosity arising from secondary polycythemia and by increased cardiac output. However, increased pulmonary capillary pressure does not contribute per se to the pathogenesis of pulmonary arterial hypertension in cor pulmonale. Hypoxemia and acidosis often aggravate independent disease of the LV and intensify respiratory insufficiency if LV failure induces pulmonary edema.

Symptoms, Signs, and Diagnosis

Cor pulmonale should be suspected in all patients with one of the underlying causes (see Etiology, above). Exertional dyspnea is the most common symptom of pulmonary hypertension. Some patients suffer syncope or fatigue on exertion, and substernal anginal pain is common. Physical signs include left parasternal systolic lift and a loud pulmonic second sound. Murmurs due to functional tricuspid and pulmonic insufficiency may occur. These signs of right heart enlargement appear early and are readily discernible in acute cor pulmonale. Chest x-rays show RV and proximal pulmonary artery enlargement with distal arterial attenuation. ECG evidence of RV hypertrophy correlates well with the degree of pulmonary hypertension. An RV gallop rhythm (S_3 and S_4), distended jugular veins (with a dominant a wave unless tricuspid regurgitation is present), hepatomegaly, and edema may occur in patients with RV failure.

Echocardiographic or radionuclide evaluation of LV and RV function is important. Arterial blood gases are helpful because appreciable hypoxemia, hypercapnia, and acidosis are unusual in left heart failure unless frank pulmonary edema is present. Because pulmonary hyperinflation and bullae cause a realignment of the heart in these patients, the physical examination, x-rays, and ECG may be relatively insensitive indicators of RV enlargement.

Diagnosis of pulmonary hypertension may require right heart catheterization. Echocardiographic measurement of RV systolic pressure is the best noninvasive method.

In cor pulmonale due to disease of the pulmonary parenchyma, clinical manifestations of the primary disease frequently overshadow those of cor pulmonale. Major symptoms and signs (dyspnea, cough, cyanosis, wheezing) also occur in left heart failure, and differentiation may require noninvasive or invasive testing.

Treatment

Therapy for primary lung disorders is discussed in §6. Therapy for right heart failure is discussed above.

Phlebotomy during hypoxic cor pulmonale has been suggested, but beneficial effects of decreased blood viscosity are not likely to outweigh the effects of reducing the O_2-carrying capacity of the blood; also, substantial polycythemia is uncommon in hypoxic cor pulmonale. Digitalis is not effective in hypoxic cor pulmonale; many patients who improve with digitalis and vasodilators may have clinically masked LV dysfunction. Diuretics can improve pulmonary gas exchange in hypoxic cor pulmonale, presumably by relieving extravascular fluid accumulation in the lungs. However, vigorous use of diuretics can lead to metabolic alkalosis, which diminishes the effectiveness of CO_2 as a respiratory stimulus. K and Cl losses must be carefully replaced when diuretics are used.

Continuous use of O_2 decreases pulmonary hypertension, prevents polycythemia in hypoxic patients, and reduces mortality. Pulmonary vasodilators (eg, hydralazine, Ca blockers, nitrous oxide, prostacyclin) have not proven effective. Patients with chronic cor pulmonale are at increased risk of venous thromboembolism, which may be reduced by long-term anticoagulation.

PRIMARY PULMONARY HYPERTENSION

A very uncommon obliterative disease of unknown cause involving medium and small pulmonary arteries resulting in right ventricular failure or fatal syncope 2 to 5 yr after detection.

Women are affected five times more often than men. The median age at diagnosis is 35 yr; younger patients have a worse prognosis. Intimal hyperplasia and consequent narrowing of the vessel lumen are always present. Areas of medial hypertrophy and hyperplasia, irreversible plexiform lesions, and necrotizing arteritis (plexogenic arteriopathy) occur in more advanced cases. Similar vascular lesions and clinical course have been observed in some patients with cirrhosis and in a few patients taking the appetite suppressant drug combination dexfenfluramine-phentermine (fen-phen), no longer marketed in the USA.

Progressive exertional dyspnea occurs in > 95% of cases. Precordial pain and syncope on exertion are less common. Raynaud's phenomenon and arthralgias occur in many patients, often years before the apparent onset of primary pulmonary hypertension.

Diagnosis and Treatment

Diagnosis is suspected on the basis of clinical manifestations, but all known causes of cor pulmonale (see above) must be excluded, especially those that may be modified by therapy (eg, pulmonary embolism). Physical examination shows, to a variable extent, the manifestations of cor pulmonale.

Echocardiography, ventilation/perfusion scanning, pulmonary function testing, and cardiac catheterization are usually necessary to exclude other causes of pulmonary hypertension. Pulmonary angiography should be undertaken if ventilation/perfusion scans show unmatched segmental or larger perfusion defects. This scan pattern is not seen in primary pulmonary hypertension but suggests chronic thrombotic occlusion of pulmonary arteries due to unresolved pulmonary embolism, which can be helped in some cases by thromboendarterectomy. Pulmonary angioscopy may reveal chronic mural thrombi, even when arteriography is

negative. The need for open lung biopsies is controversial.

A few patients can respond to vasodilators (eg, prostacyclin, nifedipine) with drastic reductions in pulmonary artery pressure. However, vasodilators should first be found effective in the cardiac catheterization laboratory. Injudicious use of these drugs has resulted in marked deterioration or fatality. Increasingly, long-term oral nifedipine is being given at dosages determined empirically during cardiac catheterization. Sustained IV infusions of prostacyclin (a vasodilator and inhibitor of platelet aggregation) via implanted catheters using portable minipumps have been effective in use for > 1 yr, improving the quality of life and reducing the urgency of lung transplantation. To prevent silent recurrent embolism or in situ thrombosis and because venous stasis can be a consequence of right heart failure, long-term oral coumarin anticoagulation is usually used if not contraindicated; the prothrombin time is kept between 1.5 and 1.75 times normal (INR, 2 to 3—see Laboratory Findings under HEMOSTASIS in Ch. 131).

Unilateral or bilateral lung transplantation has become an established procedure in primary pulmonary hypertension.

204 / SHOCK

A state in which blood flow to and perfusion of peripheral tissues are inadequate to sustain life because of insufficient cardiac output or maldistribution of peripheral blood flow, usually associated with hypotension and oliguria.

Shock may be due to hypovolemia, vasodilation, or cardiogenic causes (poor cardiac output) or a combination. The fundamental defect in shock is reduced perfusion of vital tissues due (usually) to hypotension, so that O_2 delivery or uptake is inadequate for aerobic metabolism, resulting in a shift to anaerobic respiration with increased production and accumulation of lactic acid. When shock persists, impaired organ function is followed by irreversible cell damage and death. The degree of systemic hypotension necessary to cause shock varies and often is related to preexisting vascular disease. Thus, a modest degree of hypotension that is tolerated well by a young, relatively healthy person might result in severe cerebral, cardiac, or renal dysfunction in a patient who has significant arteriosclerosis.

Hypovolemic shock: Hypovolemic shock is associated with inadequate intravascular volume (absolute or relative), which produces diminished ventricular filling and reduced stroke volume. Unless compensated for by increased heart rate, it results in decreased cardiac output.

A common cause is acute hemorrhage (eg, from trauma, peptic ulcer, esophageal varices, or aortic aneurysm). Hemorrhage may be apparent (eg, hematemesis or melena) or concealed (eg, ruptured ectopic pregnancy).

Hypovolemic shock may also follow increased losses of body fluids other than blood (see TABLE 204–1). Hypovolemia usually takes several hours to develop and may be associated with a rising Hb or Hct (due to hemoconcentration).

Hypovolemic shock may be due to inadequate fluid intake, resulting in dehydration, often with increases in fluid loss. Frequently, because of neurologic or physical disability, patients cannot respond to thirst by increasing fluid intake. In hospitalized patients, hypovolemia can be compounded if early signs of circulatory insufficiency are incorrectly ascribed to heart failure and fluids are withheld or diuretics given.

Vasodilatory shock: Vasodilatory shock results from a relative inadequacy of intravascular volume caused by vasodilation. Circulating blood volume is normal but insufficient for adequate cardiac filling. Various conditions may cause widespread venous or arteriolar dilation; eg, severe cerebral trauma or hemorrhage (neurogenic shock), liver failure, or ingestion of certain drugs or poisons. Shock associated with bacterial infection (bacteremic or septic shock—see Ch. 156) may be partly due to the vasodilatory effects of endotoxin or other chemical mediators on resistance vessels, thereby decreasing vascular resistance. In addition, some patients with acute MI and shock appear to have inadequate compensatory vasoconstriction in response to decreased cardiac output. If cardiac output does not increase commensurate with the reduction in vascular resistance, arterial hypotension develops. Below a critical systemic BP, vital organs will be inadequately perfused. Myocardial dysfunction secondary to inadequate coronary perfusion or other mechanisms (eg, release of myocardial depressant factor or other toxic substances) may complicate shock due to vasodilation.

TABLE 204–1. LOSS OF BODY FLUID IN HYPOVOLEMIC SHOCK

Nature of Loss	Mechanism of Loss
Fluid lost from the body surface area	Thermal or chemical injury
Fluid sequestered in the peritoneal cavity	In generalized peritonitis after perforation of the GI tract or pancreatitis
Fluid pooled within or lost from the GI tract	Vomiting or diarrhea resulting from small- or large-bowel obstruction, paralytic ileus, or gastroenteritis
Excessive renal fluid loss	In diabetes mellitus or insipidus, in adrenal insufficiency, in "salt-losing" nephritis, in the polyuric phase after acute tubular damage, and with potent diuretics
Intravascular fluid lost to the extravascular space	Increased capillary permeability secondary to anoxia, cardiac arrest, or acute hypersensitivity (anaphylactic) reactions in which shock is also due to arteriolar vasodilation

Cardiogenic shock: A relative or absolute reduction in cardiac output due to factors other than inadequate intravascular volume may result in shock. Causes are described in TABLE 204–2.

Symptoms and Signs

Symptoms and signs may be due to shock itself or to the underlying disease process. Mentation may be preserved, but lethargy, confusion, and somnolence are common. The hands and feet are cold, moist, and often cyanotic and pale. Capillary filling time is prolonged, and, in extreme cases, a bluish reticular pattern may appear over large areas. The pulse is weak and rapid unless heart block or terminal bradycardia is present; sometimes, only femoral or carotid pulses can be felt. Tachypnea and hyperventilation are present, but apnea may be a terminal event when the respiratory center fails due to inadequate cerebral perfusion. BP taken by cuff tends to be low (< 90 mm Hg systolic) or unobtainable, but direct measurement by intra-arterial cannula often gives significantly higher values.

In **septic shock,** a type of vasodilatory shock (see also Ch. 156), fever, usually preceded by chills, is generally present. Elevated cardiac output is associated with diminished total peripheral resistance, possibly accompanied by hyperventilation and respiratory alkalosis. Thus, early symptoms may include a shaking chill, a rapid rise in temperature, warm flushed skin, a bounding pulse, and falling and rising BP (hyper-

TABLE 204–2. MECHANISMS THAT CAUSE CARDIOGENIC SHOCK

Mechanism	Cause
Mechanical interference with ventricular filling or preload	Tension pneumothorax, cardiac tamponade, atrial tumor or clot
Interference with ventricular emptying or afterload	Pulmonary embolism, prosthetic valve malfunction
Impaired myocardial contractility	Myocardial ischemia or MI, myocarditis, drugs
Abnormalities of cardiac rhythm	Tachycardia, bradycardia
Excessive volume demands	Acute mitral or aortic regurgitation, ruptured interventricular septum

引用非特許文献

特許出願の番号	特願２００７－５０８６７９
作成日	平成２３年　５月３０日
作成者	川嵜　洋祐　　４７６５　４Ｃ００
発明の名称	心筋の病気を治療するための方法および組成物

J Physiol (2003), 549.3, pp. 667–672
© The Physiological Society 2003

DOI: 10.1113/jphysiol.2003.043976
www.jphysiol.org

Journal of Physiology

Rapid Report

Inhibition of HERG K^+ current and prolongation of the guinea-pig ventricular action potential by 4-aminopyridine

J. M. Ridley, J. T. Milnes, Y. H. Zhang, H. J. Witchel and J. C. Hancox

Department of Physiology and Cardiovascular Research Laboratories, School of Medical Sciences, University Walk, Bristol BS8 1TD, UK

4-Aminopyridine (4-AP) has been used extensively to study transient outward K^+ current ($I_{TO,1}$) in cardiac cells and tissues. We report here inhibition by 4-AP of HERG (the human *ether-à-go-go*-related gene) K^+ channels expressed in a mammalian cell line, at concentrations relevant to those used to study $I_{TO,1}$. Under voltage clamp, whole cell HERG current (I_{HERG}) tails following commands to +30 mV were blocked with an IC_{50} of 4.4 ± 0.5 mM. Development of block was contingent upon HERG channel gating, with a preference for activated over inactivated channels. Treatment with 5 mM 4-AP inhibited peak I_{HERG} during an applied action potential clamp waveform by ~59%. It also significantly prolonged action potentials and inhibited resurgent I_K tails from guinea-pig isolated ventricular myocytes, which lack an $I_{TO,1}$. We conclude that by blocking the α-subunit of the I_{Kr} channel, millimolar concentrations of 4-AP can modulate ventricular repolarisation independently of any action on $I_{TO,1}$.

(Received 27 March 2003; accepted after revision 1 May 2003; first published online 9 May 2003)
Corresponding author J. C. Hancox: Department of Physiology and Cardiovascular Research Laboratories, School of Medical Sciences, University Walk, Bristol BS8 1TD, UK. Email: jules.hancox@bristol.ac.uk

4-Aminopyridine (4-AP) has been used extensively in cardiac electrophysiology to study the physiological roles of transient outward potassium current ($I_{TO,1}$; Wang *et al.* 1991; Gillis *et al.* 1998; Elizalde *et al.* 1999; Lei *et al.* 2000; Kocic *et al.* 2002) and, in recent years, of the 'ultra-rapid' delayed rectifier current (I_{Kur}; Li *et al.* 1996; Yue *et al.* 1996). 4-AP is generally considered selective for these currents in the heart, with micromolar concentrations being used to block I_{Kur} (Li *et al.* 1996) and millimolar concentrations to block $I_{TO,1}$ (typically 0.5 to 10 mM; e.g. Wang *et al.* 1991; Gillis *et al.* 1998; Elizalde *et al.* 1999; Lei *et al.* 2000; Kocic *et al.* 2002). However, limited published data raise the possibility that 4-AP may not be entirely selective for $I_{TO,1}$ over the rapid delayed rectifier K^+ current (I_{Kr}) at concentrations used to study $I_{TO,1}$ (Mitcheson & Hancox, 1999; Liu *et al.* 1999; Zhang *et al.* 2000). Given the importance of I_{Kr} in regulating action potential repolarization and duration (Mitcheson & Sanguinetti, 1999), a non-selective effect of 4-AP on I_{Kr} would significantly influence the interpretation of data from experiments in which 4-AP is applied to cardiac muscle cells or tissues. The aim of this study was to determine whether or not 4-AP inhibits ionic current (I_{HERG}) carried by K^+ channels encoded by *HERG* (the human *ether-à-go-go*-related gene, which encodes the α-subunit of the I_{Kr} channel; Warmke & Ganetzky, 1994). 4-AP was found both to inhibit I_{HERG} recorded from human embryonic kidney cells and to prolong action potentials from guinea-pig ventricular myocytes, which lack $I_{TO,1}$. These findings have widespread implications for the use of 4-AP as an investigative tool in cardiac muscle electrophysiology.

METHODS

Maintenance of a mammalian cell line stably expressing HERG

Measurements of I_{HERG} were made from human embryonic kidney (HEK 293) cells stably expressing HERG (cell line generously donated by Professor Craig January, University of Wisconsin; Zhou *et al.* 1998). Cells were passaged using a non-enzymatic agent (Splittix, AutogenBioclear) and plated out onto fragments of sterilized glass coverslips in 30 mm petri dishes containing a modification of Dulbecco's modified Eagle's medium with Glutamax-1 (DMEM; Gibco), supplemented with 10% fetal bovine serum, 400 $\mu g\ ml^{-1}$ gentamicin (Gibco) and 400 $\mu g\ ml^{-1}$ geneticin (G418; Gibco). Cells were incubated at 37°C (5% CO_2) for a minimum of 2 days prior to any electrophysiological study.

Isolation of guinea-pig ventricular myocytes

Male adult guinea-pigs were killed by cervical dislocation (a Schedule 1 procedure according to the Home Office UK Animals (Scientific Procedures) Act 1986) and ventricular myocytes were enzymatically dispersed from both ventricles using a method described previously (Levi & Issberner, 1996). Prior to use, the isolated cells were kept at 4°C in Kraft-Brühe medium (Isenberg & Klockner, 1982).

Electrophysiological recordings
Cells were superfused with a normal Tyrode solution, which contained (mM): 140 NaCl, 4 KCl, 2.5 $CaCl_2$, 1 $MgCl_2$, 10 glucose, 5 Hepes, (titrated to pH 7.45 with NaOH). Experimental solutions were applied using a home-built, warmed solution delivery system capable of changing the bathing solution surrounding a cell in <1 s. Patch-pipettes were fire-polished to a resistance of 3.5–5 MΩ. The pipette solution for I_{HERG} measurement contained (mM): 130 KCl, 1 $MgCl_2$, 5 EGTA, 5 MgATP, 10 Hepes (titrated to pH 7.2 with KOH). A K^+-based, EGTA-free pipette solution containing 10 mM NaCl was used for action potential recordings. The 'pipette-to-bath' liquid junction potential was small (−3.2 mV) and was uncorrected. Series resistance (R_s) values lay typically between 4–7 MΩ and were compensated by > 70 %. The expected voltage drop across residual uncompensated R_s during I_{HERG} measurements was therefore only small (~3.5 mV or less) and no correction was made for this. Measurements were made at 37 ± 1 °C.

Drugs
4-AP powder (Sigma) was dissolved directly in normal Tyrode solution to make test solutions of different concentrations referred to in the Results; pH was corrected to 7.45 with HCl.

Voltage protocols and analysis
Measurements were made using an Axopatch 200 or 200A amplifier (Axon Instruments) and a CV-201/2A headstage. Voltage-clamp commands were generated using 'WinWCP' (John Dempster, Strathclyde University, UK) or pCLAMP (v 6.0, Axon Instruments). Data were recorded via a Digidata interface (Axon Instruments) and stored on the hard disk of a personal computer.

Concentration–response relationships
I_{HERG} tails were measured on repolarization to −40 mV after 1 s depolarizing voltage commands to +30 mV. 4-AP concentrations between 100 μM and 100 mM were each applied to a minimum of five different cells. The mean fractional blockade was obtained as:

$$\text{Fractional block} = 1 - \left(\frac{I_{HERG(4\text{-}AP)}}{I_{HERG(CONTROL)}}\right), \quad (1)$$

where $I_{HERG(4\text{-}AP)}$ and $I_{HERG(CONTROL)}$ represent tail current amplitudes in the presence and absence of 4-AP, respectively. The agent was rapidly acting (maximal effects of a given concentration typically being observed within ~2–4 pulses), and its effects could be observed without any marked overlying current run-down. Concentration–response data were fitted by the equation:

$$\text{Fractional block} = \frac{1}{\left(1 + \left(\frac{IC_{50}}{[4\text{-}AP]}\right)^h\right)}, \quad (2)$$

where IC_{50} is [4-AP] producing half-maximal inhibition of the I_{HERG} tail and h is the Hill coefficient for the fit.

I_{HERG} inhibition at different voltages
From −80 mV, 2 s depolarizations were applied to potentials between −40 and +40 mV. I_{HERG} tails were measured on repolarization to −40 mV. Current–voltage (I–V) relations (not shown) were constructed for each of eight cells in the absence and presence of 5 mM 4-AP. Half-maximal activation voltages were obtained by fitting each I–V relation with a modified Boltzmann equation:

$$I = \frac{I_{max}}{1 + \exp\left(\frac{(V_h - V_m)}{k}\right)}, \quad (3)$$

where I = I_{HERG} tail amplitude following test potential V_m, I_{max} is the maximal I_{HERG} tail current observed, V_h is the potential at which I_{HERG} was half-maximally activated and k is the slope factor describing I_{HERG} activation.

Voltage-dependent activation curves for I_{HERG} were obtained by calculating activation variables at 2 mV intervals between −80 and +40 mV. Values for V_h and k derived from fits to experimental I–V data with eqn (3) were inserted into the following equation:

$$\text{Activation parameter} = \frac{1}{1 + \exp\left(\frac{(V_h - V_m)}{k}\right)}, \quad (4)$$

where the 'activation parameter' at any test potential, V_m, occurs within the range 0 to 1 and V_h and k have similar meanings to those in eqn (3).

Envelope of tails
From −80 mV, membrane potential was stepped to +40 mV for varying time periods between 12.5 and 600 ms and was repolarized to −40 mV in order to monitor I_{HERG} tail amplitude. After control measurements, each cell was equilibrated in 4-AP-containing solution while at the holding potential and the protocol was then reapplied. For each cell, the fractional block of I_{HERG} tails at each test pulse duration was determined using eqn (1). The plot of mean fractional block *versus* test pulse duration was then fitted with an equation of the form:

$$\text{Fractional block} = A - \left(A \exp\left(\frac{-x}{\tau}\right)\right), \quad (5)$$

where A represents maximal fractional block, x represents pulse duration and τ is the time constant of development of blockade (ms).

Action potential voltage clamp and measurements from guinea-pig ventricular myocytes
For action potential clamp measurements of I_{HERG} from HEK cells, the command waveform used was the same as that employed in previous studies of I_{HERG} from our laboratory (Hancox *et al.* 1998*a*,*b*).

Action potentials were elicited from guinea-pig ventricular myocytes by brief suprathreshold current pulses at 15 s intervals. For measurements of guinea-pig I_K tails, membrane potential was held at −80 mV, depolarized to −40 mV for 20 ms, then depolarized to +20 mV for 300 ms. I_K tails were measured during subsequent repolarization to −40 mV.

Data analysis and presentation
Data are presented as means ± S.E.M. Statistical comparisons were made using Student's paired t test or one-way analysis of variance (ANOVA) with a Bonferroni *post hoc* test. P values of less than 0.05 were taken as significant.

RESULTS

Figure 1A shows that 4-AP produced a concentration-dependent inhibition of I_{HERG} and Fig. 1B shows the mean concentration–response relationship for this effect. The IC_{50} derived from the data was 4.4 ± 0.5 mM (Hill coefficient 0.7 ± 0.1). The voltage dependence of the effect was assessed by applying commands to a range of test potentials (Fig. 1Ci and Cii). No I_{HERG} tail inhibition was evident after pre-pulses to −30 mV and −20 mV, whilst at more positive potentials marked inhibition of I_{HERG} was observed (Fig. 1Ci and Cii). Mean data are shown in Fig. 1D, which also contains mean activation curves in control (continuous line) and 4-AP (dashed line). In the presence of 4-AP a leftward shift in the half-maximal activation voltage ($V_{0.5}$) by −7.4 ± 0.9 mV, $n = 8$; $P < 0.0001$, t test) was observed. The activation shift may account for the apparent augmentation/ lack of blockade of by 4-AP observed at −30 and −20 mV. The voltage range over which inhibition was voltage dependent corresponded with that over which voltage-dependent activation of I_{HERG} developed (Mergenthaler *et al.* 2001; Paul *et al.* 2001). Treatment with 5 mM 4-AP did not significantly alter the mean deactivation time course of tails measured at −40 mV, following a voltage command to +30 mV.

The dependence of I_{HERG} inhibition by 4-AP upon duration of depolarization was studied using an 'envelope of tails' protocol (Trudeau *et al.* 1995) (see Fig. 2A and B). Figure 2A shows representative current traces obtained in control (Fig. 2Ai) and in 4-AP (Fig. 2Aii); Fig. 2B shows a plot of the resulting mean levels of fractional block against pulse duration. The time course of development of blockade was described by a mono-exponential curve that intersected the origin, with a time constant of 32.3 ± 6.4 ms ($n = 5$). Considered collectively with Fig. 1D these data demonstrate that inhibition of I_{HERG} by 4-AP requires channel gating to occur.

An additional protocol (see Fig. 3A, lower trace) was employed to ascertain whether or not 4-AP showed a preference for activated or inactivated HERG channels. In

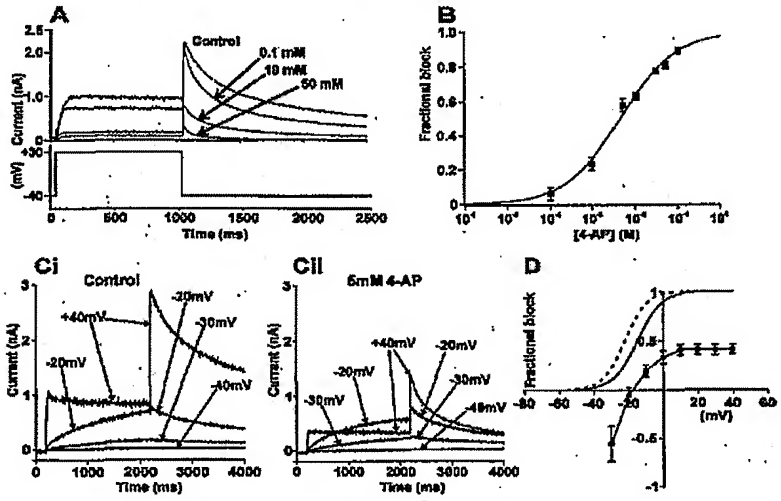

Figure 1. Concentration and voltage-dependent inhibition of I_{HERG} by 4-AP

A, upper traces show representative current traces illustrating the effect of different concentrations of 4-AP. Lower trace represents voltage protocol used. *B*, concentration response relation for I_{HERG} tail blockade by 4-AP ($n = 5$–8 cells at each concentration). *C*, representative records in the absence (*Ci*) and presence (*Cii*) of 5 mM 4-AP. *D*, the mean (± S.E.M.) fractional block of I_{HERG} by 5 mM 4-AP over a range of potentials ($n = 8$ cells). I_{HERG} activation curves are shown in the absence (continuous line) and presence (dashed line) of 5 mM 4-AP.

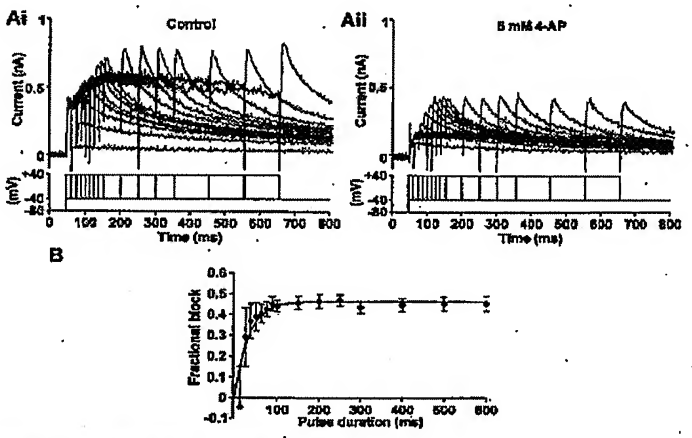

Figure 2. Time dependance of I_{Kslow} block by 4-AP

A, traces from an 'envelope of tails' protocol, in the absence (*Ai*) and presence (*Aii*) of 5 mM 4-AP. Lower traces represent the voltage protocol used. *B*, the mean (± S.E.M.) fractional block of I_{Kslow} with varying pulse duration ($n = 5$ cells). The τ for development of inhibition was 32.3 ± 6.4 ms ($n = 5$).

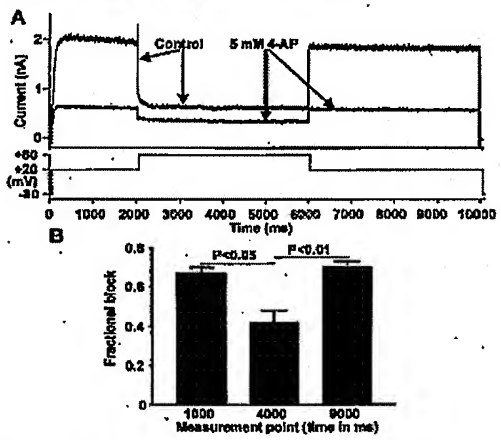

Figure 3. Effect of strong depolarisation on the action of 4-AP

A, current records (upper traces) elicited by the voltage protocol shown (lower trace), applied from a holding potential of −80 mV. Arrows indicate traces obtained in control and 4-AP. *B*, bar charts ($n = 5$ cells) compare the mean level of blockade at 1000 ms into protocol (at +20 mV), at 4000 ms (at +80 mV) and at 9000 ms (after membrane potential was returned to +20 mV).

control solution, I_{HERG} amplitude decreased markedly during a depolarisation from +20 to +80 mV (Fig. 3*A*, upper traces, Control) as a consequence of increased I_{HERG} inactivation. In the presence of 5 mM 4-AP, blockade of I_{HERG} at +20 mV was greater than that at +80 mV (Fig. 3*A*, upper traces, 4-AP). Mean data shown in Fig. 3*B* indicate that blockade during the +80 mV step ('4000 ms') was significantly lower than that at +20 mV ('1000 ms' and 9000 ms'). Thus, when I_{HERG} was reduced by extensive I_{HERG} inactivation the blocking effect of 4-AP was diminished. This observation suggests that 4-AP binds preferentially to activated over inactivated HERG channels. In further experiments we observed an acceleration of the rate of development of I_{HERG} inactivation by 4-AP (data not shown). This effect is in marked contrast with that reported for externally applied tetraethylammonium ions (TEA), which slow the distinctive, rapidly developing C-type inactivation of I_{HERG} (Smith *et al.* 1996). This action of 4-AP could have resulted either from a genuine modification of inactivation gating, or from the rapid development of open-channel block during the protocol used to study inactivation.

The effect of 4-AP on I_{HERG} elicited by an applied ventricular action potential waveform was also determined (Fig. 4*A*). In control solution, I_{HERG} amplitude increased progressively through the action potential plateau and was maximal near −30 mV (−30.2 ± 3.4 mV; $n = 5$; cf. Hancox *et al.* 1998*a*). Treatment with 5 mM 4-AP attenuated current throughout the action potential command, inhibiting maximal I_{HERG} by 58.5 ± 4.1 % ($n = 5$). Also, the voltage at which I_{HERG} peaked was shifted by −10.6 ± 4.1 mV, consistent with the voltage shift in current activation described in Fig. 1. These data suggest that 4-AP might increase the action potential duration in native cardiac tissue through blockade of native I_{Kr}, independent of any inhibitory action on $I_{TO,1}$. Therefore, we measured action potentials from guinea-pig ventricular myocytes, which lack $I_{TO,1}$ (Corabœuf *et al.* 1998). 4-AP exerted little effect immediately after the action potential peak, but the times to reach both 50 % and 90 % repolarization (APD_{50} and APD_{90}, respectively) were significantly prolonged by 4-AP (Fig. 4*B*; in control: mean $APD_{50} = 162.2 \pm 12.2$ ms and $APD_{90} = 184.3 \pm 12.2$ ms; in 4-AP: $APD_{50} = 210.9 \pm 14.6$ ms and $APD_{90} = 243.1 \pm 14.8$ ms, $n = 8$; $P < 0.01$ and $P < 0.001$, respectively). In complementary voltage-clamp experiments, resurgent I_K tails (sensitive to the I_{Kr} blocker E-4031) from guinea-pig myocytes were also inhibited by 4-AP (Fig. 4*C*).

DISCUSSION

The dependence of HERG blockade by 4-AP upon channel gating observed in this study differs from the mechanism underlying its blockade of cardiac $I_{TO,1}$, which depends considerably upon the agent binding to the closed channel (Castle & Slawsky, 1993; Wang *et al.* 1995). $I_{TO,1}$ from rat, rabbit and human have been reported to be blocked by 4-AP with IC_{50} values of 0.14, 0.33 and 0.67 mM, respectively, whilst Kv 4.3 current exhibits an IC_{50} of 1.54 mM (Xu *et al.* 1998; Paivre *et al.* 1999; Lei *et al.* 2000). Therefore, whilst 4-AP is clearly a low affinity HERG blocker, its IC_{50} for I_{HERG} inhibition falls within a 4-AP concentration range used to block $I_{TO,1}$ selectively in previous studies (typically 0.5–10 mM; Wang *et al.* 1991; Gillis *et al.* 1998; Elizalde *et al.* 1999; Lei *et al.* 2000; Kocic *et al.* 2002). The fact that some level of I_{Kr} blockade may also have occurred in such experiments is supported by the present data from guinea-pig myocytes, which lack $I_{TO,1}$, and by previous data regarding reduction of I_K tails from rabbit nodal cells (Mitcheson & Hancox, 1999). On the basis of our findings, we conclude that millimolar concentrations of 4-AP can block I_{HERG}/I_{Kr} and, thereby, prolong cardiac action potential repolarization independently of any action on $I_{TO,1}$. In light of these observations, it may be necessary to consider carefully the

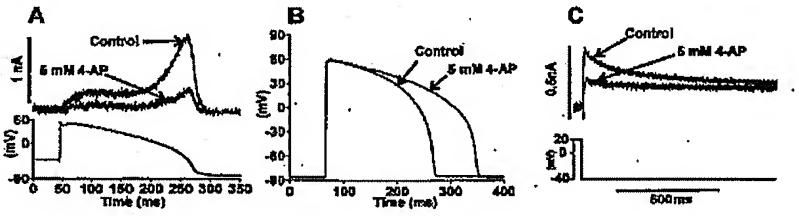

Figure 4. Effect of 4-AP under action potential conditions

A, representative records of I_{HERG} after P/4 leak subtraction, (upper traces) activated by ventricular action potential command (lower trace), in control and in the presence of 5 mM 4-AP. *B*, effect of 5 mM 4-AP on action potentials from guinea-pig ventricular myocytes. *C*, effect of 4-AP on resurgent I_K tails from a guinea-pig ventricular myocyte (upper traces; lower trace shows a section of the voltage protocol. A mean inhibition of 71.1 ± 4.3 % was observed ($n = 6$).

interpretation of experiments in which millimolar 4-AP has been used as a pharmacological tool to study cardiac $I_{to,1}$ in species that also exhibit I_{Kr}. Of course, *in vitro* data must only be extrapolated to the *in vivo* situation with caution and there is evidence that 4-AP infusion regimens used to study the role of $I_{to,1}$ in the dog (del Balzo & Rosen, 1992) may actually attain submillimolar plasma levels (Nattel *et al.* 2000). Our data are concordant with the notion that micromolar 4-AP may justifiably be used to study I_{Kur} in cells that exhibit I_{Kr}, as comparatively little I_{Kr} blockade would be expected at the low concentration levels (e.g. Yue *et al.* 1996) required to inhibit I_{Kur}.

REFERENCES

Castle NA & Slawsky MT (1993). Characterization of 4-aminopyridine block of the transient outward K^+ current in adult rat ventricular myocytes. *J Pharmacol Exp Ther* **265**, 1450–1459.

Corabocuf E, Coulombe A, Deroubaix E, Hatem S & Mercadier JJ (1998). Transient outward potassium current and repolarization of cardiac cells. *Bull Acad Natl Med* **182**, 325–333.

del Balzo U & Rosen MR (1992). T wave changes persisting after ventricular pacing in canine heart are altered by 4-aminopyridine but not by lidocaine. Implications with respect to phenomenon of cardiac 'memory'. *Circulation* **85**, 1464–1472.

Elizal de A, Barajas H, Navarro-Polanco R & Sanchez-Chapula J (1999). Frequency-dependent effects of 4-aminopyridine and almokalant on action-potential duration of adult and neonatal rabbit ventricular muscle. *J Cardiovasc Pharmacol* **33**, 352–359.

Palvre JE, Calmels TP, Rouanet S, Javre JL, Cheval B & Bril A (1999). Characterization of Kv4.3 in HEK293 cells: comparison with the rat ventricular transient outward potassium current. *Cardiovasc Res* **41**, 188–199.

Gillis AM, Geonzon RA, Mathison HJ, Kulisz E, Lester WM & Duff HJ (1998). The effects of barium, dofetilide and 4-aminopyridine (4-AP) on ventricular repolarization in normal and hypertrophied rabbit heart. *J Pharmacol Exp Ther* **285**, 252–270.

Hancox JC, Levi AJ & Witchel HJ (1998*a*). Time course and voltage dependence of expressed HERG current compared with native 'rapid' delayed rectifier K current during the cardiac ventricular action potential. *Pflugers Arch* **436**, 843–853.

Hancox JC, Witchel HJ & Varghese A (1998*b*). Alteration of HERG current profile during the cardiac ventricular action potential, following a pore mutation. *Biochem Biophys Res Commun* **253**, 719–724.

Isenberg G & Klockner U (1982). Calcium tolerant ventricular myocytes prepared by preincubation in a 'KB medium'. *Pflugers Arch* **395**, 6–18.

Kodic I, Hirano Y & Hiraoka M (2002). Rate-dependent changes in action potential duration and membrane currents in hamster ventricular myocytes. *Pflugers Arch* **443**, 353–361.

Lei M, Honjo H, Kodama I & Boyett MR (2000). Characterisation of the transient outward K^+ current in rabbit sinoatrial node cells. *Cardiovasc Res* **46**, 433–441.

Levi AJ & Issberner J (1996). Effect on the fura-2 transient of rapidly blocking the Ca^{2+} channel in electrically stimulated rabbit heart cells. *J Physiol* **493**, 19–37.

Li GR, Feng J, Yue L, Carrier M & Nattel S (1996). Evidence for two components of delayed rectifier K^+ current in human ventricular myocytes. *Circ Res* **78**, 689–696.

Liu XK, Wang W, Ebert SN, Franz MR, Katchman A & Woosley RL (1999). Female gender is a risk factor for torsades de pointes in an *in vitro* animal model. *J Cardiovasc Pharmacol* **34**, 287–294.

Mergenthaler J, Haverkamp W, Huttenhofer A, Skrzypiec BV, Munthoff U, Borggrefe M, Speckmann EJ, Breithardt G & Madeja M (2001). Blocking effects of the antiarrhythmic drug propafenone on the HERG potassium channel. *Naunyn Schmiedebergs Arch Pharmacol* **363**, 472–480.

Mitcheson JS & Hancox JC (1999). Characteristics of a transient outward current (sensitive to 4-aminopyridine) in Ca^{2+}-tolerant myocytes isolated from the rabbit atrioventricular node. *Pflugers Arch* **438**, 68–78.

Mitcheson JS & Sanguinetti MC (1999). Biophysical properties and molecular basis of cardiac rapid and slow delayed rectifier potassium channels. *Cell Physiol Biochem* **9**, 201–216.

Nattel S, Matthews C, De Blasio E, Han W, Li D & Yue L (2000). Dose-dependence of 4-aminopyridine plasma concentrations and electrophysiological effects in dogs: potential relevance to ionic mechanisms *in vivo*. *Circulation* **101**, 1179–1184.

Paul AA, Witchel HJ & Hancox JC (2001). Inhibition of HERG potassium channel current by the class Ia antiarrhythmic agent disopyramide. *Biochem Biophys Res Commun* **280**, 1243–1250.

Smith PL, Baukrowitz T & Yellen G (1996). The inward rectification mechanism of the HERG cardiac potassium channel. *Nature* **379**, 833–836.

Trudeau MC, Warmke JW, Ganetzky B & Robertson GA (1995). HERG, a human inward rectifier in the voltage-gated potassium channel family. *Science* **269**, 92–95.

Wang ZG, Fermini B & Nattel S (1991). Repolarization differences between guinea pig atrial endocardium and epicardium: evidence for a role of Ito. *Am J Physiol* **260**, H1501–1506.

Wang Z, Fermini B & Nattel S (1995). Effects of flecainide, quinidine, and 4-aminopyridine on transient outward and ultrarapid delayed rectifier currents in human atrial myocytes. *J Pharmacol Exp Ther* **272**, 184–196.

Warmke JW & Ganetzky B (1994). A family of potassium channel genes related to eag in *Drosophila* and mammals. *Proc Natl Acad Sci USA* **91**, 3438–3442.

Xu WH, Li W, Yue HW & Wang XL (1998). Characteristics of transient outward K^+ current in human atrial cardiomyocytes. *Zhongguo Yao Li Xue Bao* **19**, 481–485.

Yue L, Feng J, Li GR & Nattel S (1996). Characterization of an ultrarapid delayed rectifier potassium channel involved in canine atrial repolarization. *J Physiol* **496**, 647–662.

Zhang H, Holden AV, Kodama I, Honjo H, Lei M, Varghese T & Boyett MR (2000). Mathematical models of action potentials in the periphery and center of the rabbit sinoatrial node. *Am J Physiol Heart Circ Physiol* **279**, H397–421.

Zhou Z, Gong Q, Ye B, Fan Z, Makielski JC, Robertson GA & January CT (1998). Properties of HERG channels stably expressed in HEK 293 cells studied at physiological temperature. *Biophys J* **74**, 230–241.

Acknowledgements

This work was supported by grants from the British Heart Foundation, Wellcome Trust and a University of Bristol PhD studentship to J.M.R. The authors thank Lesley Arberry for technical assistance and Dr Andrew James for comments on the manuscript.

Author's present address

Y. H. Zhang: Department of Cardiovascular Medicine, University of Oxford, John Radcliffe Hospital, Oxford, UK.

引用非特許文献

特許出願の番号	特願２００７－５０８６７９
作成日	平成２３年　５月３０日
作成者	川嵜　洋祐　　４７６５　４Ｃ００
発明の名称	心筋の病気を治療するための方法および組成物

Targeted Replacement of Kv1.5 in the Mouse Leads to Loss of the 4-Aminopyridine–Sensitive Component of $I_{K,slow}$ and Resistance to Drug-Induced QT Prolongation

Barry London, Weinong Guo, Xiang-hua Pan, Joon S. Lee, Vladimir Shusterman, Christopher J. Rocco, Diomedes A. Logothetis, Jeanne M. Nerbonne, Joseph A. Hill

Abstract—The K^+ channel mKv1.5 is thought to encode a 4-aminopyridine (4-AP)–sensitive component of the current $I_{K,slow}$ in the mouse heart. We used gene targeting to replace mKv1.5 with the 4-AP–insensitive channel rKv1.1 (SWAP mice) and directly test the role of Kv1.5 in the mouse ventricle. Kv1.5 RNA and protein were undetectable, rKv1.1 was expressed, and Kv2.1 protein was upregulated in homozygous SWAP hearts. The density of the K^+ current $I_{K,slow}$ (depolarizations to +40 mV, pA/pF) was similar in left ventricular myocytes isolated from SWAP homozygotes (17±1, n=27) and littermate controls (16±2, n=19). The densities and properties of I_{peak}, $I_{to,f}$, $I_{to,s}$, and I_{ss} were also unchanged. In homozygous SWAP myocytes, the 50-μmol/L 4-AP–sensitive component of $I_{K,slow}$ was absent (n=6), the density of the 20-mmol/L tetraethylammonium-sensitive component of $I_{K,slow}$ was increased (9±1 versus 5±1, $P<0.05$), and no 100- to 200-nmol/L α-dendrotoxin–sensitive current was found (n=8). APD_{90} in SWAP myocytes was similar to controls at baseline but did not prolong in response to 30 μmol/L 4-AP. Similarly, QTc (ms) was not prolonged in anesthetized SWAP mice (64±2, homozygotes, n=9; 62±2, controls, n=9), and injection with 4-AP prolonged QTc only in controls (63±1, homozygotes; 72±2, controls; $P<0.05$). SWAP mice had no increase in arrhythmias during ambulatory telemetry monitoring. Thus, Kv1.5 encodes the 4-AP–sensitive component of $I_{K,slow}$ in the mouse ventricle and confers sensitivity to 4-AP–induced prolongation of APD and QTc. Compensatory upregulation of Kv2.1 may explain the phenotypic differences between SWAP mice and the previously described transgenic mice expressing a truncated dominant-negative Kv1.1 construct. (*Circ Res.* 2001;88:940-946.)

Key Words: potassium channels ■ heart ■ genetically engineered mice
■ drug-induced long-QT syndrome ■ arrhythmias

Transgenic and gene-targeting technologies have led to marked advances in the understanding of the molecular basis of cardiac repolarization in the mouse.[1,2] Dominant-negative transgenic mice overexpressing mutated Kv1.x, Kv2.x, Kv4.x, and HERG α subunits have less repolarizing K^+ current, varying degrees of cardiac action potential duration (APD) and QT prolongation, and arrhythmias.[3-7] In these experiments, the transgene may interact with several related K^+ channels in the heart, the phenotype may depend on the details of the transgene design,[3,6] and the relationship of individual gene products to the phenotype may be unclear. Gene targeting of K^+ channels using embryonic stem (ES) cells circumvents several of these difficulties by directly knocking out a single gene product.[8-13] However, gene targeting usually leads to loss of the gene in multiple organs and throughout development and is still subject to compensatory upregulation of other genes. Cross-mating lines of mice with different mutations provides one mechanism to sort out these interactions.[14]

We previously reported dominant-negative transgenic mice that overexpress in the heart an N-terminal fragment of the rat brain K^+ channel rKv1.1, have QT prolongation, and lack a rapidly activating, slowly inactivating, 4-aminopyridine (4-AP)–sensitive K^+ current, $I_{K,slow}$, in their ventricular myocytes.[3,15] These mice have both spontaneous and inducible ventricular arrhythmias, attributable at least in part to increased dispersion of repolarization and refractoriness between the apex and the base of the heart.[16,17] Although these mice have decreased protein levels of Kv1.5, the transgene may disrupt other cardiac K^+ channels, including Kv1.4, which has been shown to encode $I_{to,f}$.[9,14] Thus, the precise role of the loss of Kv1.5 in the pathogenesis of the phenotype is uncertain. In addition, nothing is known about the relationship of Kv1.5 to Kv2.x, the subunits responsible for the 4-AP–resistant component of $I_{K,slow}$.[4]

Original received August 11, 2000; revision received April 3, 2001; accepted April 3, 2001.
From the Cardiovascular Institute (B.L., X.-h.P., J.S.L., V.S., C.J.R.), University of Pittsburgh, Pittsburgh, Pa; Washington University School of Medicine (W.G., J.M.N.), St. Louis, Mo; Mount Sinai School of Medicine (D.A.L.), New York, NY; and University of Iowa College of Medicine and Department of Veterans Affairs (J.A.H.), Iowa City, Iowa.
Correspondence to Barry London, MD, PhD, Cardiovascular Institute, University of Pittsburgh, BST 1744, 200 Lothrop St, Pittsburgh, PA 15213. E-mail londonb@msx.upmc.edu

Circulation Research is available at http://www.circresaha.org

Here we report gene-targeted mice in which mKv1.5 is replaced by the 4-AP–insensitive channel subunit rKv1.1 (SWAP mice). The 4-AP–sensitive component of $I_{K,slow}$ is absent in ventricular myocytes isolated from these animals, proving definitively that Kv1.5 underlies this current. Of note, total $I_{K,slow}$ is unchanged at least in part because of the upregulation of the tetraethylammonium (TEA)-sensitive component encoded by Kv2.1. As a result, SWAP mice have normal cellular APDs and QT intervals on baseline electrocardiograms (EKGs) and resistance to drug-induced prolongation of APD and QT intervals after exposure to 4-AP.

Materials and Methods

All animal experiments were approved by the Institutional Animal Care and Use Committees at the University of Pittsburgh or Washington University School of Medicine.

Gene Targeting

The mouse Kv1.5 gene (*mKv1.5*) was cloned (genomic SV129 library, Stratagene), restriction-mapped, and sequenced. A targeting construct was engineered using a 2-kb 3′ arm consisting of the promoter and 5′-untranslated region (UTR) of *mKv1.5*, the rat Kv1.1 K^+ channel (rKv1.1) tagged with the 9-amino-acid hemagglutinin tag (HA) and cloned into the SmaI site located at position −6 of *mKv1.5* (relative to the ATG start codon), a neomycin resistance cassette (Neo_R), a 3-kb 3′ arm starting at the XbaI site in the 3′-UTR of *mKv1.5*, and the thymidine kinase gene (TK) for negative selection (Figure 1A). Homologous recombination with this construct should yield rKv1.1 driven by the mKv1.5 promoter, although the effect of the Neo_R cassette is unknown, and any 3′ regulatory elements may be lost.

Electroporation of ES cells, identification of ES cell lines heterozygous for the targeted allele, blastocyst injection to obtain chimeras, and mating with C57BL/6 mice to obtain germ-line transmission and mice heterozygous for the targeted allele (SWAP heterozygotes) were done as previously described.[8] Mice were backcrossed into the C57BL/6 line two additional generations. Male and female SWAP heterozygotes were then mated to yield the 2- to 7-month-old SWAP homozygotes, SWAP heterozygotes, and wild-type littermate controls used in the subsequent experiments. All mice were genotyped using genomic Southern blots.

Electrophysiology

The coding region of mKv1.5 was cloned into the high-expression oocyte vector pGH19K after addition of a Kozak consensus sequence.[18] The HA epitope was added to the 3′ end of rKv1.1 by polymerase chain reaction (PCR) (rKv1.1-HA). Channel properties were tested in *Xenopus* oocytes injected with in vitro transcribed cRNA (50 ng/oocyte) using the 2-microelectrode voltage-clamp technique as previously described.[19]

Single ventricular myocytes were isolated either from the entire left ventricle or separately from the left ventricular apex and septum, and whole-cell voltage- and current-clamp studies were performed at room temperature or 35°C using a Dagan 3900A (Dagan Corporation) or an Axopatch-1D (Axon Instruments) patch-clamp amplifier interfaced to a microcomputer equipped with a Digidata 1200 Series analog-to-digital interface and pClamp 7 software (Axon Instruments).[9,20] Membrane capacitance and series resistance were compensated electronically (>85%). Voltage errors were <6 mV and not corrected. Only data from cells with input resistances >0.7 GΩ were analyzed.

EKGs and Ambulatory Telemetry

Three lead EKGs (leads I, II, and AP) were performed on mice anesthetized with avertin (0.5 mg/kg) using subcutaneous electrodes, a differential amplifier (Warner DP301), and an analog-to-digital converter (MacLab, ADInstruments). Signals were digitized at 1 kHz and stored on computer. QT interval (ms) was determined as the time to 95% return to baseline by an individual blinded to genotype and corrected for heart rate using the formula $QTc = QT/(\sqrt{RR/100})$.[9,21] At least 6 days after implantation of the telemetry device (TA10ETA-F20, Data Sciences), 24-hour ambulatory EKG recordings were performed digitized at 400 Hz, stored on disk, and analyzed by hand for arrhythmias and using custom software designed to determine heart rate and heart rate variability.

Data Analysis

Voltage-clamp data were analyzed using Clampfit 6.0.5 (Axon Instruments), and current densities, normalized for cell capacitance (pA/pF), are reported. The amplitudes of the $I_{K,slow}$, I_{sus}, I_{to1}, and I_{ss} were determined by fitting the decay phase of the outward K^+ currents to the sum of two or three exponentials, as described previously.[9,14,20] Correlation coefficients were determined, and the χ^2 test was used to assess the quality of the fits. The amplitudes of the drug-sensitive currents were obtained by offline digital subtraction of the records obtained before and after drug application. All data are presented as mean±SEM. Statistical significance was determined using one-way ANOVA followed by Student-Newman-Keuls test for comparison between groups or Student's t test with correction for multiple comparisons, with $P<0.05$ defined as significant.

Results

Expression of mKv1.5 and rKv1.1-HA In Vitro

In vitro transcribed cRNA from mKv1.5 yielded delayed rectifier currents with minimal inactivation (Figure 1B). Steady-state inactivation curves (generated in 50 mmol/L rubidium chloride from isochronal tail current measurements) gave a total gating valence ($z=4.6\pm0.1$ e^-) and a voltage of 10% activation ($V_{10\%}=-32\pm2$ mV) ($n=6$). This gating valence is 23% lower and $V_{10\%}$ is shifted 20 mV to the right compared with rKv1.1 ($P<0.01$).

Addition of the 9-amino-acid HA epitope to rKv1.1 did not affect the currents when injected into *Xenopus* oocytes. We subcloned rKv1.1-HA into the prokaryotic/eukaryotic vector pBK-CMV (Stratagene, California) and transfected the construct into COS cells. The HA epitope was easily detected using monoclonal antibodies both on Western blots and by immunofluorescence (data not shown).

Properties of SWAP Mice

Two lines of targeted ES cells were identified (SWAPL77 and SWAPL46; Figure 1C). Additional insertion sites of the rKv1.1 transgene were excluded by genomic Southern blot using a probe within the transgene. The targeted band in the SWAPL46 ES line was reproducibly weaker than the native band, suggesting that the targeted allele was less abundant. This could result from either a mixed population of ES cells or a degree of aneuploidy. Both ES lines underwent germ-line transmission, however, and heterozygotes had one copy of each allele in equal abundance. Experimental results were confirmed on both lines of mice.

SWAP homozygotes from both lines appeared phenotypically normal, and there was no evidence of increased mortality. Hearts were not hypertrophied, and histology of the hearts was normal (data not shown). No overt neurological phenotype was evident in the mice.

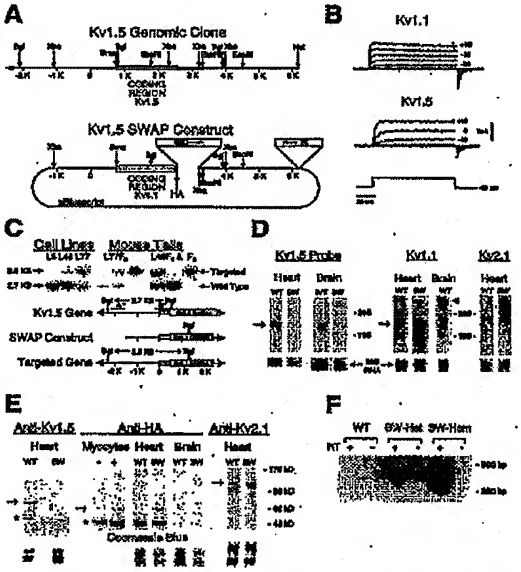

Figure 1. Targeted replacement of mKv1.5 by rKv1.1. A, Schematic representation of the mouse Kv1.5 genomic clone (top) and the targeting construct (bottom). The coding regions of Kv1.5 and Kv1.1 are labeled, and the heavier black line indicates the untranslated regions of Kv1.5 (5'-UTR and 3'-UTR). NEO and TK represent the neomycin resistance cassette and the thymidine kinase cassette, respectively. B, Expression of rKv1.1 and mKv1.5 in *Xenopus* oocytes; 100-ms depolarizing steps to the voltage indicated were used. C, Genomic Southern blots of BglII-digested DNA from 3 NEO- and TK-resistant cell lines (top left) and from mouse tails (top right). A schematic diagram showing the expected band sizes and location of the probes is shown below. Probe A (A*) was used for the blot shown. Note that only lines L77 and L46 underwent targeting events and that the targeted allele for the L46 cell line appears less abundant than the wild-type allele (see text). Mouse tail DNA for the L77 line comes from an F_2 cross of 2 heterozygotes, whereas the tail DNA for the L46 line comes from the F_1 and F_2 offspring. D, Northern blot analysis with 25 μg/lane of total RNA from the heart and brain of a wild-type mouse (WT) and a SWAP homozygote (SW) probed with cDNA fragments from the N-terminal part of the Kv1.5 coding region (left), the Kv1.1 coding region (middle), and the 3' end of Kv2.1 (right). Arrows point to native Kv1.5 expression and to rKv1.1 transgene expression, whereas the arrowhead points to expression of the native mKv1.1 gene. Note that faint expression of mKv1.1 is present in the whole-heart RNA; this may represent Kv1.1 in cells other than myocytes. Results were repeated using at least 3 mice from each line. To correct for loading during quantitative measurements, Kv2.1 signals were measured on a PhosphorImager and normalized to the signals obtained when the blots were reprobed with α-actin. E, Representative Western blot using a rabbit polyclonal anti-Kv1.5 antibody (Upstate Biotechnology, New York, NY), an antibody to the HA epitope (anti-HA, Sigma Immunochemicals, St Louis, Mo), and an anti-Kv2.1 antibody (Alomone Laboratories, Jerusalem, Israel) on crude membrane preparations (100 to 200 μg of protein/lane) from hearts and brains of a wild-type mice, SWAP homozygotes, and cultured rat neonatal cardiac myocytes transfected with either an empty plasmid (−) or a construct containing rKv1.1-HA driven by the α-myosin heavy chain promoter (+).[2,8] Identical results were obtained on hearts from both lines of mice. Arrows indicate the bands specific for Kv1.5, Kv1.1-HA, and Kv2.1, whereas asterisks indicate nonspecific bands. Equal protein loading from tissue samples is confirmed by Coomassie blue–stained gels. F, RT-PCR on cDNA from hearts of wild-type mice, SWAP heterozygotes (SW-Het), and SWAP homozygotes (SW-Hom). PCR was performed using a sense primer in the 5'-UTR of Kv1.5 and an antisense primer in the coding region of Kv1.1, followed by Southern transfer of the products and probing with a radiolabeled oligonucleotide in the 5'-UTR of Kv1.5. Parallel reactions were performed in the absence of RT to exclude genomic contamination. Note that only Kv1.1 expression driven by the transgene would be detected by this technique.

K^+ Channel Expression in SWAP Mice

Kv1.5 RNA and protein were absent in hearts from SWAP homozygotes (Figures 1D and 1E). KV1.1 RNA was detected in SWAP homozygotes by Northern blot (Figure 1D), and reverse transcriptase (RT)-PCR was used to confirm the expression of the transgene (Figure 1F). Using antibodies against the HA epitope, we detected a specific band at ≈62 kDa in the hearts of SWAP mice that was identical in size to the band produced by transfecting rat neonatal cardiac myocytes with rKv1.1-HA (Figure 1E). We did not detect rKv1.1-HA protein in the brain, although native mKv1.1 protein was quite abundant and runs at ≈72 kDa, as previously described (data not shown).[22]

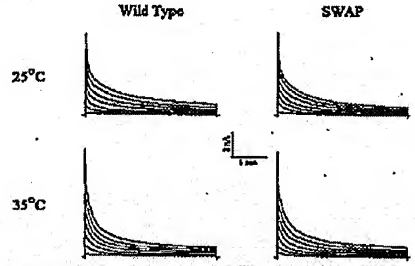

Figure 2. Voltage-gated outward K^+ currents from left ventricular myocytes isolated from wild-type and homozygous SWAP mice appear similar. From a holding potential of −70 mV, currents were elicited using 4-second depolarizing pulses to potentials between −20 and +40 mV presented at 10-second intervals. Current recordings from the same cells at both 25°C and 35°C are illustrated. Note that the inactivation of the outward currents is accelerated at 35°C.

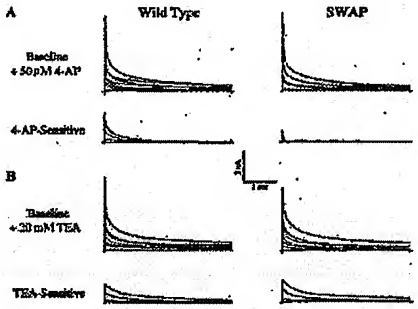

Figure 3. The 4-AP–sensitive component of $I_{K,slow}$ is absent and the TEA-sensitive component of $I_{K,slow}$ is upregulated in myocytes from SWAP homozygotes. A, Outward currents of myocytes isolated from wild-type and homozygous SWAP mice before (black) and after (red) application of 50 μmol/L 4-AP. Cells were depolarized from the holding potential of −70 mV to between −30 and +30 mV in 20-mV steps at 25°C. Note that the 4-AP–sensitive component of $I_{K,slow}$ is absent in myocytes from homozygous SWAP mice and that the residual rapidly inactivating current represents the small fraction of I_{to} blocked by the low concentration of 4-AP. B, Outward K^+ currents before and after application of 20 mmol/L TEA. The TEA-sensitive component of $I_{K,slow}$ is increased in the myocytes from Kv1.5-targeted SWAP mice.

Kv2.1 RNA expression was not significantly changed in homozygous SWAP compared with control ventricles (0.95±0.14, n=3 each; Figure 1D), but Kv2.1 protein was increased by Western blot analysis (n=3 each; Figure 1E).

K^+ Current Densities Are Unchanged in SWAP Myocytes

Figure 2 shows representative currents from voltage-clamped, randomly dispersed, left ventricular myocytes isolated from SWAP homozygotes and wild-type controls obtained using 4-second depolarizing steps from a holding potential of −70 mV to potentials between −20 and +40 mV. No differences are apparent in the amplitudes or inactivation rates at either 25°C or 35°C. The mean±SEM peak outward K^+ current densities at +40 mV at 25°C were 46±2 pA/pF in cells isolated from SWAP homozygotes (n=27), 45±2 pA/pF in cells from SWAP heterozygotes (n=8), and 47±3 pA/pF in cells from littermate controls (n=19).

The decay phases of the outward currents recorded from these left ventricular myocytes were well-fitted by the sum of 2 exponentials, consistent with the expression of $I_{to,f}$, $I_{K,slow}$, and the steady-state noninactivating current I_{ss}.[9,20] The density of $I_{K,slow}$ (at +40 mV) was similar for cells from SWAP homozygotes (17±1 pA/pF; n=27), SWAP heterozygotes (14±2 pA/pF; n=8), and controls (16±2 pA/pF; n=19). In addition, the decay time constants for $I_{K,slow}$ (at +40 mV) were indistinguishable for cells isolated from SWAP homozygotes (1259±51 ms; n=27), SWAP heterozygotes (1177±82 ms; n=8), and controls (1270±48 ms; n=19).

Similar experiments were performed on cells isolated separately from either the left ventricular apex or septum of SWAP mice. The mean±SEM peak outward K^+ current densities in the left ventricular apex (n=14) and septum (n=8) were 60±6 and 29±3 pA/pF, respectively. These values, as well as the densities of $I_{to,f}$, $I_{K,slow}$, and I_{ss}, are indistinguishable from those measured in wild-type apex and septal cells.[9,14,20] In addition, analysis of the currents in septal cells isolated from SWAP mice revealed that the mean±SEM $I_{to,f}$ density (8.2±0.8 pA/pF) and inactivation time constant (τ_{decay}=199±21 ms) are not significantly different from those determined for $I_{to,f}$ in wild-type cells.[9,14,20] These results are consistent with previous findings demonstrating that Kv1.4 underlies $I_{to,f}$ and does not contribute to $I_{K,slow}$. They also suggest that Kv1.5 and Kv1.4 do not coassemble to form functional heteromultimeric voltage-gated K^+ channels in mouse ventricular myocytes.

4-AP–Sensitive Component of $I_{K,slow}$ Is Absent in SWAP Myocytes

After exposure to 50 μmol/L 4-AP, wild-type myocytes showed a marked decrease in $I_{K,slow}$ (Figure 3A), as has been

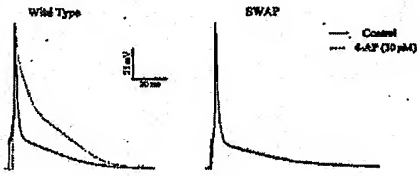

Figure 4. Action potentials in myocytes isolated from SWAP homozygotes are not prolonged by low concentrations of 4-AP. In the current-clamp mode, action potentials were evoked by 3-ms suprathreshold current injections at a rate of 1 Hz. Recordings obtained at 25°C before (solid line) and after (dashed line) application of 50 μmol/L 4-AP are superimposed.

shown in previous studies.[3,4,9,15,20] This low concentration of 4-AP also blocked $I_{to,f}$ by ~20%, an observation also consistent with previous studies.[20] The 50-μmol/L 4-AP–sensitive component of $I_{K,slow1}$, however, was completely absent in myocytes isolated from SWAP homozygotes (n=6). This provides strong evidence that Kv1.5 encodes an α subunit necessary for this current. In contrast, the component of $I_{K,slow}$ sensitive to 20 mmol/L TEA (at +40 mV; Figure 3B) was increased in myocytes from SWAP homozygotes (9±1 pA/pF, n=11) compared with controls (5±1 pA/pF, n=6; $P<0.05$). At this concentration, TEA partially blocks the component of $I_{K,slow}$ encoded by Kv2.1 channels.[4,20] Together with the Western blot data (Figure 1E), these findings suggest that functional Kv2.1 channels are upregulated in response to the loss of Kv1.5.

We were unable to identify any currents in myocytes from either wild-type or SWAP mice that were sensitive to 100 to 200 nmol/L α-dendrotoxin (DTX, n=8). Because Kv1.1 is highly sensitive to DTX, this suggests that functional Kv1.1 channels are not expressed at significant levels in SWAP myocytes.

Action Potentials in SWAP Myocytes Are Insensitive to 4-AP

APD_{90} values determined at 1-Hz stimulation were similar in current-clamped myocytes isolated from SWAP homozygotes (35±2 ms, n=8, at 25°C; 27±3 ms, n=7, at 35°C) and wild-type controls (36±3 ms, n=16, at 25°C; 25±1 ms, n=13; P=NS). As previously reported, wild-type myocytes show marked APD prolongation in response to low concentrations of 4-AP (Figure 4).[15,20] As predicted from the voltage-clamp studies, myocytes from SWAP mice were insensitive to 30 μmol/L 4-AP (n=3).

QT Interval in SWAP Mice Is Insensitive to 4-AP

The effects of 4-AP on QT intervals are shown in Figure 5. Baseline QT interval and QTc were not prolonged in anesthetized homozygous SWAP mice compared with age- and strain-matched controls (QTc: 64±2 ms, homozygotes, n=9; 60±2 ms, heterozygotes, n=4; 62±2 ms, controls, n=9). Injection with 4-AP (10 μmol/kg IP) prolonged QTc in controls but not in SWAP homozygotes (63±1 ms, homozygotes; 66±2 ms, heterozygotes; 72±2 ms, controls; $P<0.05$). The heterozygotes had an intermediate degree of QTc prolongation when injected with 4-AP. Injection with 4-AP did not induce arrhythmias in either control or SWAP mice. Heart rate was not significantly changed in anesthetized SWAP homozygotes compared with controls, and injection with saline had no effect on QTc (data not shown).

SWAP Mice Have No Increase in Arrhythmias

Mean heart rate, measured using ambulatory telemetry monitors in unanesthetized untethered mice, was similar in SWAP homozygotes compared with littermate controls (610 versus 622 bpm, n=3 each). Standard deviation of cycle length over 24 hours, a gross measure of heart rate variability, was also similar in these mice (11±1 versus 10±7 ms). In addition, SWAP homozygotes had no increase compared with littermate controls (n=4 each) in the frequency of premature atrial complexes (11±3 versus 9±6 per day), premature ventricular complexes (5±1 versus 5±2 per day), or episodes of second-degree atrioventricular block (18±10 versus 22±5 per day). During the 192 hours of telemetry screened, one SWAP homozygote had an atrial couplet and a ventricular triplet, whereas one control mouse had a ventricular couplet.

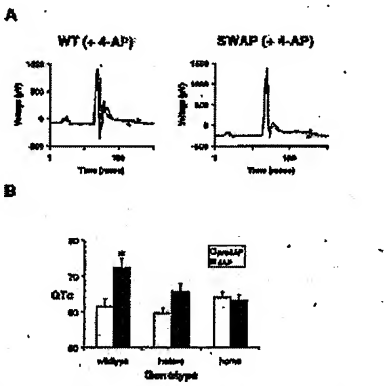

Figure 6. Homozygous SWAP mice are resistant to 4-AP–induced QT prolongation. A, EKG tracings using an anteroposterior lead from wild-type (left) and homozygous SWAP (right) mice before (black) and 15 minutes after (red) injection with 10 μmol/kg 4-AP. Records are signal averages of 5 consecutive tracings during a period with no heart rate variation. The anteroposterior lead was chosen because of the monophasic nature of the ST segment in this lead. Arrowheads show the point of 95% return to baseline. B, QTc before and after injection with 4-AP. QTc is similar in all mice before 4-AP injection but prolongs only in wild-type mice. hetero indicates SWAP heterozygotes; homo, SWAP homozygotes. *$P<0.05$ for 4-AP–treated wild-type mice compared with before treatment or with 4-AP–treated homozygotes.

Discussion

Kv1.5 Encodes the 4-AP–Sensitive Component of $I_{K,slow}$

The mouse cardiac K^+ channel subunit mKv1.5 encodes a rapidly activating, very slowly inactivating current when heterologously expressed in *Xenopus* oocytes (Figure 1B). Similar Kv1.5 channel subunits have been cloned from rat and human and are highly sensitive to 4-AP and resistant to TEA.[23–25] On the basis of these pharmacological and kinetic characteristics, Kv1.5 channels were proposed as the molecular basis for I_{Kur} in human atrium and $I_{K,slow}$ in mouse ventricle.[26,27] Antisense experiments in cultured heart cells have provided direct experimental evidence that Kv1.5 contributes to I_{Kur} in rat and human.[28,29]

We previously used a dominant-negative transgenic strategy to disrupt channels of the Kv1.x family in the heart, leading to a mouse that lacks the 4-AP–sensitive component of $I_{K,slow}$.[3,15] These mice have decreased protein levels of

Kv1.5, probably because of increased degradation. The transgene does, however, affect other channels, and these experiments do not completely prove the relationship between mKv1.5 and $I_{K,slow}$. In the present study, we have used gene targeting to selectively eliminate mKv1.5 and showed the selective loss of the 4-AP–sensitive portion of $I_{K,slow}$. We chose the strategy to replace Kv1.5 with the pharmacologically different channel Kv1.1 with the intention of minimizing other potential changes. The findings presented here definitively link Kv1.5 to a component of $I_{K,slow}$ in the mouse ventricle.

Ectopic Expression of Kv1.1 in the Hearts of SWAP Mice

Kv1.1 mRNA and protein are expressed in the hearts of transgenic SWAP mice under the control of the Kv1.5 promoter. (Figures 1D through 1F). We were not able to detect any DTX-sensitive currents, however. This suggests that very few functional Kv1.1 channels are present on the extracellular membranes of mouse ventricular myocytes and that the mouse is functionally acting as a Kv1.5 knockout, although we cannot fully exclude the possibility that heteromultimeric channels containing Kv1.1 are not DTX-sensitive. The smaller size of the rKv1.1 protein expressed in the mouse heart (62 kDa) compared with native mKv1.1 in the brain (72 kDa) points to tissue-specific differences in posttranslational processing.[22] Recent studies have highlighted the importance of helper proteins and β subunits in transporting K^+ channels to the surface membrane.[30,31] Kv1.1 is not normally expressed at high levels in the heart (Figure 1D), and the mechanism to process and successfully insert physiological levels of expressed channels into the surface membrane may be absent.

Kv2.1 Upregulation Compensates for the Loss of Kv1.5 in the Hearts of SWAP Mice

Despite the loss of the 50 μmol/L 4-AP component of $I_{K,slow}$ in myocytes isolated from SWAP mice, there was no decrease in the overall density of $I_{K,slow}$ or of the total outward current compared with controls. SWAP myocytes had an increased density of the 20 mmol/L TEA-sensitive component of $I_{K,slow}$, and Western blots showed increased Kv2.1 protein in SWAP hearts. Kv2.1 α subunits produce slowly activating, slowly inactivating, or noninactivating K^+ currents when expressed heterologously in tissue culture, and antibodies to Kv2.1 block currents of this type in hippocampal neurons.[32] Previous studies have shown that the TEA-sensitive component of the rapidly activating, slowly inactivating cardiac current $I_{K,slow}$ is selectively eliminated in transgenic mice overexpressing the dominant-negative Kv2.1N216Flag construct in the heart.[4] Taken together, these data suggest that upregulation of Kv2.1 is one compensatory mechanism for the loss of Kv1.5 in the ventricles of the SWAP mice. We cannot be certain that the entire compensation in $I_{K,slow}$ is attributable to upregulation of Kv2.1. In addition, the differences in the time- and voltage-dependent properties of Kv2.1 between tissue culture cells, hippocampal neurons, and cardiac myocytes likely reflect differences in accessory subunits or posttranslational processing.

Kv2.1 RNA levels are not changed in the SWAP mice, whereas protein levels are increased. The mechanism by which the loss of Kv1.5 leads to postranscriptional upregulation of Kv2.1 is unknown. The feedback could be based on the action potential shape and ionic currents. Alternatively, proteins that bind to the ion channel subunits could directly mitigate subunit processing, transport to the membrane, or stability.

Difference Between Dominant-Negative Transgenic and Gene-Targeted Mice

Both Kv1.x dominant-negative transgenic and Kv1.5 homozygous SWAP mice lack the 4-AP–sensitive component of $I_{K,slow}$.[3,15] The Kv1.x dominant-negative transgenic mice have QT prolongation and arrhythmias.[3,15–17] In this study, we show that targeted mice lacking *mKv1.5* have no QT interval prolongation and no arrhythmias. In fact, these mice are resistant to QT prolongation on exposure to the Kv1.5-blocking agent 4-AP. Likely explanations for the differences include both the effect of the Kv1.x transgene on other cardiac K^+ channels known to be important for repolarization, such as Kv1.4,[8,9,14] and compensatory regulation of other K^+ channels, such as Kv2.1, in the SWAP mouse. Clearly, loss of Kv1.5 alone is insufficient to lead to a highly arrhythmogenic phenotype. These findings highlight the fact that transgenic and gene-targeting techniques give different and complementary information on the role of ion channels in cardiac function.

Additional study of both models, along with mating of different strains to form double mutants, should lead to both a better understanding of the role of individual genes in repolarization and susceptibility to arrhythmias and to insights into the mechanisms by which K^+ channel gene expression is regulated in vivo in the heart.

Acknowledgments

These studies were supported in part by National Heart, Lung, and Blood Institute grants R01 HL58030 (to B.L.), R01 34161 (to J.M.N.), and K08 HL03908 (to J.A.H.); a Grant-in-Aid (to B.L.), Scientist Development Grant (to V.S.), and Postdoctoral Research Fellowship (to W.G.) from the American Heart Association; and grants from the Veterans Administration, Procter & Gamble Corporation, and the Roy J. Carver Charitable Trust (to J.A.H.). The sequence of the *mKv1.5* genomic clone is available in GenBank (accession No. AF302768). We would like to thank Dr Alexandra F.R. Stewart for his assistance and suggestions.

References

1. London B. Use of transgenic and gene-targeted mice to study K^+ channel function in the cardiovascular system. In: Archer SA, Rusch NJ, ed. *Potassium Channels in Cardiovascular Biology*. New York, NY: Plenum Publishing. In press.
2. Nerbonne JM. Molecular basis of the functional voltage-gated K^+ channel diversity in mammalian myocardium. *J Physiol (Lond)*. 2000;525:285–298.
3. London B, Jeron A, Zhou J, Buckett P, Han X, Mitchell GF, Koren G. Long QT and ventricular arrhythmias in transgenic mice expressing the N terminus and first transmembrane segment of a voltage-gated potassium channel. *Proc Natl Acad Sci USA*. 1998;95:2926–2931.
4. Xu H, Barry DM, Li H, Brunet S, Guo W, Nerbonne JM. Attenuation of the slow component of the delayed rectification, action potential prolongation, and triggered activity in mice expressing a dominant-negative Kv2 α subunit. *Circ Res*. 1999;85:623–633.

5. Barry DM, Xu H, Schuessler RB, Nerbonne JM. Functional knockout of the transient outward current, long QT syndrome, and cardiac remodeling in mice expressing a dominant-negative Kv4 α subunit. *Circ Res*. 1998; 83:560–567.
6. Wickenden AD, Lee P, Sah R, Huang Q, Fishman GE, Backx PH. Targeted expression of a dominant-negative Kv4.2 K^+ channel subunit in the mouse heart. *Circ Res*. 1999;85:1067–1076.
7. Babij P, Askew GR, Nieuwenhuijsen B, Su CM, Bridal TR, Jow B, Argentieri TM, Kulik J, DeGennaro LJ, Spinelli W, Colatsky TJ. Inhibition of cardiac delayed rectifier K^+ current by overexpression of the long-QT syndrome HERG G628S mutation in transgenic mice. *Circ Res*. 1998;83:668–678.
8. London B, Wang DW, Hill JA, Bennett PB. The transient outward current in mice lacking the potassium channel gene *Kv1.4*. *J Physiol (Lond)*. 1998;509:171–182.
9. Guo W, Xu H, London B, Nerbonne JM. Molecular basis of transient outward current diversity in mouse ventricular myocytes. *J Physiol (Lond)*. 1999;521:587–599.
10. Wickman K, Nemec J, Gendler SJ, Clapham DE. Abnormal heart rate regulation in GIRK4 knockout mice. *Neuron*. 1998;20:103–114.
11. Drici MD, Arrighi I, Chouabe C, Mann JR, Lazdunski M, Romey G, Barhanin J. Involvement of IsK-associated K^+ channel in heart rate control of repolarization in a murine engineered model of Jervell and Lange-Nielsen syndrome. *Circ Res*. 1998;83:95–102.
12. Kupershmidt S, Yang T, Anderson ME, Wessels A, Niswender KD, Magnuson MA, Roden DM. Replacement by homologous recombination of the minK gene with lacZ reveals restriction of minK expression to the mouse cardiac conduction system. *Circ Res*. 1999;84:146–152.
13. Zaritsky JJ, Schwarz TL. Targeted disruption of the Kir2.1 and Kir2.2 genes in mice and the physiological consequences to the heart. *Circulation*. 1999;100(suppl I):I-351. Abstract.
14. Guo W, Li H, London B, Nerbonne JM. Functional elimination of $I_{to,f}$ and $I_{to,s}$ early afterdepolarizations, atrioventricular block and ventricular arrhythmias in mice lacking Kv1.4 and expressing a dominant-negative Kv4 α subunit. *Circ Res*. 2000;87:73–79.
15. Zhou J, Jeron A, London B, Han X, Koren G. Characterization of a slowly inactivating outward current in adult mouse ventricular myocytes. *Circ Res*. 1998;83:806–814.
16. Jeron A, Mitchell GF, Zhou J, Murata M, London B, Buckett P, Wiviott SD, Koren G. Inducible polymorphic ventricular tachycardia in a transgenic mouse model with a long Q-T phenotype. *Am J Physiol*. 2000;278:H1891–H1898.
17. Baker LC, London B, Choi B-R, Koren G, Salama G. Enhanced dispersion of repolarization and refractoriness in transgenic mouse hearts promotes reentrant ventricular tachycardia. *Circ Res*. 2000;86:396–407.
18. London B, Trudeau MC, Newton KP, Beyer AK, Copeland NG, Gilbert DJ, Jenkins NA, Satler CA, Robertson GA. Two isoforms of the mouse *ether-a-go-go*-related gene coassemble to form channels with properties similar to the rapidly activating component of the cardiac delayed rectifier K^+ current. *Circ Res*. 1998;81:870–878.
19. Logothetis DE, Kammen BF, Lindpaintner K, Bisbas D, Nadal-Ginard B. Gating charge differences between two voltage-gated K^+ channels are due to the specific charge content of their respective S4 region. *Neuron*. 1993;10:1121–1129.
20. Xu H, Guo W, Nerbonne JM. Four kinetically distinct depolarization-activated K^+ currents in adult mouse ventricular myocytes. *J Gen Physiol*. 1999;113:661–678.
21. Mitchell GF, Jeron A, Koren G. Measurement of heart rate and Q-T interval in the conscious mouse. *Am J Physiol*. 1998;274:H747–H751.
22. Wang H, Kunkel DD, Martin TM, Schwartzkroin PA, Tempel BL. Heteromultimeric K^+ channels in terminal and juxtaparanodal regions of neurons. *Nature*. 1993;365:75–79.
23. Fedida D, Wible B, Wang Z, Fermini B, Faust F, Nattel S, Brown AM. Identity of a novel delayed rectifier current from human heart with a cloned K^+ channel current. *Circ Res*. 1993;73:210–216.
24. Snyders DJ, Tamkun MM, Bennett PB. A rapidly activating and slowly inactivating potassium channel cloned from human heart: functional analysis after stable mammalian cell culture expression. *J Gen Physiol*. 1993;101:513–543.
25. Matsubara H, Liman ER, Hess P, Koren G. Preassociational mechanism determine the type of potassium channels expressed in the rat skeletal and cardiac muscles. *J Biol Chem*. 1991;266:13324–13328.
26. Wang Z, Fermini B, Nattel S. Sustained depolarization-induced outward current in human atrial myocytes: evidence for a novel delayed rectifier K^+ current similar to Kv1.5 cloned channel currents. *Circ Res*. 1993;73: 1061–1076.
27. Fiset C, Clark RB, Larsen TS, Giles WR. A rapidly activating sustained K^+ current modulates repolarization and excitation-contraction coupling in adult mouse ventricle. *J Physiol (Lond)*. 1997;504:557–563.
28. Feng J, Wible B, Li GR, Wang Z, Nattel S. Antisense oligodeoxynucleotides directed against Kv1.5 mRNA specifically inhibit ultrarapid delayed rectifier K^+ current in cultured human atrial myocytes. *Circ Res*. 1997;80:572–579.
29. Bou-Abboud E, Nerbonne JM. Molecular correlates of the calcium-independent, depolarization-activated K^+ currents in rat atrial myocytes. *J Physiol (Lond)*. 1999;517:407–420.
30. Wible BA, Yang Q, Kuryshev YA, Accili EA, Brown AM. Cloning and expression of a novel K^+ channel regulatory protein, KChAP. *J Biol Chem*. 1998;273:11745–11751.
31. Li D, Takimoto K, Levitan ES. Surface expression of Kv1 channels is governed by a C-terminal motif. *J Biol Chem*. 2000;275:11597–11602.
32. Murakoshi H, Trimmer JS. Identification of the Kv2.1 K^+ channel as a major component of the delayed rectifier K^+ current in rat hippocampal neurons. *J Neurosci*. 2000;19:1728–1735.

This Review is part of a thematic series on **Unanswered Questions in Heart Failure**, which includes the following articles:

Is Depressed Myocyte Contractility Centrally Involved in Heart Failure?

What Is the Role of β-Adrenergic Signaling in Heart Failure?

What Causes Sudden Death in Heart Failure?

Is Abnormal Cell Growth and Hypertrophy the Cause of Heart Failure?

Does Energy Starvation Cause Heart Failure?

What Mechanisms Underlie Diastolic Dysfunction in Heart Failure?

Steven Houser, Guest Editor

What Is the Role of β-Adrenergic Signaling in Heart Failure?

Martin J. Lohse, Stefan Engelhardt, Thomas Eschenhagen

Abstract—This review addresses open questions about the role of β-adrenergic receptors in cardiac function and failure. Cardiomyocytes express all three β-adrenergic receptor subtypes—β_1, β_2, and, at least in some species, β_3. The β_1 subtype is the most prominent one and is mainly responsible for positive chronotropic and inotropic effects of catecholamines. The β_2 subtype also increases cardiac function, but its ability to activate nonclassical signaling pathways suggests a function distinct from the β_1 subtype. In heart failure, the sympathetic system is activated, cardiac β-receptor number and function are decreased, and downstream mechanisms are altered. However, in spite of a wealth of data, we still do not know whether and to what extent these alterations are adaptive/protective or detrimental, or both. Clinically, β-adrenergic antagonists represent the most important advance in heart failure therapy, but it is still debated whether they act by blocking or by resensitizing the β-adrenergic receptor system. Newer experimental therapeutic strategies aim at the receptor desensitization machinery and at downstream signaling steps. (***Circ Res.*** **2003;93:896-906.)**

Key Words: β-adrenergic receptors ■ G proteins ■ transgenic mice ■ cardiac hypertrophy ■ apoptosis

The human heart expresses β_1- and β_2-adrenergic receptors at a ratio of about 70:30; both subtypes increase cardiac frequency and contractility.[1,2] In addition, β_3-receptors have been described to mediate negative inotropic effects,[3] but their role remains uncertain.[4] All three subtypes appear to occur in cardiomyocytes, but they seem to possess distinct intracellular signaling and functional properties.[5,6]

Two well-established lines of evidence suggest that the β-adrenergic receptor system plays a major role in heart failure. First, there is a pronounced activation of the sympathetic system in patients with heart failure that is inversely correlated with survival.[7] Second, cardiac β-receptors, in particular the β_1 subtype, are downregulated in heart failure,[1,8] and the remaining receptors are uncoupled from G_s, presumably via increased activity of the receptor kinases GRK2 and/or GRK5.[9–11] Furthermore, an increase in $G\alpha_i$ subunits antagonizes β-adrenergic signaling.[12–14] Clinically, the use of β-receptor antagonists in heart failure, pioneered in the 1970s,[15] is now standard treatment.[16–19]

In spite of these major advances, many fundamental questions have remained unanswered. Why does the heart express three different β-receptors and what are the differences between the subtypes? Are the alterations of the β-receptors in heart failure detrimental or beneficial? Does the β-receptor system contribute to the pathogenesis of heart failure? And why are β-blockers effective in the treatment of

Original received May 21, 2003; revision received October 3, 2003; accepted October 8, 2003.

From the Institute of Pharmacology (M.J.L., S.E.), Wuerzburg, Germany; Institute of Experimental and Clinical Pharmacology (T.E.), Universitaetsklinikum Hamburg-Eppendorf, Germany.

Correspondence to Martin Lohse, Institute of Pharmacology, Versbacher Straße 9, 97078 Wuerzburg, Germany. E-mail lohse@toxi.uni-wuerzburg.de

Circulation Research is available at http://www.circresaha.org

DOI: 10.1161/01.RES.0000102042.83024.CA

heart failure? This review will attempt to elucidate open questions in understanding myocardial β-adrenergic signaling with respect to its role in cardiac hypertrophy and failure.

β-Adrenergic Receptor Subtypes and Their Signaling

β-Adrenergic Receptors in the Heart

The classical subdivision of β-receptors defines the β_1 subtype as the one that stimulates cardiac muscle, and the β_2 subtype that relaxes smooth muscle.[20] Both receptors couple to G_s and thereby elevate cAMP, but distinct downstream signaling decreases contractility in smooth muscle cells and increases it in cardiomyocytes. However, the β_1-receptor contributes to relaxation of blood vessels[21] and the β_2-receptor to cardiac contractility.[2] Even though the predominant cardiac β_1 subtype (≈70% to 80% depending on species) is the strongest stimulus for cardiac function, the expression levels are quite small: no more than 50 to 70 fmol/mg membrane protein in most species. Therefore, there is little receptor reserve.

Expression of the β_3 subtype is essentially limited to adipose tissue,[22] but several groups have reported β_3-receptor effects and mRNA in human, guinea pig, and canine heart and cardiomyocytes.[3,23,24] However, in contrast to its G_s-mediated signaling in adipose tissue, these reports suggest coupling to a nonclassical G_i/nitric oxide pathway mediating negative inotropic effects. In mice, cardiac-specific overexpression of β_3-receptors enhanced cardiac contractility,[25] and experiments with β_1/β_2 knockout mice provided no or very modest β_3-receptor effects.[4,26,27] Thus, the importance of this subtype remains to be defined.

A fourth receptor subtype, β_4, had been postulated to mediate cardiostimulatory effects of the antagonist CGP12177. However, studies with β_1- and β_2-receptor knockout mice have led to the conclusion that the β_4 effects are mediated by the β_1-receptor.[28,29]

β-Receptors occur also on nonmyocyte cells in the heart, and these cells can—eg, by paracrine effects—affect cardiomyocyte function and fate. The communication between these cells will constitute a major research topic.

β-Adrenergic Receptor Signaling

Why should the heart express several different subtypes of β-adrenergic receptors? Evidence has been accumulating that subtype differences are important for cardiac function and failure.

First, the three receptor subtypes have different affinities for their ligands (Figure 1). Second, there is increasing evidence for specific subcellular localizations and distinct signaling pathways. The basic hypothesis is that spatial segregation of receptors allows their association with other—equally segregated—proteins to form "signalosomes" that mediate subtype-specific responses.

Signaling by cardiac β-receptors has been studied in great detail (Figures 1 and 2). The classical common pathway is activation of adenylyl cyclases via G_s, resulting in increased cAMP levels. The primary target for cAMP is protein kinase A (PKA). PKA phosphorylates several proteins that are

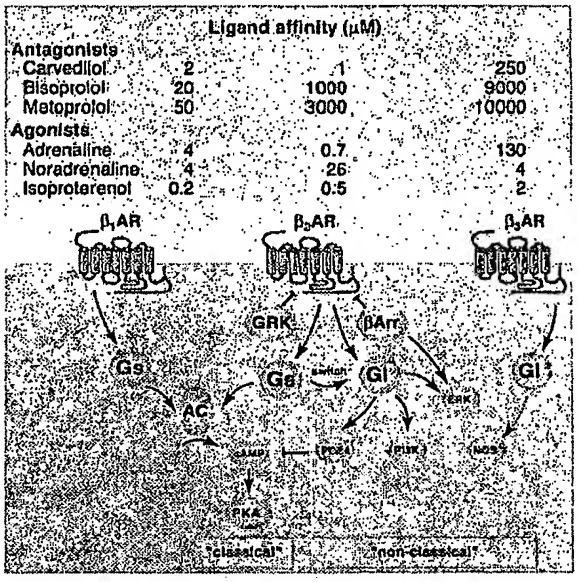

Figure 1. Agonist activation and coupling/signaling properties of β-adrenergic receptor subtypes. GRK indicates G protein–coupled receptor kinase; βArr, β-arrestin; PDE, phosphodiesterase; PI3K, phosphatidylinositol 3-kinase; and AC, adenylyl cyclase. Data from Hoffmann et al.[164]

essential for cardiac function: L-type calcium channels,[30,31] phospholamban,[32] troponin I,[33] ryanodine receptors,[34] myosin binding protein-C (MyBP-C),[35] and protein phosphatase inhibitor-1.[36] This affects cardiomyocyte contractile behavior by increasing Ca^{2+} influx (L-type channel), increasing Ca^{2+} reuptake into the sarcoplasmic reticulum (phospholamban/SERCA), and modulating myofilament Ca^{2+} sensitivity (troponin I, MyBP-C). Another target of cAMP are cAMP-gated HCN pacemaker channels.[37]

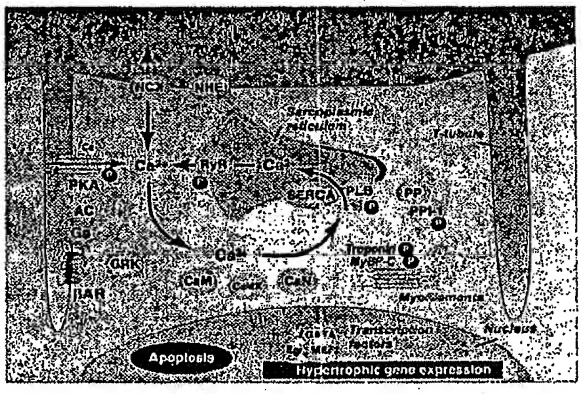

Figure 2. Calcium cycling in cardiac myocytes and regulation by PKA. AC indicates adenylyl cyclase; RyR, ryanodine receptor; PLB, phospholamban; SERCA, sarcoplasmic reticulum calcium ATPase; CaM, calmodulin; CaMK, calmodulin-dependent kinase; CaN, calcineurin; GRK, G protein–coupled receptor kinase; NCX, sodium-calcium exchanger; NHE, sodium-proton exchanger; and PP, protein phosphatase.

Most studies agree that in cardiomyocytes the cAMP pathway is stimulated through β_1- as well as β_2-receptors. However, even though the β_2 subtype causes greater adenylyl cyclase stimulation than the β_1 subtype in transfected cells[38,39] and in cardiomyocytes,[40,41] the β_1 subtype confers greater functional effects in cardiomyocytes.[2] One explanation for this difference is that cAMP generated by β_2-receptor stimulation is not equivalent to cAMP-generated via β_1-receptors. Another explanation is the existence of additional signaling pathways that modify the G_s/adenylyl cyclase/PKA pathway.

Such additional nonclassical signaling is particularly important for the β_2 (and perhaps the β_3) subtype, but less for the β_1-receptor. Many coupling proteins have been identified for the three β-receptor subtypes,[42] but only a few of them have been demonstrated in the heart (Figure 1). Nonclassical signaling for the β_1-adrenergic receptor—studied less—may include a calcium signal not inhibitable by inactive cAMP analogues.[43] It will be a major task to elucidate the physiological role(s) of these nonclassical signaling pathways.

Compartmentation of β-Adrenergic Signaling

Receptor-generated signals are usually measured as global changes in second messenger concentrations, which are implicitly assumed to change in a uniform manner. This simplistic view would mean that intracellular signaling uses neither spatial nor temporal information. However, evidence is accumulating that this is not the case, and that compartmentation of intracellular signaling may be more than an excuse for results that are difficult to interpret.

Studies on intact hearts and isolated cardiomyocytes helped to establish this concept.[44,45] Work in the 1970s suggested that PKA activation by prostaglandin E and isoprenaline exerted differential effects on glycogen phosphorylase phosphorylation in rat heart.[46] Similarly, cAMP accumulation via the glucagon-like peptide receptor was recently found to be completely uncoupled from inotropic effects in cardiomyocytes.[47] Different "efficacies" of cAMP generated via β-receptor activation or via direct adenylyl cyclase stimulation with forskolin further suggested spatial compartmentation of cAMP in cardiomyocytes.[48] Recent electrophysiological studies showed that localized stimulation of β-receptors on frog cardiomyocytes activated L-type Ca^{2+} channels in the vicinity of the receptors, whereas forskolin activated also distant Ca^{2+} channels.[49] Inhibition of isoprenaline effects by acetylcholine[50] and NO were also locally restricted.[51] Imaging of cAMP in neonatal cardiomyocytes showed that the noradrenaline-induced cAMP signal diffused only ≈1 μm, but phosphodiesterase inhibition led to generalized cAMP elevation.[52] Thus, cAMP degradation by phosphodiesterases may spatially limit cAMP signals.

Several pieces of evidence point toward differences in compartmentation between β_1- and β_2-receptors.[5,6] First, β_2-receptors can couple, in addition to G_s, also to G_i, whereas β_1-receptors couple only to G_s.[53] G_i coupling is enhanced by PKA-mediated β_2-receptor phosphorylation. Second, the PKA phosphorylation pattern induced by β_1- and β_2-receptor stimulation seems different, at least in some species. Two groups found only β_1-induced troponin I phosphorylation in rats,[54,55] whereas others described phosphorylation via both subtypes in human heart.[56] Phospholamban phosphorylation has been reported after β_1- but not β_2-receptor activation in canine and human cardiomyocytes,[54,57] while in other studies, particularly in human heart, both subtypes caused phosphorylation.[55,56] β_1-Receptor stimulation increased PKA activity in the particulate fraction of cardiomyocytes, whereas after β_2-receptor stimulation this increase was limited to the soluble fraction.[55] In adult rat cardiomyocytes, the complete absence of a cAMP signal after β_2-receptor stimulation has been reported.[58]

Which mechanisms permit spatial compartmentation of cardiomyocyte β-adrenergic signaling? First, receptors might have different cell surface localizations. In one study, the β_2 subtype was copurified with cardiomyocyte caveolae, while the β_1 subtype was more evenly distributed.[59] In another study, the β_1 subtype was preferentially localized in caveolae on rat neonatal cardiomyocytes, and this was taken as a reason for efficient adenylyl cyclase coupling.[40] Second, the receptors are probably embedded into large signalosomes, which might differ between the β_1 and the β_2 subtype. β_2-Receptor signalosomes containing an entire signaling chain have recently been demonstrated in neurons.[60] And third, postreceptor signaling may also be spatially organized.[61] cAMP signals might be spatially regulated via their site of generation (receptor localization) and via localized destruction (phosphodiesterases). Several experiments show loss of spatial localization after phosphodiesterase inhibition.[48,52,62] β_2 Receptors can actively recruit phosphodiesterase 4 to the plasma membrane.[63] Downstream signaling proteins also have specific localizations. In particular, PKA is spatially localized via binding to A-kinase anchoring proteins[64] and the same applies for protein phosphatases[65] and possibly their inhibitors.

In addition to spatial compartmentation, β-receptor coupling is also temporally regulated. First, β-receptors desensitize. This is most prominent for the β_2 subtype and small for the β_3 subtype.[66,67] Desensitization occurs via receptor phosphorylation either by PKA or by G protein–coupled receptor kinases, GRKs,[68,69] plus β-arrestins.[70] Both mechanisms uncouple receptors from G proteins.[71] In addition, the receptor/β-arrestin complex recruits several proteins that initiate nonclassical signaling pathways. Since the GRK/β-arrestin mechanism is most prominent for the β_2 subtype, this explains why nonclassical signaling pathways are most prominent for this subtype. Furthermore, PKA-induced phosphorylation of β_2-receptors promotes switching from G_s to G_i.[27,72] And finally, prolonged stimulation results in receptor downregulation, ie, a reduction in receptor number.[73] In summary, β-receptor signaling is a multifaceted process, and our current understanding seems still incomplete.

Alterations of the β-Adrenergic System in Heart Failure

Numerous studies show alterations of the cardiac β-receptor system in failing hearts.[1,2,74–76] They include a reduction of the β_1 subtype and its mRNA by up to ≈50%, correlated to disease severity,[75,76] while the β_2-receptor levels remained unchanged in most studies. It is still not clear why downregu-

lation in heart failure is specific for the β_1 subtype. The remaining β-receptors are desensitized, presumably mostly via GRKs (see below). In addition, up to 2-fold increases of $G\alpha_i$—particularly $G\alpha_{i2}$—and its mRNA occur early in heart failure[12–14,77] and may cause reduced responsiveness of many G_s-coupled receptor systems.[78–81] In addition, canine heart failure models show downregulation of $G\alpha_s$[82] and of adenylyl cyclases V and VI,[83] which are rate-limiting in the β-receptor system.[84] Heart failure–induced elevated catecholamine levels most likely cause all these alterations that functionally limit the contractile reserve.

Even though these changes have been confirmed repeatedly, their interpretation is uncertain. They can be interpreted either as a beneficial mechanism that protects the heart from the detrimental effects of chronic β-receptor stimulation, including arrhythmias, energy dysbalance, hypertrophy, and apoptosis—even though they deprive the heart from the benefits of short-term β-adrenergic responsiveness. Alternatively, they may lead to further deterioration of heart failure, since they disable the heart to meet its demands. Depending on these interpretations, therapeutic strategies might attempt either to inhibit the β-receptor system even further or to restore its sensitivity. Both apparently contrasting strategies are currently being pursued.

Role of GRKs in Heart Failure

Increased GRK activity appears to be a major factor contributing to β-receptor desensitization in failing hearts.[85,86] Numerous studies have demonstrated upregulation of GRK activity and GRK2 mRNA in patients and animal models of heart failure and hypertrophy.[11,87,88] This has led to the hypothesis that cardiac function might be restored by inhibiting GRKs.[86] No GRK inhibitors have so far been described that would allow a testing of this hypothesis, but several studies with the C-terminus of GRK2 ("βARKct") appear to support it. This 184 amino acid C-terminus inhibits GRK-mediated receptor phosphorylation,[89] and its overexpression has led to reduction of heart failure in several heart failure models.[86,90,91]

However, again the alternative hypothesis is that increased GRK activity is part of a protective adaptation. This hypothesis would be compatible with the long-term damage caused by chronic stimulation or transgenic β_1-receptor overexpression,[92,93] and with the beneficial effects of β-blockers in heart failure patients.[16] In this case, the beneficial effects of βARKct might be mediated by mechanisms distinct from GRK2 inhibition.

In fact, βARKct impairs many Gβγ pathways, and several lines of evidence suggest that Gβγ inhibition ("scavenging") is important for its effects. First, the detrimental β-receptor–mediated effects appear to be due more to the cAMP than to nonclassical signaling since (1) transgenic overexpression of the β_1 subtype is more detrimental than that of the β_2 subtype[93,94] even though the β_1 subtype activates essentially only the cAMP pathway and does not internalize well,[6,95] and (2) the detrimental effects of β_1-receptor overexpression are very similar to those of overexpression of $G\alpha_s$ or PKA.[96–98] Second, GRK2 transgenic mice show no overt cardiac pathology,[99] arguing against a detrimental role of GRK activity per se. Third, in a transgenic mouse model of heart failure, β-blockers conferred a benefit in addition to βARKct, suggesting an unrelated mechanism of action for the two principles.[91] And fourth, the protective effects of βARKct on heart failure progression have been reproduced with N-terminally truncated phosducin,[100] a supposedly "pure" Gβγ-binding protein[101] that did not restore the cAMP signal.

Thus, β-receptor blockade and βARKct might be regarded as independent and complementary therapeutic principles in heart failure. The usefulness and the mechanisms of βARKct and of "pure" GRK inhibitors will be questions for future investigations.

Cardiac β-Adrenergic Receptor Transgenic Mice

Transgenic cardiac overexpression of β_2-receptors in mice at 20 to 30 pmol/mg protein led to marked enhancement of basal contractility[94] but caused no overt cardiac pathology.[102] Adenovirus-mediated β_2-receptor overexpression enhanced myocardial contractility in a rabbit heart failure model.[103] However, later studies showed that 50-fold overexpression of β_2-receptors was well tolerated, whereas 350-fold overexpression induced cardiac pathology.[104] High-density β_2-receptor overexpression rescued left ventricular contractility after myocardial infarction[105] but worsened cardiac function after aortic banding[106] and negatively affected several genetic heart failure models,[86] including $G\alpha_q$ overexpression.[107] Lower levels (30-fold overexpression) had beneficial effects in the same model,[107] suggesting an expression optimum for enhancing cardiac function via β_2-receptors.

Cardiac overexpression of β_1-receptors in transgenic mice caused cardiomyocyte hypertrophy, followed by fibrosis and heart failure.[93,108] Calcium transients were prolonged, and expression of the sarcoplasmic reticulum (SR) protein junction was reduced.[109] Interestingly, β_1-receptor transgenic mice develop marked cardiomyocyte hypertrophy without a major increase in heart weight,[93] indicating a dramatic loss of ventricular cardiomyocytes, perhaps via apoptosis.[108] β_1 as well as α_1 agonists have long been known to cause hypertrophy.[110] These data indicate that the β_1-receptor system is ideally suited for short-term increases in cardiac function but causes marked damage after prolonged activation.

The differences reported between β_1- versus β_2-receptor overexpression are remarkable. Since both subtypes activate cAMP signaling, they must be due to nonclassical, receptor-specific pathways such as β_2-receptor coupling to G_i and mitogen-activated protein (MAP) kinases.[72,111,112] In addition, compartmentation of cAMP signals might cause differences between β_1 and β_2-receptor–generated cAMP.[98] The potential clinical implications of these differences are obvious. For example, β_1-selective antagonists might be superior to nonselective blockers in heart failure, because they would leave the β_2-receptor operational. And increasing β_2-receptors to an optimum level might also be beneficial.[103]

Which Mechanisms Mediate Detrimental β_1-Receptor Effects?

Candidate Downstream Targets

The potentially β_1-selective damage must be mediated via β_1-initiated signals. Since the major β_1 signal in cardiomyo-

cytes is the cAMP/PKA pathway, the prime suspects are the targets of PKA-mediated phosphorylation. Identifying the relevant targets is difficult since our knowledge is mostly derived from acute β-receptor stimulation, while in heart failure β-adrenergic activation lasts for years. Adaptive changes and transcriptional/translational alterations may dominate long-term responses. A striking example of opposite effects of short- versus long-term β-adrenergic stimulation is the sodium proton exchanger NHE1.

Phospholamban

The most prominent cardiac target of PKA is phospholamban (PLB), a 52 amino acid phosphoprotein that controls SR Ca^{2+} uptake by inhibiting SERCA.[32] PKA-mediated phosphorylation of PLB relieves this inhibition. Experiments with PLB knockout mice indicate that PLB mediates the positive lusitropic and part of the positive inotropic β-receptor effects.[113,114] Even though phospholamban is a major PKA target in cardiomyocytes, it is probably not responsible for the detrimental β_1-receptor effects. First, PLB knockout rescued several (but not all[115,116]) heart failure models including β_1-receptor transgenic mice,[117] suggesting that phospholamban inhibition by PKA is not detrimental. Second, gene therapy approaches inhibiting phospholamban[118,119] or augmenting SERCA[120,121] ameliorated several heart failure models. However, there may be important differences between mice and humans, since two inactivating mutations of phospholamban have recently been reported to cause heart failure in patients.[122,123] At present, it is unclear how these findings can be integrated.

Other Calcium Regulatory Proteins

Ryanodine receptor (RyR) hyperphosphorylation by PKA leading to increased open probability has been implicated in the pathogenesis of heart failure.[34] Others have disputed this observation[124] or attributed the PKA-induced increase in SR Ca^{2+} release to an indirect mechanism involving phospholamban.[125] Thus, the role of RyR phosphorylation in heart failure awaits clarification.[126]

PKA-mediated phosphorylation opens L-type Ca^{2+} channels triggering SR Ca^{2+} release through the RyR.[114] Basal L-type currents are maintained[127] in heart failure, but single-channel recordings show an increased open probability.[128] Further PKA targets are MyBP-C and troponin I, which may disinhibit myosin actin interaction[35] and reduce Ca^{2+} sensitivity of myofilaments,[129] respectively. It is not clear whether these effects contribute to heart failure.

A functional imbalance between pathways in or decreasing diastolic Ca^{2+} might lead to elevated cytosolic Ca^{2+} levels as a common final pathway in failing cardiomyocytes.[130] The downstream mechanisms exerting possible detrimental Ca^{2+} effects and the roles of Ca^{2+}-dependent proteins such as calcineurin and CaM kinase remain to be elucidated.[131]

Protein Phosphatases and Protein Phosphatase Inhibitor-1

Recent evidence indicates a regulatory role for phosphatases in cardiomyocytes.[132] Phosphatase 2A occurs in β_2-receptor signalosomes in neurons[60] and colocalizes with the RyR.[34] Heart failure is accompanied by increased global protein phosphatase (PP) activity.[132] The protein phosphatase inhibitor-1, PPI-1, inhibits PP1 only in its PKA-phosphorylated form and seems to amplify β-adrenergic signaling in cardiomyocytes.[133,134] PPI-1 mRNA, protein, and phosphorylation are reduced by 2- to 5-fold in failing human hearts,[134,135] leading to reduced PP1 inhibition.[132] Expression of constitutively active PPI-1 rescued the function of failing cardiomyocytes.[133] In order to delineate a role of PPI-1 in heart failure, the proteins regulated by PPI-1–sensitive dephosphorylation need to be identified.

Sodium Proton Exchanger NHE1

A remarkable example of how fundamentally short- and long-term effects can differ is the involvement of the cardiac sodium proton exchanger NHE1 in the detrimental effects of chronic β-receptor stimulation. Acute β-receptor stimulation may inhibit NHE1.[136] However, in β_1-receptor transgenic mice NHE1 is upregulated, and pharmacological NHE1 inhibition prevented the development of hypertrophy, fibrosis, and heart failure.[137] The mechanisms of the protective effects of NHE1 inhibition, the roles of intracellular sodium and calcium, and NHE1 regulation remain to be investigated.[137,138]

Apoptosis

β-Receptor stimulation causes apoptosis of isolated rat cardiomyocytes. Different approaches demonstrate proapoptotic effects of β_1 and antiapoptotic effects of β_2-receptors.[139–141] These in vitro studies are paralleled by findings in transgenic mice where β_1-receptor and $G\alpha_s$ overexpression markedly increased cardiomyocyte apoptosis.[108,142] However, the studies differ as to the responsible intracellular signaling pathways. β_2-Receptor–mediated stimulation of p38 MAP kinase[111] and activation of Akt kinase via G_i[141] have been proposed as antiapoptotic mediators. The proapoptotic effect of β_1-receptors has been found to be dependent on reactive oxygen species,[143] while others imply PKA-independent activation of CaMK.[43] Thus, the mechanistic links for the opposing effects of β_1- versus β_2-receptor stimulation on cardiomyocyte apoptosis remain uncertain. Nor is it clear how much β_1-receptor–mediated apoptosis contributes to heart failure.[144]

Impact on Clinical Medicine

β-Adrenergic Receptor Polymorphisms

Genes for all three β-receptor subtypes contain single nucleotide polymorphisms. Eighteen β_1-receptor variants[145] and 13 β_2-receptor variants have been described,[146] but only two β_1 and three β_2 variant genes are common and have been extensively studied with respect to cardiovascular function (Table). Two attractive hypotheses arise from these studies.

First, the β_1-receptor Gly^{389} variant (allele frequency 25% in whites, 42% in blacks) shows reduced cAMP signals[147] and may represent an impaired variant of the potentially harmful β_1-receptor. Clinical studies have given mixed results (Table), suggesting that the more active Arg^{389} variant may be detrimental in some contexts. For example, the risk for heart failure in blacks was increased for the Arg^{389} variant only when combined with the α_{2C}-receptor deletion polymorphism

Cardiovascular Role of β_1-Receptor $Arg^{389}Gly$ and β_2-Receptor $Thr^{164}Ile$ Polymorphisms

Parameter	Experimental System/Subjects	n	Effect Greater for Arg^{389} or Gly^{389}
β_1-Receptor $Arg^{389}Gly$ polymorphism			
Adenylyl cyclase activity[147]	Stable cell line		$Arg^{389}>>Gly^{389}$
Inotropic/cAMP response to noradrenaline[168]	Isolated human atria	22–30	$Arg^{389}>Gly^{389}$
Inotropic response to noradrenaline[169]	Isolated human atria (mostly β-blocker–treated)	87+20	$Arg^{389}=Gly^{389}$ $Ser^{49}Ser=Ser^{49}Gly$
Heart rate/RR response to exercise[170]	Healthy volunteers	17	$Arg^{389}=Gly^{389}$
Heart rate/QS_{2c}/renin response to exercise[171]	Healthy volunteers	24	$Arg^{389}=Gly^{389}$
RR response to atenolol[172]	Healthy volunteers	34	$Arg^{389}>Gly^{389}$
Baseline heart rate and RR[173]	Dobutamine stress echocardiographic patients	142	$Arg^{389}>Gly^{389}$ carriers
Exercise capacity (peak $\dot{V}o_2$)[174]	Heart failure patients	263	$Arg^{389}>Gly^{389}$ $Arg^{389}Gly^{49}>>Gly^{389}Ser^{49}$
Left ventricular mass[175]	Renal failure patients	249	$Arg^{389}>Gly^{389}$
Hypertension frequency[176]	Case/control and sibling pair analysis	292+265 102 pairs	$Arg^{389}>Gly^{389}$
RR response to β-blocker[172,177]	Retrospective, hypertension	92+55	$Arg^{389}=Gly^{389}$
	Healthy volunteers	21+13	$Arg^{389}>Gly^{389}$
Heart failure frequency[178]	Case/control, idiopathic dilated cardiomyopathy	426+395	No association
Heart failure frequency[148]	Case/control in blacks (few whites)	15+2	$Arg^{389}>>Gly^{389}$ only in combination $\alpha_{2C del}$-receptor
Coronary event risk[179]	Retrospective analysis of WOSCOP study population	1554	No association
β_2-Adrenergic receptor $Thr^{164}Ile$ polymorphism			
Adenylyl cyclase activity[38]	Fibroblasts		$Thr^{164}>>Ile^{164}$
Heart rate/adenylyl cyclase activity[180]	Transgenic mice		$Thr^{164}>>Ile^{164}$
Heart rate/QS_{2c} response to terbutaline[181]	Healthy volunteers	12+6	$Thr^{164}Thr>Thr^{164}Ile$
Exercise capacity (peak $\dot{V}o_2$)[182]	Heart failure patients	18+18	$Thr^{164}Thr>Thr^{164}Ile$
Survival[183]	Heart failure patients	10+247	$Thr^{164}Thr>Thr^{164}Ile$

(allele frequency 4% in whites, 38% in blacks),[148] which is a risk factor by itself.[149] Large cohort studies investigating more complete sets of such polymorphisms including complete haplotypes will be needed for an answer.

Second, the β_2-receptor Ile^{164} variant is a rare variant of the potentially protective β_2-receptor displaying reduced agonist-binding and activity when expressed in fibroblasts[38] or transgenic mice.[150] Healthy volunteers or patients heterozygous for the Ile^{164} variant exhibited lower chronotropic and inotropic response to the β_2 agonist terbutaline, reduced exercise capacity, and decreased survival in heart failure (Table). These findings support the hypothesis that an impaired β_2-receptor represents a risk factor for cardiovascular disease and particularly heart failure.

The Gly^{16} and the Gln^{27} variants of the β_2-receptor may exhibit altered agonist-induced downregulation and have been associated with decreased exercise capacity. These data are inconsistent and have been discussed elsewhere.[151]

β-Blockade in Heart Failure

Since the pioneering work in the 1970s,[152] it took two decades until β-blockers turned from contraindication to standard treatment in heart failure.[16] Blocking β-receptors when cardiac function depends on sympathoadrenergic drive long appeared counterintuitive. Today, three large studies with bisoprolol, metoprolol, and carvedilol show a similar reduction in the risk of death by a third or more, a benefit greater than of any other drug used in heart failure.[16]

Why Do β-Blockers Work in Heart Failure?

How can long-term application of negative inotropic compounds increase cardiac index, exercise capacity, and survival? Two basic mechanisms might explain this paradox: a block of the detrimental consequences of sustained β_1-receptor stimulation or resensitization of the cardiac β-receptor system. We are not aware of studies that would permit a definitive decision, but several arguments support the role of blocking detrimental β_1 effects.

First, β-blockers showed benefits in all patient subgroups, including those with high and low heart rate, blood pressure, and ejection fraction.[18] Thus, the benefit is not restricted to patients with high heart rate. Second, β-blockers exert antiarrhythmic effects, which may explain why they caused larger reductions in sudden deaths than in total mortality. Antiarrhythmic effects are particularly important since altered calcium handling makes failing hearts very susceptible to arrhythmias. Third, β-blockers might prevent the hypertrophic, proapoptotic, and pronecrotic effects of cardiomyocyte β_1-receptor stimulation. Fourth, β-blockers might improve the energy balance in failing hearts, which show energy

starvation[153] and high-energy phosphate depletion,[154] since they reduce heart rate and improve diastolic filling and blood flow. β-Blockers apparently induce a partial switch from fatty acid to glucose metabolism by inhibiting carnitine palmitoyl transferase.[7] And finally, β-blockers reverse failure-specific alterations in cardiac gene expression, which may be involved in progression of the disease.[155–158]

The resensitization hypothesis is supported by the fact β-blockers upregulate β-receptor levels and normalize elevated GRK and $G\alpha_i$ levels.[155–159] While these receptors are partially available even in the continued presence of β-blockers,[160] it is doubtful whether their increase is functionally relevant.[161,162] However, resensitization of downstream elements does result in enhanced responses to phosphodiesterase inhibitors.[161]

Differences Between β-Blockers

Bisoprolol, carvedilol, and metoprolol have been shown to be beneficial in heart failure, and others may follow. Metoprolol and bisoprolol are β_1-selective and have modest inverse activity (ie, they decrease the spontaneous activity of the receptor in the absence of agonist),[163] whereas carvedilol is nonselective, shows no inverse activity,[163] dissociates slowly from the receptor,[164] and is a radical scavenger and α_1-receptor antagonist. All three compounds led to similar clinical results, but carvedilol was superior to metoprolol in the recent COMET trial.[165] Methodological criticism aside, this trial does not answer the questions of possibly protective β_2-receptors and whether the additional properties of carvedilol are important. A role for intrinsic activity is supported by the observations that the strong partial agonist xamoterol[163] was detrimental in heart failure,[19] and the weak partial agonist bucindolol[166] was ineffective in the BEST trial.[167] The beneficial β-blockers are neutral (carvedilol) or inverse agonistic (bisoprolol, metoprolol).[163] However, because of the low constitutive activity of the β_1-receptor, it is uncertain how important inverse agonism is. Taken together, the question is still open which pharmacological properties of β-blockers make them effective in heart failure.

Conclusions

Overwhelming evidence supports a major role for the β-adrenergic system in heart failure. While this system is ideally suited for short-term increases in cardiac performance, its long-term activation is apparently detrimental. These damaging effects appear to be mainly due to stimulation of the β_1 subtype, but the responsible signaling pathways need to be identified. Relevant beneficial effects of the β_2 subtype remain to be confirmed, again together with the elucidation of the responsible—presumably nonclassical—signaling pathways. And the role of the β_3-receptor in the heart is still unclear.

The many changes in the β-adrenergic system in heart failure are most likely a protective adaptation. β-Blockers presumably act by (further) inhibiting the detrimental effects of β_1-receptor stimulation, but perhaps also by resensitizing downstream signaling elements. Future questions include the role of resensitization, the essential properties of clinically effective β-blockers, and the importance of the many downstream signaling steps in finding new strategies for the treatment of heart failure.

References

1. Brodde OE. β-Adrenoceptors in cardiac disease. *Pharmacol Ther.* 1993; 60:405–430.
2. Brodde OE, Michel MC. Adrenergic and muscarinic receptors in the human heart. *Pharmacol Rev.* 1999;51:651–690.
3. Gauthier C, Langin D, Balligand JL. β_3-Adrenoceptors in the cardiovascular system. *Trends Pharmacol Sci.* 2000;21:426–431.
4. Heubach JF, Rau T, Eschenhagen T, Ravens U, Kaumann AJ. Physiological antagonism between ventricular β_1-adrenoceptors and α_1-adrenoceptors but no evidence for β_2- and β_3-adrenoceptor function in murine heart. *Br J Pharmacol.* 2002;136:217–229.
5. Xiao RP, Cheng H, Zhou YY, Kuschel M, Lakatta EG. Recent advances in cardiac β_2-adrenergic signal transduction. *Circ Res.* 1999;85: 1092–1100.
6. Steinberg SF. The molecular basis for distinct β-adrenergic receptor subtype actions in cardiomyocytes. *Circ Res.* 1999;85:1101–1111.
7. Packer M. Neurohormonal interactions and adaptations in congestive heart failure. *Circulation.* 1988;77:721–730.
8. Bristow MR, Ginsburg R, Minobe W, Cubicciotti RS, Sageman WS, Lurie K, Billingham ME, Harrison DC, Stinson EB. Decreased catecholamine sensitivity and β-adrenergic-receptor density in failing human hearts. *N Engl J Med.* 1982;307:205–211.
9. Ping P, Anzai T, Gao M, Hammond HK. Adenylyl cyclase and G protein receptor kinase expression during development of heart failure. *Am J Physiol.* 1997;273:H707–H717.
10. Ungerer M, Parruti G, Bohm M, Puzicha M, DeBlasi A, Erdmann E, Lohse MJ. Expression of β-arrestins and β-adrenergic receptor kinases in the failing human heart. *Circ Res.* 1994;74:206–213.
11. Ungerer M, Bohm M, Elce JS, Erdmann E, Lohse MJ. Altered expression of β-adrenergic receptor kinase and β_1-adrenergic receptors in the failing human heart. *Circulation.* 1993;87:454–463.
12. Feldman AM, Cates AE, Veazey WB, Hershberger RE, Bristow MR, Baughman KL, Baumgartner WA, Van Dop C. Increase of the 40,000-mol wt pertussis toxin substrate (G protein) in the failing human heart. *J Clin Invest.* 1988;82:189–197.
13. Neumann J, Schmitz W, Scholz H, von Meyerinck L, Doring V, Kalmar P. Increase in myocardial G_i-proteins in heart failure. *Lancet.* 1988;2: 936–937.
14. Bohm M, Gierschik P, Jakobs KH, Pieske B, Schnabel P, Ungerer M, Erdmann E. Increase of $G_{i\alpha}$ in human hearts with dilated but not ischemic cardiomyopathy. *Circulation.* 1990;82:1249–1265.
15. Waagstein F, Hjalmarson A, Varnauskas E, Wallentin I. Effect of chronic β-adrenergic receptor blockade in congestive cardiomyopathy. *Br Heart J.* 1975;37:1022–1036.
16. Bristow MR. β-Adrenergic receptor blockade in chronic heart failure. *Circulation.* 2000;101:558–569.
17. CIBIS II Investigators and Committees. The Cardiac Insufficiency Bisoprolol Study II (CIBIS-II): a randomised trial. *Lancet.* 1999;353:9–13.
18. Effect of metoprolol CR/XL in chronic heart failure: metoprolol CR/XL Randomised Intervention Trial in Congestive Heart Failure (MERIT-HF). *Lancet.* 1999;353:2001–2007.
19. Xamoterol in Severe Heart Failure Study Group. Xamoterol in severe heart failure. *Lancet.* 1990;336:1–6.
20. Lands AM, Arnold A, McAuliff JP, Luduena FP, Brown TG Jr. Differentiation of receptor systems activated by sympathomimetic amines. *Nature.* 1967;214:597–598.
21. Chruscinski A, Brede ME, Meinel L, Lohse MJ, Kobilka BK, Hein L. Differential distribution of β-adrenergic receptor subtypes in blood vessels of knockout mice lacking β_1- or β_2-adrenergic receptors. *Mol Pharmacol.* 2001;60:955–962.
22. Krief S, Lonnqvist F, Raimbault S, Baude B, Van Spronsen A, Arner P, Strosberg AD, Ricquier D, Emorine LJ. Tissue distribution of β_3-adrenergic receptor mRNA in man. *J Clin Invest.* 1993;91:344–349.
23. Kitamura T, Onishi K, Dohi K, Okinaka T, Isaka N, Nakano T. The negative inotropic effect of β_3-adrenoceptor stimulation in the beating guinea pig heart. *J Cardiovasc Pharmacol.* 2000;35:786–790.
24. Cheng HJ, Zhang ZS, Onishi K, Ukai T, Sane DC, Cheng CP. Upregulation of functional β_3-adrenergic receptor in the failing canine myocardium. *Circ Res.* 2001;89:599–606.
25. Kohout TA, Takaoka H, McDonald PH, Perry SJ, Mao L, Lefkowitz RJ, Rockman HA. Augmentation of cardiac contractility mediated by the

human β_3-adrenergic receptor overexpressed in the hearts of transgenic mice. *Circulation*. 2001;104:2485–2491.
26. Tavernier G, Galitzky J, Bousquet-Melou A, Montastruc JL, Berlan M. The positive chronotropic effect induced by BRL 37344 and CGP 12177, two β_3 adrenergic agonists, does not involve cardiac β-adrenoceptors but baroreflex mechanisms. *J Pharmacol Exp Ther*. 1992;263:1083–1090.
27. Devic E, Xiang Y, Gould D, Kobilka B. β-Adrenergic receptor subtype-specific signaling in cardiac myocytes from β_1 and β_2 adrenoceptor knockout mice. *Mol Pharmacol*. 2001;60:577 583.
28. Konkar AA, Zhai Y, Granneman JG. β_1-Adrenergic receptors mediate β_3-adrenergic-independent effects of CGP 12177 in brown adipose tissue. *Mol Pharmacol*. 2000;57:252–258.
29. Kaumann AJ, Engelhardt S, Hein L, Molenaar P, Lohse M. Abolition of (−)−CGP 12177-evoked cardiostimulation in double β_1/β_2-adrenoceptor knockout mice. *Naunyn Schmiedebergs Arch Pharmacol*. 2001;363:87–93.
30. Zhao XL, Gutierrez LM, Chang CF, Hosey MM. The α_1-subunit of skeletal muscle L-type Ca channels is the key target for regulation by A-kinase and protein phosphatase-1C. *Biochem Biophys Res Commun*. 1994;198:166–173.
31. Gerhardstein BL, Puri TS, Chien AJ, Hosey MM. Identification of the sites phosphorylated by cyclic AMP-dependent protein kinase on the β2 subunit of L-type voltage-dependent calcium channels. *Biochemistry*. 1999;38:10361–10370.
32. Simmerman HK, Jones LR. Phospholamban: protein structure, mechanism of action, and role in cardiac function. *Physiol Rev*. 1998; 78:921–947.
33. Sulakhe PV, Vo XT. Regulation of phospholamban and troponin-I phosphorylation in the intact rat cardiomyocytes by adrenergic and cholinergic stimuli. *Mol Cell Biochem*. 1995;149–150:103–126.
34. Marx SO, Reiken S, Hisamatsu Y, Jayaraman T, Burkhoff D, Rosemblit N, Marks AR. PKA phosphorylation dissociates FKBP12.6 from the calcium release channel (ryanodine receptor): defective regulation in failing hearts. *Cell*. 2000;101:365–376.
35. Kunst G, Kress KR, Gruen M, Uttenweiler D, Gautel M, Fink RH. Myosin binding protein C, a phosphorylation-dependent force regulator in muscle that controls the attachment of myosin heads by its interaction with myosin S2. *Circ Res*. 2000;86:51–58.
36. Zhang ZY, Zhou B, Xie L. Modulation of protein kinase signaling by protein phosphatases and inhibitors. *Pharmacol Ther*. 2002;93:307–317.
37. Biel M, Schneider A, Wahl C. Cardiac HCN channels: structure, function, and modulation. *Trends Cardiovasc Med*. 2002;12:206–212.
38. Green SA, Holt BD, Liggett SB. β_1- and β_2-Adrenergic receptors display subtype-selective coupling to G_s. *Mol Pharmacol*. 1992;41:889–893.
39. Levy FO, Zhu X, Kaumann AJ, Birnbaumer L. Efficacy of β_1-adrenergic receptors is lower than that of β_2-adrenergic receptors. *Proc Natl Acad Sci U S A*. 1993;90:10798–10802.
40. Ostrom RS, Gregorian C, Drenan RM, Xiang Y, Regan JW, Insel PA. Receptor number and caveolar co-localization determine receptor coupling efficiency to adenylyl cyclase. *J Biol Chem*. 2001;276: 42063–42069.
41. Bristow MR, Hershberger RE, Port JD, Minobe W, Rasmussen R. β_1- and β_2-Adrenergic receptor-mediated adenylate cyclase stimulation in nonfailing and failing human ventricular myocardium. *Mol Pharmacol*. 1989;35:295–303.
42. Hall RA, Lefkowitz RJ. Regulation of G protein-coupled receptor signaling by scaffold proteins. *Circ Res*. 2002;91:672–680.
43. Zhu WZ, Wang SQ, Chakir K, Yang D, Zhang T, Brown JH, Devic E, Kobilka BK, Cheng H, Xiao RP. Linkage of β_1-adrenergic stimulation to apoptotic heart cell death through protein kinase A-independent activation of Ca^{2+}/calmodulin kinase II. *J Clin Invest*. 2003;111:617–625.
44. Zaccolo M, Magalhaes P, Pozzan T. Compartmentalisation of cAMP and Ca^{2+} signals. *Curr Opin Cell Biol*. 2002;14:160–166.
45. Steinberg SF, Brunton LL. Compartmentation of G protein-coupled signaling pathways in cardiac myocytes. *Annu Rev Pharmacol Toxicol*. 2001;41:751–773.
46. Keely SL. Activation of cAMP-dependent protein kinase without a corresponding increase in phosphorylase activity. *Res Commun Chem Pathol Pharmacol*. 1977;18:283–290.
47. Vila Petroff MG, Egan JM, Wang X, Sollott SJ. Glucagon-like peptide-1 increases cAMP but fails to augment contraction in adult rat cardiac myocytes. *Circ Res*. 2001;89:445–452.
48. Hohl CM, Li QA. Compartmentation of cAMP in adult canine ventricular myocytes: relation to single-cell free Ca^{2+} transients. *Circ Res*. 1991;69:1369–1379.
49. Jurevicius J, Fischmeister R. cAMP compartmentation is responsible for a local activation of cardiac Ca^{2+} channels by β-adrenergic agonists. *Proc Natl Acad Sci U S A*. 1996;93:295–299.
50. Jurevicius J, Fischmeister R. Acetylcholine inhibits Ca^{2+} current by acting exclusively at a site proximal to adenylyl cyclase in frog cardiac myocytes. *J Physiol*. 1996;491:669–675.
51. Dittrich M, Jurevicius J, Georget M, Rochais F, Fleischmann B, Hescheler J, Fischmeister R. Local response of L-type Ca^{2+} current to nitric oxide in frog ventricular myocytes. *J Physiol*. 2001;534:109–121.
52. Zaccolo M, Pozzan T. Discrete microdomains with high concentration of cAMP in stimulated rat neonatal cardiac myocytes. *Science*. 2002; 295:1711–1715.
53. Kuschel M, Zhou YY, Cheng H, Zhang SJ, Chen Y, Lakatta EG, Xiao RP. G_i protein-mediated functional compartmentalization of cardiac β_2-adrenergic signaling. *J Biol Chem*. 1999;274:22048–22052.
54. Kuschel M, Zhou YY, Spurgeon HA, Bartel S, Karczewski P, Zhang SJ, Krause EG, Lakatta EG, Xiao RP. β_2-Adrenergic cAMP signaling is uncoupled from phosphorylation of cytoplasmic proteins in canine heart. *Circulation*. 1999;99:2458–2465.
55. Bartel S, Krause E-G, Wallukat G, Karczewski P. New insights into β_2-adrenoceptor signalling in the adult rat heart. *Cardiovasc Res*. 2003; 57:694–703.
56. Molenaar P, Bartel S, Cochrane A, Vetter D, Jalali H, Pohlner P, Burrell K, Karczewski P, Krause EG, Kaumann A. Both β_2- and β_1-adrenergic receptors mediate hastened relaxation and phosphorylation of phospholamban and troponin I in ventricular myocardium of Fallot infants, consistent with selective coupling of β_2-adrenergic receptors to G_s-protein. *Circulation*. 2000;102:1814–1821.
57. Altschuld RA, Starling RC, Hamlin RL, Billman GE, Hensley J, Castillo L, Fertel RH, Hohl CM, Robitaille PM, Jones LR, et al. Response of failing canine and human heart cells to β_2-adrenergic stimulation. *Circulation*. 1995;92:1612–1618.
58. Kuznetsov V, Pak E, Robinson RB, Steinberg SF. β_2-Adrenergic receptor actions in neonatal and adult rat ventricular myocytes. *Circ Res*. 1995;76:40–52.
59. Rybin VO, Xu X, Lisanti MP, Steinberg SF. Differential targeting of β-adrenergic receptor subtypes and adenylyl cyclase to cardiomyocyte caveolae. *J Biol Chem*. 2000;275:41447–41457.
60. Davare MA, Avdonin V, Hall DD, Peden EM, Burette A, Weinberg RJ, Horne MC, Hoshi T, Hell JW. A β_2-adrenergic receptor signaling complex assembled with the Ca^{2+} channel Cav1.2. *Science*. 2001;293: 98–101.
61. Zaccolo M, Magalhaes P, Pozzan T. Compartmentalisation of cAMP and Ca^{2+} signals. *Curr Opin Cell Biol*. 2002;14:160–166.
62. Rich TC, Fagan KA, Tse TE, Schaack J, Cooper DM, Karpen JW. A uniform extracellular stimulus triggers distinct cAMP signals in different compartments of a simple cell. *Proc Natl Acad Sci U S A*. 2001; 98:13049–13054.
63. Perry SJ, Baillie GS, Kohout TA, McPhee I, Magiera MM, Ang KL, Miller WE, McLean AJ, Conti M, Houslay MD, Lefkowitz RJ. Targeting of cyclic AMP degradation to β_2-adrenergic receptors by β-arrestins. *Science*. 2002;298:834–836.
64. Michel JJ, Scott JD. AKAP mediated signal transduction. *Annu Rev Pharmacol Toxicol*. 2002;42:235–257.
65. Bauman AL, Scott JD. Kinase- and phosphatase-anchoring proteins: harnessing the dynamic duo. *Nat Cell Biol*. 2002;4:E203–E206.
66. Lohse MJ. Molecular mechanisms of membrane receptor desensitization. *Biochim Biophys Acta*. 1993;1179:171–188.
67. Nantel F, Bonin H, Emorine LJ, Zilberfarb V, Strosberg AD, Bouvier M, Marullo S. The human β_3-adrenergic receptor is resistant to short term agonist-promoted desensitization. *Mol Pharmacol*. 1993;43:548–555.
68. Lohse MJ, Krasel C, Winstel R, Mayor F Jr. G-protein-coupled receptor kinases. *Kidney Int*. 1996;49:1047–1052.
69. Pitcher JA, Freedman NJ, Lefkowitz RJ. G protein-coupled receptor kinases. *Annu Rev Biochem*. 1998;67:653–692.
70. Lohse MJ, Benovic JL, Codina J, Caron MG, Lefkowitz RJ. β-Arrestin: a protein that regulates β-adrenergic receptor function. *Science*. 1990; 248:1547–1550.
71. Lohse MJ, Andexinger S, Pitcher J, Trukawinski S, Codina J, Faure JP, Caron MG, Lefkowitz RJ. Kinase dependence and receptor specificity of β-arrestin and arrestin in the β_2-adrenergic receptor and rhodopsin systems. *J Biol Chem*. 1992;267:8558–8564.

72. Daaka Y, Luttrell LM, Lefkowitz RJ. Switching of the coupling of the β_1-adrenergic receptor to different G proteins by protein kinase A. *Nature*. 1997;390:88–91.
73. Danner S, Lohse MJ. Regulation of β-adrenergic receptor responsiveness modulation of receptor gene expression. *Rev Physiol Biochem Pharmacol*. 1999;136:183–223.
74. Bristow MR, Ginsburg R, Minobe W, Cubicciotti RS, Sageman WS, Lurie K, Billingham ME, Harrison DC, Stinson EB. Decreased catecholamine sensitivity and β-adrenergic-receptor density in failing human hearts. *N Engl J Med*. 1982;307:205–211.
75. Kiuchi K, Shannon RP, Komamura K, Cohen DJ, Bianchi C, Homcy CJ, Vatner SF, Vatner DE. Myocardial β-adrenergic receptor function during the development of pacing-induced heart failure. *J Clin Invest*. 1993;91:907–914.
76. Engelhardt S, Bohm M, Erdmann E, Lohse MJ. Analysis of β-adrenergic receptor mRNA levels in human ventricular biopsy specimens by quantitative polymerase chain reactions. *J Am Coll Cardiol*. 1996;27:146–154.
77. Eschenhagen T. G proteins and the heart. *Cell Biol Int*. 1993;17:723–749.
78. Bohm M, Beuckelmann D, Brown L, Feller G, Lorenz B, Nabauer M, Kemkes B, Erdmann E. Reduction of β-adrenoceptor density and evaluation of positive inotropic responses in isolated, diseased human myocardium. *Eur Heart J*. 1988;9:844–852.
79. Donahue JK, Heldman AW, Fraser H, McDonald AD, Miller JM, Rade JJ, Eschenhagen T, Marban E. Focal modification of electrical conduction in the heart by viral gene transfer. *Nat Med*. 2000;6:1395–1398.
80. Janssen PM, Schillinger W, Donahue JK, Zeitz O, Emami S, Lehnart SE, Weil J, Eschenhagen T, Hasenfuss G, Prestle J. Intracellular β-blockade: overexpression of $G\alpha_{i2}$ depresses the β-adrenergic response in intact myocardium. *Cardiovasc Res*. 2002;55:300–308.
81. Rau T, Nose M, Remmers U, Weil J, Weissmuller A, Davia K, Harding S, Peppel K, Koch WJ, Eschenhagen T. Overexpression of wild-type $G\alpha_{i2}$ suppresses β-adrenergic signaling in cardiac myocytes. *FASEB J*. 2003;17:523–525.
82. Longabaugh JP, Vatner DE, Vatner SF, Homcy CJ. Decreased stimulatory guanosine triphosphate binding protein in dogs with pressure-overload left ventricular failure. *J Clin Invest*. 1988;81:420–424.
83. Ishikawa Y, Sorota S, Kiuchi K, Shannon RP, Komamura K, Katsushika S, Vatner DE, Vatner SF, Homcy CJ. Downregulation of adenylyl-cyclase types V and VI mRNA levels in pacing-induced heart failure in dogs. *J Clin Invest*. 1994;93:2224–2229.
84. Ostrom RS, Post SR, Insel PA. Stoichiometry and compartmentation in G protein-coupled receptor signaling: implications for therapeutic interventions involving G_s. *J Pharmacol Exp Ther*. 2000;294:407–412.
85. Lohse MJ. G-protein coupled receptor kinases and the heart. *Trends Cardiovasc Med*. 1995;5:63–68.
86. Rockman HA, Koch WJ, Lefkowitz RJ. Seven-transmembrane-spanning receptors and heart function. *Nature*. 2002;415:206–212.
87. Leineweber K, Brandt K, Wludyka B, Beilfuss A, Ponicke K, Heinroth-Hoffmann I, Brodde OE. Ventricular hypertrophy plus neurohumoral activation is necessary to alter the cardiac β-adrenoceptor system in experimental heart failure. *Circ Res*. 2002;91:1056–1062.
88. Choi DJ, Koch WJ, Hunter JJ, Rockman HA. Mechanism of β-adrenergic receptor desensitization in cardiac hypertrophy is increased β-adrenergic receptor kinase. *J Biol Chem*. 1997;272:17223–17229.
89. Inglese J, Luttrell LM, Iniguez-Lluhi JA, Touhara K, Koch WJ, Lefkowitz RJ. Functionally active targeting domain of the β-adrenergic receptor kinase: an inhibitor of $G\beta\gamma$-mediated stimulation of type II adenylyl cyclase. *Proc Natl Acad Sci U S A*. 1994;91:3637–3641.
90. Rockman HA, Chien KR, Choi DJ, Iaccarino G, Hunter JJ, Ross J Jr, Lefkowitz RJ, Koch WJ. Expression of a β-adrenergic receptor kinase 1 inhibitor prevents the development of myocardial failure in gene-targeted mice. *Proc Natl Acad Sci U S A*. 1998;95:7000–7005.
91. Harding VB, Jones LR, Lefkowitz RJ, Koch WJ, Rockman HA. Cardiac βARK1 inhibition prolongs survival and augments β-blocker therapy in a mouse model of severe heart failure. *Proc Natl Acad Sci U S A*. 2001;98:5809–5814.
92. Hein L, Altman JD, Kobilka BK. Two functionally distinct α_2-adrenergic receptors regulate sympathetic neurotransmission. *Nature*. 1999;402:181–184.
93. Engelhardt S, Hein L, Wiesmann F, Lohse MJ. Progressive hypertrophy and heart failure in β_1-adrenergic receptor transgenic mice. *Proc Natl Acad Sci U S A*. 1999;96:7059–7064.
94. Milano CA, Allen LF, Rockman HA, Dolber PC, McMinn TR, Chien KR, Johnson TD, Bond RA, Lefkowitz RJ. Enhanced myocardial function in transgenic mice overexpressing the β_2-adrenergic receptor. *Science*. 1994;264:582–586.
95. Suzuki T, Nguyen CT, Nantel F, Bonin H, Valiquette M, Frielle T, Bouvier M. Distinct regulation of β_1- and β_2-adrenergic receptors in Chinese hamster fibroblasts. *Mol Pharmacol*. 1992;41:542–548.
96. Iwase M, Bishop SP, Uechi M, Vatner DE, Shannon RP, Kudej RK, Wight DC, Wagner TE, Ishikawa Y, Homcy CJ, Vatner SF. Adverse effects of chronic endogenous sympathetic drive induced by cardiac $G_{\alpha s}$ overexpression. *Circ Res*. 1996;78:517–524.
97. Antos CL, Frey N, Marx SO, Reiken S, Gaburjakova M, Richardson JA, Marks AR, Olson EN. Dilated cardiomyopathy and sudden death resulting from constitutive activation of protein kinase a. *Circ Res*. 2001;89:997–1004.
98. Lohse MJ, Engelhardt S. Protein kinase a transgenes: the many faces of cAMP. *Circ Res*. 2001;89:938–940.
99. Koch WJ, Rockman HA, Samama P, Hamilton RA, Bond RA, Milano CA, Lefkowitz RJ. Cardiac function in mice overexpressing the β-adrenergic receptor kinase or a βARK inhibitor. *Science*. 1995;268:1350–1353.
100. Li Z, Laugwitz KL, Pinkernell K, Pragst I, Baumgartner C, Hoffmann E, Rosport K, Münch G, Moretti A, Humrich J, Lohse MJ, Ungerer M. Effects of two βγ-binding proteins–N-terminally truncated phosducin and β-adrenergic receptor kinase C terminus (βARKct)–in heart failure. *Gene Ther*. 2003;10:1354–1361.
101. Bauer PH, Muller S, Puzicha M, Pippig S, Obermaier B, Helmreich EJ, Lohse MJ. Phosducin is a protein kinase A-regulated G-protein regulator. *Nature*. 1992;358:73–76.
102. Koch WJ, Lefkowitz RJ, Rockman HA. Functional consequences of altering myocardial adrenergic receptor signaling. *Annu Rev Physiol*. 2000;62:237–260.
103. Akhter SA, Skaer CA, Kypson AP, McDonald PH, Peppel KC, Glower DD, Lefkowitz RJ, Koch WJ. Restoration of β-adrenergic signaling in failing cardiac ventricular myocytes via adenoviral-mediated gene transfer. *Proc Natl Acad Sci U S A*. 1997;94:12100–12105.
104. Liggett SB, Tepe NM, Lorenz JN, Canning AM, Jantz TD, Mitarai S, Yatani A, Dorn GW 2nd. Early and delayed consequences of β_2-adrenergic receptor overexpression in mouse hearts: critical role for expression level. *Circulation*. 2000;101:1707–1714.
105. Du XJ, Gao XM, Jennings GL, Dart AM, Woodcock EA. Preserved ventricular contractility in infarcted mouse heart overexpressing β_2-adrenergic receptors. *Am J Physiol Heart Circ Physiol*. 2000;279:H2456–H2463.
106. Du XJ, Autelitano DJ, Dilley RJ, Wang B, Dart AM, Woodcock EA. β_2-Adrenergic receptor overexpression exacerbates development of heart failure after aortic stenosis. *Circulation*. 2000;101:71–77.
107. Dorn GW 2nd, Tepe NM, Lorenz JN, Koch WJ, Liggett SB. Low- and high-level transgenic expression of β_2-adrenergic receptors differentially affect cardiac hypertrophy and function in $G\alpha_q$-overexpressing mice. *Proc Natl Acad Sci U S A*. 1999;96:6400–6405.
108. Bisognano JD, Weinberger HD, Bohlmeyer TJ, Pende A, Raynolds MV, Sastravaha A, Roden R, Asano K, Blaxall BC, Wu SC, Communal C, Singh K, Colucci W, Bristow MR, Port DJ. Myocardial-directed overexpression of the human β_1-adrenergic receptor in transgenic mice. *J Mol Cell Cardiol*. 2000;32:817–830.
109. Engelhardt S, Boknik P, Keller U, Neumann J, Lohse MJ, Hein L. Early impairment of calcium handling and altered expression of junction in hearts of mice overexpressing the β_1-adrenergic receptor. *FASEB J*. 2001;15:2718–2720.
110. Zierhut W, Zimmer HG. Significance of myocardial α- and β-adrenoceptors in catecholamine-induced cardiac hypertrophy. *Circ Res*. 1989;65:1417–1425.
111. Communal C, Colucci WS, Singh K. p38 Mitogen-activated protein kinase pathway protects adult rat ventricular myocytes against β-adrenergic receptor-stimulated apoptosis. *J Biol Chem*. 2000;275:19395–19400.
112. Luttrell LM, Ferguson SS, Daaka Y, Miller WE, Maudsley S, Della Rocca GJ, Lin F, Kawakatsu H, Owada K, Luttrell DK, Caron MG, Lefkowitz RJ. β-Arrestin-dependent formation of β_2 adrenergic receptor-Src protein kinase complexes. *Science*. 1999;283:655–661.
113. Luo W, Grupp IL, Harrer J, Ponniah S, Grupp G, Duffy JJ, Doetschman T, Kranias EG. Targeted ablation of the phospholamban gene is associated with markedly enhanced myocardial contractility and loss of β-agonist stimulation. *Circ Res*. 1994;75:401–409.

114. Bers DM. Cardiac excitation-contraction coupling. *Nature*. 2002;415:198–205.
115. Song Q, Schmidt AG, Hahn HS, Carr AN, Frank B, Pater L, Gerst M, Young K, Hoit BD, McConnell BK, Haghighi K, Seidman CE, Seidman JG, Dorn GW 2nd, Kranias EG. Rescue of cardiomyocyte dysfunction by phospholamban ablation does not prevent ventricular failure in genetic hypertrophy. *J Clin Invest*. 2003;111:859–867.
116. Delling U, Sussman MA, Molkentin JD. Re-evaluating sarcoplasmic reticulum function in heart failure. *Nat Med*. 2000;6:942–943.
117. Engelhardt S, Hein L, Kranias E, Lohse MJ. Phospholamban is critically involved in β-adrenergic receptor induced hypertrophy and heart failure. *Naunyn Schmiedebergs Arch Pharmacol*. 2003;367:R93. Abstract.
118. Hoshijima M, Ikeda Y, Iwanaga Y, Minamisawa S, Date MO, Gu Y, Iwatate M, Li M, Wang L, Wilson JM, Wang Y, Ross J Jr, Chien KR. Chronic suppression of heart-failure progression by a pseudophosphorylated mutant of phospholamban via in vivo cardiac rAAV gene delivery. *Nat Med*. 2002;8:864–871.
119. del Monte F, Harding SE, Dec GW, Gwathmey JK, Hajjar RJ. Targeting phospholamban by gene transfer in human heart failure. *Circulation*. 2002;105:904–907.
120. del Monte F, Harding SE, Schmidt U, Matsui T, Kang ZB, Dec GW, Gwathmey JK, Rosenzweig A, Hajjar RJ. Restoration of contractile function in isolated cardiomyocytes from failing human hearts by gene transfer of SERCA2a. *Circulation*. 1999;100:2308–2311.
121. del Monte F, Williams E, Lebeche D, Schmidt U, Rosenzweig A, Gwathmey JK, Lewandowski ED, Hajjar RJ. Improvement in survival and cardiac metabolism after gene transfer of sarcoplasmic reticulum Ca^{2+}-ATPase in a rat model of heart failure. *Circulation*. 2001;104:1424–1429.
122. Schmitt JP, Kamisago M, Asahi M, Li GH, Ahmad F, Mende U, Kranias EG, MacLennan DH, Seidman JG, Seidman CE. Dilated cardiomyopathy and heart failure caused by a mutation in phospholamban. *Science*. 2003;299:1410–1413.
123. Haghighi K, Kolokathis F, Pater L, Lynch RA, Asahi M, Gramolini AO, Fan GC, Tsiapras D, Hahn HS, Adamopoulos S, Liggett SB, Dorn GW 2nd, MacLennan DH, Kremastinos DT, Kranias EG. Human phospholamban null results in lethal dilated cardiomyopathy revealing a critical difference between mouse and human. *J Clin Invest*. 2003;111:869–876.
124. Jiang MT, Lokuta AJ, Farrell EF, Wolff MR, Haworth RA, Valdivia HH. Abnormal Ca^{2+} release, but normal ryanodine receptors, in canine and human heart failure. *Circ Res*. 2002;91:1015–1022.
125. Li Y, Kranias EG, Mignery GA, Bers DM. Protein kinase A phosphorylation of the ryanodine receptor does not affect calcium sparks in mouse ventricular myocytes. *Circ Res*. 2002;90:309–316.
126. Eisner DA, Trafford AW. Heart failure and the ryanodine receptor: does Occam's razor rule? *Circ Res*. 2002;91:979–981.
127. Chen X, Piacentino V 3rd, Furukawa S, Goldman B, Margulies KB, Houser SR. L-type Ca^{2+} channel density and regulation are altered in failing human ventricular myocytes and recover after support with mechanical assist devices. *Circ Res*. 2002;91:517–524.
128. Schroder F, Handrock R, Beuckelmann DJ, Hirt S, Hullin R, Priebe L, Schwinger RH, Weil J, Herzig S. Increased availability and open probability of single L-type calcium channels from failing compared with nonfailing human ventricle. *Circulation*. 1998;98:969–976.
129. Kentish JC, McCloskey DT, Layland J, Palmer S, Leiden JM, Martin AF, Solaro RJ. Phosphorylation of troponin I by protein kinase A accelerates relaxation and crossbridge cycle kinetics in mouse ventricular muscle. *Circ Res*. 2001;88:1059–1065.
130. Beuckelmann DJ, Nabauer M, Erdmann E. Intracellular calcium handling in isolated ventricular myocytes from patients with terminal heart failure. *Circulation*. 1992;85:1046–1055.
131. Frey N, McKinsey TA, Olson EN. Decoding calcium signals involved in cardiac growth and function. *Nat Med*. 2000;6:1221–1227.
132. Neumann J. Altered phosphatase activity in heart failure, influence on Ca^{2+} movement. *Basic Res Cardiol*. 2002;97:I91–I95.
133. Carr AN, Schmidt AG, Suzuki Y, del Monte F, Sato Y, Lanner C, Breeden K, Jing SL, Allen PB, Greengard P, Yatani A, Hoit BD, Grupp IL, Hajjar RJ, DePaoli-Roach AA, Kranias EG. Type 1 phosphatase, a negative regulator of cardiac function. *Mol Cell Biol*. 2002;22:4124–4135.
134. El-Armouche A, Rau T, Zolk O, Ditz D, Pamminger T, Zimmermann WH, Jackel E, Harding SE, Boknik P, Neumann J, Eschenhagen T. Evidence for protein phosphatase inhibitor-1 playing an amplifier role in β-adrenergic signaling in cardiac myocytes. *FASEB J*. 2003;17:437–439.
135. Pamminger T, El-Armouche A, Eschenhagen T. Evidence for decreased expression and activity of phosphatase inhibitor-1 in human heart failure. *Naunyn Schmiedebergs Arch Pharmacol*. 2003;367:R91. Abstract.
136. Lagadic-Gossmann D, Vaughan-Jones RD. Coupling of dual acid extrusion in the guinea-pig isolated ventricular myocyte to α_1- and β-adrenoceptors. *J Physiol*. 1993;464:49–73.
137. Engelhardt S, Hein L, Keller U, Klambt K, Lohse MJ. Inhibition of Na^+-H^+-exchange prevents hypertrophy, fibrosis, and heart failure in β_1-adrenergic receptor transgenic mice. *Circ Res*. 2002;90:814–819.
138. Baartscheer A, Schumacher CA, van Borren MM, Belterman CN, Coronel R, Fiolet JW. Increased Na^+/H^+-exchange activity is the cause of increased Na^+_i and underlies disturbed calcium handling in the rabbit pressure and volume overload heart failure model. *Cardiovasc Res*. 2003;57:1015–1024.
139. Communal C, Singh K, Sawyer DB, Colucci WS. Opposing effects of β_1- and β_2-adrenergic receptors on cardiac myocyte apoptosis: role of a pertussis toxin-sensitive G protein. *Circulation*. 1999;100:2210–2212.
140. Chesley A, Lundberg MS, Asai T, Xiao RP, Ohtani S, Lakatta EG, Crow MT. The β_2-adrenergic receptor delivers an antiapoptotic signal to cardiac myocytes through G_i-dependent coupling to phosphatidylinositol 3′-kinase. *Circ Res*. 2000;87:1172–1179.
141. Zhu WZ, Zheng M, Koch WJ, Lefkowitz RJ, Kobilka BK, Xiao RP. Dual modulation of cell survival and cell death by β_2-adrenergic signaling in adult mouse cardiac myocytes. *Proc Natl Acad Sci U S A*. 2001;98:1607–1612.
142. Geng YJ, Ishikawa Y, Vatner DE, Wagner TE, Bishop SP, Vatner SF, Homcy CJ. Apoptosis of cardiac myocytes in G_{α_s} transgenic mice. *Circ Res*. 1999;84:34–42.
143. Remondino A, Kwon SH, Communal C, Pimentel DR, Sawyer DB, Singh K, Colucci WS. β-Adrenergic receptor-stimulated apoptosis in cardiac myocytes is mediated by reactive oxygen species/c-Jun NH2-terminal kinase-dependent activation of the mitochondrial pathway. *Circ Res*. 2003;92:136–138.
144. Sabbah HN, Sharov VG, Gupta RC, Todor A, Singh V, Goldstein S. Chronic therapy with metoprolol attenuates cardiomyocyte apoptosis in dogs with heart failure. *J Am Coll Cardiol*. 2000;36:1698–1705.
145. Podlowski S, Wenzel K, Luther HP, Muller J, Bramlage P, Baumann G, Felix SB, Speer A, Hetzer R, Kopke K, Hoehe MR, Wallukat G. β_1-Adrenoceptor gene variations: a role in idiopathic dilated cardiomyopathy? *J Mol Med*. 2000;78:87–93.
146. Drysdale CM, McGraw DW, Stack CB, Stephens JC, Judson RS, Nandabalan K, Arnold K, Ruano G, Liggett SB. Complex promoter and coding region β_2-adrenergic receptor haplotypes alter receptor expression and predict in vivo responsiveness. *Proc Natl Acad Sci U S A*. 2000;97:10483–10488.
147. Mason DA, Moore JD, Green SA, Liggett SB. A gain-of-function polymorphism in a G-protein coupling domain of the human β_1-adrenergic receptor. *J Biol Chem*. 1999;274:12670–12674.
148. Small KM, Wagoner LE, Levin AM, Kardia SL, Liggett SB. Synergistic polymorphisms of β_1- and α_{2C}-adrenergic receptors and the risk of congestive heart failure. *N Engl J Med*. 2002;347:1135–1142.
149. Brede M, Wiesmann F, Jahns R, Hadamek K, Arnolt C, Neubauer S, Lohse MJ, Hein L. Feedback inhibition of catecholamine release by two different α_2-adrenoceptor subtypes prevents progression of heart failure. *Circulation*. 2002;106:2491–2496.
150. Turki J, Lorenz JN, Green SA, Donnelly ET, Jacinto M, Liggett SB. Myocardial signaling defects and impaired cardiac function of a human β2-adrenergic receptor polymorphism expressed in transgenic mice. *Proc Natl Acad Sci U S A*. 1996;93:10483–10488.
151. Small KM, McGraw DW, Liggett SB. Pharmacology and physiology of human adrenergic receptor polymorphisms. *Annu Rev Pharmacol Toxicol*. 2003;43:381–411.
152. Swedberg K, Hjalmarson A, Waagstein F, Wallentin I. Prolongation of survival in congestive cardiomyopathy by β-receptor blockade. *Lancet*. 1979;1:1374–1376.
153. Katz AM. Metabolism of the failing heart. *Cardioscience*. 1993;4:199–203.
154. Spindler M, Engelhardt S, Niebler R, Wagner H, Hein L, Lohse MJ, Neubauer S. Alterations in the myocardial creatine kinase system precede the development of contractile dysfunction in β_1-adrenergic receptor transgenic mice. *J Mol Cell Cardiol*. 2003;35:389–397.
155. Sigmund M, Jakob H, Becker H, Hanrath P, Schumacher C, Eschenhagen T, Schmitz W, Scholz H, Steinfath M. Effects of meto-

prolol on myocardial β-adrenoceptors and G_{in}-proteins in patients with congestive heart failure. *Eur J Clin Pharmacol.* 1996;51:127–132.
156. Gilbert EM, Olsen SL, Renlund DG, Bristow MR. β-Adrenergic receptor regulation and left ventricular function in idiopathic dilated cardiomyopathy. *Am J Cardiol.* 1993;71:23C–29C.
157. Kubo H, Margulies KB, Piacentino V 3rd, Gaughan JP, Houser SR. Patients with end-stage congestive heart failure treated with β-adrenergic receptor antagonists have improved ventricular myocyte calcium regulatory protein abundance. *Circulation.* 2001;104: 1012–1018.
158. Lowes BD, Gilbert EM, Abraham WT, Minobe WA, Larrabee P, Ferguson D, Wolfel EE, Lindenfeld J, Tsvetkova T, Robertson AD, Quaife RA, Bristow MR. Myocardial gene expression in dilated cardiomyopathy treated with β-blocking agents. *N Engl J Med.* 2002;346: 1357–1365.
159. Heilbrunn SM, Shah P, Bristow MR, Valantine HA, Ginsburg R, Fowler MB. Increased β-receptor density and improved hemodynamic response to catecholamine stimulation during long-term metoprolol therapy in heart failure from dilated cardiomyopathy. *Circulation.* 1989;79: 483–490.
160. Wellstein A, Belz GG, Palm D. β-Adrenoceptor subtype binding activity in plasma and β-blockade by propranolol and β_1 selective bisoprolol in humans: evaluation with Schild-plots. *J Pharmacol Exp Ther.* 1988;246: 328–337.
161. Metra M, Nodari S, D'Aloia A, Muneretto C, Robertson AD, Bristow MR, Dei Cas L. β-Blocker therapy influences the hemodynamic response to inotropic agents in patients with heart failure: a randomized comparison of dobutamine and enoximone before and after chronic treatment with metoprolol or carvedilol. *J Am Coll Cardiol.* 2002;40: 1248–1258.
162. Gilbert EM, Abraham WT, Olsen S, Hattler B, White M, Mealy P, Larrabee P, Bristow MR. Comparative hemodynamic, left ventricular functional, and antiadrenergic effects of chronic treatment with metoprolol versus carvedilol in the failing heart. *Circulation.* 1996;94: 2817–2825.
163. Engelhardt S, Grimmer Y, Fan GH, Lohse MJ. Constitutive activity of the human β_1-adrenergic receptor in β_1-receptor transgenic mice. *Mol Pharmacol.* 2001;60:712–717.
164. Flesch M, Ettelbruck S, Rosenkranz S, Maack C, Cremers B, Schluter KD, Zolk O, Bohm M. Differential effects of carvedilol and metoprolol on isoprenaline-induced changes in β-adrenoceptor density and systolic function in rat cardiac myocytes. *Cardiovasc Res.* 2001;49:371–380.
165. Poole-Wilson PA, Swedberg K, Cleland JG, Di Lenarda A, Hanrath P, Komajda M, Lubsen J, Lutiger B, Metra M, Remme WJ, Torp-Pedersen C, Scherhag A, Skene A. Comparison of carvedilol and metoprolol on clinical outcomes in patients with chronic heart failure in the Carvedilol Or Metoprolol European Trial (COMET): randomised controlled trial. *Lancet.* 2003;362:7–13.
166. Maack C, Böhm M, Vlaskin L, Dabew E, Lorenz K, Schäfers H-J, Lohse MJ, Engelhardt S. Partial agonist activity of bucindolol is dependent on the activation state of the human β_1-adrenergic receptor. *Circulation.* 2003;108:348–353.
167. Beta-Blocker Evaluation of Survival Trial Investigators. A trial of the beta-blocker bucindolol in patients with advanced chronic heart failure. *N Engl J Med.* 2001;344:1659–1667.
168. Sandilands AJ, O'Shaughnessy KM, Brown MJ. Greater inotropic and cyclic AMP responses evoked by noradrenaline through Arg389 β_1-adrenoceptors versus Gly389 β_1-adrenoceptors in isolated human atrial myocardium. *Br J Pharmacol.* 2003;138:386–392.
169. Molenaar P, Rabnott G, Yang I, Fong KM, Savarimuthu SM, Li L, West MJ, Russell FD. Conservation of the cardiostimulant effects of (−)−norepinephrine across Ser49Gly and Gly389Arg β_1-adrenergic receptor polymorphisms in human right atrium in vitro. *J Am Coll Cardiol.* 2002;40:1275–1282.
170. Xie HG, Dishy V, Sofowora G, Kim RB, Landau R, Smiley RM, Zhou HH, Wood AJ, Harris P, Stein CM. Arg389Gly β_1-adrenoceptor polymorphism varies in frequency among different ethnic groups but does not alter response in vivo. *Pharmacogenetics.* 2001;11:191–197.
171. Buscher R, Belger H, Eilmes KJ, Tellkamp R, Radke J, Dhein S, Hoyer PF, Michel MC, Insel PA, Brodde OE. In-vivo studies do not support a major functional role for the Gly389Arg β_1-adrenoceptor polymorphism in humans. *Pharmacogenetics.* 2001;11:199–205.
172. Sofowora GG, Dishy V, Muszkat M, Xie HH, Kim RR, Harris PP, Prasad HH, Byrne DD, Nair UU, Wood AA, Stei CC. A common β_1-adrenergic receptor polymorphism (Arg389Gly) affects blood pressure response to β-blockade. *Clin Pharmacol Ther.* 2003;73: 366–371.
173. Humma LM, Puckett BJ, Richardson HE, Terra SG, Andrisin TE, Lejeune BL, Wallace MR, Lewis JF, McNamara DM, Picoult-Newberg L, Pepine CJ, Johnson JA. Effects of β_1-adrenoceptor genetic polymorphisms on resting hemodynamics in patients undergoing diagnostic testing for ischemia. *Am J Cardiol.* 2001;88:1034–1037.
174. Wagoner LE, Craft LL, Zengel P, McGuire N, Rathz DA, Dorn GW 2nd, Liggett SB. Polymorphisms of the β_1-adrenergic receptor predict exercise capacity in heart failure. *Am Heart J.* 2002;144:840–846.
175. Stanton T, Inglis GC, Padmanabhan S, Dominiczak AF, Jardine AG, Connell JM. Variation at the β_1 adrenoceptor gene locus affects left ventricular mass in renal failure. *J Nephrol.* 2002;15:512–518.
176. Bengtsson K, Melander O, Orho-Melander M, Lindblad U, Ranstam J, Rastam L, Groop L. Polymorphism in the β_1-adrenergic receptor gene and hypertension. *Circulation.* 2001;104:187–190.
177. O'Shaughnessy KM, Fu B, Dickerson C, Thurston D, Brown MJ. The gain-of-function G389R variant of the β_1-adrenoceptor does not influence blood pressure or heart rate response to β-blockade in hypertensive subjects. *Clin Sci (Lond).* 2000;99:233–238.
178. Tesson F, Charron P, Peuchmaurd M, Nicaud V, Cambien F, Tiret L, Poirier O, Desnos M, Jullieres Y, Amouyel P, Roizes G, Dorent R, Schwartz K, Komajda M. Characterization of a unique genetic variant in the β_1-adrenoceptor gene and evaluation of its role in idiopathic dilated cardiomyopathy. *J Mol Cell Cardiol.* 1999;31:1025–1032.
179. White HL, Maqbool A, McMahon AD, Yates L, Ball SG, Hall AS, Balmforth AJ. An evaluation of the β_1-adrenergic receptor Arg389Gly polymorphism in individuals at risk of coronary events. *Eur Heart J.* 2002;23:1087–1092.
180. Turki J, Lorenz JN, Green SA, Donnelly ET, Jacinto M, Liggett SB. Myocardial signaling defects and impaired cardiac function of a human β_1-adrenergic receptor polymorphism expressed in transgenic mice. *Proc Natl Acad Sci U S A.* 1996;93:10483–10488.
181. Brodde OE, Buscher R, Tellkamp R, Rudke J, Dhein S, Insel PA. Blunted cardiac responses to receptor activation in subjects with Thr164Ile β_2-adrenoceptors. *Circulation.* 2001;103:1048–1050.
182. Wagoner LE, Craft LL, Singh B, Suresh DP, Zengel PW, McGuire N, Abraham WT, Chenier TC, Dorn GW 2nd, Liggett SB. Polymorphisms of the β_2-adrenergic receptor determine exercise capacity in patients with heart failure. *Circ Res.* 2000;86:834–840.
183. Liggett SB, Wagoner LE, Craft LL, Hornung RW, Hoit BD, McIntosh TC, Walsh RA. The Ile164 β_2-adrenergic receptor polymorphism adversely affects the outcome of congestive heart failure. *J Clin Invest.* 1998;102:1534–1539.
184. Hoffmann C, Leitz MR, Oberdorf-Maass S, Lohse MJ, Klotz KNK. Comparative pharmacology at human β-adrenergic receptor subtypes. *Naunyn Schmiedebergs Arch Pharmacol.* In press.

PHOSPHOLAMBAN DOWN-REGULATION OR SERCA2A OVEREXPRESSION: INTERACTION WITH βAR STIMULATION IN RABBIT MYOCYTES.

Babar Chaudhri, Kerry Davia, *Federica del Monte, *Roger Hajjar, Sian E. Harding, ICSM, London and *CVRC, Harvard Med. School, Boston, MA, USA

Increasing heart force and speeding relaxation by SERCA2a overexpression using adenoviral vectors has shown promising results in failing human and animal myocytes. However, it has been suggested that stimulation by down-regulation of phospholamban might be preferable, since the maximum effect should be similar to that produced by βARs, avoiding supraphysiological effects. We have compared directly the effects of SERCA2a overexpression (5-fold) with those of phospholamban down-regulation using antisense (Plb-AS), both mediated by adenovirus. Adult rabbit myocytes were studied 48 h after infection with adenovirus: co-expression of GFP was used to identify infected myocytes. Inotropic responses to Iso were unaffected by Ad.SERCA2a or Ad.Plb-AS (maximum contraction amplitude; control, 8.6 ± 0.5 % shortening; Ad.SERCA2a, 8.1 ± 0.4%; Ad.Plb-AS, 9.2 ± 0.7%, n=9 preparations). EC_{50} values were not significantly different between groups. Both Ad.SERCA2a and Ad.Plb-AS accelerated relaxation ($P<0.02$) (Time-to-50% relaxation (R50), non-infected: 204 ± 22 ms, Ad.SERCA2a: 106 ± 15 ms, Ad.Plb-AS: 135 ± 15 ms). After maximal isoproterenol stimulation (1 μM) R50 values were, non-infected: 94 ± 7 ms, Ad.SERCA2a: 70 ± 8 ms and Ad.Plb-AS: 74 ± 5ms. Additivity with βAR stimulation is therefore similar for Plb down-regulation and SERCA2a overexpression, suggesting that other limitations within the cell prevent SERCA2a from producing supraphysiological acceleration of relaxation.

BIOCHEMICAL CHARACTERIZATION OF THE SARCOPLASMIC RETICULUM MEMBRANE IN CARDIAC FAILURE DUE TO VOLUME OVERLOAD.

Rita Chávez and Mauricio Díaz-Muñoz. Dept. of Molecular and Cellular Neurobiology. Neurobiology Center, National University of México. Juriquilla, Qro. México.

Modifications in the composition of biological membranes, including the Sarcoplasmic Reticulum (SR), have been known to happen under certain physiological or pathological conditions. SR proteins such as the calcium ATPase (SERCA) have shown to be modulated according to the phospholipidic phase they are immersed in. In volume overload, heart failure occurs as a consequence of contractility impairment. Intracellular calcium has been found to be regulated in an unusual way by all the elements involved in it, like receptors and channels. It is our intention to demonstrate that this uncoupling of the elements responsible of calcium handling is partly because of the alterations occurring within the composition of the SR membrane. Volume overload was achieved by an aorto-caval shunt as described by Garcia and Diebold (1990) with male Wistar rats weighing between 180-220 g. After 12 weeks of treatment, rats were evaluated with the following tests: systolic blood pressure, blood creatinine, optic and electronic microscopy. By using the Langendorff Model we determine the left ventricular pressure, all the electrocardiogram parameters like heart rate, qrs complex and a-v conductance. After this, we obtained enriched SR membranes from each heart and performed the biochemical assays. In this matter we made binding assays for the ryanodine receptor, enzymatic activity analysis of the SERCA pump and preliminary quantification of membrane phospholipids. The results reflect that our treated rats show mild cardiac failure according to the Langendorff Model, this is, only left ventricle pressure augmented without interfering with heart performance. However, the biochemical results exhibit interesting features like a significant raise in ryanodine binding and a clear diminution in the enzyme activity for the SERCA pump. Analysis of the fatty acids content of the SR membrane phospholipids showed to be significantly modified.

XP-002458611

PHOSPHODIESTERASE III (PDE III) INHIBITION POTENTIATES Ca-INDUCED, NOT VOLTAGE-GATED, SARCOPLASMIC RETICULUM Ca RELEASE

Xiongwen Chen, Valentino Piacentino III, and Steven R. Houser, CVRG, Temple University, Philadelphia, PA

BACKGROUND: Sarcoplasmic reticulum (SR) Ca release is triggered by the L-type Ca current ($I_{Ca,L}$). In addition, cAMP-dependent direct voltage gating has also been described with amrinone, a PDE III inhibitor, proposed as a preferential activator. We studied the effects of PDE III inhibition on $I_{Ca,L}$-induced and voltage-gated SR Ca release in feline ventricular myocytes (FeVM). **METHODS:** $I_{Ca,L}$ and contractions (37°C) were measured in FeVM with whole-cell voltage clamp and video-microscopy, respectively. Perforated patch was employed in some experiments to eliminate dialysis of the cytoplasm. The voltage-dependence of contraction (V-C) and the cadmium ($I_{Ca,L}$ inhibitor)-sensitive $I_{membrane}$ were measured before and after amrinone (AMR, 100-500 μM). **RESULTS:** The V-C relationship was bell-shaped under control (Cnt) conditions. AMR increased the rate and magnitude of contraction and the inward current. The V-C relationship broadened, but was still bell-shaped. In Na- and K-free conditions, AMR caused a significant increase in $I_{Ca,L}$ during steps to +10 mV (Cnt, 9.3±1.2 vs. AMR, 13.7±1.8 pA/pF, $p<0.05$). AMR also caused a leftward shift in the voltage-dependence of $I_{Ca,L}$ activation ($p<0.05$). **CONCLUSIONS:** AMR increases $I_{Ca,L}$ and SR Ca loading in FeVM. The bell-shaped V-C relationship in the presence of AMR is only consistent with $I_{Ca,L}$-induced SR Ca release. There is no direct voltage-gated SR Ca release in mammalian cardiac myocytes.

FUNCTIONAL SIGNIFICANCE OF β_3-ADRENERGIC RECEPTOR ACTIVATION IN HEART FAILURE

Heng-Jie Cheng, Zhu-Shan Zhang, Katsuya Onishi, Tomohiko Ukai, David C. Sane, Che-Ping Cheng, Dept of Cardiology, Wake Forest University School of Medicine, Winston-Salem, NC.

We compared cardiomyocyte steady-state β_3-adrenergic receptors (AR) mRNA and protein levels, myocyte contractile performance, $[Ca^{2+}]_i$ transient, and Ca^{2+} current ($I_{Ca,L}$) responses to BRL-37344 (BRL, 10^{-5} M), a β_3-AR agonist, in freshly isolated LV cardiomyocyte obtained from 5 instrumented dogs before and after pacing-induced CHF. Using RT-PCR with designed primers, we detected β_3-AR mRNA from myocyte total RNA in each animal both before and after CHF. β_3-AR mRNA expression and protein levels, assessed by Northern blot and Western blot, were significantly increased in CHF myocytes than in normal myocytes. Importantly, these changes were associated with enhanced β_3-AR-mediated negative modulation on myocyte contractile response and $[Ca^{2+}]_i$ regulation. Compared with normal myocytes, CHF myocytes had much greater decreases in the velocity of shortening and relengthening with BRL, accompanied by larger reductions in the peak systolic $[Ca^{2+}]_i$ transient and $I_{Ca,L}$. These responses were not modified by pretreating myocytes with metoprolol (a β_1-AR antagonist) or nadolol (a β_1- and β_2-AR antagonist), but were nearly prevented by bupranolol (a β_3-AR antagonist) or by PTX incubation. We conclude that in dogs with pacing-induced CHF, gene expression and functional response of cardiac β_3-AR are up-regulated. This factor may contribute to progression of functional impairment in CHF.

PHOSPHOLAMBAN DOWN-REGULATION OR SERCA2A OVEREXPRESSION: INTERACTION WITH βAR STIMULATION IN RABBIT MYOCYTES.

Babar Chaudhri, Kerry Davia, *Federica del Monte, *Roger Hajjar, Stan E. Harding, ICSM, London and *CVRC, Harvard Med. School, Boston, MA, USA

Increasing heart force and speeding relaxation by SERCA2a overexpression using adenoviral vectors has shown promising results in failing human and animal myocytes. However, it has been suggested that stimulation by down-regulation of phospholamban might be preferable, since the maximum effect should be similar to that produced by βARs, avoiding supraphysiological effects. We have compared directly the effects of SERCA2a overexpression (5-fold) with those of phospholamban down-regulation using antisense (Plb-AS), both mediated by adenovirus. Adult rabbit myocytes were studied 48 h after infection with adenovirus: co-expression of GFP was used to identify infected myocytes. Inotropic responses to Iso were unaffected by Ad.SERCA2a or Ad.Plb-AS (maximum contraction amplitude; control, 8.6 ± 0.5 % shortening; Ad.SERCA2a, 8.1 ± 0.4%; Ad.Plb-AS, 9.2 ± 0.7%, n=8 preparations). EC_{50} values were not significantly different between groups. Both Ad.SERCA2a and Ad.Plb-AS accelerated relaxation ($P<0.02$) (Time-to-50% relaxation (R50), non-infected: 204 ± 22 ms, Ad.SERCA2a: 106 ± 15 ms, Ad.Plb-AS: 135 ± 15 ms). After maximal isoproterenol stimulation (1 μM) R50 values were, non-infected: 94 ± 7 ms, Ad.SERCA2a: 70 ± 8 ms and Ad.Plb-AS: 74 ± 5ms. Additivity with βAR stimulation is therefore similar for Plb down-regulation and SERCA2a overexpression, suggesting that other limitations within the cell prevent SERCA2a from producing supraphysiological acceleration of relaxation.

BIOCHEMICAL CHARACTERIZATION OF THE SARCOPLASMIC RETICULUM MEMBRANE IN CARDIAC FAILURE DUE TO VOLUME OVERLOAD.

Rita Chávez and Mauricio Díaz-Muñoz. Dept. of Molecular and Cellular Neurobiology. Neurobiology Center, National University of México. Juriquilla, Qro. México.

Modifications in the composition of biological membranes, including the Sarcoplasmic Reticulum (SR), have been known to happen under certain physiological or pathological conditions. SR proteins such as the calcium ATPase (SERCA) have shown to be modulated according to the phospholipidic phase they are immersed in. In volume overload, heart failure occurs as a consequence of contractility impairment. Intracellular calcium has been found to be regulated in an unusual way by all the elements involved in it, like receptors and channels. It is our intention to demonstrate that this uncoupling of the elements responsible of calcium handling is partly because of the alterations occurring within the composition of the SR membrane. Volume overload was achieved by an aorto-caval shunt as described by Garcia and Diebold (1990) with male Wistar rats weighing between 180-220 g. After 12 weeks of treatment, rats were evaluated with the following tests: systolic blood pressure, blood creatinine, cpbs and electronic microscopy. By using the Langendorff Model we determine the left ventricular pressure, all the electrocardiogram parameters like heart rate, qrs complex and a-v conductance. After this, we obtained enriched SR membranes from each heart and performed the biochemical assays. In this matter we made binding assays for the ryanodine receptor, enzymatic activity analysis of the SERCA pump and preliminary quantification of membrane phospholipids. The results reflect that our treated rats show mild cardiac failure according to the Langendorff Model, this is, only left ventricle pressure augmented without interfering with heart performance. However, the biochemical results exhibit interesting features like a significant raise in ryanodine binding and a clear diminution in the enzyme activity for the SERCA pump. Analysis of the fatty acids content of the SR membrane phospholipids showed to be significantly modified.

PHOSPHODIESTERASE III (PDE III) INHIBITION POTENTIATES Ca-INDUCED, NOT VOLTAGE-GATED, SARCOPLASMIC RETICULUM Ca RELEASE

Xiongwen Chen, Valentino Piacentirio III, and Steven R. Houser, CVRG, Temple University, Philadelphia, PA

BACKGROUND: Sarcoplasmic reticulum (SR) Ca release is triggered by the L-type Ca current ($I_{Ca,L}$). In addition, cAMP-dependent direct voltage gating has also been described with amrinone, a PDE III inhibitor, proposed as a preferential activator. We studied the effects of PDE III inhibition on $I_{Ca,L}$-induced and voltage-gated SR Ca release in feline ventricular myocytes (FeVM). **METHODS:** $I_{Ca,L}$ and contractions (37°C) were measured in FeVM with whole-cell voltage clamp and video-microscopy, respectively. Perforated patch was employed in some experiments to eliminate dialysis of the cytoplasm. The voltage-dependence of contraction (V-C) and the cadmium ($I_{Ca,L}$ inhibitor)-sensitive $I_{membrane}$ were measured before and after amrinone (AMR, 100-500 μM). **RESULTS:** The V-C relationship was bell-shaped under control (Cnt) conditions. AMR increased the rate and magnitude of contraction and the inward current. The V-C relationship broadened, but was still bell-shaped. In Na- and K-free conditions, AMR caused a significant increase in $I_{Ca,L}$ during steps to +10 mV (Cnt, 9.3±1.2 vs. AMR, 13.7±1.8 pA/pF, $p<0.05$). AMR also caused a leftward shift in the voltage-dependence of $I_{Ca,L}$ activation ($p<0.05$). **CONCLUSIONS:** AMR increases $I_{Ca,L}$ and SR Ca loading in FeVM. The bell-shaped V-C relationship in the presence of AMR is only consistent with $I_{Ca,L}$-induced SR Ca release. There is no direct voltage-gated SR Ca release in mammalian cardiac myocytes.

FUNCTIONAL SIGNIFICANCE OF β_3-ADRENERGIC RECEPTOR ACTIVATION IN HEART FAILURE

Heng-Jie Cheng, Zhu-Shan Zhang, Katsuya Onishi, Tomohiko Ukai, David C. Sane, Che-Ping Cheng, Dept of Cardiology, Wake Forest University School of Medicine, Winston-Salem, NC.

We compared cardiomyocyte steady-state β_3-adrenergic receptors (AR) mRNA and protein levels, myocyte contractile performance, $[Ca^{2+}]_i$ transient, and Ca^{2+} current ($I_{Ca,L}$) responses to BRL-37344 (BRL, 10^{-5} M), a β_3-AR agonist, in freshly isolated LV cardiomyocyte obtained from 5 instrumented dogs before and after pacing-induced CHF. Using RT-PCR with designed primers, we detected β_3-AR mRNA from myocyte total RNA in each animal both before and after CHF. β_3-AR mRNA expression and protein levels, assessed by Northern blot and Western blot, were significantly increased in CHF myocytes than in normal myocytes. Importantly, these changes were associated with enhanced β_3-AR-mediated negative modulation on myocyte contractile response and $[Ca^{2+}]_i$ regulation. Compared with normal myocytes, CHF myocytes had much greater decreases in the velocity of shortening and relengthening with BRL, accompanied by larger reductions in the peak systolic $[Ca^{2+}]_i$ transient and $I_{Ca,L}$. These responses were not modified by pretreating myocytes with metoprolol (a β_1-AR antagonist) or nadolol (a β_1- and β_2-AR antagonist), but were nearly prevented by bupranolol (a β_3-AR antagonist) or by PTX incubation. We conclude that in dogs with pacing-induced CHF, gene expression and functional response of cardiac β_3-AR are up-regulated. This factor may contribute to progression of functional impairment in CHF.

PubMed

Display Settings: Abstract

Klin Wochenschr. 1981 Jun 15;59(12):639-45.

[Treatment of severe congestive heart failure with the beta-agonist fenoterol (author's transl)].

[Article in German]

Irmer M, Wollschläger H, Just H.

Abstract

The acute hemodynamic effects of the semiselective beta 2-stimulating compound Fenoterol were studied in 7 patients with severe congestive heart failure (IV NYHA) as a result of a low-output-syndrome of varying aetiology (coronary heart disease/cardiomyopathy). The continuous infusion of Fenoterol (2.5 micrograms/min for 60 min) induced the following changes in parameters of pump function: a slight but not yet significant fall of PCPm which we considered as a reference value of LVEDP from 24 +/- 9 to 20 +/- 6 mm Hg (13%); a highly significant increase in CI from 1.96 +/- 04 to 2.71 +/- 0.53 l/min . m2 (39%; p less than 0.001) and in SVI from 18.7 +/- 4.9 to 24.8 +/- 8.1 ml/m2 (32%; p less than 0.01); a clear reduction of TPR from 1374 +/- 427 to 977 +/- 282 dyn . s . cm-5 (28%; p less than 0.001). PVR was reduced from 245 +/- 158 to 192 +/- 85 dyn . s . cm-5 (n.s.). There were no significant changes in right ventricular filling pressure (15 +/- 8 to 15 +/- 9 mm Hg), mean arterial pressure (76 +/- 17 to 75 +/- 16 mm Hg) and heart rate (107 +/- 13 to 117 +/- 23 beats/min). The study indicates that the "selective" beta 2-agonist Fenoterol in severe congestive heart failure produces a significant improvement in pump function. We assume the increase in SV to be due to a positive inotropic effect -- caused by beta 1-stimulation -- and a reduction of impedance to left ventricular ejection by decrease in TPR -- caused by beta 2-stimulation. Thus Fenoterol seems to be useful in treatment of severe congestive heart failure with elevated TPR.

PMID:6114186[PubMed - indexed for MEDLINE]

Publication Types, MeSH Terms, Substances

LinkOut - more resources

Recent Developments in the Design of Orally Bioavailable β3-Adrenergic Receptor Agonists

Masaaki Sawa* and Hiroshi Harada

Chemistry Research Laboratories, Drug Research Division, Dainippon Sumitomo Pharma Co., Ltd., 33-94 Enoki-cho, Suita, Osaka 564-0053, Japan

Abstract: The β_3-adrenergic receptor (β_3-AR) has been shown to mediate various pharmacological and physiological effects such as lipolysis, thermogenesis, and relaxation of the urinary bladder. Activation of the β_3-AR is thought to be a possible approach for the treatment of obesity, type 2 diabetes mellitus, and frequent urination. Therefore, the β_3-AR is recognized as an attractive target for drug discovery. On the other hand, activation of the β_1- or β_2-AR can cause undesirable side effects such as increased heart rate or muscle tremors. Consequently, a number of recent efforts in this field have been directed toward the design of selective agonists for the β_3-AR. This review summarizes recent advances in β_3-AR agonists with an emphasis on recent attempts to create potent, selective and orally bioavailable small-molecule agonists.

Keywords: β_3-adrenergic receptor, G protein-coupled receptor, agonist, obesity, type2 diabetes mellitus, frequent urination, lipolysis, thermogenesis.

INTRODUCTION

β-adrenoceptors (β-ARs) belong to the superfamily of G protein-coupled receptors that consist of seven membrane-spanning domains, three intra- and three extracellular loops, one extracellular N-terminal domain, and one intracellular C-terminal tail [1]. At present three different β-AR subtypes have been identified using pharmacological methods and through cloning of the receptors [1, 2]. β-ARs were originally sub-classified into two different subtypes, β_1- and β_2-ARs by Lands *et al.* in 1967 based on the different physiologic effects of their ligands [3]. This classification has greatly contributed to the elimination of adverse effects as seen with former β-agonists and led to the development of selective β_1- and β_2-AR agonists/antagonists which have been useful in treating cardiovascular diseases and asthma nowadays [4]. In the early 1980s, the existence of a novel β-AR (β_3-AR) was reported primarily in rat adipose tissue [5]. Subsequently, Emorine *et al.* was first to clone human β_3-AR in 1989 and revealed that it mediated metabolic effects such as lipolysis and thermogenesis in adipose tissues [6]. Accordingly, this third β-AR has come to occupy an important position in drug discovery highlighted by its potential role in obesity through its modulation of fat metabolism.

The β_3-AR is mainly located on the surface of both white and brown adipocytes and is stimulated by its endogenous ligands, catecholamines, adrenalin, and noradrenaline. Recent studies indicate that β_3-AR also exists in human heart, gall bladder, gastrointestinal tract, prostate, and urinary bladder detrusor tissues [2]. It has been suggested that stimulation of β_3-AR results in various pharmacological effects such as lipolysis and thermogenesis in adipocytes, reducing of colonic motility, and relaxation of the urinary bladder detrusor. Therefore, a number of laboratories have been engaged in developing β_3-AR agonists for the treatment of metabolic, gastrointestinal and urologic diseases such as obesity, type 2 diabetes, irritable bowel syndrome, and frequent urination and urinary incontinence [For recent reviews, see Ref. 7-12].

During the early stage of β_3-agonist development (represented hereby, BRL-37344, **1**, CL 316,243, **2** and CGP-12177A, **3**), the optimization of agonists was conducted in rodent models for the modulation of adipose tissue in human. These compounds showed potent anti-obesity and anti-diabetic effects in rodent type-II diabetic models and subsequently entered clinical trials. However, these clinical studies have been discontinued because of insufficient efficacy, lack of selectivity (some adverse effects were observed such as increased heart rate and muscle tremors), and/or poor pharmacokinetics [12]. It was not revealed until later that, with experiments using cloned human receptors, these compounds not only had partial β_3-agonistic activity but also showed moderate subtype selectivity because of structural differences between human and rodent β_3-ARs [2, 13]. These facts have led us to recognize the importance of using a cloned human receptor assay and that efficacy in the rodent model does not always effectively translate into the human system. Another important issue in the first generation of β_3-agonists was their poor pharmacokinetics that seemed to result from their characteristic ethanolamine and carboxylic acids [14]. In succeeding years, a large number of β_3-agonists have been synthesized and evaluated using cloned human receptors to ensure efficacy [7-9, 11]. In this review, we summarize recent attempts to create potent, selective and orally bioavailable β_3-AR agonists.

DEVELOPMENT OF β_3-AR AGONISTS

To date, numerous β_3-AR agonists have been identified and evaluated *in vitro* and *in vivo*. The most important feature of these agonists is an aminoalcohol function flanked

*Address correspondence to this author at the Chemistry Research Laboratories, Drug Research Division, Dainippon Sumitomo Pharma Co., Ltd., 33-94 Enoki-cho, Suita, Osaka 564-0053, Japan; E-mail : masaaki-sawa@ds-pharma.co.jp

0929-8673/06 $50.00+.00

by two aromatic regions, which corresponds to the pharmacophore of the endogenous ligands of ARs. Most early β_3-agonists were designed to have carboxylic acids on the right-hand side (RHS) aromatic region since an acid functionality was found to enhance β_3-AR selectivity [15, 16]. However, developments of those agonists were often hampered because of low oral bioavailability. This low bioavailability is most likely due to poor oral absorption which may be attributed to its highly hydrophilic portions, the aminoalcohol and acid moieties. Consequently, recent efforts in this field have been directed toward mainly the optimization of the RHS region to find orally bioavailable β_3-agonists since the aminoalcohol functionality is thought to be necessary for β_3-AR binding. As for the left-hand side (LHS) aromatic region, a minimal variety of successful modifications has been reported thus far. This region, however, also contributes largely to both agonistic and intrinsic activity (IA). In the following discussion, we summarize progress in the optimization of both the LHS and RHS and also in the discovery of novel β_3-AR agonist scaffolds.

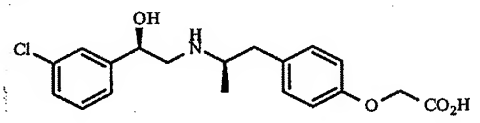

1 (BRL 37344)

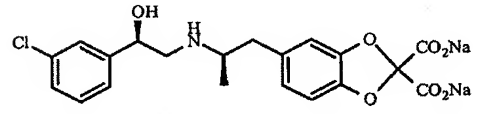

2 (CL 316,243)

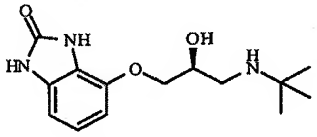

3 (CGP 12177A)

Fig. (1). Representative First Generation of β_3-AR Agonists.

Modification of RHS

Researchers at Merck explored a series of benzenesulfonamide β_3-agonists and identified potent, selective and orally bioavailable compounds [17-26]. A hexylurea derivative **4** (L-757,793) was found to be a potent agonist of human β_3-AR (EC_{50} = 6.3 nM) with high selectivity over β_1- and β_2-ARs (>1000-folds) [17]. The urea moiety, however, was detrimental to oral absorption due to its high polar property. When this compound was administered orally (10 mg/kg) to dogs, no serum glycerol response was recorded. Cyclization of the urea moiety in **4**, to reduce the polarity, produced the cyclic ureido derivatives **5** (L-760,087) and **6** (L-764,646). Although these compounds maintained potency and selectivity, they still showed poor oral bioavailabilities (7% in dogs) [18]. Introduction of a cyclopentane moiety at the terminal alkyl group (**7**, L-766,892) [19] and further optimization afforded the tetrazolone benzenesulfonamide analogue **8** (L-770,644) [20]. L-770,644 was a potent and selective β_3-agonist (EC_{50} = 13 nM, IA = 75%) with high selectivity over β_1- (EC_{50} = 1900 nM, IA = 33%) and β_2-ARs (EC_{50} = 1800 nM, IA = 26%), and showed >100-fold selectivity against a panel of receptors and ion channels. In addition, this compound had significantly superior pharmacokinetics and its oral bioavailability was found to be 27% in both dogs and rats. Subsequent studies in the replacement of the tetrazolone with heterocyclics produced a number of potent β_3-agonists [21-26]. Among them, 4-(trifluoromethyl)phenyl thiazole analogue **9** (L-796,568) was a potent and selective agonist (EC_{50} = 3.6 nM, IA = 94% for β_3-AR; >1300 and >600-fold selectivity against β_1- and β_2-ARs, respectively) [26]. This compound displayed good oral bioavailability in both dogs (%F = 27) and rats (%F = 17), but low bioavailability in monkeys (%F = 4). It also had an exceptionally long half-life (t1/2 >8h) in all species tested [27]. This compound was >100-fold selective for β_3-AR when tested against a panel of receptors and ion channels, and therefore, was chosen as a clinical candidate. Further modification of the benzenesulfonamide group produced indoline analogues **10** [28] and **11** [29]. Indolinesulfonamide **10** had an EC_{50} value of 0.93 nM (IA = 86%) and showed high subtype selectivity (IC_{50} = 2600 and 1300 nM for β_1- and β_2-ARs, respectively). In an *in vivo* study, i.v. administration of compound **10** in anesthetized rhesus monkeys evoked dose-dependent increases in lipolysis and energy expenditure [30]. Despite its high selective profile for monkey β_3-AR (EC_{50} = 0.43 nM, IA = 80% for monkey β_3-AR, >700-fold selective against monkey β_1- and β_2-ARs), compound **10** elicited facial flushing *via* peripheral vasodilatation and reflex

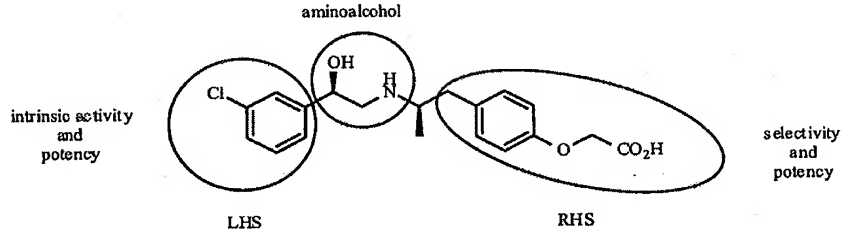

Fig. (2).

tachycardia. It is not certain whether this β_3-AR-evoked vasodilatation was a direct effect of β_3-AR activation in the peripheral vasculature or was a secondary effect to the release or generation of an endogenous vasodilator.

CL 316,243 (**2**) was identified by American Cyanamid (now Wyeth) to have potent activity for the rodent β_3-AR [31], but was subsequently found to be a weak and partial agonist against the human β_3-AR (EC_{50} = 1.15 μM, IA = 63%) [32]. In addition, CL 316,243 showed low oral bioavailability mainly due to the dicarboxylic acid on the RHS [14]. In an effort to enhance potency for human β_3-AR, further exploration was conducted by using a human receptor assay, and compound **12**, possessing a unique piperidine ring on the RHS, was discovered as a lead. After subsequent optimization of **12**, phenylpiperidines **13** [32] and **14** [33], in which the acid moieties were replaced by 2,4-thiazolidinedione and oxadiazolidinedione respectively, were found to be potent and selective human β_3-AR agonists. In *in vivo* tests, both compounds showed significant thermogenic effects (30% increase in thermogenesis) in human β_3-AR transgenic mice (Tg mice) when administered at a dose of 10 mg/kg. Further investigation of substituents on the RHS afforded sulfonamide **15**, with a β_3-agonistic activity (EC_{50} = 4 nM, IA = 100%) and >500-fold selectivity over β_1- and β_2-ARs [34]. Concurrent studies on the optimization of the piperidine analogues gave another series of analogues which possess amino acids on the RHS [35]. Leucine analogue **16** (EC_{50} = 8 nM, IA = 96%) showed an excellent agonistic profile and selectivity for β_3-AR (Ki = >100 and 3.4 μM against β_1 and β_2, respectively). Moreover, compound **16** elicited significant thermogenesis (53% increase) in Tg mice *in vivo*.

The Wyeth group also examined other possible modifications to the piperidine scaffold and disclosed 4-aminomethylpiperidine **17** [36] and 4-aminopiperidine urea **18** [37]. Both compounds were potent β_3-agonists with good selectivity and exhibited thermogenesis effects *in vivo*.

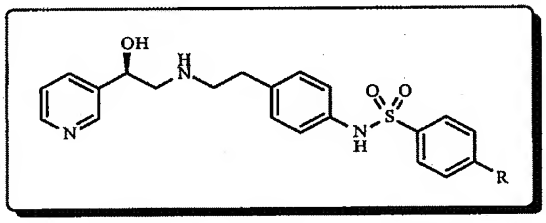

4: R = (L-757,793)

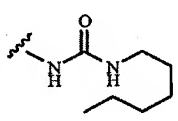

EC_{50} (IA)	β_3	6.3 nM (70%)
	β_1	7300 nM (31%)
	β_2	(0%@1000nM)
IC_{50}	β_3	44 nM
	β_1	8000 nM
	β_2	3000 nM

5: R = (L-760,087)

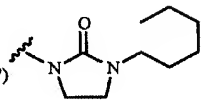

EC_{50} (IA)	β_3	18 nM (62%)
IC_{50}	β_1	5000 nM
	β_2	2300 nM

6: R = (L-764,646)

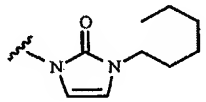

EC_{50} (IA)	β_3	14 nM (56%)
IC_{50}	β_3	81 nM
	β_1	18000 nM
	β_2	12000 nM

7: R = (L-766,892)

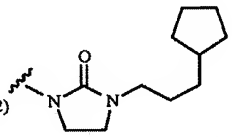

EC_{50} (IA)	β_3	5.7 nM (64%)
IC_{50}	β_1	2400 nM
	β_2	760 nM

8: R = (L-770,644)

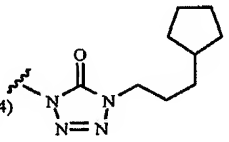

EC_{50} (IA)	β_3	13 nM (75%)
	β_1	1900 nM (33%)
	β_2	1800 nM (26%)
IC_{50}	β_3	92 nM
	β_1	3400 nM
	β_2	1600 nM

9: R = (L-796,568)

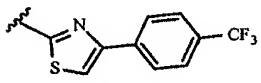

EC_{50} (IA)	β_3	3.6 nM (94%)
	β_1	4800 nM (24%)
	β_2	2400 nM (25%)
IC_{50}	β_3	46 nM
	β_1	2300 nM
	β_2	2300 nM

Fig. (3). Structures of Benzenesulfonamide β_3-AR Agonists and Their Activity towards Human β-ARs.

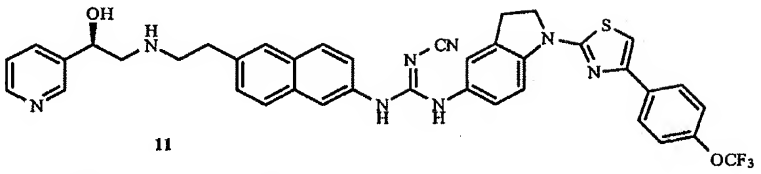

11

EC_{50} (IA)	β_3	19 nM (62%)
	β_1	(2%@10000nM)
	β_2	(11%@10000nM)
IC_{50}	β_1	2300 nM
	β_2	7100 nM

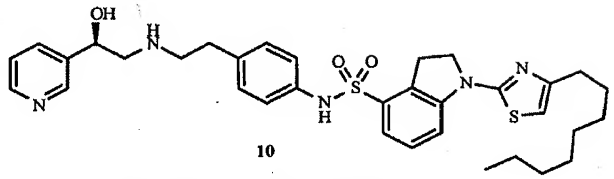

10

EC_{50} (IA)	β_3	0.93 nM (86%)
IC_{50}	β_1	2600 nM
	β_2	1300 nM

Fig. (4). Structures of Indolinesulfonamide β_3-AR Agonists and Their Activity towards Human β-ARs.

Researchers at Bristol-Myers Squibb screened their compound library and identified a subset of hit compounds which were a structurally related series of 4-hydroxy-3-methylsulfonanilidoethanolamines. Optimization of a lead compound having a phenethyl moiety on the RHS led to diarylethylamine **19** (BMS-194449) [38]. This compound showed potent activity for β_3-AR (Ki = 160 nM, IA = 77%) and good selectivity (Ki = 1280 and 1120 nM against β_1- and β_2-ARs, respectively). However, BMS-194449 had an unfavorable pharmacokinetic profile in rats; its oral bioavailability was less than 2%, mainly due to glucuronidation of benzylic and phenolic hydroxyl groups.

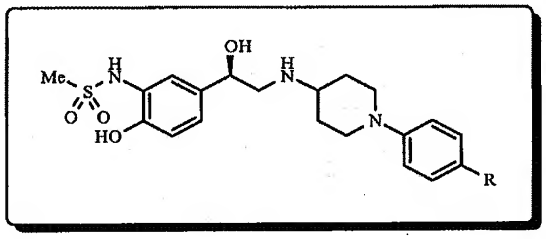

12: R = —COOH

EC_{50} (IA)	β_3	220 nM (120%)

13: R =

EC_{50} (IA)	β_3	10 nM (119%)
	β_1	1190 nM (67%)
	β_2	2720 nM (82%)
Ki	β_1	3280 nM
	β_2	1570 nM

14: R =

EC_{50} (IA)	β_3	20 nM (100%)
	β_1	5180 nM (59%)
	β_2	14900 nM (29%)
Ki	β_1	9490 nM
	β_2	74000 nM

15: R =

EC_{50} (IA)	β_3	4 nM (100%)
	β_1	5000 nM (45%)
	β_2	2000 nM (51%)

16: R =

EC_{50} (IA)	β_3	8 nM (96%)
	β_1	(0.08%)
	β_2	(0.06%)
Ki	β_1	>100000 nM
	β_2	3400 nM

Fig. (5). Structures of Phenylpiperidine β_3-AR Agonists and Their Activity towards Human β-ARs.

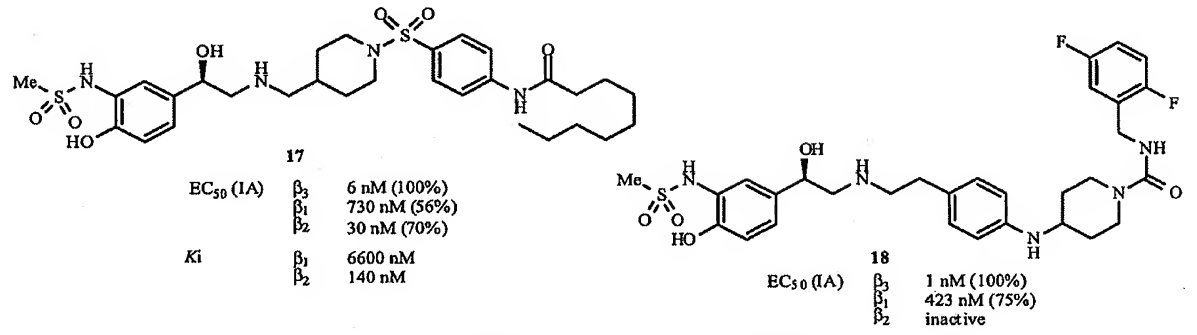

Fig. (6). Structures of Piperidine β_3-AR Agonists and Their Activity towards Human β-ARs.

Intravenous administration of BMS-194449 to 6 volunteers showed no separation between the onset of lipolysis and β_2-AR mediated prolongation of the QT interval. Thus, further studies with BMS-194449 were terminated.

Further optimization of the phenethyl analogue produced compounds **20** (BMS-196085, *Ki* =25 nM, IA = 95%) with an excellent selectivity against β_1 and β_2-ARs (*Ki* = 756 and 125 nM, respectively) [39]. Unfortunately, BMS-196085 showed poor oral bioavailability (<5%) because of extensive glucuronidation in monkeys. In an initial clinical proof-of-concept study, bolus i.v. administration of BMS-196085 evoked increased levels of free fatty acids in the blood plasma. However, a 2-week continuous i.v. infusion of BMS-196085 resulted in tachycardia and failed to produce statistically significant changes in the resting metabolic rate.

Further explorations of this phenethyl lead compound led to the identification of diethyl phosphonate **21** (BMS-201620), a potent β_3-agonist (*Ki* = 93 nM, IA = 93%) with excellent subtype selectivity (*Ki* = 4732 and 18042 nM for β_1- and β_2-ARs, respectively) [40]. In an *in vivo* study in anesthetized African green monkeys, BMS-201620 showed a large safety margin between separation of β_3-mediated effects and β_1- and β_2-dependent events. This margin was superior to that of BMS-1944493 and BMS-196085. BMS-201620, however, showed unfavorable biophysical and PK profiles in rats and African green monkeys, in a similar manner as former clinical candidates; its oral bioavailability was less than 1–2%. Despite its unfavorable PK profile, this compound was chosen as a clinical candidate. Intravenous administration of BMS-201620 to 6 volunteers produced no separation between the onset of lipolysis and prolongation of the QT interval, and thus, further studies were terminated.

Glaxo Wellcome (now GlaxoSmithKline) disclosed a series of β_3-agonists having an anilinophenylacetic acid on the RHS as exemplified by GR9803 (**22**) [41]. This compound was a potent full agonist of human β_3-AR (EC_{50} = 16 nM, IA = 117%) but showed moderate subtype selectivity. After an extensive structure-activity relationship (SAR) study on the RHS substituents, compound **23**, which has an acylsulfonamide moiety as a carboxylic acid isostere, was identified as a potent and selective β_3-agonist (EC_{50} = 1.3 nM, IA = 98%) [42]. Despite its relatively short half-life (1.0 h) in dogs, compound **23** was found to be orally active in mice thermogenesis studies.

In the early 1990s, Dainippon (now Dainippon Sumitomo) identified a series of indolylalkylamines as potent β_3-agonists. Extensive SAR study on substituents of the indole ring produced a potent and selective β_3-agonist, AJ-9677 (**24**) [43, 44]. Interestingly, it is not only a potent full agonist of human β_3-AR (EC_{50} = 0.062 nM, IA =

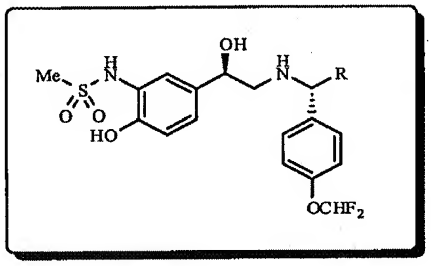

19: R = 4-CHF_2O-Phenyl (BMS-194449)

Ki (IA) β_3 160 nM (77%)
β_1 1280 nM
β_2 1120 nM

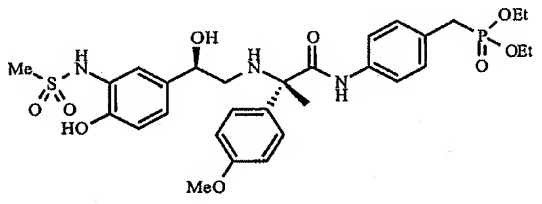

20: R = Benzyl (BMS-196085)

Ki (IA) β_3 25 nM (95%)
β_1 756 nM (63%)
β_2 125 nM (45%)

21 (BMS-201620)

Ki (IA) β_3 93 nM
β_1 4743 nM
β_2 18042 nM

Fig. (7). Structures of β_3-AR Agonists developed by Bristol-Myers Squibb.

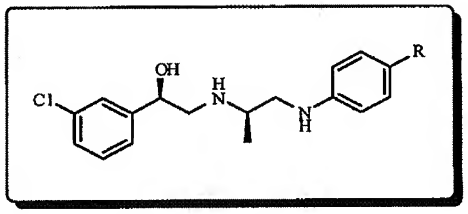

22: R = CH_2CO_2H (GR-9803)

EC_{50} (IA)	β_3	16 nM (117%)
	β_1	79 nM (24%)
	β_2	50 nM (90%)
IC_{50}	β_1	1000 nM
	β_2	800 nM

23: R =

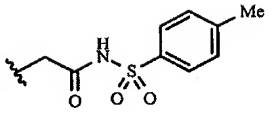

EC_{50} (IA)	β_3	1.3 nM (98%)
	β_1	630 nM (23%)
	β_2	79 nM (34%)
IC_{50}	β_1	2000 nM
	β_2	5000 nM

Fig. (8). Structures of β_3-AR Agonists developed by GlaxoSmithKline.

116%) but also a strong full agonist of rodent β_3-AR (EC_{50} = 0.016 nM, IA = 110%). Chronic oral administration of AJ-9677 to genetically diabetic obese KK-Ay/TA mice for 14 days significantly inhibited body weight gain and decreased glucose, insulin, free fatty acid (FFA), and triglyceride concentrations in plasma [45]. Moreover, AJ-9677 resulted in a marked increase in the expression of uncoupling protein-1 (UCP-1) in white adipose tissues (20- to 80-fold) and upregulation of GLUT4 mRNA and protein levels in both white and brown adipose tissues. AJ-9677 reduced the total weight of white adipose tissue by converting large adipocytes into small adipocytes through increased lipolysis and the induction of UCPs that are associated with the reduction of TNF-α and FFA levels. On the basis of this pharmacological profile, AJ-9677 entered into clinical development as a drug for the treatment of type 2 diabetes and obesity in 1999. Unfortunately, while there has been no safety concerns during the course of the trials, these clinical studies have not been able to show enough efficacy to continue the further development of this agent [46].

Subsequent optimization of the indole derivatives identified a thiophenesulfonamide derivative **25**, which substituted a methansulfonate group in place of the terminal carboxylic acid [47]. Compound **25** was found to be a highly potent β_3-AR agonist (EC_{50} = 0.21 nM, IA = 97%) with excellent selectivity for β_3-AR over β_1- and β_2-ARs (210- and 86-fold, respectively). Unfortunately, this compound had extremely low oral bioavailability due to the lack of cellular permeability. Further effort investigating the

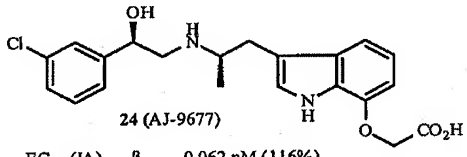

24 (AJ-9677)

EC_{50} (IA)	β_3	0.062 nM (116%)
	β_1	6.4 nM (26%)
	β_2	13 nM (26%)

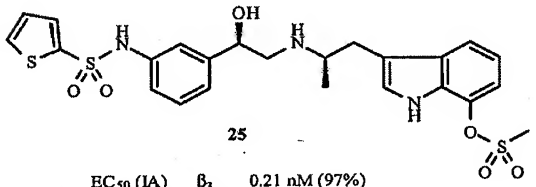

25

EC_{50} (IA)	β_3	0.21 nM (97%)
	β_1	44 nM (36%)
	β_2	18 nM (50%)
Ki	β_3	4.0 nM
	β_1	66 nM
	β_2	48 nM

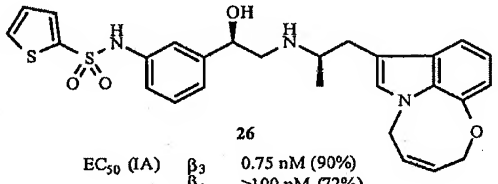

26

EC_{50} (IA)	β_3	0.75 nM (90%)
	β_1	>100 nM (72%)
	β_2	(27%@1000nM)
Ki	β_3	3.1 nM
	β_1	550 nM
	β_2	150 nM

Fig. (9). Structures of Indole-based β_3-AR Agonists and Their Activity towards Human β-ARs.

effect of various substituents on the indole ring identified a series of 1,7-cyclized indole analogues [48]. Among them, compound **26**, an eight-membered ring analogue with a double bond on its 1,7-linker portion, was found to be a potent β_3-AR agonist (EC_{50} = 0.75 nM, IA = 90%) with extremely high selective profiles for β_3-AR over β_1- and β_2-ARs. In addition, this series of 1,7-cyclized indole derivatives all showed high cellular permeability in Caco-2 cell membrane assays. These results revealed the potential of 1,7-linked tricyclic indole-based derivatives as a new leading set of candidates for human β_3-AR agonists with good oral bioavailability.

Researchers at Pfizer have developed a series of sulfamide-based human β_3-AR agonists [49]. cis-3,5-Dimethylmorpholinylsulfamide **27** was found to be a potent β_3-agonist (EC_{50} = 8 nM, IA = 85%) and showed high selectivity against β_1- and β_2-ARs (>1300- and >200-fold, respectively). Although the bioavailability of compound **27** was not determined, this compound showed low human microsomal intrinsic clearance. *In vivo*, compound **27** produced a 35% increase in oxygen consumption relative to the control animals when dosed orally in rats at 30 mg/kg. The fact that a similar *in vivo* response was seen from intraperitoneal administration suggests compound **27** has good oral absorption.

Phenylurea **28**, discovered by the Fujisawa group (now Astellas), is a highly potent agonist of human β_3-AR (EC_{50} = 0.5 nM) with excellent selectivity over β_1- and β_2-ARs (40- and >200-fold, respectively) [50]. Interestingly, this compound has a characteristic hydroxymethyl group at the alpha position of the aminoalcohol, and removal of this hydroxymethyl group resulted in a decrease of both potency and selectivity. Pharmacokinetic studies of compound **28** revealed that it has different oral bioavailability between rats and dogs (F = 1.1% and 20.3%, respectively). These results were attributed to differences in metabolic stability between species.

Benzodioxine derivative **29** (N-5984), synthesized by the Nisshin Flour Milling group, showed good agonistic potency for β_3-AR (EC_{50} = 1.7 nM) but partial intrinsic activity (IA = 52%) [51]. In the binding assay, the *Ki* value of N-5984 (*Ki* = 30 nM) was 14 and 220 times more potent than those of BRL37344 and CL 316,243, respectively. N-5984 is currently under clinical evaluation.

In the early 1990s, Sanofi-Midy (now Sanofi-Aventis) identified a series of phenylethanolaminotetralins (PEATs) as selective β_3-AR agonists in rodents [52]. In the series of PEATs, SR-58611A (**30**) was found to have an excellent profile as a β_3-AR agonist [53]. SR-58611A was a potent inhibitor of rat colonic motility (EC_{50} = 3.5 nM) with

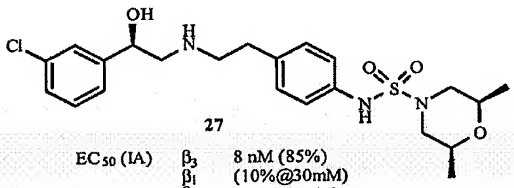

27

EC_{50} (IA)	β_3	8 nM (85%)
	β_1	(10%@30mM)
	β_2	(8%@30mM)
Ki	β_3	7 nM
	β_1	9750 nM
	β_2	1400 nM

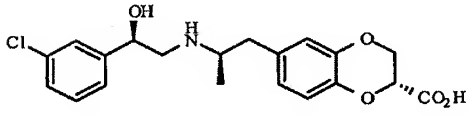

29 (N-5984)

EC_{50} (IA)	β_3	1.7 nM (52%)
Ki	β_3	30 nM
	β_1	2200 nM
	β_2	600 nM

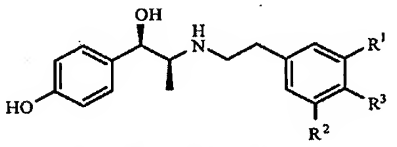

31 (Ritodrine): R^1 = H, R^2 = H, R^3 = OH
32: R^1 = R^2 = Cl, R^3 = $NHCH_2CO_2H$
33 (KUL-7211): R^1 = R^2 = H R^3 = OCH_2CO_2H

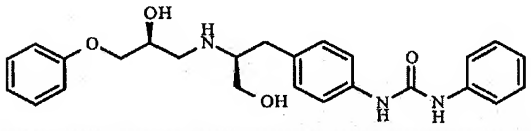

28

EC_{50}	β_3	0.5 nM
	β_1	20 nM
	β_2	>100 nM

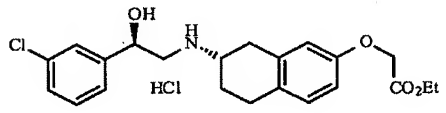

30 (SR-58611A)

EC_{50} (IA)	β_3	25 nM (123%)
	β_1	12000 nM (96%)
	β_2	36 nM (87%)
Ki	β_3	6640 nM
	β_1	38500 nM
	β_2	187 nM

Fig. (10). Structures of β_3-AR Agonists and Their Activity towards Human β-ARs.

minimal cross-reactivity on guinea-pig atrium or rat uterus ($EC_{50} \geq 30000$ and 500 nM, respectively). *In vivo* studies showed that SR-58611A had a good bioavailabiliy and colonic selectivity in conscious rats and dogs. SR-58611A was developed as a potential treatment for irritable bowel syndrome and obesity, and then for depression. In a clinical study for assessment of the effects of SR-58611A on rectal sensory thresholds and compliance during isobaric distension (40 or 240 mg, p.o.), SR-58611A significantly increased the threshold for pain compared with placebo ($p < 0.01$). Neither dose significantly affected rectal compliance [54].

Recently, it has been suggested that β_3-ARs play a significant role in urinary storage [55-60]. In order to discover a new approach for the treatment of urinary bladder dysfunction, the Kissei group has employed ritodrine **31** (a β_2-AR agonist), as a lead compound and synthesized a series of the ritodrine derivatives [61-64]. Dichloroaniline **32** (EC_{50} = 14 nM, IA = 85%) exhibited potent β_3-AR-mediated relaxation of ferret detrusors and high subtype selectivity based on experiments using rat atriums (β_1-AR, 2071-fold) and rat uterus (β_2-AR, 1000-fold) [61]. Compound **32** also showed nearly full agonistic activity to the cloned human β_3-AR. The intravenous administration of this compound significantly reduced urinary bladder pressure in anesthetized male rats (ED_{50} = 48 μg/kg) without cardiovascular side effects due to β_1- or β_2-AR mediation.

A more recent study showed that both β_2- and β_3-ARs coexist in the human ureter and that these receptors mediate relaxation induced by adrenergic stimulation. β_2- and β_3-AR dual agonists therefore might prove clinically useful for relieving ureteral colic and promoting stone passage [65, 66]. Phenoxyacetic acid **33** (KUL-7211) was found to be a potent and selective β_2- and β_3-dual agonist in an isolated rat organ assay [64]. They determined the selectivity of this dual agonist for both β_2 and β_3-AR against β_1-AR based on the ratio of inhibition of spontaneous uterine contraction (*via* β_2-AR stimulation) or inhibition of colonic contraction (*via* β_3-AR stimulation) versus an increase in atrial rate (*via* β_1-AR stimulation), respectively. The selectivity of KUL-7211 for β_2 and β_3-AR were 56.3 and 242.2-folds, respectively. In addition, KUL-7211 relaxed KCl-induced tonic contractions in both rabbit (EC_{50} = 1.4 μM, whose ureteral relaxation is mediated *via* β_2-AR stimulation) and canine (EC_{50} = 0.30 μM, *via* β_3-AR stimulation) isolated ureters in a concentration dependent manner. Currently, clinical evaluation of KUL-7211 is ongoing.

Modification of LHS

The majority of β_3-AR agonists described to date possess a 3-chlorophenyl group attached directly to the aminoalcohol framework. This was discovered by Beecham as the first β_3-AR agonist, BRL37344 [5, 67, 68]. Bristol-Myers Squibb and Wyeth independently have reported a series of 4-hydroxy-3-methylsulfonanilidoethanolamine derivatives, which are potent agonists of human β_3-AR as described above. Researchers at Dainippon reported a series of arylsulfonamide derivatives such as compound **25** [47, 69], which have excellent agonistic profiles *in vitro* but poor oral bioavailability in rats due to low cell permeability [70]. In an effort to improve their oral bioavailability, the effect on both their agonistic potency and Caco-2 cell permeability by replacing the sulfonamide portion on the LHS was investigated [70]. Replacement of the benzenesulfonamide moiety on the LHS with benzenesulfonate, benzyloxy, benzylamine, or methylation of the N-H proton on the benzenesulfonamide resulted in remarkable improvements in cell permeability. This indicated that the sulfonamide portion is detrimental to cell permeability. Introduction of cinnamylamine on the LHS provided compound **34**, which is a potent agonist of β_3-AR (EC_{50} = 1.0 nM, IA = 97%) and exhibited good oral bioavailability in rats (21%).

Aryloxypropanolamines are another structural class of β_3-AR agonists originally derived from β-blocker agents. Several groups have explored aryloxypropanolamine derivatives and disclosed potent and selective agonists of human β_3-AR [50, 71-81]. Aryloxypropanolamines, however, often exhibit strong antagonistic activity towards β_1 and β_2 receptors which may cause unwanted side effects [32, 77]. CGP 12177 (**3**) was initially described as a high-affinity antagonist of β_1- and β_2-ARs [82, 83], and later it was demonstrated to be a partial agonist of the rodent and human β_3-AR [84-86]. The relatively high potency of CGP 12177 has prompted the development of other β_3-AR selective aryloxypropanolamines with higher efficacies, such as LY-362884 (**35**), which was developed by Eli Lilly [79]. Further optimization on the left-hand side of LY-362884 produced compound **36** (LY-377604), an orally available carbazole analogue with a potent β_3-AR agonistic activity (EC_{50} = 4 nM) [80, 81]. LY-377604 entered into clinical development as a drug for the treatment of type 2 diabetes and obesity.

The Wyeth group has reported novel cyclic sulfonamide derivatives with aryloxymethyl groups on the LHS, **37** and **38**, that are potent β_3-AR agonists and have excellent selectivity against β_1- and β_2-AR [77, 78]. Compound **37** was active *in vivo* in β_3 transgenic mice with a 30% increase in thermogenesis when dosed intraperitoneally at 10 mg/kg [77].

In 1998, Merck proposed a series of aryloxypropanolamines with an arylsulfonamide on the RHS [72-74]. The n-hexyl urea analogue **39** (L-755,507), displayed an excellent activity profile as an extremely potent human β_3-AR agonist (EC_{50} = 0.43 nM), with >440-fold selectivity over β_1 and β_2 binding [73]. Furthermore, it was only a weak partial agonist of β_1- and β_2-AR (IA = 25 and 2%, respectively). Acute exposure of rhesus monkeys to L-555,507 elicited lipolysis and metabolic rate elevation, and chronic exposure (4 weeks) increased UCP-1 expression in rhesus brown adipose tissue [87]. Unfortunately, this compound had extremely poor oral bioavailability (<1% in dogs) presumably due to the polar and highly solvated urea moiety [74].

Substitution of both the phenol on the LHS and the urea portion on the RHS led to 3-pyridyloxypropanolamine **40** (L-750,355), which was a selective partial agonist of the human β_3-AR (EC_{50} = 10 nM, IA = 49%) [74]. While the oral bioavailability in rats of L-750,355 was still low (4%), significant improvement in its oral bioavailability was observed in dogs (47%). This result indicated that the replacement of the phenol in the phenoxypropanolamine series with a pyridine moiety results in an increased oral

bioavailability, particularly, in dogs. Despite its highly selective profiles in monkeys, intravenous administration of L-750,355 to anesthetized rhesus monkeys evoked dose-dependent glycerolemia and tachycardia [88]. The β-blocker, propranolol, completely inhibited L-750355-induced tachycardia but did not block L-750355-induced lipolysis, suggesting that the increase in heart rate was mediated *via* activation of β_1-AR. These observations suggested that L-750355-induced tachycardia may not have been mediated *via* direct activation of cardiac β_1-AR. Rather, it might be reflexogenic in origin, consequent upon evoked increases in metabolic rate and direct β_3-AR mediated peripheral vasodilatation [30].

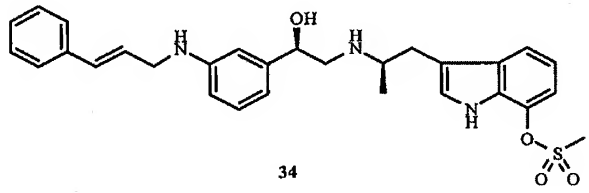

34

EC_{50} (IA) β_3 1.0 nM (97%)
β_1 (36%@1000nM)
β_2 13 nM (81%)

Ki β_3 15 nM
β_1 48 nM
β_2 25 nM

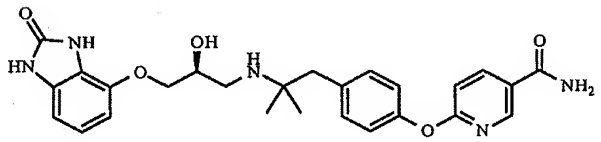

35
(LY-362884)

EC_{50} (IA) β_3 30 nM (98%)

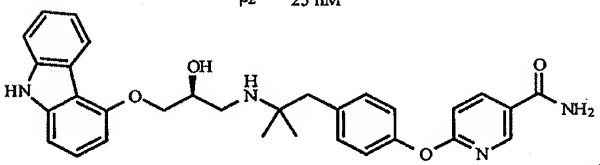

36
(LY-377604)

EC_{50} (IA) β_3 4.3 nM

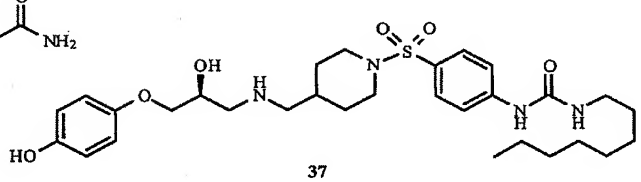

37

EC_{50} (IA) β_3 49 nM (110%)
β_1 887 nM (16%)

IC_{50} β_1 6156 nM
β_2 268 nM

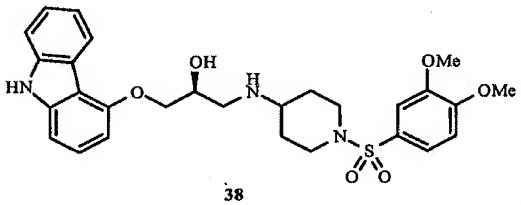

38

EC_{50} (IA) β_3 20 nM (120%)
β_1 >100000 nM (14%)
β_2 >100000 nM (2%)

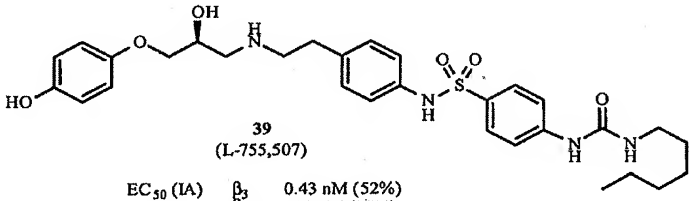

39
(L-755,507)

EC_{50} (IA) β_3 0.43 nM (52%)
β_1 580 nM (25%)
β_2 >10000 nM (2%)

IC_{50} β_3 13 nM
β_1 200 nM
β_2 190 nM

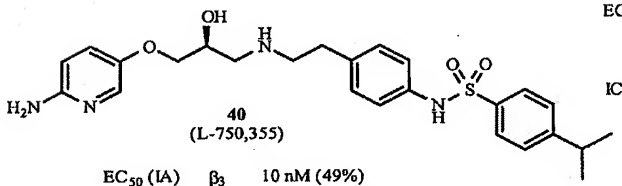

40
(L-750,355)

EC_{50} (IA) β_3 10 nM (49%)
β_1 3175 nM (33%)
β_2 >10000 nM (3.7%)

IC_{50} β_3 49 nM
β_1 3180 nM
β_2 526 nM

Fig. (11). Structures of β_3-AR Agonists having various LHS and Their Activity towards Human β-ARs.

Development of New Scaffolds

It would be of great interest to investigate alternative scaffolds to the aminoalcohols used in typical β_3-AR agonists because the highly hydrophilic aminoalcohol moiety is often detrimental to oral absorption. Trimetoquinol **41** (TMQ), used clinically in Japan as a bronchorelaxant, is a known potent β_3-AR agonist (EC_{50} = 1.7 nM, IA = 92%) [89, 90], but exhibits only marginal selectivity over the β_1 and β_2-ARs [91]. Some laboratories, therefore, have focused on structural modifications of TMQ in order to develop selective β_3-AR agonists [91-93].

Merck has disclosed a novel series of β_3-AR agonists derived from TMQ [91]. 4,4-Biphenyl derivative **42** is of particular interest because it was a very potent β_3-AR agonist (EC_{50} = 6 nM, IA = 91%) and exhibits excellent selectivity over binding to β_1- and β_2-ARs (>300-folds).

Researchers at the University of Tennessee have investigated catechol bioisosteres in an effort to improve the selectivity of TMQ [92, 93]. Aminothiazole **43** was found to be a partial agonist of β_3-AR (EC_{50} = 112 nM, IA = 67%) and did not activate β_1- and β_2-ARs. It had, however, weak binding affinity for β_3-AR (*Ki* = 1480 nM), and thus, did not show any selectivity over binding to β_1- and β_2-ARs (*Ki* = 724 and 427 nM, respectively) [92].

CONCLUDING REMARKS

To date, numerous β_3-AR agonists have been identified, of which several compounds have entered clinical trials for different indications including type 2 diabetes, obesity, depression, irritable bowel syndrome, and overactive bladder. Several excellent reviews on these compounds in clinical trials have been published [2, 10-12, 94]. Nevertheless, most clinical studies of early β_3-agonists have been discontinued because of a lack of efficacy and/or oral bioavailability. The failure of most clinical trials with these early β_3-agonists seems to be attributed to the lack of agonistic activity and/or moderate selectivity for the human receptors since these compounds were developed based on rodent models. Namely, antagonistic and/or agonistic activity for β_1- and β_2-receptors results in unwanted side effects such as tachycardia and/or tremors [95, 96] that limits the treatment dose. These clinical findings reinforced the importance of developing selective β_3-AR agonists using cloned human receptor assays.

Although clinical developments of the early β_3-agonists were disappointing, several orally active β_3-agonists are still currently under clinical trails as shown in Table **1**. Despite the promising effects of β_3-AR agonists in rodents, some clinical trials for the treatment of obesity and diabetes have been halted presumably due to lack of efficacy in humans [94]. In rodents, β_3-ARs are abundantly expressed in white and brown adipose tissues [97]. In humans, however, β_3-ARs are abundant in brown adipose tissues, but only modest amounts of β_3-AR mRNA have been detected in white adipose tissues [98]. Consequently, therapeutic use of β_3-AR agonists for the treatment of obesity and diabetes in humans seems to be open to questions. Recent studies indicate that the amount of brown adipose tissues in human, the key tissues for energy expenditure, may be insufficient to

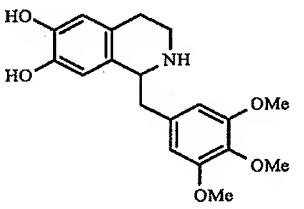

41 (Trimetoquinol, TMQ)

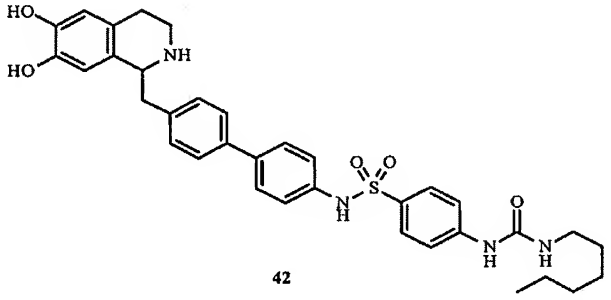

42

EC_{50} (IA)	β_3	6 nM (91%)
	β_1	1800 nM (44%)
	β_2	340 nM (67%)
IC_{50}	β_3	9.4 nM
	β_1	3000 nM
	β_2	3400 nM

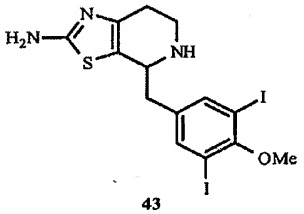

43

EC_{50} (IA)	β_3	112 nM (67%)
	β_1	(<5%)
	β_2	(<5%)
Ki	β_3	1480 nM
	β_1	724 nM
	β_2	427 nM

Fig. (12). Structures of TMQ-based β_3-AR Agonists and Their Activity towards Human β-ARs.

Table 1. Summary of β_3-AR Agonists in Current Clinical Trials

Product [Ref.]	Company	Highest Development Phase	Indication
SR-58611 [99]	Sanofi-Aventis	Phase III	Depression
Solabegron (GW-427353) [101]	GlaxoSmithKline	Phase II	Type 2 diabetes, Overactive bladder
L-796568 [104, 105]	Merck	Phase II	Obesity
LY-377604 [106]	Eli Lilly	Phase I	Type 2 diabetes, Obesity
YM-178 [102]	Astellas	Phase II	Overactive bladder
KUC-7483 [103]	Kissei (Originator) Boehringer Ingelheim	Phase I	Overactive bladder, Urinary incontinence
KUL-7211 [103]	Kissei	Phase I	Urolithiasis
N-5984 [107]	Nisshin Kyorin	Phase II	Type 2 diabetes, Obesity

produce satisfactory metabolic effects by β_3-AR agonists. More fundamental information will be necessary to elucidate whether or not more satisfactory results can be achieved with β_3-AR agonists for the treatment of obesity and Type 2 diabetes.

Other potential therapeutic uses of β_3-AR agonists are for the treatment of depression, irritable bowel syndrome, and overactive bladder (Table 1). SR-58611 is currently being evaluated in Phase III trials for depression in France [99]. In a Phase IIa trial in patients with severe recurrent depression, SR-58611 was well tolerated and showed superior efficacy compared to fluoxetine (Selective Serotonin Reuptake Inhibitor, SSRI). A Phase IIb study demonstrated comparable efficacy and tolerability to paroxetine (SSRI). However, it is still unclear whether the antidepressant effect by SR-58611 is mediated *via* β_3-AR activation because β_3-ARs appear to be absent in the brain in both rodents and humans [2, 100]. SR-58611 was also in phase II clinical trials for irritable bowel syndrome in France but no recent development has been reported for this indication [99]. Solabegron (GW-427353) [101], YM-178 [102], KUL-7211 and KUC-7483 [103] are currently in Phase I/II clinical trials for the treatment of overactive bladder, urinary incontinence, or urolithiasis but no detailed information is available.

Continuing clinical studies will clarify the physiologic effects mediated by β_3-AR and elucidate the potential therapeutic uses of β_3-AR agonists in humans.

ACKNOWLEDGEMENT

We would like to thank Ms. Junko Nishino for her considerable assistance with reference database searches.

REFERENCES

[1] Strosberg, A.D. *Protein. Sci.*, **1993**, *2*, 1198.
[2] Strosberg, A.D. *Annu. Rev. Pharmacol. Toxicol.*, **1997**, *37*, 421.
[3] Lands, A.M.; Arnold, A.; McAuliff, J.P.; Luduena, F.P.; Brown, T.G. Jr. *Nature*, **1967**, *214*, 597.
[4] Emilien, G.; Maloteaux, J.M. *Eur. J. Clin. Pharmacol.*, **1998**, *53*, 389.
[5] Arch, J.R.; Ainsworth, A.T.; Cawthorne, M.A.; Piercy, V.; Sennitt, M.V.; Thody, V.E.; Wilson, C.; Wilson, S. *Nature*, **1984**, *309*, 163.
[6] Emorine, L.J.; Marullo, S.; Briend-Sutren, M.M.; Patey, G.; Tate, K.; Delavier-Klutchko, C.; Strosberg, A.D. *Science*, **1989**, *245*, 1118.
[7] Dow, R.L. *Exp. Opin. Invest. Drugs*, **1997**, *6*, 1811.
[8] Weber, A.E. *Ann. Rep. Med. Chem.*, **1998**, *33*, 193.
[9] Kordik, C.P.; Reitz, A.B. *J. Med. Chem.*, **1999**, *42*, 181.
[10] Weyer, C.; Gautier, J.F.; Danforth, E. Jr. *Diabet.. Metab.*, **1999**, *25*, 11.
[11] Hu, B.; Jennings, L.L. *Prog. Med. Chem.*, **2003**, *41*, 167.
[12] de Souza, C.J.; Burkey, B.F. *Curr. Pharm. Des.*, **2001**, *7*, 1433.
[13] Strosberg, A.D.; Pietri-Rouxel, F. *Trends. Pharmacol. Sci.*, **1996**, *17*, 373.
[14] Sum, F.W.; Gilbert, A.; Venkatesan, A.M.; Lim, K.; Wong, V.; O'Dell, M.; Francisco, G.; Chen, Z.; Grosu, G.; Baker, J.; Ellingboe, J.; Malamas, M.; Gunawan, I.; Primeau, J.; Largis, E.; Steiner, K. *Bioorg. Med. Chem. Lett.*, **1999**, *9*, 1921.
[15] Beeley, L.J.; Berge, J.M.; Chapman, H.; Dean, D.K.; Kelly, J.; Lowden, K.; Kotecha, N.R.; Morgan, H.K.A.; Rami, H.K.; Thompson, M.; Vongb, A.K.K.; Ward, R.W. *Bioorg. Med. Chem. Lett.*, **1997**, *7*, 219.
[16] Sher, P.M.; Mathur, A.; Fisher, L.G.; Wu, G.; Skwish, S.; Michel, I.M.; Seiler, S.M.; Kenneth, E. J.; Dickinson, K.E.J. *Bioorg. Med. Chem. Lett.*, **1997**, *7*, 1583.
[17] Naylor, E.M.; Colandrea, V.J.; Candelore, M.R.; Cascieri, M.A.; Colwell, L.F. Jr.; Deng, L.; Feeney, W.P.; Forrest, M.J.; Hom, G.J.; MacIntyre, D.E.; Strader, C.D.; Tota, L.; Wang, P.R.; Wyvratt, M.J.; Fisher, M.H.; Weber, A.E. *Bioorg. Med. Chem. Lett.*, **1998**, *8*, 3087.
[18] Parmee, E.R.; Naylor, E.M.; Perkins, L.; Colandrea, V.J.; Ok, H.O.; Candelore, M.R.; Cascieri, M.A.; Deng, L.; Feeney, W.P.; Forrest, M.J.; Hom, G.J.; MacIntyre, D.E.; Miller, R.R.; Stearns, R.A.; Strader, C.D.; Tota, L.; Wyvratt, M.J.; Fisher, M.H.; Weber, A.E. *Bioorg. Med. Chem. Lett.*, **1999**, *9*, 749.
[19] Naylor, E.M.; Parmee, E.R.; Colandrea, V.J.; Perkins, L.; Brockunier, L.; Candelore, M.R.; Cascieri, M.A.; Colwell, L.F. Jr.; Deng, L.; Feeney, W.P.; Forrest, M.J.; Hom, G.J.; MacIntyre, D.E.; Strader, C.D.; Tota, L.; Wang, P.R.; Wyvratt, M.J.; Fisher, M.H.; Weber, A.E. *Bioorg. Med. Chem. Lett.*, **1999**, *9*, 755.
[20] Shih, T.L.; Candelore, M.R.; Cascieri, M.A.; Chiu, S.H.; Colwell, L.F. Jr.; Deng, L.; Feeney, W.P.; Forrest, M.J.; Hom, G.J.; MacIntyre, D.E.; Miller, R.R.; Stearns, R.A.; Strader, C.D.; Tota, L.; Wyvratt, M.J.; Fisher, M.H.; Weber, A.E. *Bioorg. Med. Chem. Lett.*, **1999**, *9*, 1251.
[21] Feng, D.D.; Biftu, T.; Candelore, M.R.; Cascieri, M.A.; Colwell, Deng; L, Feeney; WP, Forrest; MJ, Hom; GJ, MacIntyre; DE, Miller; RR, Stearns; RA, Strader; CD, Tota; L, Wyvratt; MJ, Fisher; MH, Weber; A.E. *Bioorg. Med. Chem. Lett.*, **2000**, *10*, 1427.
[22] Biftu, T.; Feng, D.D.; Liang, G.B.; Kuo, H.; Qian, X.; Naylor, E.M.; Colandrea, V.J.; Candelore, M.R.; Cascieri, M.A.; Colwell,

L.F. Jr.; Forrest, M.J.; Hom,; G.J.; MacIntyre, D.E.; Stearns, R.A.; Strader, C.D.; Wyvratt, M.J.; Fisher, M.H.; Weber, A.E. *Bioorg. Med. Chem. Lett.*, **2000**, *10*, 1431.

[23] Ok, H.O.; Reigle, L.B.; Candelore, M.R.; Cascieri, M.A.; Colwell, L.F.; Deng, L.; Feeney, W.P.; Forrest, M.J.; Hom, G.J.; MacIntyre, D.E.; Strader, C.D.; Tota, L.; Wang, P.; Wyvratt, M.J.; Fisher, M.H.; Weber, A.E. *Bioorg. Med. Chem. Lett.*, **2000**, *10*, 1531.

[24] Mathvink, R.J.; Tolman, J.S.; Chitty, D.; Candelore, M.R.; Cascieri, M.A.; Colwell, L.F. Jr.; Deng, L.; Feeney, W.P.; Forrest, M.J.; Hom, G.J.; MacIntyre, D.E.; Tota, L.; Wyvratt, M.J.; Fisher, M.H.; Weber, A.E. *Bioorg. Med. Chem. Lett.*, **2000**, *10*, 1971.

[25] Brockunier, L.L.; Parmee, E.R.; Ok, H.O.; Candelore, M.R.; Cascieri, M.A.; Colwell, L.F. Jr.; Deng, L.; Feeney, W.P.; Forrest, M.J.; Hom, G.J.; MacIntyre, D.E.; Tota, L.; Wyvratt, M.J.; Fisher, M.H.; Weber, A.E. *Bioorg. Med. Chem. Lett.*, **2000**, *10*, 2111.

[26] Mathvink, R.J.; Tolman, J.S.; Chitty, D.; Candelore, M.R.; Cascieri, M.A.; Colwell, L.F. Jr.; Deng, L.; Feeney, W.P.; Forrest, M.J.; Hom, G.J.; MacIntyre, D.E.; Miller, R.R.; Stearns, R.A.; Tota, L.; Wyvratt, M.J.; Fisher, M.H.; Weber, A.E. *J. Med. Chem.*, **2000**, *43*, 3832.

[27] Stearns, R.A.; Miller, R.R.; Tang, W.; Kwei, G.Y.; Tang, F.S.; Mathvink, R.J.; Naylor, E.M.; Chitty, D.; Colandrea, V.J.; Weber, A.E.; Colletti, A.E.; Strauss, J.R.; Keohane, C.A.; Feeney, W.P.; Iliff, S.A.; Chiu, S.H. *Drug. Metab. Dispos.*, **2002**, *30*, 771.

[28] Mathvink, R.J.; Barritta, A.M.; Candelore, M.R.; Cascieri, M.A.; Deng, L.; Tota, L.; Strader, C.D.; Wyvratt, M.J.; Fisher, M.H.; Weber, A.E. *Bioorg. Med. Chem. Lett.*, **1999**, *9*, 1869.

[29] Brockunier, L.L.; Candelore, M.R.; Cascieri, M.A.; Liu, Y.; Tota, L.; Wyvratt, M.J.; Fisher, M.H.; Weber, A.E.; Parmee, E.R. *Bioorg. Med. Chem. Lett.*, **2001**, *11*, 379.

[30] Hom, G.J.; Forrest, M.J.; Bach, T.J.; Brady, E.; Candelore, M.R.; Cascieri, M.A.; Fletcher, D.J.; Fisher, M.H.; Iliff, S.A.; Mathvink, R.; Metzger, J.; Pecore, V.; Saperstein, R.; Shih, T.; Weber, A.E.; Wyvratt, M.; Zafian, P.; MacIntyre, D.E. *J. Pharmacol. Exp. Ther.*, **2001**, *297*, 299.

[31] Bloom, J.D.; Dutia, M.D.; Johnson, B.D.; Wissner, A.; Burns, M.G.; Largis, E.E.; Dolan, J.A.; Claus, T.H. *J. Med. Chem.*, **1992**, *35*, 3081.

[32] Hu, B.; Ellingboe, J.; Gunawan, I.; Han, S.; Largis, E.; Li, Z.; Malamas, M.; Mulvey, R.; Oliphant, A.; Sum, F.W.; Tillett, J.; Wong, V. *Bioorg. Med. Chem. Lett.*, **2001**, *11*, 757.

[33] Hu, B.; Malamas, M.; Ellingboe, J.; Largis, E.; Han, S.; Mulvey, R.; Tillett, J. *Bioorg. Med. Chem. Lett.*, **2001**, *11*, 981.

[34] Hu, B.; Ellingboe, J.; Han, S.; Largis, E.; Lim, K.; Malamas, M.; Mulvey, R.; Niu, C.; Oliphant, A.; Pelletier, J.; Singanallore, T.; Sum, F.W.; Tillett, J.; Wong, V. *Bioorg. Med. Chem.*, **2001**, *9*, 2045.

[35] Hu, B.; Ellingboe, J.; Han, S.; Largis, E.; Mulvey, R.; Oliphant, A.; Sum, F.W.; Tillett, J. *J. Med. Chem.*, **2001**, *44*, 1456.

[36] Steffan, R.J.; Ashwell, M.A.; Solvibile, W.R.; Matelan, E.; Largis, E.; Han, S.; Tillet, J.; Mulvey, R. *Bioorg. Med. Chem. Lett.*, **2002**, *12*, 2963.

[37] Ashwell, M.A.; Solvibile, W.R. Jr.; Han, S.; Largis, E.; Mulvey, R.; Tillet, J. *Bioorg. Med. Chem. Lett.*, **2001**, *11*, 3123.

[38] Washburn, W.N.; Sher, P.M.; Poss, K.M.; Girotra, R.N.; McCann, P.J.; Gavai, A.V.; Mikkilineni, A.B.; Mathur, A.; Cheng, P.; Dejneka, T.C.; Sun, C.Q.; Wang, T.C.; Harper, T.W.; Russell, A.D.; Slusarchyk, D.A.; Skwish, S.; Allen, G.T.; Hillyer, D.E.; Frohlich, B.H.; Abboa-Offei, B.E.; Cap, M.; Waldron, T.L.; George, R.J.; Tesfamariam, B.; Ciosek, C.P. Jr.; Ryono, D.; Young, D.A.; Dickinson, K.E.; Seymour, A.A.; Arbeeny, C.M.; Gregg, R.E. *Bioorg. Med. Chem. Lett.*, **2001**, *11*, 3035.

[39] Gavai, A.V.; Sher, P.M.; Mikkilineni, A.B.; Poss, K.M.; McCann, P.J.; Girotra, R.N.; Fisher, L.G.; Wu, G.; Bednarz, M.S.; Mathur, A.; Wang, T.C.; Sun, C.Q.; Slusarchyk, D.A.; Skwish, S.; Allen, G.T.; Hillyer, D.E.; Frohlich, B.H.; Abboa-Offei, B.E.; Cap, M.; Waldron, T.L.; George, R.J.; Tesfamariam, B.; Harper, T.W.; Ciosek, C.P. Jr.; Young, D.A.; Dickinson, K.E.; Seymour, A.A.; Arbeeny, C.M.; Washburn, W.N. *Bioorg. Med. Chem. Lett.*, **2001**, *11*, 3041.

[40] Washburn, W.N.; Sun, C.Q.; Bisacchi, G.; Wu, G.; Cheng, P.T.; Sher, P.M.; Ryono, D.; Gavai, A.V.; Poss, K.; Girotra, R.N.; McCann, P.J.; Mikkilineni, A.B.; Dejneka, T.C.; Wang, T.C.; Merchant, Z.; Morella, M.; Arbeeny, C.M.; Harper, T.W.; Slusarchyk, D.A.; Skwish, S.; Russell, A.D.; Allen, G.T.; Tesfamariam, B.; Frohlich, B.H.; Abboa-Offei, B.E.; Cap, M.; Waldron, T.L.; George, R.J.; Young, D.; Dickinson, K.E.; Seymour, A.A. *Bioorg. Med. Chem. Lett.*, **2004**, *14*, 3525.

[41] Foxton, M.W. PCT Patent Application. WO 9533724, **1995**.

[42] Uehling, D.E.; Donaldson, K.H.; Deaton, D.N.; Hyman, C.E.; Sugg, E.E.; Barrett, D.G.; Hughes, R.G.; Reitter, B.; Adkison, K.K.; Lancaster, M.E.; Lee, F.; Hart, R.; Paulik, M.A.; Sherman, B.W.; True, T.; Cowan, C. *J. Med. Chem.*, **2002**, *45*, 567.

[43] Harada, H.; Hirokawa, Y.; Suzuki, K.; Hiyama, Y.; Oue, M.; Kawashima, H.; Yoshida, N.; Furutani, Y.; Kato, S. *Bioorg. Med. Chem. Lett.*, **2003**, *13*, 1301.

[44] Harada, H.; Hirokawa, Y.; Suzuki, K.; Hiyama, Y.; Oue, M.; Kawashima, H.; Kato, H.; Yoshida, N.; Furutani, Y.; Kato, S. *Chem. Pharm. Bull.*, **2005**, *53*, 184.

[45] Kato, H.; Ohue, M.; Kato, K.; Nomura, A.; Toyosawa, K.; Furutani, Y.; Kimura, S.; Kadowaki, T. *Diabetes*, **2001**, *50*, 113.

[46] Dainippon Pharmaceuticals, *News Release (September 2003)*.

[47] Mizuno, K.; Sawa, M.; Harada, H.; Tateishi, H.; Oue, M.; Tsujiuchi, H.; Furutani, Y.; Kato, S. *Bioorg. Med. Chem. Lett.*, **2004**, *14*, 5959.

[48] Mizuno, K.; Sawa, M.; Harada, H.; Taoka, I.; Yamashita, H.; Oue, M.; Tsujiuchi, H.; Arai, Y.; Suzuki, S.; Furutani, Y.; Kato, S. *Bioorg. Med. Chem.*, **2005**, *13*, 855.

[49] Dow, R.L.; Paight, E.S.; Schneider, S.R.; Hadcock, J.R.; Hargrove, D.M.; Martin, K.A.; Maurer, T.S.; Nardone, N.A.; Tess, D.A.; DaSilva-Jardine, P. *Bioorg. Med. Chem. Lett.*, **2004**, *14*, 3235.

[50] Nakajima, Y.; Hamashima, H.; Washizuka, K.; Tomishima, Y.; Ohtake, H.; Imamura, E.; Miura, T.; Kayakiri, H.; Kato, M. *Bioorg. Med. Chem. Lett.*, **2005**, *15*, 251.

[51] Yanagisawa, T.; Sato, T.; Yamada, H.; Sukegawa, J.; Nunoki, K. *Tohoku. J. Exp. Med.*, **2000**, *192*, 181.

[52] Bianchetti, A.; Manara, L. *Br. J. Pharmacol.*, **1990**, *100*, 831.

[53] Cecchi, R.; Croci, T.; Boigegrain, R.; Boveri, S.; Baroni, M.; Boccardi, G.; Guimbard, J.P.; Guzzi, U. *Eur. J. Med. Chem.*, **1994**, *29*, 259.

[54] Delvaux, M.; Louvel, D.;Peronnet, P.; Bouloux, C.; Frexinos, J. *Gastroenterology*, **1995**, *108*, A589.

[55] Igawa, Y.; Yamazaki, Y.; Takeda, H.; Akahane, M.; Ajisawa, Y.; Yoneyama, T.; Nishizawa, O. *Acta Physiol. Scand.*, **1998**, *164*, 117.

[56] Igawa, Y.; Yamazaki, Y.; Takeda, H.; Hayakawa, K.; Akahane, M.; Ajisawa, Y.; Yoneyama, T.; Nishizawa, O.; Andersson, K.-E. *Br. J. Pharmacol.*, **1999**, *126*, 819.

[57] Takeda, M.; Obara, K.; Mizusawa, T.; Tomita, Y.; Arai, K.; Tsutsui, T.; Hatano, A.; Takahashi, K.; Nomura, S. *J. Pharmacol. Exp. Ther.*, **1999**, *288*, 1367.

[58] Fujimura, T.; Tamura, K.; Tsutsumi, T.; Yamamoto, T.; Nakamura, K.; Koibuchi, Y.; Kobayashi, M.; Yamaguchi, O. *J. Urol.*, **1999**, *161*, 680.

[59] Takeda, H.; Yamazaki, Y.; Igawa, Y.; Kaidoh, K.; Akahane, S.; Miyata, H.; Nishizawa, O.; Akahane, M.; Andersson, K.-E. *Neurourol. Urodyn.*, **2002**, *21*, 558.

[60] Kaidoh, K.; Igawa, Y.; Takeda, H.; Yamazaki, Y.; Akahane, S.; Miyata, H.; Ajisawa, Y.; Nishizawa, O.; Andersson, K.-E. *J. Urol.*, **2002**, *168*, 1247.

[61] Tanaka, N.; Tamai, T.; Mukaiyama, H.; Hirabayashi, A.; Muranaka, H.; Akahane, S.; Miyata, H.; Akahane, M. *J. Med. Chem.*, **2001**, *44*, 1436.

[62] Tanaka, N.; Tamai, T.; Mukaiyama, H.; Hirabayashi, A.; Muranaka, H.; Ishikawa, T.; Akahane, S.; Akahane, M. *Bioorg. Med. Chem.*, **2001**, *9*, 3265.

[63] Tanaka, N.; Tamai, T.; Mukaiyama, H.; Hirabayashi, A.; Muranaka, H.; Ishikawa, T.; Kobayashi, J.; Akahane, S.; Akahane, M. *J. Med. Chem.*, **2003**, *46*, 105.

[64] Tomiyama, Y.; Murakami, M.; Hayakawa, K.; Akiyama, K.; Yamazaki, Y.; Kojima, M.; Shibata, N.; Akahane, M. *J. Pharmacol. Sci.*, **2003**, *92*, 411.

[65] Park, Y.C.; Tomiyama, Y.; Hayakawa, K.; Akahane, M.; Ajisawa, Y.; Miyatake, R.; Kiwamoto, H.; Sugiyama, T.; Kurita, T. *J. Urol.*, **2000**, *164*, 1364.

[66] Tomiyama, Y.; Hayakawa, K.; Murakami, M.; Akahane, M.; Ajisawa, Y.; Park, Y.-C.; Kurita, T. *J. Urol.*, **1999**, *161*, 83.

[67] Cawthorne, M.A.; Sennitt, M.V.; Arch, J.R.; Smith, S.A. *Am. J. Clin. Nutr.*, **1992**, *55*, 252S.

[68] Oriowo, M.A.; Chapman, H.; Kirkham, D.M.; Sennitt, M.V.; Ruffolo, R.R., Jr.; Cawthorne, M.A. *J. Pharmacol. Exp. Ther.*, **1996**, *277*, 22.

[69] Sawa, M.; Tateishi, H.; Mizuno, K.; Harada, H.; Oue, M.; Tsujiuchi, H.; Furutani, Y.; Kato, S. *Bioorg. Med. Chem. Lett.*, **2004**, *14*, 5963.
[70] Sawa, M.; Mizuno, K.; Harada, H.; Tateishi, H.; Arai, Y.; Suzuki, S.; Oue, M.; Tsujiuchi, H.; Furutani, Y.; Kato, S. *Bioorg. Med. Chem. Lett.*, **2005**, *15*, 1061.
[71] Fisher, L.G.; Sher, P.M.; Skwish, S.; Michel, I.M.; Seiler, S.M.; Dickinson, K.E.J. *Bioorg. Med. Chem. Lett.*, **1996**, *16*, 2253.
[72] Weber, A.E.; Mathvink, R.J.; Perkins, L.; Hutchins, J.E.; Candelore, M.R.; Tota, L.; Strader, C.D.; Wyvratt, M.J.; Fisher, M.H. *Bioorg. Med. Chem. Lett.*, **1998**, *8*, 1101.
[73] Parmee, E.R.; Ok, H.O.; Candelore, M.R.; Tota, L.; Deng, L.; Strader, C.D.; Wyvratt, M.J.; Fisher, M.H.; Weber, A.E. *Bioorg. Med. Chem. Lett.*, **1998**, *8*, 1107.
[74] Weber, A.E.; Ok, H.O.; Alvaro, R.F.; Candelore, M.R.; Cascieri, M.A.; Chiu, S.H.; Deng, L.; Forrest, M.J.; Hom, G.J.; Hutchins, J.E.; Kao, J.; MacIntyre, D.E.; Mathvink, R.J.; McLoughlin, D.; Miller, R.R.; Newbold, R.C.; Olah, T.V.; Parmee, E.R.; Perkins, L.; Stearns, R.A.; Strader, C.D.; Szumiloski, J.; Tang, Y.S.; Tota, L.; Fisher, M.H. *Bioorg. Med. Chem. Lett.*, **1998**, *8*, 2111.
[75] Malams, M.S.; Largis, E.; Gunawan, I.; Li, Z.; Tillett, J.; Han, S.C.-H.; Mulvey, R. *Med. Chem. Res.*, **2000**, *10*, 164.
[76] Aubriot, S.; Nicolle, E.; Lattier, M.; Morel, C.; Cao, W.; Daniel, K.W.; Collins, S.; Leclerc, G.; Faure, P. *Bioorg. Med. Chem. Lett.*, **2002**, *12*, 209.
[77] Steffan, R.J.; Ashwell, M.A.; Solvibile, W.R.; Matelan, E.; Largis, E.; Han, S.; Tillet, J.; Mulvey, R. *Bioorg. Med. Chem. Lett.*, **2002**, *12*, 2957.
[78] Sum, F.W.; Wong, V.; Han, S.; Largis, E.; Mulvey, R.; Tillett, J. *Bioorg. Med. Chem. Lett.*, **2003**, *13*, 2191.
[79] Jesudason, C.D.; Bell, M.G.; Crowell, T.A.; Cusick, T.; Droste, C.A.; Gritton, W.H.; Jones, C.D.; Kim, G.; Kriauciunas, A.V.; Matthews, D.P.; McDonald, J.H.; Neel, D.A.; Peters, M.K.; Rito, C.J.; Shuker, A.J.; Siegel, M.G.; Stephens, T.J.; Winter, M.A. *216th ACS National Meeting*, Boston, MA, **1998**, MEDI-025.
[80] Shuker, A.J.; Bell, M.G.; Bloomquist, W.; Calligaro, D.O.; Cohen, M.L.; Crowell, T.A.; Cusick, T.S.; Droste, C.A.; Evrard, D.A.; Hahn, P.J.; Heiman, M.L.; Jesudason, C.D.; Jones, C.D.; Kim, G.; Kriaucinus, A.V.; Matthews, D.P.; McDonald, J.H.; Neel, D.A.; Palkowitz, A.D.; Peters, M.K.; Rito, C.J.; Siegel, M.G.; Stephens, T.W.; Winter, M.A.; Dananberg, J. *217th ACS National Meeting*, Anaheim, CA, **1999**, MEDI-159.
[81] Jesudason, C.D.; Bell, M.G.; Crowell, T.A.; Droste, C.A.; Jones, C.D.; Kim, G.; Matthews, D.P.; Neel, D.A.; Rito, C.J.; Shuker, A.J.; Winter, M.A.; Bryant, R.D.; Fisher, J.W.; Peters, M.K.; Trankle, W.G.; Heiman, M.L.; Kriauciunas, A.V.; Tinsley, F.C.; Dananberg, J.; Miller, J.W. *220th ACS National Meeting*, Washington, DC, **2000**, MEDI-300.
[82] Staehelin, M.; Simons, P. *EMBO J.*, **1982**, *1*, 187.
[83] Staehelin, M.; Simons, P.; Jaeggi, K.; Wigger, N. *J. Biol. Chem.*, **1983**, *258*, 3496.
[84] Mohell, N.; Dicker, A. *Biochem. J.*, **1989**, *261*, 401.
[85] Granneman, J.G.; Lahners, K.N.; Chaudhry, A. *Mol. Pharmacol.*, **1991**, *40*, 885.
[86] Granneman, J.G.; Lahners, K.N.; Chaudhry, A. *Mol. Pharmacol.*, **1993**, *44*, 264.
[87] Fisher, M.H.; Amend, A.M.; Bach, T.J.; Barker, J.M.; Brady, E.J.; Candelore, M.R.; Carroll, D.; Cascieri, M.A.; Chiu, S.H.; Deng, L.; Forrest, M.J.; Hegarty-Friscino, B.; Guan, X.M.; Hom, G.J.; Hutchins, J.E.; Kelly, L.J.; Mathvink, R.J.; Metzger, J.M.; Miller, R.R.; Ok, H.O.; Parmee, E.R.; Saperstein, R.; Strader, C.D.; Stearns, R.A.; MacIntyre, D.E. *J. Clin. Invest.*, **1998**, *101*, 2387.
[88] Forrest, M.J.; Hom, G.; Bach, T.; Candelore, M.R.; Cascieri, M.A.; Strader, C.; Tota, L.; Fisher, M.H.; Szumiloski, J.; Ok, H.O.; Weber, A.E.; Wyvratt, M.; Vicario, P.; Marko, O.; Deng, L.; Cioffe, C.; Hegarty-Friscino, B.; MacIntyre, E. *Eur. J. Pharmacol.*, **2000**, *407*, 175.
[89] Iwasawa, Y.; Kiyomoto, A. *Jpn. J. Pharmacol.*, **1967**, *17*, 143.
[90] Shonk, R.F.; Miller, D.D.; Feller, D.R. *Biochem. Pharmacol.*, **1971**, *20*, 3403.
[91] Parmee, E.R.; Brockunier, L.L.; He, J.; Singh, S.B.; Candelore, M.R.; Cascieri, M.A.; Deng, L.; Liu, Y.; Tota, L.; Wyvratt, M.J.; Fisher, M.H.; Weber, A.E. *Bioorg. Med. Chem. Lett.*, **2000**, *10*, 2283.
[92] Zheng, W.; Nikulin, V.I.; Konkar, A.A.; Vansal, S.S.; Shams, G.; Feller, D.R.; Miller, D.D. *J. Med. Chem.*, **1999**, *42*, 2287.
[93] He, Y.; Nikulin, V.I.; Vansal, S.S.; Feller, D.R.; Miller, D.D. *J. Med. Chem.*, **2000**, *43*, 591.
[94] Nisoli, E.; Tonello, C.; Carruba, M.O. *Curr. Med. Chem. – Central Nervous System Agents*, **2003**, *3*, 257.
[95] Connacher, A.A.; Lakie, M.; Powers, N.; Elton, R.A.; Walsh, E.G.; Jung, R.T. *Br. J. Clin. Pharmacol.*, **1990**, *30*, 613.
[96] Wheeldon, N.M.; McDevitt, D.G.; Lipworth, B.J. *Br. J. Clin. Pharmacol.*, **1994**, *7*, 363.
[97] Granneman, J.G.; Lahners, K.N.; Chaudhry, A. *Mol. Pharmacol.*, **1991**, *40*, 895.
[98] Krief, S.; Lönnqvist, F.; Raimbault, S.; Baude, B.; Van Spronsen, A.; Arner, P.; Strosberg, A.D.; Ricquier, D.; Emorine, L.J. *J. Clin. Invest.*, **1993**, *91*, 344.
[99] *Drugs R. D.*, **2003**, *4*, 380.
[100] Nisoli, E.; Tonello, C.; Benarese, M.; Carruba, M.O. *J. Neurochem.*, **1995**, *65*, 1580.
[101] GlaxoSmithKline, *Product Development Pipeline (February 2005)*, available at: http://science.gsk.com/
[102] Astellas Pharma, *R&D Pipeline List (May 2005)*, available at: http://www.astellas.com/
[103] Kissei Pharmaceutical, *Annual Reprot* **2004**, available at: http://www.kissei.co.jp/
[104] Larsen, T.M.; Toubro, S.; van Baak, M.A.; Gottesdiener, K.M.; Larson, P.; Saris, W.H.; Astrup, A. *Am. J. Clin. Nutr.*, **2002**, *76*, 780.
[105] van Baak, M.A.; Hul, G.B.; Toubro, S.; Astrup, A.; Gottesdiener, K.M.; DeSmet, M.; Saris, W.H. *Clin. Pharmacol. Ther.*, **2002**, *71*, 272.
[106] Miller, J.W.; Farid, N.A.; Johnson, R.D.; Smith, B.P.; Dananberg, J. *Obes. Res.*, **1999**, *7*, 121S.
[107] Kyorin Pharmaceutical, *R&D activities (November 2004)*, available at: http://www.kyorin-pharm.co.jp/

Received: June 17, 2005 **Revised: October 08, 2005** **Accepted: October 10, 2005**

Available online at www.sciencedirect.com
SCIENCE DIRECT
Pharmacology & Therapeutics 111 (2006) 652–673
Pharmacology & Therapeutics
www.elsevier.com/locate/pharmthera

Associate editor: P. Molenaar

β_3-Adrenoceptors in the cardiovascular system: Putative roles in human pathologies

Bertrand Rozec [a,b,1], Chantal Gauthier [a,c,*]

[a] *Inserm U533, L'institut du thorax, Nantes, France*
[b] *Département d'anesthésie et de réanimation chirurgicale, CHRU G et R Laënnec, Nantes, France*
[c] *Université de Nantes, Faculté des Sciences et Techniques, Nantes, France*

Abstract

The sympathetic nervous system is central for the neurohumoral regulation of the cardiovascular system and is largely involved in many cardiovascular diseases affecting millions of people around the world. It is classically admitted that β-adrenoceptors (β-AR) of the β_1 and β_2 subtypes mediate the effects of catecholamines on the force of contraction of cardiac muscle, and on the relaxation of vascular smooth muscle. However, the molecular characterization in 1989 of a third β-AR subtype, β_3, and later its identification in human heart has changed the classically admitted paradigm on the regulation of heart function by the β-adrenergic system. In blood vessels, β_3-AR, like β_1 and β_2, produced a relaxation. But at the present time, the physiological role of β_3-AR is not clearly identified. Thus, the purpose of this review is to summarize the pharmacological and molecular evidence supporting the functional roles of β_3-AR in cardiovascular tissues of various species, including humans. In addition, this review discusses the potential role of β_3-AR in several cardiovascular diseases and emphasizes their putative involvement as new therapeutic targets.

Keywords: β-adrenergic receptors; Heart; Vessels; Contractility; Heart failure; Hypertension

Abbreviations: β-AR, β-adrenoceptor; cAMP, cyclic adenosine monophosphate; BRL 37344, 4-[-[2-hydroxy-(3-chlorophenyl)ethyl-amino]propyl]phenoxyacetate; CHO, Chinese hamster ovary; CL 316 243, 5-(2-{[2-(3-chlorophenyl)-2-hydroxyethyl]-amino}propyl)-1,3-benzodioxole-2,2-dicarboxylate; cGMP, cyclic guanosine monophosphate; CGP 12177A, 4-[3-*t*-butylamino-2-hydroxypropoxy]benzimidazol-2-one; CFTR, cystic fibrosis transmembrane conductance regulator; eNOS, endothelial nitric oxide synthase; L-748,328, (*S*)-*N*-[4-[2-[[3-[3-(ami-nosulphonyl)phenoxy]-2-hydroxypropyl]-amino]ethyl]phenyl]benzenesulfonamide; L-748,337, (*S*)-*N*-[4-[2-[[3-[3-(acetamidomethyl)phenoxy]-2-hydroxypropyl]amino]ethyl]phenyl]benzenesulfonamide; L-NMMA, N^G-monomethyl-L-arginine monoacetate; NO, nitric oxide; PCR, polymerase chain reaction; PKA, cAMP-dependent protein kinase; SR 58611A, (*RS*)-*N*-[(2*S*)-7-ethoxycarbonylmethoxy-1,2,3,4-tetrahydronapht-2-yl]-(2)-2-(3-chlorophenyl)-2 hydroethanamide hydrochloride; SR 59230A, 3-(2-ethylphenoxy)-1-[(1*S*)1,2,34-tetrahydronapht-1-ylaminol]-(2*S*)-2-propanol oxalate; TGβ3, mice overexpressing human β_3-adrenoceptors in cardiomyocytes.

Contents

* Corresponding author. Inserm U533, l'institut du thorax, Faculté de Médecine, 1 rue Gaston Veil, BP 53508, F-44035 Nantes, France. Tel.: +33 2 40 08 33 94; fax: +33 2 40 41 29 50.
E-mail address: chantal.gauthier@nantes.inserm.fr (C. Gauthier).
[1] Present address: Unit of Pharmacology and Therapeutics, Department of Medicine, University of Louvain Medical School, Brussels, Belgium.

0163-7258/$ - see front matter © 2006 Elsevier Inc. All rights reserved.
doi:10.1016/j.pharmthera.2005.12.002

1. Introduction

The sympathetic nervous system is central for the neurohumoral regulation of the cardiovascular system and is largely involved in many cardiovascular diseases affecting millions of people around the world. During the 1980s, the classification of β-adrenoceptors (β-AR) into 2 subtypes (β_1 and β_2) (Lands et al., 1967) was challenged. Thus, it is now known that 3 different subtypes, β_1-, β_2- and β_3-AR, could at least participate in the regulation of cardiovascular function. β_3-AR differs from β_1- and β_2-AR subtypes by its molecular structure and pharmacological profile. Its stimulation produces specific effects in the cardiovascular system. This review will present an overview of characteristics of β_3-AR and reports on the presence and the roles of β_3-AR in the cardiovascular system and their potential involvement in different pathologies.

2. Structure and characteristics of β_3-adrenoceptors

2.1. Gene

The gene encoding human β_3-AR was cloned in 1989 (Emorine et al., 1989). Since then, the gene has been cloned in rat, mice, bovine, monkey, dog (for review, see Strosberg, 1997), sheep and goat (Forrest & Hickford, 2000). Unlike the genes encoding β_1- and β_2-AR, the gene encoding β_3-AR contains introns. The existence of several exons raises the possibility of alternative splicing and thus of different receptor isoforms with putative distinct pharmacological properties. Among the different species previously cited, variations in length and amino acid content of the sequence of the C-terminus tail have been reported (Fig. 1).

In human, the gene is localized on chromosome 8. The number of exons and introns is controversial. The first structure proposed was 2 exons and 1 intron. The first exon of 1.7 kb has a high homology with rodents. It encodes for the first 402 amino acids of the receptor. The second exon encodes the last 6 amino acids of the C-terminus tail and the 3′ region not translated from the mRNA (Granneman et al., 1992, 1993; Van Spronsen et al., 1993). This structure of 2 exons and 1 intron has also been described in dogs and monkeys (Walston et al., 1997; Lenzen et al., 1998). Thus, 2 putative isoforms with various C-terminus tails could exist (Fig. 1): an isoform of 402 amino acids (isoform A) and an isoform with 6 additional amino acids (isoform C). Another structure with 3 exons and 2 introns has also been proposed for the human gene (Fig. 1; Levasseur et al., 1995). However, the alternative splicing site for the second exon seems to be not functional (Granneman et al., 1992) and strengthens the first hypothesis of a structure with 2 exons.

In rats and mice, the gene encoding β_3-AR contains 3 exons and 2 introns. The first exon of 1.4 kb encodes the first 388 amino acids. In rat, the second exon of 0.7 kb encodes the last 12 amino acids of the C terminus tail. In this species, 2 isoforms of β_3-AR could be expressed: A and B isoforms of 388 and 400 amino acids, respectively (Fig. 1; Van Spronsen et al., 1993). In mice, 2 sites in the exon 2 allow an alternative splicing leading to 2 isoforms, β_{3a} and β_{3b} (Evans et al., 1999). The β_{3b}-AR encoded by the alternately spliced mRNA has a C-terminus that has 17 amino acids following the sequence encoded by the first exon region compared to 13 in the known receptor (β_{3a}-AR) (Fig. 1). β_{3b}-AR mRNA is differentially expressed in mouse tissues, with levels relative to β_{3a}-AR mRNA highest in hypothalamus, cortex and white adipose tissue, and lower in ileum smooth muscle and brown adipose tissue (Evans et al., 1999).

2.2. Protein

The β_3-AR, as well as β_1- and β_2-AR, belongs to the G protein-coupled receptors characterized by 7 transmembrane

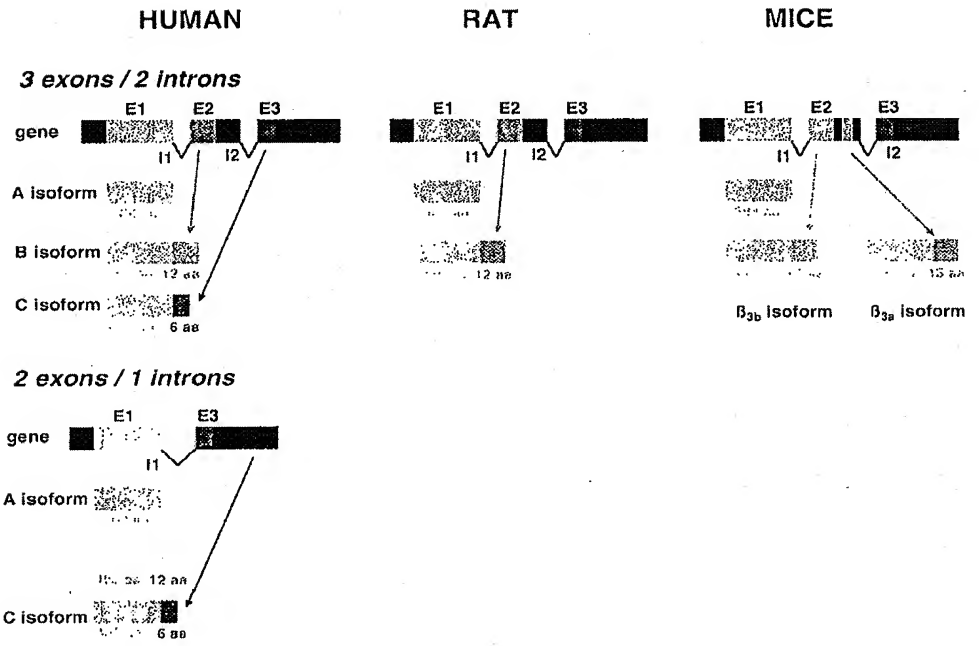

Fig. 1. Putative structures of β_3-AR isoforms obtained after alternative splicing in human, rat and mice. aa: amino acid; E: exon; I: intron.

domains of 22–28 amino acids and having 3 intracellular and 3 extracellular loops (Fig. 2). The N-terminus of all 3 β-AR is extracellular and glycosylated, whereas the C-terminus is intracellular. The transmembrane domains, TM3, TM4, TM5 and TM6 are essential for ligand binding (Strosberg & Pietri-Rouxel, 1996). The disulphide bond between Cys110 in the second and Cys189 in the third extracellular loops is essential for ligand binding and activity of the receptor (Moffett et al., 1993). Amino acid sequence homology between β_1-, β_2- and β_3-AR is 40–50% in both man and rat and is restricted almost exclusively to the 7 transmembrane segments and to most of the membrane-proximal regions of intracellular loops. The rat and human β_3-AR are 79% identical; the biggest homology is in the transmembrane domains (94%) whereas the lowest homology is observed in the C-terminus tail and the third intracellular loop.

β_3-AR differ from classical β_1- and β_2-AR in their regulatory properties. It is known that desensitization of β_1- and β_2-AR responses upon agonist stimulation involves

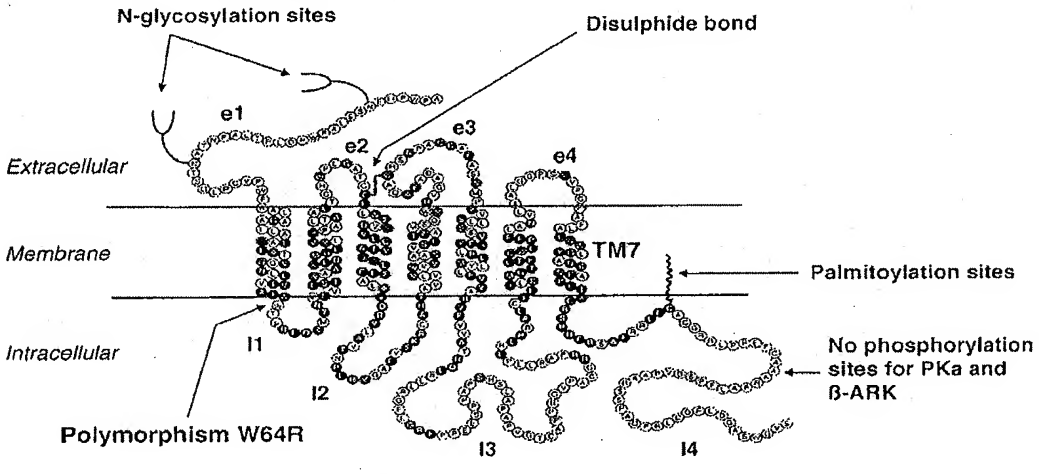

Fig. 2. Primary structure of human β_3-AR. The dark circles represent amino acids identical in the three β-AR subtypes. e: extracellular region; i: intracellular region; TM: transmembrane domain.

phosphorylation of occupied receptors, uncoupling and internalization (Summers et al., 1997). Both β_1- and β_2-AR have serine and threonine residues in the C-terminus tail that act as substrates for G protein-coupled receptor kinases, and consensus sequences for phosphorylation by cyclic adenosine monophosphate (cAMP)-dependent protein kinase (PKA). The β_3-AR lacks a PKA phosphorylation site, and has fewer serine and threonine residues in the C-terminus tail. It has been shown that the β_3-AR was resistant to short term agonist-promoted desensitization. Studies on chimeric β_2/β_3-AR show that domains within the C-terminus tail and in second and third intracellular loops of the β_2-AR were the major determinants of desensitization (Liggett et al., 1993; Jockers et al., 1996). Thus, in human myometrium, β_2-AR undergoes functional desensitization after long-term exposure to salbutamol, which is associated with a significant reduction of the number of β_2-AR binding sites. In contrast, a sustained stimulation of β_3-AR did not modify their subsequent functional effects and the number of β_3-AR binding sites remained unchanged after such treatment (Rouget et al., 2004). Thus, these data suggest that following prolonged activation by the sympathetic nervous system, the β_3-adrenergic response may be preserved while the β_1- and β_2-adrenergic responses are diminished.

In mice, it has been shown that the β_{3b}-AR differs from the β_{3a}-AR by the presence in the C-terminal tail of 2 additional serine residues. These are potentially important targets for phosphorylation and may thereby mediate desensitization of the β_{3b}-AR (Evans et al., 1999). Thus, it will be of interest to determine whether the mouse β_{3b}-AR demonstrates a greater tendency towards phosphorylation and associated desensitization. To the best of our knowledge, the desensitization has been mainly studied in Chinese hamster ovary (CHO), adipocytes and digestive tract, and no data are presently available in the cardiovascular system.

Quantification of the β_3-AR protein in comparison with other β-AR subtypes has been proved to be difficult. Radioligand binding studies have been performed with [^{125}I] cyanopindolol and [^{3}H] 4-[3-*t*-butylamino-2-hydroxypropoxy] benzimidazol-2-one (CGP 12177A). However, those compounds showed low potency for the β_3-AR and bound to β_1/β_2-AR and also to the low affinity state of β_1-AR. A tritiated enantiomer of the β_3-AR agonist, 4-[-[2-hydroxy-(3-chlorophenyl)ethyl-amino]propyl]phenoxyacetate (BRL 37344), was shown to bind a single population of sites in rat brown adipose tissue but its use has not been reported in tissues with lower expression levels (Klaus et al., 1995).

3. Pharmacology of β_3-adrenoceptors

β_3-AR are pharmacologically characterized by a set of criteria that include (1) high affinity and potency of selective agonists such as BRL 37344, 5-(2-{[2-(3-chlorophenyl)-2-hydroxyethyl]-amino}propyl)-1,3-benzodioxole-2,2-dicarboxylate (CL 316 243) and (*RS*)-*N*-[(2S)-7-ethoxycarbonylmethoxy-1,2,3,4-tetrahydronapht-2-yl]-(2)-2-(3-chlorophenyl)-2 hydroethanamide hydrochloride (SR 58611A) (Arch & Kaumann, 1993; Emorine et al., 1994; Strosberg & Pietri-Rouxel, 1996); (2) partial agonistic activity of several β_1- and/or β_2-AR antagonists, such as CGP 12177A (Liggett, 1992; Blin et al., 1993; Kaumann & Molenaar, 1996), bucindolol (Blin et al., 1993) and pindolol (Blin et al., 1993); (3) atypically low affinity for conventional β-AR antagonists such as propranolol and nadolol. For a long time, β_3-AR has been also characterized by an atypically low stereoselectivity index for reference agonist and antagonist enantiomers as compared to those reported for β_1- and β_2-AR (Arch & Kaumann, 1993; De Ponti et al., 1996). However, some studies performed with β_3-AR antagonists show different effects between *S,S* enantiomer (3-(2-ethylphenoxy)-1-[(1*S*) 1,2,34-tetrahydronapht-1-ylaminol]-(2*S*)-2-propanol oxalate, SR 59230A) and *R,R* enantiomer (SR 59483A) (De Ponti et al., 1996; Manara et al., 1996). More recently, it has been shown that the degree of stereoselectivity varied between species: the human β_3-AR displayed higher affinities and enantiomeric ratios than the mouse or rat β_3-AR. The degree of stereoselectivity was relatively low for the agonists, isoproterenol and norepinephrine, but was higher for antagonists and, in particular, tertatolol and propranolol (Popp et al., 2004).

3.1. Agonists

β_3-AR is activated by catecholamines (Table 1) but at higher concentrations than β_1- and β_2-AR with a K_i of 1 μM

Table 1
Chemical structure of several β_3-AR agonists and antagonists

Catecholamines:

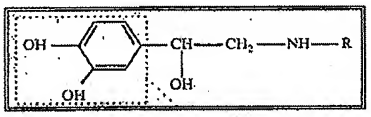

No selective β-AR agonists (β_1/ β_2/ β_3): norepinephrine, epinephrine, isoproterenol

Phenylethanolamines:

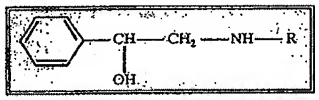

Preferential β_3-AR agonists: BRL 37344, SR 58611A, CL 316 243

Aryloxypropanolamines:

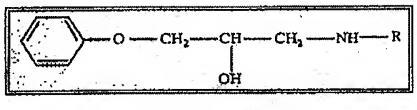

Preferential β_3-AR agonists: L 755,507, ICI 201,651
Partial β_3-AR agonists: CGP 12177A, L 755,507, pindolol

No selective β-AR antagonists: [illegible]
Selective β-AR antagonists: [illegible]

R is specific of a given compound.

(Strosberg, 1997) suggesting that β_3-AR could be activated in situations where catecholamine tone is high. β_3-AR are activated with high affinity and potency by selective agonists belonging to 2 different classes. The first class comprises the phenylethanolamines (Table 1), including BRL 37344 (Arch et al., 1984), SR 58611A (Bianchetti & Manara, 1990) and CL 316 243 (Dolan et al., 1994). However, some of those compounds such as BRL 37344 and SR 58611A also possess low affinity for β_1- and β_2-AR (Dolan et al., 1994). The second class includes the aryloxypropanolamines (Table 1), such as CGP 12177A (Pietri-Rouxel & Strosberg, 1995, Lenzen et al., 1998) and cyanopindolol. CGP 12177A is a β_1- and β_2-AR antagonist, and a weak β_3-AR agonist. As it is generally observed with agonists of G protein-coupled receptors, the efficacy and potency of CGP 12177A as a β_3-AR agonist varies dramatically with the expression level of the β_3-AR (Wilson et al., 1996). It is important to note that mouse β_{3a}-AR and β_{3b}-AR expressed in CHO cells shared similar affinity and potency for all β-AR ligands examined (Hutchinson et al., 2002).

Studies performed in vitro and in vivo described the complexity of β_3-AR pharmacology suggesting a pronounced inter-species variability and the heterogeneous pharmacological profiles of β_3-AR agonists in a given species. For example, agonists display significant differences in efficacy and potency between rodent and human β_3-AR. In addition, affinity and potencies differ according to the assay. Some β_3-AR agonists have been evaluated by measuring cAMP accumulation in whole cells transfected with the human β_3-AR, whereas others were tested in isolated membranes to measure cAMP production by adenylyl cyclase (Sennitt et al., 1998). Not only were agonists usually more potent in the whole cell assay, but relative potencies differed between the 2 assays; the phenylethanolamine being more potent relative to the aryloxypropanolamine in the whole cells compared to the membrane assay. Moreover, in binding assays employing [^{125}I]-iodocyanopindolol as the labeled ligand, the relative potencies of a series of agonists were almost the complete opposite of their relative potencies as stimulants of cAMP accumulation (Arch, 2002).

3.2. Antagonists

β_3-AR are blocked by nonselective β-AR antagonists such as bupranolol (Langin et al., 1991; Galitzky et al., 1993). As described for β_3-AR agonists, β_3-AR antagonist potencies may also vary. The β_3-AR is also blocked by the selective β_3-AR antagonist SR 59230A (Table 1). However, whereas this compound may be a selective antagonist of the rodent β_3-AR (Kaumann & Molenaar, 1996; Manara et al., 1996; Kubo et al., 1997), its utility as a selective antagonist of the human β_3-AR is less certain (Arch, 2002). Two selective antagonists (Table 1) of the human cloned β_3-AR, (*S*)-*N*-[4-[2-[[3-[3-(ami-nosulphonyl) phenoxy]-2-hydroxypropyl]-amino]ethyl]phenyl]benzenesulfonamide (L-748,328) and (*S*)-*N*-[4-[2-[[3-[3-(acetamidomethyl) phenoxy]-2-hydroxypropyl]amino]ethyl]phenyl]benzenesulfonamide (L-748,337), have also been described, but in this assay, both compounds show a weak affinity for rodent β_3-AR (Candelore et al., 1999).

4. β_3-adrenoceptors in the heart

In the heart, β-AR pathways are the primary means of increasing cardiac performance in response to acute or chronic stress. Until last decade, only β_1- and β_2-AR were described in the heart with a β_1/β_2-AR ratio of approximately 80:20 (Bristow et al., 1986). The effects of β_1- and β_2-AR are well established both in human and other mammals. Their stimulation produces positive chronotropic and inotropic effects. For β_1-AR stimulation, the linear G_s-adenylyl cyclase–cAMP–PKA signaling cascade has been classically corroborated. Recent works using recombinant β-AR subtypes, as well as β-AR-deficient mice, have established the existence of a lower state of the β_1-AR, which was guanine nucleotide-sensitive state pre-coupled to stimulatory G proteins. This state was called low affinity state of the β_1-AR (Granneman, 2001). In the heart, its stimulation produced a positive inotropic effect by activation of the cAMP pathway (Sarsero et al., 2003).

The data concerning the signaling pathway mediating the contractile effect of β_2-AR in the heart is not so clear. Like β_1-AR, β_2-AR are linked to G_s protein. In human heart, it has been reported that β_2-AR mediated maximal or near maximal (positive inotropic, lusitropic) effects by coupling to $G_{s\alpha}$ protein–cAMP–PKA pathway (Kaumann et al., 1999). In addition to G_s, β_2-AR coupled to pertussis toxin-sensitive G_i proteins (Xiao et al., 1999) and activated the cytosolic phospholipase A_2/arachidonic acid pathway (Pavoine et al., 1999; Pavoine & Defer, 2005). The involvement of cardiac β_2-AR–$G_{i\alpha}$ pathway may be more important in rodents compared to human. However, in pathological conditions, it has been suggested in human failing heart that this pathway could substitute for a deficient G_s–adenylyl cyclase pathway in mediating β_2-AR responses (Pavoine et al., 2003). Finally, a direct agonist-promoted association of the β_2-AR with the Na/H exchanger regulatory factor (NHE-RF), a protein that regulates the activity of the Na/H exchanger type 3, has been reported (Hall et al., 1998). This interaction may be critical for a rapid and specific signal transduction from the receptor to its effector in a compartmentalized fashion. However, the physiological relevance of that mechanism remains to elucidate.

In the human heart and in some other species, another β-AR subtype, β_3, has been described. Interestingly, in full contrast with other β-AR subtypes, their stimulation produced a marked decrease in cardiac contractility (Gauthier et al., 2000).

4.1. Contractiles effects

In human, in vivo studies have shown that β_3-AR agonists produced positive chronotropic effects, which were prevented by β_1- or β_2-AR antagonists and are likely due to baroreflex activation in response to β_3-AR agonist-induced vasodilation (Wheeldon et al., 1993, 1994). In human endomyocardial biopsies from transplanted hearts, we have shown that the classical positive inotropic effect of isoproterenol was inverted to a negative inotropic effect (Gauthier et al., 1996), in the presence of nadolol, a β_1- and β_2-AR antagonist with a low affinity for the native and recombinant β_3-AR (Emorine et al.,

1989; Galitzky et al., 1993). Similar negative inotropic effects were obtained with several β_3-AR agonists including BRL 37344, SR 58611A and CL 316 243. These agonists decreased contractility at concentrations ranging from 0.1 nM to 1 μM with nanomolar potency. The relative rank order of potency of these β_3-AR agonists (BRL 37344>SR 58611A≈CL 316 243≫CGP 12177A) (Gauthier et al., 1996) was similar to that observed in CHO cells expressing human β_3-AR (Pietri-Rouxel & Strosberg, 1995). CGP 12177A, the partial β_3-AR agonist having β_1- and β_2-AR antagonistic and low-affinity β_1-AR agonistic properties, exerted a cardiodepressant effect which was weaker than that elicited by the preferential β_3-AR agonists (Gauthier et al., 1996). Importantly, effects of β_3-AR agonists can be reproduced with the naturally occurring catecholamine, norepinephrine, at concentrations close to pathophysiologically relevant levels, and in the presence of blockade of the α_1- and β_1-, β_2-AR with prazosine and nadolol, respectively (Gauthier et al., 1998). Furthermore, the cardiodepressant effect of β_3-AR agonists was unaffected by metoprolol (a β_1-AR antagonist) or nadolol, but was antagonized by bupranolol (Gauthier et al., 1996) which combines β_1-, β_2- and β_3-AR antagonistic properties (Langin et al., 1991; Galitzky et al., 1993). The presence of β_3-AR was strengthened by detection of transcripts encoding for this receptor by polymerase chain reaction (PCR) assays (Gauthier et al., 1996) and β_3-AR proteins, by Western blotting and immunohistochemistry in ventricles from nonfailing human hearts (Moniotte et al., 2001).

In contrast, another group did not report cardiodepressant effects with β_3-AR agonists including BRL 37344 in the presence of nadolol both in human atrium and ventricle (Kaumann & Molenaar, 1997; Molenaar et al., 1997). Furthermore, in human atrium, (−)-pindolol which possessed partial β_3-AR and low affinity state of β_1-AR agonistic properties only produced positive inotropic effects that were not blocked by a selective β_3-AR antagonist, L-748,337 (Joseph et al., 2003) suggesting that this effect did not result from an action on β_3-AR. However, using a selective monoclonal antibody directed against the human β_3-AR (Mab 72c), Chamberlain et al. (1999) showed a positive immunostaining in myocardial cells of human atria, demonstrating the presence of β_3-AR in human atrial tissue. More recently, it has been shown that BRL 37344 produced an increase of contractility of human right atrial trabeculae. However, this effect was abolished in the presence of nadolol indicating that BRL 37344 induced an effect on β_1/β_2-AR in human atria (Pott et al., 2003) and fails to directly induce a negative inotropic effect as in human ventricle (Gauthier et al., 1996). Thus, the presence as well as the functional roles of β_3-AR in human normal atria remains to be clarified.

The cardiac effects of several preferential β_3-AR agonists have also shown substantial variability across species and the pharmacological profile of β_3-AR agonists obtained on the human myocardium cannot be extrapolated from usual animal models. Furthermore, using different approaches provide contradictory data. Thus, in guinea-pig atrium, SR 58611A (Bianchetti & Manara, 1990) and CL 316 243 (Dolan et al., 1994) did not modify contractility and heart rate whereas in Langendorff-perfused guinea pig heart, β_3-adrenergic stimulation induced a negative inotropic effect (Kitamura et al., 2000).

In dogs, intravenously administrated β_3-AR agonists induced a positive chronotropic effect (Tavernier et al., 1992). Because a positive chronotropic effect was not observed in denervated animals, it was concluded that the tachycardia resulted from a baroreceptor-mediated reflex in response to a drop in blood pressure caused by the vasodilatory effect of β_3-AR agonists (Berlan et al., 1994; Shen et al., 1994, 1996). However, in the latter study, after combined autonomic blockade, CL 316 243 still induced a positive inotropic effect in the conscious dog, but its effect on heart rate was lost (Shen et al., 1996). Positive chronotropic and inotropic effects were also reported in isolated dog atrium perfused with blood from a donor dog injected with a β_3-AR agonist, BRL 37344. These effects were attributed to β_1-AR stimulation (Takayama et al., 1993) and could result from baroreceptor activation and catecholamine release in the donor dog. In canine papillary muscles, several β_3-AR agonists produced a negative inotropic effect less pronounced than in human myocardium (about 30% and 50%, respectively). However, the rank order of potency of the β_3-AR agonists was very different from that observed in human myocardium (CGP 12177A>BRL 37344≈SR 58611A≫CL 316 243) (Gauthier et al., 1999). The negative inotropic effect of these β_3-AR agonists was associated with the detection of β_3-AR transcripts in the same tissues (Gauthier et al., 1999). In canine myocytes, BRL 37344 produced a concentration-dependent decrease of contraction and relaxation. Those effects were not modified by pretreatment of myocytes with β_1- and β_1/β_2-AR antagonists, indicating that this response was not mediated by β_1- and β_2-AR. By contrast, they were completely blocked by β_3-AR antagonists, bupranolol and L-748,337, indicating that the negative inotropic action of BRL 37344 resulted from an action on β_3-AR. The relevance of those data has been later strengthened by the detection of β_3-AR transcripts and proteins in dogs (Cheng et al., 2001).

In rat atrium, several preferential β_3-AR agonists (CL 316 243, ZD 2079 and SR 58611A) used at micromolar concentrations did not change chronotropy and inotropy whereas they produced a relaxation of colonic smooth muscle at lower (nanomolar) concentrations (Kaumann & Molenaar, 1996). Likewise, no effect of several β_3-AR agonists was found in rat atria (Cohen et al., 1999) and in rat ventricular preparation except a small effect of BRL 37344 (Gauthier et al., 1999). The relevance of those functional data were reinforced by the absence or the very low expression of β_3-AR found in the rat myocardium (Gauthier et al., 1999). In another study, β_3-AR transcripts and proteins were detected in normal heart (Dincer et al., 2001). However, this report did not exclude the possibility that the β_3-AR originated from brown adipose tissue as no investigation was performed with adipose tissue markers such as adipsin. In rat neonatal cardiomyocytes, no functional response was observed (Germack & Dickenson, 2006) suggesting the absence of β_3-AR.

In wild-type mice, β_3-AR agonists induced no significant effects on contractility. This was corroborated by the absence of

detection of β_3-AR proteins (Tavernier et al., 2003). However, cardiac overexpression of the human β_3-AR in mice (TGβ_3) reproduced ex vivo the negative inotropic effects obtained with β_3-AR stimulation in human ventricular tissues (Tavernier et al., 2003). By contrast, in another study performed in vivo in a similar TGβ_3 mouse model, the administration of a β_3-AR agonist, L-755,507, produced a positive inotropic response (Kohout et al., 2001). The different experimental approaches, ex vivo versus in vivo, and the genetic background of the mice (B6D2/F1 vs. B6S/F1 hybrid in the studies of Tavernier et al., 2003 and Kohout et al., 2001, respectively) could partly explain the discrepancy. Furthermore, a single line of mice was investigated in the former study whereas data were collected from several transgenic lines in the latter one. Moreover, the choice of the β_3-AR agonists may be subject to controversy regarding their nature and concentrations used.

4.2. Electrophysiological effects

The mechanisms of β_3-AR-mediated attenuation of cardiac contractility are largely unknown, but the current evidence suggests the involvement of alterations in excitation–contraction coupling and transmembrane ions channels activities. Cardiac electrophysiological effects of the β_3-AR stimulation have not been investigated extensively. In canine and rat cardiomyocytes and in beating guinea-pig heart, the negative inotropic effect of BRL 37344 was associated with an inhibition of L-type calcium channels (Fig. 3) and a decreased amplitude of the intracellular calcium transients (Kitamura et al., 2000; Cheng et al., 2001; Zhang et al., 2005b). In human endomyocardial biopsies, β_3-AR agonists induced a reduction in the amplitude and an acceleration in the repolarization phase of the ventricular action potential in the same range of concentrations that altered mechanical responses (Gauthier et al., 1996). These effects were not observed in ventricular tissues obtained from patients with cystic fibrosis (Leblais et al., 1999), a pathology caused by mutations in the cystic fibrosis transmembrane conductance regulator (CFTR) gene (Riordan et al., 1989). As CFTR protein is expressed in the human heart (Levesque et al., 1992; Warth et al., 1996), the discordant results obtained with β_3-AR agonists in ventricular action potential of noncystic fibrosis and cystic fibrosis patients could result in part from the activation of a chloride repolarizing current flowing through CFTR channels not functional in cystic fibrosis cardiac muscle. In a heterologous expression system co-expressing human β_3-AR and CFTR, β_3-AR agonists induced CFTR activation through a cAMP–PKA-independent pathway (Leblais et al., 1999). The modulation of action potential repolarization by β_3-AR stimulation could also result from an effect on potassium channels. However, controversial data exist regarding the role of potassium currents. In a recombinant system, it was suggested that β_3-AR activated the potassium channel KvLQT1/MinK (Kathofer et al., 2000). However, in this study, preferential β_3-AR agonists were not used. In guinea-pig cardiomyocytes, BRL 37344 inhibited the potassium channel I_{Ks} leading to an increase in action potential duration (Bosch et al., 2002). Further work will be needed to determine the putative role of β_3-AR in the regulation of cardiac repolarization.

Concerning the regulation of heart rate by the β_3-AR stimulation, several in vivo studies using preferential β_3-AR agonists such as BRL 37344 and CL 316 243, reported a positive chronotropic effect in dogs and rats (Tavernier et al., 1992; Shen et al., 1994, 1996). However, these effects resulted probably from reflex mechanisms rather than from a direct stimulation of cardiac β_3-AR as they were abolished after sinoaortic denervation in conscious dogs (Tavernier et al., 1992) or after β_1- and β_2-AR blockade in dogs and rats (Shen et al., 1996). Likewise, in humans, the positive β_3-AR-related chronotropic effects described by Wheeldon et al. (1993, 1994) were prevented by β_1- or β_2-AR antagonists and were likely due to baroreflex activation secondary to the vasodilation induced by the β_3-AR agonist. In TGβ_3 mice, heart rate was significantly increased (Tavernier et al., 2003) whereas in another study wild-type and TGβ_3 mice presented similar heart rate (Kohout et al., 2001). The increase in heart rate reported by

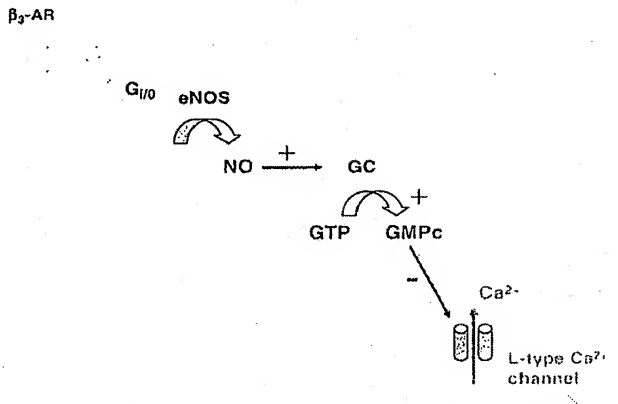

Fig. 3. Signaling pathway of β_3-AR in cardiomyocytes. β_3-AR: β_3-adrenoceptor; Ca^{2+}: calcium; cGMP: cyclic guanosine monophosphate; eNOS: endothelial nitric oxide synthase; $G_{i/o}$: $G_{i/o}$ protein; GTP: guanosine triphosphate; GC: guanylyl cyclase; NO: nitric oxide; +: stimulation; −: inhibition.

Tavernier et al. (2003) could result from the activation of KvLQT1 which is expressed in the mice conduction system (Wang et al., 1996) or by the presence of constitutively active β_3-AR due to their overexpression as previously described for the β_2-AR (Milano et al., 1994). By contrast, as I_{Ks} is absent in adult mice heart (Kupershmidt et al., 1999), this potassium current could not be involved in the effects observed on heart rate. Then, future works will have to be performed to clarify the role of β_3-AR in heart rate regulation.

4.3. Signaling pathways

In the heart, contrary to β_1- and β_2-AR, β_3-AR are not coupled to G_s proteins, but to G_i proteins (Fig. 3). The pretreatment by pertussis toxin of human ventricular tissues, canine and rat cardiomyocytes abolished the negative inotropic effect induced by β_3-AR stimulation (Gauthier et al., 1996; Cheng et al., 2001; Zhang et al., 2005b). In rodent adipocytes, β_3-AR could be coupled both to G_i and G_s proteins (Chaudhry et al., 1994; Begin-Heick, 1995). Recently, it has been shown in a recombinant system that the mice β_{3b}-AR isoform coupled to both G_s and G_i, while the β_{3a}-AR coupled only to G_s (Hutchinson et al., 2002). At the present time, no study has evaluated the signaling pathways activated by the stimulation of β_{3a} and β_{3b} isoforms in native systems as well as the existence of those 2 isoforms in the heart.

In human ventricle, the activation of G_i proteins did not appear to cause an inhibition of adenylyl cyclase, but rather an activation of the nitric oxide (NO) pathway, probably implicating the endothelial nitric oxide synthase (eNOS) (Fig. 3; Gauthier et al., 1998), which is expressed both in endothelial cells and ventricular cardiomyocytes (Schulz et al., 2006). In β_3-AR knockout mice, the cardiac contractility in response to isoproterenol was increased compared to wild-type mice. Albeit this response was not modified after NO synthase inhibition by N^G-monomethyl-L-arginine monoacetate (L-NMMA) in knock-out mice, but was potentiated in wild-type mice (Varghese et al., 2000). As no β_3-AR transcript and protein has been detected in wild-type mouse heart, this effect could result from the presence of β_3-AR in vessels. Furthermore, this study suggests that β_3-AR/NO pathway could act as a negative feedback mechanism opposing the positive inotropic influences of catecholamines in the heart.

The NO production produces an activation of soluble guanylyl cyclase leading to an increase in intracellular cyclic guanosine monophosphate (cGMP) (Fig. 3; Gauthier et al., 1998). Similar results demonstrating an involvement of the same pathway were obtained in canine and rat cardiomyocytes (Cheng et al., 2001; Zhang et al., 2005b). The cGMP elevation could activate different targets: (1) the cGMP-dependent protein kinase, which decreases calcium current through regulation of L-type calcium channels (Mery et al., 1991; Wahler & Dollinger, 1995) or down-regulates the contractile response of myofilament proteins independently of changes in calcium transients (Shah et al., 1994; Goldhaber et al., 1996; Yasuda & Lew, 1997), and (2) the cGMP-stimulated phosphodiesterases (PDE II; Beavo, 1995) which decreases cAMP levels (Mery et al., 1993). Alternatively, NO might regulate cardiac function in a cGMP-independent manner through covalent modifications of key proteins such as the cytochrome c oxydase (Torres et al., 1995), the creatine phosphokinase (Gross et al., 1996) or L-type calcium channels (Campbell et al., 1996). However, the mechanism involved in the inhibition of L-type calcium current by the β_3-AR stimulation observed in canine and rat cardiomyocytes (Cheng et al., 2001; Zhang et al., 2005b) is not yet elucidated.

In human atrial trabeculae, BRL 37344 did not modify the force of contraction by activating β_3-AR. However, it stimulated directly eNOS activity leading to an increase in NO production (Pott et al., 2003). This study suggests that β_3-AR stimulation in human atrium do not have the same functional significance as in ventricular myocardium. This could be explained by (i) a different coupling in human atrium and ventricle, (ii) a lower β_3-AR expression in right atrium than in left ventricle, where studies are classically performed, and (iii) an overexpression of eNOS in atrium (Bloch et al., 1999). It has been suggested that the atrial β_3-AR system might provide a protective negative feed back mechanism against arrhythmia and sinusal tachycardia resulting from an excessive β_1/β_2-AR stimulation. However, this hypothesis is not in agreement with the results obtained in TGβ_3 mice, which presented an increase of the basic heart rate (Tavernier et al., 2003). This discrepancy could be explained by the fact that right atrial tissues were obtained from patients with either valvular or coronary disease and the β_3-AR response could be influenced by disease state and/or medication. Further work will be needed to evaluate the putative role of atrial β_3-AR in arrhythmia and sinusal tachycardia.

5. β_3-adrenoceptors in blood vessels

Over the last 20 years, knowledge of vascular physiology and pharmacology has dramatically changed, mainly because of the recognition of the role of endothelium in vasomotor control. Activation of endothelial receptors induces either vasodilation (Furchgott & Zawadzki, 1980) or vasoconstriction (De Mey & Vanhoutte, 1982). Furthermore, recent work suggests a new perspective of β-AR signaling in the vessels partly in relation with the description of the third β-AR subtype. Stimulation of β-AR leads to a relaxation of vascular smooth muscle, thereby controlling the blood flow distribution in different organs. Both β_1-AR and β_2-AR are involved in vasodilation. Classically, the β_2-AR are the predominant β-AR in the peripheral vessels (Lands et al., 1967), but the involvement of each β-AR subtype varies according to vascular bed and species (Osswald & Guimaraes, 1983). For instance, β_1-AR seem to be predominant in coronary and cerebral arteries (Edvinsson & Owman, 1974; O'Donnell & Wanstall, 1985). Moreover, Krauss et al. (1992) showed that the magnitude of β-AR-mediated responses of epicardial coronary arteries was inversely related to the size of the vessel. Even in a given model, contradictory results can be observed. Thus, in the rat aorta, endothelium-independence, or partial and total dependence for isoprenaline-induced vasodilation, was demonstrated (Konishi & Su, 1983; Brawley et al.,

2000). To explain these contradictory results, Guimaraes and Moura (2001) suggested that the β-AR induced relaxation might be differently observed according to: (i) the precontractive agent used, (ii) the precontraction level and (iii) the expression amount of β-AR.

In this context, the discovery of β_3-AR increases the complexity of the sympathetic regulation in the vascular system.

5.1. In vivo studies

In vivo studies have been conducted to establish the effect of β_3-AR agonist on systemic hemodynamics and regional blood flow distribution in different models.

In conscious rats, Shen et al. (1994, 1996) showed that CL 316 243 and BRL 37244 induced hypotension and peripheral vasodilation, which persisted after blockade of β_1- and β_2-AR, suggesting that BRL 37344 was a potent β_3-AR agonist but less selective than CL 316 243 (Shen et al., 1996). Tracer microspheres were used to evaluate the effect of β_3-AR agonists on some regional blood flow in anesthetized rat. Neither CL 316 243 nor BRL 26830A induced significant blood pressure variation in rat. Nevertheless, blood flow was increased by CL 316 243 in pancreatic islet (Atef et al., 1996) and by BRL 26380A in brown adipose tissue (Takahashi et al., 1992). In addition, several β_3-AR agonists (BRL 35135, CL 316 243, SR 58611A) increased antral gastric mucosal blood flow in rats anesthetized with halothane (Kuratani et al., 1994).

Genetic knockout techniques have allowed investigations to delineate subtype-specific contributions of β-AR in mouse. Rohrer et al. (1999) observed compensatory vascular β_3-AR responsiveness in β_1/β_2-AR double knockout mice. Thus, in those anesthetized mice, CL 316 243 induced an exaggerated hypotensive response comparatively to wild-type mice.

In conscious dogs, Tavernier et al. (1992) demonstrated that BRL 37344 induced hypotension. Similar hypotension has also been observed with BRL 37344 and CL 316 243 in normal and sinoaortic denervated dogs (Berlan et al., 1994). The evaluation of cutaneous blood flow using Laser-Döppler technology showed an increase of skin perfusion. In conscious dogs instrumented and after combined pharmacological blockade, the evaluation of regional blood flow pattern induced by BRL 37344 using radioactive microspheres confirmed the decrease of blood pressure related to peripheral conductance increase and vasodilation in fat tissue and skin (Shen et al., 1994). In the same way, in normal dogs, infusion of SR 58611A induced hypotensive effect by peripheral vasodilation, which was resistant to β_1/β_2-AR blockade (Donckier et al., 2001). As in the rat, CL 316 243 seems to be a more specific β_3-AR agonist than BRL 37344 in the dog (Shen et al., 1996). More importantly, the vascular effects of β_3-AR stimulation was most profound in dogs than in other species studied (Shen et al., 1996).

Anecdotally, BRL 37344 induced dose-dependent increases in nasal arterial blood flow and volume of the nasal mucosa (reflecting capacitance vessel function) in anesthetized pigs (Lacroix et al., 1995).

Few works evaluated the effects of β_3-AR stimulation in the cardiovascular system in human and nonhuman primate. In the latter, CL 316 243 and BRL 37344 elicited almost no effect on cardiovascular parameters in conscious monkeys and baboons (Shen et al., 1996). In humans, CGP 12177A, a partial β_3-AR agonist, induced a weaker effect in the control of lipolysis and nutritive blood flow in human subcutaneous abdominal adipose tissue (Barbe et al., 1996). In human healthy volunteers, Wheeldon et al. (1994) evaluated the effects of another β_3-AR agonist BRL 35315. BRL 35315 is rapidly converted to the de-esterified acid metabolite, BRL 37344, in vivo and it is believed that effects of BRL 35135 are actually mediated by BRL 37344. This study suggested that BRL 35135 produced most effects by β_2-AR stimulation. To be exhaustive, a recent published placebo-controlled randomized trial showed that a 28 days treatment with L-796,568, a β_3-AR agonist, did not induce any significant cardiovascular changes (Larsen et al., 2002).

5.2. Conductive arteries

In rat thoracic aorta, Clark and Bertholet (1983) have shown that pindolol, a nonspecific β-AR agonist with partial β_3-AR agonistic activity induced vasodilation resistant to pretreatment with propranolol, suggesting the presence of an atypical β-AR receptor. In the same way, some studies demonstrated that isoproterenol-induced relaxation was resistant to β_1/β_2-AR blockade in rat carotid and thoracic aorta (Oriowo, 1994; MacDonald et al., 1999; Trochu et al., 1999).

In thoracic aorta, BRL 37344 induced a concentration-dependent vasorelaxation in phenylephrine (α_1-AR agonist)-preconstricted arterial rings (Oriowo, 1995). Similar relaxant effects were obtained with SR 58611A, which were not modified by pretreatment with nadolol but were antagonized by SR 59230A, a β_3-AR antagonist (Trochu et al., 1999). Endothelium removal strongly reduced the β_3-AR-induced relaxation, indicating that β_3-AR were mainly located on endothelial cells in rat thoracic aorta (Trochu et al., 1999). Endothelial cell localization was latter confirmed by molecular and immunohistochemical approaches (Rautureau et al., 2002). However, these results have been contested. Thus, in the same vascular bed, Brahmadevara et al. (2003) showed that in phenylephrine-constricted rings, but not PGF2α-constricted ones, relaxations to isoproterenol presented a propranolol-resistant component. In phenylephrine-constricted rings, the selective β_3-AR antagonist, SR 59230A, did not antagonize relaxation to BRL 37344 and SR 58611A. In addition, CL 316 243 failed to produce relaxation. In PGF2α-constricted rings, only SR 58611A produced relaxation, which was not affected by SR 59230A. Recently, a study demonstrated that SR 58611A and nebivolol (a selective β_1-AR antagonist with partial β_3-AR agonistic properties) induced a vasodilation in endothelin 1-constricted rings. Vasodilation was antagonized by a selective β_3-AR antagonist (L-748,337) (Rozec et al., in press). This study confirms the fact that nebivolol-induced NO-dependent vasorelaxation in rat thoracic aorta resulted, at least in part, from a β_3-AR agonistic effect (de Groot et al., 2003). In summary, multidisciplinary approaches indicate that β_3-AR are present in

rat thoracic aorta, but its vasodilating effects are affected by the constricting agent used. Hence, as suggested by some workers (see for instance, Kozlowska et al., 2005), the constrictor agent should be chosen with great caution for the investigation of the role of β-AR in vessels. Recently, it has been suggested that β_3-AR were involved in the β-AR-mediated relaxation of rat abdominal aorta smooth muscle (Matsushita et al., 2003). However, those data should be taken with caution because the use of only a partial β_3-AR agonist and the endothelial removal was not tested.

In rat isolated carotid artery, as in aorta, propranolol shifted the isoproterenol concentration relaxation curve to the right without changing the maximum response. Moreover, BRL 37344 also produced a concentration-dependent relaxation of norepinephrine-precontracted artery segments. This relaxation was endothelium-independent and was not affected by propranolol (Oriowo, 1994). Comparable results have been obtained with U-44619 (a thromboxane A2 homolog)-constricted rat isolated carotid arteries (MacDonald et al., 1999). Nevertheless, in the latter study, it was suggested that there may be a different contribution of endothelium of classical β- and β_3-AR-mediated effects, with lesser involvement of endothelium in the β_3-AR-mediated relaxation. In the main mesenteric artery, the presence of atypical β-AR and the lack of β_3-AR have been reported (Kozlowska et al., 2003). The fact that β_3-AR agonists caused relaxation might suggest the involvement of β_3-AR rather than atypical β-AR in this effect. However, a detailed comparison of the order of potencies argued for the opposite conclusion instead.

In mice lacking β_1- or β_2-AR subtypes (β_1-KO, β_2-KO), isoproterenol induced relaxation of segments from thoracic aorta, carotid, femoral arteries. In contrast, in double β_1/β_2-KO mice, isoprenaline-relaxation was abolished, suggesting no β_3-AR effect (Chruscinski et al., 2001). Interestingly, in the same double β_1/β_2-KO mice, an in vivo study showed that the response to the β_3-AR agonist, CL 316 243, alone was significantly increased in the β_1/β_2-AR double KO (Rohrer et al., 1999). The results of this study suggested that all β-AR subtypes can mediate vasodilatory responses in vivo and that an enhancement of β_3-AR responsiveness is present in mice lacking both β_1- and β_2-AR.

The most popular human conductive vessel used in organ bath studies is the internal mammary artery harvested during coronary artery bypass graft. In endothelium-denuded internal mammary artery precontracted with phenylephrine, BRL 37344 produced a concentration-dependent relaxation suggesting the presence of an atypical β-AR, perhaps β_3-AR, located in smooth muscle cells (Shafiei et al., 2000). Recently, using molecular and biochemical approaches, the presence of β_3-AR was confirmed, but with an endothelial localization (Rozec et al., 2005). Its activation by SR 58611A induced a vasodilating NO-dependent response, unaffected by β_1/β_2-blockade, but antagonized by L-748,337, a selective β_3-AR antagonist (Rozec et al., 2005). The tocolytic effect of β_3-AR agonists leads some authors to explore effects of β_3-AR agonists on umbilical and placental vascular beds. In human umbilical artery, BRL 37344 induced a weak vasodilation (Dennedy et al., 2002). In human placental artery obtained from women with uncomplicated or pre-eclamptic pregnancies, SR 59119A induced relaxation. The functional presence of β_3-AR was strengthened by molecular and biochemical approaches (Rouget et al., 2005).

5.3. Resistive arteries

Few studies have been carried out concerning β_3-AR in arteries with diameters between 2 and 300 μm, referred to as resistance arteries.

In rat mesenteric microarteries, relaxation mediated by β-AR is due mainly to the stimulation of β_1-AR present throughout the smooth muscle cell layer, with a partial intracellular location (Briones et al., 2005). In this work, evidence against the participation of β_2- and β_3-AR is also reported. Thus, in phenylephrine-precontracted arteries, although salbutamol (β_2-AR agonist), BRL 37344 (β_3-AR agonist) and CGP 12177A (agonist of the low affinity state of β_1-AR) caused relaxation (with a less potency than isoproterenol), CL 316 243 was ineffective. In arteries precontracted with 5-HT or U-46619, isoproterenol produced a concentration-dependent relaxation whereas salbutamol, BRL 37344, CGP 12177A and CL 316243 did not. Furthermore, in phenylephrine-precontrated arteries, the vasodilation induced by BRL 37344 and SR 59230A could be explain by a competitive α_1-AR antagonism.

In mice lacking β_1- and/or β_2-adrenergic receptor subtypes, several resistive arteries, including distal branches of the femoral artery, epigastric, and mesenteric arteries, were investigated to determine whether they showed a β-adrenergic vasorelaxation (Chruscinski et al., 2001). Among these different vessels, isoproterenol caused relaxation only in the mesenteric artery, and this relaxation was mediated only by the β_1-AR subtype because the effect of isoproterenol was completely absent in vessels from β_1-KO mice. However, in another vascular bed, using videomicroscopy, it has been recently shown that nebivolol (a selective β_1-AR antagonist with partial β_3-AR agonistic properties) dose-dependently relaxed mice coronary resistance microarteries precontracted with prostaglandin F2α. This relaxation was sensitive to NO synthase inhibition, unaffected by the β_1/β_2-AR antagonist, nadolol, and prevented by the $\beta_1/\beta_2/\beta_3$-AR antagonist, bupranolol. Importantly, nebivolol failed to relax microarteries from β_3-AR-deficient mice (Dessy et al., 2005).

In human coronary microartery preparations, β_3-AR transcripts and protein have been detected. The presence of β_3-AR was confirmed by the vasodilation induced by BRL 37344 and nebivolol in endothelin-1-preconstricted microarteries. This relaxation was not affected by pretreatment with nadolol, thereby ruling out a β_1/β_2-AR-mediated effect, but was fully abrogated by bupranolol (Dessy et al., 2004, 2005).

In human corpus cavernosum, β_3-AR are localized mainly in smooth muscle cells. Their activation by a preferential β_3-AR agonist, BRL 37344, relaxed longitudinal strips precontracted with phenylephrine. This relaxation was selectively blocked by a specific β_3-AR antagonist, SR 59230A (Cirino et al., 2003).

5.4. Pulmonary circulation

The pulmonary circulation differs from the systemic one in several important aspects, the most important being the hypoxic pulmonary vasoconstriction. The precise mechanisms underlying hypoxic pulmonary vasoconstriction are far from clear. The vasodilator profiles of 3 selective β_3-AR agonists, SR 59104A, SR 59119A and SR 58611A, on the hypoxic vasoconstriction have been investigated in the rat isolated perfused lung preparation (Dumas et al., 1998). The 3 β_3-AR agonists caused concentration-dependent relaxation during the pulmonary pressure response. SR 59230A, a β_3-AR antagonist, inhibited vasorelaxant effects of SR 59104A but failed, as with propranolol, to oppose those of SR 59119A and SR 58611A. Based on these results, the authors suggested the existence of an atypical β-AR in rat pulmonary vessels. In the same species, intralobar pulmonary artery precontracted with PGF2α, isoproterenol induced vasorelaxation which was not fully abolished by pre-treatment with nadolol. However, the remaining dilation was not further inhibited by SR 59230A. Moreover, BRL 37344, SR 58611A and CGP 12177A did not elicit vasorelaxation, suggesting the absence of β_3-AR in this vascular bed (Pourageaud et al., 2005). Nevertheless, according to the size of the vessels, β-AR subtypes could be different as suggested by the fact that β-AR mediated vasorelaxation in large arteries was largely NO-dependent, whereas in small arteries a significant proportion of relaxation was NO-independent (Priest et al., 1997).

In isolated canine pulmonary arterial rings precontracted with norepinephrine, CL 316 243 and BRL 37344 produced a concentration-dependent relaxation, but with a lower potency than isoproterenol and salbutamol suggesting the functional presence of β_3-AR in canine pulmonary artery smooth muscle (Tagaya et al., 1999).

5.5. Venous system

In isolated segments of the rat portal vein, BRL 37344 produced a concentration-dependent inhibition of electrically-induced contractions. This inhibitory effect of BRL 37344 was not antagonized by propranolol. In addition, BRL 37344 inhibited adrenergic transmission in this vascular bed via atypical β-AR that were distinct from β_3-AR and were located pre-junctionally (Yousif & Oriowo, 2002).

In equine digital veins, several β_3-AR agonists, SR 58611A, ZD 2079 and ZM 215001, induced concentration-dependent relaxation. SR 58611A-induced relaxation were unaffected by nadolol (β_1/β_2-blocker) but significantly reduced by ZM 215001 used at a high concentration (2 μM) and behaved as a β_3-AR antagonist, by endothelium removal or pre-treatment with a NO synthase inhibitor suggesting the presence of β_3-AR

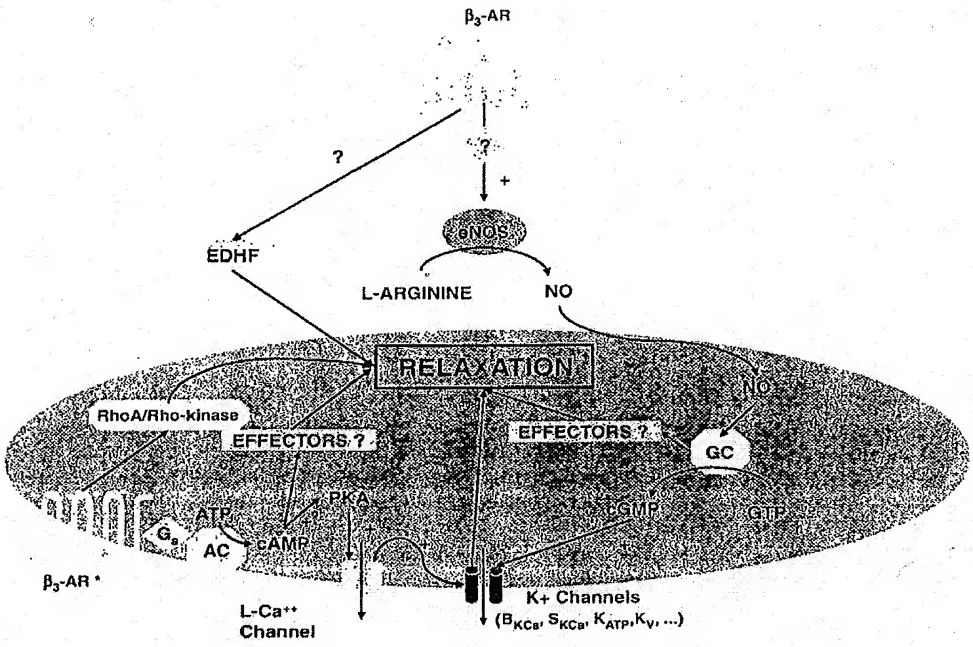

Fig. 4. Main signaling pathways of β_3-AR in the vessels, including all hypothesis regardless the species and vascular beds. AC: adenylyl cyclase; ATP: adenosine triphosphate; $[Ca^{2+}]_i$: intracellular calcium concentration; cAMP: cyclic adenosine monophosphate; cGMP: cyclic guanosine monophosphate; EDHF: endothelial derived hyperpolarising factor; eNOS: endothelial nitric oxide synthase; GC: guanylyl cyclase; GTP: guanosine triphosphate; G_s: stimulatory G protein; NO: nitric oxide; PKA: cAMP-dependent protein kinase.

in equine digital veins (Mallem et al., 2003). However, their roles have yet to be determined.

5.6. Signaling pathways in vascular tissue

Few studies have been carried out to determine the precise signaling pathways involved in vascular β_3-AR activation. As mentioned previously, the cellular localization of β_3-AR varied according to the vascular bed, the vessel size and the species. In the rat thoracic aorta, β_3-AR are mainly located in endothelial cells, and act in conjunction with β_1- and β_2-AR to mediate relaxation through activation of a NO synthase pathway and a subsequent increase in intracellular cGMP levels (Fig. 4; Trochu et al., 1999). In the same model, Rautureau et al. (2002) demonstrated that the β_3-AR-mediated effect, in contrast to the heart, did not result from the activation of a pertussis toxin-sensitive G protein. In this vascular bed, β_3-AR-mediated relaxation involved several potassium channels. The pre-treatment of aortic rings by iberiotoxin, glibenclamide, tolbutamide or 4-aminopyridine, significantly reduced the SR 58611A-mediated vasorelaxation, suggesting that B_{KCa}, K_{ATP} and K_v, respectively, are effectors of the vasorelaxation produced by β_3-AR stimulation in rat thoracic aorta (Fig. 4). However, this inhibition was not complete in each experimental condition suggesting the participation of several classes of potassium channels in this global effect. An involvement of potassium channels in the relaxant effect of β_3-AR was also reported in the rat isolated perfused lung preparation. β_3-AR vasodilated the pulmonary vascular bed, partly through B_{KCa} and S_{KCa} channels activation and NO release (Dumas et al., 1999). In rat portal vein myocytes, the activation of β_3-AR stimulated L-type calcium channels through a $G_{\alpha s}$-induced stimulation of the cAMP/PKA pathway leading to the subsequent phosphorylation of those channels (Viard et al., 2000). However, it is important to note that in this study, no preferential β_3-AR agonist was tested but only CGP 12177A, which combines partial β_3-AR and low affinity β_1-AR agonistic properties.

The involvement of the cAMP pathway was also suggested in the canine pulmonary artery. In this vessel, the dilating effect of CL 316 243 was endothelium-independent and produced an increased in intracellular cAMP level (Tamaoki et al., 1998).

In the human internal mammary artery, SR 58611A induced an endothelium- and NO-dependent relaxation (Fig. 4; Rozec et al., 2005). In human coronary microarteries precontracted with KCl (thereby preventing vessel hyperpolarization), the relaxation to BRL 37344 was reduced and totally abrogated by the NO synthase inhibitor, L-omega-nitroarginine, confirming the participation of a NO-mediated relaxation (Dessy et al., 2004). The NO synthase-independent relaxation was completely inhibited by calcium-activated potassium channel inhibitors, apamin and charybdotoxin, consistent with an additional endothelium-derived hyperpolarizing factor-like response. Accordingly, membrane potential recordings demonstrated a hyperpolarization in response to β_3-AR stimulation. In human placental arteries, SR 59119A induced an endothelium-independent vasodilation mediated by an intracellular cAMP increase without modification in the cGMP level (Rouget et al., 2005).

In the human corpus cavernosum, β_3-AR relaxation resulted from the inhibition of the RhoA/Rho-kinase pathway (Cirino et al., 2003).

6. Involvement of β_3-adrenoceptors in cardiovascular pathologies

6.1. Heart failure

The failing human heart is characterized by a sustained activation of the sympathetic nervous system. The higher catecholamine levels help to maintain cardiac performance over the short-term by increasing contractility and heart rate. At first, the increase of cardiac adrenergic drive is beneficial, but ultimately damaging to the myocardium.

In all models investigated, β_3-AR are upregulated in human heart failure (Moniotte et al., 2001) as well as in cardiomyocytes from dog with pacing-induced cardiac heart failure (Morimoto et al., 2004). However, changes in contractile response did not strictly parallel with β_3-AR abundance. In human, the negative inotropic effect induced by BRL 37344 was blunted in failing heart tissue compared to responses observed in nonfailing heart tissue (Moniotte et al., 2001). In animal models, the upregulation of β_3-AR observed in heart failure was correlated with an increase in the negative inotropic effect induced by the β_3-AR stimulation (Cheng et al., 2001; Morimoto et al., 2004; Zhang et al., 2005b). This discrepancy might result from several factors such as species difference in β_3-AR, variation in severity of heart failure, or the effect of pharmacotherapy on the human failing heart. The rat model of heart failure was associated with a 40–48% mortality during the investigated period (4 months) without precision about the stage of heart failure (Zhang et al., 2005b), which is much higher than would be expected in a population of human heart failing patients. In addition, in the rat and dog models, the authors examined a single left ventricular myocyte obtained from isoproterenol-induced failing rat hearts (Zhang et al., 2005b) or from dog with pacing-induced cardiac heart failure (Morimoto et al., 2004), whereas Moniotte et al. (2001) studied ventricular strips obtained from dilated or ischemia-caused failing human hearts. To support this discrepancy, it is important to note that heart failure is also characterized by an alteration of the vasomotor tonus leading to a decreased vasodilation at baseline and in response to β-AR stimulation. Those alterations lead to impaired peripheral vasodilation and an inappropriate vasoconstriction. This effect is due to the activation of neuro-hormonal systems and endothelial dysfunction. Thus, it is important to take into account the role of endothelial cells in the cardiac response.

Comparing the expression of the different β-AR subtypes, we previously noted that the human failing heart contained a relatively high proportion of β_2-AR due to selective down-regulation of β_1-AR, without change in the total β_2-AR density. In this context, the importance of β_3-AR in the pathogenesis of heart failure is supported by several features: (i) β_3-AR are

coupled to $G_{i/o}$ proteins that are upregulated during heart failure (El-Armouche et al., 2003); (ii) β_3-AR is relatively resistant to desensitization following activation by an agonist (Strosberg, 1997); (iii) β_3-AR is also resistant to heterologous desensitization, because it lacks the consensus sequences for phosphorylation by PKA and β-ARK (Strosberg, 1997); (iv) β_3-AR is activated at higher catecholamine concentrations than β_1- and β_2-Ar (Pietri-Rouxel & Strosberg, 1995) and finally (v) β_3-AR are upregulated at end stage of human heart failure (Moniotte et al., 2001) and in cardiomyocytes from dog with pacing-induced cardiac heart failure (Morimoto et al., 2004). Therefore, in heart failure with the sustained activation of the sympathetic system, the β_3-AR-mediated response may be probably preserved, when β_1- and β_2-AR-mediated responses are reduced (Moniotte & Balligand, 2002). The regulation of cardiac contractility by catecholamines in heart failure indicates opposite compensatory modifications between β_1/β_2- and β_3-AR. Several studies also report similar opposite modifications in cardiac β-AR subtypes. Kohout et al. (2001) have reported that β_1-AR expression was lower in TGβ_3 mice. In contrast, β_3-AR knockout mice exhibited an increase in β_1-AR mRNA in white and brown adipose tissue (Susulic et al., 1995). Recently, in neonatal rat cardiomyocytes following chronic exposure to norepinephrine, β_3-AR are functionally up-regulated whereas β_1- and β_2-AR are down-regulated (Gennack & Dickenson, 2006).

The opposite changes that occurred in β_1- and β_3-AR (2- to 3-fold increase) abundance in the human failing left ventricle, with an imbalance between their inotropic influences, may underlie the functional degradation of the human failing heart. However, at earlier stages of the disease, the upregulation of the β_3-AR could be viewed as a compensatory mechanism to prevent further cardiomyocyte damage. In TGβ_3 mice, no histological evidence of myocyte hypertrophy or fibrogenesis was observed (Tavernier et al., 2003), suggesting that the activation of β_3-AR was not responsible for cardiac damage during heart failure. Furthermore, in contrast, Engelhardt et al. (2002) showed that chronic stimulation of β_1-AR lead to hypertrophy, interstitial fibrosis and heart failure in β_1-AR transgenic mice. Thus, over-expression of β_3-AR might protect cardiac damage induced by the high catecholamine level present in heart failure, particularly during the early stages of the disease. The β_3-adrenergic stimulation related-cardiac protection might result from (i) a reduction of the activation of L-type calcium channels and thus, of calcium overload, (ii) a better diastolic function due to NO production, (iii) a preservation of intracellular ATP and creatine phosphate content related to the negative inotropic effect and finally (iv) the vasodilating effects, because arteriolar and venous dilatation would reduce afterload and preload, respectively, and improve the O_2/MVO_2 balance. In a similar way, in normal heart, the negative inotropic effect induced by the β_3-adrenergic stimulation might play a role of a «safety-valve» during intense adrenergic stimulation (stress, important physical effort, etc.). Conversely, as heart failure progresses to a later stage, the activation of β_3-AR might become deleterious, with a persistent negative inotropic effect enhancing myocardial depression. In rat failing heart, the effect of β_3-AR agonists aggravated markedly cardiac function and stimulated cardiac myocytes apoptosis. Thus, if the levels of β_3-AR were too high, they might contribute to the loss of cardiac function and provide the basis of the functional degradation of failing heart (Kong et al., 2004). Further experiments, using complementary approaches (in vitro, ex vivo and in vivo) and appropriate animal models, will be needed to evaluate the involvement of β_3-AR at early and end stages of heart failure.

The beneficial effects of β_3-AR stimulation is further suggested by recent findings concerning the use of 3rd generation β-blockers in heart failure treatment. Thus, although β-AR blockade has been found to improve survival in patients with heart failure, the mechanism responsible for the beneficial effects of blocking β-AR activation could actually be due to the effects of these agents on the vasculature. The β-blockers of 3rd generation have vasodilator action (Toda, 2003) and may be more efficient to treat heart failure than nonvasodilatory ones. The use of such drugs might be particularly relevant to improve tolerability in elderly patients with heart failure, when endothelial vasodilator reserve is limited, age-associated fibrotic changes in the sinus node occur, and higher risk of hypotension and bradychardia are present. Some recent clinical trials are already quite encouraging (Flather et al., 2005). Furthermore, patients with left ventricular hypertrophy seem to be particularly sensitive to the beneficial effect of NO on diastolic function (Matter et al., 1999) and trials in patients with left ventricular dysfunction had already shown a greater improvement in the parameters of diastolic function, associated with an increase in exercise capacity, with nebivolol administration, compared with the traditional β-blockers (Nodari et al., 2003). Moreover, any blockers that could induce NO release and chelate oxygen radicals may provide additional useful actions by blunting apoptosis, necrosis and/or proliferation of myocardial cells. In fact, some of those β-blockers, such as bucindolol and nebivolol, have been described as β_3-AR agonists, with endothelium-dependent vasodilating properties (Gosgnach et al., 2001; De Groot et al., 2003; Rozec et al., in press). A trial using bucindolol in patients with advanced chronic heart failure produced no significant overall survival benefit leading to stop the trial and to withdraw bucindolol (Beta-Blocker Evaluation of Survival Trial Investigators, 2001). However, it is difficult to draw conclusions regarding the absence of benefit of bucindolol because this trial was performed on a demographically diverse group of patients with NYHA class III and IV heart failure, due to primary or secondary dilated cardiomyopathy, and associated with a left ventricular ejection fraction of 35% or lower.

6.2. *Hypertension*

Hypertension results essentially from an imbalance between the vasoconstrictive and vasodilatory mechanisms, partly due to pre- and post-synaptic sympathetic dysfunctions (De Champlain, 2001). A generalized decrease of the β-adrenergic response has been recognized in systemic hypertension in human (Michel et al., 1990) and in various animal models (Feldman, 1987; Michel et al., 1990; Doggrell & Surman, 1995). The main defects identified include β-AR

down-regulation, alteration of G protein levels and impairment of β-AR-G protein-effectors coupling (Werstiuk & Lee, 2000). However, some studies described that β-AR-mediated relaxation of thoracic aorta and mesenteric arteries of hypertensive rats was unchanged (Borkowski et al., 1992; Boonen et al., 1993) or enhanced (Carvalho et al., 1987) in comparison with what was observed in normotensive rats. Several explanations may exist for those controversial findings regarding β-AR-induced relaxation in arterial hypertension. Thus, the β-AR-mediated relaxation was dependent on: (1) the stage of hypertension (Borkowski et al., 1992), (2) the agent used for preconstraction of vessels (Konishi & Su, 1983; Carvalho et al., 1987) and (3) the precontraction level (Konishi & Su, 1983; Carvalho et al., 1987). It is important to note that in all those studies, the β-AR relaxant responses have been investigated by using isoproterenol, a nonselective β-AR agonist, and the contribution of each β-AR subtype in the β-adrenergic-mediated relaxation was not determined. There are only few data about the potential role of vascular β_3-AR in hypertension. In a canine perinephritic hypertension model, β_3-adrenergic stimulation has been shown to be beneficial (Donckier et al., 2001). In 12-week-old spontaneously hypertensive rats, we have described an up-regulation of the β_3-AR expression, albeit it was not associated with an increase in the β_3-adrenergic-induced vasorelaxation (Mallem et al., 2004).

Concerning the role of β-blockers in the hypertensive treatment, nebivolol which also possesses β_3-AR agonistic properties, seems the most appropriate β-AR blocker for the management of patients with mild to moderate essential hypertension (Czuriga et al., 2003). In addition, only nebivolol, a β-blocker with NO donor properties, has been shown to improve endothelial function, but this effect results from the increase in NO and not from the β-AR blocking properties of the drug (Thuillez & Richard, 2005).

A missense mutation of the β_3-AR gene, resulting in replacement of tryptophan by arginine at codon 64 (*W64R*), has been described (Walston et al., 1995; Widen et al., 1995; Clement et al., 1995). This single nucleotide polymorphism has been associated with insulin resistance (Widen et al., 1995), obesity in both adults (Clement et al., 1995; Kurabayashi et al., 1996; Mitchell et al., 1998) and children (Endo et al., 2000), hyperinsulinemia (Xiang et al., 1998), an increased capacity to gain weight (Clement et al., 1995), and fasting concentrations of high-density lipoprotein (Thomas et al., 2000) and glucose (Corella et al., 2001). This polymorphism has also been associated with hypertension (Table 2; Tonolo et al., 1999; Ringel et al., 2000; Hao et al., 2004). A study carried out in a large unselected sample of a white male working population in Southern Italy showed that the Trp64Arg variant of the β_3-AR predicts a greater tendency to develop abdominal adiposity and high blood pressure with advancing age (Strazzullo et al.,

Table 2
Trp64Arg polymorphism in human β_3-AR and hypertension

Population	*n*	Association	Comments	References
Caucasian population (Hungary)	147 healthy/295 obese children	Yes	Although the prevalence of this polymorphism was similar in children, it seems to be associated with increased adiposity and higher fasting insulin levels	Erhardt et al., 2005
Japanese young	160 non-obese normotensive men	Yes	BP elevation over 5 years	Masuo et al., 2005
European origin student	175 adolescents: 121 normotensive and 54 hypertensive	No	Trp64Arg variant of the β_3-AR gene may favor the central adiposity gain	Porto et al., 2004
Japanese population	1685; 935 women and 750 men of the cohort of Funagata Diabetes study	No	Genotype Arg/Arg was associated with obesity and type 2 diabetes	Oizumi et al., 2001
Caucasian population (Spain) with essential hypertension	87	No	Trp64Arg related with a different membrane lipid composition and erythrocyte sodium lithium counter transport values it	Pamies-Andreu et al., 2000
Caucasian population (German) with diabetes type 2	417	Yes in men	No association with vascular complications	Ringel et al., 2000
Southern Chinese	802	No	No involvement in the development of diabetes, hypertension or dyslipidaemia, but do suggest a relationship with obesity	Thomas et al., 2000
Sardinian	494	Yes	Association with higher serum triglyceride levels	Tonolo et al., 1999
Japanese with diabetes type 2	83	No		Baba et al., 1998
Caucasian population (Germany)	6450	No	No association with obesity, type 2 diabetes mellitus, dyslipidemia	Buettner et al., 1998
Caucasian (eastern Finland)	375	No	No association with resting metabolic rate, abdominal obesity, increased lipid oxidation, or earlier development of NIDDM	Rissanen et al., 1997
Japanese	173	No	Not associated with essential hypertension, insulin sensitivity, or plasma catecholamine levels in hypertensive subjects	Fujisawa et al., 1997

2001). In a clinical trial (randomized, double-blind fashion), the effect of administration of norepinephrine was compared between 8 nondiabetic normotensive subjects with the Trp64Arg variant and 8 without. The Trp64Arg amino acid variant of the β_3-AR seemed to confer increased sensitivity to the pressure effect of norepinephrine (Melis et al., 2002). This polymorphism seems to facilitate the development of hypertension in the presence of high adrenergic tone. Nevertheless, caution should be taken when associating gene polymorphism with and a multifactorial disease like hypertension. An account of environmental conditions and eventual synergistic polymorphism to explain apparent contradictory results. Hypertension is a complex genetic disorder caused by interplay between several 'risk' genes and environmental factors (genetic heritability approximately 30%). Most genetic studies of hypertension use a candidate gene approach and 2 conclusions have been made: (i) there is no association or linkage with the genes studied, or (ii) the hypertension phenotype is heterogeneous and subgroups with hypertension related to certain polymorphisms cannot be identified because of background noise. Studies using intermediate phenotypes suggest the latter is most likely (Agarwal et al., 2005).

In the specific case of eclampsia, pre-eclampsia has been associated with an impairment of β_3-AR responsiveness (Rouget et al., 2005). The Trp64Arg polymorphism of the β_3-AR did not seem to predispose to pre-eclampsia (Malina et al., 2004). Nevertheless, Zhang et al. (2005a) highlighted a puzzling relationship between the polymorphism and the risk of pre-eclampsia.

6.3. Obesity and diabetes mellitus

Obesity has now become a major target for drug development not only for affecting obesity per se, but also for managing and preventing comorbid conditions such as diabetes and cardiovascular disease. Under investigation are agents that increase energy expenditure, that is β_3-AR agonists. On the other hand, diabetes mellitus is a prevalent disease often associated with vascular complications, such as microangiopathy and atherosclerosis. Although the mechanisms of vascular dysfunction are poorly understood, several studies provide data suggesting alterations in vascular responses to vasoactive agents. Moreover, studies carried out in animals (Turner & White, 1996) and humans (Johnstone et al., 1993) showed that endothelium-dependent vasodilation is impaired in diabetes mellitus. In diabetic rat, the effects of β-AR stimulation on diastolic blood pressure was fully abolished (Gallego et al., 2002). It has been shown as for heart failure, β_1-AR and β_3-AR density decreased and increased respectively in hearts of long-term diabetic rats. This could explain, at least in part, the impairment in cardiac function in chronic diabetes (Dincer et al., 2001). It has been suggested that selective β_3-AR agonists exerted potent antidiabetic effects in rodent models when given chronically (Arch & Wilson, 1996).

Molecular variations of β_3-AR may also lead to obesity, insulin resistance and type II diabetes mellitus (Table 3). The Trp64Arg polymorphism has been associated with early onset of type II diabetes (Walston et al., 1995), diabetic retinopathy and nephropathy in Japanese type II diabetes patients (Sakane et al., 1997, 1998). More recently, it has been shown that the homozygote of β_3-AR gene Trp64Arg mutation was related with diabetes (Xiu et al., 2004). These various results open new research fields concerning the implication of β-AR, and particularly the β_3-AR subtype in the cardiovascular complication of the diabetes mellitus.

Diabetic retinopathy is the number 1 cause of blindness in humans between the ages of 20 and 74 years (Klein, 1996). Age-related macular degeneration is the predominant cause of blindness in the elderly population (O'Shea, 1996; Harris et al., 1999). Although both diseases involve abnormal blood vessel growth in the eye, the mechanisms underlying this growth remain unknown. Results from these studies demonstrate for the first time that β_3-AR exist in human retinal endothelial cells. Alterations in sympathetic nerve activity may contribute to vascular complications of diabetes and diabetic retinopathy might result in changes in the β_3-AR signaling (Steinle et al., 2003, 2005). If these in vitro studies on cultured cells can be extrapolated to the intact retinal circulation, the β_3-AR signaling might initiate retinal endothelial cell proliferation

Table 3
Trp64Arg polymorphism in human β_3-AR and coronary heart disease

Population	n	Association	Comments	References
Caucasian population (German)	1000 angiographically confirmed Coronary heart disease/1000 control	No	No effect modification by gender and atherogenic risk factors	Stangl et al., 2001
Indo-Mauritian patients	338 with premature coronary heart disease/148 control subjects	No direct link	β_3-AR gene variant seems to modulate the effects of β-AR blockers on triglyceride and HDL cholesterol concentrations	Manraj et al., 2001
White Americans	271 with incident CHD cases/700 control subjects	Not predictive of incident CHD	Trp64Arg polymorphism is not a major predictor of atherosclerosis	Morrison et al., 1999
Caucasian (Finland)	185 nondiabetic subjects with angiographically confirmed CHD/119 subject with diabetes type 2 and CHD	No	not significantly related to insulin resistance	Pulkkinen et al., 1999
Japanese	428	No		Tanaka et al., 1999
Chinese	137 patients with angiographically documented coronary heart disease/188 normal subjects	No	No association with the insulin resistance syndrome	Sheu et al., 1999

and migration, both of which being critical stages of angiogenesis.

6.4. Coronary artery disease

The localisation of β_3-AR on microcoronary arteries in humans indicates a potential role in coronaropathy (Dessy et al., 2004). Furthermore, nebivolol could induce an angiogenic response related to its β_3-AR agonistic properties (Dessy et al., 2005). It would therefore provide additional cardiovascular benefits in patients with ischemic cardiac or peripheral diseases. However, the roles of β_3-AR in ischaemia and reperfusion and whether their stimulation is protective or deleterious has not been determined. β_3-AR stimulation, which has a negative inotropic effect could therefore spare the heart of excessive oxygen demand, and may therefore be cardioprotective.

A study with a large sample of clinically well-characterized patients indicated that the Trp64Arg polymorphism did not represent a major risk factor for angiographically confirmed coronary artery disease (Stangl et al., 2001). In the same way, this polymorphism is neither a major predictor of atherosclerosis or coronary incidents in a sample of middle-aged white Americans (Morrison et al., 1999).

After coronary artery bypass, the vascular β-AR responses are markedly abnormal, due in part to the exposure of vessels to endogenous catecholamines (Friedman et al., 1995; Sellke et al., 1997). Several mechanisms were suggested to explain β-AR dysfunction after coronary artery bypass: (i) uncoupling of β-AR from the G_s-protein–adenylyl cyclase complex (attributed to the rapid phosphorylation of the receptor); and/or (ii) impairment of the adenylyl cyclase moiety (Schranz et al., 1993; Booth et al., 1998). In contrast, β_3-AR are only activated by high concentrations of catecholamines such as isoproterenol (Pietri-Rouxel & Strosberg, 1995). Furthermore, β_3-AR have been shown to be relatively resistant to desensitization (Iwase et al., 2000). The effect of β_3-AR stimulation could increase the graft and the coronary flow after coronary artery bypass graft and the negative inotropic effect induced by β_3-AR agonists in the human heart could reduce the myocardial oxygen consumption (Gauthier et al., 1996). It may result in an improvement of the heart oxygen supply/consumption ratio and thus accommodate for a reduced perfusion more especially as β_3-AR is present in human microcoronary arteries (Dessy et al., 2004).

The IMA malperfusion syndrome is a critical complication of coronary artery bypass graft operations (1.9% and up to 20% after primary coronary bypass and reoperation, respectively) and can have devastating effects on the outcome of a cardiac operation (Carrel et al., 1995). The aetiology of the syndrome is multifactorial, but a spasm of the graft has been frequently suggested and thus, the treatment implicated the use of vasodilator and inotropic drugs (Gaudino et al., 1997). However, the vasoconstrictive effects of inotropic substances could reduce arterial graft flow and worsen the situation (He et al., 1994). In this regard, when β-AR agonists were nevertheless used in the perioperative period, drugs were usually nonselective and presented α-AR properties (epinephrine, norepinephrine, dobutamine, isoproterenol). Furthermore, it was admitted that internal mammary arteries exhibited moderate β_1/β_2-AR function, which implied that use of β-AR agonists was not appropriate to reverse vasospasm (Uydes-Dogan et al., 1996). Thus, new β-AR agonists, having β_3-AR agonistic properties, might help to maintain the coronary artery bypass graft flow. However, the balance between global vasodilatory β-AR effect and potential negative inotropic effect of β_3-AR agonistic component must be evaluated, as no in vivo human study has definitevely shown a negative inotropic effect of such drugs. Moreover, the specific changes in β-AR pathway in post-operative period constitute another field of investigation, particularly in the case of low post-operative cardiac output.

The routine use of β-AR blockers have been considered for patients who undergo revascularization after acute myocardial infarction in order to reduce mortality (Chen et al., 2000). Although most patients are made asymptomatic after coronary artery bypass, there is evidence that blood flow through internal mammary artery grafts is inadequate for maximal exercise (Kawasuji et al., 1993). The development of a third generation of β-blockers with vasodilating properties resulting from a β_3-AR agonistic effect (nebivolol, bucindolol) might constitute an interesting new way of investigation (de Groot et al., 2003; Toda, 2003; Rozec et al., in press).

7. Conclusion

The characterization of functional β_3-AR in the heart opens new fields of investigations. A lot remains to be done to fully characterize their intracellular signaling pathway(s), in particular the involvement of different ion channels in their cardiac responses as well as their physiological roles in the regulation of the cardiac function in the normal heart. At present time, no hypothesis could explain the discrepancies of β_3-adrenergic effects on cardiac contractility observed in vitro and in vivo. Thus, this point must be clarified. Furthermore, the levels of expression of β_3-AR, relative to those of β_1- and β_2-AR need to be examined across the different cardiac chambers and at different stages of the life. In addition, the factors regulating the abundance of each receptor subtype need to be identified, as well as neural, endocrine or metabolic factors governing the tissue-specific expression of putative β_3-AR isoforms.

In vessels, the presence of 3 β-AR subtypes that all produce a vasorelaxation, raises several questions. From a physiological point of view, as vascular β_3-AR are only stimulated by very high doses of catecholamines, they could be reserve receptors that are only activated during extreme or stressful conditions and exercise in order to reduce the blood pressure in response to physiological catecholamines. However, future studies are needed to confirm this hypothesis.

In all cardiovascular pathologies investigated, β_3-AR were increased suggesting that they play an important role in those diseases. A better characterization of β_3-AR and the development of new compounds (agonists and antagonists) acting on β_3-AR could lead to identify new therapeutic targets and to better control the adrenergic system in those pathologies.

Acknowledgments

Chantal Gauthier is supported by the "Institut National de la Santé et de la Recherche Médicale", the "Fédération Française de Cardiologie", the "Fondation de France" and the "Fondation Langlois". Bertrand Rozec was supported by grants from the "Société Française d'Anesthésie et de Réanimation" and the "Fondation de la Recherche Médicale". We thank Dr. Jacques Noireaud for critical reading. We are grateful to the Departments of Cardiology and the Departments of Cardiovascular Surgery of Laënnec Hospital in Nantes for continuous support.

References

Agarwal, A., Williams, G. H., & Fisher, N. D. (2005). Genetics of human hypertension. *Trends Endocrinol Metab 16*(3), 127–133.

Arch, J. R. (2002). Beta(3)-adrenoceptor agonists: potential, pitfalls and progress. *Eur J Pharmacol 440*(2–3), 99–107.

Arch, J. R., Ainsworth, A. T., Cawthorne, M. A., Piercy, V., Sennitt, M. V., Thody, V. E., et al. (1984). Atypical beta-adrenoceptor on brown adipocytes as target for anti-obesity drugs. *Nature 309*(5964), 163–165.

Arch, J. R., & Kaumann, A. J. (1993). Beta 3 and atypical beta-adrenoceptors. *Med Res Rev 13*(6), 663–729.

Arch, J. R., & Wilson, S. (1996). Beta 3-adrenoceptors and the regulation of metabolism in adipose tissues. *Biochem Soc Trans 24*(2), 412–418.

Atef, N., Lafontan, M., Double, A., Helary, C., Ktorza, A., & Penicaud, L. (1996). A specific beta 3-adrenoceptor agonist induces increased pancreatic islet blood flow and insulin secretion in rats. *Eur J Pharmacol 298*(3), 287–292.

Baba, T., Nakajima, S., & Yajima, Y. (1998). Beta3-adrenergic receptor gene polymorphism is not associated with hypertension in NIDDM patients without nephropathy. *Horm Metab Res 30*(10), 629–632.

Barbe, P., Millet, L., Galitzky, J., Lafontan, M., & Berlan, M. (1996). In situ assessment of the role of the beta 1-, beta 2- and beta 3-adrenoceptors in the control of lipolysis and nutritive blood flow in human subcutaneous adipose tissue. *Br J Pharmacol 117*(5), 907–913.

Beavo, J. A. (1995). cGMP inhibition of heart phosphodiesterase: is it clinically relevant? *J Clin Invest 95*(2), 445.

Begin-Heick, N. (1995). Beta 3-adrenergic activation of adenylyl cyclase in mouse white adipocytes: modulation by GTP and effect of obesity. *J Cell Biochem 58*(4), 464–473.

Berlan, M., Galitzky, J., Bousquet-Melou, A., Lafontan, M., & Montastruc, J. L. (1994). Beta-3 adrenoceptor-mediated increase in cutaneous blood flow in the dog. *J Pharmacol Exp Ther 268*(3), 1444–1451.

Beta-Blocker Evaluation of Survival Trial Investigators. (2001). A trial of the beta-blocker bucindolol in patients with advanced chronic heart failure. *N Engl J Med 344*(22), 1659–1667.

Bianchetti, A., & Manara, L. (1990). In vitro inhibition of intestinal motility by phenylethanolaminotetralines: evidence of atypical beta-adrenoceptors in rat colon. *Br J Pharmacol 100*(4), 831–839.

Blin, N., Camoin, L., Maigret, B., & Strosberg, A. D. (1993). Structural and conformational features determining selective signal transduction in the beta 3-adrenergic receptor. *Mol Pharmacol 44*(6), 1094–1104.

Bloch, W., Fleischmann, B. K., Lorke, D. E., Andressen, C., Hops, B., Hescheler, J., et al. (1999). Nitric oxide synthase expression and role during cardiomyogenesis. *Cardiovasc Res 43*(3), 675–684.

Boonen, H. C., Daemen, M. J., Eerdmans, P. H., Fazzi, G. E., van Kleef, E. M., Schiffers, P. M., et al. (1993). Mesenteric small artery changes after vasoconstrictor infusion in young rats. *J Cardiovasc Pharmacol 22*(3), 388–395.

Booth, J. V., Landolfo, K. P., Chesnut, L. C., Bennett-Guerrero, E., Gerhardt, M. A., & Atwell, D. M. (1998). Acute depression of myocardial beta-adrenergic receptor signaling during cardiopulmonary bypass: impairment of the adenylyl cyclase moiety. Duke Heart Center Perioperative Desensitization Group. *Anesthesiology 89*(3), 602–611.

Borkowski, K. R., Gros, R., & Schneider, H. (1992). Vascular beta-adrenoceptor-mediated responses in hypertension and ageing in rats. *J Auton Pharmacol 12*(6), 389–401.

Bosch, R. F., Schneck, A. C., Kiehn, J., Zhang, W., Hambrock, A., Eigenberger, B. W., et al. (2002). Beta3-adrenergic regulation of an ion channel in the heart-inhibition of the slow delayed rectifier potassium current I(Ks) in guinea pig ventricular myocytes. *Cardiovasc Res 56*(3), 393–403.

Brahmadevara, N., Shaw, A. M., & MacDonald, A. (2003). Evidence against beta 3-adrenoceptors or low affinity state of beta 1-adrenoceptors mediating relaxation in rat isolated aorta. *Br J Pharmacol 138*(1), 99–106.

Brawley, L., Shaw, A. M., & MacDonald, A. (2000). Role of endothelium/nitric oxide in atypical beta-adrenoceptor-mediated relaxation in rat isolated aorta. *Eur J Pharmacol 398*(2), 285–296.

Briones, A. M., Daly, C. J., Jimenez-Altayo, F., Martinez-Revelles, S., Gonzalez, J. M., McGrath, J. C., et al. (2005). Direct demonstration of beta(1)- and evidence against beta(2)- and beta(3)-adrenoceptors, in smooth muscle cells of rat small mesenteric arteries. *Br J Pharmacol*.

Bristow, M. R., Ginsburg, R., Umans, V., Fowler, M., Minobe, W., Rasmussen, R., et al. (1986). Beta 1- and beta 2-adrenergic-receptor subpopulations in nonfailing and failing human ventricular myocardium: coupling of both receptor subtypes to muscle contraction and selective beta 1-receptor down-regulation in heart failure. *Circ Res 59*(3), 297–309.

Campbell, D. L., Stamler, J. S., & Strauss, H. C. (1996). Redox modulation of L-type calcium channels in ferret ventricular myocytes. Dual mechanism regulation by nitric oxide and S-nitrosothiols. *J Gen Physiol 108*(4), 277–293.

Candelore, M. R., Deng, L., Tota, L., Guan, X. M., Amend, A., Liu, Y., et al. (1999). Potent and selective human beta(3)-adrenergic receptor antagonists. *J Pharmacol Exp Ther 290*(2), 649–655.

Carrel, T., Kujawski, T., Zund, G., Schwitter, J., Amann, F. W., Gallino, A., et al. (1995). The internal mammary artery malperfusion syndrome: incidence, treatment and angiographic verification. *Eur J Cardiothorac Surg 9*(4), 190–195.

Carvalho, M. H., Scivoletto, R., Fortes, Z. B., Nigro, D., & Cordellini, S. (1987). Reactivity of aorta and mesenteric microvessels to drugs in spontaneously hypertensive rats: role of the endothelium. *J Hypertens 5*(3), 377–382.

Chamberlain, P. D., Jennings, K. H., Paul, F., Cordell, J., Berry, A., Holmes, S. D., et al. (1999). The tissue distribution of the human beta3-adrenoceptor studied using a monoclonal antibody: direct evidence of the beta3-adrenoceptor in human adipose tissue, atrium and skeletal muscle. *Int J Obes Relat Metab Disord 23*(10), 1057–1065.

Chaudhry, A., MacKenzie, R. G., Georgic, L. M., & Granneman, J. G. (1994). Differential interaction of beta 1- and beta 3-adrenergic receptors with Gi in rat adipocytes. *Cell Signal 6*(4), 457–465.

Chen, J., Radford, M. J., Wang, Y., Marciniak, T. A., & Krumholz, H. M. (2000). Are beta-blockers effective in elderly patients who undergo coronary revascularization after acute myocardial infarction? *Arch Intern Med 160*(7), 947–952.

Cheng, H. J., Zhang, Z. S., Onishi, K., Ukai, T., Sane, D. C., & Cheng, C. P. (2001). Upregulation of functional beta(3)-adrenergic receptor in the failing canine myocardium. *Circ Res 89*(7), 599–606.

Chruscinski, A., Brede, M. E., Meinel, L., Lohse, M. J., Kobilka, B. K., & Hein, L. (2001). Differential distribution of beta-adrenergic receptor subtypes in blood vessels of knockout mice lacking beta(1)- or beta(2)-adrenergic receptors. *Mol Pharmacol 60*(5), 955–962.

Cirino, G., Sorrentino, R., di Villa, B. R., Popolo, A., Palmieri, A., Imbimbo, C., et al. (2003). Involvement of beta 3-adrenergic receptor activation via cyclic GMP-but not NO-dependent mechanisms in human corpus cavernosum function. *Proc Natl Acad Sci USA 100*(9), 5531–5536.

Clark, B. J., & Bertholet, A. (1983). Effects of pindolol on vascular smooth muscle. *Gen Pharmacol 14*(1), 117–119.

Clement, K., Vaisse, C., Manning, B. S., Basdevant, A., Guy-Grand, B., Ruiz, J., et al. (1995). Genetic variation in the beta 3-adrenergic receptor and an increased capacity to gain weight in patients with morbid obesity. *N Engl J Med 333*(6), 352–354.

Cohen, M. L., Bloomquist, W., Kriauciunas, A., Shuker, A., & Calligaro, D. (1999). Aryl propanolamines: comparison of activity at human beta3

receptors, rat beta3 receptors and rat atrial receptors mediating tachycardia. *Br J Pharmacol 126*(4), 1018–1024.

Corella, D., Guillen, M., Portoles, O., Sorli, J. V., Alonso, V., Folch, J., et al. (2001). Gender specific associations of the Trp64Arg mutation in the beta3-adrenergic receptor gene with obesity-related phenotypes in a Mediterranean population: interaction with a common lipoprotein lipase gene variation. *J Intern Med 250*(4), 348–360.

Czuriga, I., Riecansky, I., Bodnar, J., Fulop, T., Kruzsicz, V., & Kristof, E. (2003). Comparison of the new cardioselective beta-blocker nebivolol with bisoprolol in hypertension: the Nebivolol, Bisoprolol Multicenter Study (NEBIS). *Cardiovasc Drugs Ther 17*(3), 257–263.

de Champlain, J. (2001). Do most antihypertensive agents have a sympatholytic action? *Curr Hypertens Rep 3*(4), 305–313.

de Groot, A. A., Mathy, M. J., van Zwieten, A., & Peters, S. L. (2003). Involvement of the beta3 adrenoceptor in nebivolol-induced vasorelaxation in the rat aorta. *J Cardiovasc Pharmacol 42*(2), 232–236.

De Mey, J. G., & Vanhoutte, P. M. (1982). Heterogeneous behavior of the canine arterial and venous wall. Importance of the endothelium. *Circ Res 51*(4), 439–447.

De Ponti, F., Gibelli, G., Croci, T., Arcidiaco, M., Crema, F., & Manara, L. (1996). Functional evidence of atypical beta 3-adrenoceptors in the human colon using the beta 3-selective adrenoceptor antagonist, SR 59230A. *Br J Pharmacol 117*(7), 1374–1376.

Dennedy, M. C., Houlihan, D. D., McMillan, H., & Morrison, J. J. (2002). Beta2- and beta3-adrenoreceptor agonists: human myometrial selectivity and effects on umbilical artery tone. *Am J Obstet Gynecol 187*(3), 641–647.

Dessy, C., Moniotte, S., Ghisdal, P., Havaux, X., & Balligand, J. L. (2004). Endothelial beta3-adrenoceptors mediate vasorelaxation of human coronary microarteries through nitric oxide and endothelium-dependent hyperpolarization. *Circulation 110*(8), 948–954.

Dessy, C., Saliez, J., Ghisdal, P., Daneau, G., Lobysheva, I. I., Frerart, F., et al. (2005). Endothelial beta3-adrenoreceptors mediate nitric oxide-dependent vasorelaxation of coronary microvessels in response to the third-generation beta-blocker nebivolol. *Circulation 112*(8), 1198–1205.

Dincer, U. D., Bidasee, K. R., Guner, S., Tay, A., Ozcelikay, A. T., & Altan, V. M. (2001). The effect of diabetes on expression of beta1-, beta2-, and beta3-adrenoreceptors in rat hearts. *Diabetes 50*(2), 455–461.

Doggrell, S. A., & Surman, A. J. (1995). Loss of maximum attenuation and receptor reserve for isoprenaline at the beta 2-adrenoceptors of the portal veins of hypertensive rats. *J Hypertens 13*(9), 1023–1029.

Dolan, J. A., Muenkel, H. A., Burns, M. G., Pellegrino, S. M., Fraser, C. M., Pietri, F., et al. (1994). Beta-3 adrenoceptor selectivity of the dioxolane dicarboxylate phenethanolamines. *J Pharmacol Exp Ther 269*(3), 1000–1006.

Donckier, J. E., Massart, P. E., Van Mechelen, H., Heyndrickx, G. R., Gauthier, C., & Balligand, J. L. (2001). Cardiovascular effects of beta 3-adrenoceptor stimulation in perinephritic hypertension. *Eur J Clin Invest 31*(8), 681–689.

Dumas, M., Dumas, J. P., Bardou, M., Rochette, L., Advenier, C., & Giudicelli, J. F. (1998). Influence of beta-adrenoceptor agonists on the pulmonary circulation. Effects of a beta3-adrenoceptor antagonist, SR 59230A. *Eur J Pharmacol 348*(2-3), 223–228.

Dumas, J. P., Goirand, F., Bardou, M., Dumas, M., Rochette, L., Advenier, C., et al. (1999). Role of potassium channels and nitric oxide in the relaxant effects elicited by beta-adrenoceptor agonists on hypoxic vasoconstriction in the isolated perfused lung of the rat. *Br J Pharmacol 127*(2), 421–428.

Edvinsson, L., & Owman, C. (1974). Pharmacological characterization of adrenergic alpha and beta receptors mediating the vasomotor responses of cerebral arteries in vitro. *Circ Res 35*(6), 835–849.

El-Armouche, A., Zolk, O., Rau, T., & Eschenhagen, T. (2003). Inhibitory G-proteins and their role in desensitization of the adenylyl cyclase pathway in heart failure. *Cardiovasc Res 60*(3), 478–487.

Emorine, L., Blin, N., & Strosberg, A. D. (1994). The human beta 3-adrenoceptor: the search for a physiological function. *Trends Pharmacol Sci 15*(1), 3–7.

Emorine, L. J., Marullo, S., Briend-Sutren, M. M., Patey, G., Tate, K., Delavier-Klutchko, C., et al. (1989). Molecular characterization of the human beta 3-adrenergic receptor. *Science 245*(4922), 1118–1121.

Endo, K., Yanagi, H., Hirano, C., Hamaguchi, H., Tsuchiya, S., & Tomura, S. (2000). Association of Trp64Arg polymorphism of the beta3-adrenergic receptor gene and no association of Gln223Arg polymorphism of the leptin receptor gene in Japanese schoolchildren with obesity. *Int J Obes Relat Metab Disord 24*(4), 443–449.

Engelhardt, S., Hein, L., Keller, U., Klambt, K., & Lohse, M. J. (2002). Inhibition of Na(+)–H(+) exchange prevents hypertrophy, fibrosis, and heart failure in beta(1)-adrenergic receptor transgenic mice. *Circ Res 90*(7), 814–819.

Erhardt, E., Czako, M., Csernus, K., Molnar, D., & Kosztolanyi, G. (2005). The frequency of Trp64Arg polymorphism of the beta3-adrenergic receptor gene in healthy and obese Hungarian children and its association with cardiovascular risk factors. *Eur J Clin Nutr 59*(8), 955–959.

Evans, B. A., Papaioannou, M., Hamilton, S., & Summers, R. J. (1999). Alternative splicing generates two isoforms of the beta3-adrenoceptor which are differentially expressed in mouse tissues. *Br J Pharmacol 127*(6), 1525–1531.

Feldman, R. D. (1987). Beta-adrenergic receptor alterations in hypertension physiological and molecular correlates. *Can J Physiol Pharmacol 65*(8), 1666–1672.

Flather, M. D., Shibata, M. C., Coats, A. J., Van Veldhuisen, D. J., Parkhomenko, A., Borbola, J., et al. (2005). Randomized trial to determine the effect of nebivolol on mortality and cardiovascular hospital admission in elderly patients with heart failure (SENIORS). *Eur Heart J 26*(3), 215–225.

Forrest, R. H., & Hickford, J. G. (2000). Rapid communication: nucleotide sequences of the bovine, caprine, and ovine beta3-adrenergic receptor genes. *J Anim Sci 78*(5), 1397–1398.

Friedman, M., Wang, S. Y., Stahl, G. L., Johnson, R. G., & Sellke, F. W. (1995). Altered beta-adrenergic and cholinergic pulmonary vascular responses after total cardiopulmonary bypass. *J Appl Physiol 79*(6), 1998–2006.

Furchgott, R. F., & Zawadzki, J. V. (1980). The obligatory role of endothelial cells in the relaxation of arterial smooth muscle by acetylcholine. *Nature 288*(5789), 373–376.

Galitzky, J., Reverte, M., Portillo, M., Carpene, C., Lafontan, M., & Berlan, M. (1993). Coexistence of beta 1-, beta 2-, and beta 3-adrenoceptors in dog fat cells and their differential activation by catecholamines. *Am J Physiol 264*(3 Pt 1), E403–E412.

Gallego, M., Espina, L., & Casis, O. (2002). Blood pressure responsiveness to sympathetic agonists in anaesthetised diabetic rats. *J Physiol Biochem 58*(2), 87–93.

Gaudino, M., Trani, C., Luciani, N., Alessandrini, F., & Possati, G. (1997). The internal mammary artery malperfusion syndrome: late angiographic verification. *Ann Thorac Surg 63*(5), 1257–1261.

Gauthier, C., Tavernier, G., Charpentier, F., Langin, D., & Le Marec, H. (1996). Functional beta3-adrenoceptor in the human heart. *J Clin Invest 98*(2), 556–562.

Gauthier, C., Leblais, V., Kobzik, L., Trochu, J. N., Khandoudi, N., Bril, A., et al. (1998). The negative inotropic effect of beta3-adrenoceptor stimulation is mediated by activation of a nitric oxide synthase pathway in human ventricle. *J Clin Invest 102*(7), 1377–1384.

Gauthier, C., Tavernier, G., Trochu, J. N., Leblais, V., Laurent, K., Langin, D., et al. (1999). Interspecies differences in the cardiac negative inotropic effects of beta(3)-adrenoceptor agonists. *J Pharmacol Exp Ther 290*(2), 687–693.

Gauthier, C., Langin, D., & Balligand, J. L. (2000). Beta3-adrenoceptors in the cardiovascular system. *Trends Pharmacol Sci 21*(11), 426–431.

Germack, R., & Dickenson, J. M. (2006). Induction of {beta}3-adrenergic receptor functional expression following chronic stimulation with noradrenaline in neonatal rat cardiomyocytes. *J Pharmacol Exp Ther 316*(1), 392–402.

Goldhaber, J. I., Kim, K. H., Natterson, P. D., Lawrence, T., Yang, P., & Weiss, J. N. (1996). Effects of TNF-alpha on $[Ca^{2+}]_i$ and contractility in isolated adult rabbit ventricular myocytes. *Am J Physiol 271*(4 Pt 2), H1449–H1455.

Gosgnach, W., Boixel, C., Nevo, N., Poiraud, T., & Michel, J. B. (2001). Nebivolol induces calcium-independent signaling in endothelial cells by a possible beta-adrenergic pathway. *J Cardiovasc Pharmacol 38*(2), 191–199.

Granneman, J. G. (2001). The putative beta4-adrenergic receptor is a novel state of the beta1-adrenergic receptor. *Am J Physiol Endocrinol Metab 280*(2), E199–E202.

Granneman, J. G., Lahners, K. N., & Chaudhry, A. (1993). Characterization of the human beta 3-adrenergic receptor gene. *Mol Pharmacol 44*(2), 264–270.

Granneman, J. G., Lahners, K. N., & Rao, D. D. (1992). Rodent and human beta 3-adrenergic receptor genes contain an intron within the protein-coding block. *Mol Pharmacol 42*(6), 964–970.

Gross, W. L., Bak, M. I., Ingwall, J. S., Arstall, M. A., Smith, T. W., Balligand, J. L., et al. (1996). Nitric oxide inhibits creatine kinase and regulates rat heart contractile reserve. *Proc Natl Acad Sci USA 93*(11), 5604–5609.

Guimaraes, S., & Moura, D. (2001). Vascular adrenoceptors: an update. *Pharmacol Rev 53*(2), 319–356.

Hall, R. A., Ostedgaard, L. S., Premont, R. T., Blitzer, J. T., Rahman, N., Welsh, M. J., et al. (1998). A C-terminal motif found in the beta2-adrenergic receptor, P2Y1 receptor and cystic fibrosis transmembrane conductance regulator determines binding to the Na+/H+ exchanger regulatory factor family of PDZ proteins. *Proc Natl Acad Sci USA 95*(15), 8496–8501.

Hao, K., Peng, S., Xing, H., Yu, Y., Huang, A., Hong, X., et al. (2004). Beta(3) adrenergic receptor polymorphism and obesity-related phenotypes in hypertensive patients. *Obes Res 12*(1), 125–130.

Harris, A., Chung, H. S., Ciulla, T. A., & Kagemann, L. (1999). Progress in measurement of ocular blood flow and relevance to our understanding of glaucoma and age-related macular degeneration. *Prog Retin Eye Res 18*(5), 669–687.

He, G. W., Acuff, T. E., Yang, C. Q., Ryan, W. H., & Mack, M. J. (1994). Middle and proximal sections of the human internal mammary artery are not "passive conduits". *J Thorac Cardiovasc Surg 108*(4), 741–746.

Hutchinson, D. S., Bengtsson, T., Evans, B. A., & Summers, R. J. (2002). Mouse beta 3a- and beta 3b-adrenoceptors expressed in Chinese hamster ovary cells display identical pharmacology but utilize distinct signalling pathways. *Br J Pharmacol 135*(8), 1903–1914.

Iwase, M., Ichikawa, K., Tashiro, K., Iino, K., Shinohara, N., Ibayashi, S., et al. (2000). Effects of monosodium glutamate-induced obesity in spontaneously hypertensive rats vs. Wistar Kyoto rats: serum leptin and blood flow to brown adipose tissue. *Hypertens Res 23*(5), 503–510.

Jockers, R., Da Silva, A., Strosberg, A. D., Bouvier, M., & Marullo, S. (1996). New molecular and structural determinants involved in beta 2-adrenergic receptor desensitization and sequestration. Delineation using chimeric beta 3/beta 2-adrenergic receptors. *J Biol Chem 271*(16), 9355–9362.

Johnstone, M. T., Creager, S. J., Scales, K. M., Cusco, J. A., Lee, B. K., & Creager, M. A. (1993). Impaired endothelium-dependent vasodilation in patients with insulin-dependent diabetes mellitus. *Circulation 88*(6), 2510–2516.

Joseph, S. S., Lynham, J. A., Molenaar, P., Grace, A. A., Colledge, W. H., & Kaumann, A. J. (2003). Intrinsic sympathomimetic activity of (−)-pindolol mediated through a (−)-propranolol-resistant site of the beta1-adrenoceptor in human atrium and recombinant receptors. *Naunyn Schmiedeberg's Arch Pharmacol 368*(6), 496–503.

Kathofer, S., Zhang, W., Karle, C., Thomas, D., Schoels, W., & Kiehn, J. (2000). Functional coupling of human beta 3-adrenoreceptors to the KvLQT1/MinK potassium channel. *J Biol Chem 275*(35), 26743–26747.

Kaumann, A. J., & Molenaar, P. (1996). Differences between the third cardiac beta-adrenoceptor and the colonic beta 3-adrenoceptor in the rat. *Br J Pharmacol 118*(8), 2085–2098.

Kaumann, A. J., & Molenaar, P. (1997). Modulation of human cardiac function through 4 beta-adrenoceptor populations. *Naunyn Schmiedeberg's Arch Pharmacol 355*(6), 667–681.

Kaumann, A., Bartel, S., Molenaar, P., Sanders, L., Burrell, K., Vetter, D., et al. (1999). Activation of beta2-adrenergic receptors hastens relaxation and mediates phosphorylation of phospholamban, troponin I, and C-protein in ventricular myocardium from patients with terminal heart failure. *Circulation 99*(1), 65–72.

Kawasuji, M., Tedoriya, T., Takemura, H., Sakakibara, N., Taki, J., & Watanabe, Y. (1993). Flow capacities of arterial grafts for coronary artery bypass grafting. *Ann Thorac Surg 56*(4), 957–962.

Kitamura, T., Onishi, K., Dohi, K., Okinaka, T., Isaka, N., & Nakano, T. (2000). The negative inotropic effect of beta3-adrenoceptor stimulation in the beating guinea pig heart. *J Cardiovasc Pharmacol 35*(5), 786–790.

Klaus, S., Muzzin, P., Revelli, J. P., Cawthorne, M. A., Giacobino, J. P., & Ricquier, D. (1995). Control of beta 3-adrenergic receptor gene expression in brown adipocytes in culture. *Mol Cell Endocrinol 109*(2), 189–195.

Klein, R. (1996). Diabetic retinopathy. *Annu Rev Public Health 17*, 137–158.

Kohout, T. A., Takaoka, H., McDonald, P. H., Perry, S. J., Mao, L., Lefkowitz, R. J., et al. (2001). Augmentation of cardiac contractility mediated by the human beta(3)-adrenergic receptor overexpressed in the hearts of transgenic mice. *Circulation 104*(20), 2485–2491.

Kong, Y. H., Li, W. M., & Tian, Y. (2004). Effect of beta3-adrenoreceptors agonist on beta3-adrenoreceptors expression and myocyte apoptosis in a rat model of heart failure. *Zhongguo Wei Zhong Bing Ji Jiu Yi Xue 16*(3), 142–147.

Konishi, M., & Su, C. (1983). Role of endothelium in dilator responses of spontaneously hypertensive rat arteries. *Hypertension 5*(6), 881–886.

Kozlowska, H., Szymska, U., Schlicker, E., & Malinowska, B. (2003). Atypical beta-adrenoceptors, different from beta 3-adrenoceptors and probably from the low-affinity state of beta 1-adrenoceptors, relax the rat isolated mesenteric artery. *Br J Pharmacol 140*(1), 3–12.

Kozlowska, H., Schlicker, E., Kozlowski, M., Siedlecka, U., Laudanski, J., & Malinowska, B. (2005). Ligands at beta2-, beta3-, and the low-affinity state of beta1-adrenoceptors block the alpha1-adrenoceptor-mediated constriction in human pulmonary and rat mesenteric arteries. *J Cardiovasc Pharmacol 46*(1), 76–82.

Krauss, S. L., Dodge, J. T., & Bevan, J. A. (1992). Magnitude of beta-adrenoceptor-mediated responses of dog epicardial coronary arteries: inverse relation to diameter. *Am J Physiol 263*(5 Pt 2), H1422–H1429.

Kubo, S., Matsuda, A., Ohnuki, T., Hattori, K., Suzuki, J., & Nagatomo, T. (1997). Assessment of beta 2- and beta 3-adrenoceptors in rat white adipose tissues by radioligand binding assay. *Biol Pharm Bull 20*(2), 142–148.

Kupershmidt, S., Yang, T., Anderson, M. E., Wessels, A., Niswender, K. D., Magnuson, M. A., et al. (1999). Replacement by homologous recombination of the minK gene with lacZ reveals restriction of minK expression to the mouse cardiac conduction system. *Circ Res 84*(2), 146–152.

Kurabayashi, T., Carey, D. G., & Morrison, N. A. (1996). The beta 3-adrenergic receptor gene Trp64Arg mutation is overrepresented in obese women. Effects on weight, BMI, abdominal fat, blood pressure, and reproductive history in an elderly Australian population. *Diabetes 45*(10), 1358–1363.

Kuratani, K., Kodama, H., & Yamaguchi, I. (1994). Enhancement of gastric mucosal blood flow by beta-3 adrenergic agonists prevents indomethacin-induced antral ulcer in the rat. *J Pharmacol Exp Ther 270*(2), 559–565.

Lacroix, J. S., Kurt, A. M., Auberson, S., & Bretton, C. (1995). Beta-adrenergic mechanisms in the nasal mucosa vascular bed. *Eur Arch Otorhinolaryngol 252*(5), 298–303.

Lands, A. M., Arnold, A., McAuliff, J. P., Luduena, F. P., Brown, T. G., et al. (1967). Differentiation of receptor systems activated by sympathomimetic amines. *Nature 214*(88), 597–598.

Langin, D., Portillo, M. P., Saulnier-Blache, J. S., & Lafontan, M. (1991). Coexistence of three beta-adrenoceptor subtypes in white fat cells of various mammalian species. *Eur J Pharmacol 199*(3), 291–301.

Larsen, T. M., Toubro, S., van Baak, M. A., Gottesdiener, K. M., Larson, P., Saris, W. H., et al. (2002). Effect of a 28-d treatment with L-796568, a novel beta(3)-adrenergic receptor agonist, on energy expenditure and body composition in obese men. *Am J Clin Nutr 76*(4), 780–788.

Leblais, V., Demolombe, S., Vallette, G., Langin, D., Baro, I., Escande, D., et al. (1999). Beta3-adrenoceptor control the cystic fibrosis transmembrane conductance regulator through a cAMP/protein kinase A-independent pathway. *J Biol Chem 274*(10), 6107–6113.

Lenzen, G., Pietri-Rouxel, F., Drumare, M. F., Amiard, A., Guillot, S., Archimbault, P., et al. (1998). Genomic cloning and species-specific properties of the recombinant canine beta3-adrenoceptor. *Eur J Pharmacol 363*(2–3), 217–227.

Levasseur, S., Pigeon, C., Reyl-Desmars, F., Caput, D., & Lewin, M. J. (1995). Stimulation of adenylate cyclase by the isoforms of human and rat beta-3 adrenergic receptor expressed in the CHO cells. *Gastroenterol Clin Biol 19*(8–9), 668–672.

Levesque, P. C., Hart, P. J., Hume, J. R., Kenyon, J. L., & Horowitz, B. (1992). Expression of cystic fibrosis transmembrane regulator Cl^- channels in heart. *Circ Res 71*(4), 1002–1007.

Liggett, S. B. (1992). Functional properties of the rat and human beta 3-adrenergic receptors: differential agonist activation of recombinant receptors in Chinese hamster ovary cells. *Mol Pharmacol 42*(4), 634–637.

Liggett, S. B., Freedman, N. J., Schwinn, D. A., & Lefkowitz, R. J. (1993). Structural basis for receptor subtype-specific regulation revealed by a chimeric beta 3/beta 2-adrenergic receptor. *Proc Natl Acad Sci USA 90*(8), 3665–3669.

MacDonald, A., McLean, M., MacAulay, L., & Shaw, A. M. (1999). Effects of propranolol and L-NAME on beta-adrenoceptor-mediated relaxation in rat carotid artery. *J Auton Pharmacol 19*(3), 145–149.

Malina, A. N., Laivuori, H. M., Agatisa, P. K., Collura, L. A., Crombleholme, W. R., Sims, C. J., et al. (2004). The Trp64Arg polymorphism of the beta3-adrenergic receptor is not increased in women with preeclampsia. *Am J Obstet Gynecol 190*(3), 779–783.

Mallem, M. Y., Gogny, M., Gautier, F., Bucas, V., & Desfontis, J. C. (2003). Evaluation of beta3-adrenoceptor-mediated relaxation in intact and endotoxin-treated equine digital veins. *Am J Vet Res 64*(6), 708–714.

Mallem, M. Y., Toumaniantz, G., Serpillon, S., Gautier, F., Gogny, M., Desfontis, J. C., et al. (2004). Impairment of the low-affinity state beta1-adrenoceptor-induced relaxation in spontaneously hypertensive rats. *Br J Pharmacol 143*(5), 599–605.

Manara, L., Badone, D., Baroni, M., Boccardi, G., Cecchi, R., Croci, T., et al. (1996). Functional identification of rat atypical beta-adrenoceptors by the first beta 3-selective antagonists, aryloxypropanolaminotetralins. *Br J Pharmacol 117*(3), 435–442.

Manraj, M., Francke, S., Hebe, A., Ramjuttun, U. S., & Froguel, P. (2001). Genetic and environmental nature of the insulin resistance syndrome in Indo-Mauritian subjects with premature coronary heart disease: contribution of beta3-adrenoreceptor gene polymorphism and beta blockers on triglyceride and HDL concentrations. *Diabetologia 44*(1), 115–122.

Masuo, K., Katsuya, T., Fu, Y., Rakugi, H., Ogihara, T., & Tuck, M. L. (2005). Beta2- and beta3-adrenergic receptor polymorphisms are related to the onset of weight gain and blood pressure elevation over 5 years. *Circulation 111*(25), 3429–3434.

Matsushita, M., Horinouchi, T., Tanaka, Y., Tsuru, H., & Koike, K. (2003). Characterization of beta3-adrenoceptor-mediated relaxation in rat abdominal aorta smooth muscle. *Eur J Pharmacol 482*(1–3), 235–244.

Matter, C. M., Mandinov, L., Kaufmann, P. A., Vassalli, G., Jiang, Z., & Hess, O. M. (1999). Effect of NO donors on LV diastolic function in patients with severe pressure-overload hypertrophy. *Circulation 99*(18), 2396–2401.

Melis, M. G., Secchi, G., Brizzi, P., Severino, C., Maioli, M., & Tonolo, G. (2002). The Trp64Arg beta3-adrenergic receptor amino acid variant confers increased sensitivity to the pressor effects of noradrenaline in Sardinian subjects. *Clin Sci (Lond) 103*(4), 397–402.

Mery, P. F., Lohmann, S. M., Walter, U., & Fischmeister, R. (1991). Ca^{2+} current is regulated by cyclic GMP-dependent protein kinase in mammalian cardiac myocytes. *Proc Natl Acad Sci USA 88*(4), 1197–1201.

Mery, P. F., Pavoine, C., Belhassen, L., Pecker, F., & Fischmeister, R. (1993). Nitric oxide regulates cardiac Ca2+ current. Involvement of cGMP-inhibited and cGMP-stimulated phosphodiesterases through guanylyl cyclase activation. *J Biol Chem 268*(35), 26286–26295.

Michel, M. C., Brodde, O. E., & Insel, P. A. (1990). Peripheral adrenergic receptors in hypertension. *Hypertension 16*(2), 107–120.

Milano, C. A., Allen, L. F., Rockman, H. A., Dolber, P. C., McMinn, T. R., Chien, K. R., et al. (1994). Enhanced myocardial function in transgenic mice overexpressing the beta 2-adrenergic receptor. *Science 264*(5158), 582–586.

Mitchell, B. D., Blangero, J., Comuzzie, A. G., Almasy, L. A., Shuldiner, A. R., Silver, K., et al. (1998). A paired sibling analysis of the beta-3 adrenergic receptor and obesity in Mexican Americans. *J Clin Invest 101*(3), 584–587.

Moffett, S., Mouillac, B., Bonin, H., & Bouvier, M. (1993). Altered phosphorylation and desensitization patterns of a human beta 2-adrenergic receptor lacking the palmitoylated Cys341. *EMBO J 12*(1), 349–356.

Molenaar, P., Sarsero, D., & Kaumann, A. J. (1997). Proposal for the interaction of non-conventional partial agonists and catecholamines with the 'putative beta 4-adrenoceptor' in mammalian heart. *Clin Exp Pharmacol Physiol 24*(9–10), 647–656.

Moniotte, S., Vaerman, J. L., Kockx, M. M., Larrouy, D., Langin, D., Noirhomme, P., et al. (2001). Real-time RT-PCR for the detection of beta-adrenoceptor messenger RNAs in small human endomyocardial biopsies. *J Mol Cell Cardiol 33*(12), 2121–2133.

Moniotte, S., & Balligand, J. L. (2002). Potential use of beta(3)-adrenoceptor antagonists in heart failure therapy. *Cardiovasc Drug Rev 20*(1), 19–26.

Morimoto, A., Hasegawa, H., Cheng, H. J., Little, W. C., & Cheng, C. P. (2004). Endogenous beta3-adrenoreceptor activation contributes to left ventricular and cardiomyocyte dysfunction in heart failure. *Am J Physiol Heart Circ Physiol 286*(6), H2425–H2433.

Morrison, A. C., Brancati, F. L., Folsom, A. R., Smith, L., & Boerwinkle, E. (1999). Beta3-adrenergic receptor Trp64Arg polymorphism does not predict incident CHD or carotid intima-media thickness in a community-based sample of whites: the ARIC study. Atherosclerosis Risk in Communities. *Hum Genet 105*(4), 314–319.

Nodari, S., Metra, M., & Dei, C. L. (2003). Beta-blocker treatment of patients with diastolic heart failure and arterial hypertension. A prospective, randomized, comparison of the long-term effects of atenolol vs. nebivolol. *Eur J Heart Fail 5*(5), 621–627.

O'Donnell, S. R., & Wanstall, J. C. (1985). Responses to the beta 2-selective agonist procaterol of vascular and atrial preparations with different functional beta-adrenoceptor populations. *Br J Pharmacol 84*(1), 227–235.

Oizumi, T., Daimon, M., Saitoh, T., Kameda, W., Yamaguchi, H., Ohnuma, H., et al. (2001). Genotype Arg/Arg, but not Trp/Arg, of the Trp64Arg polymorphism of the beta(3)-adrenergic receptor is associated with type 2 diabetes and obesity in a large Japanese sample. *Diabetes Care 24*(9), 1579–1583.

O'Shea, J. G. (1996). Age-related macular degeneration: a leading cause of blindness. *Med J Aust 165*(10), 561–564.

Oriowo, M. A. (1994). Atypical beta-adrenoceptors in the rat isolated common carotid artery. *Br J Pharmacol 113*(3), 699–702.

Oriowo, M. A. (1995). Different atypical beta-adrenoceptors mediate isoprenaline-induced relaxation in vascular and non-vascular smooth muscles. *Life Sci 56*(15), L269–L275.

Osswald, W., & Guimaraes, S. (1983). Adrenergic mechanisms in blood vessels: morphological and pharmacological aspects. *Rev Physiol Biochem Pharmacol 96*, 53–122.

Pamies-Andreu, E., Garcia-Lozano, R., Palmero-Palmero, C., Garcia-Morillo, S., Alonso-ARcas, A., Stiefel, P., et al. (2000). Genetic variation in the beta-3-adrenergic receptor in essential hypertension. *Life Sci 67*(4), 391–397.

Pavoine, C., & Defer, N. (2005). The cardiac beta2-adrenergic signalling a new role for the cPLA2. *Cell Signal 17*(2), 141–152.

Pavoine, C., Behforouz, N., Gauthier, C., Le Gouvello, S., Roudot-Thoraval, F., Martin, C. R., et al. (2003). Beta2-adrenergic signaling in human heart: shift from the cyclic AMP to the arachidonic acid pathway. *Mol Pharmacol 64*(5), 1117–1125.

Pavoine, C., Magne, S., Sauvadet, A., & Pecker, F. (1999). Evidence for a beta2-adrenergic/arachidonic acid pathway in ventricular cardiomyocytes. Regulation by the beta1-adrenergic/cAMP pathway. *J Biol Chem 274*(2), 628–637.

Pietri-Rouxel, F., & Strosberg, A. D. (1995). Pharmacological characteristics and species-related variations of beta 3-adrenergic receptors. *Fundam Clin Pharmacol 9*(3), 211–218.

Popp, B. D., Hutchinson, D. S., Evans, B. A., & Summers, R. J. (2004). Stereoselectivity for interactions of agonists and antagonists at mouse, rat and human beta3-adrenoceptors. *Eur J Pharmacol 484*(2–3), 323–331.

Porto, P. I., Garcia, S. I., Dieuzeide, G., Gonzalez, C., Landa, M. S., & Pirola, C. J. (2004). Clinical features of the metabolic syndrome in adolescents: minor role of the Trp64Arg beta3-adrenergic receptor gene variant. *Pediatr Res 55*(5), 836–841.

Pott, C., Brixius, K., Bundkirchen, A., Bolck, B., Bloch, W., Steinritz, D., et al. (2003). The preferential beta3-adrenoceptor agonist BRL 37344 increases force via beta1/beta2-adrenoceptors and induces endothelial nitric oxide synthase via beta3-adrenoceptors in human atrial myocardium. *Br J Pharmacol 138*(3), 521–529.

Pourageaud, F., Leblais, V., Bellance, N., Marthan, R., & Muller, B. (2005). Role of beta(2)-adrenoceptors (ss-AR), but not ss(1)-, beta(3)-AR and endothelial nitric oxide, in beta-AR-mediated relaxation of rat intrapulmonary artery. *Naunyn Schmiedeberg's Arch Pharmacol 372*(1), 14–23.

Priest, R. M., Hucks, D., & Ward, J. P. (1997). Noradrenaline, beta-adrenoceptor mediated vasorelaxation and nitric oxide in large and small pulmonary arteries of the rat. *Br J Pharmacol 122*(7), 1375–1384.

Pulkkinen, A., Kareinen, A., Saarinen, L., Heikkinen, S., Lehto, S., & Laakso, M. (1999). The codon 64 polymorphism of the beta3-adrenergic receptor gene is not associated with coronary heart disease or insulin resistance in nondiabetic subjects and non-insulin-dependent diabetic patients. *Metabolism 48*(7), 853–856.

Rautureau, Y., Toumaniantz, G., Serpillon, S., Jourdon, P., Trochu, J. N., & Gauthier, C. (2002). Beta 3-adrenoceptor in rat aorta: molecular and biochemical characterization and signalling pathway. *Br J Pharmacol 137*(2), 153–161.

Ringel, J., Kreutz, R., Distler, A., & Sharma, A. M. (2000). The Trp64Arg polymorphism of the beta3-adrenergic receptor gene is associated with hypertension in men with type 2 diabetes mellitus. *Am J Hypertens 13*(9), 1027–1031.

Riordan, J. R., Rommens, J. M., Kerem, B., Alon, N., Rozmahel, R., Grzelczak, Z., et al. (1989). Identification of the cystic fibrosis gene: cloning and characterization of complementary DNA. *Science 245*(4922), 1066–1073.

Rohrer, D. K., Chruscinski, A., Schauble, E. H., Bernstein, D., & Kobilka, B. K. (1999). Cardiovascular and metabolic alterations in mice lacking both beta1- and beta2-adrenergic receptors. *J Biol Chem 274*(24), 16701–16708.

Rouget, C., Breuiller-Fouche, M., Mercier, F. J., Leroy, M. J., Loustalot, C., Naline, E., et al. (2004). The human near-term myometrial beta 3-adrenoceptor but not the beta 2-adrenoceptor is resistant to desensitisation after sustained agonist stimulation. *Br J Pharmacol 141*(5), 831–841.

Rouget, C., Barthez, O., Goirand, F., Leroy, M. J., Breuiller-Fouche, M., Rakotoniaina, Z., et al. (2005). Stimulation of the ADRB3 adrenergic receptor induces relaxation of human placental arteries: influence of pre-eclampsia. *Biol Reprod*.

Rozec, B., Serpillon, S., Toumaniantz, G., Seze, C., Rautureau, Y., & Baron, O. (2005). Characterization of beta3-adrenoceptors in human internal mammary artery and putative involvement in coronary artery bypass management. *J Am Coll Cardiol 46*(2), 351–359.

Rozec, B., Tran Quang, T., Noireaud, J., & Gauthier, C. (in press). Mixed beta 3-adrenoceptor agonist and alpha 1-adrenoceptor antagonist properties of nebivolol in rat thoracic aorta. *Br J Pharmacol*.

Sakane, N., Yoshida, T., Yoshioka, K., Nakamura, Y., Umekawa, T., Kogure, A., et al. (1997). Beta 3-adrenoreceptor gene polymorphism: a newly identified risk factor for proliferative retinopathy in NIDDM patients. *Diabetes 46*(10), 1633–1636.

Sakane, N., Yoshida, T., Yoshioka, K., Nakamura, Y., Umekawa, T., Kogure, A., et al. (1998). Trp64Arg mutation of beta3-adrenoceptor gene is associated with diabetic nephropathy in Type II diabetes mellitus. *Diabetologia 41*(12), 1533–1534.

Sarsero, D., Russell, F. D., Lynham, J. A., Rabnott, G., Yang, I., Fong, K. M., et al. (2003). (−)-CGP 12177 increases contractile force and hastens relaxation of human myocardial preparations through a propranolol-resistant state of the beta 1-adrenoceptor. *Naunyn Schmiedeberg's Arch Pharmacol 367*(1), 10–21.

Schranz, D., Droege, A., Broede, A., Brodermann, G., Schafer, E., Oelert, H., et al. (1993). Uncoupling of human cardiac beta-adrenoceptors during cardiopulmonary bypass with cardioplegic cardiac arrest. *Circulation 87*(2), 422–426.

Schulz, R., Rassaf, T., Massion, P. B., Kelm, M., & Balligand, J. L. (2006). Recent advances in the understanding of the role of nitric oxide in cardiovascular homeostasis. *Pharmacol Ther 108*(3), 225–256.

Sellke, F. W., Tofukuji, M., Stamler, A., Li, J., & Wang, S. Y. (1997). Beta-adrenergic regulation of the cerebral microcirculation after hypothermic cardiopulmonary bypass. *Circulation 96*(9 Suppl), II-10.

Sennitt, M. V., Kaumann, A. J., Molenaar, P., Beeley, L. J., Young, P. W., Kelly, J., et al. (1998). The contribution of classical (beta1/2-) and atypical beta-adrenoceptors to the stimulation of human white adipocyte lipolysis and right atrial appendage contraction by novel beta3-adrenoceptor agonists of differing selectivities. *J Pharmacol Exp Ther 285*(3), 1084–1095.

Shafiei, M., Omrani, G., & Mahmoudian, M. (2000). Coexistence of at least three distinct beta-adrenoceptors in human internal mammary artery. *Acta Physiol Hung 87*(3), 275–286.

Shah, A. M., Spurgeon, H. A., Sollott, S. J., Talo, A., & Lakatta, E. G. (1994). 8-Bromo-cGMP reduces the myofilament response to Ca^{2+} in intact cardiac myocytes. *Circ Res 74*(5), 970–978.

Shen, Y. T., Cervoni, P., Claus, T., & Vatner, S. F. (1996). Differences in beta 3-adrenergic receptor cardiovascular regulation in conscious primates, rats and dogs. *J Pharmacol Exp Ther 278*(3), 1435–1443.

Shen, Y. T., Zhang, H., & Vatner, S. F. (1994). Peripheral vascular effects of beta-3 adrenergic receptor stimulation in conscious dogs. *J Pharmacol Exp Ther 268*(1), 466–473.

Shieu, W. H., Lee, W. J., Yao, Y. E., Jeng, C. Y., Young, M. M., & Chen, Y. T. (1999). Lack of association between genetic variation in the beta3-adrenergic receptor gene and insulin resistance in patients with coronary heart disease. *Metabolism 48*(5), 651–654.

Stangl, K., Cascorbi, I., Laule, M., Stangl, V., Meisel, C., & Wernecke, K. D. (2001). The beta3-adrenergic receptor Trp64Arg mutation is not associated with coronary artery disease. *Metabolism 50*(2), 184–188.

Steinle, J. J., Booz, G. W., Meininger, C. J., Day, J. N., & Granger, H. J. (2003). Beta 3-adrenergic receptors regulate retinal endothelial cell migration and proliferation. *J Biol Chem 278*(23), 20681–20686.

Steinle, J. J., Zamora, D. O., Rosenbaum, J. T., & Granger, H. J. (2005). Beta 3-adrenergic receptors mediate choroidal endothelial cell invasion, proliferation, and cell elongation. *Exp Eye Res 80*(1), 83–91.

Strazzullo, P., Iacone, R., Siani, A., Cappuccio, F. P., Russo, O., Barba, G., et al. (2001). Relationship of the Trp64Arg polymorphism of the beta3-adrenoceptor gene to central adiposity and high blood pressure: interaction with age. Cross-sectional and longitudinal findings of the Olivetti Prospective Heart Study. *J Hypertens 19*(3), 399–406.

Strosberg, A. D. (1997). Structure and function of the beta 3-adrenergic receptor. *Annu Rev Pharmacol Toxicol 37*, 421–450.

Strosberg, A. D., & Pietri-Rouxel, F. (1996). Function and regulation of the beta 3-adrenoceptor. *Trends Pharmacol Sci 17*(10), 373–381.

Summers, R. J., Kompa, A., & Roberts, S. J. (1997). Beta-adrenoceptor subtypes and their desensitization mechanisms. *J Auton Pharmacol 17*(6), 331–343.

Susulic, V. S., Frederich, R. C., Lawitts, J., Tozzo, E., Kahn, B. B., Harper, M. E., et al. (1995). Targeted disruption of the beta 3-adrenergic receptor gene. *J Biol Chem 270*(49), 29483–29492.

Tagaya, E., Tamaoki, J., Takemura, H., Isono, K., & Nagai, A. (1999). Atypical adrenoceptor-mediated relaxation of canine pulmonary artery through a cyclic adenosine monophosphate-dependent pathway. *Lung 177*(5), 321–332.

Takahashi, H., Yoshida, T., Nishimura, M., Nakanishi, T., Kondo, M., & Yoshimura, M. (1992). Beta-3 adrenergic agonist, BRL-26830A, and alpha/beta blocker, arotinolol, markedly increase regional blood flow in the brown adipose tissue in anesthetized rats. *Jpn Circ J 56*(9), 936–942.

Takayama, S., Furukawa, Y., Ren, L. M., Inoue, Y., Sawaki, S., & Chiba, S. (1993). Positive chronotropic and inotropic responses to BRL 37344, a beta 3-adrenoceptor agonist in isolated, blood-perfused dog atria. *Eur J Pharmacol 231*(3), 315–321.

Tamaki, S., Iwai, N., Tsujita, Y., Nakamura, Y., Ohmichi, N., & Kinoshita, M. (1999). Variant of the beta3-adrenergic receptor gene and coronary atherosclerosis in Japanese subjects. *Int J Cardiol 69*(3), 309–311.

Tamaoki, J., Tagaya, E., Isono, K., & Nagai, A. (1998). Atypical adrenoceptor-mediated relaxation of canine pulmonary artery through a cAMP-dependent pathway. *Biochem Biophys Res Commun 248*(3), 722–727.

Tavernier, G., Galitzky, J., Bousquet-Melou, A., Montastruc, J. L., & Berlan, M. (1992). The positive chronotropic effect induced by BRL 37344 and CGP 12177, two beta-3 adrenergic agonists, does not involve cardiac beta adrenoceptors but baroreflex mechanisms. *J Pharmacol Exp Ther 263*(3), 1083–1090.

Tavernier, G., Toumaniantz, G., Erfanian, M., Heymann, M. F., Laurent, K., Langin, D., et al. (2003). Beta3-adrenergic stimulation produces a decrease

of cardiac contractility ex vivo in mice overexpressing the human beta3-adrenergic receptor. *Cardiovasc Res 59*(2), 288–296.

Thomas, G. N., Tomlinson, B., Chan, J. C., Young, R. P., & Critchley, J. A. (2000). The Trp64Arg polymorphism of the beta3-adrenergic receptor gene and obesity in Chinese subjects with components of the metabolic syndrome. *Int J Obes Relat Metab Disord 24*(5), 545–551.

Thuillez, C., & Richard, V. (2005). Targeting endothelial dysfunction in hypertensive subjects. *J Hum Hypertens 19*(Suppl 1), S21–S25.

Toda, N. (2003). Vasodilating beta-adrenoceptor blockers as cardiovascular therapeutics. *Pharmacol Ther 100*(3), 215–234.

Tonolo, G., Melis, M. G., Secchi, G., Atzeni, M. M., Angius, M. F., Carboni, A., et al. (1999). Association of Trp64Arg beta 3-adrenergic-receptor gene polymorphism with essential hypertension in the Sardinian population. *J Hypertens 17*(1), 33–38.

Torres, J., Darley-Usmar, V., & Wilson, M. T. (1995). Inhibition of cytochrome c oxidase in turnover by nitric oxide: mechanism and implications for control of respiration. *Biochem J 312*(Pt 1), 169–173.

Trochu, J. N., Leblais, V., Rautureau, Y., Beverelli, F., Le Marec, H., Berdeaux, A., et al. (1999). Beta 3-adrenoceptor stimulation induces vasorelaxation mediated essentially by endothelium-derived nitric oxide in rat thoracic aorta. *Br J Pharmacol 128*(1), 69–76.

Turner, N. C., & White, P. (1996). Effects of streptozotocin-induced diabetes on vascular reactivity in genetically hyperinsulinaemic obese Zucker rats. *J Cardiovasc Pharmacol 27*(6), 884–890.

Uydes-Dogan, B. S., Nebigil, M., Aslamaci, S., Onuk, E., Kanzik, I., & Akar, F. (1996). The comparison of vascular reactivities of arterial and venous grafts to vasodilators: management of graft spasm. *Int J Cardiol 53*(2), 137–145.

van Spronsen, A., Nahmias, C., Krief, S., Briend-Sutren, M. M., Strosberg, A. D., & Emorine, L. J. (1993). The promoter and intron/exon structure of the human and mouse beta 3-adrenergic-receptor genes. *Eur J Biochem 213*(3), 1117–1124.

Varghese, P., Harrison, R. W., Lofthouse, R. A., Georgakopoulos, D., Berkowitz, D. E., & Hare, J. M. (2000). Beta(3)-adrenoceptor deficiency blocks nitric oxide-dependent inhibition of myocardial contractility. *J Clin Invest 106*(5), 697–703.

Viard, P., Macrez, N., Coussin, F., Morel, J. L., & Mironneau, J. (2000). Beta-3 adrenergic stimulation of L-type Ca(2+) channels in rat portal vein myocytes. *Br J Pharmacol 129*(7), 1497–1505.

Wahler, G. M., & Dollinger, S. J. (1995). Nitric oxide donor SIN-1 inhibits mammalian cardiac calcium current through cGMP-dependent protein kinase. *Am J Physiol 268*(1 Pt 1), C45–C54.

Walston, J., Silver, K., Bogardus, C., Knowler, W. C., Celi, F. S., Austin, S., et al. (1995). Time of onset of non-insulin-dependent diabetes mellitus and genetic variation in the beta 3-adrenergic-receptor gene. *N Engl J Med 333*(6), 343–347.

Walston, J., Lowe, A., Silver, K., Yang, Y., Bodkin, N. L., Hansen, B. C., et al. (1997). The beta3-adrenergic receptor in the obesity and diabetes prone rhesus monkey is very similar to human and contains arginine at codon 64. *Gene 188*(2), 207–213.

Wang, Q., Curran, M. E., Splawski, I., Burn, T. C., Millholland, J. M., VanRaay, T. J., et al. (1996). Positional cloning of a novel potassium channel gene: KVLQT1 mutations cause cardiac arrhythmias. *Nat Genet 12*(1), 17–23.

Warth, J. D., Collier, M. L., Hart, P., Geary, Y., Gelband, C. H., Chapman, T., et al. (1996). CFTR chloride channels in human and simian heart. *Cardiovasc Res 31*(4), 615–624.

Werstiuk, E. S., & Lee, R. M. (2000). Vascular beta-adrenoceptor function in hypertension and in ageing. *Can J Physiol Pharmacol 78*(6), 433–452.

Wheeldon, N. M., McDevitt, D. G., & Lipworth, B. J. (1993). Investigation of putative cardiac beta 3-adrenoceptors in man. *Q J Med 86*(4), 255–261.

Wheeldon, N. M., McDevitt, D. G., & Lipworth, B. J. (1994). Cardiac effects of the beta 3-adrenoceptor agonist BRL35135 in man. *Br J Clin Pharmacol 37*(4), 363–369.

Widen, E., Lehto, M., Kanninen, T., Walston, J., Shuldiner, A. R., & Groop, L. C. (1995). Association of a polymorphism in the beta 3-adrenergic-receptor gene with features of the insulin resistance syndrome in Finns. *N Engl J Med 333*(6), 348–351.

Wilson, S., Chambers, J. K., Park, J. E., Ladurner, A., Cronk, D. W., Chapman, C. G., et al. (1996). Agonist potency at the cloned human beta-3 adrenoceptor depends on receptor expression level and nature of assay. *J Pharmacol Exp Ther 279*(1), 214–221.

Xiang, K., Jia, W., Lu, H., Zheng, T., Lu, J., & Tang, J. (1998). Effects of Trp64Arg mutation in the beta 3-adrenergic receptor gene on body fat, plasma glucose level, lipid profile, insulin secretion and action in Chinese. *Zhonghua Yi Xue Yi Chuan Xue Za Zhi 15*(6), 337–340.

Xiao, R. P., Cheng, H., Zhou, Y. Y., Kuschel, M., & Lakatta, E. G. (1999). Recent advances in cardiac beta(2)-adrenergic signal transduction. *Circ Res 85*(11), 1092–1100.

Xiu, L. L., Weng, J. P., Sui, Y., Wang, J., Yan, J. H., & Huang, Z. M. (2004). Common variants in beta 3-adrenergic-receptor and uncoupling protein-2 genes are associated with type 2 diabetes and obesity. *Zhonghua Yi Xue Za Zhi 84*(5), 375–379.

Yasuda, S., & Lew, W. Y. (1997). Lipopolysaccharide depresses cardiac contractility and beta-adrenergic contractile response by decreasing myofilament response to Ca2+ in cardiac myocytes. *Circ Res 81*(6), 1011–1020.

Yousif, M. H., & Oriowo, M. A. (2002). BRL 37344 inhibited adrenergic transmission in the rat portal vein via atypical beta-adrenoceptors. *Pharmacol Res 45*(4), 313–317.

Zhang, C., Williams, M. A., Edwards, K. L., & Austin, M. A. (2005a). Trp64Arg polymorphism of the beta3-adrenergic receptor gene, pre-pregnancy obesity and risk of pre-eclampsia. *J Matern Fetal Neonatal Med 17*(1), 19–28.

Zhang, Z. S., Cheng, H. J., Onishi, K., Ohte, N., Wannenburg, T., & Cheng, C. P. (2005b). Enhanced inhibition of L-type Ca^{2+} current by {beta}3-adrenergic stimulation in failing rat heart. *J Pharmacol Exp Ther 315*(3), 1203–1211.

Available online at www.sciencedirect.com
ScienceDirect
Life Sciences 79 (2006) 1234–1241
Life Sciences
www.elsevier.com/locate/lifescie

ENOS is not activated by nebivolol in human failing myocardium

Klara Brixius [a,b], Qiaofeng Song [a], Alock Malick [a], Birgit Boelck [a], Klaus Addicks [c], Wilhelm Bloch [b], Uwe Mehlhorn [d], Robert H.G. Schwinger [a,e,*]

[a] *Laboratory of Muscle Research and Molecular Cardiology, Department of Internal Medicine III, University of Cologne, Germany*
[b] *Department of Molecular and Cellular Sport Medicine, German Sport University, Cologne, Germany*
[c] *Institute I of Anatomy, University of Cologne, Germany*
[d] *Clinic for Cardiothoracic Surgery, University of Cologne, Germany*
[e] *Klinikum Weiden, Weiden i.d. Opf., Germany*

Received 15 November 2005; accepted 21 March 2006

Abstract

Nebivolol is a highly selective β_1-adrenoceptor blocker with additional vasodilatory properties, which may be due to an endothelial-dependent β_3-adrenergic activation of the endothelial nitric oxide synthase (eNOS). β_3-adrenergic eNOS activation has been described in human myocardium and is increased in human heart failure. Therefore, this study investigated whether nebivolol may induce an eNOS activation in cardiac tissue. Immunohistochemical stainings were performed using specific antibodies against eNOS translocation and eNOS serine^{1177} phosphorylation in rat isolated cardiomyocytes, human right atrial tissue (coronary bypass-operation), left ventricular non-failing (donor hearts) and failing myocardium after application of the β-adrenoceptor blockers nebivolol, metoprolol and carvedilol, as well as after application of BRL 37344, a specific β_3-adrenoceptor agonist. BRL 37344 (10 μM) significantly increased eNOS activity in all investigated tissues (either via translocation or phosphorylation or both). None of the beta-blockers (each 10 μM), including nebivolol, increased either translocation or phosphorylation in any of the investigated tissues. In human failing myocardium, nebivolol (10 μM) decreased eNOS activity. In conclusion, nebivolol shows a tissue-specific eNOS activation. Nebivolol does not activate the endothelial eNOS in end-stage human heart failure and may thus reduce inhibitory effects of NO on myocardial contractility and on oxidative stress formation. This mode of action may be of advantage when treating heart failure patients.

Keywords: eNOS; Nebivolol; Carvedilol; Metoprolol; Heart failure; BRL 37344

Introduction

Nebivolol is a specific β_1-adrenoceptor blocker, which has been shown to cause vasodilation in various animal species and humans (Bowman et al., 1994; Cockcroft et al., 1995; Gosgnach et al., 2001). It has been suggested that this effect is mediated by an endothelial-dependent release of nitric oxide (NO), because the nebivolol-induced vasodilation can be prevented by mechanically disrupting the endothelium (Gao et al., 1991) or by inhibition of NO synthase (NOS) (Bowman et al., 1994).

Recently, it was shown that the β_3-adrenergic pathways may be involved in the nebivolol-induced vasodilation/eNOS activation of rat aorta and human umbilical vein endothelial cells (Gosgnach et al., 2001). Additionally, it was shown a few years ago that cardiac β_3-adrenergic stimulation also results in a release of nitric oxide, which decreases force of contraction, especially in human failing myocardium (Gauthier et al., 1996, 1998). This β-adrenergic increase of NO may further depress cardiac contractility in end-stage heart failure.

Several mechanisms for eNOS activation have been discussed (for review see Fleming and Busse, 2003). Under basal conditions, eNOS is located at the cellular membrane close to caveolin. Upon receptor stimulation the caveolin/eNOS

* Corresponding author. Laboratory of Muscle Research and Molecular Cardiology, Department of Internal Medicine III, Joseph-Stelzmann-Str. 9, 50924 Cologne, Germany. Tel.: +49 221 4783138; fax: +49 221 4783746.
E-mail address: Robert.Schwinger@medizin.uni-koeln (R.H.G. Schwinger).

0024-3205/$ - see front matter © 2006 Elsevier Inc. All rights reserved.
doi:10.1016/j.lfs.2006.03.030

interaction is initiated and eNOS may translocate from the cell membrane into the cytosol. Besides translocation, eNOS activity can be altered by phosphorylation of the enzyme. Phosphorylation at eNOS serine^{1177} has been linked to an increase in eNOS activity, whereas a simultaneous phosphorylation of eNOS serine^{1177} and -threonine^{495} may be associated with a decline of NO-liberation (Dimmeler et al., 1999; Fleming et al., 2001). Phosphorylation of eNOS at serine^{114} may induce a functional uncoupling of eNOS resulting in an increased release of superoxide anions (Fleming and Busse, 2003).

β_3-adrenergic stimulation induces different mechanisms of eNOS activation depending on the cardiac region investigated. In human right atrial myocardium, β_3-adrenergic stimulation induces a translocation and a phosphorylation of the eNOS enzyme at serine^{1177}, whereas in human left ventricular non-failing myocardium only a phosphorylation of the eNOS enzyme at serine^{1177} was observed. β_3-adrenergic stimulation was not followed by a phosphorylation of eNOS threonine^{495} or serine^{114} (Pott et al., 2003; Brixius et al., 2004).

This study investigates whether application of nebivolol may be associated with an increase in the cardiac eNOS activation in rat and human non-failing myocardium and whether this response is enhanced in end-stage heart failure.

Materials and methods

Isolated rat cardiomyocytes

We isolated adult rat cardiomyocytes from healthy male Wistar rats (body weight 220–250 g, n=4). The rats were euthanized by cervical dislocation; the heart was excised, rapidly cannulated and perfused with Powell medium. (in mM: NaCl 110, KCl 2.5, $MgSO_4$ 1.3, KH_2PO_4 1.18, $NaHCO_3$ 3.25, pH 7.4, 37 °C, equilibrated with 95% O_2 : 5% CO_2) for 10 min with a modified Langendorff apparatus. Hearts were enzymatically digested with collagenase type II (Biochrom) in Powell buffer for 12–15 min and subjected to increasing concentration of calcium. Isolated cardiomyocytes were cultured on laminin coated culture dishes (laminin natural mouse, Coll. Biomedical) in supplemented medium M199 (Gibco) containing per 500 ml Pen/Strep (Sigma) 5 ml; insulin H (Höchst) 7.2 I.E.; non-essential amino-acids (Gibco) 5 ml; MEM-vitamins (Gibco) 10 ml).

Human myocardial tissue

Human non-failing ventricular trabeculae were obtained from 4 non-failing donor hearts (males, age: 52±2) that could not be transplanted due to technical reasons. No cardiac catheterization had been performed in the organ donor group, but none of the donors had a history of heart disease and all had normal left ventricular function as measured by echocardiography.

Failing myocardial tissue was obtained from explanted hearts of 5 recipients at transplantation who had idiopathic dilated cardiomyopathy (stadium D, 4 males, 1 female, age: 50±3).

Right atrial myocardium was obtained from patients (7 male, 5 female; age 72.1±7.2 years) who underwent coronary artery bypass grafting operations for coronary heart disease (n=8) or valve disease operations (n=4). None had clinical signs of heart failure. Medical treatment of right atrial tissue donors consisted of statins, nitrates, angiotensin-converting enzyme inhibitors, platelet inhibitors, diuretics and/or β-adrenoceptor antagonists. The drugs used for general anaesthesia were flunitrazepam, fentanyl and pancuronium bromide with propofol.

The study was approved by the local ethics committee and conforms with the Helsinki Declaration.

Immunohistochemistry

Pre-treatment of rat cardiomyocytes

In order to investigate eNOS activation, we performed incubation procedures with rat cardiomyocytes by adding nebivolol (10 μmol/l) or BRL 37344 (10 μmol/l). We then fixed the cells in 4% paraformaldehyde (PFA) for 20 min. Finally, we rinsed each dish in 0.1 M phosphate buffered saline (PBS, in mmol/l: Na_2HPO_4 0.08, NaH_2PO_4 0.019, NaCl 0.15) buffer at least three times and stored at 4 °C until further immunocytochemical investigation.

Pre-treatment and fixation of human myocardium

The human myocardial samples were immediately placed in ice-cold pre-aerated modified Tyrode's solution and delivered to the laboratory within 10 min. In order to investigate eNOS activation, we performed pre-incubation procedures with freshly obtained tissue. Muscle strips of right atrial or left ventricular myocardium were suspended in separate organ baths for at least 30 min at 37 °C with oxygenated Tyrode's solution (in mM: NaCl 119.8, KCl 5.4, $MgCl_2$ 1.05, $CaCl_2$ 1.8, NaH_2PO_4 0.42, glucose 5.05, ascorbic acid 0.28, Na_2EDTA 0.05, pH: 7.4, 95% O_2, 5% CO_2). We then incubated the myocardium for 5 min with either nebivolol, metropolol, carvedilol, BRL 37344 (each 10 μM) or the solvent, before fixing in 4% paraformaldehyde for 4 h. Previous experiments have shown that maximum eNOS activation was reached after 5 min incubation (Pott et al., 2003; Brixius et al., 2004).

After the PFA-incubation, the cardiac tissue was rinsed in 0.1 M PBS for 24 h. Specimens were stored for another 18 h in PBS solution with 18% sucrose for cryoprotection and afterwards frozen at −80 °C with the help of a tissue tek embedding console system.

Immunocytochemistry

Prior to immunohistochemical examination, 10 μm slices of pre-treated myocardial tissue and the dishes with rat cardiomyocytes were placed in a bathing solution of 3% H_2O_2 and 80% methanol for 30 min. We then permeabilized them with 0.2% Triton-X 100 in 0.1 mol/l PBS. Thereafter, specimens were treated with 5% bovine serum albumine (BSA) solution in PBS. Prior to each step, the sections were rinsed in PBS buffer

at least three times. Incubation with the primary antibody was performed in a PBS-based solution of 0.8% BSA for 12 h at 4 °C. After rinsing with PBS, the sections were incubated with the corresponding secondary biotinylated goat anti-rabbit antibody for 1 h at room temperature. A streptavidin–horseradish peroxidase complex was then applied as a detection system (1:100 dilution) for 1 h. Finally, staining was developed for 3–15 min with 3,3-diaminobenzidine tetrahydrochloride (DAB) in 0.05 mol/l TRIS–HCl buffer and 0.1% H_2O_2. Negative control sections were incubated without the primary antibody.

TV-densitometry

For intensity analysis of immunostaining in rat cardiomyocytes and human myocardial samples, we measured the grey values of 30 cardiomyocytes from 6 randomly selected areas of each slice. The intensity of immunostaining was reported as a percentage of the mean of measured cardiomyocyte grey value minus the background grey value (%mArGV), where 0% was defined as totally white and 100% as totally black. The background grey value was measured at a cell free area of the slice. For staining intensity detection a Nikon microscope coupled to a black and white video camera connected to a frame grabber was used. The analysis was performed using the Optimas 6.01 image analysis program.

We consequently excluded vascular structures.

Materials

The following primary antibodies were used for immunohistochemistry: 1) rabbit anti-eNOS antibody against the bovine eNOS peptide (599–613) plus additional C-terminal Cys conjugated to KLH (PYNSSPREQHKSYKC) (Biomol, Hamburg, Germany). This antibody has been previously shown to be specific in detecting the eNOS protein after dissociation from caveolin, i.e. after translocation (Bloch, 2001); 2) anti-phospho-eNOS^{Ser1177} (Upstate, Lake Placid, USA), corresponding to amino acids 1172–1183 of human eNOS.

As secondary antibody, a biotinylated goat anti-rabbit was used for accentuation. Nebivolol was generously provided by Berlin-Chemie AG, Berlin, Germany; Metoprolol by Astra Gmbh, Wedel, Germany; Carvedilol by Boehringer Mannheim, Germany. The preferential β_3-AR agonist BRL 37344 was obtained from Tocris (Bristol, United Kingdom).

Statistical analysis

All data are presented as mean±SEM. Data were analyzed using Student's *t*-test for paired and unpaired data. Significance was considered at p value <0.05.

Results

Rat cardiomyocytes

To investigate whether nebivolol may influence eNOS activation in cardiac myocytes, possibly due to a β_3-adrenoceptor agonistic activity, we performed immunohistochemical staining using an antibody which specifically detects the activated form of the eNOS protein (Bloch et al., 2001). In addition, eNOS phosphorylation was measured at serine^{1177}, a phosphorylation site which has been demonstrated to increase eNOS activity (Dimmeler et al.,

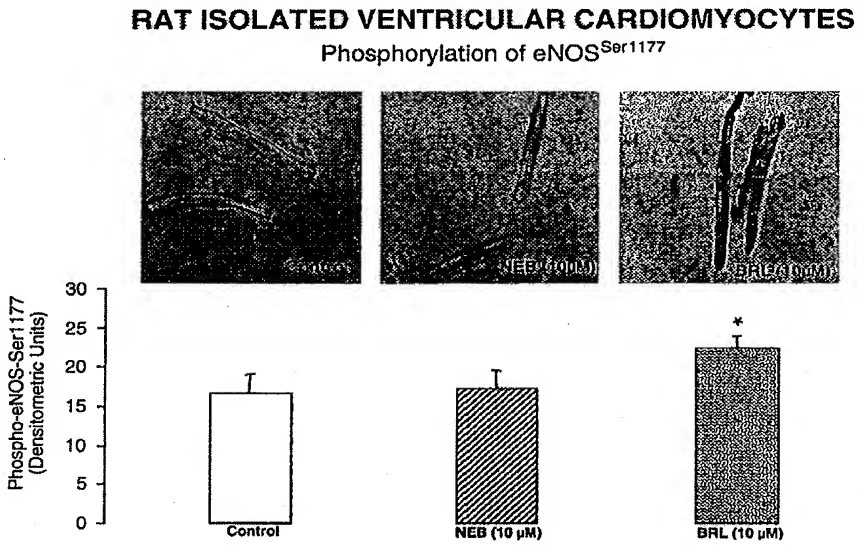

Fig. 1. Immunohistochemical detection of eNOS phosphorylation at serine^{1177} (p-eNOS^{Ser1177}) in rat ventricular cardiomyocytes. No increase in p-eNOS^{Ser1177} staining occurs in rat cardiomyocytes under control conditions and in the presence of nebivolol (NEB, 10 µM, 5 min, $n=4$ dishes, 30 cells per dish). After application of BRL 37344 (BRL, 10 µM, 5 min, $n=4$ dishes, 30 cells per dish), an increase in p-eNOS^{Ser1177} can be observed. *$p<0.05$.

1999). For comparison, we studied eNOS activation in isolated cardiomyocytes after application of BRL 37344 (10 μM), a preferential β_3-adrenoceptor agonist, which has been previously shown to induce an eNOS activation via translocation and eNOS phosphorylation at Ser^{1177}. Fig. 1 shows original pictures taken from the experiments and summarizes the results.

No alterations of eNOS translocation were observed after application of nebivolol or BRL 37344. $eNOS^{Ser1177}$ phosphorylation was only increased after application of BRL 37344.

Human right atrial myocardium

Species differences may exist regarding the activation of the β-adrenergic and the eNOS system. In addition, regional differences have been described for eNOS activation following β_3-adrenergic stimulation (Brixius et al., 2004). In order to investigate whether β-adrenoceptor blockers may influence eNOS activation in right atrial human myocardium, we performed immunohistochemical eNOS staining in isolated, electrically stimulated human right atrial myocardium under control conditions (t=0 min) and after application of nebivolol, metoprolol or carvedilol (10 μM, t=5 min). For comparison, experiments were performed in the presence of BRL 37344 (10 μM, t=5 min). Figs. 2 and 3 present pictures taken from original immunostainings and summarize the results.

No eNOS activation via translocation or $eNOS^{Ser1177}$ phosphorylation was observed in human right atrial myocardium myocytes after application of nebivolol, metoprolol or carvedilol. Only in the presence of BRL 37344 was a significant translocation and $eNOS^{Ser1177}$ phosphorylation detected in human right atrial myocardium.

Influence of beta-blockers on eNOS activation in human non-failing and failing left ventricular myocardium

Immunohistochemical studies were performed in isolated left ventricular trabeculae of human non-failing and failing left ventricular myocardium in the absence and presence nebivolol, metoprolol, carvedilol or BRL 37344 (each 10 μM, 5 min).

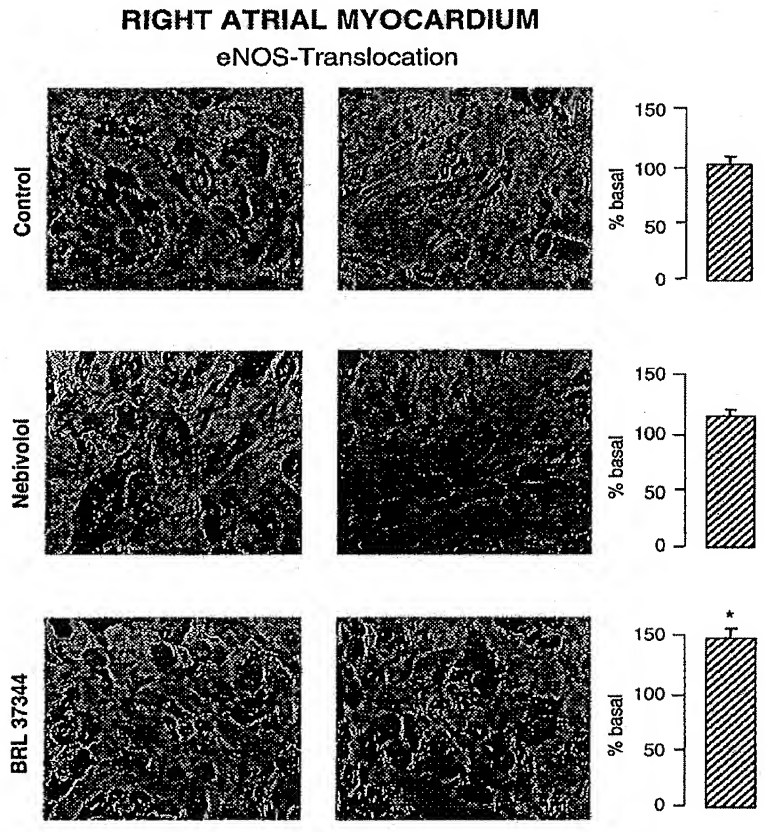

Fig. 2. eNOS translocation in human right atrial myocardium. Only after application of BRL 37344 (10 μM, 5 min), can an increase in eNOS translocation be observed. *$p<0.05$.

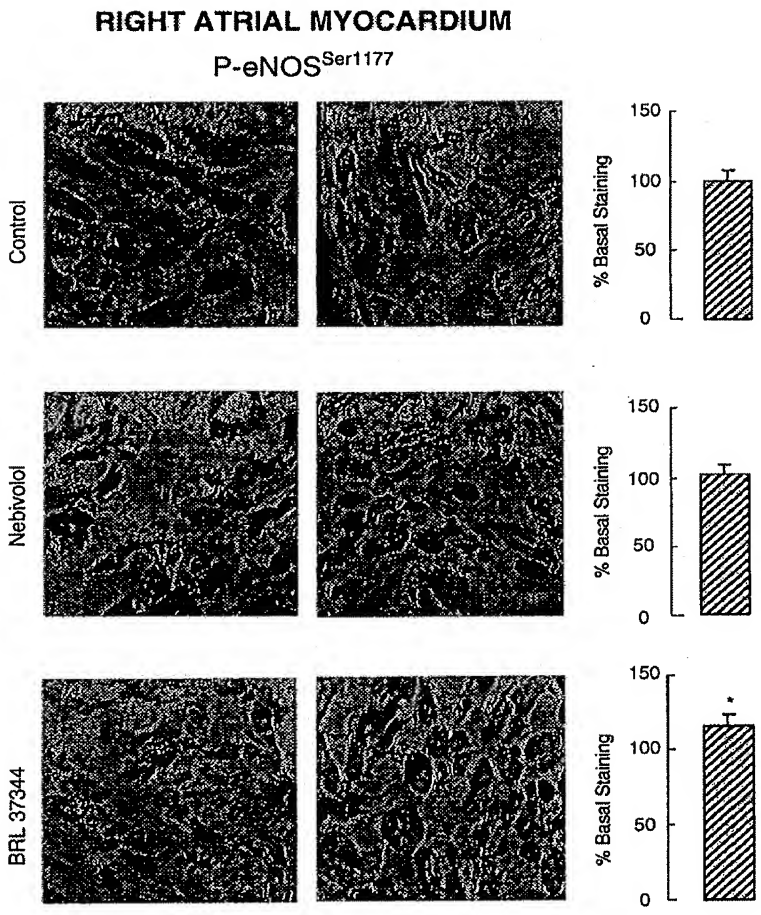

Fig. 3. Immunohistochemical detection of p-eNOS^{Ser1177} protein in human right atrial myocardium. Only after application of BRL 37344 (10 μM, 5 min), can an increase in eNOS phosphorylation at serine^{1177} be observed. *$p<0.05$.

Fig. 4 summarizes the results obtained in human non-failing myocardium. None of the β-adrenoceptor blockers altered eNOS translocation and eNOS^{Ser1177} phosphorylation in human non-failing left ventricular cardiac myocytes.

Figs. 5 and 6 show original pictures and summarize the data obtained in human failing myocardium. Only BRL 37344 significantly increased eNOS translocation and Ser^{1177} phosphorylation, whereas nebivolol decreased the two parameters compared to control. Metoprolol and carvedilol did not alter eNOS activity.

Discussion

This study investigated the influence of nebivolol, carvedilol and metoprolol on eNOS activation in rat cardiomyocytes and human non-failing and failing myocardium. Whereas there was a clear reaction of BRL 37344, a preferential β_3-adrenoceptor agonist, on eNOS activation in cardiac tissue, nebivolol, carvedilol and metoprolol did not alter eNOS activity in cardiac tissue. In human failing myocardium eNOS activation was depressed by nebivolol.

Nebivolol is a specific β_1-adrenoceptor blocker, which has been shown to cause an endothelial-dependent vasodilation by liberation of nitric oxide in various animal species and humans due – at least partly – to a stimulation of the β_3-adrenoceptors (Bowman et al., 1994; Cockcroft et al., 1995; Gosgnach et al., 2001). The eNOS protein is also expressed in cardiomyocytes and there is an indication that β_3-adrenergic stimulation by BRL 37344 may decrease cardiac contractility, especially in human failing myocardium due to eNOS activation and NO liberation (Gauthier et al., 1996, 1998). In this study, nebivolol did not alter eNOS activity in human non-failing myocardium and even depressed eNOS activation in the failing heart. A depression of eNOS activation may be beneficial in human end-stage failing hearts since it may reduce the impairment of cardiac contractility (Gauthier et al., 1996, 1998) and may also depress any oxidative stress which may result from an uncoupling of the eNOS protein (Dixon et al., 2003).

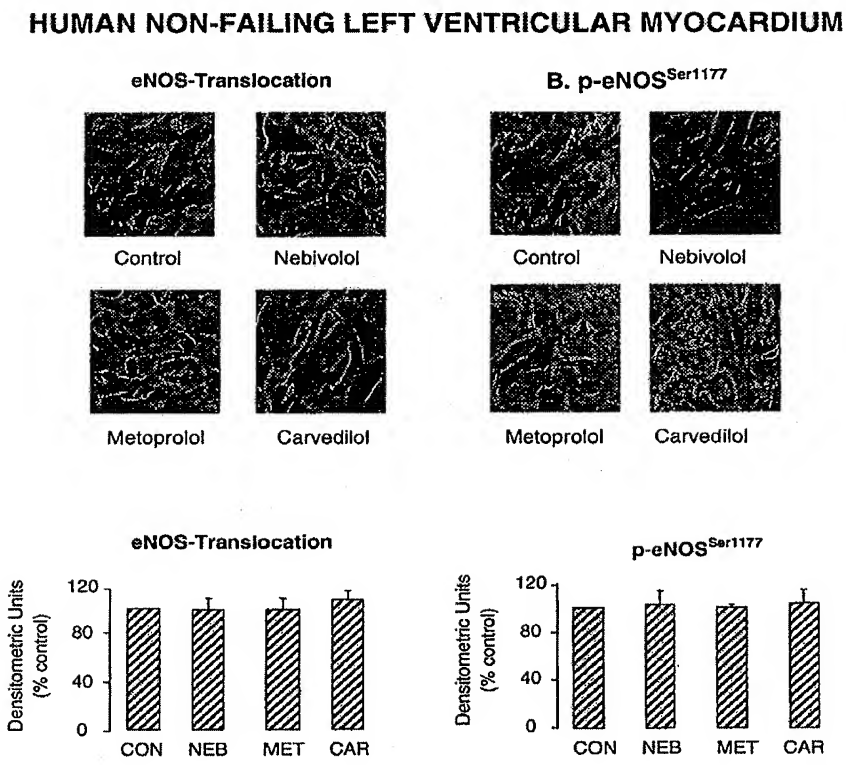

Fig. 4. eNOS translocation and p-eNOS^{Ser1177} protein in human left ventricular non-failing myocardium. No alterations were observed in the presence of nebivolol, metoprolol, and carvedilol (each 10 μM, 5 min) compared to control.

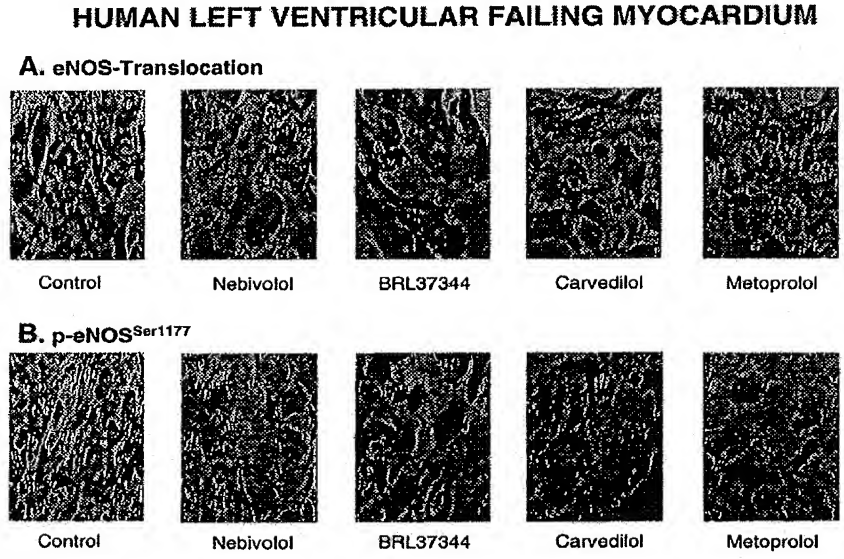

Fig. 5. Immunohistochemical detection of eNOS translocation and p-eNOS^{Ser1177} protein in human left ventricular failing myocardium. Only in the presence of BRL 37344 (10 mM, 5 min) was a significant increase in eNOS translocation and phosphorylation detected. Application of nebivolol decreased eNOS translocation and Ser^{1177} phosphorylation. No alterations were observed in the presence of metoprolol or carvedilol (each 10 μM, 5 min) compared to control.

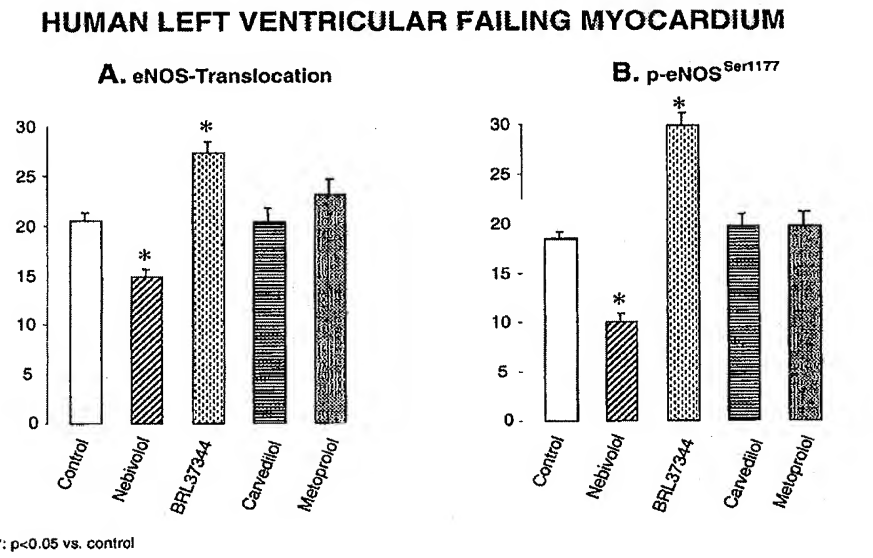

Fig. 6. Summarized data on the immunohistochemical detection of eNOS translocation and p-eNOS^{Ser1177} protein in human left ventricular failing myocardium.

The tissue specific lack of eNOS activation by nebivolol in contrast to BRL 37344 may be due to nebivolol's β_1-adrenoceptor selective blocking properties. In contrast to nebivolol, β_1- and β_2-adrenoceptor agonistic properties have been described for BRL 37344, especially in human atrial myocardium (Pott et al., 2003). Thus, an interaction may exist between the three β-adrenoceptor subtypes which may either facilitate or decrease eNOS activation depending on the mechanisms by which the adrenoceptors are influenced by each drug. However, this has to be investigated in further studies.

Although we detected no clear mechanism to explain the lack of cardiac eNOS activation by nebivolol, the high vasoselectivity of NO-liberation by nebivolol may be of great importance regarding the NO- and β_3-adrenoceptor-mediated alterations of heart rate. In clinical settings, β_3-adrenoceptor agonists were shown to increase heart rate and blood pressure in humans (Wheeldon et al., 1994). In addition, in isolated, electrically stimulated human right atrial appendages CGP 12177 (in the presence of 200 nM propranolol to block β_1- and β_2-adrenoceptors) has been shown to cause positive chronotropic effects (Kaumann, 1996).

In conclusion, this study shows that nebivolol, metoprolol and carvedilol do not affect cardiac eNOS activation in human non-failing myocardium and even suppress eNOS activation in human failing myocardium. These vasoselective NO-liberating properties of nebivolol may be of special advantage when treating cardiovascular patients.

Acknowledgements

The authors thank Esra Köroglu, Katja Rösler, and Kerstin Schenk for their excellent technical help. This work contains data from the doctoral thesis of Q.S.

References

Bloch, W., Mehlhorn, U., Krahwinkel, A., Reiner, M., Dittrich, M., Schmidt, A., Addicks, K., 2001. Ischemia increases detectable endothelial nitric oxide synthase in rat and human myocardium. Nitric Oxide 5, 317–333.

Bowman, A.J., Chen, C.P., Ford, G.A., 1994. Nitric oxide mediated venodilator effects of nebivolol. British Journal of Clinical Pharmacology 38, 199–204.

Brixius, K., Bloch, W., Pott, C., Napp, A., Krahwinkel, A., Ziskoven, C., Koriller, M., Mehlhorn, U., Hescheler, J., Fleischmann, B., Schwinger, R.H.G., 2004. Mechanisms of beta 3-adrenoceptor-induced eNOS activation in right atrial and left ventricular human myocardium. British Journal of Pharmacology 143, 1014–1022.

Cockcroft, J.R., Chowienczyk, P.J., Brett, S.E., Chen, C.P., Dupont, A.G., Van Nueten, L., Wooding, S.J., Ritter, J.M., 1995. Nebivolol vasodilates human forearm vasculature: evidence for an L-arginine/NO-dependent mechanism. Journal of Pharmacology and Experimental Therapeutics 274, 1067–1071.

Dimmeler, S., Fleming, I., Fisslthaler, B., Hermann, C., Busse, R., Zeiher, A.M., 1999. Activation of nitric oxide synthase in endothelial cells by Akt-dependent phosphorylation. Nature 399, 601–605.

Dixon, L.J., Morgan, D.R., Hughes, S.M., McGrath, L.T., El-Sherbeeny, N.A., Plumb, R.D., Devine, A., Leahey, W., Johnston, G.D., McVeigh, G.E., 2003. Functional consequences of endothelial nitric oxide synthase uncoupling in congestive cardiac failure. Circulation 107, 1725–1728.

Fleming, I., Busse, R., 2003. Molecular mechanisms involved in the regulation of the endothelial nitric oxide synthase. American Journal of Physiology 284, R1–R12.

Fleming, I., Fisslthaler, B., Dimmeler, S., Kemp, B.E., Busse, R., 2001. Phosphorylation of Thr(495) regulates Ca(2+)/calmodulin-dependent endothelial nitric oxide synthase activity. Circulation Research 88, E68–E75.

Gao, Y.S., Nagao, T., Bond, R.A., Janssens, W.J., Vanhoutte, P.M., 1991. Nebivolol induces endothelium-dependent relaxations of canine coronary arteries. Journal of Cardiovascular Pharmacology 17, 964–969.

Gauthier, C., Tavernier, G., Charpentier, F., Langin, D., Le Marec, H., 1996. Functional beta3-adrenoceptor in the human heart. Journal of Clinical Investigation 98, 556–562.

Gauthier, C., Leblais, V., Kobzik, L., Trochu, J.N., Khandoudi, N., Bril, A., Balligand, J.L., Le Marec, H., 1998. The negative inotropic effect of beta3-adrenoceptor stimulation is mediated by activation of a nitric oxide synthase

pathway in human ventricle. Journal of Clinical Investigation 102, 1377–1384.
Gosgnach, W., Boixel, C., Nevo, N., Poiraud, T., Michel, J.B., 2001. Nebivolol induces calcium-independent signaling in endothelial cells by a possible beta-adrenergic pathway. Journal of Cardiovascular Pharmacology 38, 191–199.
Kaumann, A.J., 1996. (−)-CGP 12177-induced increase of human atrial contraction through a putative third beta-adrenoceptor. British Journal of Pharmacology 117, 93–98.
Pott, C., Brixius, K., Bundkirchen, A., Bolck, B., Bloch, W., Steinritz, D., Mehlhorn, U., Schwinger, R.H.G., 2003. The preferential beta3-adrenoceptor agonist BRL 37344 increases force via beta1-/beta2-adrenoceptors and induces endothelial nitric oxide synthase via beta3-adrenoceptors in human atrial myocardium. British Journal of Pharmacology 138, 521–529.
Wheeldon, N.M., McDevitt, D.G., McDevitt, D.G., Lipworth, B.J., 1994. Cardiac effects of the beta 3-adrenoceptor agonist BRL35135 in man. British Journal of Clinical Pharmacology 37, 363–369.

THE JOURNAL OF BIOLOGICAL CHEMISTRY VOL. 285, NO. 18, pp. 13712–13720, April 30, 2010

Activation of cAMP-dependent Signaling Induces Oxidative Modification of the Cardiac Na^+-K^+ Pump and Inhibits Its Activity*

Received for publication, December 1, 2009, and in revised form, February 24, 2010 Published, JBC Papers in Press, March 1, 2010, DOI 10.1074/jbc.M109.090225

Caroline N. White[‡§], Chia-Chi Liu[‡], Alvaro Garcia[‡§], Elisha J. Hamilton[‡], Karin K. M. Chia[‡§], Gemma A. Figtree[‡§1], and Helge H. Rasmussen[‡§2]

From the [‡]North Shore Heart Research Group, Kolling Institute, University of Sydney, Sydney 2065 and the [§]Department of Cardiology, Royal North Shore Hospital, Sydney 2065, Australia

Cellular signaling can inhibit the membrane Na^+-K^+ pump via protein kinase C (PKC)-dependent activation of NADPH oxidase and a downstream oxidative modification, glutathionylation, of the β_1 subunit of the pump α/β heterodimer. It is firmly established that cAMP-dependent signaling also regulates the pump, and we have now examined the hypothesis that such regulation can be mediated by glutathionylation. Exposure of rabbit cardiac myocytes to the adenylyl cyclase activator forskolin increased the co-immunoprecipitation of NADPH oxidase subunits $p47^{phox}$ and $p22^{phox}$, required for its activation, and increased superoxide-sensitive fluorescence. Forskolin also increased glutathionylation of the Na^+-K^+ pump β_1 subunit and decreased its co-immunoprecipitation with the α_1 subunit, findings similar to those already established for PKC-dependent signaling. The decrease in co-immunoprecipitation indicates a decrease in the α_1/β_1 subunit interaction known to be critical for pump function. In agreement with this, forskolin decreased ouabain-sensitive electrogenic Na^+-K^+ pump current (arising from the 3:2 Na^+:K^+ exchange ratio) of voltage-clamped, internally perfused myocytes. The decrease was abolished by the inclusion of superoxide dismutase, the inhibitory peptide for the ϵ-isoform of PKC or inhibitory peptide for NADPH oxidase in patch pipette solutions that perfuse the intracellular compartment. Pump inhibition was also abolished by inhibitors of protein kinase A and phospholipase C. We conclude that cAMP- and PKC-dependent inhibition of the cardiac Na^+-K^+ pump occurs via a shared downstream oxidative signaling pathway involving NADPH oxidase activation and glutathionylation of the pump β_1 subunit.

The membrane Na^+-K^+ pump transports three Na^+ ions out of and two K^+ ions into cells against their electrochemical gradient using energy derived from hydrolysis of ATP. The Na^+ and K^+ ion gradients generated by the pump serve in secondary co- and counter-transport processes that maintain gradients for H^+, Ca^{2+}, Cl^-, and various organic molecules. Changes in the intracellular Na^+ concentration can have wide-ranging effects on the intracellular milieu and, hence, cell function, including excitability, energy metabolism, and excitation-contraction coupling. Regulation of the Na^+-K^+ pump is, therefore, important for cell homeostasis.

The Na^+-K^+ pump is a heterodimer that consists of a large α subunit and a much smaller β subunit. Each exists in several isoforms with α_1 and β_1 the most abundantly expressed (1). Hydrolysis of ATP and transport of Na^+ and K^+ are mediated by the α subunit. The β subunit has a chaperone role in mediating membrane integration of newly synthesized α subunits. In addition, it influences transport properties of the assembled α/β heterodimer. A conformational rearrangement of the heterodimer during the catalytic cycle may couple the β subunit to function (2).

Oxidative stimuli induce glutathionylation, a reversible oxidative modification, of Cys-46 of the β_1 subunit. Glutathionylation and an associated pump inhibition are abolished by mutation of Cys-46 indicating a causal relationship between the oxidative modification and pump function. This is supported by the absence of an effect of oxidative stimuli when expressed pump heterodimers contain wild-type β_2 or β_3 subunits that do not have a Cys-46 (3). The physiological relevance of glutathionylation is suggested by its coupling to hormone receptors and kinase-dependent signaling pathways. Exposure of cardiac myocytes to angiotensin II (Ang II)[3] increases glutathionylation and inhibits pump activity via protein kinase C (PKC)-dependent activation of NADPH oxidase (3, 4). Conversely, exposure of myocytes to β_3 adrenergic receptor agonists decreases glutathionylation from base line and stimulates pump activity via activation of nitric oxide (NO) synthase and NO-dependent downstream pathways (5).[4] Thus, pump stimulation and inhibition are mediated by decreasing or increasing the degree of Cys-46 glutathionylation from base line.

Cyclic AMP-dependent messenger pathways have also been reported to regulate the Na^+-K^+ pump. Such regulation occurs in many different tissues (6), including the heart (7–16), and is

* The work was supported by grants from the North Shore Heart Research Foundation and the National Health and Medical Research Council.

[1] Supported by a Royal Australian College of Physicians/High Blood Pressure Research Foundation Fellowship and the University of Sydney Medical Foundation.

[2] To whom correspondence should be addressed: Dept. of Cardiology, Royal North Shore Hospital, St. Leonards, NSW, 2065, Australia. Tel.: 61-2-9926-8684; Fax: 61-2-9926-6521; E-mail: helge.rasmussen@sydney.edu.au.

[3] The abbreviations used are: Ang II, angiotensin II; PKC, protein kinase C; PKA, protein kinase A; $PLMI_p$, electrogenic Na^+-K^+ pump current; RACK, receptor for activated kinase; DHE, dihydroethidium; SOD, superoxide dismutase; PLC, phospholipase C; Epac, exchange protein directly activated by cAMP.

[4] H. Bundgaard, C. Liu, A. Garcia, E. J. Hamilton, Y. Huang, K. K. Chia, S. H. Hunyor, G. A. Figtree, and H. H. Rasmussen, submitted for publication.

reported to cause either pump stimulation or inhibition. In this study we show that the adenylyl cyclase activator forskolin can induce glutathionylation of the β_1 Na^+-K^+ pump subunit in cardiac myocytes. As expected from the glutathionylation of the subunit (3), exposure of voltage-clamped myocytes to forskolin decreased electrogenic Na^+-K^+ pump current (I_p). Parallel studies on intact myocytes and functional studies on voltage-clamped, internally perfused myocytes implicated the same oxidative signaling pathway in the forskolin-induced glutathionylation of the β_1 subunit and decrease in I_p.

EXPERIMENTAL PROCEDURES

Cells—Ventricular myocytes were isolated from rabbit hearts as described previously (17). They were stored at room temperature until used for experimentation and were used on the day of isolation only. Experimental protocols were approved by our institutional animal ethics and care committee.

Protein Co-immunoprecipitation and Detection of Glutathionylated Protein—Cells were lysed in ice-cold buffer containing 150 mmol/liter NaCl, 50 mmol/liter Tris·HCl (pH 8.0), EDTA, and 1% Triton X-100. Protease inhibitors were added. The lysates were clarified by centrifugation at 16,000 × *g* for 20 min and incubated with monoclonal antibody to the protein of interest or control IgGs. Protein A/G plus-agarose beads (40 μl of a 50% slurry) were added to the supernatant for a further incubation of 1 h at 4 °C. Immunoprecipitated proteins were eluted by boiling for 5 min in Laemmli sample buffer. Immune complexes were analyzed by SDS/PAGE and Western blot by probing with antibodies to εPKC (BD Biosciences), the receptor for the activated kinase (εRACK, BD Biosciences), $p22^{phox}$ (Santa Cruz Biotechnology), $p47^{phox}$ (Santa Cruz Biotechnology), and the α_1 or β_1 subunit of Na^+-K^+-ATPase (Upstate Biotechnology). To detect *S*-glutathionylation of pump subunits, myocytes were loaded with biotinylated glutathione (GSH). After lysis, the biotin-tagged glutathionylated subfraction was precipitated using streptavidin-Sepharose beads (18) and immunoblotted for α_1 and β_1 Na^+-K^+ pump subunits. In separate experiments the β_1 subunit immunoprecipitate was immunoblotted with an antibody against glutathionylated protein (anti-GSH antibody, Invitrogen). Western blots were quantified by densitometry using a Las-4000 image reader and Multi Gauge 3.1 software (Fuji Photo Film Co., Ltd.) and normalized against relevant control. Exposure times were adjusted to ensure that the variation in signal intensity was in the linear dynamic range.

Fluorescence Microscopy—The oxidative fluorescent dye dihydroethidium (DHE) was used to image intracellular $O_2^{\cdot-}$ as described previously (19, 20). Myocytes were incubated in the dark in Krebs solution containing 2 μmol/liter DHE for 20 min at 37 °C. In some experiments they were preincubated in 170 IU/ml pegylated superoxide dismutase (pegylated SOD, covalently attached polyethylene glycol polymer chain to SOD, which enhances cell association of the enzyme), 10 μmol/liter apocynin, or 10 μmol/liter myristoylated εPKC inhibitory peptide for 20 min before loading with DHE. Myocytes were then exposed to control solutions or solutions containing 100 nmol/liter forskolin for 10 min before fixation in 2% paraformaldehyde on ice for 4 min. They were washed and mounted on poly-L-lysine-coated glass slides in Vectashield and examined under a laser scanning confocal microscope (Nikon C1) equipped with an argon-krypton laser. The excitation wavelength was 488 nm, and the emission wavelength was 585 nm. The fluorescence images were obtained using constant settings of scanning speed, pinhole diameter, and voltage gain. Myocytes representative of each experimental condition were selected randomly for quantification of fluorescence intensity (Photoshop, Adobe). Only myocytes with clear striations and a rod-like shape were included in the analysis. The average intensity for cells from each experiment was normalized against its control (100%).

Measurement of I_p in Voltage-clamped Myocytes—Solutions and voltage clamp protocol were designed to minimize non-pump membrane currents in voltage-clamped myocytes. We used wide-tipped patch pipettes (4–5 μm) filled with solutions containing 5 mmol/liter HEPES, 2 mmol/liter MgATP, 5 mmol/liter EGTA, 70 mmol/liter potassium glutamate, 10 mmol/liter sodium glutamate, and 80 mmol/liter tetramethylammonium chloride. The solution also contained 0.01 mmol/liter L-arginine when indicated. Myocytes were initially superfused with solution containing 140 mmol/liter NaCl, 5.6 mmol/liter KCl, 2.16 mmol/liter $CaCl_2$, 1 mmol/liter $MgCl_2$, 10 mmol/liter glucose, 0.44 mmol/liter NaH_2PO_4, 10 mmol/liter HEPES, and subsequently with a solution that was nominally Ca^{2+}-free and contained 2 mmol/liter $BaCl_2$ and 0.2 mmol/liter $CdCl_2$. Na^+-containing compounds in this solution were replaced with *N*-methyl-D-glutamine (21) to avoid transmembrane Na^+ influx that might cause an increase in the intracellular Na^+ concentration and secondary pump stimulation. This solution also included 100 nmol/liter forskolin when indicated. Because forskolin is expected to activate a large Cl^- current, we voltage-clamped myocytes at the equilibrium potential for Cl^-, calculated from the composition of the superfusate and pipette solution (−14 mV). I_p was identified as the difference between stable holding current before and after Na^+-K^+ pump blockade with100 μmol/liter ouabain. Na^+-K^+ pump currents are small relative to other membrane currents, and it is important for their accurate measurement that holding currents are stable before and after superfusion of ouabain. We used predetermined criteria for stability of holding currents, and the shift in the currents was induced by ouabain (22). I_p was normalized for membrane capacitance and, hence, cell size. We switched to the ouabain-containing superfusate 8–10 min after the whole-cell configuration had been established in all experiments. As the effect of ouabain is not reversible within the time frame that stable holding currents can be reliably measured (22, 23), the suspension of myocytes was removed at the conclusion of the experimental protocol, and a new aliquot of myocytes was added to the tissue bath in ouabain-free solution. As a consequence, only one myocyte was studied per bath.

Statistical Analysis—Results are expressed as the mean ± S.E. One-way analysis of variance was used for analysis of co-immunoprecipitation data, and a Student's *t* test was used for paired data, with single tail distribution for analysis of differences in DHE fluorescence intensity levels between experiments and controls. Student's *t* test for unpaired data was used for analysis of patch clamp data. $p < 0.05$ is regarded as significant in all comparisons.

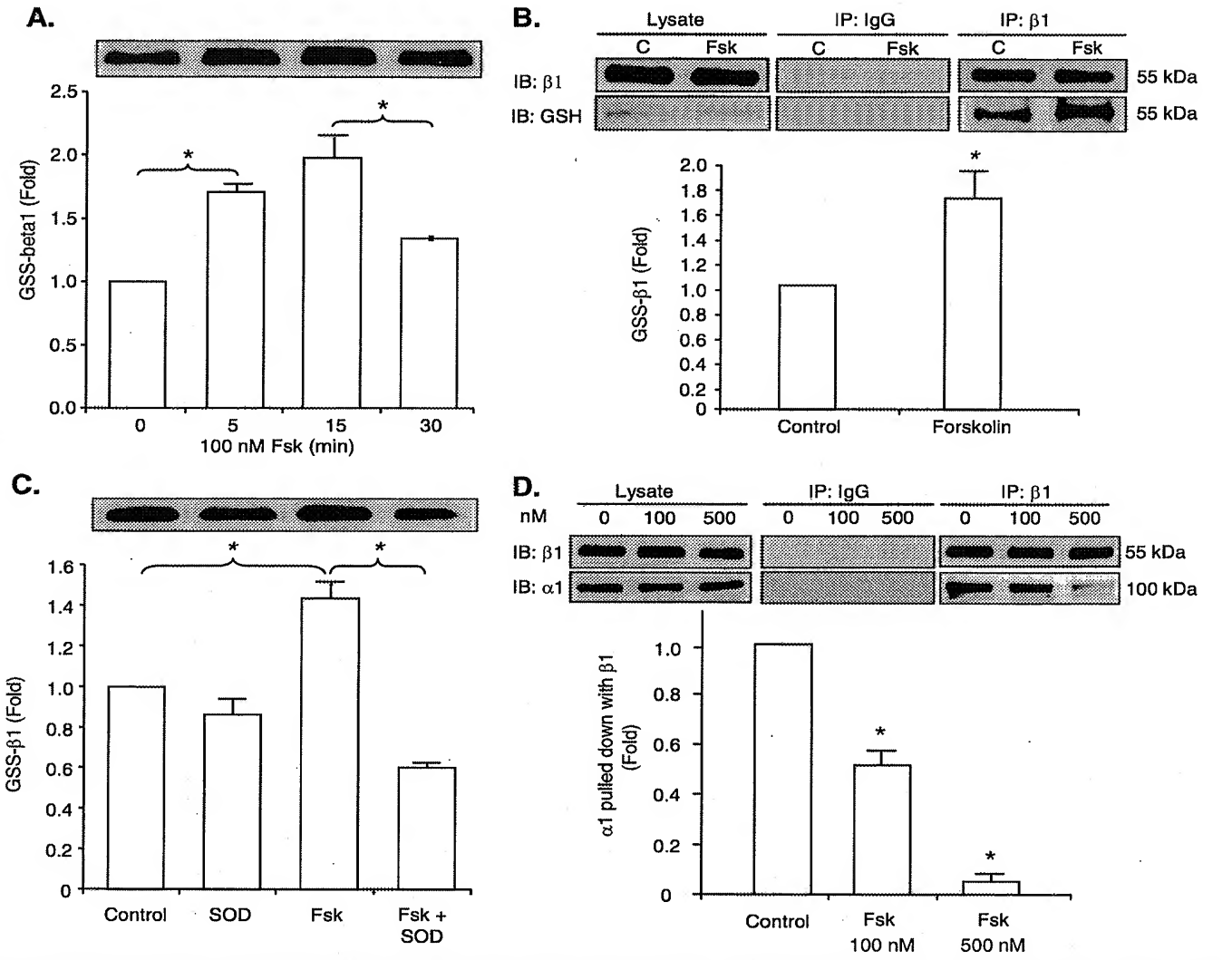

FIGURE 1. **Effect of forskolin on glutathionylation of the Na^+-K^+ pump β_1 subunit and α_1/β_1 subunit interaction.** *A*, the immunoblot shows biotinylated GSS-β_1 subunit after exposure of myocytes loaded with biotin-GSH to forskolin for 5, 15, or 30 min or vehicle control. *B*, shown is the effect of forskolin on glutathionylation of the β_1 subunit as shown by immunoblotting (*IB*) the β_1 subunit immunoprecipitate (*IP*) with GSH antibody. The immunoblot of the cell lysate and non-immune IgG control are also shown. *C*, control. *C*, shown is the effect of SOD on forskolin-induced glutathionylation as detected by the biotin-GSH technique. *D*, shown is the effect of forskolin on Na^+-K^+ pump α_1/β_1 subunit co-immunoprecipitation. Representative α_1 and β_1 subunit immunoblots after immunoprecipitation with β_1 subunit antibody are shown. The histograms show mean densitometry of blots from three-four experiments, each normalized against control (%). *IP* indicates the antibody used for immunoprecipitation. *IB* indicates the antibody used for immunoblot. The *asterisk* indicates significant difference *versus* control.

RESULTS

Forskolin Induces Glutathionylation of the β_1 Pump Subunit and Decreases Its Co-immunoprecipitation with the α_1 Subunit—To examine the effect of cAMP-dependent signaling on glutathionylation of the pump β_1 subunit (3), myocytes were loaded with biotin-tagged GSH. They were then exposed to control solution or solution containing 100 nmol/liter forskolin for 5, 15, or 30 min. The cells were lysed, and the glutathionylated protein subfraction was pulled down with streptavidin beads and immunoblotted with β_1 subunit antibody. Fig. 1*A* shows that there was an increase in glutathionylation of the β_1 subunit after 5 min of exposure to forskolin. The increase was sustained with exposure for 15 min, but there was a subsequent decrease by 30 min.[5] Fig. 1*B* shows that forskolin also increased glutathionylation of the β_1 subunit as detected by the independent GSH antibody technique (3). As shown in Fig. 1*C*, preincubation of myocytes in solutions containing pegylated SOD abolished the forskolin-induced glutathionylation.

The interaction of the pump β subunit with the catalytic α subunit is important for function, and glutathionylation of the β_1 subunit is associated with a reduction in its co-immunoprecipitation with the α_1 subunit (3). We examined the effect of forskolin on α_1/β_1 subunit co-immunoprecipitation. Myocytes

[5] Results of molecular, DHE fluorescence, and patch clamp studies used in this study are summarized and compared in Fig. 7.

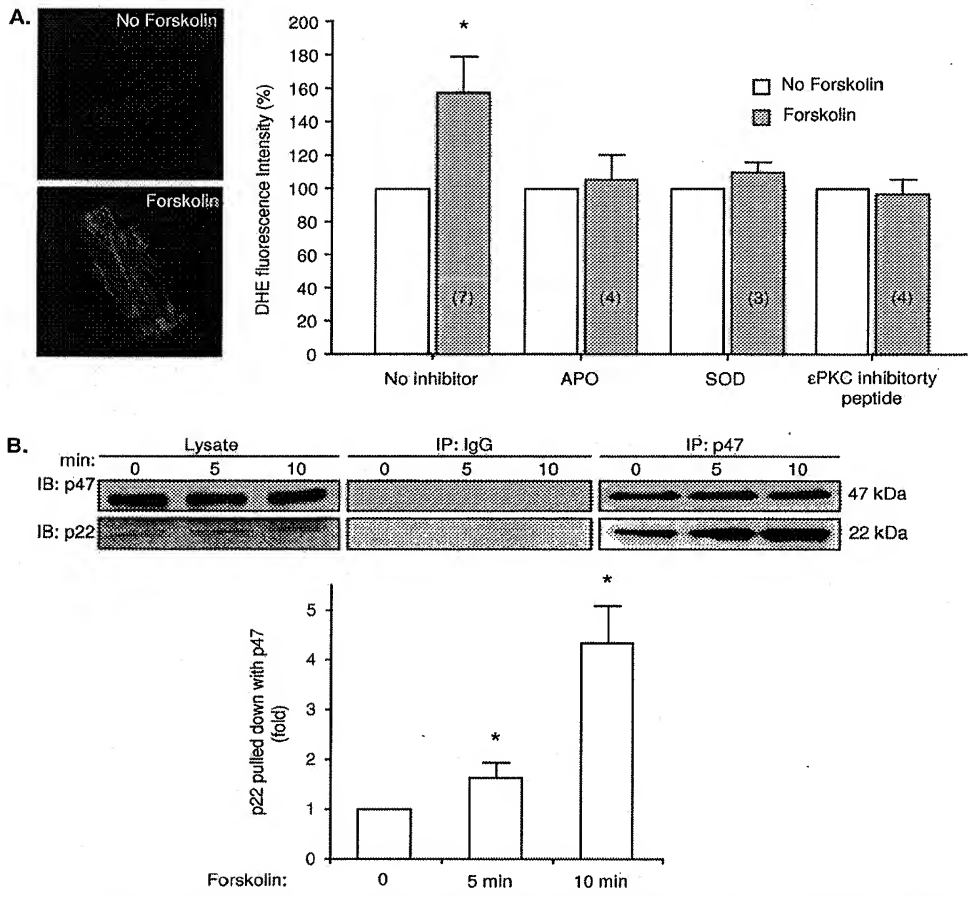

FIGURE 2. **Effect of forskolin on myocyte O_2^--sensitive DHE fluorescence and NADPH oxidase activation.** *A*, confocal fluorescent micrographs and mean DHE-fluorescence intensity of control myocytes and myocytes exposed to forskolin are shown. Forskolin increased the fluorescence intensity. This increase was abolished by pegylated-SOD, apocynin (*APO*), or myristoylated εPKC inhibitory peptide. The number of experiments is shown in *parentheses*. *B*, shown is co-immunoprecipitation of $p47^{phox}$ and $p22^{phox}$ subunits of NADPH oxidase. Representative immunoblots of $p47^{phox}$ and $p22^{phox}$ immunoprecipitated with antibody to the $p47^{phox}$ subunit after exposure of myocytes to forskolin are shown. *IP* indicates the antibody used for immunoprecipitation. *IB* indicates the antibody used for immunoblot. The histogram shows the mean densitometric measurements of immunoblots from three experiments standardized to the value of control samples. The *asterisk* represents significant difference compared with control.

were exposed to 100 or 500 nmol/liter forskolin for 15 min before lysis. The lysate was immunoprecipitated with β_1 subunit antibody and immunoblotted with α_1 subunit antibody. Fig. 1*D* shows that forskolin reduced α_1/β_1 subunit co-immunoprecipitation.

Forskolin Induces εPKC-dependent Activation of NADPH Oxidase—As the Na^+-K^+ pump subunits co-immunoprecipitate with the membrane-associated $p22^{phox}$ subunits of NADPH oxidase in cardiac myocytes (4) and SOD abolished the forskolin-induced glutathionylation, we examined if forskolin activates NADPH oxidase. Two techniques were used, O_2^--sensitive DHE fluorescence and co-immunoprecipitation of the cytosolic $p47^{phox}$ NADPH oxidase subunit with $p22^{phox}$, reflecting the translocation that is necessary for activation. We loaded myocytes with DHE and exposed them to 100 nmol/liter forskolin for 10 min or to control solutions. Representative micrographs and a summary histogram are shown in Fig. 2*A*. Forskolin increased the intensity of DHE fluorescence. Preincubation of myocytes in solutions containing 170 IU/ml pegylated SOD or 10 μmol/liter NADPH oxidase inhibitor apocynin blocked the increase in fluorescence supporting the specificity of the fluorescence signal and implicating the source of O_2^-. Phosphorylation of the $p47^{phox}$ by PKC, but not PKA, can activate NADPH oxidase (24), and we have previously found that activation of NADPH oxidase can be inhibited by an εPKC-inhibitory peptide (4). To examine if the forskolin-induced increase in DHE fluorescence might be dependent on εPKC, we incubated myocytes with 10 μmol/liter membrane-permeable, myristoylated εPKC inhibitory peptide. It abolished the forskolin-induced increase in fluorescence. To examine if forskolin increases co-immunoprecipitation of the $p47^{phox}$ NADPH oxidase subunit with the $p22^{phox}$ subunit, we exposed myocytes to 100 nmol/liter forskolin or to control solutions for 15 min. Cell lysate was immunoprecipitated with antibody to the $p47^{phox}$ subunit, and the precipitate was immunoblotted with antibody to $p22^{phox}$. Fig. 2*B* shows that forskolin increased the co-immunoprecipitation.

Forskolin Inhibits I_p in Cardiac Myocytes—The forskolin-induced increase in glutathionylation of the β_1 subunit of the Na^+-K^+ pump in cardiac myocytes shown in Fig. 1 is expected to cause pump inhibition (3) and is, therefore, difficult to reconcile with the pump stimulation widely reported to be mediated by cAMP-dependent pathways. We examined the effect of forskolin on I_p measured in myocytes with the whole-cell patch clamp technique. With this technique, the intracellular compartment is perfused with patch pipette solutions, and the concentration of some low molecular weight substances is expected to be altered. L-Arginine is of particular interest as either a decrease or an increase in its concentration may promote oxidation; a reduction in L-arginine levels may uncouple nitric-oxide synthase to preferentially synthesize superoxide rather than NO. Conversely, NO synthesized from supplemental L-arginine may combine with superoxide to form the highly oxidant species peroxynitrite. To minimize risk of an experimental artifact resulting from alterations in intracellular L-arginine concentrations, initial experiments were performed with and without L-arginine included in patch pipette solutions. In a first series of experiments we included 10 μmol/liter L-arginine in pipette solutions, a con-

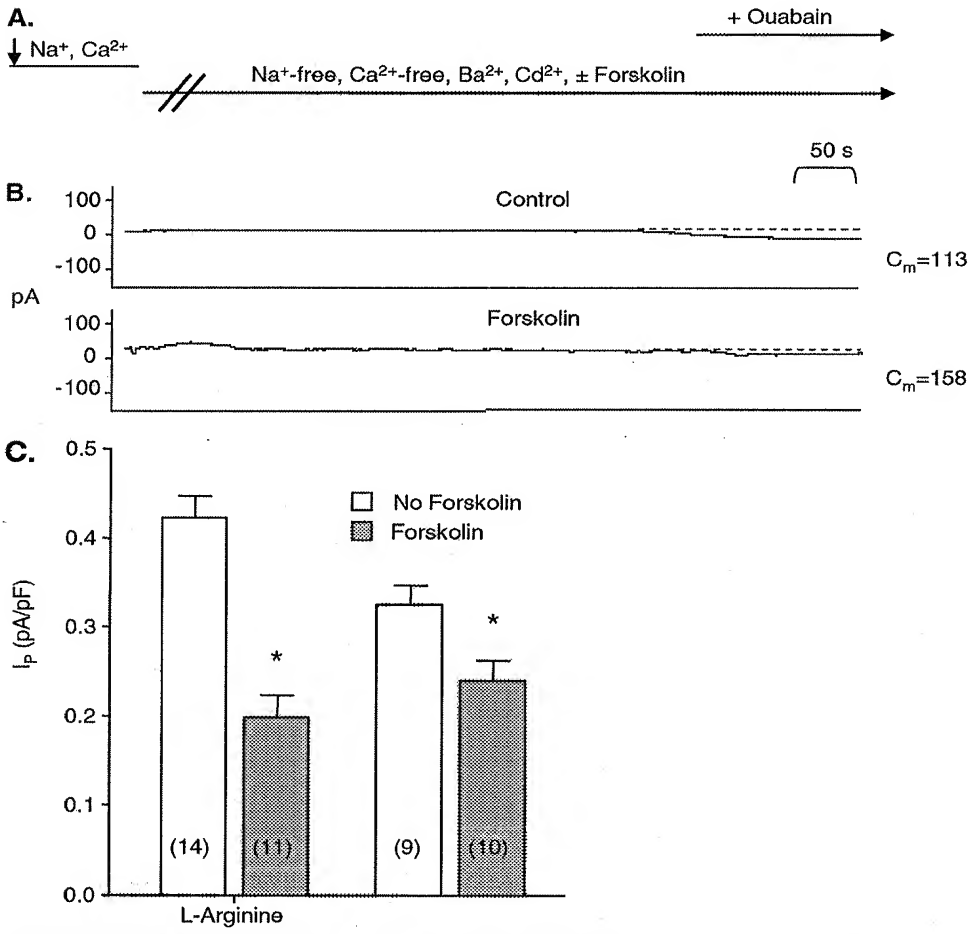

FIGURE 3. **Effect of forskolin on Na^+-K^+ pump current in myocytes.** *Panel A* shows the timing of changes in the composition of superfusates. The *arrow on the left side of the panel* indicates establishment of the whole-cell configuration and, hence, perfusion of the intracellular compartment with pipette solution. The switch from a Ca^{2+}-containing, forskolin-free solution in the tissue bath to a nominally Ca^{2+}-free solution containing Ba^{2+}, Cd^{2+}, and forskolin and the switch to a solution also containing ouabain (the *arrow on the right side of the panel*) are shown. *Panel B* shows examples of holding currents. Large changes in the currents that occur the first 1–2 min after the switch to Na^+- and Ca^{2+}-free Ba^{2+}- and Cd^{2+}-containing superfusate before currents stabilize are not shown. Stable holding currents before exposure of myocytes to ouabain are important for the measurement of I_p. Stability of the currents as well as the ouabain-induced shift in them was identified from the read-out of an electronic cursor. C_m indicates membrane capacitance in picofarads (*pF*). *Panel C* shows the mean I_p normalized for membrane capacitance. The pipette solution contained L-arginine where indicated. The numbers of myocytes in each group are indicated in *parentheses*. The *asterisk* indicates a significant difference between the means of I_p.

centration ~10-fold above the K_D for relevant nitric-oxide synthase isoforms (19). The myocytes were superfused with forskolin-free "standard" Na^+- and Ca^{2+}-containing Tyrode solution, whereas the whole-cell configuration was established. We then switched to a nominally Na^+-free superfusate to rule out influx of Na^+ that might cause secondary pump stimulation. This superfusate was also nominally Ca^{2+}-free. It contained forskolin or was forskolin-free in control experiments. Fig. 3*A* shows the timing of changes in the composition of superfusates. Fig. 3*B* shows currents of a control myocyte and a myocyte exposed to forskolin. I_p was smaller for the myocyte exposed to forskolin than for the control myocyte. Fig. 3*C* shows that forskolin induced a statistically significant decrease in mean I_p. An independent set of experiments was performed using an identical protocol with the exception that pipette solutions did not contain L-arginine. Results are included in Fig. 3*C*. In agreement with our previous study (19), I_p in control experiments was smaller than in experiments performed using patch pipettes containing L-arginine. However, forskolin again significantly reduced I_p. Holding currents after Na^+-K^+ pump blockade with ouabain in both sets of experiments were very small and similar for control myocytes and myocytes exposed to forskolin, consistent with use of the calculated equilibrium potential for chloride as the test potential. Although qualitatively similar, the forskolin-induced decrease in I_p appeared larger when L-arginine was included in pipette solutions. To avoid a bias in favor of Na^+-K^+ pump inhibition that we expected from the β_1 subunit glutathionylation and to facilitate comparisons with previous studies, we used patch pipette solutions without added L-arginine in all subsequent experiments.

Effect of H-89 and ϵPKC Inhibitory Peptide on the Forskolin-induced Na^+-K^+ Pump Inhibition—We next included 500 nmol/liter H-89, an inhibitor of PKA, in patch pipette solutions and exposed myocytes to superfusate with or without forskolin. Fig. 4 shows that H-89 abolished the decrease in I_p. Because cross-talk between the ϵPKC and PKA has been reported (25), we included 100 nmol/liter ϵPKC inhibitory peptide in patch pipette solutions (26). It abolished the forskolin-induced decrease in I_p. PKA-dependent activation of PKC is mediated by phospholipase C (PLC) in non-cardiac tissues (25, 27, 28). We, therefore, included the PLC inhibitor U-73,122 in pipette solutions in a concentration of 1 μmol/liter. This abolished the forskolin-induced decrease in I_p as shown in Fig. 4.

Functional studies in myocytes internally perfused with patch pipette solution supported a role for ϵPKC in forskolin-induced pump inhibition. We examined if forskolin increases co-immunoprecipitation of ϵPKC with ϵRACK in intact myocytes. Ang II, a known activator of ϵPKC in cardiac myocytes (4), was used as a positive control. Myocytes were exposed to 100 nmol/liter forskolin, 100 nmol/liter Ang II, or vehicle control solutions for 15 min. The lysate was immunoprecipitated with antibodies to ϵPKC, and the precipitate was immunoblotted with antibodies to ϵRACK. Fig. 5 shows that both Ang II

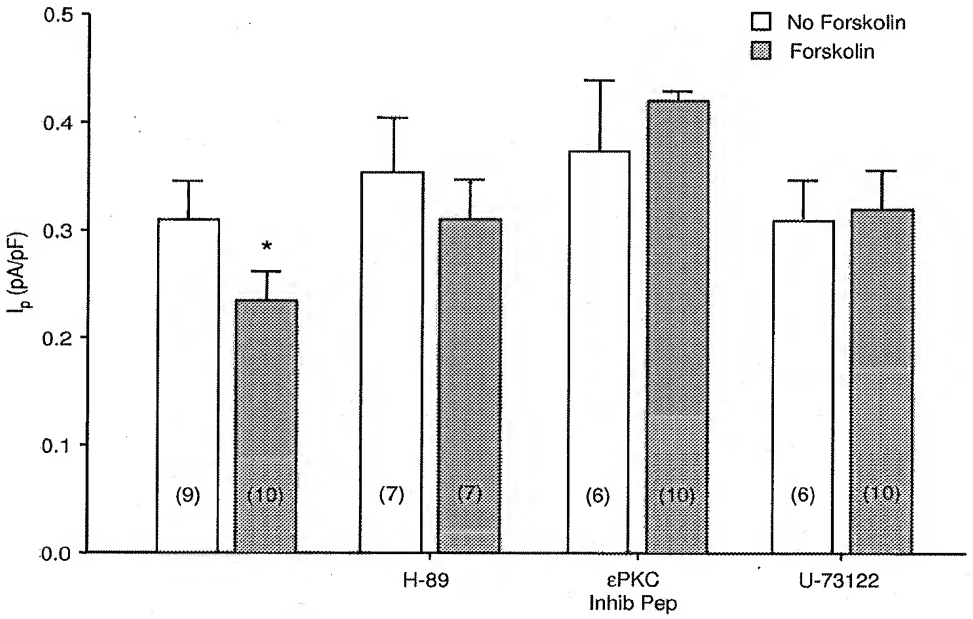

FIGURE 4. **Effects of inhibitors of PKA, εPKC and PLC on forskolin-induced Na^+-K^+ pump inhibition.** Myocytes were perfused with pipette solutions containing H89, εPKC inhibitory peptide, or U-73122 as indicated. The data from myocytes not exposed to inhibitors, previously presented in Fig. 1, is included for reference. The numbers of myocytes in each group are indicated in *parentheses*. The *asterisk* indicates a significant difference compared with control. *pF*, picofarads.

and forskolin induced an increase in co-immunoprecipitation of εPKC with εRACK. Preincubation of myocytes with 500 nmol/liter H-89 prevented the forskolin-, but not the Ang II-induced increase in co-immunoprecipitation. These results suggest activation of εPKC is sensitive to H-89, consistent with the functional effects of both H-89 and the εPKC inhibitory peptide to abolish the forskolin-induced decrease in I_p shown in Fig. 4.

Oxidative Signaling Mediates the Forskolin-induced Decrease in I_p—We next examined the role of NADPH oxidase and oxidant signaling in the forskolin-induced decrease in I_p. To examine the role of $O_2^{\cdot-}$, we included 200 IU/ml SOD in patch pipette solutions and measured I_p after exposing the patch-clamped myocytes to superfusates containing forskolin or to control superfusates. Fig. 6 shows that SOD abolished the forskolin-induced decrease in I_p. In another series of experiments we inhibited NADPH oxidase. We exposed myocytes to 10 μmol/liter apocynin, included in the superfusate because it is readily membrane-permeable, or we used the gp91ds peptide to inhibit docking of $p47^{phox}$ and, hence, activation of NADPH oxidase. The gp91ds peptide is usually considered a low efficacy inhibitor when combined with the *tat* peptide that is used to facilitate transmembrane entry into intact cells (29). However, the whole cell patch clamp technique allowed us to directly perfuse the intracellular compartment with a *tat*-free compound. We included it in patch pipette solutions in a concentration of 10 μmol/liter, a concentration expected to prevent activation of NADPH oxidase (4). As shown in Fig. 6, forskolin-induced pump inhibition was abolished by apocynin or gp91ds peptide.

DISCUSSION

Na^+-K^+ pump inhibition mediated by cAMP-dependent pathways in cardiac myocytes was reported in early studies (8, 9), but many more recent studies have reported that these pathways mediate pump stimulation either by increasing maximal pump rate or by increasing pump affinity for intracellular Na^+ (7, 11–16, 30). In our study, forskolin induced glutathionylation of the Na^+-K^+ pump β_1 subunit. Because glutathionylation of the subunit is causally related to Na^+-K^+ pump inhibition (3), this is concordant with the forskolin-induced pump inhibition we demonstrated in functional studies.

We used the whole-cell patch clamp technique to examine functional effects of cAMP-dependent pathways on the Na^+-K^+ pump, as have most previous studies. If wide-tipped patch pipettes are used, the technique will in principle allow control of membrane voltage and the concentration of Na^+-K^+ pump ligands on both sides of the membrane in a largely intact cell. However, sources of error from transmembrane Na^+ influx (31) or unstable base-line membrane currents can easily contaminate measurement of the small pump currents. Even when wide-tipped patch pipettes are used, agonist-induced Na^+ influx and secondary pump stimulation can cause a large increase in the I_p that is measured (32). We used wide-tipped patch pipettes to optimize control of the intracellular milieu, and we used Na^+-free superfusates to eliminate errors from transmembrane Na^+ influx. Activation of the cAMP-dependent Cl^- current might change the intracellular Cl^- concentration and, hence, the electrochemical driving force for the $Na^+/K^+/2Cl^-$ co-transporter. Activation of the co-transporter in turn can alter the ouabain-sensitive current that defines I_p (32). We used the calculated equilibrium potential for Cl^- as the test potential to eliminate a net change in cAMP-dependent Cl^- channel fluxes. As indicated by the similar holding currents after superfusion of ouabain in experiments performed with and without forskolin, this objective was achieved.

Experimental activation of cAMP-dependent pathways in previous studies on the cardiac myocyte Na^+-K^+ pump has been achieved by exposing myocytes to a β adrenergic receptor agonist or by directly activating adenyl cyclase with exposure to forskolin. Receptor activation is the most physiologically relevant of the two approaches. However, available agonists have poor selectivity against the three different β adrenergic receptor subtypes (33), and the compounds used in some previous studies may have activated the β_3 adrenergic receptor that is coupled to activation of nitric-oxide synthase. We have found

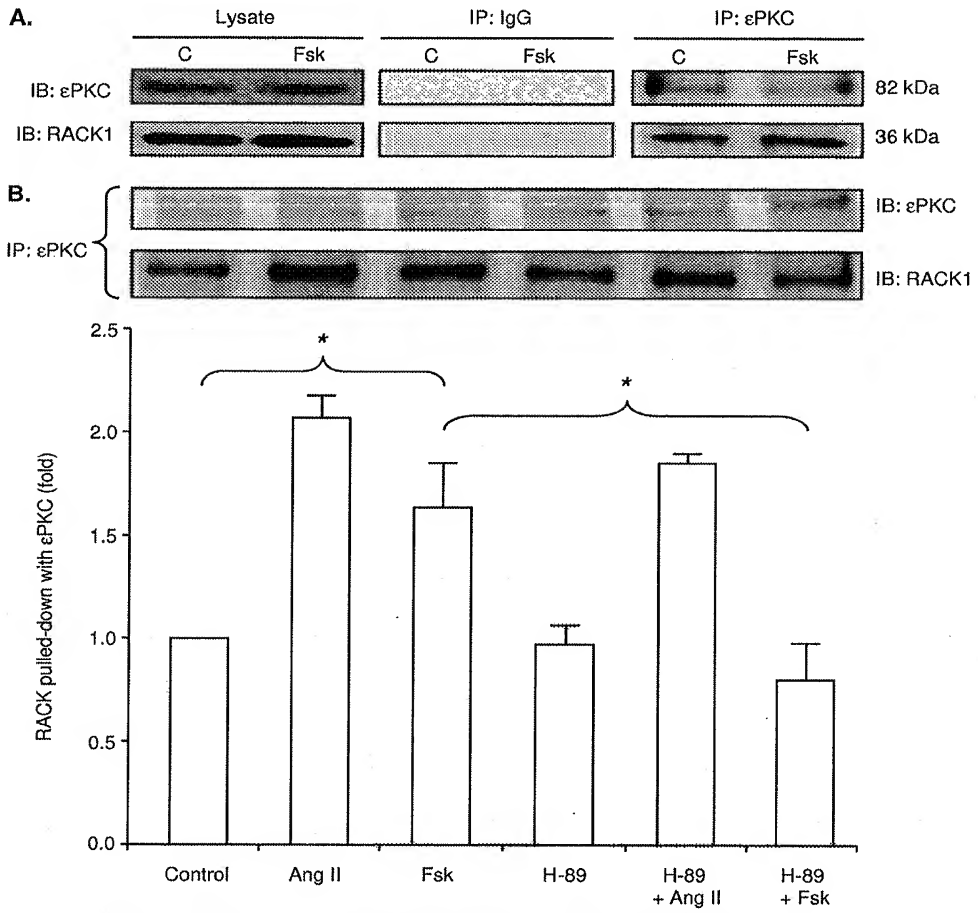

FIGURE 5. **Effect of forskolin on co-immunoprecipitation of εPKC with RACK.** Myocytes exposed to Ang II (positive control), forskolin, or vehicle control were lysed before co-immunoprecipitation. εPKC immunoprecipitate (*IP*) was immunoblotted (*IB*) for εPKC or RACK. The histogram shows the mean densitometric measurements of immunoblots from three experiments standardized to the value of control samples. Ang II induced an increase in εPKC/RACK co-immunoprecipitation that was insensitive to H-89. Forskolin also induced an increase in εPKC/RACK co-immunoprecipitation, but this was abolished by H-89. The *asterisk* indicates significant differences compared with control. *C*, control.

the β_3 adrenergic receptor mediates stimulation of the Na^+-K^+ pump in cardiac myocytes (5).[5] We, therefore, used forskolin, as have most of the recent studies (7, 11, 12, 15, 16).

Data from functional Na^+-K^+ pump studies, studies on myocyte DHE fluorescence, and molecular studies implicated the pathway summarized at the top of Fig. 7. Although effects of cAMP-dependent pathways are classically attributed to PKA-mediated phosphorylation of effector proteins, the exchange protein directly activated by cAMP (Epac) has also become recognized as important. PKA and Epac can act independently of each other, in synergy or antagonistically (34). The effect of H-89 to block the forskolin-induced decrease in I_p and increase in co-immunoprecipitation of εPKC with RACK suggests a requirement for PKA activation but does not necessarily rule out a synergistic role of Epac.

PLC β- and ε-isoforms can be activated downstream from PKA (25) or Epac (35), and the effect of U-73,122 to abolish the forskolin-induced decrease in I_p is consistent with a role for PLC activation in our study. An increase in diacylglycerol levels in turn may activate PKC. These results are also consistent with studies in the kidney showing PKA/PKC cross-talk-dependent Na^+-K^+ pump inhibition attributed to PLC activation (27).

The forskolin-induced increase in εPKC/RACK co-immunoprecipitation implicates PKC. The effect of the εPKC inhibitor peptide to abolish both an increase in DHE fluorescence and a decrease in I_p supports the functional role of PKC activation. PKC-dependent phosphorylation of the cytosolic NADPH oxidase subunit $p47^{phox}$ induces its translocation to the membranous $p22^{phox}$ subunit that is required for activation of NADPH oxidase (24). Consistent with NADPH oxidase activation, forskolin induced an increase in co-immunoprecipitation of $p47^{phox}$ with $p22^{phox}$, and apocynin abolished the forskolin-induced increase in DHE fluorescence. The effect of the gp91ds peptide used to block docking of $p47^{phox}$ is also consistent with a downstream NADPH oxidase dependence of Na^+-K^+ pump inhibition. Because proximity to a source of oxidants is important for the specific oxidative modification of target proteins (36), the co-localization of the NADPH oxidase complex with the Na^+-K^+ pump we have reported previously (4) should facilitate glutathionylation of the pump β_1 subunit and the functional equivalent of inhibition.

Perfusion of the intracellular compartment using patch pipettes with particularly wide tips in our study might have altered signaling pathways. However, the concordance of results in voltage-clamped, internally perfused myocytes and intact myocytes studied with fluorescence and molecular techniques, summarized in Fig. 7, suggest that signaling domains are not readily susceptible to changes induced by myocyte perfusion. This may reflect compartmentalization of signaling and perhaps anchoring of key signaling molecules. Taken together, the results suggest the signaling pathway shown in Fig. 7 is plausible, and the consistency of results obtained with different techniques supports the overall validity of the study.

The time dependence of the forskolin-induced increase in glutathionylation shown in Fig. 1*A* suggests that effects are not sustained long term. This may reflect a cellular homeostatic response to activation of cAMP-dependent signaling that terminates a phosphorylation-dependent part of the signal as discussed previously (37). For the variable we measure here, mechanisms that inactivate the downstream oxidative signaling pathway or directly activate deglutathionylation may have addi-

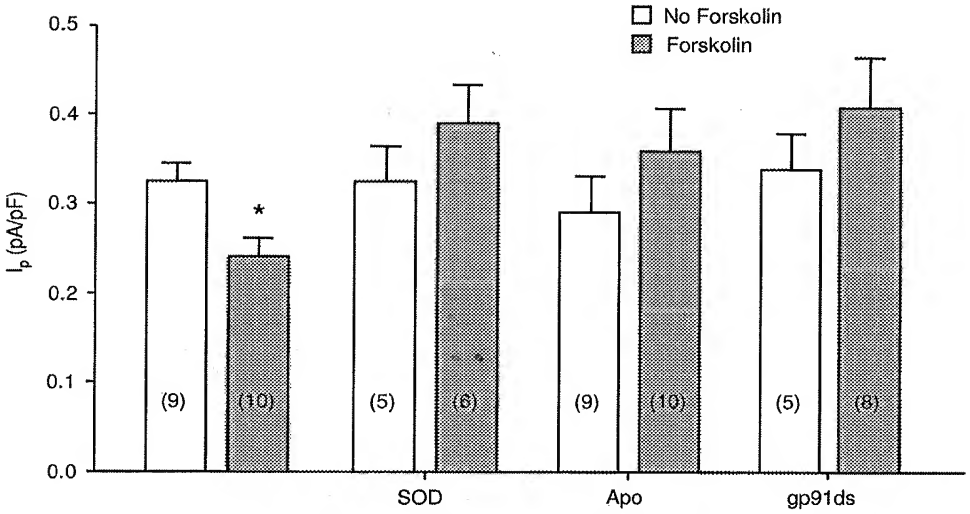

FIGURE 6. **Role of superoxide and NADPH oxidase in forskolin-induced Na^+-K^+ pump inhibition.** Myocytes were perfused with pipette solutions containing SOD, apocynin (*Apo*), or the gp91ds peptide as indicated. The data from myocytes not exposed to inhibitors, previously presented in Fig. 1, is included for reference. Numbers of myocytes in each group are indicated in *parentheses*. The *asterisk* indicates a significant difference compared with control. *pF*, picofarads.

⊕ PKA → ⊕ PLC → ⊕ εPKC → ⊕ NADPH Oxidase → ⊖ Na-K pump

Molecular	H-89 ⊗↑co-IP of PKC/RACK		↑ PKC/RACK co-IP	↑ $p47^{phox}$/$p22^{phox}$ co-IP	↑ GSS-β_1 ↓ α_1/β_1 co-IP
Fluorescence			PKC inhib pep ⊗ ↑ DHE fluorescence	Apocynin and SOD ⊗ ↑ DHE fluorescence	
Functional	H-89 ⊗↓ Ip	U73122 ⊗↓ Ip	PKC inhib pep ⊗↓ Ip	Apocynin and gp91ds ⊗ ↓ Ip	↓ Ip

FIGURE 7. **Summary of molecular, fluorescence, and patch clamp studies on effects of forskolin.** Steps in the signaling pathway that are implicated are shown at the top with stimulation and inhibition indicated by + and −. Blocks of responses to forskolin are indicated below by ×. Glutathionylation of the β_1 subunit is indicated by GSS-β_1, and Na^+-K^+ pump current is indicated by I_p. *co-IP*, co-immunoprecipitation.

tional effects on the time course. However, our *in vitro* study cannot accurately reflect the complex structural, mechanical, and neurohormonal *in vivo* milieu of the beating heart, and it will be important to determine the effects of cAMP-dependent signaling on Na^+-K^+ pump function and β_1 subunit glutathionylation *in vivo* in future studies.

The effect of cAMP-dependent signaling on Na^+-K^+ pump function has important implications for our understanding of excitation-contraction coupling in the heart under physiological and pathophysiological conditions. In the normal heart, pump inhibition with an increase in adrenergic drive is expected to increase intracellular Na^+ and, hence, Ca^{2+} levels and act in synergy with the well recognized positive inotropic effect of cAMP on Ca^{2+} entry and intracellular Ca^{2+} handling. However, although a modest increase in intracellular Na^+ levels enhances contractility, the high levels typically seen in heart failure can have the opposite effect and are believed to contribute adversely to its phenotype (38, 39). It is of particular importance for the present study that adverse effects of NADPH oxidase-dependent redox signaling may also contribute (40). Efficacy of treatments that target dysregulation of adrenergic signaling in heart failure trials are consistent with an *in vivo* relevance of our results. Blockade of adenyl cyclase-coupled receptors by "β-blockers" may exert some of its benefit (41) by reducing oxidative stress, reversing Na^+-K^+ pump inhibition, and hence, reducing cellular Na^+ overload. This contrasts with the long term detrimental effect of activation of cAMP-dependent signaling by a β_1 adrenergic receptor agonist (42) or a phosphodiesterase III inhibitor (43) documented in clinical trials. The common role of PKC-dependent NADPH oxidase activation in both Ang II- and cAMP-induced Na^+-K^+ pump inhibition may contribute to the well established therapeutic synergy between angiotensin-converting enzyme inhibitors and β-blockers in heart failure (41). Their combined use is expected to inhibit the shared oxidative signaling pathway more effectively than either group of drugs used alone.

Acknowledgments—We acknowledge the facilities as well scientific and technical assistance from the staff at the NANO Major National Research Facility at the Electron Microscopy Unit, the University of Sydney. In particular, the assistance from Ellie Kable, and Professor Filip Braet was greatly appreciated. We also greatly appreciate advice from Dr. Ron Clarke about implications of Na^+-K^+ pump kinetics.

REFERENCES

1. Blanco, G., and Mercer, R. W. (1998) *Am. J. Physiol.* **275**, F633–F650
2. Geering, K. (2008) *Curr. Opin. Nephrol. Hypertens.* **17**, 526–532
3. Figtree, G. A., Liu, C. C., Bibert, S., Hamilton, E. J., Garcia, A., White, C. N., Chia, K. K., Cornelius, F., Geering, K., and Rasmussen, H. H. (2009) *Circ. Res.* **105**, 185–193
4. White, C. N., Figtree, G. A., Liu, C. C., Garcia, A., Hamilton, E. J., Chia, K. K., and Rasmussen, H. H. (2009) *Am. J. Physiol. Cell Physiol* **296**, C693–C700
5. Garcia, A., Bundgaard, H., Hamilton, E., Liu, C., Chia, K. K., Figtree, G. A., and Rasmussen, H. H. (2008) *12th International ATPase Conference, Aarhus, Denmark, August 5–10, 2008*, abstract 157
6. Therien, A. G., and Blostein, R. (2000) *Am. J. Physiol. Cell Physiol* **279**, C541–C566
7. Kockskämper, J., Sendhoff, K., Erlenkamp, S., Bordusa, F., Cerovsky, V., and Glitsch, H. G. (2001) *Pflugers Arch* **441**, 807–815
8. Gao, J., Mathias, R. T., Cohen, I. S., and Baldo, G. J. (1992) *J. Physiol.* **449**, 689–704
9. Gao, J., Cohen, I. S., Mathias, R. T., and Baldo, G. J. (1998) *Pflugers Arch.* **435**, 479–484
10. Despa, S., Bossuyt, J., Han, F., Ginsburg, K. S., Jia, L. G., Kutchai, H., Tucker, A. L., and Bers, D. M. (2005) *Circ. Res.* **97**, 252–259
11. Erlenkamp, S., Glitsch, H. G., and Kockskämper, J. (2002) *Pflugers Arch.* **444**, 251–262

12. Silverman, B. Z., Fuller, W., Eaton, P., Deng, J., Moorman, J. R., Cheung, J. Y., James, A. F., and Shattock, M. J. (2005) *Cardiovasc. Res.* **65,** 93–103
13. Despa, S., Tucker, A. L., and Bers, D. M. (2008) *Circulation* **117,** 1849–1855
14. Bossuyt, J., Despa, S., Han, F., Hou, Z., Robia, S. L., Lingrel, J. B., and Bers, D. M. (2009) *J. Biol. Chem.* **284,** 26749–26757
15. Fuller, W., Howie, J., McLatchie, L. M., Weber, R. J., Hastie, C. J., Burness, K., Pavlovic, D., and Shattock, M. J. (2009) *Am. J. Physiol. Cell Physiol* **296,** C1346–C1355
16. Kockskamper, J., Erlenkamp, S., and Glitsch, H. G. (2000) *J. Physiol.* **523,** 561–574
17. Hool, L. C., Whalley, D. W., Doohan, M. M., and Rasmussen, H. H. (1995) *Am. J. Physiol.* **268,** C366–C375
18. Adachi, T., Weisbrod, R. M., Pimentel, D. R., Ying, J., Sharov, V. S., Schöneich, C., and Cohen, R. A. (2004) *Nat Med* **10,** 1200–1207
19. White, C. N., Hamilton, E. J., Garcia, A., Wang, D., Chia, K. K., Figtree, G. A., and Rasmussen, H. H. (2008) *Am. J. Physiol. Cell Physiol.* **294,** C572–C578
20. Kim, Y. M., Guzik, T. J., Zhang, Y. H., Zhang, M. H., Kattach, H., Ratnatunga, C., Pillai, R., Channon, K. M., and Casadei, B. (2005) *Circ. Res.* **97,** 629–636
21. Hansen, P. S., Buhagiar, K. A., Gray, D. F., and Rasmussen, H. H. (2000) *Am. J. Physiol. Cell Physiol.* **278,** C546–C553
22. William, M., Vien, J., Hamilton, E., Garcia, A., Bundgaard, H., Clarke, R. J., and Rasmussen, H. H. (2005) *J. Physiol.* **565,** 815–825
23. Despa, S., and Bers, D. M. (2007) *Am. J. Physiol. Cell Physiol.* **293,** C321–C327
24. Park, J. W., Hoyal, C. R., Benna, J. E., and Babior, B. M. (1997) *J. Biol. Chem.* **272,** 11035–11043
25. Yao, L., Fan, P., Jiang, Z., Gordon, A., Mochly-Rosen, D., and Diamond, I. (2008) *Mol. Pharmacol.* **73,** 1105–1112
26. Buhagiar, K. A., Hansen, P. S., Bewick, N. L., and Rasmussen, H. H. (2001) *Am. J. Physiol. Cell Physiol.* **281,** C1059–C1063
27. Gomes, P., and Soares-da-Silva, P. (2002) *Am. J. Physiol. Renal Physiol.* **282,** F1084–F1096
28. Gomes, P., and Soares-da-Silva, P. (2004) *Eur. J. Pharmacol.* **488,** 51–59
29. Bedard, K., and Krause, K. H. (2007) *Physiol. Rev.* **87,** 245–313
30. Bibert, S., Roy, S., Schaer, D., Horisberger, J. D., and Geering, K. (2008) *J. Biol. Chem.* **283,** 476–486
31. Nakao, M., and Gadsby, D. C. (1989) *J. Gen. Physiol.* **94,** 539–565
32. Mihailidou, A. S., Buhagiar, K. A., and Rasmussen, H. H. (1998) *Am. J. Physiol.* **274,** C175–C181
33. Hoffmann, C., Leitz, M. R., Oberdorf-Maass, S., Lohse, M. J., and Klotz, K. N. (2004) *Naunyn Schmiedebergs Arch. Pharmacol.* **369,** 151–159
34. Cheng, X., Ji, Z., Tsalkova, T., and Mei, F. (2008) *Acta Biochim. Biophys. Sin.* **40,** 651–662
35. Oestreich, E. A., Wang, H., Malik, S., Kaproth-Joslin, K. A., Blaxall, B. C., Kelley, G. G., Dirksen, R. T., and Smrcka, A. V. (2007) *J. Biol. Chem.* **282,** 5488–5495
36. Winterbourn, C. C. (2008) *Nat. Chem. Biol.* **4,** 278–286
37. Feschenko, M. S., Stevenson, E., and Sweadner, K. J. (2000) *J. Biol. Chem.* **275,** 34693–34700
38. Pieske, B., and Houser, S. R. (2003) *Cardiovasc. Res.* **57,** 874–886
39. Pieske, B., Houser, S. R., Hasenfuss, G., and Bers, D. M. (2003) *Cardiovasc. Res.* **57,** 871–872
40. Murdoch, C. E., Grieve, D. J., Cave, A. C., Looi, Y. H., and Shah, A. M. (2006) *Curr. Opin. Pharmacol.* **6,** 148–153
41. Klein, L., O'Connor, C. M., Gattis, W. A., Zampino, M., de Luca, L., Vitarelli, A., Fedele, F., and Gheorghiade, M. (2003) *Am. J. Cardiol.* **91,** 18F–40F
42. The Zamoterol in Severe Heart Failure Group (1990) *Lancet* **336,** 1–6
43. Packer, M., Carver, J. R., Rodeheffer, R. J., Ivanhoe, R. J., DiBianco, R., Zeldis, S. M., Hendrix, G. H., Bommer, W. J., Elkayam, U., and Kukin, M. L. (1991) *N. Engl. J. Med.* **325,** 1468–1475

A Selective Human β_3 Adrenergic Receptor Agonist Increases Metabolic Rate in Rhesus Monkeys

Michael H. Fisher,* Angela M. Amend,§ Thomas J. Bach,‡ Jeanne M. Barker,** Edward J. Brady,‡ Mari R. Candelore,§ Dayna Carroll,‡ Margaret A. Cascieri,§ Shuet-Hing Lee Chiu,‖ Liping Deng,§ Michael J. Forrest,‡ Bonnie Hegarty-Friscino,¶ Xiao-Ming Guan,§ Gary J. Hom,‡ Jennifer E. Hutchins,* Linda J. Kelly,§ Robert J. Mathvink,* Joseph M. Metzger,‡ Randall R. Miller,‖ Hyun O. Ok,* Emma R. Parmee,* Richard Saperstein,‡ Catherine D. Strader,§ Ralph A. Stearns,‖ G. Marie Thompson,§ Laurie Tota,§ Pasquale P. Vicario,§ Ann E. Weber,* John W. Woods,** Matthew J. Wyvratt,* Peter T. Zafian,‡ and D. Euan MacIntyre‡

*Department of Medicinal Chemistry, ‡Department of Pharmacology, §Department of Molecular Pharmacology and Biochemistry, ‖Department of Drug Metabolism, ¶Department of Laboratory Animal Resources, and **Department of Inflammation Research, Merck Research Laboratories, Rahway, New Jersey 07065

Abstract

Activation of β_3 adrenergic receptors on the surface of adipocytes leads to increases in intracellular cAMP and stimulation of lipolysis. In brown adipose tissue, this serves to up-regulate and activate the mitochondrial uncoupling protein 1, which mediates a proton conductance pathway that uncouples oxidative phosphorylation, leading to a net increase in energy expenditure. While chronic treatment with β_3 agonists in nonprimate species leads to uncoupling protein 1 up-regulation and weight loss, the relevance of this mechanism to energy metabolism in primates, which have much lower levels of brown adipose tissue, has been questioned. With the discovery of L-755,507, a potent and selective partial agonist for both human and rhesus β_3 receptors, we now demonstrate that acute exposure of rhesus monkeys to a β_3 agonist elicits lipolysis and metabolic rate elevation, and that chronic exposure increases uncoupling protein 1 expression in rhesus brown adipose tissue. These data suggest a role for β_3 agonists in the treatment of human obesity. (*J. Clin. Invest.* 1998. 101:2387–2393.) Key words: obesity • lipolysis • brown fat • uncoupling protein • energy metabolism

Introduction

Obesity constitutes a major risk-factor in the development of non–insulin-dependent diabetes and cardiovascular disease. This condition is difficult to control by food restriction alone because compensatory decreases in metabolic rate follow reductions in body weight imposed by reduced caloric intake (1). Thus, to offset this metabolic resistance to weight loss, an increase in energy expenditure (stimulation of metabolic rate) would be a desirable component of antiobesity therapy. A unique β adrenergic receptor subtype has been identified on the surface of rat adipocytes. Activation of this receptor, subsequently termed β_3, leads to increases in cellular cAMP and stimulation of lipolysis (2). In brown adipose tissue (BAT),[1] these serve to up-regulate and activate the mitochondrial uncoupling protein (UCP1), which mediates a proton conductance pathway that uncouples oxidative phosphorylation from fatty acid β oxidation, leading to a net increase in energy utilization (3). There is an ongoing debate as to whether UCP1 acts directly as a proton transporter, or as a fatty acid anion transporter where the free fatty acids function as cycling protonophores (3, 4). A number of rat-selective β_3 agonists have been discovered (2, 3, 5, 6) and shown to cause increases in metabolic rate, weight loss, and an improvement in glucose tolerance in dogs and rats (5–8). The observed weight loss resulted from a decrease in body lipids with no decrease in muscle mass (8). However, the relevance of this mechanism of energy metabolism in primates, which have much lower levels of BAT, has been questioned (3). Studies with these compounds in humans were inconclusive at best, and were complicated by side-effects of tremors and tachycardia, presumably via stimulation of β_2 and β_1 receptors, respectively (9, 10). The reason for these failures became clear with the identification and cloning of a human β_3 receptor (11, 12) and the demonstration of pharmacological differences between the rat and human β_3 receptors (13). Our own unpublished results show that all of the β_3 agonists tested in the clinic to date are only weak partial agonists of the human β_3 receptor, and are not selective for the β_3 receptor over the β_1 and β_2 receptors in humans. Thus our research focused on the discovery of β_3 agonists selective for the human receptor.

Several groups have utilized CGP12177, a β_1 and β_2 adrenergic receptor antagonist and a weak β_3 adrenergic receptor agonist, to demonstrate that β_3 adrenergic agonists will stimulate lipolysis in humans and some species of nonhuman primates (14, 15). As is generally observed with agonists of G protein–coupled receptors, the efficacy and potency of CGP12177 as a β_3 agonist varies dramatically with the level of expression of the β_3 receptor (16). Accordingly, we have assessed β_3 agonist activity in cell lines expressing low levels (< 100 fmol/mg) of the β_3 receptor, which mimic the pharmacology observed in human adipocyes.

Address correspondence to Michael H. Fisher, Merck Research Laboratories, RY121-108, P.O. Box 2000, Rahway, NJ 07065. Phone: 732-594-5945; FAX: 732-594-1185; E-mail: mike_fisher@merck.com Catherine D. Strader's present address is Department of Cardiovascular and Neuroscience Research, Schering Plough Research Institute, 2015 Galloping Hill Road, Kenilworth, NJ 07033.

Received for publication 12 December 1997 and accepted in revised form 1 April 1998.

J. Clin. Invest.

0021-9738/98/06/2387/07 $2.00
Volume 101, Number 11, June 1998, 2387–2393
http://www.jci.org

1. *Abbreviations used in this paper:* BAT, brown adipose tissue; RQ, respiratory quotient; UCP, uncoupling protein; WAT, white adipose tissue.

Methods

Unless otherwise noted, all chemical reagents were purchased from Sigma Chemical Co. (St. Louis, MO).

Functional assays. The human β_3 receptor was obtained from Dr. J. Grannemann (Wayne State University, Detroit, MI), and other receptors were cloned as previously described (17, 18). Human and rhesus monkey β_1, β_2, and β_3 receptors were expressed in mammalian cell lines for the primary screening assays. CHO cells, stably transfected with the cloned β-adrenergic receptors were harvested in enzyme-free dissociation media (Specialty Media, Lavallette, NJ) 3 d after plating. Cells were counted and distributed in the assay tubes, after being resuspended in ACC buffer (75 mM Tris, pH 7.4, 250 mM sucrose, 12.5 mM $MgCl_2$, 1.5 mM EDTA), containing the antioxidant sodium metabisulfite at a concentration of 0.2 mM and a phosphodiesterase inhibitor (0.6 mM IBMX). The cAMP production reaction was initiated by mixing cells with 20 μl of a 6× stock of the ligand to be tested. Tubes were shaken at 275 rpm for 45 min at room temperature, and the reaction stopped by boiling the tubes for 3 min. The cAMP produced in response to the ligand was measured in the lysate by competing against [^{125}I]-cAMP for binding to a cAMP-directed antibody using an automated RIA machine (ATTOFLO; Atto Instruments, Baltimore, MD). The cAMP level was determined by comparison to a standard curve.

Binding assays. CHO cells expressing the cloned human and rhesus β receptors were grown in selective media for 3 d and membranes prepared by hypotonic lysis in 1 mM Tris, pH 7.2. Receptor binding assays were carried out in a final volume of 250 μl containing 5–10 μg of membrane protein, the radioligand [^{125}I]-cyanopindolol at a concentration of 45 pM, and the compound of interest at various concentrations. Binding reactions were carried out for 1 h at 23°C, and terminated by filtration over GF/C filters using a 96-well cell harvester from Inotech (Lansing, MI).

Lipolysis assays. Rhesus adipose tissue was obtained by surgical biopsy of subcutaneous adipose depots and used immediately. Adipose cells were harvested from the tissue after digestion with collagenase D (Boehringer Mannheim, Indianapolis, IN) as described by Rodbell (19) or performed directly on minced tissue pieces (50–100 mg/assay). The incubation mixture was shaken gently in an incubator under 5% CO_2 atmosphere for 2 h. The infranatant was collected for glycerol determination. The glycerol content of the samples was determined by the glycerol kinase procedure, using the Sigma Chemical Co. kit 337A.

Western analysis. Antibodies were generated in rabbits after immunization with the peptide corresponding to residues 232–247 of the human UCP1. This sequence is homologous to the corresponding sequence in the rhesus protein. Tissue homogenates were electrophoresed using SDS-PAGE, and transferred to nitrocellulose before incubation with antibody. The signals were quantitated on a fluorimager (Molecular Dynamics, Sunnyvale, CA) using the substrate Attophos™ (JBL Scientific Inc., San Luis Obispo, CA). Western analysis using increasing concentrations of homogenized tissue produced a linear response. Analysis of each sample was performed on three separate gels. Data for samples on each gel were normalized to one post-treatment vehicle sample before averaging the three values for each sample. Protein concentrations were determined using the Bradford reagent. Data were analyzed using the GraphPad Prism program (San Diego, CA).

Measurement of lipolysis and heart rate in vivo. All animal procedures were reviewed and approved by the Merck Research Laboratories Institutional Animal Care and Use Committee. Male lean rhesus monkeys (4–7 kg body weight; age 3–5 yr) were fasted for 24 h and were lightly anesthetized with ketamine (10 mg/kg, i.m.; Fort Dodge Labs, Fort Dodge, IA). A 22-gauge intravenous catheter (Becton Dickinson & Co., Sandy, UT) was placed in a saphenous vein for the administration of test compounds after which the animals were administered Nembutal (25 mg/kg, i.v.; Abbott Labs, North Chicago, IL). A 20-gauge angiocatheter, connected to a TNF-R pressure transducer (Ohmeda Medical Device Systems, Madison, WI), was placed in a femoral artery for monitoring blood pressure. ECG leads were connected for the continuous measurement of heart rate. Heart rate and blood pressure were monitored for ~ 30 min until stable baseline values were obtained, at which time animals were administered a series of rising dose infusions (0.1 ml/min) of agonists (isoproterenol, L-755,507), or an equivalent volume of vehicle over a 15-min period. Infusion periods were separated by an interval of ~ 20 s. Blood samples (2 ml) were collected from the femoral artery 1 min before the initiation of infusions and 14 min into each infusion period. Serum glycerol was measured using an enzymatic colorimetric assay and serum potassium was determined using an ion specific electrode.

Measurement of metabolic rate in vivo. Male lean rhesus monkeys (4–8 kg body weight; age 3–6 yr) were fasted and prepared as described above. An endotracheal tube was inserted into the trachea and a 6-mm diameter vacuum line was attached to the outlet of the endotracheal tube in order to sample exhaled air. Exhaled air was drawn into the mixing chamber of a respiratory analyzer (Oxyscan model OXS-1RM O_2/CO_2 respiratory gas analyzer; Omnitech Electronics Inc., Columbus, OH) at a rate of 1 liter/min. Energy expenditure was calculated from the volume of O_2 consumed and the volume of CO_2 generated. L-755,507 was administered after a stabilization period of 30–40 min after anesthesia, and metabolic rate was monitored for an additional 60 min. Heart rate was recorded continuously, and blood samples were collected from the femoral artery at the times indicated for determination of serum glycerol.

Results

In vitro potency and selectivity of β_3 receptor agonist L-755,507. Benzenesulfonamide derivative L-755,507 is a partial agonist

Table I. Activity of L-755,507 at the Cloned Human and Rhesus β Adrenergic Receptors

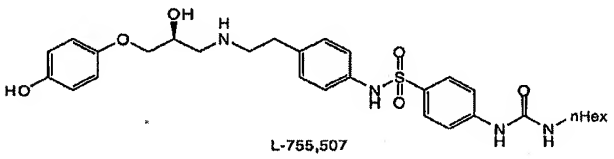

L-755,507

	β_3		β_1		β_2	
Species	EC_{50} (% act)	IC_{50}	EC_{50} (% act)	IC_{50}	EC_{50} (% act)	IC_{50}
	nM	*nM*	*nM*	*nM*	*nM*	*nM*
Human	0.43±0.31 (52±16)	13±7.2	580±300 (25±7)	200±40	> 10000 (2)	190±110
Rhesus	2.2±1.0 (68±14)	130±27	> 10000 (33±20)	2300±920	> 10000 (0)	1500±960

The receptors were expressed in CHO cells at receptor densities of 46–88 fmol/mg (*β_3 receptors*) or 300–500 fmol/mg (*β_1 and β_2 receptors*). Agonist potency (EC_{50}) and efficacy (*% act*) were assessed by measurement of intracellular cAMP levels, and the latter is expressed relative to the maximum response evoked by isoproterenol in each cell type. Binding affinities were quantified as inhibition of [^{125}I]-cyanopindolol binding in each cell type. Data are mean±SD of ≥ 3 determinations, and are expressed as nanomolar values. The sequence for the rhesus β_3 adrenergic receptor that we have cloned and utilized is identical to that recently deposited in GenBank (U63591 and U63592). The homology between the human and rhesus β_3 receptors is 99% within the transmembrane spanning regions, and between the human and rhesus β_1 and β_2 receptors the homology is 100% within this same region.

for the human β_3 receptor, with maximal activation 52% of that evoked by isoproterenol. L-755,507 activates the human β_3 receptor with an EC_{50} of 0.43 nM and inhibits ligand binding to β_1 and β_2 receptors with IC_{50}'s of 200 and 190 nM (Table I). It has weak agonist activity at the human β_1 receptor, but is > 1,000-fold selective for activation of the β_3 receptor versus activation of the β_1 receptor. L-755,507 has no measurable β_2 agonist activity. In contrast, CGP12177 activates the β_3 receptor in these cells with an EC_{50} of 5,300 nM and inhibits binding to β_1 and β_2 receptors with IC_{50}'s of 2.6 and 2.9 nM. Thus, under these conditions of receptor expression, L-755,507 is > 10,000-fold more potent than CGP12177 as a β_3 agonist. Moreover, L-755,507 is > 400-fold selective for the β_3 receptor (as reported by activation of the β_3 receptor versus activation of or binding to β_1 and β_2 receptors), while CGP12177 is a potent β_1 and β_2 receptor antagonist.

L-755,507 is also a potent and selective β_3 partial agonist in rhesus monkeys as assessed by its affinity for the cloned β adrenergic receptors from this species (Table I). It activates the rhesus monkey β_3 receptor with an EC_{50} of 2.2 nM with maximal activation 68% of the maximal activation of isoproterenol. It has weak activity at the rhesus monkey β_1 receptor with 33% of the maximal activity of isoproterenol at the highest concentration tested (10 μM), and it has no measurable activity at the rhesus monkey β_2 receptor. Thus, although the compound is fivefold less potent at the rhesus monkey β_3 receptor than at the human β_3 receptor, its selectivity for activation of β_3 receptors versus binding to or activation of β_1 and β_2 receptors is > 400-fold in both species. In addition, L-755,507 stimulates lipolysis in rhesus adipocytes in vitro with an EC_{50} = 3.9 nM, and a maximal effect 23% of that of isoproterenol (Fig. 1).

L-755,507 was selected for further evaluation since this compound shows broad selectivity for the β_3 receptor versus other biogenic amine G protein–coupled receptors. L-755,507 is at least 300-fold selective for the human β_3 adrenergic receptor vs the human alpha 1a, alpha 1b, alpha 1d, alpha 2a, alpha 2b, alpha 2c, dopamine D3 and D4 receptors, and is 46-fold selective for the dopamine D2 receptor (data not shown). As expected, the structure activity relationship for affinity at the β_3 receptor varies independently of the structure activity relationship for these other G protein–coupled receptors, and optimization of this selectivity is both critical and challenging, but is attainable.

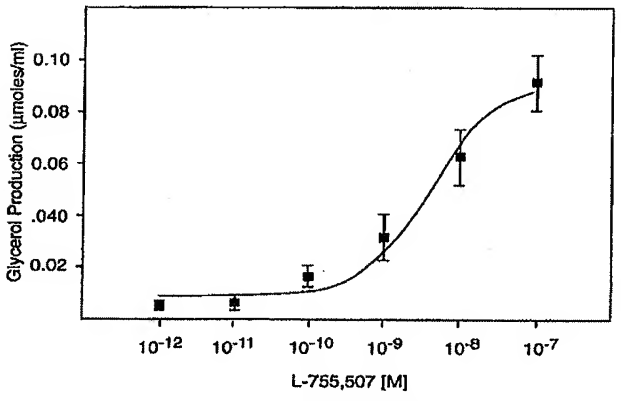

Figure 1. Stimulation of lipolysis in isolated rhesus adipocytes. Adipose tissue from subcutaneous depots was obtained from anesthetized rhesus monkeys by surgical biopsy. Adipocytes were isolated by collagenase digestion as described in Methods, and incubated with isoproterenol or L-755,507 for 2 h at 37°C before determination of glycerol levels in the incubation media.

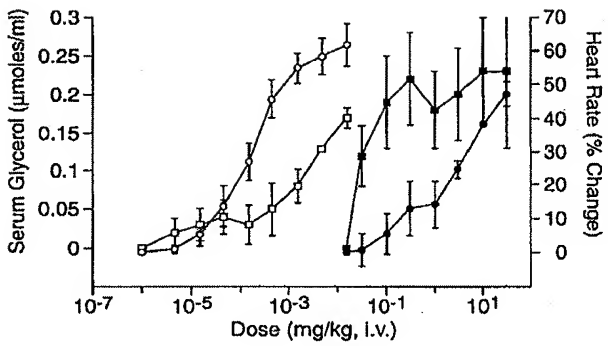

Figure 2. The effects of isoproterenol (*open symbols*) and L-755,507 (*closed symbols*), administered by intravenous infusion, on serum glycerol (*squares*) and heart rate (*circles*) were determined in anesthetized rhesus. Each point represents the mean of determinations in two to five animals and the vertical bars the standard error of the mean.

Effects of L-755,507 on lipolysis and heart rate in the rhesus monkey. L-755,507 and isoproterenol were administered as sequential rising dose infusions over 15 min into catheterized and instrumented barbiturate anesthetized monkeys (Fig. 2). Although these studies were conducted in male animals, preliminary studies indicated that the profile of activity of L-755,507 was similar in male and female rhesus. For L-755,507, the ED_{50} for glycerolemia (dose producing 50% maximal increase in serum glycerol) was 0.03 mg/kg and the ED_{50} for tachycardia (dose producing 50% maximal increase in heart rate, i.e., ~ 40 bpm) was 2.5 mg/kg. For isoproterenol, the ED_{50} for glycerolemia was 0.003 mg/kg and the ED_{50} for tachycardia was 0.0002 mg/kg. No changes in mean arterial pressure or serum potassium were evident in L-755,507–treated animals, but at higher doses of isoproterenol (≥ 0.003 mg/kg), hypokalemia and hypotension were observed (data not shown).

Effects of L-755,507 on metabolic rate in the rhesus monkey. L-755,507 stimulates metabolic rate by ~ 30% after acute bolus intravenous administration of 0.1 mg/kg to rhesus monkeys. The response peaked within 30 min and was sustained for at least 60 min, the duration of the monitoring period. Under these conditions, lipolysis and tachycardia accompanied the metabolic rate increase: lipolysis was maximal within 15 min of agonist administration, whereas the tachycardia, which occurred in the absence of changes in mean arterial pressure, was slowly developing and peaked (~ 15% increase in heart rate) at 40 min after L-755,507 administration (Fig. 3). Note that the profile of the tachycardia evoked by L-755,507 is markedly different from that elicited by β_1 agonists such as isoproterenol, as the latter is rapid in onset and is maximal within 60 s of agonist addition. Evaluation of the dose dependence of these responses indicated that significant increases in metabolic rate and lipolysis were evident at a dose of L-755,507

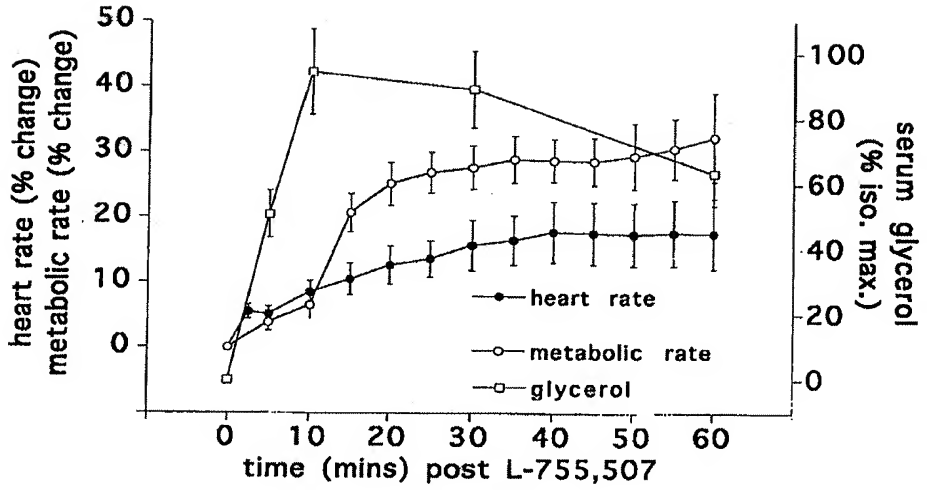

Figure 3. The effects of L-755,507 (0.1 mg/kg, i.v.) on metabolic rate (*open circles*), serum glycerol (*open squares*), and heart rate (*solid circles*) were determined in the anesthetized rhesus. Metabolic rate and heart rate are expressed as the percent change from baseline values, and serum glycerol is expressed as a percentage of the response evoked by a maximally effective dose of isoproterenol in the same animals. No changes in any of the parameters were evident after vehicle administration in place of L-755,507. Each point represents the mean of determinations in three to four animals and the vertical bars the standard error of the mean.

($\leq$ 0.01 mg/kg) at which no significant tachycardia was evident (Fig. 4).

Chronic exposure of rhesus monkeys to L-755,507. Female rhesus monkeys were administered vehicle (25% ethanol, 25% polyethylene glycol 400, 50% saline, 1 ml/kg, i.v., twice daily) or L-755,507 (3 mg/kg, i.v., twice daily) daily for up to 28 d. Samples of axillary brown adipose tissue, so defined because of the presence of UCP1, multilocular lipid droplets, and a significant cytoplasm: lipid ratio (vide infra), were obtained before and at 2 and 4 wk after initiation of treatment, and the morphology of, and UCP1 levels in axillary BAT were determined.

As shown in Fig. 5, UCP1 levels were increased by 62% (P = 0.04) and 132% (P = 0.05) after 2 and 4 wk of administration of L-755,507, respectively. No changes in UCP2 expression were noted. Histological examination of samples of BAT obtained 4 wk after administration of vehicle or L-755,507 revealed changes at both the light and electron microscopic levels (Fig. 6). Light micrographs (Fig. 6, *A* and *B*) demonstrate that, in comparison to vehicle treated control animals, treatment with L-755,507 results in a decrease in the size of intracellular lipid droplets coupled with an increase in the number of droplets per cell. Moreover, the cytoplasm:lipid ratio is increased in the tissue from animals treated with the β_3 agonist. A further structural effect of chronic exposure to L-755,507, which is evident when specimens are observed by electron microscopy (Fig. 6, *C* and *D*), is that there are many more cristae within the mitochondria of tissue from L-755,507–treated animals. In tissue from β_3 agonist–treated animals, the cristae are usually found as tightly packed arrays of parallel membranes

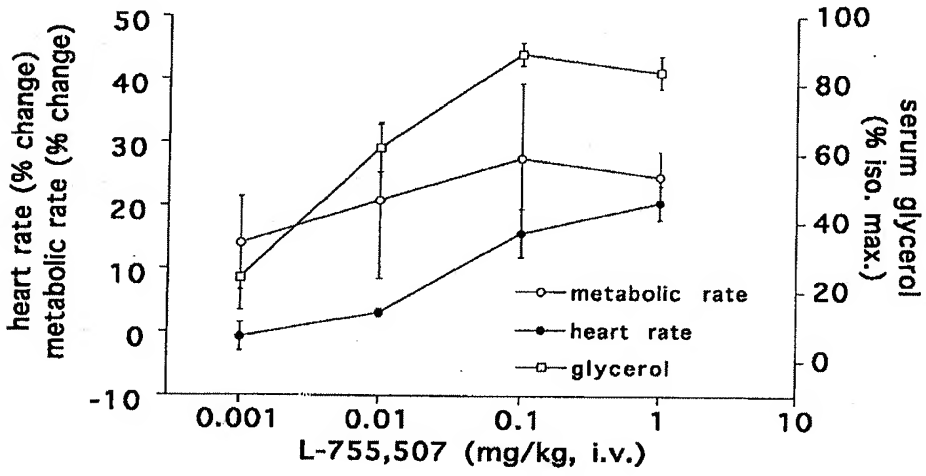

Figure 4. The dose dependence of the effects of L-755,507 (0.001–1 mg/kg, i.v.) on metabolic rate (*open circles*), serum glycerol (*open squares*), and heart rate (*solid circles*) were determined in the anesthetized rhesus, and the data reported are those obtained 30 min after compound administration. Metabolic rate and heart rate are expressed as the percent change from baseline values, and serum glycerol is expressed as a percentage of the response evoked by a maximally effective dose of isoproterenol in the same animals. No changes in any of the parameters were evident after vehicle administration in place of L-755,507. Each point represents the mean of determinations in three to four animals and the vertical bars the standard error of the mean.

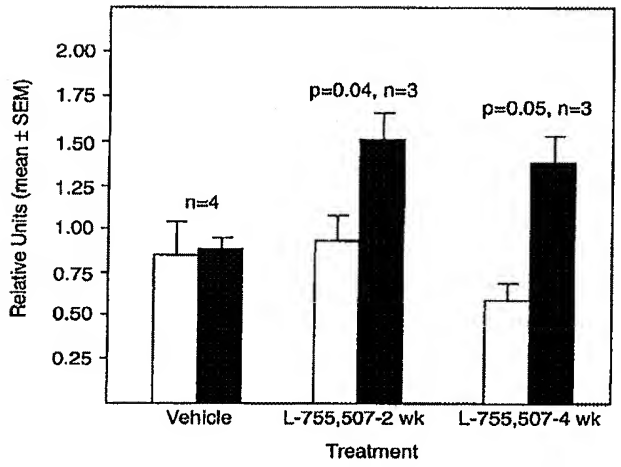

Figure 5. Effects of chronic administration of L-755,507 on mitochondrial UCP levels in axillary brown adipose tissue. UCP levels were determined by Western analysis of membrane fractions from BAT obtained by surgical biopsy before (*open bars*) and after (*closed bars*) 2 or 4 wk of administration of vehicle or L-755,507 (3 mg/kg, i.v., twice daily). Analysis was performed three times for each tissue sample, and data for samples on each gel were normalized to one posttreatment vehicle sample before averaging the three values for each sample. Data shown are the mean±SEM for the normalized data for each animal within a treatment group (four vehicle-treated animals, three L-755,507–treated animals for 2 or 4 wk). Statistical analysis was performed using a 1-tailed paired *t* test.

whereas in tissue from vehicle-treated animals there are fewer cristae per mitochondria and they generally fill only a portion of the mitochondrial volume.

Discussion

Using cloned human receptors for screening, a novel β_3 adrenergic receptor agonist, L-755,507, was discovered. This compound is a potent β_3 agonist at both the human and rhesus receptors, and is > 1,000-fold selective for activation of the β_3 receptor versus activation of the β_1 receptor in both species. Selectivity is > 400-fold in both species when quantified with respect to activation of the β_3 receptor and activation of or binding to β_1 and β_2 receptors.

We and others (20–22) have shown that it is only possible to detect β_3 adrenergic receptor mRNA in omental white adipose tissue (WAT) and in BAT from humans and rhesus monkeys by reverse transcription PCR. However, β_1 and β_2 adrenergic receptor mRNA can be detected by Northern blots. Thus, in contrast to rodent adipocytes, the β_3 adrenergic receptor is a minor component of the complement of β adrenergic receptors expressed on primate adipocytes. However, CGP12177 stimulates triglyceride breakdown in human abdominal WAT consistent with its activation of β_3 receptors (15). In addition, we have evaluated the effects of L-755,507 and 14 other selective β_3 agonists on lipolysis in human abdominal WAT and demonstrated that lipolytic activity correlates well with their affinity for the human β_3 adrenergic receptor ($r^2 = 0.34$, slope = 0.38 [$P = 0.02$]). In contrast, there is no correlation between their lipolytic potential and their affinity

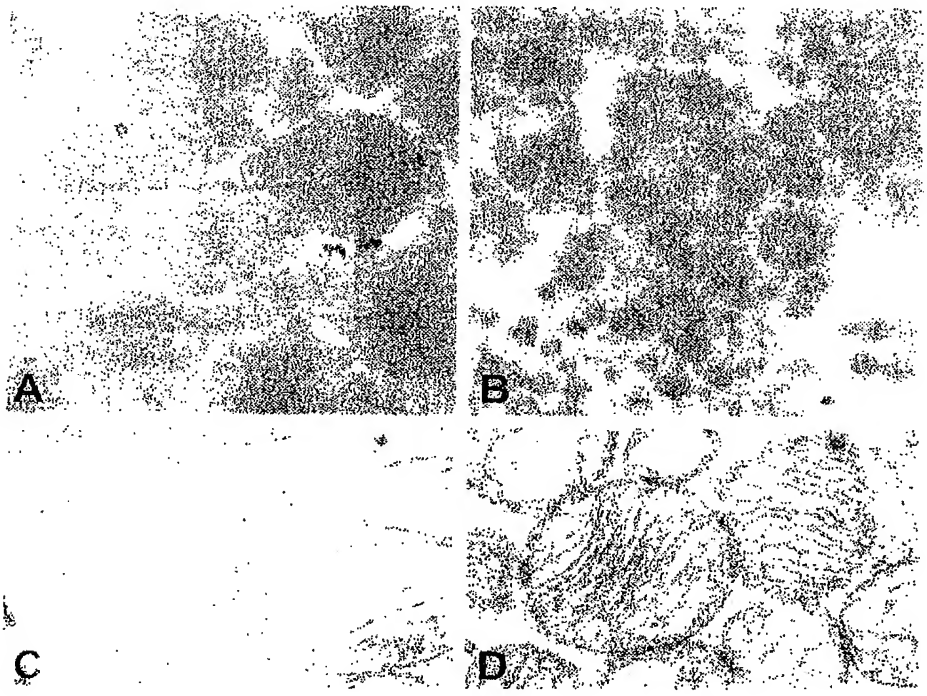

Figure 6. Structural observation of axillary brown adipose tissue collected from rhesus which had been treated for 28 d with L-755,507 (3 mg/kg, i.v., twice daily) (B and D) or vehicle (A and C). Magnification, *A* and *B* = 900, *C* and *D* = 70,000.

for the human β_1 or β_2 adrenergic receptors (r^2 = 0.02 and 0.08, slope = 0.08 [P = 0.6] and 0.24 [P = 0.3], respectively). The stimulation of lipolysis in human WAT by compounds selective for the human β_3 receptor suggests that the β_3 receptor is expressed at levels sufficient to be pharmacologically exploited to selectively activate adipose tissue.

L-755,507 is potent and efficacious at the rhesus β_3 receptor, and was thus chosen for more detailed studies. Preliminary pharmacokinetic analyses in various species indicated that this class of compounds was poorly orally bioavailable, with relatively short terminal half lives. Accordingly, the profile of activity of the compound in rhesus was evaluated after intravenous administration. When administered as sequential rising dose infusions over 15 min into catheterized and instrumented barbiturate anesthetized monkeys, L-755,507 and isoproterenol dose dependently stimulated lipolysis and tachycardia. For L-755,507, the dose–response curve for glycerolemia lies significantly to the left of that for tachycardia, whereas the converse is true for isoproterenol. Although L-755,507 is less potent than isoproterenol in stimulating lipolysis, the maximum extents of glycerolemia evoked by L-755,507 and isoproterenol are similar when measured in the same animal, indicating that the compound behaves as a full agonist with respect to lipolysis in vivo. These data indicate that the profile of activity of L-755,507 in vivo in the rhesus monkey differs markedly from that of the nonselective β agonist isoproterenol.

L-755,507 stimulates metabolic rate after acute bolus intravenous administration to rhesus monkeys. The maximum increase in metabolic rate (~ 30% above baseline) was evident at 0.1 mg/kg L-755,507, and was accompanied by lipolysis and slowly developing tachycardia. However, significant increases in metabolic rate and lipolysis were evident at a dose of L-755,507 (≤ 0.01 mg/kg) at which no significant tachycardia was evident. In these lean animals baseline respiratory quotient (RQ) is ~ 0.8, indicating predominance of fat over carbohydrate as substrates for oxidation in the fasted state. No reductions in RQ were evident after L-755,507 administration, presumably because of the low RQ before β_3 agonist administration. In support of this contention, we have shown that other β_3 agonists can reduce RQ in conscious fed animals, where baseline RQ is ~ 0.9 (unpublished observations). Activation of lipolysis and metabolic rate elevation in nonhuman primates by L-755,507 at doses which fail to elicit significant tachycardia (a β_1 effect) or hypokalemia (a β_2 effect) suggest that human-selective β_3 receptor agonists will display an improved side-effect profile, in comparison to rodent-selective β_3 agonists, in humans.

As noted above, L-755,507 shows only very weak agonist activity at the rhesus β_1 receptor in vitro. This, together with the observation that the tachycardia evoked by bolus L-755,507 is much slower in onset than that evoked by isoproterenol, suggests that the tachycardia observed in rhesus monkeys after L-755,507 administration may not be a direct effect of activation of cardiac β_1 receptors by the β_3 agonist. Additional studies, to be described elsewhere, using selective human β_3 agonists in anesthetized and conscious rhesus monkeys established that the tachycardia evoked by β_3 agonists is reflexogenic in origin, consequent upon evoked increases in metabolic rate and direct β_3 receptor–mediated peripheral vasodilatation which occurs in the absence of changes in mean arterial pressure.

To evaluate the sequelae of chronic exposure to L-755,507, female rhesus monkeys were administered vehicle or L-755,507 (3 mg/kg, i.v., twice daily) daily for up to 28 d. Preliminary studies in conscious rhesus monkeys established that L-755,507 does not elicit significant direct β_1 receptor activation, as reported by rapidly developing tachycardia, but produces a peak increase (~ 20%) in metabolic rate, that is relatively transient and returns to the baseline value within 3 h. From the extent and duration of the L-755,507-induced increase in metabolic rate, as measured acutely over 3 h, we estimate the maximum increase in 24-h energy expenditure that could be achieved using this dosing regimen of L-755,507 is ~ 5%. Accordingly, we chose not to attempt to measure 24-h energy expenditure in the chronically dosed animals using doubly labeled water, because in primates the sensitivity of the technique is sufficient to report increases in energy expenditure that are at least 10–15%. Consistent with the predicted small increases in 24-h energy expenditure, where a 5% increase (i.e., ~ 24 kcal/d) deriving from increased fat metabolism (calorific value = 9.3 kcal/gram) would yield a weight loss of < 3 grams/d in rhesus monkeys, there were no differences in weight loss between vehicle-treated and L-755,507–treated animals. To place these observations in rhesus monkeys in proper perspective, we estimate that a 10% increase in 24-h energy expenditure in humans will yield a clinically meaningful weight loss at the rate of ~ 1 kg per month.

A significant increase in UCP1 levels was observed after 2 and 4 wk of administration of L-755,507. In addition, morphologic changes in the axillary fat of treated animals were consistent with BAT activation. Studies using other β_3 agonists in male rhesus indicate that the morphological effects of chronic β_3 agonist administration in the rhesus are not gender specific. Consistent with previous reports in rodents (23), chronic exposure of rhesus monkeys to this selective β_3 agonist did not alter expression of the newly discovered homolog UCP2 in axillary BAT.

Given the relative paucity (but not absence) of BAT in primates, including humans (24), it is likely that the acute lipolytic and metabolic rate effects of β_3 agonists such as L-755,507 are mediated predominantly, if not exclusively, via activation of β_3 receptors on white adipocytes. The evoked thermogenesis may derive in part from uncoupling of fatty acid β oxidation from ATP generation via the intermediation of UCP1, UCP2, and/or UCP3 (25) in BAT, or from UCP2 and/or UCP3 in WAT. This concept is consistent with the observations in transgenic mice where the acute effects of β_3 agonists on O_2 consumption are more marked in animals which express β_3 receptors exclusively in WAT than in BAT (26). As we have shown that chronic exposure to β_3 agonists upregulates BAT in rhesus, the presumption is that under these conditions BAT would make a greater contribution to the increase in metabolic rate. β_3 agonists also cause sustained metabolic effects, including up-regulation of nascent BAT and weight loss in other species (e.g., dogs) which, like humans and nonhuman primates, have relatively sparse BAT in adulthood (5, 24, 27). Moreover, hibernomata and pheochromocytoma in humans are associated with BAT expansion and up-regulation, respectively, and both are accompanied by marked weight loss (24). It remains to be shown whether chronic therapy with β_3 agonists in humans elicits up-regulation of BAT with resulting negative energy balance and weight loss.

Conclusions. L-755,507 is the first β_3 agonist demonstrated to be potent and selective for the receptor in humans and

rhesus monkeys, and is the first selective compound to activate lipolysis in adipocytes isolated from these species. Thus, although the expression levels of β_3 receptors found in primate adipocytes are quite low, and reportedly variable among primate species (14, 28), activation of these receptors by selective agonists produces the desired pharmacological response in rhesus monkeys. In addition, our data demonstrate that pharmacological activation of β_3 receptors in primates acutely stimulates lipolysis in vivo and increases metabolic rate, suggesting that responses to appropriate β_3 agonists in primates mimic the responses previously seen in rodents. Finally, in a manner similar to that previously observed in rodents and dogs, chronic administration of these compounds activates and differentiates rhesus monkey BAT, as evidenced by increased UCP1 expression, which process is controlled by β_3 receptor activation (29). Thus, the data suggest that selective β_3 agonists with high affinity for the human receptor may be useful for increasing energy expenditure and inducing weight loss in humans.

Acknowledgments

We thank MaryAnn Haas for technical preparation of the manuscript.

References

1. Leibel, R.L., M. Rosenbaum, and J. Hirsch. 1995. Changes in energy expenditure resulting from altered body weight. *N. Engl. J. Med.* 332:621–628.

2. Arch, J.R.S., A.T. Ainsworth, M.A. Cawthorne, V. Piercy, M.V. Sennitt, V.E. Thody, C. Wilson, and S. Wilson. 1984. Atypical beta-adrenoceptor on brown adipocytes as target for anti-obesity drugs. *Nature.* 309:163–165.

3. Lowell, B.B., and J.S. Flier. 1997. Brown adipose tissue, beta3-adrenergic receptors, and obesity. *Annu. Rev. Med.* 48:307–316.

4. Garlid, K.D., D.E. Orosz, M. Modriansky, S. Vassanelli, and P. Jezek. 1996. On the mechanism of fatty acid-induced proton transport by mitochondrial uncoupling protein. *J. Biol. Chem.* 271:2615–2620.

5. Holloway, B.R. 1989. Selective β-agonists of brown fat and thermogenesis. *In* Hormones, Thermogenesis and Obesity. H.A. Lardy and F.W. Stratman, editors. Elsevier, New York. 477–484.

6. Bloom, J.D., M.D. Dutia, B.D. Johnson, A. Wissner, M.G. Burns, E.E. Largis, J.A. Dolan, and T.H. Claus. 1992. Disodium (R,R,)-5-[2-[[2-(3-chlorophenyl)-2-hydroxyethyl]-amino]propyl]-1,3-benzodioxole-2,2-dicarboxylate (CL 316,243). A potent beta-adrenergic agonist virtually specific for beta-3 receptors. A promising antidiabetic and antiobesity agent. *J. Med. Chem.* 35: 3081–3084.

7. Croci, T., R. Cecchi, A. Tarantino, G. Aureggi, A. Bianchetti, R. Boigegrain, and L. Manara. 1988. Inhibition of rat colon motility by stimulation of atypical beta-adrenoceptors with new gut-specific agents. *Pharmacol. Res. Commun.* 20:147–151.

8. Arch, J.R.S., M.A. Cawthorne, K.A. Coney, B.A. Gusterson, V. Piercy, M.V. Sennitt, S.A. Smith, J. Wallace, and S. Wilson. 1991. β-Adrenoceptor-mediated control of thermogenesis, body composition and glucose homeostasis. *In* Obesity and Cachexia. N.J. Rothwell and M.J. Stock, editors. John Wiley & Sons, Ltd., New York. 242–268.

9. Connacher, A.A., R.T. Jung, and P.E.G. Mitchell. 1988. Weight loss in obese subjects on a restricted diet given BRL26830A, a new atypical beta-adrenoceptor agonist. *Br. Med. J. Clin. Res. Ed.* 296:1217–1220.

10. Wheeldon, N.M., D.G. McDevitt, and B.J. Lipworth. 1994. Cardiac effects of the beta 3-adrenoceptor agonist BRL35135 in man. *Br. J. Clin. Pharmacol.* 37:363–369.

11. Emorine, L.J., S. Marullo, M.M. Breind-Sutren, G. Patey, K. Tate, C. Delavier-Kluthko, and A.D. Strosberg. 1989. Molecular characterization of the human beta 3-adrenergic receptor. *Science.* 245:1118–1121.

12. Granneman, J.G., K.N. Lahners, and D.D. Rao. 1992. Rodent and human beta 3-adrenergic receptor genes contain an intron within the protein-coding block. *Mol. Pharmacol.* 42:964–970.

13. Liggett, S.B. 1992. Functional properties of the rat and human beta 3-adrenergic receptors: differential agonist activation of recombinant receptors in Chinese hamster ovary cells. *Mol. Pharmacol.* 42:634–637.

14. Meyers, D.S., S. Skwish, K.E.J. Dickinson, B. Kienzle, and C.M. Arbeeny. 1997. Beta 3-adrenergic receptor-mediated lipolysis and oxygen consumption in brown adipocytes from cynomolgus monkeys. *J. Clin. Endocrinol. Metab.* 82:395–401.

15. Enocksson, S., M. Shimizu, F. Lonnqvist, J. Nordenstrom, and P. Arner. 1995. Demonstration of an in vivo functional beta 3-adrenoceptor in man. *J. Clin. Invest.* 95:2239–2245.

16. Wilson, S., J.K. Chambers, J.E. Park, A. Ladurner, D.W. Cronk, C.G. Chapman, H. Kallender, M.J. Browne, G.J. Murphy, and P.W. Young. 1996. Agonist potency at the cloned human beta-3 adrenoceptor depends on receptor expression level and nature of assay. *J. Pharmacol. Exp. Ther.* 279:214–221.

17. Frielle, T., S. Collins, K.W. Daniel, M.G. Caron, R.J. Lefkowitz, and B.K. Kobilka. 1987. Cloning of the cDNA for the human beta 1-adrenergic receptor. *Proc. Natl. Acad. Sci. USA.* 84:7920–7924.

18. Kobilka, B.K., R.A. Dixon, T. Frielle, H.G. Dohlman, M.A. Bolanoski, I.S. Sigal, T.L. Yan-Feng, U. Francke, M.G. Caron, and R.J. Lefkowitz. 1987. cDNA for the human beta 2-adrenergic receptor: a protein with multiple membrane-spanning domains and encoded by a gene whose chromosomal location is shared with that of the receptor for platelet-derived growth factor. *Proc. Natl. Acad. Sci. USA.* 84:46–50.

19. Rodbell, M. 1964. Effects of hormones on glucose metabolism and lipolysis. *J. Biol. Chem.* 239:375–380.

20. Lonnqvist, F., S. Krief, A.D. Strosberg, B. Nyberg, J. Emorine, and P. Arner. 1993. Evidence for a functional beta 3-adrenoceptor in man. *Br. J. Pharmacol.* 110:929–936.

21. Tavernier, G., P. Barbe, J. Galitzky, M. Berlan, D. Caput, M. Lafontan, and D. Langin. 1996. Expression of beta 3-adrenoceptors with low lipolytic action in human subcutaneous white adipocytes. *J. Lipid Res.* 37:87–97.

22. Revelli, J.-P., P. Muzzin, A. Paolini, M. Moinat, and J.-P. Giacobino. 1993. Expression of the beta 3-adrenergic receptor in human white adipose tissue. *J. Mol. Endocrinol.* 10:193–197.

23. Fleury, C., M. Neverova, S. Collins, S. Raimbault, O. Champigny, C. Levi-Meyrueis, F. Bouillaud, M.F. Seldin, R.S. Surwit, D. Ricquier, and C.H. Warden. 1997. Uncoupling protein-2: a novel gene linked to obesity and hyperinsulinemia. *Nat. Genet.* 15:269–272.

24. Lean, M.E.J. 1992. Evidence for brown adipose tissue in humans. *In* Obesity. P. Bjorntorp and B.N. Brodoff, editors. J.B. Lippincott Co., Philadelphia, 117–129.

25. Gong, D.-W., Y. He, M. Karas, and M. Reitman. 1997. Uncoupling protein-3 is a mediator of thermogenesis regulated by thyroid hormone, β3-adrenergic agonists, and leptin. *J. Biol. Chem.* 272:24129–24132.

26. Grujic, D., V.S. Susulic, M.-E. Harper, J. Himms-Hagen, B.A. Cunningham, B.E. Corkey, and B.B. Lowell. 1997. β3-Adrenergic receptors on white and brown adipocytes mediate β3-selective agonist-induced effects on energy expenditure, insulin secretion, and food intake. *J. Biol. Chem.* 272:17686–17693.

27. Champigny, O., D. Ricquier, O. Blondel, R.M. Mayers, M.G. Briscoe, and B.R. Holloway. 1991. β3-Adrenergic receptor stimulation restores message and expression of brown-fat mitochondrial uncoupling protein in adult dogs. *Proc. Natl. Acad. Sci. USA.* 88:10774–10777.

28. Bousquet-Melou, A., J. Galitzky, C. Carpene, M. Lafontan, and M. Berlan. 1994. Beta-adrenergic control of lipolysis in primate white fat cells: a comparative study with nonprimate mammals. *Am. J. Physiol.* 267:115–123.

29. Cannon, B., A. Jacobsson, S. Rehnmark, and J. Nedergaard. 1996. Signal transduction in brown adipose tissue recruitment: noradrenaline and beyond. *Int. J. Obesity.* 20:36–42.

Effect of a 28-d treatment with L-796568, a novel β_3-adrenergic receptor agonist, on energy expenditure and body composition in obese men[1–3]

Thomas M Larsen, Søren Toubro, Marleen A van Baak, Keith M Gottesdiener, Patrick Larson, Wim HM Saris, and Arne Astrup

ABSTRACT

Background: Stimulation of energy expenditure (EE) with selective thermogenic β-adrenergic agonists may be a promising approach for treating obesity.

Objective: We analyzed the effects of the highly selective human β_3-adrenergic agonist L-796568 on 24-h EE, substrate oxidation, and body composition in obese, weight-stable men.

Design: In this 2-center, double-blind, randomized, parallel-group study, we measured 24-h EE before and after 28 d of treatment with L-796568 (375 mg/d) or placebo during weight maintenance (ie, without dietary intervention) in nondiabetic, nonsmoking men aged 25–49 y with body mass index (in kg/m^2) of 28–35 (n = 10 subjects per treatment group).

Results: The mean change in 24-h EE from before to after treatment did not differ significantly between groups (92 ± 586 and 86 ± 512 kJ/24 h for the L-796568 and placebo groups, respectively). The change in 24-h nonprotein respiratory quotient from before to after treatment did not differ significantly between groups (0.009 ± 0.021 and 0.009 ± 0.029, respectively). No changes in glucose tolerance were observed, but triacylglycerol concentrations decreased significantly with L-796568 treatment compared with placebo (−0.76 ± 0.76 and 0.42 ± 0.31 mmol/L, respectively; $P < 0.002$). Overall, treatment-related changes in body composition were not observed, but higher plasma L-796568 concentrations in the L-796568 group were associated with greater decreases in fat mass ($r = -0.69$, $P < 0.03$).

Conclusions: Treatment with L-796568 for 28 d had no major lipolytic or thermogenic effect but it lowered triacylglycerol concentrations. This lack of chronic effect on energy balance is likely explained by insufficient recruitment of β_3-responsive tissues in humans, down-regulation of the β_3-adrenergic receptor–mediated effects with chronic dosing, or both. *Am J Clin Nutr* 2002;76:780–8.

KEY WORDS L-796568, β_3-adrenergic receptor, β_3-adrenergic receptor agonist, β_3 agonist, selectivity, energy expenditure, lipolysis, respiratory quotient, indirect calorimetry, triacylglycerol, obesity, obese men

INTRODUCTION

Several sympathomimetic agents are currently being used to treat human obesity. These agents have potential anorectic and thermogenic effects. However, the earlier use of nonselective β-adrenergic compounds was associated with adverse reactions such as tachycardia and tremor, which were attributable to β_1 and β_2 stimulation, respectively. The characterization of the β_3-adrenergic receptor, mainly expressed in white adipose tissue (WAT) and brown adipose tissue (BAT) (1, 2), evoked hope for a new potential target in the pharmacologic treatment of obesity and diabetes.

A marked thermogenic response to selective β_3-adrenergic receptor agonists was found in rodents (3, 4). When administered over a period of weeks, these agonists induce weight loss and have antidiabetic effects (3, 5). Furthermore, in addition to their thermogenic effects, β_3 agonists may promote fat loss by stimulating fatty acid mobilization and, directly or indirectly, fat oxidation. Studies of isolated human fat cells show lipolytic activity not involving the β_1 and β_2 receptors (6, 7), and in vivo studies in humans show lipolytic activity of the partial β_3-adrenergic receptor agonist CGP12177. This effect was not inhibited by the combined β_1 and β_2 antagonist propranolol (8), and it was suggested that the β_3-adrenergic receptor may be responsible for a substantial proportion of the lipolytic response to norepinephrine in humans (9).

Among the β_3 agonists tested in human clinical trials to date, only the compound CL 316 243 has been recognized as weakly potent, but selective, toward the human β_3-adrenergic receptor (10). In an 8-wk study in lean male subjects, this partial β_3-adrenergic receptor agonist significantly increased insulin-stimulated glucose disposal, fasting plasma fatty acid concentrations, and 24-h fat oxidation without any side effects mediated by β_1 or β_2; however, no effects on energy expenditure or body weight were observed.

L-796568, a novel β_3-adrenergic receptor agonist for the human β_3-adrenergic receptor, shows potency as a selective human β_3 agonist when tested in cyclic AMP assays on Chinese hamster

[1] From the Research Department of Human Nutrition, The Royal Veterinary and Agricultural University, Copenhagen (TML, ST, and AA); the Nutrition and Toxicology Research Institute (NUTRIM), Department of Human Biology, Maastricht University, Maastricht, Netherlands (MAVB and WHMS); and Merck & Co, Rahway, NJ (KMG and PL).

[2] Supported by Merck & Co Inc, Whitehouse Station, NJ.

[3] Address reprint requests to TM Larsen, Research Department of Human Nutrition, The Royal Veterinary and Agricultural University, Rolighedsvej 30, 1958 Frederiksberg, Copenhagen, Denmark. E-mail: tml@kvl.dk.

Received January 1, 2001.

Accepted for publication October 24, 2001.

Am J Clin Nutr 2002;76:780–8. Printed in USA.

ovary cells transfected with the human β_3-adrenergic receptor, and the compound has an EC_{50} = 3.6 nmol/L (94% activation compared with isoprenaline) with >600-fold selectivity over the human β_1 and β_2 receptors (11). A related β_3 agonist that has similar potency, L-755507, elicited a dose-dependent rise in metabolic rate and lipolysis in rhesus monkeys; there was an ≈30% increase in metabolic rate after intravenous bolus administration. Chronic treatment with L-755507 was also accompanied by significant increases in BAT and uncoupling protein 1 expression (12). Human studies with L-796568 showed dose-dependent increases in plasma glycerol and fatty acid concentrations (K Gottesdiener and Merck & Co, unpublished observations, 1999). More importantly, in obese subjects who had fasted overnight, an ≈8% acute thermogenic effect of a single 1000-mg dose of L-796568 was found (13). The purpose of the present study was to test whether this acute effect was maintained after 28 d of chronic treatment with a dosing regimen (375 mg L-796568 once daily with food) that was shown in a separate study to achieve plasma concentrations of L-796568 similar to or higher than those achieved with a single 1000-mg dose of L-796568 administered in the fasted state.

SUBJECTS AND METHODS

Study design

This double-blind, randomized, placebo-controlled, parallel-group study was performed at 2 centers, Copenhagen and Maastricht. A total of 20 male subjects were randomly assigned to receive either 375 mg L-796568 or placebo, administered once daily with breakfast. In each treatment group (placebo or L-796568) there were 10 subjects (5 at each study site).

Energy expenditure (EE) and substrate oxidation rates were determined with indirect calorimetry in respiration chambers on a fixed physical-activity protocol. L-796568 was administered at 0915 in the respiration chamber after a meal. The study consisted of a baseline 24-h measurement (0915 to 0915) on day 0 (the day before treatment began) and a second measurement obtained with an identical protocol on day 27. At the baseline visit, the measurement was continued for 6 h after each subject ingested his first dose of study medication to evaluate a possible acute effect of the compound. To investigate a possible drug effect during particular periods of the day, the 24-h measurement period (0915–0915) was divided into the following specific intervals: sleep EE (0300–0600), basal metabolic rate (0730–0830), daytime EE (0915–1315), exercise EE (1430–1445), and postdinner EE (1915–2215).

Subjects

All subjects underwent a full physical examination with an electrocardiogram, medical history, and routine hematology, biochemistry, and urine screening tests. All were found to be in good health (except for their obesity), without previous or current endocrine, cardiovascular, or hepatic diseases. The subjects reported no acute illnesses within the 2 wk immediately preceding the start of the trial. None of the subjects were dieting or took any medication regularly. They were all nonsmokers, aged 25–49 y, with a body mass index (BMI; in kg/m^2) between 28 and 35 and stable weight (±4 kg) for ≥3 mo before the study.

All subjects were carefully instructed to maintain their usual dietary habits and body weight throughout the study. During the 28-d treatment period, the subjects consumed breakfasts with a consistent composition each morning (1620 kJ, 30% of energy from fat) to improve drug absorption (≈3-fold increase in area under the curve when administered with food). They also avoided excessive or strenuous physical activity and consumed no more than 2 units (24 g) of alcohol and 4 cups of caffeinated beverages/d. Alcohol intake was prohibited for 48 h before the respiration chamber sessions. No other medication was allowed, and subjects were instructed to report any additional medication used during this period. The study was approved by the Ethics Committee of Frederiksberg and Copenhagen (Copenhagen site) and the Medical Ethics Committee of Maastricht University (Maastricht site). The subjects gave their written, informed consent according to the Helsinki Declaration.

Anthropometry

Body weight was measured in light clothing on a decimal scale on days 0, 7, 14, and 28 (in Copenhagen: Lindeltronic 8000, Lindells Inc, Kristianstad, Sweden; in Maastricht: Sauter model D-7440, Sauter Inc, Ebingen, Germany). Body composition was estimated with dual-energy X-ray absorptiometry within 7 d before treatment (prestudy) and again within 2 d after the last treatment day (poststudy) (both sites: Lunar DPX-IQ; General Electric, Madison, WI) and with the bioelectrical impedance method (Copenhagen: Animeter; HTS-Engineering Inc, Odense, Denmark and Maastrict: Hydra ECF/ICF model 4200; Xitron Technologies, San Diego). Heart rate and blood pressure were measured with an automatic device (both sites: Omron Automatic HEM-705CP; Omron Electronics GmbH, Hamburg, Germany).

Indirect calorimetry

EE and substrate oxidation were measured in open-circuit respiration chambers. At the Copenhagen site, the floor area and volume were 6.5 m^2 and 14.7 m^3, respectively (14), whereas at the Maastricht site, the floor area and volume were 7.0 m^2 and 14.0 m^3, respectively (15). The room temperature was maintained at 24 °C during the daytime and 18 °C at night. The oxygen and carbon dioxide exchange was determined by taking measurements of the oxygen fraction (Copenhagen: Magnos 4G; Hartman and Braun, Frankfurt, Germany and Maastricht: Magnos 6G, Hartman and Braun, in combination with OA184A; Servomex, Crowborough, United Kingdom) and carbon dioxide fraction (both sites: Uras 3G; Hartman and Braun) at the inlet and outlet of the chamber and from the flow of the outgoing air.

Urine was collected for a 24-h period on days 0 and 27 and also during the 6-h period after the first dose. Urine samples were used to estimate protein oxidation by assessing nitrogen excretion. Protein oxidation was calculated on the basis of the assumption that 6.25 g protein is combusted per gram of nitrogen excreted. Subsequently, nonprotein oxygen and carbon dioxide exchanges were calculated on the basis of the assumption that 0.952 L O_2 is consumed and 0.795 L CO_2 is produced per gram of protein oxidized. Carbohydrate and fat oxidation were then calculated by using the constants published by Elia and Livesey (16).

Spontaneous physical activity in the respiration chambers was assessed with 2 microwave radar instruments (Sisor Mini-Radar; Static Input System SA, Lausanne, Switzerland) at the Copenhagen site and with an analogue ultrasound system (Aritech Advisor DU160; Aritech BV, Roermond, Netherlands) at the Maastricht site. The spontaneous physical activity scores were used to

redefine the sleeping period if spontaneous physical activity exceeded 2% during the prescribed period.

During the subjects' stays in the respiration chamber, the activity protocols (ie, fixed meal times and sessions of physical activity) were similar at the 2 sites. Two 15-min sessions of bicycling at a work output of 75 W were included in the protocol at 1430 and 1630. To ensure adherence to the protocol, the subjects were monitored constantly by a laboratory technician during the daytime. To accustom the subjects to the respiration chamber environment, they spent the night (Copenhagen) or at least some hours (Maastricht) in the chamber before the experiments.

Diet

To achieve energy balance (defined as energy intake − EE, ± 0.5 MJ) during the stay in the respiration chamber, the appropriate dietary energy content (kJ/24 h) was individually calculated by using the subjects' fat-free mass (FFM) in the following equation: 136.1 kJ/kg × FFM in kg + 2154 kJ (17). FFM was calculated with an algorithm determined on the basis of impedance measurements in men (18). The dietary composition was similar at the 2 study sites, providing an average of 50% of energy from carbohydrates (range: 48.6–53.6%), 35% from fat (32.2–35.6%), and 15% from protein (13.4–16.9%). The diet had a calculated respiratory quotient (RQ; derived from the dietary macronutrient composition) of ≈0.881, depending on the actual energy intake. Dietary energy content and composition were calculated by using BECEL dietary assessment software (Unilever, Rotterdam, Netherlands) and the Dutch Food Composition Table at the Maastricht site. At the Copenhagen site, we used DANKOST dietary assessment software, version 2.0 (Danish Catering Center Denmark). Both software programs use the Atwater factors for metabolizable energy. Any food not consumed by the subjects was reweighed and subtracted to calculate actual energy and macronutrient intakes. A maximum of 2 cups tea or coffee was allowed during the respiratory chamber measurements, and intake during the baseline measurement was replicated during the second measurement.

Blood and urine sample collection

While the subjects were in a fasted state and resting, blood samples were obtained from a forearm vein; this was done before subjects entered the chamber on day 0 and after they left the chamber on day 28. The blood was analyzed for norepinephrine, epinephrine, fatty acids, triacylglycerol, glycerol, lactate, ketones (β-hydroxybutyrate), total cholesterol, HDL cholesterol, LDL cholesterol, VLDL cholesterol, and leptin. In addition, fasting triacylglycerol, fatty acids, glycerol, and total cholesterol were measured on day 14. We also obtained blood samples to be analyzed for L-796568 concentration on day 0 and before the dose of L-796568 on days 21, 25, and 28; subjects were fasting when the blood was drawn.

A 24-h urine sample was collected for measurement of nitrogen and catecholamines from 0900 on day 0 to 0900 on day 1 and again from 0900 on day 27 to 0900 on day 28. In addition, urine was collected on day 1 from 0900 to 1500.

Blood and urine analyses

For the analyses of plasma glycerol and fatty acid concentrations, 2 mL blood was drawn into a tube containing EDTA, kept on ice, and centrifuged within 1 h at 1200 × *g* for 15 min at 4 °C; the plasma was stored at −70 °C until analyzed. The analysis was done with an automated spectrophotometric procedure (19). For the analyses of serum leptin, 4 mL blood was drawn into a tube, kept on ice, and centrifuged within 1 h at 1200 × *g* for 15 min at 20 °C. The serum was stored at −70 °C until analyzed with the DSL-23100 leptin immunoradiometric assay kit (Diagnostic Systems Laboratories, Webster, TX).

For the analyses of plasma catecholamines, 6 mL blood was drawn and immediately transferred into a fresh solution of reduced glutathione; this was centrifuged at 806 × *g* for 10 min at 4 °C. The plasma was immediately frozen in liquid nitrogen and stored at −70 °C until analyzed by using HPLC with electrochemical detection (20). For the analyses of plasma L-796568, 5 mL blood was drawn into a tube containing heparin, placed on ice, and centrifuged at 1670 × *g* for 15 min at 4 °C. The plasma was stored at −20 °C until analyzed by using solid-liquid extraction, electrospray liquid chromatography–tandem mass spectrophotometry (LC-MS/MS) method (Merck & Co, West Point, PA).

For the analyses of serum or plasma lipids, 4 mL blood was drawn into a tube, centrifuged at 2000 × *g* for 10 min at 4 °C, and kept at −18 °C until analyzed. At the Copenhagen site, we measured serum triacylglycerols with an enzymatic method (21) and serum HDL cholesterol with an enzymatic method (22); serum LDL cholesterol was calculated (23). At the Maastricht site, serum triacylglycerols and serum total cholesterol were measured with an enzymatic method (24), plasma HDL cholesterol was measured with an enzymatic method (25), and plasma LDL cholesterol was calculated (23).

For the analyses of β-hydroxybutyrate and lactate, at the Copenhagen site 5 mL blood was drawn into a tube containing EDTA and mixed, 4 mL ice-cold perchloric acid was added, and the solution was kept at −18 °C until analyzed. β-hydroxybutyrate concentration was analyzed with a colorimetric method (Boehringer Mannheim, Mannheim, Germany), and blood lactate was measured with enzymatic determination (26). At the Maastricht site, serum β-hydroxybutyrate was analyzed with an enzymatic method (27) automated on a Cobas Fara centrifugal analyzer (Roche, Basel, Switzerland). Plasma lactate was analyzed via enzymatic determination (YSI model 2300 glucose and lactate analyzer; Yellow Springs Instruments Inc, Yellow Springs, OH).

Subjects underwent a 120-min oral-glucose-tolerance test (OGTT) with 75 g glucose on 2 occasions: within the 7 d before the study and on day 28 (the end of the study). Both OGTTs were performed in the fasting state, but on day 28 the glucose was consumed with 375 mg L-796568. For the analyses of glucose and insulin concentrations, at the Copenhagen site 4 mL blood was drawn into a gel tube, allowed to coagulate, and centrifuged at 2000 × *g* for 10 min at 4 °C. The serum was kept at 18 °C until analyzed. Serum insulin was measured with a radioimmunoassay kit from Pharmacia AS, Copenhagen and serum glucose was measured with enzymatic glucose oxidase (21). At the Maastricht site, serum insulin was analyzed with an Autodelfia fluoroimmunoassay kit from Perkin-Elmer Wallac Inc, Oy, Finland, and plasma glucose was measured with an enzymatic method (28). For the analyses of plasma glucagon, at the Copenhagen site 5 mL blood was drawn into a tube containing EDTA, stored at 4 °C for < 30 min, and centrifuged at 2000 × *g* for 10 min at 4 °C. The plasma layer was transferred into a glass tube holding 1.500 kallikrein-inactivating units (KIE) of Trasylol (Bayer Pharma, Lyngby, Denmark). The sample was stored at 25 °C until analyzed with a radioimmunoassay kit from Diagnostic Products Corp, Los Angeles. At the Maastricht site, serum glucagon was analyzed with a radioimmunoassay kit (glucagon double antibody; DPC Biermann GmbH, Bad Nauheim, Germany).

TABLE 1
Anthropometric and cardiovascular measures at baseline and energy expenditure (EE) and nonprotein respiratory quotient (RQ_{np}) during the baseline stay in the respiration chamber[1]

	Placebo group (n = 10)	L-796568 group (n = 10)
Age (y)	35 ± 8	37 ± 6
Height (cm)	184 ± 8	181 ± 5
Body weight (kg)	102.7 ± 12.7	103.5 ± 7.9
BMI (kg/m^2)	30.3 ± 2.2	31.5 ± 2.1
Fat-free mass (kg)[2]	74.9 ± 10.7	70.9 ± 4.6
Fat mass (kg)[2]	28.7 ± 5.2	31.7 ± 5.0
Systolic BP (mm Hg)	128 ± 7	126 ± 6
Diastolic BP (mm Hg)	76 ± 9	81 ± 7
Heart rate (beats/min)	63 ± 6	63 ± 11
24-h EE (kJ/min)	8.13 ± 0.93	8.10 ± 0.45
24-h RQ_{np}	0.846 ± 0.021	0.858 ± 0.020
Sleeping EE (kJ/min)	6.03 ± 0.93	5.92 ± 0.33
Basal metabolic rate (kJ/min)	7.48 ± 1.14	7.05 ± 0.73
Daytime RQ_{np}	0.806 ± 0.028	0.838 ± 0.035[3]

[1] $\bar{x}$ ± SD. BP, blood pressure.
[2] Determined within the 7 d before the baseline stay in the respiration chamber.
[3] Significantly different from the placebo group, $P = 0.04$.

For the analyses of urinary nitrogen, urine was collected in bottles containing 10 mL sulfuric acid (2 mol/L); 8 mL was transferred into scintillation vials and stored at −20 °C before analysis via oxidative decomposition with heat conductance detection (Heraeus CHN-O-RAPID; Heraeus GmbH, Hanau, Germany). For the analyses of urinary norepinephrine and epinephrine, 3 mL acidified urine was stored at −70 °C before analysis via HPLC with electrochemical detection (20).

Appetite profiles

Subjects were asked to complete appetite questionnaires during both stays in the respiration chamber (29). The questionnaires include questions related to hunger and satiety, both of which were rated on a 100-mm visual analogue scale. Subjects recorded their responses before lunch (while fasting), every hour for the 3 h after lunch, before dinner, and every hour for the 3 h after dinner (a total of 8 times).

Statistical analyses

The effect of treatment with L-796568 on 24-h EE was the primary endpoint of this study. Within each treatment group, changes over time relative to baseline were tested by using a paired t test. Mean (±SD) changes over time (eg, from day 0 to day 27) were calculated and group differences were tested by using a two-sample unpaired t test. If the group differences were significant or nearly significant ($P < 0.10$) at baseline, group differences from day 0 to day 27 were recalculated with a general linear model univariate analysis with baseline values added as cofactors. Changes in OGTT response were tested with a general linear model on the basis of a repeated-measures analysis of variance model, and significant group-by-time interaction effects were subsequently analyzed with an unpaired t test. Correlations were determined by using simple correlation analysis. Because body weight and FFM were stable throughout the treatment periods, these factors were not included in the analyses. Analyses were performed with SPSS 10.0 for Windows (SPSS Inc, Chicago). $P < 0.05$ was regarded as statistically significant.

TABLE 2
Blood and urine variables at baseline[1]

	Placebo group (n = 10)	L-796568 group (n = 10)
Blood		
Glucose (mmol/L)	5.35 ± 0.67	5.46 ± 0.52
Insulin (pmol/L)	64 ± 28	87 ± 56
Glucagon (pmol/L)	19 ± 5	26 ± 13
Fatty acids (μmol/L)	324 ± 93	415 ± 122[2]
Glycerol (μmol/L)	45 ± 12	58 ± 21
Triacylglycerols (mmol/L)	1.23 ± 0.64	2.03 ± 0.89[3]
Lactate (μmol/L)	720 ± 210	913 ± 180[3]
Ketones (μmol/L)	87.7 ± 79.5	115.7 ± 73.6
Leptin (ng/mL)	11 ± 5	14 ± 10
Norepinephrine (nmol/L)	2.45 ± 1.40	2.00 ± 0.82
Epinephrine (pmol/L)	156 ± 80	147 ± 84
Total cholesterol (mmol/L)	4.9 ± 0.8	5.7 ± 1.2[2]
HDL cholesterol (mmol/L)	1.1 ± 0.3	1.0 ± 0.2
LDL cholesterol (mmol/L)	3.2 ± 0.8	3.6 ± 1.0
Urine		
Norepinephrine (μg/24 h)	47.4 ± 13.3	56.5 ± 39.2
Epinephrine (μg/24 h)	6.77 ± 2.44	6.94 ± 3.25

[1] $\bar{x}$ ± SD.
[2] Tendency toward group difference, $P < 0.10$.
[3] Significantly different from placebo group, $P < 0.05$.

RESULTS

All subjects completed the study in accordance with our protocol. The 2 groups were well matched with regard to anthropometric and indirect calorimetry measures at baseline (**Table 1**). There were no significant differences at baseline between the groups in biochemical variables, except for triacylglycerol and lactate, which were significantly higher ($P < 0.05$) in subjects allocated to the L-796568 treatment. There was also a tendency ($P < 0.10$) for higher total cholesterol and fatty acid concentrations in the L-796568 group (**Table 2**).

In both groups, there were no significant changes in body weight, body composition, heart rate, or blood pressure from day 0 to day 28. The magnitude of the changes in these variables from day 0 to day 28 did not differ significantly between groups (**Table 3**).

TABLE 3
Changes from day 0 (baseline) to day 28 (day 28 value minus day 0 value) for body weight, body composition, and cardiovascular measures[1]

	Placebo group (n = 10)	L-796568 group (n = 10)
Body weight (kg)	−0.2 ± 1.2	−0.5 ± 1.6
Fat-free mass (kg)[2]	−1.7 ± 2.8	0.4 ± 2.0
Fat mass (kg)[2]	1.0 ± 2.6	0.2 ± 1.5
Fat mass:fat-free mass[2]	0.02 ± 0.05	−0.00 ± 0.03
Systolic BP (mm Hg)	5 ± 8	3 ± 11
Diastolic BP (mm Hg)	3 ± 5	−2 ± 6
Heart rate (beats/min)	2 ± 5	−3 ± 13

[1] $\bar{x}$ ± SD. BP, blood pressure. There were no significant differences between the 2 groups in the magnitude of the change from day 0 to day 28.
[2] Determined within the 7 d before the baseline stay in the respiration chamber.

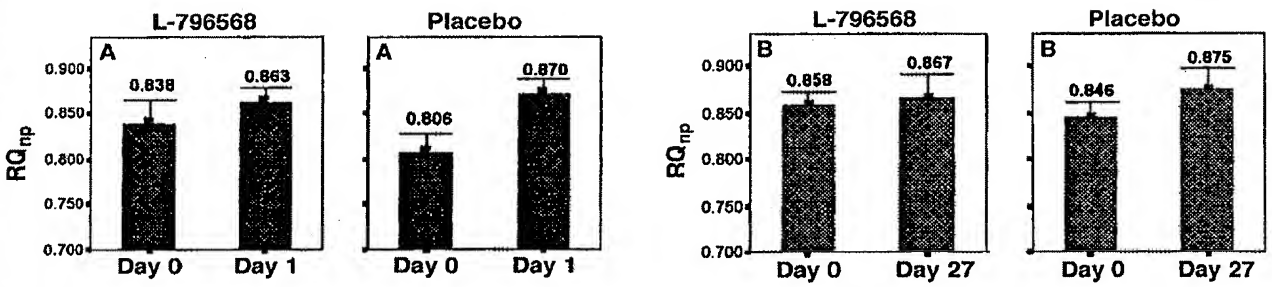

FIGURE 1. Acute effect (A): change in daytime nonprotein respiratory quotient (RQ_{np}) between day 0 (baseline) and day 1 (measured from 0 to 4 h postdose). There was a significant between-group difference without correction for baseline values ($P < 0.02$); however, when baseline data were included as a cofactor the difference was not significant ($P = 0.21$). Chronic effect (B): change in 24-h RQ_{np} between day 0 and day 27 ($P = 0.09$). $n = 10$ per group.

When we compared day 0 with day 1 to test for an acute effect, we observed no between-group differences in daytime EE (0.37 ± 0.47 and 0.41 ± 0.58 kJ/min for the placebo and L-796568 groups, respectively), but there was a significantly smaller increase ($P < 0.02$) in daytime nonprotein respiratory quotient (RQ_{np}) in the L-796568 group (0.025 ± 0.041) than in the placebo group (0.064 ± 0.021) (**Figure 1**). However, the difference was not significant ($P = 0.21$) when the higher baseline RQ_{np} values for the L-796568 group were included as a cofactor in the analysis. The same tendency was observed for RQ_{np} during exercise, although the difference was not significant (0.000 ± 0.040 and −0.039 ± 0.055 for the placebo and L-796568 groups, respectively).

For all the time intervals (ie, 24 h, sleep, daytime, postdinner, during exercise, and basal metabolic rate), changes in EE and RQ_{np} from day 0 to day 27 were not significantly different between the 2 groups (with or without adjustment for changes in FFM and energy balance), except for a significantly smaller increase in daytime RQ_{np} in the L-796568 group (unadjusted for energy balance; 0.044 ± 0.031 and 0.001 ± 0.040 in the placebo and L-796568 groups, respectively; $P < 0.02$) (**Table 4**). However, this significant difference in daytime RQ_{np} for the chronic response was no longer significant ($P = 0.15$) when the higher baseline RQ_{np} values for the L-796568 group were included as a cofactor in the analysis.

Compliance was assured by observation of daily dosing and by measurement of the mean predose plasma L-796568 concentrations on days 21, 25, and 28 (3-d mean ± SD = 77.2 ± 30.3 nmol/L); these values were as predicted on the basis of previous studies. Even though there was no overall difference between groups in the body composition variables, there was a significant inverse correlation between the change in fat mass (poststudy minus prestudy) and the average predose plasma L-796568 concentration in the L-796568 group ($r = -0.69$, $P < 0.03$), ie, higher L-796568 concentrations were associated with greater decreases in fat mass (**Figure 2**). The decreases in fat mass were small,

TABLE 4
Changes from day 0 (baseline) to day 27 (day 27 value minus day 0 value) for energy expenditure (EE) and nonprotein respiratory quotient (RQ_{np})[1]

	Placebo group ($n = 10$)	L-796568 group ($n = 10$)
24-h EE (kJ/min)	0.06 ± 0.36	0.06 ± 0.41
Sleeping EE (kJ/min)	0.01 ± 0.44	0.15 ± 0.32
Basal metabolic rate (kJ/min)	−0.14 ± 0.60	0.14 ± 0.62
Daytime EE (kJ/min)	0.17 ± 0.40	0.03 ± 0.44
Postdinner EE (kJ/min)	0.10 ± 0.48	0.16 ± 0.86
Exercise EE (kJ/min)[2]	−3.49 ± 5.64	−0.52 ± 1.60
24-h RQ_{np}	0.029 ± 0.021	0.009 ± 0.029
Sleeping RQ_{np}	0.046 ± 0.041	0.041 ± 0.037
Basal RQ_{np}	0.067 ± 0.039	0.044 ± 0.050
Daytime RQ_{np}[3]	0.044 ± 0.031	0.001 ± 0.040
Postdinner RQ_{np}	0.025 ± 0.031	0.029 ± 0.063
Exercise RQ_{np}	−0.027 ± 0.077	−0.045 ± 0.056

[1] $\bar{x}$ ± SD.
[2] Exercise value was measured during a 15-min session of cycling (1430–1445).
[3] Without the cofactor, $P < 0.02$ for the difference between the 2 groups in the magnitude of change from day 0 to day 27. With the baseline value as a cofactor, $P = 0.15$.

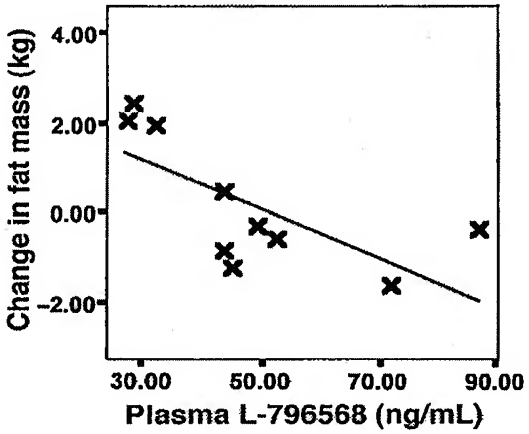

FIGURE 2. Correlation between mean predose plasma L-796568 concentration on days 21, 25, and 28 and change in fat mass from pretreatment to posttreatment ($r = -0.69$, $P < 0.03$); $n = 10$. Each × represents the mean L-796568 concentration for 1 subject on the 3 measurement days.

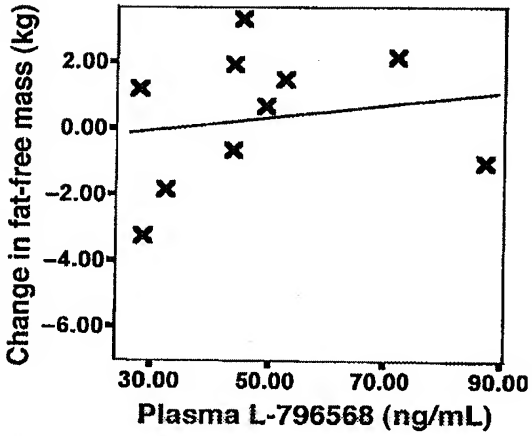

FIGURE 3. Correlation between mean predose plasma L-796568 concentration on days 21, 25, and 28 and change in fat-free mass from pretreatment to posttreatment ($r = 0.21$, $P = 0.56$); $n = 10$. Each × represents the mean L-796568 concentration for 1 subject on the 3 measurement days.

however. No significant correlations were found between plasma L-796568 concentration and changes in FFM (**Figure 3**) or other endpoints, including changes in 24-h EE ($r = -0.08$, $P = 0.98$), 24-h RQ_{np} ($r = 0.56$, $P = 0.09$), and the ratio of fat mass to FFM ($r = -0.52$, $P = 0.13$).

The results of the OGTTs showed no significant differences between the treatment groups in the changes in the incremental areas under the curve for plasma glucose, insulin, or glucagon responses. However, a time × day × group interaction effect was found ($P < 0.02$) for the glucose response, and subsequent unpaired t test analysis at each time point showed a significantly higher glucose concentration at the 120-min time point in the L-796568 group than in the placebo group on day 28 ($P < 0.03$) (**Figure 4**).

On day 14, fasting triacylglycerol, total cholesterol, and fatty acid concentrations were significantly decreased in the L-796568 group compared with the placebo group, but only the decrease in total cholesterol was significant when baseline values were included as a covariate ($P < 0.005$) (data not shown). There were no significant differences in the changes in glycerol between the groups.

For triacylglycerol and total cholesterol, there were significant decreases in the L-796568 group compared with the placebo group from baseline (day 0) to day 28 (**Table 5**). When the higher baseline values of the L-796568 group were taken into account, only the change in triacylglycerol remained significantly different between the groups (-0.76 ± 0.76 and 0.42 ± 0.31 mmol/L for the L-796568 and placebo groups, respectively; $P < 0.002$).

We found no significant differences between groups for blood concentrations of LDL cholesterol, HDL cholesterol, ketones, lactate, leptin, norepinephrine, or epinephrine, or for urinary nitrogen or catecholamine excretion. The 2 groups did

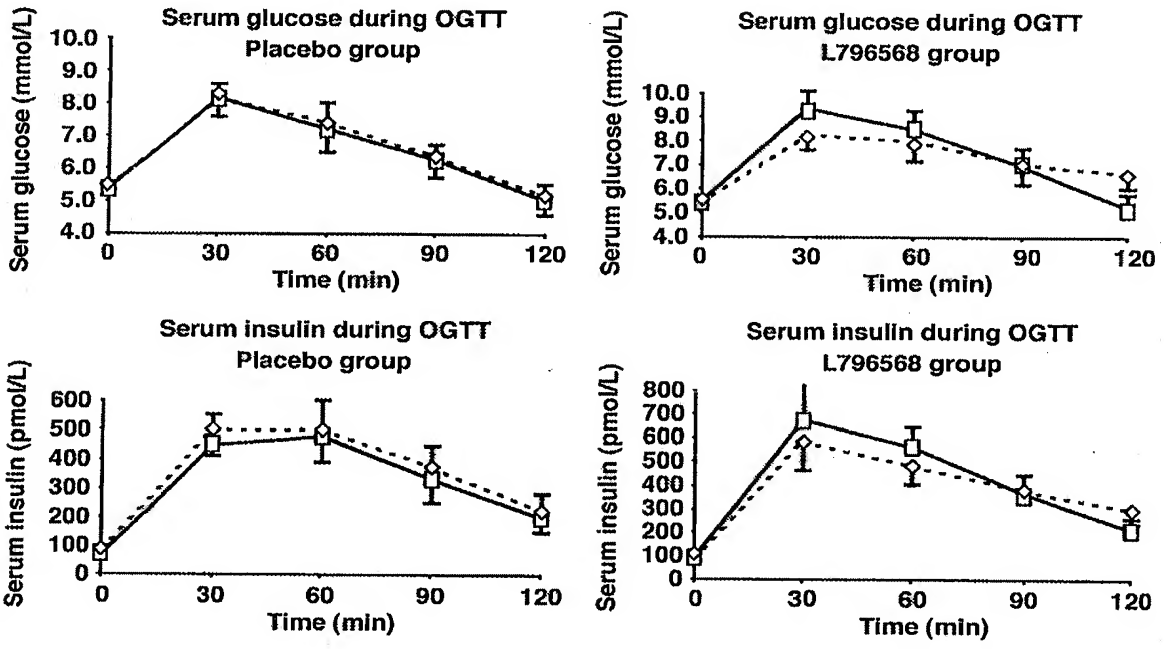

FIGURE 4. Glucose and insulin responses during oral-glucose-tolerance tests (OGTTs) performed pretreatment (□) and on day 28 (◆); $n = 10$ per group. No significant changes were found in the incremental area under the curve, but there was a significant time × day × group interaction effect ($P < 0.02$; general linear model for repeated-measures ANOVA) for glucose, with higher serum glucose at 120 min in the L-796568 group than in the placebo group on day 28 ($P < 0.03$).

TABLE 5
Changes in blood lipids from day 0 (baseline) to days 14 and 28

	Placebo group (n = 10)	L-796568 group (n = 10)	P^1	
			No cofactor	With cofactor
Fatty acids (μmol/L)				
Day 14 − day 0	14 ± 31[2]	−11 ± 11	<0.03	0.07
Day 28 − day 0	−17 ± 128	−8 ± 215	0.91	—
Glycerol (μmol/L)				
Day 14 − day 0	21 ± 50	5 ± 19	0.34	—
Day 28 − day 0	−4 ± 15	−6 ± 19	0.81	—
Triacylglycerols (mmol/L)				
Day 14 − day 0	0.19 ± 0.55	−0.84 ± 0.88	<0.01	0.13
Day 28 − day 0	0.42 ± 0.31	−0.76 ± 0.76	<0.001	<0.002
Total cholesterol (mmol/L)				
Day 14 − day 0	0.2 ± 0.5	−0.8 ± 0.6	<0.002	<0.005
Day 28 − day 0	0.1 ± 0.7	−0.7 ± 0.6	<0.02	0.07

[1] P values are for differences between groups (unpaired t test); the cofactor was the baseline value.
[2] $\bar{x}$ ± SD.

not differ significantly with regard to hunger or satiety ratings at lunch or dinner.

Nine subjects in the L-796568 group and 2 in the placebo group reported gastrointestinal side effects, primarily diarrhea, during the treatment period. No subjects reported tremor (data not shown).

DISCUSSION

Previous pharmacologic studies have used a variety of approaches to try to elucidate the thermogenic potential of β_3 receptors in humans, but these studies have reported conflicting results. One approach has been to study EE with nonspecific β agonists in the presence of β_1 and β_2 antagonists to isolate any effects caused by β_3 agonist stimulation. In one study, 43% of the thermogenic effect of ephedrine (which potentiates the synaptic release of noradrenaline) remained after pretreatment with the β_1 and β_2 antagonist nadolol (30). Other studies showed that isoprenaline and BRL35135 (nonspecific β_3 agonists) have thermogenic effects that are not completely abolished by nadolol (31, 32). However, these findings were not confirmed in other studies that used a similar approach (33, 34). A second approach has been to investigate the effect of putative β_3 agonists. Of all the previous studies on this topic, the one that seems the most informative evaluated the effect of the β_3 agonist CL316 243, at a dose of 1500 mg/d, on EE and RQ (10). CL316 243 is a partial but selective human β_3 agonist (60% activity compared with isoprenaline; > 1500-fold selectivity over β_1 and β_2) (35), but is ≈1000-fold less potent (EC_{50} = 3700 nmol/L) than is L-796568 (K Gottesdiener and Merck & Co, unpublished observations, 1999). Plasma concentrations in the study were low compared with its EC_{50} value, and CL316 243 failed to increase EE after 8 wk of chronic administration.

In the present study of obese subjects, 375 mg of the human β_3-adrenergic receptor agonist L-796568, taken once daily, had no effect on 24-h EE or on EE during any other time interval, neither acutely nor after 28 d of administration. These results were surprising, because an acute 8% increase in EE was observed after administration of a single 1000-mg dose of L-796568 to obese subjects who had fasted overnight (13). The lack of acute effect on EE on the first treatment day in this study was less surprising, because the present study had a different design in which subjects were not resting and were served a large breakfast during the measurements; these factors are both likely to increase variability.

One explanation for the lack of chronic effect of L-796568 on EE could be that the plasma concentrations were too low. Overall, we think this is unlikely for the following reasons: *1*) L-796568 is a very potent (EC_{50} ≈3.6 nmol/L) and full agonist of the human β_3-adrenergic receptor and average plasma concentrations were ≈77 nmol/L, or > 20-fold higher than EC_{50} values, throughout the day; *2*) lower plasma concentrations were associated with significant increases in EE in the rhesus monkey (K Gottesdiener and Merck & Co, unpublished observations, 1999); and *3*) in a separate study, this dosing regimen (375 mg with food) resulted in peak plasma concentrations of ≈175 nmol/L, which is well above the peak plasma concentrations (≈100 nmol/L) achieved in the acute study that led to an 8% increase in EE (13).

An alternative explanation for the lack of chronic effect on EE might be that the agonist- induced BAT proliferative capability of β_3 receptor–responsive tissues in humans was too low during chronic stimulation. BAT, the primary tissue that responds to β_3 stimulation in rodents and possibly in rhesus monkeys, is only present in very limited amounts in adult humans and has questionable functional capacity. Thus, an acute β_3-stimulated increase in EE in humans is less likely to be dependent on BAT and might be mediated directly by WAT and perhaps indirectly by the liver and muscles. This is consistent with studies in transgenic mice that showed that the major part of acute β_3-agonist-induced thermogenesis and lipolysis is mediated by WAT and not by BAT (36). Compared with β_1 and β_2 receptors, β_3 receptors have quite low expression in human WAT (37), yet seem capable of producing an acute increase in EE. In addition, BAT might be up-regulated after chronic β_3 receptor stimulation. One study showed that 28 d of treatment with the β_3 adrenergic receptor agonist L-755507 was sufficient to induce significant BAT proliferation and uncoupling protein 1 up-regulation in rhesus monkeys (12). If humans are similar to rhesus monkeys in this respect, this 28-d study might have led to BAT proliferation, uncoupling protein 1 up-regulation, and increases in EE that exceeded the acute effects.

Another likely explanation for the lack of chronic effect on EE is down-regulation of β_3 receptors, even though previous in vivo studies in rodents showed no signs of β_3-adrenergic receptor

agonist–induced down-regulation (38, 39). If down-regulation is the cause of the lack of chronic β_3-adrenergic receptor–mediated thermogenesis, this suggests that a different β_3-adrenergic receptor–desensitizing mechanism occurs in humans. However, we also cannot rule out the possibility that some type of negative feedback occurs, possibly via inhibition of lipolysis with indirect effects on EE. Studies in humans showed increased thermogenesis during intravenous infusions of lipid plus heparin (ie, increased fatty acids) (40), suggesting that mobilization of fatty acids may be the major determinant of β_3-agonist-induced thermogenesis. However, an attenuated response of β_3 agonist-mediated increases in plasma fatty acid concentrations was observed after 9 d of treatment with 375 mg L-796568 in healthy volunteers; the acute increases measured on the first treatment day were completely absent after 9 d of treatment (K Gottesdiener and Merck & Co, unpublished observations, 1999).

Interestingly, however, we did not find any β_3 agonist–induced changes in catecholamine concentrations or excretion, suggesting that there was no major influence on lipolysis via changes in endogenous catecholamine metabolism. The lack of effect of the agonist under conditions when food intake is not altered does not exclude the possibility that the drug may show thermogenic efficacy in preventing the fall in EE under conditions of hypocaloric dieting, ie, when sympathetic activity is low and there is a tendency for adrenergic receptors to be up-regulated.

In the present weight-maintenance study, FFM and fat mass did not differ significantly between groups. However, the observed changes in body fat mass in the L-796568 group were inversely correlated with plasma L-796568 concentrations measured at the end of the study period, suggesting sustained increased fat oxidation. After 28 d of treatment, there was no sustained increase in the mobilization of fatty acids, as assessed by measuring fasting concentrations of fatty acids and glycerol.

When baseline RQ_{np} values were included as a cofactor in the analysis, there was no significant effect of L-796568 on substrate partitioning represented by RQ or nonprotein RQ, but regarding acute induced thermogenesis, any acute effect on daytime RQ_{np} may be masked by interference induced by diet and physical activity. However, among all the measuring periods, daytime RQ_{np} shows the largest decrease and thus indicates an acute stimulatory effect of a drug on fat oxidation, which may be dependent on fatty acid mobilization. On the contrary, we did not find a significant chronic effect on substrate partitioning, as indicated by the lack of effect on 24-h RQ_{np} (Figure 1).

Treatment with L-796568 reduced plasma triacylglycerol and total cholesterol concentrations to a greater extent than did placebo after 14 d. In L-796568 studies conducted in dogs and monkeys, decreased triacylglycerol concentrations were also found (K Gottesdiener and Merck & Co, unpublished observations, 1999), and chronically decreased triacylglycerol concentrations were observed previously in selective β_3 agonist studies in obese mice (41). β_3 agonists were shown to improve glucose tolerance in humans (10, 42), but in this study, we found no significant effect of L-796568 on glucose tolerance. The plasma glucose profile over time in the L-796568 group shows lower and more sustained concentrations, which may have been caused by decreased gastric emptying resulting from the known effects of β_3 agents on gastric motility (43–45).

There was no evidence in this study that L-796568 had effects on β_1 and β_2 receptors, as indicated by the absence of tachycardia, tremor, and increased blood pressure and the lack of effects on plasma potassium. Significantly more subjects in the L-796568 group had gastrointestinal side effects such as diarrhea, an effect which was previously found in dogs (K Gottesdiener and Merck & Co, unpublished observations, 1999) but not in human studies of CL316243 (C Weyer, personal communication, 2001). In animal models, β_3 agonists had anorectic effects, but L-796568 did not seem to have any effect on appetite parameters assessed during the subjects' stays in the respiration chamber.

In conclusion, no chronic thermogenic effect of L-796568 was found in obese, nondiabetic young men. There was also no evidence of stimulation of fat oxidation by L-796568, although changes in fat mass correlated negatively with drug concentrations, suggesting some potential activity at the β_3 receptor. In addition, triacylglycerol concentrations decreased substantially in the L-796568 group. In contrast with most studies of nonspecific β_3 agonists, there was no evidence of β_1 or β_2 stimulation to confound these results. The lack of chronic effects most likely resulted from down-regulation of β_3 effects (indirectly or directly via down-regulation of receptors) or a lack of recruitment of BAT in humans, or both.

At the Copenhagen site, we thank the kitchen staff, Inge Timmermann, Kirsten Bryde Rasmussen, Martin Kreutzer, John Lind, and Benjamin Buemann and at the Maastricht site, we thank Gabby Hul, Paul Schoffelen, Joan Senden, and Jos Stegen.

REFERENCES

1. Krief A, Lönnqvist F, Raimbault S, et al. Tissue distribution of β_3-adrenergic receptor mRNA in man. J Clin Invest 1993;91:344–9.
2. Berkowitz DE, Nardone NA, Smiley RM, et al. Distribution of β_3-adrenoceptor mRNA in human tissues. Eur J Pharmacol 1995;289: 223–8.
3. Yoshida T, Sakane N, Wakabayashi Y, Umekawa T, Kondo M. Anti-obesity and anti-diabetic effects of CL316,243, a highly specific β_3-adrenoceptor agonist, in yellow KK mice. Life Sci 1994;54: 491–8.
4. Himms-Hagen J, Cui J, Danforth E, et al. Effect of CL-316,243, a thermogenic β_3-agonist, on energy balance and brown and white adipose tissues in rats. Am J Physiol 1994;266:R1371–82.
5. Arbeeny CM, Meyers DS, Hillyer DE, Bergquist KE. Metabolic alterations associated with the antidiabetic effect of β_3-adrenergic receptor agonists in obese mice. Am J Physiol 1995;268: E678–84.
6. Hoffstedt J, Lönnqvist F, Shimuzu M, Blaak E, Arner P. Effects of several putative β_3-adrenoceptor agonists on lipolysis in human omental adipocytes. Int J Obes Relat Metab Disord 1996;20: 428–34.
7. Galitzky J, Langin D, Verwaerde P, Montastruc J-L, Lafontan M, Berlan M. Lipolytic effects of conventional β_3-adrenoceptor agonists and of CGP 12,177 in rat and human fat cells: preliminary pharmacological evidence for a putative β_4-adrenoceptor. Br J Pharmacol 1997;122:1244–50.
8. Enocksson S, Shimizu M, Lönnqvist F, Nordenström J, Arner P. Demonstration of an in vivo functional β_3-adrenoceptor in man. J Clin Invest 1995;95:2239–45.
9. Zaagsma J, Nahorski SR. Is the adipocyte beta-adrenoceptor a prototype for the recently cloned atypical 'beta-3 adrenoceptor'? Trends Pharmacol Sci 1990;11:3–7.
10. Weyer C, Tataranni PA, Snitker S, Danforth E, Ravussin E. Increase in insulin action and fat oxidation following treatment with CL 316,243, a highly selective beta$_3$-adrenoceptor agonist in humans. Diabetes 1998;47:1555–61.
11. Mathvink RJ, Tolman JS, Chitty D, et al. Discovery of a potent, orally

bioavailable β_3 adrenergi receptor agonist, (R)-*N*-[4-[2[[2-hydroxy-2-(3-pyridinyl)ethyl]amino]ethyl]phenyl]-4-[4-[4-(trifluoromethyl)phenyl]-thiazol-2-yl]benzensulfonamide. J Med Chem 2000;43:3832–6.

12. Fisher MH, Amend AM, Bach TJ, et al. A selective human β_3 adrenergic receptor agonist increases metabolic rate in rhesus monkeys. J Clin Invest 1998;101:2387–93.
13. van Baak MA, Hul GB, Toubro S, et al. Acute effect of L-796568, a novel β_3-adrenergic receptor agonist, on energy expenditure in obese men. Clin Pharmacol Ther 2002;71:272–9.
14. Astrup A, Thorbek G, Lind J, Isaksson B. Prediction of 24-h energy expenditure and its components from physical characteristics and body composition in normal-weight humans. Am J Clin Nutr 1990; 52:777–83.
15. Schoffelen PFM, Westerterp K, Saris W, Ten Hoor F. A dual-respiration chamber system with automatic calibration. J Appl Physiol 1997;83: 2064–72.
16. Elia M, Livesey G. Energy expenditure and fuel selection in biological systems: the theory and practice of calculations based on indirect calorimetry and tracer methods. World Rev Nutr Diet 1992;70: 68–131.
17. Klausen B, Toubro S, Astrup A. Age and sex effects on energy expenditure. Am J Clin Nutr 1997;65:895–907.
18. Heitmann BL. Prediction of body water and fat in adult Danes from measurements of electrical impedance. A validation study. Int J Obes 1990;14:789–802.
19. Li R, Keymulen B, Gerlo E. Determination of glycerol in plasma by an automated enzymatic spectrophotometric procedure. Clin Chem Lab Med 2001;39:20–4.
20. Smedes F, Kraak JC, Poppe H. Simple and fast solvent extraction system for selective and quantitative isolation of adrenaline, noradrenaline and dopamine from plasma and urine. J Chromatogr 1982;231:25–39.
21. Trinder P. Determination of glucose in blood using glucose oxidase with an alternative oxygen receptor. Ann Clin Biochem 1969;6: 24–7.
22. Sugiuchi H, Uji Y, Okabe H, et al. Direct measurement of high-density lipoprotein cholesterol in serum with polyethylene glycol-modified enzymes and sulphated alpha-cyclodextrin. Clin Chem 1995;41:717–23.
23. Friedewald WT, Levy RI, Fredrickson DS. Estimation of the concentration of low-density lipoprotein cholesterol in plasmas, without use of the preparative ultracentrifuge. Clin Chem 1972;18:499–502.
24. Tietz NW, ed. Clinical guide to laboratory tests. 2nd ed. Philadelphia: WB Saunders, 1990.
25. Tietz NW, ed. Fundamentals of clinical chemistry. 3rd ed. Philadelphia: WB Saunders, 1987.
26. Lundholm L, Lundholm EM, Vamos N. Lactic acid assay with L(+) lactic acid dehydrogenase from rabbit muscle. Acta Physiol Scand 1963:58;243–9.
27. Elia M, Folmer P, Schlatman A, Goren A, Austen S. Carbohydrate, fat and protein metabolism in muscle and in the whole body after mixed meal ingestion. Metabolism 1988;37:542–51.
28. Burtis CA, Ashwood ER, eds. Tietz textbook of clinical chemistry. 2nd ed. Philadelphia: WB Saunders, 1994.
29. Flint A, Raben A, Blundell JE, Astrup A. Reproducibility, power and validity of visual analogue scales in assessment of appetite sensations in single test meal studies. Int J Obes Relat Metab Disord 1999; 23:1–11.
30. Liu Y-L, Toubro S, Astrup A, Stock MJ. Contribution of β_3-adrenoceptor activation to epinephrine-induced thermogenesis in humans. Int J Obes Relat Metab Disord 1995;19:678–85.
31. Wheeldon NM, McDevitt DG, Lipworth BJ. Do beta 3-adrenoceptors mediate metabolic responses to isoprenaline. Q J Med 1993;86: 595–600.
32. Wheeldon NM, Mcdevitt DG, Mcfarlane LC, Lipworth BJ. Beta-adrenoceptor subtypes mediating the metabolic effects of BRL 35135 in man. Clin Sci (Colch) 1994;86:331–7.
33. Blaak EE, van Baak MA, Kempen KPG, Saris WHM. Role of α- and β-adrenoceptors in sympathetically mediated thermogenesis. Am J Physiol 1993;264:E11–7.
34. Schiffelers SL, Blaak EE, Saris WH, van Baak MA. In vivo beta3-adrenergic stimulation of human thermogenesis and lipid use. Clin Pharmacol Ther 2000;67:558–66.
35. Dolan JA, Muenkel HA, Burns MG, et al. Beta-3 adrenoceptor selectivity of the dioxolane dicarboxylate phenethanolamines. J Pharmacol Exp Ther 1994;269:1000–6.
36. Grujic D, Susulic VS, Harper M-E, et al. β_3-adrenergic receptors on white and brown adipocytes mediate β_3-selective agonist-induced effects on energy expenditure, insulin secretion and food intake. J Biol Chem 1997;272:17686–93.
37. Revelli J-P, Muzzin P, Paoloni A, Moinat M, Giacobino J-P. Expression of the β_3-adrenergic receptor in human white adipose tissue. J Mol Endocrinol 1993;10:193–7.
38. Thomas RF, Holt BD, Schwinn OA, Liggett SB. Long-term agonist exposure induces up-regulation of β_3-adrenergic receptor expression via multiple cAMP response elements. Proc Natl Acad Sci U S A 1992;89:4490–4.
39. Yoshida T, Umekawa T, Sakane Nkogure A, Kondo M. Long-term exposure of a β_3-adrenoceptor agonist induces up-regulation of β_3-, but not β_1-adrenoceptor in adipose tissue in OLEFT rats with obesity and diabetes. Int J Obes Relat Metab Disord 1998;22:S187 (abstr).
40. Schiffelers SLH, Saris WHM, van Baak MA. The effect of an increased NEFA concentration on thermogenesis and substrate oxidation in obese and lean men. Int J Obes Relat Metab Disord 2001; 25:33–8.
41. Yoshitomi H, Yamazaki K, Abe S, Tanaka I. Differential regulation of mouse uncoupling proteins among brown adipose tissue, white adipose tissue, and skeletal muscle in chronic β_3 adrenergic receptor agonist treatment. Biochem Biophys Res Commun 1998; 253:85–91.
42. Mitchell TH, Ellis RMD, Smith SA, Robb G, Cawthorne MA. Effects of BRL 35135, a β-adrenoceptor agonist with novel selectivity in obese subjects. Int J Obes 1989;13:757–66.
43. Fletcher DS, Candelore MR, Grujic D, et al. Beta-3 adrenergic receptor agonists cause an increase in gastrointestinal transit time in wild-type mice, but not in mice lacking the beta-3 adrenergic receptor. J Pharmacol Exp Ther 1998;287:720–4.
44. De Ponti F, Modini C, Gibelli G, Crema F, Frigo G. Atypical β-adrenoceptors mediating relaxation in the human colon: functional evidence for β_3- rather than β_4-adrenoceptors. Pharmacol Res 1999; 39:345–8.
45. Manara L, Croci T, Aureggi G, et al. Functional assessment of β adrenoceptor subtypes in human colonic circular and longitudinal (taenia coli) smooth muscle. Gut 2000;47:337–42.

Acute effect of L-796568, a novel β_3-adrenergic receptor agonist, on energy expenditure in obese men

Objective: Our objective was to investigate the thermogenic efficacy of single oral doses of the novel β_3-adrenergic receptor agonist L-796568 [(*R*)-*N*-[4-[2-[[2-hydroxy-2-(3-pyridinyl)ethyl]amino]ethyl]-phenyl]-4-[4-[4-(trifluoromethyl)phenyl]thiazol-2-yl]-benzenesulfonamide, dihydrochloride] in humans.
Methods: Twelve healthy overweight to obese men participated in this 2-center, 3-period, randomized, placebo-controlled, crossover trial. In each period subjects received 250 mg L-796568, 1000 mg L-796568, or placebo. Energy expenditure and respiratory quotient were determined by indirect calorimetry; blood samples were taken; and ear temperature, heart rate, and blood pressure were measured at baseline and during the 4-hour period after administration.
Results: Energy expenditure increased significantly after the 1000-mg dose (about 8%) and this was accompanied by an increase in plasma glycerol and free fatty acid concentrations. Systolic blood pressure also increased significantly. No changes in heart rate, diastolic blood pressure, ear temperature, plasma catecholamine, potassium, or leptin were found.
Conclusions: Single-dose administration of 1000 mg of the novel β_3-adrenergic receptor agonist L-796568 increased lipolysis and energy expenditure in overweight men. This is the first study to show such an effect of β_3-adrenergic receptor agonists in humans without significant evidence for β_2-adrenergic receptor involvement. (Clin Pharmacol Ther 2002;71:272-9.)

Marleen A. van Baak, PhD, Gabby B. J. Hul, MSc, Søren Toubro, PhD, Arne Astrup, MD, PhD, Keith M. Gottesdiener, MD, Marina DeSmet, PharmD, PhD, and Wim H. M. Saris, MD, PhD *Maastricht, The Netherlands, Copenhagen, Denmark, and Rahway, NJ*

The prevalence of obesity is increasing in many countries all over the world.[1] The health risks associated with obesity, such as type 2 diabetes, hypertension, coronary artery disease, gallbladder disease, and arthritis, form a serious public health problem for the years to come if no effective strategies to prevent and treat it are developed.[1] Comprehensive weight management programs, including a reduction of energy intake through an energy-restricted diet and an increase in energy expenditure through increased levels of physical activity in combination with a behavior modification program, have been developed. In many cases such programs lead to considerable short-term weight loss. However, long-term maintenance of the reduced weight often fails to occur. Current pharmacologic approaches to the treatment of obesity focus on reinforcement of these programs and they have been shown to improve long-term weight maintenance success.[2,3] The pharmacologic agents currently available for the management of obesity (orlistat and sibutramine) are effective through decreased nutrient absorption and appetite suppression, respectively. The approach of increased energy expenditure has been less well explored.

The peripheral sympathetic nervous system plays an important role in the regulation of energy expenditure.[4] Stimulation of sympathetic activity results in an

From the Nutrition and Toxicology Research Institute (NUTRIM), Department of Human Biology, Maastricht University; the Research Department of Human Nutrition, Royal Veterinary and Agricultural University, Copenhagen; and Merck & Co, Inc, Rahway.
Supported by Merck & Co. Inc. Rahway, NJ.
Received for publication July 19, 2001; accepted Dec 29, 2001.
Reprint requests: Marleen A. van Baak, PhD, Department of Human Biology. Maastricht University, PO Box 616, 6200 MD Maastricht, The Netherlands.
E-mail: *m.vanbaak@hb.unimaas.nl*

0009-9236/2002/$35.00 + 0 **13/1/122527**
doi:10.1067/mcp.2002.122527

increase of resting energy expenditure in humans, which is mediated by β-adrenergic receptors.[5] Both β_1- and β_2-adrenergic receptors lead to thermogenesis on stimulation.[6,7] Obesity appears to be associated with a blunted response to sympathetic stimulation that is probably caused mainly by β_2-adrenergic receptor malfunction.[7,8] However, treatment of obesity with the classic nonselective or β_2-selective agonists is not possible, because of the many unacceptable side effects of these drugs.

The discovery of a third β-adrenergic receptor subtype in humans, which in animal models has been shown to stimulate lipolysis in brown and white adipose tissue and lead to thermogenesis in brown adipocytes, has opened new possibilities for treatment of human obesity by selective β_3-adrenergic receptor stimulation. In humans the presence of β_3-adrenergic receptor mRNA has been shown in brown and white adipose tissue and the gall bladder, colon, stomach, small intestine, prostate gland, and heart but not in skeletal muscle or the liver, lung, kidney, thyroid, or lymphocytes.[9-12] One study has more recently provided evidence for the presence of the β_3-adrenergic receptor protein in human gastrocnemius muscle and the right atrium.[13] Although most of the currently available β_3-adrenergic receptor agonists are only weak partial agonists of the human β_3-adrenergic receptor and usually not very selective, a functional role for the β_3-receptor in adipocyte lipolysis has been suggested by studies in isolated human omental and subcutaneous fat cells[14,15] and in vivo in microdialysis studies with such agonists.[16-18] Because these drugs are not available for intravenous or oral administration in humans, their thermogenic efficacy is unknown. Indirect studies that used combinations of different sympathomimetics and blockers to dissect out the contribution of the β_3-receptor to human thermogenesis have yielded inconsistent results.[19-22]

L-796568 [(*R*)-*N*-[4-[2-[[2-hydroxy-2-(3-pyridinyl) ethyl]amino]ethyl]-phenyl]-4-[4-[4-(trifluoromethyl)phenyl]thiazol-2-yl]-benzenesulfonamide, dihydrochloride] is a newly developed β_3-adrenergic receptor agonist with high affinity (concentration that produces 50% of the maximum possible response [EC_{50}], 3.6 ± 2.2 nmol/L) and efficacy (94% ± 10% of maximal cyclic adenosine monophosphate accumulation by isoproterenol [INN, isoprenaline]) for the cloned human β_3-adrenergic receptor transfected in Chinese hamster ovary cells.[23] L-796568 is a weak partial agonist at the human β_1-receptor and β_2-receptor, with EC_{50} values of 4.8 and 2.4 μmol/L, respectively, and efficacy of 25% of isoproterenol activity.[23] Phase I human studies showed that L-796568 was well tolerated in doses up to 1500 mg. Administration of L-796568 therefore allows us to study, for the first time, the effects of a specific human β_3-adrenergic receptor agonist on in vivo lipolysis and thermogenesis in humans. This study was designed to investigate the thermogenic efficacy of single oral doses of 250 and 1000 mg L-796568 in obese men.

METHODS

Subjects. Twelve healthy, nonsmoking male volunteers between 18 and 45 years old (mean ± SD, 34.4 ± 5.8 years) were included in the study. All of the subjects had maintained a stable weight (±4 kg) and had a body mass index between 28 and 34 kg/m^2 (mean ± SD, 30.7 ± 2.1 kg/m^2). None of the volunteers had participated in an organized weight loss program during the previous 3 months. All had normal blood pressure measurements (90 to 150 mm Hg systolic and 50 to 95 mm Hg diastolic blood pressure) and resting heart rates (<90 beats/min). Habitual heavy consumers of coffee (>4 cups per day) were excluded. Current or anticipated use of any prescription or nonprescription drugs was not allowed.

Experimental protocol. The study was a 2-center, 3-period, randomized, placebo-controlled, crossover trial. In each period subjects received 250 mg L-796568, 1000 mg L-796568, or placebo in a balanced fashion. All drug supplies were provided as a "double dummy," so investigators and subjects were blinded to the treatment regimen. A washout period of 6 to 8 days between study periods allowed plasma levels of L-796568 to dissipate. Prestudy procedures included a medical history and a physical examination that included vital signs, determination of body mass index, measurement of thyroid function parameters, a safety laboratory panel for blood and urine, and a 12-lead electrocardiogram (ECG).

On the test days the subjects came to the laboratory in the morning after an overnight fast. Urine was collected for the safety panel. Subjects rested in a semirecumbent position, and a catheter was inserted into a forearm vein of each subject for blood sampling (100 minutes before dosing). Continuous heart rate and blood pressure monitoring was started, and heart rate and blood pressure were registered at 65 and 20 minutes before dosing. At 10 minutes before dosing, blood samples were taken for plasma catecholamine concentration (heparinized tubes that contained glutathione), plasma free fatty acids and glycerol concentration (ethylenediaminetetra-acetic acid tubes), plasma potassium (lithium-heparin tubes), and serum leptin concentration (serum tubes), as well as for the safety laboratory panel.

At 0 minutes before dosing, another blood sample was obtained for free fatty acids and glycerol concentration and for serum leptin concentration. After all blood was drawn, the catheter was flushed with saline solution. Ear temperature was determined at 60 minutes before dosing. Energy expenditure was measured for 30 minutes, from 60 minutes before dosing to 30 minutes before dosing, as a predose baseline.

After the baseline measurements, each subject was given a single oral dose of the study drug (250 mg or 1000 mg L-796568 or placebo) with 240 ml water and continued to fast and rest in a semisupine position for 4 hours. During this period, energy expenditure was measured during the last 20 minutes of each half hour. The first 10 minutes of each half hour was used for either blood sampling or calibration or both. Blood pressure and heart rate continued to be monitored and were recorded every 30 minutes. Blood samples for potassium, free fatty acids, and glycerol were obtained at 1, 2, 3, and 4 hours after dosing. Blood samples were obtained 1.5 and 4 hours after dosing for plasma catecholamines and 4 hours after dosing for leptin. The catheter was flushed with saline solution after each blood sample was drawn. Four hours after dosing, ear temperature was measured and a 12-lead ECG was obtained.

Methods. Energy expenditure was determined by indirect calorimetry with use of a ventilated hood system. Flow through the hood was set at approximately 50 L/min and was measured with a dry gas meter (Maastricht: Schlumberger, Dordrecht, The Netherlands; Copenhagen: Oxycon-beta, Mijnhardt, The Netherlands). $\dot{V}O_2$ and $\dot{V}CO_2$ were determined every 15 seconds from flow through the hood and the difference in oxygen (Maastricht: paramagnetic oxygen analyzer, Servomex, Crowborough, United Kingdom; Copenhagen: Oxycon-beta) and carbon dioxide (Maastricht: paramagnetic CO_2 analyzer, Servomex; Copenhagen: Oxycon-beta) concentrations between ingoing and outgoing air. Identical calibration procedures were used in the two centers. Respiratory quotient was calculated as $\dot{V}CO_2/\dot{V}O_2$. Energy expenditure was calculated from $\dot{V}O_2$ and $\dot{V}CO_2$ with the abbreviated Weir formula.[24]

Blood pressure and heart rate were measured with a semiautomated device (Maastricht: Omron 705 CP, Hamburg, Germany; Copenhagen: digital blood pressure meter model UA-743, A & D Company, Tokyo, Japan). Heart rate monitoring was performed by means of a 3-lead ECG monitor (Maastricht: Cardiolife, Nikon-Kohden, Tokyo, Japan; Copenhagen: Diascope 2, model 211, Simonsen & Weel, Copenhagen, Denmark). The 12-lead ECG was registered by means of a Cardiette Daedalus View H, H&C Medical Devices, Cavareno, Italy (Maastricht), or a Microsmart MC, Marquette Hellige, Freiburg, Germany (Copenhagen).

Analytic methods. Blood for serum leptin was allowed to clot at least 30 minutes and was then centrifuged for 15 minutes at 1200*g* at room temperature. All other blood samples were centrifuged immediately at 4°C for 15 minutes at 1200*g* except for the sample for potassium, which was centrifuged at room temperature. Plasma and serum were stored at –80°C until analysis.

Plasma free fatty acids,[25] glycerol,[26] potassium (direct potentiometry with an ion-selective electrode), and serum leptin[27] were analyzed at the Department of Clinical Chemistry, Academic Hospital of the Free University of Brussels (Brussels, Belgium). Plasma catecholamine concentrations (norepinephrine and epinephrine) were analyzed at the Department of Human Biology in Maastricht by HPLC with electrochemical detection by use of a kit from Recipe (München, Germany).[28]

Data analysis. Data are presented as mean values ± SD, unless stated otherwise. For all variables, mean values at baseline (ie, predose for each treatment period) and at 4 hours after dosing were calculated. Within-treatment changes from baseline to 4 hours after dosing were computed by subtracting the baseline value from the 4-hour postdose value [Δ4-0 h]). In addition, mean energy expenditure during the 4-hour postdose period (mean 0-4 h) and 1-hour peak values were calculated for energy expenditure (for each treatment the two 20-minute measurements within each hour were averaged and the highest 1-hour mean value was chosen as the 1-hour peak value). The 3 treatments were compared by ANOVA for repeated measures (baseline values, 4-hour postdose values, and changes over the 4-hour postdose period [Δ4-0 h]). In case of a significant overall ANOVA outcome ($P < .050$), post hoc comparisons between the 250- and 1000-mg doses of L-796568 and placebo were performed by paired *t* tests. Within-treatment differences between the 4-hour postdose and baseline measurements were analyzed by paired *t* tests. A *P* value <.050 was considered to be statistically significant.

RESULTS

L-796568 was generally well tolerated in this study. Side effects were reported by 7 subjects, were of mild to moderate intensity, and had disappeared within 24 hours. No tremor was reported. No significant changes in safety laboratory parameters or urine composition were found in any subjects during the course of the study, except in 1 subject in whom low total cholesterol was found that appeared to be unrelated to the drug. At baseline there were no statistically significant differences for any of the variables among conditions.

Table I. Values of all variables (mean ± SD) at baseline (0 h) and at 4 hours after dosing (4 h) and the change during the 4-hour postdose period (Δ4-0 h)

Variable and treatment	*0 h*	*4 h*	*Δ4-0 h*
Energy expenditure (kJ/min)			
Placebo	6.05 ± 0.55	6.14 ± 0.59	0.09 ± 0.36
250 mg	6.11 ± 0.53	6.16 ± 0.48	0.06 ± 0.21
1000 mg	5.97 ± 0.58	6.43 ± 0.52**	0.46 ± 0.31**
ANOVA	$P = .38$	$P < .050$	$P < .001$
Ear temperature			
Placebo	36.6°C ± 0.5°C	36.7°C ± 0.7°C	0.13°C ± 0.40°C
250 mg	36.5°C ± 0.4°C	36.7°C ± 0.6°C	0.15°C ± 0.48°C
1000 mg	36.4°C ± 0.5°C	36.8°C ± 0.5°C	0.33°C ± 0.22°C
ANOVA	$P = .35$	$P = .80$	$P = .19$
Plasma free fatty acids (mmol/L)			
Placebo	0.341 ± 0.115	0.542 ± 0.144	0.183 ± 0.138
250 mg	0.303 ± 0.123	0.585 ± 0.115	0.283 ± 0.166
1000 mg	0.327 ± 0.100	0.780 ± 0.185**	0.444 ± 0.224**
ANOVA	$P = .63$	$P < .001$	$P < .010$
Plasma glycerol (μmol/L)			
Placebo	48.0 ± 17.3	60.8 ± 17.9	11.6 ± 21.4
250 mg	41.1 ± 9.6	63.4 ± 13.8	23.1 ± 14.8*
1000 mg	41.4 ± 10.1	78.7 ± 20.7**	36.3 ± 19.6**
ANOVA	$P = .20$	$P < .001$	$P < .001$
Respiratory quotient			
Placebo	0.803 ± 0.062	0.793 ± 0.034	−0.010 ± 0.035
250 mg	0.834 ± 0.052	0.796 ± 0.027	−0.038 ± 0.034
1000 mg	0.818 ± 0.040	0.783 ± 0.015	−0.035 ± 0.040
ANOVA	$P = .26$	$P = .39$	$P = .08$
Plasma potassium (mmol/L)			
Placebo	4.01 ± 0.24	3.97 ± 0.21	−0.04 ± 0.14
250 mg	4.10 ± 0.28	3.87 ± 0.14	−0.23 ± 0.24
1000 mg	4.18 ± 0.59	3.94 ± 0.14	−0.24 ± 0.55
ANOVA	$P = .56$	$P = .22$	$P = .29$
Heart rate (beats/min)			
Placebo	62.8 ± 11.1	59.4 ± 12.5	−3.5 ± 7.1
250 mg	60.3 ± 8.1	62.0 ± 7.0	1.5 ± 5.7
1000 mg	61.2 ± 8.2	61.4 ± 9.0	−0.2 ± 4.4
ANOVA	$P = .43$	$P = .62$	$P = .14$
Systolic blood pressure (mm Hg)			
Placebo	128.6 ± 6.6	130.1 ± 12.6	1.1 ± 10.0
250 mg	132.4 ± 6.2	135.6 ± 12.2*	3.2 ± 8.6
1000 mg	126.8 ± 9.7	139.1 ± 13.0**	12.2 ± 14.2**
ANOVA	$P = .16$	$P < .050$	$P < .010$
Diastolic blood pressure (mm Hg)			
Placebo	82.9 ± 6.7	85.7 ± 7.6	2.6 ± 5.8
250 mg	85.5 ± 7.1	87.3 ± 10.0	1.8 ± 6.1
1000 mg	81.9 ± 6.8	88.8 ± 10.5	6.8 ± 8.6
ANOVA	$P = .12$	$P = .29$	$P = .13$
Plasma norepinephrine (ng/L)			
Placebo	262 ± 70	271 ± 92	9.0 ± 54.1
250 mg	258 ± 108	278 ± 113	20.5 ± 64.1
1000 mg	289 ± 90	324 ± 129	34.8 ± 114.5
ANOVA	$P = .29$	$P = .16$	$P = .69$
Plasma epinephine (ng/L)			
Placebo	28 ± 14	38 ± 20	9.8 ± 21.0
250 mg	27 ± 21	32 ± 19	4.9 ± 12.3
1000 mg	28 ± 14	30 ± 14	2.2 ± 17.9
ANOVA	$P = .97$	$P = .21$	$P = .43$
Serum leptin (μg/L)			
Placebo	12.6 ± 7.6	11.8 ± 6.7	−0.78 ± 1.61
250 mg	14.0 ± 7.4	12.8 ± 6.6	−1.18 ± 1.17
1000 mg	11.9 ± 6.7	11.0 ± 6.9	−0.87 ± 0.54
ANOVA	$P = .18$	$P = .10$	$P = .70$

ANOVA *P* value refers to overall between-groups ANOVA outcome.
*$P < .05$, **$P < .001$, versus placebo (post hoc paired *t* tests).

Thermogenic effects. The changes in energy expenditure from baseline during the 4-hour postdose period are shown in Fig 1. At 4 hours after dosing, energy expenditure was significantly different among the 3 conditions ($P < .05$, between-treatments overall ANOVA; Table I). Energy expenditure increased significantly from baseline to 4 hours after dosing (by 0.46 ± 0.31 kJ/min, 7.8%) after the 1000-mg dose ($P < .001$, within-treatment paired t test). No statistically significant changes were found after the 250-mg dose (0.06 ± 0.21 kJ/min, 1.0%; $P = .35$, within-treatment paired t test) or after placebo (0.09 ± 0.36 kJ/min, 1.5%; $P = .41$, within-treatment paired t test). The changes differed significantly among the 3 conditions ($P < .001$, between-treatments overall ANOVA; $P < .001$ for 1000 mg versus placebo; $P = .67$ for 250 mg versus placebo; Table I). Comparison of the 1-hour peak energy expenditures or mean energy expenditure during the period from baseline to 4 hours after dosing among the 3 treatments did not yield statistically significant differences ($P = .32$ for 1000 mg versus placebo; $P = .88$ for 250 mg versus placebo; between-treatments overall ANOVA).

Ear temperature values at different time points are shown in Table I. No statistically significant differences were found at any time point, and the 4-hour postdose changes did not differ among treatments ($P = .19$, between-treatments overall ANOVA).

Metabolic effects. The plasma concentrations of free fatty acids and glycerol showed a dose-dependent increase during the 4-hour postdose period (Fig 2), which differed statistically significantly among conditions ($P < .010$ for Δ4-0 h, between-treatments overall ANOVA). The changes after the 250-mg dose (0.283 ± 0.166 mmol/L for Δ4-0 h free fatty acids; 23 ± 15 μmol/L for Δ4-0 h glycerol) and after the 1000-mg dose (0.444 ± 0.224 mmol/L for Δ4-0 h free fatty acids; 36 ± 20 μmol/L for Δ4-0 h glycerol) differed significantly from those after placebo (0.183 ± 0.138 mmol/L for Δ4-0 h free fatty acids; 12 ± 21 μmol/L for Δ4-0 h glycerol) (Δ4-0 h free fatty acids: $P < .010$, between-treatments overall ANOVA; $P = .09$ for 250 mg versus placebo; $P < .005$ for 1000 mg versus placebo; Δ4-0 h glycerol: $P < .001$, between-treatments overall ANOVA; $P < .050$ for 250 mg versus placebo; $P < .005$ for 1000 mg versus placebo; Table I).

The respiratory quotient at 4 hours after dosing did not differ statistically significantly among treatments ($P = .39$, between-treatments overall ANOVA; Table I), although there was a tendency toward a reduction in the respiratory quotient after the 250-mg (–0.038 ± 0.034) and 1000-mg (–0.035 ± 0.040) doses compared with placebo (–0.010 ± 0.035), but the difference among treatments did not reach statistical significance (Δ4-0 h respiratory quotient: $P = .08$, between-treatments overall ANOVA). Plasma potassium concentrations showed no statistically significant changes during any of the treatments (Table I).

Cardiovascular effects. There were no statistically significant differences in heart rate between the 3 treatments at any time point, and the changes during the 4-hour postdose period did not differ significantly. At 4 hours after dosing, there was a statistically significant difference in systolic blood pressure among treatments ($P < .050$, between-treatments overall ANOVA; Table I). The increase in systolic blood pressure during the 4-hour postdose period was 1.5 ± 10.4 mm Hg after placebo, 3.2 ± 8.7 mm Hg after 250 mg L-796568, and 12.2 ± 13.7 mm Hg after 1000 mg L-796568 ($P < .005$, between-treatments ANOVA; $P = .41$ for 250 mg versus placebo; $P < .010$ for 1000 mg versus placebo; Table I). No statistically significant differences in diastolic blood pressure were observed during the study period (Table I).

Hormonal effects. No differences in plasma norepinephrine, epinephrine, or serum leptin concentrations were found among treatments during the 4-hour study period (Table I).

DISCUSSION

Despite the very clear role of β_3-adrenergic receptors in the regulation of energy expenditure in several animal models, their importance in human thermogenesis has not yet been convincingly shown. Several β_3-adrenergic receptor agonists have been tested in humans, but because of their poor selectivity and efficacy, the results so far have not been convincing.[29-32] In contrast to these compounds, L-796568 is both a highly selective and a highly effective agonist of the human β_3-adrenergic receptor in vitro.[23] This study clearly showed that L-796568 also has lipolytic and thermogenic activity in vivo after single-dose administration to obese men. At 4 hours after administration, the 1000-mg dose had increased energy expenditure by about 8%. The time to peak plasma concentration of L-796568 has been shown to be about 4 to 5 hours.[33] In this study the plasma concentration of L-796568 therefore probably had not reached its peak in all individuals after the 4-hour period, and a further thermogenic effect by L-796568 after 4 hours is likely.

In vitro the EC_{50} of L-796568 for stimulation of the human β_3-adrenergic receptor was 3.6 nmol/L. The EC_{50} values of L-796568 for human β_1-adrenergic receptor (4770 nmol/L) and β_2-adrenergic receptor stimulation (2405 nmol/L) were much higher than

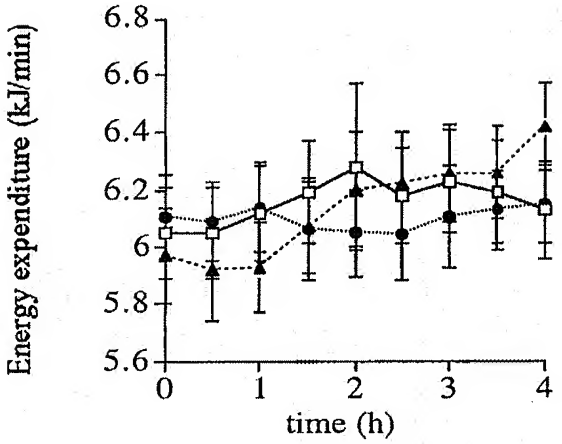

Fig 1. Energy expenditure (mean ± SEM) after placebo *(squares)*, 250 mg L-796568 *(circles)*, and 1000 mg L-796568 *(triangles)*.

those for human β_3-adrenergic receptor stimulation.[23] In another study it was found that the peak plasma concentration of L-796568 was about 28.5 nmol/L after a single 250-mg dose and about 89.4 nmol/L after a single 1000-mg dose in lean healthy volunteers (Merck Research Laboratories. Data on file). Both concentrations were well above the EC_{50} of β_3-adrenergic receptor stimulation, and the highest concentration was still >25-fold lower than the EC_{50} for β_2-adrenergic receptor stimulation and >50-fold lower than the EC_{50} for β_1-adrenergic receptor stimulation. However, a significant contribution of β_2- or β_1-adrenergic receptor-mediated stimulation cannot be fully excluded only on the basis of comparisons with in vitro EC_{50} values. Tremor and hypokalemia, indicators of β_2-adrenergic receptor stimulation, were not evident and it is unlikely that the effects of L-796568 were the result of stimulation of sympathetic nervous system activity because plasma catecholamine concentrations did not change.

Several in vitro studies have shown that human subcutaneous adipose tissue and especially omental adipose tissue express functional β_3-adrenergic receptors.[14,15] Microdialysis studies have shown that these receptors are also functional in situ.[16-18] This study confirms that systemic administration of a β_3-adrenergic receptor agonist is also capable of stimulating lipolysis in vivo. In a recent study we showed that increased plasma concentrations of free fatty acids induced thermogenesis in lean and obese subjects in the absence of stimulation by the sympathetic nervous system.[33] It is

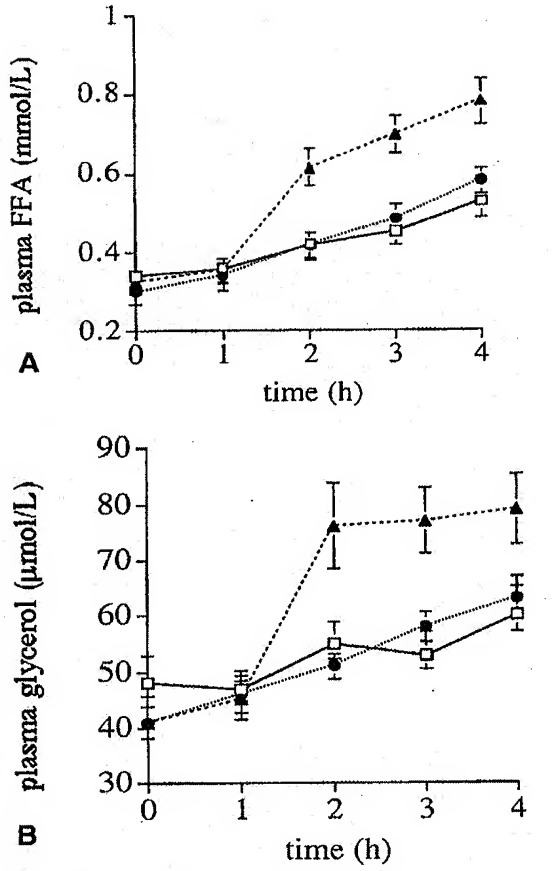

Fig 2. Mean ± SEM plasma free fatty acid concentrations (FFA; **A**) and glycerol concentrations **(B)** after placebo *(squares)*, 250 mg L-796568 *(circles)*, and 1000 mg L-796568 *(triangles)*.

therefore conceivable that the thermogenic response after L-796568 administration is caused by the β_3-adrenergic receptor-mediated stimulation of lipolysis and does not involve any further β_3-adrenergic receptor-mediated effects.

Systolic blood pressure increased significantly after L-796568. In the absence of an increase in heart rate, this suggests increased contractility of the heart or an increase in total peripheral resistance. However, diastolic blood pressure did not increase significantly, which does not support an increase in peripheral resistance. Moreover, in vivo and in vitro experiments in different animal species suggest a vasodilatory effect

of β_3-adrenergic agonists.[34] The presence of β_3-adrenergic receptors in the human heart has been reported for the right atrium[13] and for the ventricular endomyocardium.[12] To date, the functional role of the atrial β_3-adrenergic receptors is unclear. Stimulation of the ventricular β_3-adrenergic receptors produces a negative inotropic effect in animals and in human ventricular endomyocardial biopsies.[12,34] On the basis of these findings, a role for the up-regulation of β_3-adrenergic receptors in human heart failure as a protection against further myocyte damage has been proposed.[34] However, a negative inotropic effect of stimulation of β_3-adrenergic receptors is not in line with the increase in systolic blood pressure that was observed in this study. On the basis of these data, an increased contractility of the heart as a result of β_1-adrenergic receptor stimulation by L-796568 cannot be fully excluded. However, the pattern of changes of the different variables after L-796568 is not identical to that after specific β_1- (or β_2)-adrenergic receptor stimulation.[33]

In conclusion, single-dose administration of 1000 mg of the novel β_3-adrenergic receptor agonist L-796568 increased lipolysis and energy expenditure in overweight men. This is the first study to show such an effect of β_3-adrenergic receptor agonists in humans, without significant evidence for β_2-adrenergic receptor involvement. Involvement of β_1-adrenergic receptor stimulation could not be fully excluded but seems to be unlikely in view of the higher EC_{50} for human β_1-adrenergic receptor stimulation than for human SYMBOLB_3-adrenergic receptor stimulation in vitro and the plasma concentrations likely to be present.

We thank Jos Stegen for his analysis of the plasma catecholamines.

References

1. World Health Organization. Obesity: preventing and managing the global epidemic. Geneva (Switzerland): World Health Organization; 2000. WHO Technical Report Series No.: 894.
2. Sjöström L, Rissanen A, Andersen T, Boldrin M, Golay A, Koppeschaar HP, et al. Randomised placebo-controlled trial of orlistat for weight loss and prevention of weight regain in obese patients. European Multicentre Orlistat Study Group. Lancet 1998;352:167-72.
3. James WP, Astrup A, Finer N, Hilsted J, Kopelman P, Rössner S, et al. Effect of sibutramine on weight maintenance after weight loss: a randomised trial. STORM Study Group. Sibutramine Trial of Obesity Reduction and Maintenance. Lancet 2000;356:2119-25.
4. van Baak MA. The peripheral sympathetic nervous system in human obesity. Obes Rev 2001;2:3-14.
5. Blaak EE, van Baak MA, Kempen KP, Saris WH. Role of α- and β-adrenoceptors in sympathetically mediated thermogenesis. Am J Physiol 1993;264:E11-7.
6. Schiffelers SL, van Harmelen VJ, de Grauw HA, Saris WH, van Baak MA. Dobutamine as selective β_2-adrenoceptor agonist in in vivo studies on human thermogenesis and lipid utilization. J Appl Physiol 1999;87:977-81.
7. Schiffelers SL, Saris WH, Boomsma F, van Baak MA. β_1- and β_2-Adrenoceptor-mediated thermogenesis and lipid utilization in obese and lean men. J Clin Endocrinol Metabol 2001;86:2191-9.
8. Blaak EE, van Baak MA, Kemerink GJ, Pakbiers MT, Heidendal AK, Saris WH. β-Adrenergic stimulation of energy expenditure and forearm skeletal muscle metabolism in lean and obese men. Am J Physiol 1994; 267:E306-15.
9. Krief S, Lönnqvist F, Raimbault S, Baude B, Van Spronsen A, Arner P, et al. Tissue distribution of β_3-adrenergic receptor mRNA in man. J Clin Invest 1993;91:344-9.
10. Berkowitz DE, Nardone NA, Smiley RM, Price DT, Kreutter DK, Fremeau RT, et al. Distribution of $\beta_3$adrenoceptor mRNA in human tissues. Eur J Pharmacol 1995;289:223-8.
11. Rodriguez M, Carillon C, Coquerel A, Le Fur G, Ferrara P, Caput D, et al. Evidence for the presence of β_3-adrenergic receptor mRNA in the human brain. Brain Res Mol Brain Res 1995;29:369-75.
12. Gauthier C, Tavernier G, Charpentier F, Langin D, Le Marec H. Functional β_3-adrenoceptor in the human heart. J Clin Invest 1996;98:556-62.
13. Chamberlain PD, Jennings KH, Paul F, Cordell J, Berry A, Holmes SD, et al. The tissue distribution of the human β_3-adrenoceptor studied using a monoclonal antibody: direct evidence of the β_3-adrenoceptor in human adipose tissue, atrium and skeletal muscle. Int J Obes Relat Metab Disord 1999;23:1057-65.
14. Lönnqvist F, Krief S, Strosberg AD, Nyberg B, Emorine LJ, Arner P. Evidence for a functional β_3-adrenoceptor in man. Br J Pharmacol 1993;110:929-36.
15. Hoffstedt J, Shimizu M, Sjöstedt S, Lönnqvist F. Determination of β_3-adrenoceptor mediated lipolysis in human fat cells. Obes Res 1995;3:447-57.
16. Enocksson S, Shimizu M, Lönnqvist F, Nordenström J, Arner P. Demonstration of an in vivo functional β_3-adrenoceptor in man. J Clin Invest 1995;95:2239-45.
17. Barbe P, Millet L, Galitzky J, Lafontan M, Berlan M. In situ assessment of the role of the β_1-, β_2- and β_3-adrenoceptors in the control of lipolysis and nutritive blood flow in human subcutaneous adipose tissue. Br J Pharmacol 1996;117:907-13.
18. Tavernier G, Barbe P, Galitzky J, Berlan M, Caput D, Lafontan M, et al. Expression of β_3-adrenoceptor with low lipolytic action in human subcutaneous white adipocytes. J Lipid Res 1996;37:87-97.
19. Wheeldon NM, McDevitt DG, Lipworth BJ. Do β_3-adrenoceptors mediate metabolic responses to isoprenaline. Q J Med 1993;86:595-600.

20. Blaak EE, Saris WH, van Baak MA. Adrenoceptor subtypes mediating catecholamine-induced thermogenesis in man. Int J Obes Relat Metab Disord 1993;17 Suppl 3:S78-81.
21. Liu YL, Toubro S, Astrup A, Stock MJ. Contribution of β_3-adrenoceptor activation to ephedrine-induced thermogenesis in humans. Int J Obes Relat Metab Disord 1995;19:678-85.
22. Schiffelers SL, Blaak EE, Saris WH, van Baak MA. In vivo β_3-adrenergic stimulation of human thermogenesis and lipid use. Clin Pharmacol Ther 2000;67:558-66.
23. Mathvink RJ, Tolman JS, Chitty D, Candelore MR, Cascieri MA, Colwell LF, et al. Discovery of a potent, orally bioavailable β_3 adrenergic receptor agonist, (R)-N-[4-[2-[[2-hydroxy-2-(3-piridinyl)ethyl]amino]ethyl]phenyl]-4-[4-[4-(trifluoromethyl)phenyl]thiazol-2-yl]benzenesulfonamide. J Med Chem 2000;43:3832-6.
24. Weir JB. New methods for calculating metabolic rate with special reference to protein metabolism. J Physiol 1949;109:1-9.
25. Demacker PN, Hymans AG, Jansen AP. Enzymatic and chemical extraction determinations of free fatty acids in serum compared. Clin Chem 1982;28:1765-8.
26. Li R, Keymeulen B, Gerlo E. Determination of glycerol in plasma by an automated enzymatic spectrophotometric procedure. Clin Chem Lab Med 2001;39:20-4.
27. Wallace AM. Measurement of leptin and leptin binding in the human circulation. Ann Clin Biochem 2000;37:244-52.
28. Smedes F, Kraak JC, Poppe H. Simple and fast solvent extraction system for selective and quantitative isolation of adrenaline, noradrenaline and dopamine from plasma and urine. J Chromatogr 1982;231:25-39.
29. Arch JR, Wilson S. Prospects for β_3-adrenoceptor agonists in the treatment of obesity and diabetes. Int J Obes Relat Metab Disord 1996;20:191-9.
30. Himms-Hagen J, Danforth E. The potential role of β_3-adrenoceptor agonists in the treatment of obesity and diabetes. Curr Opinion Endocrinol Diabetes 1996;3:59-65.
31. Weyer C, Tataranni PA, Snitker S, Danforth E, Ravussin E. Increase in insulin action and fat oxidation after treatment with CL 316,243, a highly selective β_3-adrenoceptor agonist in humans. Diabetes 1998;47:1555-61.
32. Buemann B, Toubro S, Astrup A. Effects of the two β_3-agonists, ZD7114 and ZD2079, on 24-hour energy expenditure and respiratory quotient in obese subjects. Int J Obes Relat Metab Disord 2000;24:1553-60.
33. Schiffelers SL, Saris WH, van Baak MA. The effect of an increased free fatty acid concentration on thermogenesis and substrate oxidation in obese and lean men. Int J Obes Relat Metab Disord 2001;25:33-8.
34. Gauthier C, Langin D, Balligand JL. β_3-Adrenoceptors in the cardiovascular system. Trends Pharmacol Sci 2000;21:426-31.

British Journal of Pharmacology (1998) 123, 371–380

Validity of (−)-[^{3}H]-CGP 12177A as a radioligand for the 'putative β_4-adrenoceptor' in rat atrium

Doreen Sarsero, [1]Peter Molenaar & *Alberto J. Kaumann

Department of Pharmacology, University of Melbourne, Parkville, 3052, Victoria, Australia and *Human Pharmacology Laboratory, The Babraham Institute, Cambridge CB2 4AT, U.K.

1 We have recently suggested the existence in the heart of a 'putative β_4-adrenoceptor' based on the cardiostimulant effects of non-conventional partial agonists, compounds that cause cardiostimulant effects at greater concentrations than those required to block β_1- and β_2-adrenoceptors. We sought to obtain further evidence by establishing and validating a radioligand binding assay for this receptor with (−)-[^{3}H]-CGP 12177A ((−)-4-(3-tertiarybutylamino-2-hydroxypropoxy) benzimidazol-2-one) in rat atrium. We investigated (−)-[^{3}H]-CGP 12177A for this purpose for two reasons, because it is a non-conventional partial agonist and also because it is a hydrophilic radioligand.

2 Increasing concentrations of (−)-[^{3}H]-CGP 12177A, in the absence or presence of 20 μM (−)-CGP 12177A to define non-specific binding, resulted in a biphasic saturation isotherm. Low concentrations bound to β_1- and β_2-adrenoceptors (pK_D 9.4±0.1, B_{max} 26.9±3.1 fmol mg^{-1} protein) and higher concentrations bound to the 'putative β_4-adrenoceptor' (pK_D 7.5±0.1, B_{max} 47.7±4.9 fmol mg^{-1} protein). In other experiments designed to exclude β_1- and β_2-adrenoceptors, (−)-[^{3}H]-CGP 12177A (1–200 nM) binding in the presence of 500 nM (−)-propranolol was also saturable (pK_D 7.6±0.1, B_{max} 50.8±7.4 fmol mg^{-1} protein).

3 The non-conventional partial agonists (−)-CGP 12177A (pK_i 7.3±0.2), (±)-cyanopindolol (pK_i 7.6±0.2), (−)-pindolol (pK_i 6.6±0.1) and (±)-carazolol (pK_i 7.2±0.2) and the antagonist (−)-bupranolol (pK_i 6.6±0.2), all competed for (−)-[^{3}H]-CGP 12177A binding in the presence of 500 nM (−)-propranolol at the 'putative β_4-adrenoceptor', with affinities closely similar to potencies and affinities determined in organ bath studies.

4 The catecholamines competed with (−)-[^{3}H]-CGP 12177A at the 'putative β_4-adrenoceptor' in a stereoselective manner, (−)-noradrenaline (pK_{iH} 6.3±0.3, pK_{iL} 3.5±0.1), (−)-adrenaline (pK_{iH} 6.5±0.2, pK_{iL} 2.9±0.1), (−)-isoprenaline (pK_{iH} 6.2±0.5, pK_{iL} 3.4±0.1), (+)-isoprenaline (pK_i < 1.7), (−)-RO363 ((−)-(1-(3,4-dimethoxyphenethylamino)-3-(3,4-dihydroxyphenoxy)-2-propranol)oxalate, pK_i 5.5±0.1).

5 The inclusion of guanosine 5-triphosphate (GTP 0.1 mM) had no effect on binding of (−)-CGP 12177A or (−)-isoprenaline to the 'putative β_4-adrenoceptor'. In competition binding studies, (−)-CGP 12177A competed with (−)-[^{3}H]-CGP 12177A for one receptor state in the absence (pK_i 7.3±0.2) or presence of GTP (pK_i 7.3±0.2). (−)-Isoprenaline competed with (−)-[^{3}H]-CGP 12177A for two states in the absence (pK_{iH} 6.6±0.3, pK_{iL} 3.5±0.1; % H 25±7) or presence of GTP (pK_{iH} 6.2±0.5, pK_{iL} 3.4±0.1; % H 37±6). In contrast, at β_1-adrenoceptors, GTP stabilized the low affinity state of the receptor for (−)-isoprenaline.

6 The specificity of binding to the 'putative β_4-adrenoceptor' was tested with compounds active at other receptors. High concentrations of the β_3-adrenoceptor agonists, BRL 37344 ((RR+SS)[4-[2-[[2-(3-chlorophenyl)-2-hydroxy-ethyl]amino]propyl]phenoxy]acetic acid, 6 μM), SR 58611A (ethyl{(7S)-7-[(2R)-2-(3-chlorophenyl)-2-hydroxyethylamino]-5,6,7,8-tetrahydronaphtyl2-yloxy} acetate hydrochloride, 6 μM), ZD 2079 ((±)-1-phenyl-2-(2-4-carboxymethylphenoxy)-ethylamino)-ethan-1-ol, 60 μM), CL 316243 (disodium (R,R)-5-[2-[2-(3-chlorophenyl)-2-hydroxyethyl-amino]propyl]- 1,3-benzodioxole-2,2-dicarboxylate, 60 μM) and antagonist SR 59230A (3-(2-ethylphenoxy)-1-[(1S)-1,2,3,4-tetrahydronaphth-1-ylamino]-2S-2-propanol oxalate, 6 μM) caused less than 22% inhibition of (−)-[^{3}H]-CGP 12177A binding in the presence of 500 nM (−)-propranolol. Histamine (1 mM), atropine (1 μM), phentolamine (10 μM), 5-HT (100 μM) and the 5-HT$_4$ receptor antagonist SB 207710 ((1-butyl-4-piperidinyl)-methyl 8-amino-7-iodo-1,4-benzodioxan-5-carboxylate, 10 nM) caused less than 26% inhibition of binding.

7 Non-conventional partial agonists, the antagonist (−)-bupranolol and catecholamines all competed for (−)-[^{3}H]-CGP 12177A binding in the absence of (−)-propranolol at β_1-adrenoceptors, with affinities (pK_i) ranging from 1.6–3.6 log orders greater than at the 'putative β_4-adrenoceptor'.

8 We have established and validated a radioligand binding assay in rat atrium for the 'putative β_4-adrenoceptor' which is distinct from β_1-, β_2- and β_3-adrenoceptors. The stereoselective interaction with the catecholamines provides further support for the classification of the receptor as 'putative β_4-adrenoceptor'.

Keywords: (−)-[^{3}H]-CGP 12177A; (−)-CGP 12177A; 'putative β_4-adrenoceptor'; atypical β-adrenoceptors; β_1-adrenoceptor; non-conventional partial agonists; catecholamines; (−)-RO363; rat atrium

Introduction

Carlsson *et al.* (1972) showed that both β_1- and β_2-adrenoceptors mediate positive chronotropic effects in cat sino-atrial node and were the first to propose the co-existence of β-adrenoceptors. Since then, the concept of co-existence of β_1- and β_2-adrenoceptors has been confirmed in various cardiac regions in many species including man (Elnatan *et al.*, 1994; Kaumann, 1997; Kaumann & Molenaar, 1997). Recently, Gauthier *et al.* (1996) provided evidence for a β_3-adrenoceptor in endomyocardial ventricular biopsies from transplanted hearts and from patients

[1]Author for correspondence.

undergoing open heart surgery. Interestingly, unlike β_1- and β_2-adrenoceptors which mediate cardiostimulant effects (Kaumann & Molenaar, 1997), stimulation of the β_3-adrenoceptor caused cardiodepressant effects (Gauthier *et al.*, 1996). However, cardiodepressant effects mediated by stimulation of β_3-adrenoceptors have not been confirmed in human right ventricular trabeculae, from explanted hearts in terminal failure, or in right ventricular septal strips, from young children with congenital defects (Kaumann & Molenaar, 1997).

For well over 20 years now, evidence has been slowly accumulating for the existence of a cardiac β-adrenoceptor which is pharmacologically distinct from the β_1-, β_2- and β_3-adrenoceptor subtypes. First described in 1973 (Kaumann, 1973), some compounds which had been classified as β_1- and β_2-adrenoceptor antagonists, caused cardiostimulant effects at much higher concentrations than those that caused antagonism. These compounds were termed non-conventional partial agonists. It was not until later (Kaumann, 1989) that it was hypothesized that non-conventional partial agonists may mediate their effects through a β-adrenoceptor distinct from β_1- and β_2-adrenoceptors. Non-conventional partial agonists also cause agonist effects on β_3-adrenoceptors of adipocytes (for review see Arch & Kaumann, 1993), leading on occasion, to the assumption that the cardiac atypical β-adrenoceptor is a β_3-adrenoceptor (Bond & Lefkowitz, 1996). However, more recently, Malinowska & Schlicker (1996) and Kaumann & Molenaar (1996) showed that the non-conventional partial agonists, CGP 12177A and cyanopindolol caused cardiostimulant effects in rat heart through a receptor that was pharmacologically distinct from β_3-adrenoceptors. Furthermore, Kaumann & Molenaar (1996) showed that the β_3-adrenoceptor agonists, BRL 37344, CL 316243, ZD 2079, SR 58611A at concentrations up to 60 μM, concentrations considerably higher than those required to relax rat colon through β_3-adrenoceptors, did not have any effect in rat left or right atrium, nor did they have any effect on cardiostimulant responses to (−)-CGP 12177A. The cardiostimulant effects of (−)-CGP 12177A were unaffected by the β_1- and β_2-adrenoceptor antagonist (−)-propranolol (200 nM), only marginally blocked by the β_3-adrenoceptor selective antagonist SR 59230A (pK_B = 5.1–5.4 compared to 6.3–7.5 at rat colonic β_3-adrenoceptors) and were blocked with moderate affinity by (−)-bupranolol (pK_B = 6.4–6.8) and CGP 20712A (pK_B = 6.3–6.4) (Kaumann & Molenaar, 1996). There is now evidence for coupling of the receptor to the Gs protein-adenylyl cyclase pathway. Positive inotropic and chronotropic effects of (−)-CGP 12177A were potentiated by the phosphodiesterase inhibitor 3-isobutyl-1-methylxanthine (IBMX; Kaumann & Lynham, 1997). Furthermore (−)-CGP 12177A enhances cyclic AMP levels (Kaumann *et al.*, 1997) and causes increased activity of cyclic AMP-dependent protein kinase in left and right atrium (Kaumann & Lynham, 1997).

Until now a radioligand binding assay for the receptor that mediates cardiostimulant effects of non-conventional partial agonists has not been available. In this study we have developed and validated a radioligand binding assay in rat atrium with (−)-[^{3}H]-CGP 12177A. In addition we have provided evidence for binding to the receptor of the endogenous catecholamines, (−)-noradrenaline and (−)-adrenaline and synthetic catecholamines, (−)-isoprenaline and (−)-RO363. We now propose that non-conventional partial agonists and catecholamines interact with the cardiac atypical β-adrenoceptor which we designate 'putative β_4-adrenoceptor'.

A preliminary account of this work was presented at the American Society for Pharmacology and Experimental Therapeutics meeting, San Diego, March, 1997 (Sarsero *et al.*, 1997).

Methods

Membrane preparation

Sprague-Dawley rats of either sex (250–300 g) were stunned by a blow on the head, exsanguinated and left and right atrium dissected. Atria were homogenized in ice-cold Tris/Mg^{2+} assay buffer (composition in mM: Tris-HCl 50, EGTA 5, EDTA 1, $MgCl_2$ 4, ascorbic acid 1 and phenylmethylsulphonyl fluoride 0.5; pH 7.4), then centrifuged for 5 min at 2,250 × *g* (4°C). The supernatant was centrifuged at 50,000 × *g* (4°C) for 15 min and the pellet resuspended in 15 volumes of ice-cold assay buffer.

Experiments were performed in assay buffer with or without guanosine 5′-triphosphate (GTP; 0.1 mM).

Association and dissociation experiments

The association of (−)-[^{3}H]-CGP 12177A (specific activity 44.5 Ci mmol^{-1}) to 'putative β_4-adrenoceptor' binding sites in rat atrium was determined at time points ranging from 0–15 min.

The dissociation of (−)-[^{3}H]-CGP 12177A from binding sites previously incubated with (−)-[^{3}H]-CGP 12177A for 20 min at 37°C was determined for time points ranging from 0–60 min after the addition of 20 μM (−)-CGP 12177A. K_1 was determined from the equation

$$B_t = B_{eq} \cdot e^{-K_{-1}t} \quad (1)$$

where B_t is specific binding at time t and B_{eq} is specific binding at equilibrium.

Saturation experiments

For binding to β_1-, β_2- and 'putative β_4-adrenoceptor' binding sites 0.01–200 nM (−)-[^{3}H]-CGP 12177A was used in the absence or presence of 20 μM (−)-CGP 12177A to define non-specific binding.

Saturation binding experiments were analysed for two binding sites by non-linear curve fitting with the equation

$$B_{eq} = (B_{max_{\beta_1AR+\beta_2AR}} \cdot [(-)\text{-}[^3\text{H}]\text{-CGP 12177A}])/(K_{D_{\beta_1AR+\beta_2AR}} + [(-)\text{-}[^3\text{H}]\text{-CGP 12177A}]) + (B_{max_{\beta_4AR}} \cdot [(-)\text{-}[^3\text{H}]\text{-CGP 12177A}])/(K_{D_{\beta_4AR}} + [(-)\text{-}[^3\text{H}]\text{-CGP 12177A}]) \quad (2)$$

where $B_{max_{\beta_1AR+\beta_2AR}}$ is the maximal density of β_1- + β_2-adrenoceptors, $B_{max_{\beta_4AR}}$ is the maximal density of 'putative β_4-adrenoceptors', $K_{D_{\beta_1AR+\beta_2AR}}$ is the dissociation constant of (−)-[^{3}H]-CGP 12177A for β_1- and β_2-adrenoceptors and $K_{D_{\beta_4AR}}$ is the dissociation constant of (−)-[^{3}H]-CGP 12177A at the 'putative β_4-adrenoceptor'.

Alternatively, for binding to β_1- and β_2-adrenoceptor binding sites only, 0.01–20 nM (−)-[^{3}H]-CGP 12177A was used in the absence or presence of 500 nM (−)-propranolol to define non-specific binding. For binding to 'putative β_4-adrenoceptor' binding sites only, 1–200 nM (−)-[^{3}H]-CGP 12177A was used in the presence of 500 nM (−)-propranolol with 20 μM (−)-CGP 12177A to define non-specific binding.

Saturation binding experiments were analysed for one binding site by non-linear curve fitting.

Assays were conducted at 37°C for 120 min.

Competition binding studies

For binding to β_1-adrenoceptor binding sites a single concentration of (−)-[^{3}H]-CGP 12177A (1.0−3.8 nM) was used in the presence of the β_2-adrenoceptor selective antagonist ICI 118,551 50 nM, a concentration which is at least 100 times greater than its affinity for β_2-adrenoceptors (Bilski *et al.*, 1983; Lemoine *et al.*, 1985). The concentrations of (−)-[^{3}H]-CGP 12177A used were higher than its pK_D value at rat atrial β_1- or β_2-adrenoceptor binding sites (pK_D 9.4, this study) and were used to obtain a clear signal between total and non-specific binding. A higher concentration (47−57 nM) was used to label 'putative β_4-adrenoceptor' binding sites in the presence of 500 nM (−)-propranolol. Non-specific binding was defined as above. Assays were conducted at 37°C for 120 min (β_1- and β_2-adrenoceptors) or 60 min ('putative β_4-adrenoceptors').

Competition binding experiments were analysed according to the equation:

$$B_{eq} = B_{nsb} + (B_{tb} - B_{nsb})/(1 + 10^{([competitor]-logIC_{50})}) \quad (3)$$

where B_{tb} = specifically bound (−)-[^{3}H]-CGP 12177A in the absence of competitor, B_{nsb} = non-specifically bound (−)-[^{3}H]-CGP 12177A and IC_{50} = the concentration of competitor causing 50% inhibition.

The pK_i for the competitor was then calculated from the Cheng and Prussoff equation (Cheng & Prussoff, 1973).

Competition binding experiments were analysed for two sites according to the equation:

$$B_{eq} = B_{nsb} + f_H(B_{tb} - B_{nsb})/(1 + 10^{([competitor]-logIC_{50H})}) + f_L(B_{tb} - B_{nsb})/(1 + 10^{([competitor]-logIC_{50L})}) \quad (4)$$

where f_H is the fraction of high affinity binding sites, f_L is the fraction of low affinity binding sites, IC_{50H} and IC_{50L} are concentrations of competitor causing 50% inhibition at high and low affinity binding sites, respectively. pK_{iH} and pK_{iL} were calculated as above.

Assays were terminated by addition of 5 ml ice-cold Tris wash buffer (Tris-HCl, 50 mM, pH 7.4) followed by rapid filtration (Brandel M-30R cell harvester) over GF/B filters. Radioactivity retained on filter paper was counted in a Packard beta-counter (Model Tri-Carb 460 CD).

Protein was determined by the method of Lowry *et al.* (1951) with bovine serum albumin as a standard.

Kinetic, saturation and competition binding data were analysed by non-linear regression by PRISM (GraphPad Software, Inc.).

Drugs used

(−)-CGP 12177A, BRL 37344, SB 207710 (SmithKline Beecham Pharmaceuticals, Welwyn, U.K.), CGP 20712A (2-hydroxy-5(2-((2-hydroxy-3-(4-((1-methyl-4-trifluoromethyl) 1H-imidazole-2-yl) -phenoxy) propyl) amino) ethoxy)-benzamide monomethane sulfphonate) (Ciba-Geigy AG, Basel, Switzerland), (±)-carazolol (Boehringer Mannheim GmbH, Mannheim, Germany), SR 58611A (Sanofi, Montpellier, France), SR 59230A (Sanofi, Milan, Italy), CL 316243 (Wyeth-Ayerst Research Princeton, NJ, USA), ZD 2079 (Zeneca Pharmaceuticals, Macclesfield, U.K.), ICI 118,551 (erythro-DL-1(7-methylindan-4-yloxy)-3-isopropylaminobutan-2-ol) (Zeneca, Wilmslow, Cheshire, U.K.), (±)-cyanopindolol, (−)-pindolol (Sandoz, Basle, Switzerland), (−)-bupranolol (Sanol, Monheim, Germany), (+)-isoprenaline (+)-bitartrate (Sterling-Winthrop Research Institute, Rensselaer, N.Y., USA), guanosine 5'-triphosphate (Boehringer Mannheim, Australia), (−)-RO363 (Institute of Drug Technology, Boronia, Australia), (−)-noradrenaline bitartrate (Research Biochemicals International, Natick, MA, USA); (−)-propranolol hydrochloride, (±)-propranolol hydrochloride, histamine dihydrochloride, (−)-adrenaline bitartrate; (−)-isoprenaline bitartrate; atropine sulphate; 5-hydroxytryptamine hydrochloride; phentolamine methanesulphonate; phenylmethysulfonyl fluoride; bovine serum albumin, (Sigma, St Louis, MO, USA); (−)-[^{3}H]-CGP 12177A (Dupont, Boston, MA, U.S.A.).

Results

Kinetic binding experiments

Specific binding of 20 nM−84 nM (−)-[^{3}H]-CGP 12177A in the presence of 500 nM (−)-propranolol to 'putative β_4-adrenoceptors' in rat atrial homogenates was time-dependent and reached over 50% of equilibrium by 15 s, our first sample point (n=6, Figure 1). Therefore, we were not able to obtain an accurate estimate of the observed association rate constant. Binding remained stable for up to 60 min (n=3). The addition of excess (−)-CGP 12177A (20 μM) caused dissociation of (−)-[^{3}H]-CGP 12177A with a dissociation rate constant, K_1 $5.9 \pm 2.2 \times 10^{-2}$ min^{-1}, n=5 (Figure 1).

Saturation binding experiments

Specific binding of increasing concentrations (0.01−200 nM) of (−)-[^{3}H]-CGP 12177A (defined with 20 μM (−)-CGP 12177A) to rat atrial homogenates was biphasic with a low Hill slope (0.77±0.05, n=6). Non-specific binding of (−)-[^{3}H]-CGP 12177A increased linearly with concentration (not shown). Specific binding was 56±4% of total binding, 72±14 d.p.m. at 60 pM; 86±1%, 311±36 dpm at 500 pM; 81±1%, 830±68 d.p.m. at 5 nM and 50±2%, 1499±79 d.p.m. at 40 nM. The curve could be resolved into two sites, one with high affinity (pK_D 9.4±0.1, B_{max} 26.9±3.1 fmol mg^{-1} protein) and another site with lower affinity (pK_D 7.5±0.1, B_{max} 47.7±4.9 fmol mg^{-1} protein, n=6). Figure 2 shows a representative saturation binding experiment.

In other saturation binding experiments, binding of low concentrations of (−)-[^{3}H]-CGP 12177A (0.01−20 nM) in the absence or presence of 500 nM (−)-propranolol to rat atrial membrane homogenates was saturable (B_{max} 30.1±1.6 fmol mg^{-1} protein, n=6) and of high affinity (pK_D 9.4±0.1, n=6) (Figure 2). This value is similar to that observed for binding to β_1- and β_2-adrenoceptor binding sites in rat ventricle by Nanoff *et al.* (1987). The presence of β_1- and β_2-adrenoceptor binding sites was confirmed by competition binding studies with the selective β_1-adrenoceptor antagonist CGP 20712A, which revealed binding to β_1-(pK_i 8.2±0.2, % β_1 78±1, n=6) and β_2-adrenoceptor binding sites (pK_i 6.1±0.1, % β_2 22±1, n=6) (Figure 3). (−)-Propranolol competed with (−)-[^{3}H]-CGP 12177A with high affinity (pK_i 8.4±0.1, n_H 0.91±0.15, n=6) (Figure 3) and was therefore used at 500 nM to block binding of (−)-[^{3}H]-CGP 12177A to β_1- and β_2-adrenoceptor binding sites.

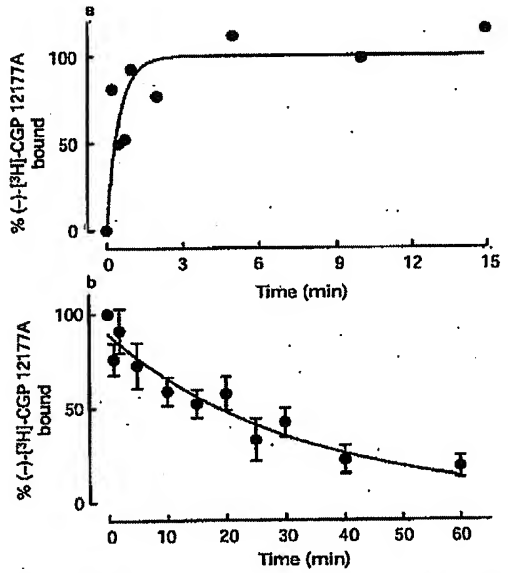

Figure 1 Kinetic analysis of (−)-[^{3}H]-CGP 12177A binding to 'putative β_4-adrenoceptor' binding sites in rat atrial membranes. (−)-[^{3}H]-CGP 12177A binding was performed in the presence of 500 nM (−)-propranolol to block β_1- and β_2-adrenoceptors. Non-specific binding was determined with 20 μM (−)-CGP 12177A. Representative association curve (a) shows specific binding of (−)-[^{3}H]-CGP 12177A (84 nM) at 37°C against time. Mean dissociation curve (b) shows specific binding at various times after addition of 20 μM (−)-CGP 12177A. Each point is expressed as a percentage of the binding occurring at equilibrium in association experiments and at time zero in dissociation experiments. Vertical lines in (b) show s.e.mean from 5 separate experiments.

(−)-[^{3}H]-CGP 12177A (1−200 nM) binding was saturable in the presence of 500 nM (−)-propranolol (B_{max} 50.8±7.4 fmol mg^{-1} protein, $n=6$) and of lower affinity (pK_D 7.6±0.1, $n=6$) (Figure 2).

The results of the separate saturation binding experiments for (−)-[^{3}H]-CGP 12177A together with competition binding experiments with CGP 20712A are consistent with the presence of high affinity β_1- and β_2 -adrenoceptor binding sites, together with a lower affinity binding site, i.e. the 'putative β_4-adrenoceptor'.

Competition binding experiments at the 'putative β_4-adrenoceptor'

The non-conventional partial agonists (−)-CGP 12177A, (±)-cyanopindolol, (−)-pindolol and (±)-carazolol and the antagonist (−)-bupranolol all competed for binding at the 'putative β_4-adrenoceptor' (Table 1, Figure 4 and 5). High concentrations of the selective β_3-adrenoceptor agonists, 6 μM BRL 37344, 60 μM ZD 2079, 60 μM CL 316243, 6 μM SR 58611A and the β_3-adrenoceptor antagonist 6 μM SR 59230A caused less than 22% inhibition (Table 2). Drugs from other classes of receptors, 1 mM histamine, 1 μM atropine, 10 μM phentolamine, 100 μM 5-HT and the 5-HT$_4$ antagonist 10 nM SB 207710 did not compete for (−)-[^{3}H]-CGP 12177A binding (Table 2).

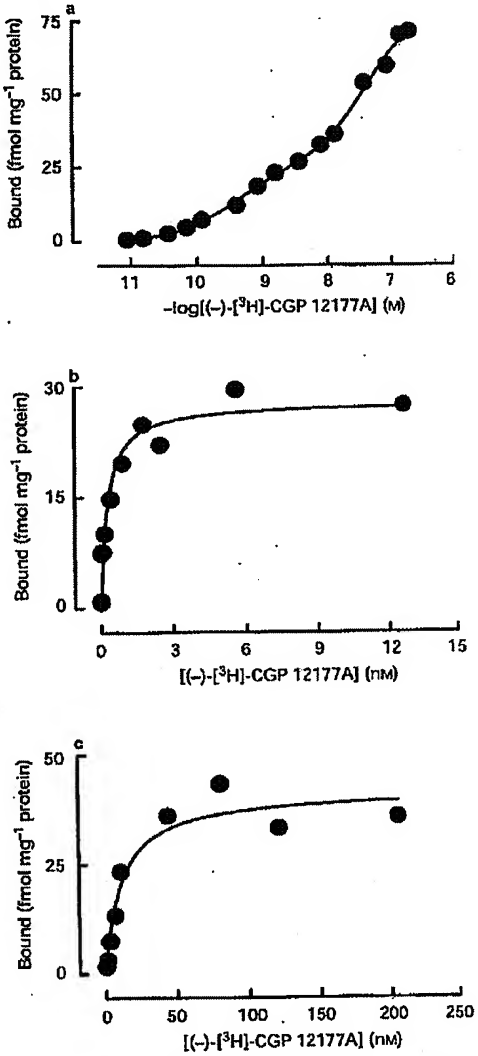

Figure 2 Individual saturation binding experiments showing specific binding in rat atrial membranes for (a) (−)-[^{3}H]-CGP 12177A (0.01−200 nM) binding to β_1-, β_2- and 'putative β_4-adrenoceptors' with non-specific binding determined by 20 μM (−)-CGP 12177A, (b) (−)-[^{3}H]-CGP 12177A (0.01−20 nM) binding to β_1- and β_2- adrenoceptors with non-specific binding determined with 500 nM (−)-propranolol and (c) (−)-[^{3}H]-CGP 12177A (1−200 nM) binding to 'putative β_4-adrenoceptors' in the presence of 500 nM (−)-propranolol, with non-specific binding determined with 20 μM (−)-CGP 12177A. In (a) the saturation binding isotherm was biphasic with one component corresponding to binding at β_1- and β_2- adrenoceptors and the other component corresponding to binding at the 'putative β_4-adrenoceptor'. Note, experiments shown in (a), (b) and (c) were performed on different batches of atrial membranes.

The catecholamines (−)-noradrenaline, (−)-adrenaline, (−)-isoprenaline, (+)-isoprenaline and (−)-RO363 competed for binding in a stereoselective manner (Table 1, Figure 6).

Competition binding experiments at β_1-adrenoceptors

Competition binding experiments were also performed at β_1-adrenoceptors. The non-conventional partial agonists and the antagonist (−)-bupranolol competed for (−)-[^{3}H]-CGP 12177A binding at β_1-adrenoceptors (Figures 4 and 5, Table 1). The catecholamines, (−)-noradrenaline, (−)-adrenaline, (−)-isoprenaline, (+)-isoprenaline and (−)-RO363 also competed at the β_1-adrenoceptor in a stereoselective manner (Figure 6, Table 1). The difference of log affinity estimates between β_1- and 'putative β_4-adrenoceptor' binding sites (log pK_i β_1-adrenoceptor-log pK_i 'putative β_4-adrenoceptor') were not consistent and ranged between 1.6 and 3.6 log units (Table 1).

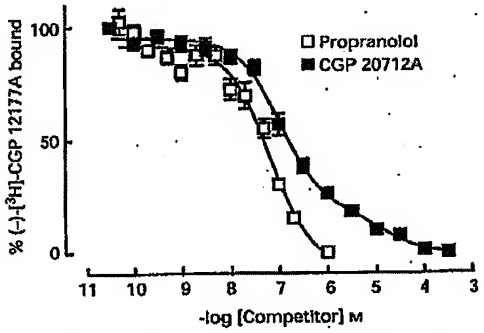

Figure 3 Mean competition binding curves between (−)-[^{3}H]-CGP 12177A and (−)-propranolol and CGP 20712A at β_1 and β_2-adrenoceptor binding sites. Competition binding curves for CGP 20712A could be resolved into a high affinity component corresponding to β_1-adrenoceptors and a low affinity component corresponding to β_2-adrenoceptors. Vertical lines show s.e.mean.

Effect of GTP on radioligand binding at β_1- and 'putative β_4-adrenoceptor' binding sites

GTP (0.1 mM) stabilized the low affinity binding site for (−)-isoprenaline at β_1-adrenoceptors. In the absence of GTP, two binding sites (pK_{iH} 8.47, pK_{iL} 6.79, % H 35.1) were identified. However, in the presence of GTP, one site only with pK_i 7.1 was detected (Figure 7, Table 1).

At 'putative β_4-adrenoceptor' binding sites, inclusion of GTP (0.1 mM) had no effect on competition binding experiments with (−)-CGP 12177A or (−)-isoprenaline (Figure 7). (−)-CGP 12177A competed with (−)-[^{3}H]-CGP 12177A for one receptor state in the absence or presence of GTP with affinity pK_i 7.3 (Figure 7, Table 1). (−)-Isoprenaline competed with (−)-[^{3}H]-CGP 12177A at two states of the receptor in the absence (pK_{iH} 6.6, pK_{iL} 3.5; % H 25.0) and presence of GTP (pK_{iH} 6.2, pK_{iL} 3.4; % H 37.5) Figure 7, Table 1).

Discussion

(−)-[^{3}H]-CGP 12177A was used to label β_1-, β_2- and 'putative β_4- adrenoceptor' binding sites in rat atrium. The design of the 'putative β_4-adrenoceptor binding assay was based on functional studies in which (−)-CGP 12177A stimulated an atypical β-adrenoceptor resistant to blockade of β_1- and β_2-adrenoceptors by (−)-propranolol in rat right and left atrium (Kaumann & Molenaar, 1996; 1997; Kaumann, 1997), which we now call the 'putative β_4-adrenoceptor'. We considered (−)-[^{3}H]-CGP 12177A to be a suitable candidate to investigate as a radioligand for the 'putative β_4-adrenoceptor' in preference to other non-conventional partial agonists, such as iodocyanopindolol or carazolol because of its low lipophilicity (Partition Dulbecco's phosphate buffer solution: octanol ratio [^{3}H]-carazolol 1:23; [^{125}I]-iodocyanopindolol 1:18; [^{3}H]-CGP 12177A 3.1:1; Staehlin *et al.*, 1983). We also considered, as did Staehlin *et al.*, (1983), that (−)-[^{3}H]-CGP 12177A was less likely than [^{3}H]-carazolol

Table 1 Comparison of competition binding data between (−)-[^{3}H]-CGP 12177A and catecholamines, non-conventional partial agonists and the antagonist (−)-bupranolol at β_1-adrenoceptors and the putative 'β_4-adrenoceptor' in the presence or absence of guanosine triphosphate (GTP, 0.1 mM).

	β_1-adrenoceptors*				Putative β_4-adrenoceptors**			
	n	pK_i	%	n_H	n	pK_i	%	n_H	ΔpK_i
+GTP (0.1 mM)									
(−)-Noradrenaline					5	6.30±0.30(H)	20.5±3.6(H)	0.58±0.07	
	4	5.89±0.12(L)	100	0.82±0.02		3.46±0.05(L)	79.5±3.6(L)		2.43
(−)-Adrenaline					5	6.51±0.19(H)	24.4±3.4(H)	0.31±0.03	
	4	5.66±0.07(L)	100	0.83±0.06		2.92±0.11(L)	75.6±3.4(L)		2.74
(−)-Isoprenaline					4	6.23±0.46(H)	37.5±6.3(H)	0.43±0.04	
	7	7.06±0.04(L)	100	0.99±0.05		3.44±0.12(L)	62.5±6.3(L)		3.62
(+)-Isoprenaline	4	3.71±0.13		0.74±0.11	6	<1.7		–	–
(−)-RO363	3	7.45±0.06		0.99±0.12	6	5.46±0.13		0.81±0.09	1.99
(−)-CGP 12177A	–				4	7.34±0.18		0.75±0.06	–
(±)-Cyanopindolol	4	10.75±0.05		0.98±0.05	6	7.56±0.17		0.65±0.09	3.19
(−)-Pindolol	4	8.69±0.04		0.91±0.09	6	6.57±0.14		0.77±0.16	2.12
(±)-Carazolol	4	9.96±0.10		1.24±0.14	6	7.23±0.22		0.85±0.21	2.73
(−)-Bupranolol	4	8.19±0.02		1.01±0.05	10	6.63±0.20		0.83±0.06	1.56
−GTP									
(−)-Isoprenaline	3	8.47±0.31(H)	35.1±7.9(H)	0.74±0.02	4	6.56±0.35(H)	25.0±6.6(H)	0.49±0.05	1.91
		6.79±0.20(L)	64.9±7.9(L)			3.50±0.07(L)	75.0±9.6(L)		3.29
(−)-CGP 12177A	–	–		–	4	7.32±0.19		0.82±0.13	–

*β_1-Adrenoceptor binding performed in the presence of the β_2-adrenoceptor antagonist ICI 118,551 50 nM.
**'Putative β_4-adrenoceptor' binding performed in the presence of (−)-propranolol 500 nM. Affinity (pK_i) and pseudo Hill coefficient values (n_H) were obtained from n individual experiments and are shown as mean±s.e.mean. ΔpK_i = pK_i (β_1-adrenoceptor) − pK_i ('putative β_4-adrenoceptor'). H: high affinity binding state; L: low affinity binding state; %: percentage of receptor in high or low affinity binding state.

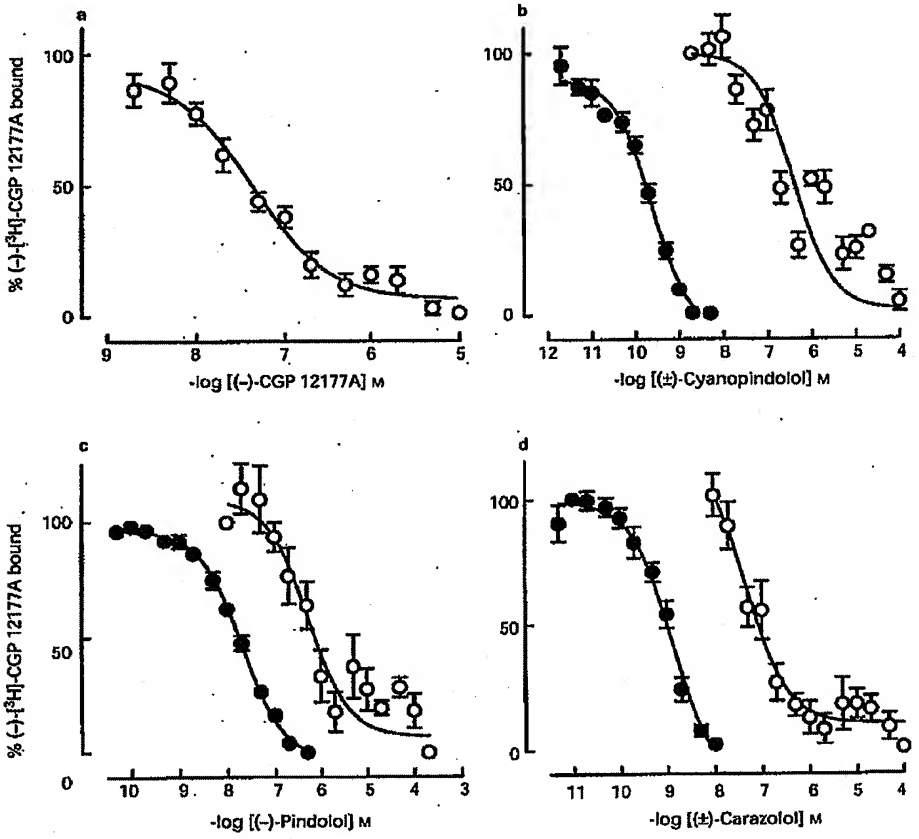

Figure 4 Mean competition binding curves between (-)-[^{3}H]-CGP 12177A and non-conventional partial agonists ((a)(−)-CGP 12177A, (b) (±)-cyanopindolol, (c) (−)-pindolol and (d) (±)-carazolol) at β_1-adrenoceptor binding sites in the presence of the selective β_2-adrenoceptor antagonist 50 nM ICI 118,551 (solid circles) and 'putative β_4-adrenoceptor' binding sites (open circles). Vertical lines show s.e.mean.

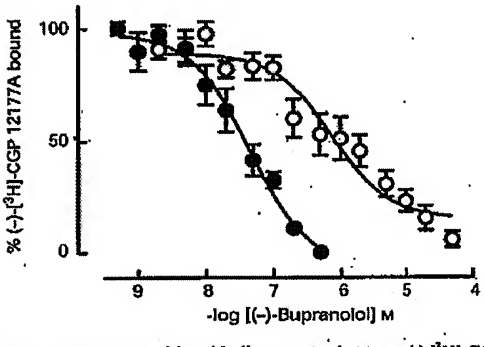

Figure 5 Mean competition binding curves between (-)-[^{3}H]-CGP 12177A and the antagonist (-)-bupranolol at β_1-adrenoceptor binding sites in the presence of the selective β_2-adrenoceptor antagonist 50 nM ICI 118,551 (solid symbols) and 'putative β_4-adrenoceptor' binding sites (open symbols). Vertical lines show s.e.mean.

or [^{125}I]-iodocyanopindolol to bind to non-specific, (−)-propranolol-resistant binding sites (Molenaar *et al.*, 1992).

The continuous saturation binding experiment with (−)-[^{3}H]-CGP 12177A in the absence or presence of 20 μM CGP 12177A was biphasic, suggesting the presence of at least two distinct receptor populations. The higher affinity site was to β_1- and β_2-adrenoceptor binding sites which we did not distinguish between. Earlier radioligand binding studies showed evidence for β_1- and β_2-adrenoceptor binding sites in rat whole heart (Minneman *et al.*, 1979a;b), ventricle (Nanoff *et al.*, 1987; Sarsero & Molenaar, 1995) and in separate (Juberg *et al.*, 1985) or combined left and right atrium, (this study). In rat ventricle, Nanoff *et al.* (1987) showed that (−)-[^{3}H]-CGP 12177A had a slightly higher affinity for β_1- (pK_i 9.5) than β_2-adrenoceptor binding sites (pK_i 9.0) which was similar to our 'combined' β_1- and β_2-adrenoceptor value. In spontaneously beating rat right atrium β_1-adrenoceptors mediate powerful chronotropic effects, but it is also possible to detect β_2-adrenoceptor-mediated chonotropic effects with either the selective β_2-adrenoceptor agonist procaterol (O'Donnell & Wanstall, 1985)

Table 2 Summary of competition binding data at the 'putative β_4-adrenoceptor' * between (−)-[^{3}H]-CGP 12177A and single concentrations of compounds active at β_3-adrenoceptors, histamine, muscarinic, α-adrenoceptors and 5-HT receptors

	n	*Inhibition %*
BRL 37344 6 μM	6	6.7±3.7
SR 58611A 6 μM	6	22.2±5.3
ZD 2079 60 μM	6	12.0±6.7
CL 316243 60 μM	6	11.3±3.3
SR 59230A 6 μM	6	16.3±4.5
Histamine 1 mM	6	25.1±4.9
Atropine 1 μM	8	25.5±9.0
Phentolamine 10 μM	6	10.0±3.9
5-HT 100 μM	6	7.4±4.2
SB 207710 10 nM	6	17.9±11.1

* 'Putative β_4-adrenoceptor' binding performed in the presence of (−)-propranolol 500 nM. Shown are percentage inhibition values obtained from n individual experiments expressed as mean±s.e.mean.

or with (−)-adrenaline using the selective β_1-adrenoceptor antagonist CGP 20712A (Kaumann, 1986).

We then set up separate saturation radioligand binding assays, one for β_1- and β_2-adrenoceptors and another for the low affinity receptor population. For β_1- and β_2-adrenoceptor binding sites, non specific binding was determined with 500 nM (−)-propranolol. There was good agreement between the two methods for the determination of β_1- and β_2-adrenoceptor density (26.9 and 30.1 fmol mg^{-1} protein) and affinity of (−)-[^{3}H]-CGP 12177A (pK_D 9.4 both assays). For the low affinity binding site, a saturation binding assay was designed with 500 nM (−)-propranolol to block β_1- and β_2-adrenoceptors and 20 μM (−)-CGP 12177A to define non-specific binding. Again there was good agreement between B_{max} and pK_D values (B_{max}, 47.7 and 50.8 fmol mg^{-1} protein; pK_D 7.5 and 7.6). These studies show the presence of a low affinity site in addition to β_1- and β_2-adrenoceptor binding sites.

We then determined whether the low affinity binding site was the 'putative β_4-adrenoceptor' binding site.

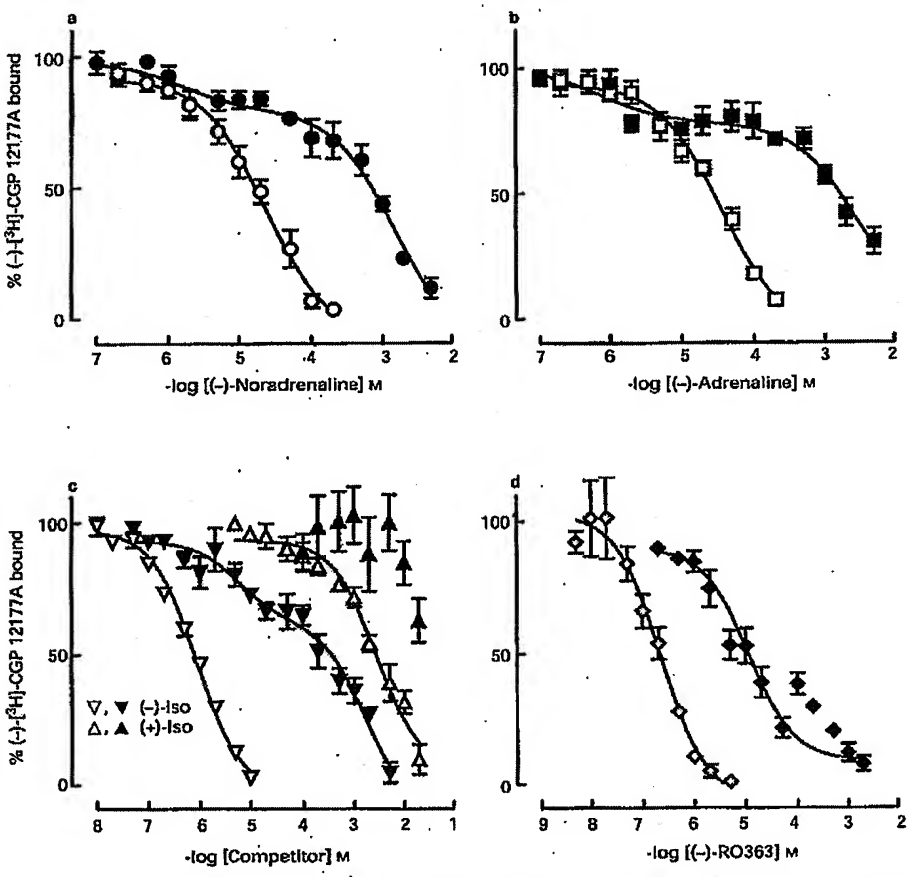

Figure 6 Mean competition binding curves between (−)-[^{3}H]-CGP 12177A and the catecholamines, (a) (−)-noradrenaline, (b) (−)-adrenaline, (c) (−)-isoprenaline ((−)-Iso) and (+)-isoprenaline ((+)-Iso) and (d) (−)-RO363 at β_1-adrenoceptor binding sites in the presence of the selective β_2-adrenoceptor antagonist 50 nM ICI 118,551 (open symbols) and 'putative β_4-adrenoceptor' binding sites (solid symbols). Vertical lines show s.e. mean.

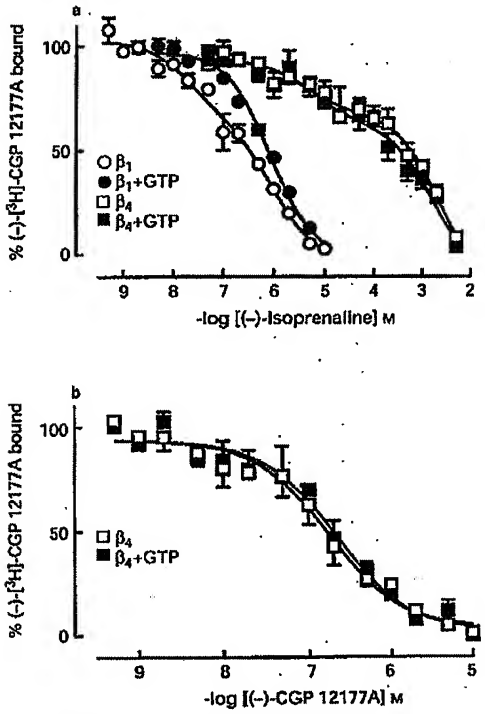

Figure 7 Effect of GTP on binding at β_1-adrenoceptor binding sites (β_1), in the presence of the selective β_2-adrenoceptor antagonist 50 nM ICI 118,551) and at the 'putative β_4-adrenoceptor' (β_4). Competition binding experiments were performed between (−)-[^{3}H]-CGP 12177A and (−)-isoprenaline (a) and (−)-CGP 12177A (b) in the absence or presence of GTP, 0.1 mM. Competition binding isotherms for (−)-isoprenaline in the absence of GTP at β_1-adrenoceptors, and for (−)-isoprenaline in the absence and presence of GTP at 'putative β_4-adrenoceptors' were fitted to a two state affinity model.

Non-conventional partial agonists

The affinities of non-conventional partial agonists were closely similar to potencies determined from organ bath studies. The affinity of (−)-CGP 12177A determined from saturation (7.5–7.6) and competition binding experiments (7.3) was similar to its pEC_{50} value in rat left (7.5) and right (7.3) atrium (Kaumann & Molenaar, 1996). The affinity of (±)-cyanopindolol (7.6) was also similar to its pEC_{50} value in rat left (7.1) and right (7.7) atrium (Kaumann & Molenaar, 1996). Similar comparisons are also valid for (−)-pindolol (pK_i 6.6, pEC_{50} guinea-pig right atrium 7.0, Walter *et al.*, 1984) and (±)-carazolol (pK_i 7.2, pEC_{50} rat right atrium 7.0, Kaumann *et al.*, 1979). The affinity of (−)-bupranolol (6.6) was also similar to its affinity in rat atrium (pK_B 6.4–6.8, Kaumann & Molenaar, 1996). These results indicate similarity of the functional receptor and binding site.

Lack of activity of ligands from other receptor classes

(−)-[^{3}H]-CGP 12177A has also been used as a radioligand for β_3-adrenoceptor binding sites in murine 3T3-F442A adipocytes and human β_3-adrenoceptors expressed in Chinese hamster ovary cells (Feve *et al.*, 1991), rat brown (D'Allaire *et al.*, 1995) and white adipocytes (Germack *et al.*, 1997). In these studies the affinities of (−)-[^{3}H]-CGP 12177A ranged from 23–80 nM. Therefore we determined whether the β_3-adrenoceptor agonists, BRL 37344 (6 μM), ZD 2079 (60 μM) SR 58611A (6 μM) and CL 316243 (60 μM) and the antagonist SR 59230A (6 μM) competed for (−)-[^{3}H]-CGP 12177A binding in rat atrium. The affinities (pK_D) of BRL 37344 range from 6.6–7.1 on the rat cloned β_3-adrenoceptor (Muzzin *et al.*, 1991; Liggett, 1992; Dolan *et al.*, 1994), CL 316243, 6.0 on rat cloned β_3-adrenoceptor (Dolan *et al.*, 1994) and SR 58611A 5.2 at the human and 5.9 at the murine cloned β_3-adrenoceptor (Blin *et al.*, 1994). These agonists did not compete for binding with (−)-[^{3}H]-CGP 12177A in rat atrium. The antagonist SR 59230A, has an affinity (pK_B) of 6.3–7.5 on rat colonic β_3-adrenoceptors (Kaumann & Molenaar, 1996) but also did not compete for (−)-[^{3}H]-CGP 12177A binding in rat atrium. These studies are in line with our previous functional studies (Kaumann & Molenaar, 1996), in which we showed that the β_3-adrenoceptor agonists did not affect basal contractile activity (left atrium) or sinoatrial rate (right atrium) and nor did they modify the cardiostimulant effects of (−)-CGP 12177A. We also determined the affinity of SR 59230A to be (pK_B) 5.1–5.4 for the 'putative β_4-adrenoceptor' in rat right and left atrium which is lower than at β_3-adrenoceptors (Kaumann & Molenaar, 1996). Our radioligand binding studies support the conclusion made from previous studies (Kaumann & Molenaar, 1996; Malinowska & Schlicker, 1996) that the receptor mediating cardiostimulant effects of CGP 12177A in rat is not a β_3-adrenoceptor.

Further specificity of (−)-[^{3}H]-CGP 12177A binding was tested with compounds which are active at histamine, muscarinic, α-adrenoceptors and 5-HT receptors. The affinity values of histamine for H_1- and H_2-receptors in guinea-pig left atrium, determined from competition binding experiments with [^{3}H]-mepyramine (H_1-) were (pK_i) 4.8 and [^{3}H]-tiotidine (H_2-) 5.1, respectively (Hattori *et al.*, 1991). Atropine has an affinity (pK_i) of 8.9 for rat atrial M_2-receptors, determined in competition binding experiments with [^{3}H]-N-methyl scopolamine (Doods *et al.*, 1987). Phentolamine has affinities (pK_i) of 8.2, 7.2 and 7.5 for α_{1a}- α_{1b}- and α_{1d}-receptors (Michel *et al.*, 1995). 5-Hydroxytryptamine (5-HT) has an affinity (pK_i) of 6.6 and SB 207710 (9.5) for piglet right atrial 5-HT_4 receptors (Kaumann *et al.*, 1995a) determined in radioligand binding experiments with [^{125}I]-SB 207710. Our studies showed that (−)-[^{3}H]-CGP 12177A does not label histamine, muscarinic, α-adrenoceptors or 5-HT receptors in rat atrium.

Interaction of catecholamines with the 'putative β_4-adrenoceptor'

We had previously observed that positive inotropic effects of the catecholamine (−)-RO363 in human right atrium *in vitro* were partially resistant to blockade by (−)-CGP 20712A (Molenaar *et al.*, 1997). We ruled out stimulation of co-existing β_2-adrenoceptors and suggested that it also stimulated the 'putative β_4-adrenoceptor' (Molenaar *et al.*, 1997). Wheeldon *et al.* (1993) also provided evidence that (−)-isoprenaline could cause inotropic and lusitropic effects in human myocardium *in vivo* by stimulation of an atypical β-adrenoceptor. The atypical β-adrenoceptor effects of (−)-isoprenaline were observed in the presence of atenolol 25 mg (p.o.), a concentration that attenuates (−)-isoprenaline-induced increases in heart rate (β_1-adrenoceptor) and nadolol 5, 20 and 80 mg (p.o), concentrations, that attenuate (−)-isoprenaline-mediated increases in heart rate (β_1-adrenoceptor) and postural finger tremor (β_2-adrenoceptor). Wheeldon *et al.* (1993) described the receptor as a β_3-adrenoceptor, but this is

not the same receptor which causes cardiodepression in ventricular endomyocardial biopsies of cardiac transplant patients or patients undergoing open heart surgery (Gauthier *et al.*, 1996). Wheeldon *et al.*, (1993) provided further evidence for a cardiostimulant atypical β-adrenoceptor which we think corresponds to the 'putative β_4-adrenoceptor'.

We have shown that the endogenous catecholamines (−)-noradrenaline, (−)-adrenaline and synthetic catecholamines, (−)-RO363, (−)-and (+)-isoprenaline bind to the 'putative β_4-adrenoceptor' in a stereoselective manner. Two affinity states of the receptor were observed for (−)-noradrenaline, (−)-adrenaline and (−)-isoprenaline. The high affinity state comprised 20–38% of the total population of receptors. These catecholamines had similar affinities for the high affinity state (pK_{iH} 6.2–6.5) and also for the low affinity state of the 'putative β_4-adrenoceptors' (pK_{iL} 2.9–3.5). The affinities of catecholamines at the low affinity state of the receptor were slightly higher than those at native β_3- adrenoceptors of rat adipocytes (Germack *et al.*, 1997). Furthermore, the overall affinity of (−)-RO363 was higher at the rat atrial 'putative β_4-adrenoceptor' (pK_i 5.5) than at the human cloned β_3-adrenoceptor (pK_i 4.5, Molenaar *et al.*, 1997). These small but consistent differences further appear to differentiate the 'putative β_4-adrenoceptor' from the β_3-adrenoceptor. The functional significance of the high and low affinity binding sites remains to be determined.

Comparison between binding at 'putative β_4-adrenoceptor' and β_1-adrenoceptor binding sites

We included 500 nM (−)-propranolol in the 'putative β_4-adrenoceptor' binding assay to block co-existing β_1- and β_2-adrenoceptor sites. In order to validate further binding to the 'putative β_4-adrenoceptor' and to ensure that it did not represent binding to β_1-adrenoceptor binding sites, we also estimated the affinities of non-conventional partial agonists and catecholamines at β_1-adrenoceptors. Affinities for all compounds tested were higher at the β_1-adrenoceptor than at the 'putative β_4-adrenoceptor'. However, the difference between pK_i values at β_1- and 'putative β_4- adrenoceptor' (pK_i β_1−−pK_i 'putative β_4-adrenoceptor') were not consistent and ranged from 1.6–3.6 log units (Table 1). This indicates that 'putative β_4-adrenoceptor' binding cannot be interpreted as β_1-adrenoceptor binding shifted to the right by (−)-propranolol. If this were the case, one would expect the same difference between (pK_i β_1−− pK_i 'putative β_4-adrenoceptor'), regardless of ligand affinity.

Agonist binding at β_1- and β_2-adrenoceptor subtypes is sensitive to guanine nucleotides. In the absence of guanine nucleotides, the receptor binding site exists in high and low affinity states and in their presence, the high affinity state is converted to the low affinity state (Lefkowitz *et al.*, 1976; 1981; Maguire *et al.*, 1976; Kaumann *et al.*, 1995b). We also showed that inclusion of GTP stabilized the low affinity state of the β_1-adrenoceptor for the agonist (−)-isoprenaline. In this assay at β_1-adrenoceptors, (−)-[^{3}H]-CGP 12177A is an antagonist. At 'putative β_4-adrenoceptors', GTP had no effect on agonist binding with (−)-isoprenaline and (−)-CGP 12177A. It is important to realize that the radioligand, (−)-[^{3}H]-CGP 12177A is an agonist at the 'putative β_4-adrenoceptor' and we do not know whether a high or low affinity receptor state is stabilized at the concentrations used for competition binding with cold ligands. Therefore, the effects of GTP on agonist binding cannot be strictly compared between β_1-adrenoceptors and the 'putative β_4-adrenoceptor'. Further clarification of the effects of guanine nucleotides on agonist binding at the 'putative β_4-adrenoceptor' will be possible with the development of an antagonist radioligand.

Conclusions and future prospects

This study has established and validated a radioligand binding assay for the cardiac atypical β-adrenoceptor. The stereoselective catecholamine binding profile and difference from β_1-, β_2- and β_3-adrenoceptors indicate that the atypical β-adrenoceptor is novel. We designate this receptor provisionally as 'putative β_4-adrenoceptor'. However, we await the cloning of the receptor for a formal classification of it. We are currently using this radioligand binding assay in human right atrium, where we have also obtained functional evidence for the existence of the 'putative β_4-adrenoceptor' (Kaumann, 1996; 1997; Kaumann & Molenaar, 1996; Sarsero *et al.*, 1996a;b; Kaumann *et al.*, 1997; Molenaar *et al.*, 1997). We are also planning quantitative receptor autoradiography studies to determine the density and distribution of 'putative β_4-adrenoceptors' in discrete regions such as rat and human sinoatrial node.

A.J.K. was supported by the British Heart Foundation. P.M. and A.J.K. were supported by the University of Melbourne (Collaborative Research Award). P.M. is an NHMRC Senior Research Fellow.

References

ARCH, J.R.S. & KAUMANN, A.J. (1993). β_3-Adrenoceptors and atypical β-adrenoceptors. *Med. Res. Rev.*, **48**, 663–729.

BILSKI, A.J., HALLIDAY, S.E., FITZGERALD, J.D. & WALE, J.L. (1983). The pharmacology of a β_2-selective adrenoceptor antagonist (ICI 118,551). *J. Cardiovasc. Pharmacol.*, **5**, 430–437.

BOND, R.A. & LEFKOWITZ, R.J. (1996). The third beta is not the charm. *J. Clin. Invest.*, **93**, 241.

BLIN, N., NAHMIAS, C., DRUMARE, M.F. & STROSBERG, A.D. (1994). Mediation of most atypical effects by species homologues of the β_3-adrenoceptor. *Br. J. Pharmacol.*, **112**, 911–919.

CARLSSON, E., ÅBLAD, B., BRÅNDSTRÖM, A. & CARLSSON, B. (1972). Differentiated blockade of the chronotropic effects of various adrenergic stimuli in the cat heart. *Life Sci.*, **11**, 953–958.

CHENG, Y. & PRUSOFF, W.H. (1973). Relationship between the inhibition constant (K_I) and the concentration of inhibitor which causes 50 per cent inhibition (I_{50}) of an enzymatic reaction. *Biochem. Pharmacol.*, **22**, 3099–3108.

D'ALLAIRE, F., ATGIÉ, C., MAURIÈGE, P., SIMARD, P.-M. & BUKKOWIECKI, L.J. (1995). Characterization of β_1- and β_3-adrenoceptors in intact brown adipocytes of the rat. *Br. J. Pharmacol.*, **114**, 275–282.

DOLAN, J.A., MUENKEL, H.A., BURNS, M.G., PELLEGRINO, S.M., FRASER, C.M., PIETRI, F., STROSBERG, A.D., LARGIS, E.E., DUTIA, M.D., BLOOM, J.D., BASS, A.S., TANIKELLA, T.K., COBUZZI, A., LAI, F.M. & CLAUS, T.H. (1994). Beta-3 adrenoceptor selectivity of the dioxolane dicarboxylate phenethanolamines. *J. Pharmacol. Exp. Ther.*, **269**, 1000–1006.

DOODS, H.N., MATHY, M.-J., DAVIDESKI, D., VAN CHARLDORP, K.J., DE JONGE, A. & VAN ZWIETEN, P.A. (1987). Selectivity of muscarinic antagonists in radioligand and *in vivo* experiments for the putative M_1, M_2 and M_3 receptors. *J. Pharmacol. Exp. Ther.*, **242**, 257–262.

ELNATAN, J., MOLENAAR, P., ROSENFELDT, F.L. & SUMMERS, R.J. (1994). Autoradiographic localization and quantitation of β_1- and β_2-adrenoceptors in the human atrioventricular conducting system: A comparison of patients with idiopathic dilated cardiomyopathy and ischemic heart disease. *J. Mol. Cell. Cardiol.*, **26**, 313-323.

FEVE, B., EMORINE, L.J., LASNIER, F., BLIN, H., BAUDE, B., NAHMIAS, C., STROSBERG, A.D. & PAIRAULT, J. (1991). Atypical β-adrenergic receptor in 3T3-F442A adipocytes. Pharmacological and molecular relationship with the human β_3-adrenergic receptor. *J. Biol. Chem.*, **266**, 20329-20336.

GAUTHIER, C., TAVERNIER, G., CHARPENTIER, F., LANGIN, D. & LE MAREC, H. (1996). Functional β_3-adrenoceptor in the human heart. *J. Clin. Invest.*, **98**, 556-562.

GERMACK, R., STARZEC, A.B., VASSY, R. & PERRET, G. (1997). β-Adrenoceptor subtype expression and function in rat white adipocytes. *Br. J. Pharmacol.*, **120**, 201-210.

HATTORI, Y., ENDOU, M., GANDO, S. & KANNO, M. (1991). Identification and characterization of histamine H_1- and H_2-receptors in guinea-pig left atrial membranes by [^{3}H]-mepyramine and [^{3}H]-tiotidine binding. *Br. J. Pharmacol.*, **103**, 1573-1579.

JUBERG, E.N., MINNEMAN, K.P. & ABEL, P.W. (1985). β_1- and β_2-adrenoceptor binding and functional response in right and left atria of rat heart. *Naunyn-Schmiedeberg's Arch. Pharmacol.*, **330**, 193-202.

KAUMANN, A.J. (1973). Adrenergic receptors in heart muscle. Two different mechanisms of β blockers as partial agonists. International Union of Biochemistry. Symposium 52. *Acta Physiol. Latamer.*, **72**, 63-82.

KAUMANN, A.J. (1986). The β_1-adrenoceptor antagonist CGP 20712 A unmasks β_2-adrenoceptors activated by (−)-adrenaline in rat sinoatrial node. *Naunyn-Schmiedeberg's Arch. Pharmacol.*, **332**, 406-409.

KAUMANN, A.J. (1989). Is there a third heart β-adrenoceptor? *Trends Pharmacol. Sci.*, **10**, 316-320.

KAUMANN, A.J. (1996). (−)-CGP 12177-induced increase of human atrial contraction through a putative third β-adrenoceptor. *Br. J. Pharmacol.*, **117**, 619-622.

KAUMANN, A.J. (1997). Four β-adrenoceptor subtypes in mammalian heart. *Trends Pharmacol. Sci.*, **18**, 70-76.

KAUMANN, A.J. & LYNHAM, J.A. (1997). (−)-CGP 12177A stimulates cyclic AMP-dependent protein kinase in rat atria through an atypical β-adrenoceptor. *Br. J. Pharmacol.*, **120**, 1187-1189.

KAUMANN, A.J., LYNHAM, J.A. & BROWN, A.M. (1995a). Labelling with [^{125}I]-SB 207710 of a small 5-HT$_4$ receptor population in piglet right atrium: functional relevance. *Br. J. Pharmacol.*, **115**, 933-936.

KAUMANN, A.J., LYNHAM, J.A., SANDERS, L., BROWN, A.M. & MOLENAAR, P. (1995b). Contribution of differential efficacy to the pharmacology of human β_1- and β_2-adrenoceptors. *Pharmacol. Commun.*, **6**, 215-222.

KAUMANN, A.J., LYNHAM, J.A., SARSERO, D. & MOLENAAR, P. (1997). The atypical cardiostimulant β-adrenoceptor is distinct from β_3-adrenoceptors and is coupled to a cyclic AMP-dependent pathway in rat and human myocardium. *Br. J. Pharmacol.*, **120**, 102P.

KAUMANN, A.J. & MOLENAAR, P. (1996). Differences between the third cardiac β-adrenoceptor and the colonic β_3-adrenoceptor in the rat. *Br. J. Pharmacol.*, **118**, 2085-2098.

KAUMANN, A.J. & MOLENAAR, P. (1997). Modulation of human cardiac function through 4 β-adrenoceptor populations. *Naunyn-Schmiedeberg's Arch. Pharmacol.*, **355**, 667-681.

KAUMANN, A.J., MORRIS, T.H. & BIRNBAUMER, L. (1979). A comparison of the influence of N-isopropyl and N-tert butyl substituents on the affinity of ligands for sinoatrial β-adrenoceptors in rat atria and β-adrenoceptors coupled to the adenylyl cyclase in kitten ventricle. *Naunyn-Schmiedeberg's Arch. Pharmacol.*, **307**, 1-8.

LEFKOWITZ, R.J., DE LEAN, A., HOFFMAN, B.B., STADEL, J.M., KENT, R., MICHEL, R. & LIMBIRD, L. (1981). Molecular pharmacology of adenylate cyclase-coupled α- and β-adrenergic receptors. *Adv. Cyclic Nucleotide Res.*, **14**, 145-161.

LEFKOWITZ, R.J., MULLIKIN, D. & CARON, M.G. (1976). Regulation of β-adrenergic receptors by guanyl-5'-yl imidodiphosphate and other purine nucleotides. *J. Biol. Chem.*, **251**, 4686-4692.

LEMOINE, H., EHLE, B. & KAUMANN, A.J. (1985). Direct labelling of β_2 adrenoceptors: Comparisons of binding potency of [^{3}H]-ICI 118,551 and blocking potency of ICI 118,551. *Naunyn-Schmiedeberg's Arch. Pharmacol.*, **331**, 40-51.

LIGGETT, S.B. (1992). Functional properties of the rat and human β_3-adrenergic receptors: Differential agonist activation of recombinant receptors in Chinese hamster ovary cells. *Mol. Pharmacol.*, **42**, 634-637.

LOWRY, O.H., ROSEBROUGH, N.J., FARR, A.L. & RANDALL, R.J. (1951). Protein measurement with the folin phenol reagent. *J. Biol. Chem.*, **193**, 265-275.

MAGUIRE, M.E., VAN ARSDALE, P.M. & GILMAN, A.G. (1976). An agonist-specific effect of guanine nucleotides on binding to the beta adrenergic receptor. *Mol. Pharmacol.*, **12**, 335-339.

MALINOWSKA, B. & SCHLICKER, E. (1996). Atypical β-adrenoceptors, different from β_3-adrenoceptors, mediate the positive chronotropic effect of CGP 12177 and cyanopindolol in the pithed rat. *Br. J. Pharmacol.*, **117**, 943-949.

MICHEL, M.C., KENNY, B. & SCHWINN, D.A. (1995). Classification of α_1-adrenoceptor subtypes. *Naunyn-Schmiedeberg's Arch. Pharmacol.*, **352**, 1-10.

MINNEMAN, K.P., HEDBERG, A. & MOLINOFF, P.B. (1979a). Comparison of *beta* adrenergic receptor subtypes in mammalian tissues. *J. Pharmacol. Exp. Ther.*, **211**, 502-508.

MINNEMAN, K.P., HEGSTRAND, L.R. & MOLINOFF, P.B. (1979b). Simultaneous determination of *beta*-1 and *beta*-2-adrenergic receptors in tissues containing both receptor subtypes. *Mol. Pharmacol.*, **16**, 34-46.

MOLENAAR, P., KOMPA, A.R., ROBERTS, S.J., PAK, H.S. & SUMMERS, R.J. (1992). Localization of (-)-[^{125}I]cyanopindolol binding in guinea-pig heart: characteristics of non-β-adrenoceptor related binding in cardiac pacemaker and conducting regions. *Neurosci. Lett.*, **136**, 118-122.

MOLENAAR, P., SARSERO, D., ARCH, J.R.S., KELLY, J., HENSON, S.M. & KAUMANN, A.J. (1997). Effects of (−)-RO363 at human atrial β-adrenoceptor subtypes, the human cloned β_3-adrenoceptor and rodent intestinal β_3-adrenoceptors. *Br. J. Pharmacol.*, **120**, 165-176.

MUZZIN, P., REVELLI, J.-P., KUHNE, F., GOCAYNE, J.D., MCCOMBIE, W.R., VENTER, J.C., GIACOBINO, J.-P. & FRASER, C.M. (1991). An adipose tissue-specific β-adrenergic receptor. Molecular cloning and down-regulation in obesity. *J. Biol. Chem.*, **266**, 24053-24058.

NANOFF, C., FREISSMUTH, M. & SCHÜTZ, W. (1987). The role of a low β_1-adrenoceptor selectivity of [^{3}H]-CGP 12177A for resolving subtype-selectivity of competitive ligands. *Naunyn-Schmiedeberg's Arch. Pharmacol.*, **336**, 519-525.

O'DONNELL, S.R. & WANSTALL, J.C. (1985). Responses to the β_2-selective agonist procaterol of vascular and atrial preparations with different functional β-adrenoceptor populations. *Br. J. Pharmacol.*, **84**, 227-235.

SARSERO, D. & MOLENAAR, P. (1995). Effects of chronic infusion of (-)-isoprenaline on rat cardiac muscarinic (M_2)-cholinoceptors and β_1- and β_2-adrenoceptors. *J. Auton. Pharmacol.*, **15**, 239-255.

SARSERO, D., MOLENAAR, P. & KAUMANN, A.J. (1996a). The human cardiac atypical β-adrenoceptor stimulates a cyclic AMP-dependent pathway. *J. Mol. Cell. Cardiol.*, **28**, A274.

SARSERO, D., MOLENAAR, P. & KAUMANN, A.J. (1996b). Stimulation of the "putative β_4-adrenoceptor" causes positive inotropic effects and hastens relaxation in human atrium and ventricle through a cAMP dependent pathway. *Proc. Aust. Soc. Clin. Exp. Pharmacol. Toxicol.*, **3**, 38.

SARSERO, D., MOLENAAR, P. & KAUMANN, A.J. (1997). (-)-[^{3}H]-CGP 12177A labels the atypical β-adrenoceptor (βAR) in rat atrium. *The Pharmacologist*, **39** (abstract 104), p 39.

STAEHELIN, M., SIMONS, P., JAEGGI, K. & WIGGER, H. (1983). CGP-12177. A hydrophilic β-adrenergic receptor radioligand reveals high affinity binding of agonists to intact cells. *J. Biol. Chem.*, **258**, 3496-3502.

WHEELDON, N.M., MCDEVITT, D.G. & LIPWORTH, B.J. (1993). Investigation of putative cardiac β_3-adrenoceptors in man. *Q. J. Med.*, **86**, 255-261.

WALTER, M., LEMOINE, H. & KAUMANN, A.J. (1984). Stimulant and blocking effects of optical isomers of pindolol on the sinoatrial node and trachea of guinea pig. Role of β-adrenoceptor subtypes in the dissociation between blockade and stimulation. *Naunyn-Schmiedeberg's Arch. Pharmacol.*, **327**, 159-175.

(Received September 8, 1997
Accepted October 15, 1997)

Research Paper

Gastroprotective effects of β_3-adrenoceptor agonists on water immersion plus restraint stress-induced gastric ulcer in rats

A. Paul,* S. Goswami, D. Santani

*Lachoo Memorial College of Science and Technology (Pharmacy Wing), Shastri Nagar, Jodhpur - 342003. India; Department of Pharmacology, L. M. College of Pharmacy, Navrangpura, Ahmedabad - 380009. India.

Received: 4.7.2003
Revised: 24.9.2003
Accepted: 2.10.2003

Correspondence to:
A. Paul
E-mail: a_paul@sancharnet.in

ABSTRACT

Objective: To evaluate the gastroprotective effects of β_3-adrenoceptor agonists CGP 12177A and SR 58611A, on water immersion plus restraint stress (WIRS)-induced gastric ulceration in rats.

Material and Methods: Drugs were administered (5, 10 and 15 mg/kg, *p.o.*) 30 min prior to the ulcerogenic procedure. Ulcer index and the score for intensity of intraluminal bleeding were determined. Gastric wall mucus content (GWMC) and mast cell counts were determined in the glandular portion of the stomach.

Results: A dose-dependent reduction in the ulcer index was observed with both the drugs. A significant rise in the GWMC in the glandular tissue at 15 mg/kg dose was caused by the β_3-adrenoceptors agonists. In the glandular tissue the mast cell count was significantly decreased at 10 and 15 mg/kg dose with both drugs.

Conclusion: The present study shows the gastroprotective effect of β_3-adrenoceptor agonists CGP 12177A and SR 58611A against WIRS-induced gastric ulceration in rats. The gastroprotective effect may be mediated by the enhancement of mucin activity and the decrease in mast cell degranulation.

KEY WORDS: CGP 12177A, SR 58611A, β_3 stimulants, stress ulcer, mucoprotectives

Introduction

Recent localization of β_3-adrenoceptors using immunohistochemical studies has confirmed the presence of β_3-adrenoceptors in human vascular and non-vascular smooth muscles of the gastrointestinal tract.[1] The presence of β_3-adrenoceptors has been well described in mast cells and basophils and the stimulation of these receptors results in the inhibition of immune-stimulated histamine release.[2,3]

Espluges *et al* [4] observed significant antiulcer activity with β-adrenergic drugs such as salbutamol, salmeterol and isoprenaline against polymixin-B-induced gastric ulcers involving histamine release. However, propranolol could only partially antagonize the isoprenaline-induced inhibitory effect on histamine release. This shows that besides β_2-adrenoceptor stimulation, these agonists inhibit histamine release through some additional mechanism other than beta-receptor stimulation. The involvement of β_1-adrenoceptors in the histamine release mechanism was ruled out by these studies. Isoprenaline was reported to be as potent as SR 58611A, a β_3-adrenoceptor agonist, in stimulating β_3-adrenoceptors in isolated rat colon.[5] β_3-adrenoceptor agonists inhibit gastric ulcer-induced by indomethacin,[5,6] pylorus ligation and ethanol[7] in rats.

Hence, this study was undertaken to evaluate the antiulcer effect of β_3-adrenoceptor agonists on water immersion plus restraint stress (WIRS)- induced gastric ulcer in rats. The study was also directed towards the elucidation of the mechanism of the antiulcer activity of β_3-adrenoceptor agonists.

Material and Methods

Wistar albino rats of either sex weighing 200-250 g were selected. Rats were fed with standard chow diet and water *ad libitum* till the end of the experimental period. Distributions of the animals in-group, sequence of trials and treatment aspects were randomized. This experiment complied with the guidelines of our laboratory for animal experimentation. The Animal Ethics Committee of the institute cleared the experimental protocols.

CGP 12177A [(±)-4-(3-t-butylamino-2-hydroxy-propoxy) benzimidazol-2-one] and SR58611A [ethyl {(7S)-7-[(2R)-2-(3-

chlorophenyl)-2-hydroxyethylamino] 5,6,7,8-tetrahydronapthalene-2-yloxy} acetate hydrochloride] were obtained as gift samples from Novartis, Switzerland and Sanofi Recherche, France respectively. Drugs dissolved in distilled water were administered orally to rats in doses of 5, 10 and 15 mg/kg. Saline treated (0.5 ml/100 g, *p.o.*) rats served as controls. The dose of β_3-adrenoceptor agonists were selected on the basis of ED_{50} values of BRL 35135, a β_3-adrenoceptor agonist on indomethacin-induced ulceration and total acid-output in pylorus-ligated rats.[5]

Water immersion plus restraint stress-induced gastric ulceration

The method described by Takagi and Okabe[6] was employed with slight modification. Rats were fasted for 12 h, care being taken to avoid coprophagy. The rats were immobilized in a restrainer and subsequently they were immersed in water up to xiphoid process for 7 h. The temperature of the water was maintained at 24± 1°C. Drugs were given orally 30 min prior to the restraint procedure. After 7 h of immobilization and water immersion the animals were taken out and killed with high-dose anesthetic ether. The stomach was removed and the severity of intraluminal bleeding was examined and expressed as score for intensity (SI) of intraluminal bleeding according to the following scale: 0, no blood detectable; 1, thin blood follows the rugae; 2, thick blood follows the rugae; 3, thick blood follows the rugae with blood clots in certain areas; 4, extensive covering of the whole of mucosal surface with thick blood.[9] After wiping the blood, the ulcer index was determined[10] and the stomach tissue was subjected to mast cell examination and analysed for gastric wall mucus content (GWMC).

Measurement of gastric wall mucus

The modified procedure of Corne *et al*[11] was used for the determination of gastric wall mucus. One half of the glandular portion of the stomach, opened along the greater curvature, was carefully separated from the rumenal part and transferred into 10 ml Alcian blue (8GX, Sigma) 0.1% (w/v) solution (Alcian blue was dissolved in 0.16 M sucrose buffered with sodium acetate 0.05 M, and finally adjusted to pH 5.8 with HCl IM). The tissue was stained for 2 h in Alcian blue solution; excess dye was removed by 2 successive rinses, soaking the tissue each time in 10 ml sucrose 0.25 M, first for 15 min and then for 45 min. Dye complexed with gastric wall mucus was then extracted with 10 ml magnesium chloride at 30 min intervals for 2 h. Four ml of the extract was shaken with an equal volume of ether until an emulsion was formed. This was centrifuged at 3600 rpm for 10 min. Ether was pipetted out and discarded, and the concentration of Alcian blue was determined in the aqueous layer. Color absorbance was recorded using a spectrophotometer (Shimadzu) at 598 nm. The quantity of Alcian blue extract per g wet glandular tissue was calculated from freshly prepared standard curves.

Examination of mast cells

Mast cells in the glandular mucosal layer were stained and measured by the method described by Cho and Ogle.[12] Following ulcer measurement, one half of the glandular stomach was fixed in freshly prepared lead acetate 4% (w/v) solution for 2 days. The tissues were then dehydrated by 1 h immersion in each of progressively increasing concentrations of 70, 95 and 100 % v/v ethanol, and cleared in xylene for 30 min. The specimens were immersed in melted paraffin at 60°C for 3 h, and finally embedded in paraffin block; 7 μm thick sections were made with an "820" Spencer microtome and were transferred to slides, using the water floatation method. The sections were oven-dried at 60°C for 3 h before deparaffinisation with 3 changes of xylene, hydrated by passing the sections at 2 min intervals through solutions of ethyl alcohol 100, 100, 100, 95 and 70% and finally water. Sections were then stained with an aqueous solution of 0.5% w/v toluidine blue for 0.5 min, dehydrated through 3 changes of tertiary butanol over a period of 1.5 min, cleared with xylene (3 changes over 3 min) and mounted in di-phenyl xylol (DPX). The mast cell count was expressed as the number of granulated metachromatically stained cells seen in 42 adjacent oil immersion fields (o.i.f., magnification 100x) covering an area of 1 mm^2. Cells that were partially stained (*i.e.*, partly degranulated) were also counted.

Statistical analysis

The results were expressed as mean ± SEM and analyzed for statistical significance by the two-tailed Student's *'t'* test and by one-way ANOVA followed by Dunnett's test. *P values < 0.05* were considered significant. The ED_{50} values for anti-ulcer activity (ulcer index) were calculated using ED_{50} plus v1.0 software.

Results

Severe hemorrhagic gastric glandular mucosal ulcers were observed in stress-induced control animals (Table 1). Significant change in the ulcer index, GWMC and mast cell count were observed in WIRS-stress as compared with non-stressed controls (Table 1).

Both the β_3-adrenoceptor agonists (CGP 12177A and SR 58611A) reduced the ulcer index in a dose-dependent manner (10 and 15 mg/kg, Table 2). ED_{50} values for antiulcer activity (ulcer index) of CGP 12177A and SR 58611A in WIRS- induced gastric ulcer model were found to be 10.25 and 10.48 mg/kg respectively.

Gastric wall mucus content was significantly higher in the CGP 12177A and SR 58611A treated group at 15 mg/kg dose as compared to controls. At 10 and 15 mg/kg doses, a significant rise in the mast cell count was observed with both the compounds (Table 2).

Discussion

The experimental stress ulcer may be considered equivalent to clinical stress ulcer which occurs after surgery, head injury or shock. An acute gastric hemorrhagic lesion in the glandular stomach characterizes a stress ulcer.[13] The present study shows anti-ulcer activity of β_3-adrenoceptor agonists (CGP 12177A and SR 58611A) which was evident from a significant decrease in the ulcer index at 10 and 15 mg/kg doses in a WIRS-induced gastric ulcer model.

The centrally-induced vascular disturbance of mucosal capillaries is being implicated in restraint-induced gastric

Table 1

Effect of water immersion plus restraint stress (WIRS) on ulcer index, gastric wall mucus content (GWMC) and mucosal mast cell count in rats

Group	*Ulcer index*	*GWMC (mg Alcian blue/ g wt. of glandular tissue)*	*Mast cell counts per 42 o.i.f.*
No stress	0.02 ± 0.02	1.85 ± 0.14	74.13 ± 5.04
WIRS- stress	1.42 ± 0.22*	0.48 ± 0.07*	23.38 ± 3.14*

*$P<0.001$ when compared with the No stress group (Student's '*t*' test). The values are mean ± SEM, n = 8 in each group.

Table 2

Effect of CGP 12177A and SR 58611A on WIRS-induced gastric ulceration in rats

Pretreatment (p.o.)	*Dose (mg/kg)*	*Ulcer index*	*GWMC (mg Alcian blue/ g wt. of glandular tissue)*	*Mast cell counts 42 (o.i.f.)*	*SI of intraluminal bleeding*
Control	Saline 0.5 ml/100 g	1.42 ± 0.22	0.48 ± 0.07	23.38 ± 3.05	2.13 ± 0.29
CGP 12177A	5	0.92 ± 0.13	0.58 ± 0.07	35.38 ± 3.20	1.63 ± 0.26
CGP 12177A	10	0.69 ± 0.12*	0.68 ± 0.08	49.25 ± 2.96*	1.50 ± 0.19
CGP 12177A	15	0.48 ± 0.10*	0.89 ± 0.07*	59.50 ± 3.26*	1.50 ± 0.19
SR 58611A	5	0.99 ± 0.15	0.62 ± 0.09	36.25 ± 3.70	1.50 ± 0.27
SR 58611A	10	0.68 ± 0.11*	0.75 ± 0.08	51.88 ± 3.32*	1.75 ± 0.25
SR 58611A	15	0.49 ± 0.10*	1.07 ± 0.10*	56.50 ± 4.28*	1.50 ± 0.19
One-way ANOVA		F 5.95	5.89	14.86	
		df 6,49	6,49	6,49	
		P *<0.05*	*<0.05*	*<0.05*	

*$P < 0.05$ when compared with the control group (Dunnett's test). The values are mean ± SEM. n=8 in each group.

bleeding[13]. β_3-adrenoceptor agonists can cause enhancement in antral gastric mucosal blood flow (GMBF) in rats.[5] The insignificant decrease in score of intensity of intraluminal bleeding caused by β_3-adrenoceptor agonists in the present study can be partly attributed to their ability to enhance antral GMBF. The specific pathophysiologic mechanism involved in stress-induced ulcers could be ultimate multifactorial impairment of mucosal defense system. An increase in gastric acid secretion, reduction of gastric mucus and alteration in the microvasculature of the gastric mucosa play a major role in the pathogenesis of stress- induced ulcers.[14,15] Our earlier study has shown that the mechanism of the anti-ulcer action of β_3-adrenoceptor agonists in the pylorus ligation model is partly attributed to a decrease in acid secretion. β-adrenoceptor agonists are known to inhibit the release of histamine.[2] Histamine has been known to induce gastric acid secretion mainly through H_2-receptor activation.[16] Gastrin-stimulated and cholinergically-mediated acid secretions require a background release of histamine from mast cells for their maximal effects. Thus any agent that reduces the release of histamine from mast cells should suppress acid secretion.[17] Therefore, the effect of β_3-adrenoceptor agonists on mucin activity and mast cell counts was also studied in the present study. In the WIRS-induced gastric ulcer model, enhanced mucin activity (GWMC) and increase in mast cell counts (*i.e.*, decrease in mast cell degranulation) caused by CGP 12177A and SR 58611A may explain the antiulcer action of β_3-adrenoceptor agonists.

In conclusion, our study shows significant gastroprotective activity of β_3-adrenoceptor agonists against WIRS-induced gastric ulcer model. The mechanism for antiulcer action is attributed to the enhancement of mucin activity and a decrease in mast cell degranulation.

Acknowledgements

The authors are thankful to M/s Novartis, Switzerland and Sanofi Recherche, France for supplying gift samples of CGP 12177A and SR 58611A.

References

1. Anthony A, Schepelmann S, Guillaume JL, Strosberg AD, Dhillon AP, Pounder RE, *et al.* Localisation of the β_3-adrenoceptors in the human gastrointestinal tract: an immunohistochemical study. Aliment Pharmacol Ther 1998;12:519-25.
2. Schleimer RP, MacGlashan DW Jr, Peters SP, Naclerio R, Proud D, Adkinson NF, *et al.* Inflammatory mediators and mechanisms of release from purified human basophils and mast cells. J Allergy Clin Immunol 1984;74:473-81.
3. Gentilini G, Grazia di Bello D, Raspanti S, Mugnai S, Zilleti L. Salmeterol inhibits anaphylactic histamine release from guinea pig isolated mast cells. J Pharm Pharmacol 1994;46:76-7.
4. Espluges J, Lloris JM, Marti-Bonmati E, Morcillo EJ. Effects of β-adrenoceptor drug stimulation on various models of gastric ulcer in rats. Br J Pharmacol 1982;76:587-94.
5. Kuratani K, Kodama H, Yamaguchi I. Enhancement of gastric mucosal blood flow by β_3-adrenergic agonists prevents indomethacin- induced antral ulcer in the rat. J Pharmacol Exp Ther 1994;270:559-65.
6. Bahl AK, Clayton NM, Coates J, Martin DP, Oakley IG, Strong P, *et al.* Comparison of the profiles of agonists as stimulants of the β_3- adrenoceptor *in vitro* with their gastroprotective effects in the conscious rat. Br J Pharmacol 1996;117:580-6.
7. Paul A, Santani DD. Preliminary study on antiulcer effect of β_3-adrenoceptor

agonists in albino rats. Indian J Pharmacol 2002;34:44-7.
8. Takagi A, Okabe S. The effects of drugs on the production and recovery processes of the stress ulcer. Jpn J Pharmacol 1968;18:9-18.
9. Hayase M, Takeuchi K. Gastric acid secretion and lesion formation in rats under water- immersion stress. Dig Dis Sci 1986;31:166-71.
10. Goswami S, Jain S, Santani DD. Antiulcer activity of cromakalim (BRL 34915), a potassium channel opener, against experimentally induced gastric and duodenal ulcers in rats and guinea-pigs. J Pharm Pharmacol 1997;49:195-9.
11. Corne SJ, Morrissey SM, Woods RJ. Proceedings: A method for the quantitative estimation of gastric barrier mucus. J Physiol 1974;242:116-7.
12. Cho CH, Ogle CW. A correlative study of antiulcer effects of zinc sulphate in stressed rats. Eur J Pharmacol 1978;48:97-105.
13. Brodie DA, Hooke KF. The effect of vasoactive agents on stress- induced gastric haemorrhage the in rat. Digestion 1971;4:193-204.
14. Kitagawa H, Fujiwara M, Osumi Y. Effect of water- immersion stress on gastric secretion and mucosal blood flow in rats. Gastroenterology 1979;77:298-302.
15. Blum AL. Therapeutic approach to ulcer healing. Am J Med 1985;79:8-14.
16. Black JW, Duncan WA, Durant CJ, Ganellin CR, Parsons EM. Definition and antagonism of histamine H_2- receptors. Nature 1972;236:385-90.
17. Stevens MH, Thirlby RC, Richardson CT, Fredrickson MA, Unger RH, Feldman M. Inhibitory effects of β-adrenergic agonists on gastric acid secretion in dogs. Am J Physiol 1986;251:453-9.

Pergamon

Bioorganic & Medicinal Chemistry Letters 8 (1998) 3087–3092

BIOORGANIC & MEDICINAL CHEMISTRY LETTERS

3-PYRIDYLETHANOLAMINES: POTENT AND SELECTIVE HUMAN β3 ADRENERGIC RECEPTOR AGONISTS

Elizabeth M. Naylor,* Vincent J. Colandrea, Mari R. Candelore, Margaret A. Cascieri, Lawrence F. Colwell, Jr., Liping Deng, William P. Feeney, Michael J. Forrest, Gary J. Hom, D. Euan MacIntyre, Catherine D. Strader,[1] Laurie Tota, Pei-Ran Wang, Matthew J. Wyvratt, Michael H. Fisher, and Ann E. Weber

Departments of Medicinal Chemistry, Biochemistry and Physiology, Pharmacology, and Laboratory Animal Resources,

Merck Research Laboratories, Rahway, New Jersey 07065, U.S.A.

Received 20 July 1998; accepted 16 September 1998

Abstract: The 3-pyridylethanolamine L-757,793 is a potent β_3 AR agonist (EC_{50} 6.3 nM, 70% activation) with 1,300- and 500-fold selectivity over binding to the β_1 and β_2 ARs, respectively. L-757,793 stimulated lipolysis in rhesus monkeys (ED_{50} 0.2 mg/kg) with a maximum response equivalent to that elicited by isoproterenol.

β_3 Adrenergic receptor agonists (AR) are potential anti-obesity drugs.[2] These agents activate specific receptors, located on the surface of adipocytes, causing stimulation of lipolysis and an increase in metabolic rate. A number of different structural classes of β_3 AR agonists have been disclosed.[3] The arylethanolamine BRL 37344 (1) was one of the first β_3 AR agonists to be discovered. In rats, BRL 37344 is a potent, selective β_3 AR agonist and was used to identify the β_3 AR in rat brown adipocytes.[4] Subsequently, cloning and expression of the human and rat β_3 ARs indicated differences in their pharmacological properties.[5] In human AR assays performed here at Merck, BR 37344 is a weak β_3 partial agonist (β_3 EC_{50} 450 nM, 23% activation) with β_1 and β_2 AR binding affinities of 5,000 and 3,000 nM, respectively.[6]

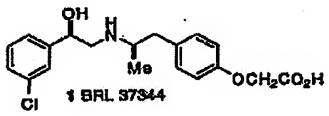

1 BRL 37344

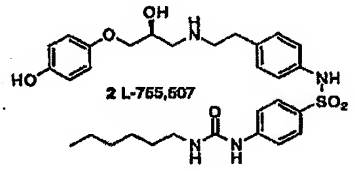

2 L-755,507

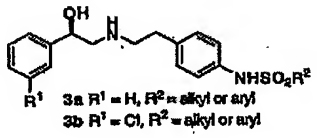

3a R^1 = H, R^2 = alkyl or aryl
3b R^1 = Cl, R^2 = alkyl or aryl

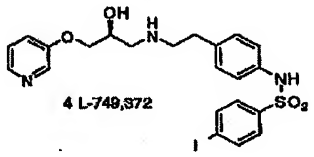

4 L-749,372

Recent publications from Merck describe a number of aryloxypropanolamines.[7–10] Aryloxypropanolamine L-755,507 (2) is a highly potent human β_3 AR agonist (β_3 EC_{50} 0.43 nM, 52% activation) with greater

0960-894X/98/$ - see front matter
PII: S0960-894X(98)00571-X

than 400-fold selectivity over binding to the β_1 and β_2 ARs, respectively.[8,9] The sulfonamide moiety present in L-755,507 and related compounds imparts significant potency and selectivity for the human β_3 AR.[7] We decided to investigate whether incorporation of a sulfonamide moiety into the arylethanolamines would have a similar effect.[11]

Series of phenethanolamines **3a** and the 3-chloro analogs **3b** were synthesized and their biological profiles examined.[12] These compounds exhibited minimal β_3 AR agonist activity (data not shown). Modification of the aryloxy group present in the L-755,507 series led to the discovery of 3-pyridyloxypropanolamine L-749,372 (**4**).[10] L-749,372 is a β_3 AR partial agonist (EC_{50} 3.6 nM, 33% activation) with 270- and 30-fold selectivity over binding to the β_1 and β_2 ARs, respectively. In view of the biological profile of L-749,372, we prepared a series of 3-pyridylethanolamines **5**. The synthesis of these compounds is illustrated in the Scheme.[13]

Scheme. Asymmetric Synthesis of 3-Pyridylethanolamines

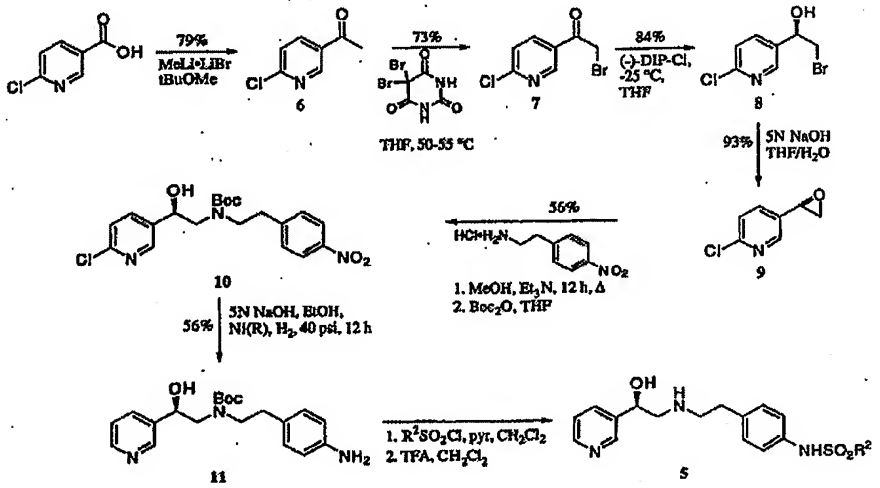

Reaction of 6-chloronicotinic acid with methyllithium lithium bromide complex gave the methyl ketone **6**.[14] The methyl ketone **6** was treated with bromobarbituric acid in refluxing tetrahydrofuran (THF) to afford the bromoketone **7**. In the absence of the chloro substituent, the bromoketone was unstable. Asymmetric reduction with (-)-DIP-Chloride™ [(-)-*B*-chlorodiisopinocampheylborane] provided the bromohydrin **8** that was converted to the epoxide **9** with base.[15] Epoxide opening with *p*-nitrophenethylamine hydrochloride followed by protection of the resultant secondary amine with di-*tert*-butyldicarbonate gave the protected ethanolamine **10**. Epoxide opening with *p*-nitrophenethylamine rather than *p*-aminophenethylamine produced an improved yield and precluded a selective protection step. Concomitant dechlorination and reduction of the nitrobenzene to aniline were effected by hydrogenation under basic conditions using Raney® nickel as catalyst. Aniline **11** was sulfonylated with the appropriate sulfonyl chloride[16] then deprotected with trifluoroacetic acid

(TFA) to afford the desired 3-pyridylethanolamines **5**. In vitro data for these compounds is shown in Tables 1 and 2.

Table 1. Comparison of the β_3 AR Agonist Activity and β_1 and β_2 Binding Affinity for Sulfonamides **5a–j**

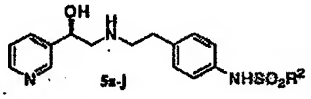

Compound	R^2	β_3 EC_{50}, nM (%act)[a]	β_1 Binding IC_{50}, nM[b]	β_2 Binding IC_{50}, nM[b]
5a	Me	(1)[c]	7,000	10,000
5b	isoPro	(1)[c]	100,000	50,000
5c	$(CH_2)_2Ph$	(12)[c]	100,000	8,000
5d	Ph	160 (55)	20,000	8,000
5e	2-Naphthyl	38 (78)	10,000	1,000
5f	3-Quinolinyl	(26)[c]	100,000	1,000
5g	4-isoPro-Ph	56 (65)	30,000	6,000
5h	4-Cl-Ph	49 (70)	30,000	10,000
5i	4-Br-Ph	77 (65)	10,000	5,000
5j	4-I-Ph	56 (86)	10,000	7,000

[a]Adenylyl cyclase activation given as % of the maximal stimulation with isoproterenol; single point data are reported in parentheses as (% activation @ concentration in nM). [b]Receptor binding assays were carried out with membranes prepared from CHO cells expressing the cloned human receptor in the presence of ^{125}I-iodocyanopindolol. [c]Single point data, % activation at 100 nM.

The methyl-, isopropyl-, and phenethylsulfonamides, **5a**, **5b**, and **5c**, respectively, were essentially inactive in the human β_3 AR assay; however, the benzenesulfonamide **5d** exhibited modest potency and efficacy. Replacement of the phenyl group by a 2-naphthyl moiety led to a 4-fold improvement in β_3 potency. A significant loss in activity was observed with the 3-quinolinylsulfonamide **5f**. Earlier SAR studies in the phenoxypropanolamine series indicated that substitution at the para position of the phenyl ring over the ortho and meta sites was generally the most preferred for β_3 potency enhancement.[7] A number of 4-substituted benzenesulfonamides were prepared and tested. The 4-halo- and 4-isopropylbenzenesulfonamides **5g–j** were all 2- to 3-fold more potent than the parent compound **5d**. These 4-substituted benzenesulfonamides were all at least 100-fold selective (with the exception of the 4-bromo analog, 65-fold selective over β_2 binding) for β_3 AR agonist potency over β_1 and β_2 binding affinity. The ability of these compounds to activate the β_1 and β_2 ARs was low (less than 35% activation at 10 μM).

Next we examined a series of 4-ureidobenzenesulfonamides **5k–o** (Table 2). Increasing the length of the alkyl chain led to enhanced β_3 AR agonist potency. The phenethyl analog **5o** (β_3 EC_{50} 1.6 nM, 55% activation) was equipotent with the octyl urea **5n**. The analogous carbamates **5p–r** and amides **5s–u** were synthesized and tested. In all cases, these compounds were found to have β_3 EC_{50} values less than or equal to their respective urea analogs; however, potencies were usually enhanced with increasingly lipophilic groups as was observed in the urea series. The ureas and amides generally exhibited good selectivity for β_3 AR agonist activity over

binding to the β_1 and β_2 ARs. The carbamates were less selective. In particular, the *n*-hexyl- and phenethylcarbamates **5q** and **5r** were only 14- and 12-fold selective over binding to the β_2 AR. The β_1 and β_2 AR efficacies for these ureas, carbamates and amides were low. The hexylurea **5m** was a weak partial agonist for the β_1 AR (EC_{50} 7,300 nM, 31% activation), and at 1 μM was inactive at the β_2 AR. This highly selective β_3 AR agonist, L-757,793 has an EC_{50} value of 6.3 nM (70% activation) and binds to the β_3 AR with an IC_{50} value of 44 nM.

Table 2. Comparison of the β_3 AR Agonist Activity and β_1 and β_2 Binding Affinity for Sulfonamides **5k–u**

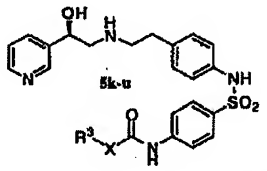

Compound	X	R^3	β_3 EC_{50}, nM (%act)[a]	β_1 Binding IC_{50}, nM[b]	β_2 Binding IC_{50}, nM[b]
5k	NH	Me	100 (63)	2,000	8,000
5l	NH	nPro	68 (33)	2,000	8,000
5m	NH	nHex	6.3 (70)	8,000	3,000
5n	NH	nOct	1.4 (60)	970	410
5o	NH	$(CH_2)_2Ph$	1.6 (55)	160	200
5p	O	nPro	150 (65)	60,000	10,000
5q	O	nHex	27 (70)	2,000	380
5r	O	$(CH_2)_2Ph$	67 (68)	7,000	820
5s	CH_2	nPro	67 (72)	60,000	9,000
5t	CH_2	nHex	18 (81)	8,000	10,000
5u	CH_2	$(CH_2)_2Ph$	18 (53)	10,000	2,000

[a]Adenylyl cyclase activation given as % of the maximal stimulation with isoproterenol. [b]Receptor binding assays were carried out with membranes prepared from CHO cells expressing the cloned human receptor in the presence of ^{125}I-iodocyanopindolol.

The urea L-757,793 **5m** was examined in a rising dose study in anesthetized rhesus monkeys.[17] L-757,793 was given by bolus injection at 15 minute intervals. L-757,793 elicited hyperglycerolemia (ED_{50} 0.2 mg/kg) with a maximum response equivalent to that of isoproterenol. No significant heart rate effects were seen up to the maximum dose tested (1 mg/kg).

When L-757,793 was administered orally (10 mg/kg) to dogs, no serum glycerol response was recorded. Plasma concentrations of L-757,793 were less than 10 nM. A large improvement was observed with the 4-iodophenyl compound **5j**. Its oral bioavailability in dogs (dosed 10 mg/kg po, 3 mg/kg iv) was 51%. This data supports our earlier findings, in the phenoxypropanolamine series,[10] that the urea moiety is detrimental to oral absorption.

In conclusion, we have shown that the 3-pyridylethanolamine L-757,793 is a potent β_3 AR agonist (EC_{50} 6.3 nM) with 1,300- and 500-fold selectivity over binding to the β_1 and β_2 ARs, respectively. Oral bioavailability of L-757,793 was poor; however, the impressive oral bioavailability (51%) of the 4-iodobenzenesulfonamide suggests that modification of the substituents on the benzenesulfonamide moiety has the potential to produce a compound with the desirable biological profile of L-757,793, and the pharmacokinetic properties necessary for an oral therapeutic agent. Work in this area is ongoing and will be published in due course.

Acknowledgment: We thank Mr. Paul Cunningham and Mr. Donald Hora, Jr. for expert technical assistance with the in vivo experiments, Ms. Amy Bernick for mass spectral analyses, Dr. Gerard Kieczykowski and Mr. Joseph Leone for preparing large quantities of key intermediates, and Professor James Grannemann (Wayne State University) for supplying the cloned human β_3 adrenergic receptor.

References and Notes

1. Present address: Schering Plough Research Institute, Kenilworth, NJ 07033, U.S.A.

2. For recent reviews see: Lowell, B. B.; Flier, J. S. *Annu. Rev. Med.* **1997**, *48*, 307; Strosberg, A. D.; Pietri-Rouxel, F. *Trends Pharmacol. Sci.* **1996**, *206*, 373; Arch, J. R. S.; Wilson, S. *Int. J. Obesity* **1996**, *20*, 191.

3. For reviews see: Dow, R. L. *Exp. Opin. Invest. Drugs* **1997**, *6*, 1811; Claus, T. H.; Bloom, J. D. *Ann. Rep. Med. Chem.* **1995**, *30*, 189.

4. Arch, J. R. S; Ainsworth, A. T.; Cawthorne, M. A.; Piercy, V.; Sennitt, M. V.; Thody, V. E.; Wilson, C.; Wilson, S. *Nature* **1984**, *309*, 163.

5. Liggett, S. B. *Mol. Pharmacol.* **1992**, *42*, 634.

6. See ref 9 for experimental details. Briefly, the human β_3 receptor was obtained from Professor J. Grannemann (Wayne State University). The human β_1 and β_2 receptors were cloned as described in Frielle, T.; Collins, S.; Daniel, K. W.; Caron, M. G.; Lefkowitz, R. J.; Kobilka, B. K. *Proc. Natl. Acad. Sci. U.S.A.* **1987**, *84*, 7920 and Kobilka, B. K.; Dixon, R. A.; Frielle, T.; Dohlman, H. G.; Bolanoski, M. A.; Sigal, I. S.; Yan-Feng, T. L.; Francke, U.; Caron, M. G.; Lefkowsitz, R. J. *Proc. Natl. Acad. Sci. U.S.A.* **1987**, *84*, 46. The receptors were expressed in CHO cells at receptor densities of 46–88 fmol/mg (β_3 receptors) or 300–500 fmol/mg (β_1 and β_2 receptors). Agonist activity and binding affinity were assessed by measurement of cellular cAMP levels relative to isoproterenol and inhibition of ^{125}I-iodocyanopindolol binding, respectively.

7. Weber, A. E.; Mathvink, R. J.; Perkins, L.; Hutchins, J. E.; Candelore, M. R.; Tota, L.; Strader, C. D.; Wyvratt, M. J.; Fisher, M. H. *Bioorg. Med. Chem. Lett.* **1998**, *8*, 1101.

8. Parmee, E. R.; Ok, H. O.; Candelore, M. R.; Tota, L.; Deng, L.; Strader, C. D.; Wyvratt, M. J.; Fisher, M. H.; Weber, A. E. *Bioorg. Med. Chem. Lett.* **1998**, *8*, 1107.

9. Fisher, M. H.; Amend, A. M.; Bach, T. J.; Barker, J. M.; Brady, E. J.; Candelore, M. R.; Carroll, D.; Cascieri, M. A.; Chiu, S.-H. L.; Deng, L.; Forrest, M. J.; Hegarty-Friscino, B.; Guan, X.-M.; Hom, G. J.; Hutchins, J. E.; Kelly, L. J.; Mathvink, R. J.; Metzger, J. M.; Miller, R. R.; Ok, H. O.; Parmee, E. R.; Saperstein, R.; Strader, C. D.; Stearns, R. A.; Thompson, G. M.; Tota, L.; Vicario, P. P.; Weber, A. E.; Woods, J. W.; Wyvratt, M. J.; Zafian, P. T.; MacIntyre, D. E. *J. Clin. Invest.* **1998**, *101*, 2387.

10. Weber, A. E.; Ok, H. O.; Alvaro, R. F.; Candelore, M. R.; Cascieri, M. A.; Chiu, S.-H. L.; Deng, L.; Forrest, M. J.; Hom, G. J.; Hutchins, J. E.; Kao, J.; MacIntyre, D. E.; Mathvink, R. J.; McLoughlin, D.; Miller,

R. R.; Newbold, R. C.; Olah, T. V.; Parmee, E. R.; Perkins, L.; Stearns, R. A.; Strader, C. D.; Szumiloski, J.; Tang, Y. S.; Tota, L.; Vicario, P. P.; Wyvratt, M. J.; Fisher, M. H. *Bioorg. Med. Chem. Lett.* 1998, *8*, 2111.

11. Presented in part at the 26th National Medicinal Chemistry Symposium, Richmond, VA, June 1998; Abstract D29.

12. The phenethanolamines **3a** and 3-chloro analogs **3b** were synthesized from the commercially available chiral epoxides in a similar manner to that reported for the aryloxypropanolamines (see ref 7). Epoxide opening with *p*-aminophenethylamine was followed by selective Boc-protection of the resultant secondary amine. Treatment with the appropriate sulfonyl chloride and deprotection with TFA afforded the desired sulfonamides **3a** and **3b**.

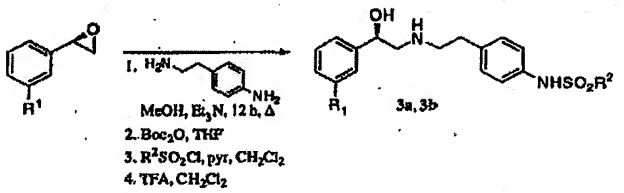

13. The 3-pyridylethanolamines **5a–u** were prepared as optically active *R* enantiomers. Several pairs of *R* and *S* enantiomers in this 3-pyridylethanolamine series have been synthesized and their β_3 AR agonist activity examined. In each case, in line with expectation, the *R* isomer was 5–190 fold more potent than the respective *S* isomer. All final compounds were characterized by NMR, mass spectrometry and HPLC. For experimental details see: Fisher, M. H.; Naylor, E. M.; Weber, A. E. U.S. Patent 5 541 197, 1996.

14. Personal communication from Dr. Sander G. Mills.

15. The enantioselectivity of the chiral reduction was determined by opening the epoxide with *S*-(-)-α-methylbenzylamine. The diasteromeric excess of the resultant ethanolamine was calculated to be 90% from the ^{1}H NMR spectrum.

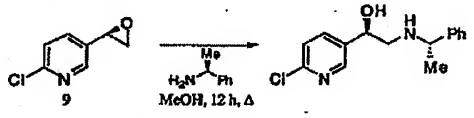

16. The 4-ureidobenzenesulfonyl chlorides were prepared either by treatment of the phenyl urea with chlorosulfonic acid or by addition of the amine to 4-(chlorosulfonyl)phenyl isocyanate. The 4-carbamoylbenzenesulfonyl chlorides were synthesized by addition of the alcohol to 4-(chlorosulfonyl)phenyl isocyanate. The 4-amidobenzenesulfonyl chlorides were prepared by treatment of the 4-amidobenzene with chlorosulfonic acid.

17. Male lean rhesus monkeys (n = 3) were fasted overnight and administered ketamine (10 mg/kg, im) for induction of anesthesia. Catheters were placed in the cephalic vein and femoral artery for intravenous drug administration and measurement of arterial pressure and heart rate. ECG leads were also attached for monitoring Lead II ECG and heart rate. While monitoring the cardiovascular parameters, Nembutal (20–25 mg/kg, iv) was given over 10 min for anesthesia. Heart rate was monitored for approximately 30 min until stable baseline values were obtained, at which time animals were administered a series of bolus doses of test compound in a vehicle consisting of 10% aqueous citric acid solution (10 mM), 30% PEG400, 60% saline. Bolus doses were separated by an interval of 15 min. Blood samples (2 mL) were collected from the femoral artery one min prior to the administration of compound and 14 min after each bolus dose. Serum glycerol was measured using an enzymatic colorimetric assay. After completion of the series of bolus doses of test compound, animals were administered an infusion of isoproterenol (100 μg/kg) over 15 min to elicit a maximal increase in serum glycerol.

Mechanism of Amelioration of Insulin Resistance by β_3-Adrenoceptor Agonist AJ-9677 in the KK-A^y/Ta Diabetic Obese Mouse Model

Hiroshi Kato, Mayumi Ohue, Kaori Kato, Akinori Nomura, Kaoru Toyosawa, Yasuji Furutani, Satoshi Kimura, and Takashi Kadowaki

The mechanism by which the specific β_3-adrenoceptor agonist AJ-9677 relieves insulin resistance in vivo was investigated by studying its effects in the white and brown adipose tissues of the KK-A^y/Ta diabetic obese mouse model. AJ-9677 reduced the total weight of white adipose tissues by reducing the size of the adipocytes, an effect associated with the normalization of tumor necrosis factor-α (TNF-α) and leptin expression levels. The levels of uncoupling protein (UCP)-1 mRNA in brown adipose tissue were increased threefold. AJ-9677 caused a marked increase (20- to 80-fold) in the expression of UCP-1 in white adipose tissues. The levels of UCP-2 mRNA were increased in both the white and brown adipose tissues of diabetic obese mice, and AJ-9677 further upregulated UCP-2 mRNA levels in brown adipose tissue, but reduced its levels in white adipose tissue. UCP-3 mRNA levels were not essentially changed by AJ-9677. However, AJ-9677 significantly (two- to four-fold) upregulated the GLUT4 mRNA and protein levels in white and brown adipose tissues and the gastrocnemius. The generation of small adipocytes, presumably mediated by increased expression of UCP-1 in addition to increased lipolysis in response to AJ-9677, was associated with decreased TNF-α and free fatty acid production and may be the mechanism of amelioration of insulin resistance in KK-A^y/Ta diabetic obese mice. *Diabetes* 50:113–122, 2001

The β_3-adrenoceptor was suspected to exist more than 15 years ago (1), and it is now known to be present in both rodent and human tissues. The human β_3-adrenoceptor was cloned and sequenced in 1989 (2). The characteristics of the β_3-adrenoceptor are quite different from those of β_1- and β_2-adrenoceptors. The β_3-adrenoceptor is expressed mainly in the white and brown adipose tissues (3), and it is important in lipolysis and thermogenesis in rodents (4). The β_3-adrenoceptor agonist BRL 26830A stimulates lipolysis in adipose tissues, and chronic treatment with an adequate dose of BRL 26830A has decreased body weight without reducing food intake (5). This weight loss was caused by the stimulation of energy expenditure and increased lipolysis (6). The effects of the β_3-adrenoceptor on thermogenesis are believed to occur through activation and upregulation of uncoupling protein (UCP)-1, which is mainly expressed in brown adipose tissues. For example, chronic treatment of yellow KK mice with the β_3-adrenoceptor agonist CL 316,243 increased expression of UCP-1 mRNA in brown adipose tissues and induced UCP-1 mRNA in white adipose tissues, the gastrocnemius, and quadriceps muscles (7). Recently, UCP-2 and -3 were identified. UCP-2 is widely expressed in humans; UCP-2 mRNA has been detected in the adipose tissues, skeletal muscles, lungs, the heart, and kidneys (8,9). UCP-3 is expressed primarily in skeletal muscles in humans and in skeletal muscles and brown adipose tissues in rodents (10,11). Regulation of the activation of UCP-2 and -3 may be different from that of UCP-1 (10,12,13), and these two proteins may be functionally involved in energy expenditure (8,10). Therefore, the increased energy expenditure induced by β_3-adrenoceptor agonists in vivo may be mediated by UCP-2 and -3 in addition to UCP-1, especially in humans.

β_3-adrenoceptor agonists have antidiabetic and antiobesity effects in rodent models of type 2 diabetes (14–17), but the molecular mechanisms of these effects, especially the antidiabetic effects, are largely unknown. Molecules secreted by hypertrophic adipocytes (e.g., tumor necrosis factor-α [TNF-α] and free fatty acids [FFAs]) may cause insulin resistance associated with obese type 2 diabetes. The expression levels of TNF-α in white adipose tissues are higher in diabetic obese models than in normal animals, and both neutralization of TNF-α (18) and target disruption of the TNF-α/TNF-α receptor (19) have prevented the development of insulin resistance despite the presence of obesity. TNF-α appears to interfere with the insulin signal transduction pathway by inhibiting the insulin receptor tyrosine kinase and the tyrosine phosphorylation of insulin receptor substrate-1 (18). Moreover, FFAs cause insulin resistance in the skeletal muscles and liver via multiple mechanisms, including the inhibition of phosphatidylinositol 3-kinase activity associated with insulin receptor substrate-1 (20), which may cause inhibition of GLUT4 translocation and glycogen synthesis stimulated by insulin. The expression levels of leptin in white adipose tissues and the plasma levels secreted from adipocytes are higher in diabetic obese models. Administration of leptin causes insulin sensitivity rather than insulin resistance (21). Leptin may be secreted from hypertrophic

From the Department of Pharmacology III (H.K., M.O., K.K., Y.F.), Discovery Research Laboratories; the Research and Development Coordination (A.N.) and the Department of Toxicology (K.T.), Developmental Research Laboratories, Dainippon Pharmaceutical Co., Osaka; and the Department of Metabolic Diseases (H.K., S.K., T.K.), Graduate School of Medicine, University of Tokyo, Tokyo, Japan.

Address correspondence and reprint requests to Hiroshi Kato, Department of Pharmacology III, Discovery Research Laboratories, Dainippon Pharmaceutical Co., Ltd., Osaka 564-0053, Japan. E-mail: hiroshi-kato@dainippon-pharm.co.jp.

ELISA, enzyme-linked immunosorbent assay; FFA, free fatty acid; NEFA, nonesterified fatty acid; OGTT, oral glucose tolerance test; PCR, polymerase chain reaction; PPAR-γ, peroxisome proliferator–activated receptor γ; PVDF, polyvinylidene difluoride; RT, reverse transcription; TNF-α, tumor necrosis factor-α; UCP, uncoupling protein.

adipocytes to compensate for the insulin resistance caused by obesity. In fact, some methods used to cause insulin resistance (e.g., lipid infusion and glucose infusion) were recently found to stimulate leptin gene expression (22). Thiazolidinediones improve insulin sensitivity in diabetic obese models. They increase the number of small white adipocytes and decrease the number of large adipocytes, thereby reducing expression levels of TNF-α and plasma FFA concentrations (23). The regulation of TNF-α expression and FFA production in white adipose tissues may be closely involved in the antidiabetic effect of β_3-adrenoceptor agonists.

Many β_3-adrenoceptor agonists have been developed, but the early compounds did not show the expected effects in humans that were seen in mice and rats. After the cloning of the human β_3-adrenoceptor, differences between the structures of the rat and human receptors were clarified. AJ-9677 was screened with Chinese hamster ovary cells expressing either the human or the rat β_3-adrenoceptor (24). We previously demonstrated that AJ-9677 could stimulate both rat and human β_3-adrenoceptors (24). The present study investigated the effects on diabetes and obesity and the molecular mechanisms of AJ-9677 in the KK-A^y/Ta diabetic obese mouse model.

RESEARCH DESIGN AND METHODS

Chemicals. AJ-9677 ([3-[(2*R*)-[[(2*R*)-(3-chlorophenyl)-2-hydroxyethyl]amino] propyl]-1*H*-indol-7-yloxy]acetic acid), a specific β_3-adrenoceptor agonist (β_1:β_2:β_3 = 1:2:210), was synthesized at Dainippon Pharmaceutical (Osaka, Japan).

Animals and drug treatment. Male 9-week-old KK-A^y/Ta and 11-week-old C57BL/6J mice were purchased from Clea Japan (Tokyo, Japan) and were allowed to adjust to the facilities and handling for 1 week before all experimental protocols. Under standardized conditions, the mice were given dry food (CE-2; Oriental Yeast, Tokyo) and water ad libitum. Mice were divided into control and treatment groups so that the mean body weight of the two groups was comparable 1 day before the starting day (day 1). The treatment group was given AJ-9677 by gavage at 0.01 mg/kg or 0.1 $mg^{-1} \cdot kg^{-1} \cdot day^{-1}$ in the morning for 14 days. The control group was given only 0.5% tragacanth solution. At 24 h after the last administration of AJ-9677, blood samples were collected from the cut ends of the tails and centrifuged to separate plasma. Blood samples from 12-week-old C57BL/6J mice were also collected by the same method. For some mice, the rectal temperature was measured after AJ-9677 administration. Some mice were killed by bleeding under anesthesia 20 h after the final administration of AJ-9677. Epididymal white adipose tissues, inguinal white adipose tissues, interscapular brown adipose tissues, and the gastrocnemius were removed and divided into segments for further studies. The same tissues from 12-week-old C57BL/6J mice were also removed. Some KK-A^y/Ta mice were administered AJ-9677 (0.1 mg/kg) after 24-h fasting to observe the acute effect on lipolytic activity in vivo. Blood samples were collected 1 h after the administration.

Oral glucose tolerance test and determination of plasma glucose, insulin, FFAs, and triglycerides. The oral glucose tolerance test (OGTT) was performed on day 15 after 24 h fasting. The mice received a 20% glucose solution (2 g/kg). Blood samples were collected just before and 0.5, 1, 2, and 3 h after glucose loading. Plasma glucose and insulin levels were determined with a Glucose C-II Test from Wako Pure Chemical Industries (Osaka, Japan) and an insulin enzyme-linked immunosorbent assay (ELISA) from Shibayagi, (Gumma, Japan). FFAs were determined with a nonesterified fatty acid (NEFA) C-Test from Wako Pure Chemical Industries, and Triglycerides were detected with a Determiner triglyceride-S555 from Kyowa Medex Co. (Tokyo, Japan).

Lipolytic activity in white adipocytes. White adipocytes were isolated from epididymal white adipose tissues of KK-A^y/Ta mice by collagenase type II (Sigma Chemical, St. Louis, MO) digestion according to the method described by Rodbell (25). Adipocytes were successively filtered through 1,000-, 500-, and 200-μm meshes and washed in Krebs-Ringer phosphate solution (pH 7.4) containing bovine serum albumin (4 g/100 ml) and glucose (1 mg/ml). Isolated adipocytes were suspended in Krebs-Ringer phosphate solution (pH 7.4) containing bovine serum albumin (1 g/100 ml), glucose (1 mg/ml), phenylisopropyl adenosine (100 nmol/l), and adenosine deaminase (1 U/ml). Adipocytes (~2.5×10^5 cells/ml) were incubated with AJ-9677 or (–)-isoproterenol for 30 min at 37°C. The reaction was terminated with 1N H_2SO_4 and neutralized with 1N NaOH. FFAs were determined with an NEFA C-Test (Wako Pure Chemical Industries). A quantity of the isolated adipocytes was mixed in chloroform-methanol (3:2), shaken vigorously, and centrifuged at 10,000*g*. The precipitate was dissolved in 1N NaOH, and protein was determined with a bicinchoninic acid protein assay reagent (Pierce, IL).

Expression of TNF-α and leptin. Measurements of TNF-α and leptin proteins secreted in isolated white adipose tissues (400–1,000 mg) were performed as described previously (26). Adipose tissues were minced into small pieces and incubated in a Krebs-Ringer phosphate solution (pH 7.4) containing endotoxin-free bovine serum albumin (4 g/100 ml) and glucose (1 mg/ml) at 37°C with rotation (100 rpm). After a 2-h incubation, the incubation mixture was centrifuged and the supernatant collected. Concentrations of TNF-α and leptin proteins were determined with a mouse TNF-α ELISA system (Amersham Pharmacia Biotech U.K., Buckinghamshire, U.K.) and a mouse leptin ELISA kit (Morinaga Bioscience Institute, Yokohama, Japan). Total DNA was also isolated from the adipose tissues as described previously (27).

Histological analysis. Small pieces of epididymal and inguinal white adipose tissues were removed and rinsed with saline. The tissues were fixed with 10% formalin and embedded in paraffin. Tissue sections were cut at a thickness of 2.5 μm and stained with hematoxylin and eosin. To examine the size of the white adipocytes, the number of adipocytes was counted in five limited areas (7×10^{-3} mm^2) of each stained specimen. The mean value of the five areas was designated as an index of the cell size (i.e., a larger number means smaller size). In this analysis, the multilocular adipocytes were excluded. For immunohistochemistry, the paraffin-embedded sections were stained with anti–cytochrome oxidase antibody (Molecular Probes, Eugene, OR). The signals were detected by a Vectastain avitin-biotin-peroxidase complex system with a diaminobenzidine substrate kit (Vector Laboratories, Burlingame, CA). For electron microscopic observations, the tissues were fixed with 2.5% glutaraldehyde and embedded in Epon 812.

Triglycerides and DNA in adipose tissues. The method for determining the triglyceride and DNA contents in the epididymal and inguinal white adipose tissues was slightly modified from the method described by Okuno et al. (23). Briefly, 50 mg adipose tissue was homogenized in 2 ml of a solution containing 150 mmol/l sodium chloride, 0.1% Triton X-100, and 10 mmol/l Tris, pH 8.0, at 50°C using a polytron homogenizer (NS-310E; Micro Tech Nichion, Chiba, Japan) for 1 min. The triglyceride content of this homogenized solution was determined by a Determiner triglyceride-S555 (Kyowa Medex). For DNA determination, the homogenized solution was mixed with SDS, proteinase K, and EDTA to final concentrations of 0.1%, 100 μg/ml, and 10 mmol/l, respectively. After a 12–16 h incubation at 37°C, the DNA was extracted by the phenol-chloroform extraction method. The DNA pellets were redissolved in a solution containing 20 μg/ml ribonuclease A, 1 mmol/l EDTA, and 10 mmol/l Tris at pH 8.0. After 20 min of incubation at 37°C, the DNA was re-extracted by the phenol-chloroform extraction method. The DNA pellets were finally dissolved with TE buffer (10 mmol/l Tris and 1 mmol/l EDTA, pH 8.0). DNA content was calculated from the absorbance at 260 nm, with the optical density at 260 nm of 50 μg/ml DNA solution taken as equal to 1.0 by a Gene Quant RNA/DNA Calculator (Amersham Pharmacia Biotech, U.K.).

Expression of mRNAs by reverse transcription–competitive polymerase chain reaction. Extraction of total RNA from tissues was carried out by homogenizing 50 mg frozen tissue in 1 ml RNAzol B (Tel-Test, Friendswood, TX). RNA pellets were obtained from the homogenate by repeated extraction with chloroform and alcohol precipitation. The mRNA of TNF-α, leptin, GLUT4, and three different subtypes of UCP were quantitatively determined by the reverse transcription (RT)–competitive polymerase chain reaction (PCR) method described by Auboeuf and Vidal (28); however, the internal standard was prepared according to the method of Celi et al. (29). Table 1 lists both the sequences of primers used for internal standards and RT-competitive PCR and the sizes of each target fragment and competitor fragment generated by RT-competitive PCR. For construction of single-strand cDNA, 1 μg of total RNA was used with the SuperScript preamplification system (Life Technologies, Gaithersburg, MD) using oligo$(dT)_{12-18}$ as a primer. The internal standards (competitors) were prepared by PCR using template cDNA constructed with total RNA from epididymal white or interscapular brown adipose tissues and a specific set of oligonucleotides as primers (i.e., forward-short [S] and reverse) (Table 1). RT-competitive PCR was performed with a constant amount of target cDNA and four different amounts of the corresponding internal standard. The PCR conditions were 20–30 cycles of denaturation at 94°C for 15 s, annealing at 55°C (or 62°C for TNF-α) for 30 s, and extension at 72°C for 30 s. The number of cycles was selected to obtain a measurable amount of products depending on the content of the target. The PCR products were subjected to agarose gel electrophoresis and ethidium bromide staining. After photographs were taken, the density of the DNA band was analyzed with the Kodak Digital Science Electrophoresis Documentation and Analysis System 120 (Eastman Kodak Company, Rochester, NY). The initial amount of the target was calculated from the plot of the density ratio of the competitor band to the target band versus the initial amount of the competitor added in the PCR reaction.

Western blot analysis of GLUT4. Crude and plasma membranes were prepared from frozen epididymal white adipose tissues using differential ultracentrifugation as described by Simpson et al. (36) and Kelada et al. (37). Proteins

TABLE 1
Primers used for RT-competitive PCR

Target molecules	Sequences for primers	Locations	Product sizes (bp)	References
UCP-1				
Forward-L	:5′ AAA GCT TGT CAA CAC TTT GG 3′	503–522,	Target : 418	(30)
Forward-S	:5′ AAA GCT TGT CAA CAC TTT GGT AAC ATA TGA CCT CAT G 3′	503–522, and 578–594	Competitor : 363	
Reverse	:5′ GTG GTA CAA TCC ACT GTC TG 3′	901–920		
UCP-2				
Forward-L	:5′ GAC CTA TGA CCT CAT CAA AGA 3′	585–605,	Target : 286	(9)
Forward-S	:5′ GAC CTA TGA CCT CAT CAA AGA CCC TTG CCA CTT CAC TTC TG 3′	585–605, and 642–661	Competitor : 250	
Reverse	:5′ GGT GAC AAA CAT CAC TAC G 3′	852–870		
UCP-3				
Forward-L	:5′ AAG CCA TGA TAC GCC TGG GAA 3′	425–445,	Target : 362	GenBank
Forward-S	:5′ AAG CCA TGA TAC GCC TGG GAA GGC CCA ACA TCA CAA GA 3′	425–445, and 536–552	Competitor : 272	AF032902
Reverse	:5′ CTG AGC CAC CAT CTT CAG CAT 3′	766–786		
Leptin				
Forward-L	:5′ GTT TTG GAG CAG TTT GGA TC 3′	2,528–2,547,	Target : 522	(32)
Forward-S	:5′ GTT TTG GAG CAG TTT GGA TCC AGG TCA TAC CCT GTG GAG 3′	2,528–2,547, and 2,652–2,670	Competitor : 418	
Reverse	:5′ GCA TAT GGG AAG TTT CAC AA 3′	3,030–3,049		
TNF-α				
Forward-L	:5′ GGG ACA GTG ACC TGG ACT GT 3′	891–910,	Target : 520	(33)
Forward-S	:5′ GGG ACA GTG ACC TGG ACT GTA GGT TGC CTC TGT CTC AGA A 3′	891–910, and 1,009–1,028	Competitor : 422	
Reverse	:5′ GCA GAG GTT CAG TGA TGT AG 3′	1,391–1,410		
GLUT4				
Forward-L	:5′ TAG AGC AGG AGG TGA AAC CC 3′	2,066–2,085,	Target : 363	(34)
Forward-S	:5′ TAG AGC AGG AGG TGA AAC CCT CCT TTC CTC TAC AGC A 3′	2,066–2,085, and 2,172–2,188	Competitor : 277	
Reverse	:5′ TGC AGA CCC CTT CTC GAA AG 3′	2,409–2,428		
β-actin (for noncoding region)				
Forward-L	:5′ GGT TGG AGC AAA CAT CCC CC 3′	1,351–1,370,	Target : 460	(35)
Forward-S	:5′ GGT TGG AGC AAA CAT CCC CCA AGT GGT TAC AGG AAG TCC C 3′	1,351–1,370, and 1,471–1,490	Competitor : 360	
Reverse	:5′ TTG TGT AAG GTA AGG TGT GC 3′	1,791–1,810		
β-actin (for coding region)				
Forward-L	:5′ CGT GGG CCG CCC TAG GCA CCA 3′	102–122,	Target : 541	(35)
Forward-S	:5′ CGT GGG CCG CCC TAG GCA CCA ACT GGG ACG ACA TGG AG 3′	102–122, and 233–249	Competitor : 431	
Reverse	:5′ CTC TTT GAT GTC ACG CAC GAT TTC 3′	619–642		

For RT-competitive PCR, forward-long (L) and reverse primers were used, except that the forward-S primer was used instead of the forward-L primer to prepare internal standard (competitor). To standardize the amount of the target molecule, the amount of β-actin mRNA was determined using either the noncoding region primer set or the coding region primer set (the latter being used only for the gastrocnemius muscle β-actin mRNA).

in crude and plasma membrane fractions were separated by SDS-PAGE on 12.5% gels using the system described by Laemmli (38). The separated proteins were transferred to polyvinylidene difluoride (PVDF) membranes at 10 V for 30 min by the semidry blotting system (Bio-Rad Laboratories, Hercules, CA). The PVDF membranes were blocked with Block Ace (Dainippon Pharmaceutical) and incubated for 1 h with polyclonal anti-GLUT4 antibody (Transformation Research, Framingham, MA). The membranes were subsequently incubated with anti–rabbit IgG antibody conjugated with horseradish peroxidase (Santa Cruz Biotechnology, Santa Cruz, CA) for 1 h. The immunolabeled signals were detected with autoradiography film using the enhanced chemiluminescence system (Amersham Pharmacia Biotech).

Statistical analysis. Values are shown as the means ± SE. The statistical significance of the values was analyzed by the Dunnett's two-tailed test when more than three groups were compared or the two-tailed Student's t test or the Welch t test when two groups were compared.

RESULTS

Effects of AJ-9677 on plasma glucose, insulin, FFA, and triglyceride levels. Control KK-A^y/Ta diabetic obese mice showed marked hyperglycemia, hyperinsulinemia, hypertriglyceridemia, and high FFA levels compared with normal C57BL/6J mice (Table 2). AJ-9677 stimulated lipolysis in vitro dose-dependently with higher potency than isoproterenol (Fig. 1). Acute administration of AJ-9677 also stimulated lipolysis, and plasma FFA levels were increased (0.77 ± 0.05 to 1.63 ± 0.05 mEq/l, $P < 0.001$, $n = 8$). However, in mice treated with AJ-9677 (0.1 mg/kg) for 14 days, hyperglycemia and high FFA levels were completely normalized and

TABLE 2
Effects of AJ-9677 treatment for 14 days on the body weight, total food intake, plasma parameters, weight of epididymal white adipose tissues, and triglyceride contents of white adipose tissues in KK-A^y/Ta diabetic obese mice and C57BL/6J mice

	KK-A^y/Ta		
	Control	AJ-9677 (0.1 mg/kg)	C57BL/6J
Body weight (g) on day 1	38.1 ± 0.6	37.8 ± 1.1	—
Body weight (g) on day 15	40.2 ± 0.7	37.8 ± 0.8	—
Body weight increase (%)	5.28 ± 0.53	0.03 ± 1.54*	—
Total food intake (g)	87.0 ± 4.0	87.0 ± 2.9	—
Plasma glucose (mg/dl)	421.1 ± 28.6	208.7 ± 10.3†	160.9 ± 9.2
Plasma insulin (ng/ml)	87.78 ± 11.84	4.15 ± 0.72†	1.35 ± 0.26
Plasma FFA (mEq/l)	0.61 ± 0.03	0.18 ± 0.01†	0.32 ± 0.04
Plasma triglyceride (mg/dl)	601.6 ± 28.1	217.1 ± 10.0†	121.0 ± 3.7
Epididymal WAT (g)	1.72 ± 0.05	0.91 ± 0.04†	0.26 ± 0.03
Triglyceride content in epididymal WAT (mg/μg DNA)	5.67 ± 0.70	3.09 ± 0.30†	2.66 ± 0.22
Triglyceride content in inguinal WAT (mg/μg DNA)	6.09 ± 0.66	3.05 ± 0.33*	1.93 ± 0.18

Data are means ± SE; n = 6–8 in KK-A^y/Ta groups and 5 in the C57BL/6J group. Blood and tissue samples were collected under well-fed conditions. *P < 0.01 and †P < 0.001 vs. the control group. WAT, white adipose tissue.

hyperinsulinemia and hypertriglyceridemia were markedly improved (Table 2). The OGTT indicated that the diabetic obese mice treated with AJ-9677 showed significantly lower glucose levels after glucose loading and significantly lower levels of plasma insulin than the untreated control mice (Fig. 2). These data clearly indicate that the AJ-9677 antidiabetic effect is mediated by the amelioration of insulin resistance in the diabetic obese mouse model. Although AJ-9677 treatment did not alter the total food intake, age-dependent weight gain was reduced in the diabetic obese mice (Table 2). These results suggest that AJ-9677 may inhibit weight gain by increasing energy expenditure. Consistent with this idea, rectal temperature was elevated by ~1°C (36.8 ± 0.2 to 37.7 ± 0.1°C, P < 0.01, n = 8) 1.5 h after the administration on day 1 of 0.1 mg/kg of AJ-9677.

Effects of AJ-9677 on white adipose tissues. The mice treated with AJ-9677 showed an ~50% reduction in the weight of epididymal white adipose tissues compared with the control mice (Table 2). Moreover, triglyceride levels in the

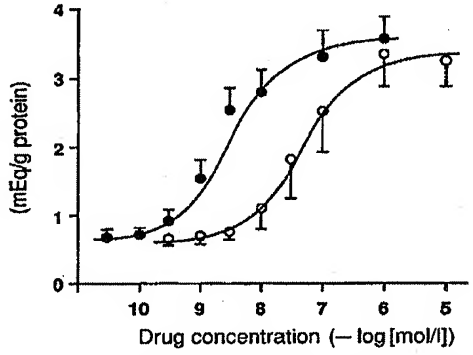

FIG. 1. Lipolytic activities of AJ-9677 in white adipocytes from KK-A^y/Ta diabetic obese mice. Isolated adipocytes were incubated with AJ-9677 (●) or isoproterenol (○). FFA concentrations were normalized to protein concentrations. The data are expressed as means ± SE of four experiments.

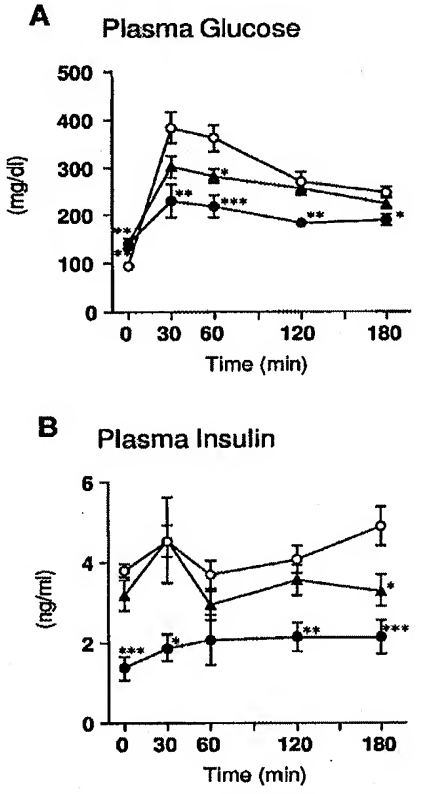

FIG. 2. Effects of AJ-9677 on glucose tolerance in KK-A^y/Ta diabetic obese mice. OGTT was performed after 24-h fasting after administration of AJ-9677 (0.01 mg^{-1} · kg^{-1} · day^{-1} or 0.1 mg^{-1} · kg^{-1} · day^{-1}) for 14 days. Blood samples were collected sequentially and plasma glucose (*A*) and insulin (*B*) were measured. ○, control; ▲, AJ-9677 (0.01 mg/kg); ●, AJ-9677 (0.1 mg/kg). The data are expressed as means ± SE; n = 6 in each group. *P < 0.05, **P < 0.01, and ***P < 0.001 compared with the control group.

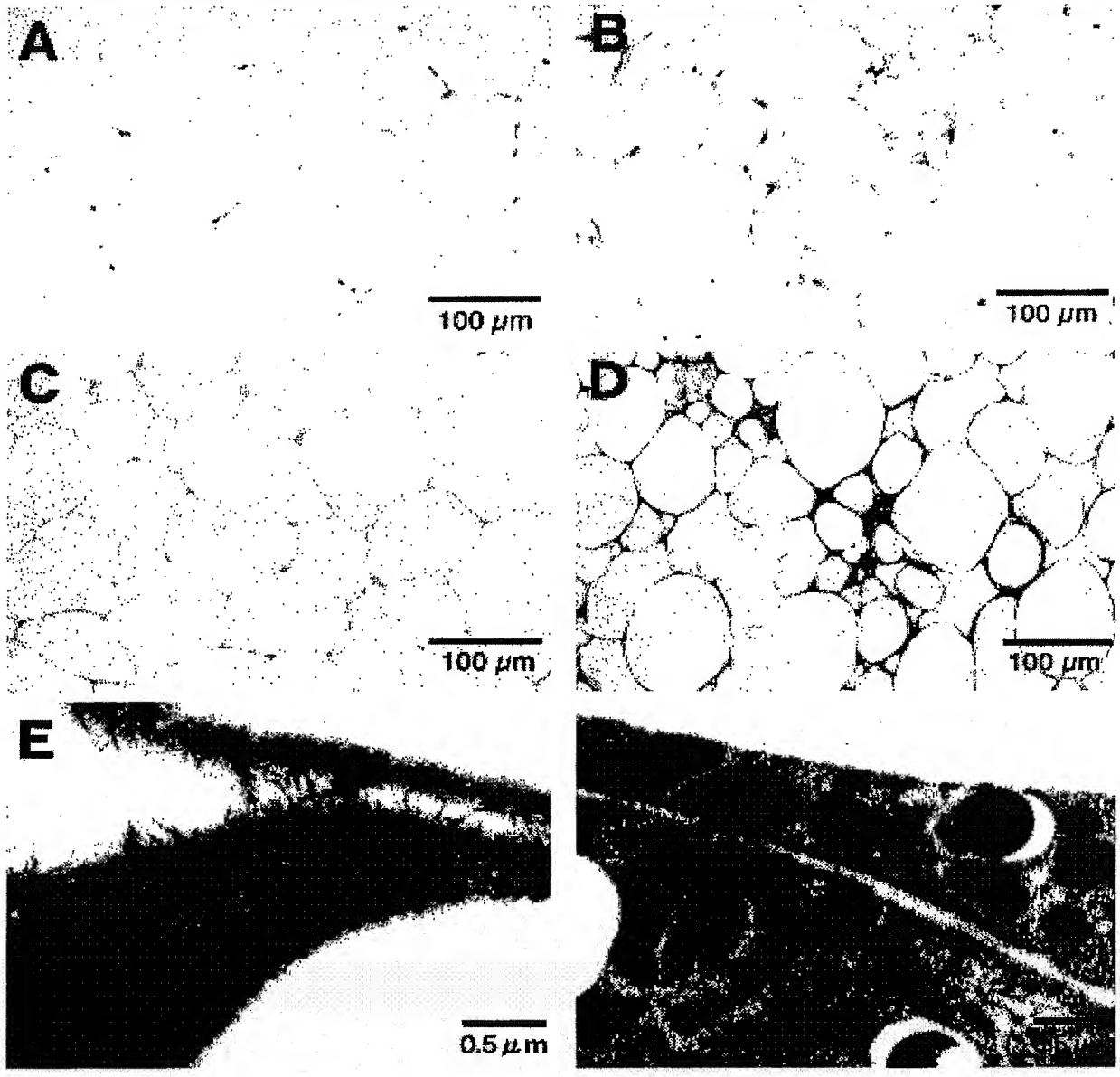

FIG. 3. Histological examination of white adipose tissues from control and AJ-9677–treated KK-A^{y}/Ta diabetic obese mice. Tissues were removed after a 14-day treatment under well-fed conditions. *A*, *C*, and *E* show control KK-A^{y}/Ta mice. *B*, *D*, and *F* show AJ-9677–treated KK-A^{y}/Ta mice. *A* and *B* show epididymal white adipose tissues stained with hematoxylin and eosin. *C* and *D* show epididymal white adipose tissues immunostained with anti-cytochrome oxidase antibody. *E* and *F* show electron microscopic observations of inguinal white adipose tissues.

epididymal white adipose tissues normalized to DNA levels (TG/DNA ratios) were also reduced by ~50%, to almost the same level as the control levels (Table 2), indicating that the triglyceride content per cell was reduced to normal. TG/DNA ratios in inguinal white adipose tissues were also reduced by ~50% by AJ-9677 treatment (Table 2).

Histological analysis of white adipose tissues. Treatment with AJ-9677 clearly reduced the size of adipocytes in the epididymal white adipose tissues (Fig. 3*A* and *B*). The number of white adipocytes in the limited area was larger in the AJ-9677–treated group than that in the control group. This effect was exerted in a dose-dependent manner (i.e., a

TABLE 3
Effects of AJ-9677 administration on the size of white adipocytes

	Number of cells (cells per 7×10^{-3} mm^2)
Experiment 1	
Control	91.7 ± 3.9
AJ-9677 (0.01 mg/kg)	111.6 ± 7.8*
Experiment 2	
Control	75.2 ± 3.1
AJ-9677 (0.1 mg/kg)	120.1 ± 2.3†

Data are means ± SE; $n = 10$ in each group.The number of cells were counted in five limited areas of each section stained with hematoxylin and eosin. *$P < 0.05$ and †$P < 0.001$ vs. the control group.

120% increase at a dosage of 0.01 mg/kg and a 160% increase at a dosage of 0.1 mg/kg) (Table 3). Moreover, the AJ-9677 treatment caused the formation of some multilocular adipocytes resembling brown adipocytes. Immunostaining of cytochrome oxidase in the AJ-9677–treated group was stronger than that in the control group (Fig. 3*C* and *D*). These results were also found in the inguinal white adipose tissues (data not shown). These observations suggest that AJ-9677 treatment caused the exaltation of mitochondrial function and the conversion of white adipocytes into brown adipocytes. Alternatively, β_3-adrenoceptor agonist treatment may cause differentiation of preadipocytes of brown adipose tissue lineage in white adipose tissues. AJ-9677 treatment caused a dramatic increase in the number of mitochondria in the cytoplasm of inguinal white adipocytes (Fig. 3*E* and *F*).

Effect of AJ-9677 treatment on the overexpression of TNF-α and leptin mRNA and protein. The TNF-α mRNA levels were markedly higher in control KK-A^y/Ta mice than in C57BL/6J mice. Treatment with AJ-9677 decreased the TNF-α mRNA level to 35% of the control level (Fig. 4*A*). This reduction of TNF-α mRNA was associated with a parallel reduction in the amount of TNF-α protein secreted from the adipocytes (Fig. 4*C*). Very similar data were obtained for leptin mRNA and protein secretion (Fig. 4*B* and *D*). AJ-9677 also reduced the mRNA expression levels and secretion of both TNF-α and leptin in the inguinal white adipose tissues (data not shown).

Effect of AJ-9677 treatment on expression of UCP-1, -2, and -3. AJ-9677 treatment caused the mRNA expression of UCP-1 in brown adipose tissues to be increased threefold (Fig. 5*A*). UCP-2 mRNA levels were increased in the brown adipose tissues of control KK-A^y/Ta mice, and AJ-9677 treatment further upregulated the expression of UCP-2 mRNA. UCP-3 mRNA levels were not changed in the brown adipose tissues of the control KK-A^y/Ta mice, and AJ-9677 treatment did not affect the expression of UCP-3 mRNA. UCP-1 was hardly expressed in the epididymal and inguinal white adipose tissues of both control KK-A^y/Ta and C57BL/6J mice. However, administration of AJ-9677 caused a 20- to 80-fold increase in UCP-1 expression levels in the epididymal (Fig. 5*B*) and inguinal (Fig. 5*C*) white adipose tissues. UCP-2 expression levels were increased three- to sixfold in both epididymal and inguinal white adipose tissues of the control KK-A^y/Ta mice, as seen in brown adipose tissues (Fig. 5*B* and *C*). However, the expression of UCP-2 mRNA was reduced and left unchanged by AJ-9677 in the epididymal and inguinal white adipose tissues, respectively, unlike the effects seen in brown adipose tissues (Fig. 5*B* and *C*). The expression of UCP-3 was not altered in white and brown adipose tissues of the control KK-A^y/Ta mice. Although AJ-9677 treatment decreased UCP-3 expression levels in epididymal white adipose tissues (Fig. 5*B*), it did not affect UCP-3 expression levels in

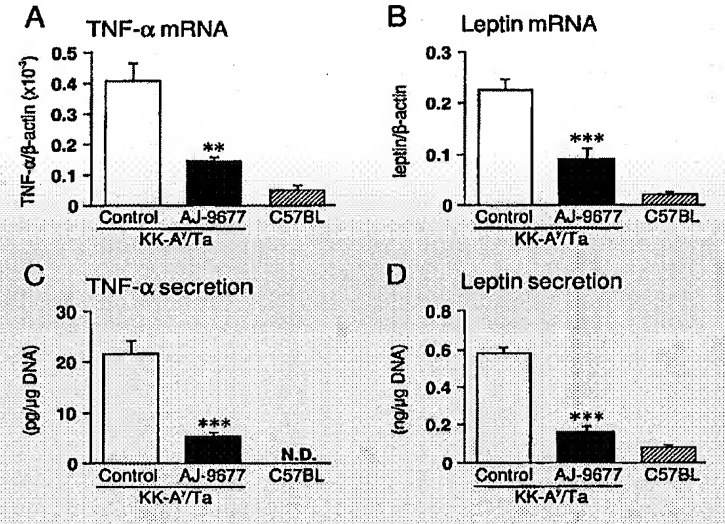

FIG. 4. Messenger RNA expression and secretion of TNF-α and leptin in epididymal white adipose tissues from control and AJ-9677–treated KK-A^y/Ta diabetic obese mice and C57BL/6J mice. Adipose tissues were removed after a 14-day treatment under well-fed conditions. *A* and *B*: TNF-α and leptin mRNA expression, respectively. The mRNA expression levels were analyzed by the RT-competitive PCR method. *C* and *D*: TNF-α and leptin protein secretion, respectively. TNF-α and leptin were measured by ELISA kits. The details of the experiments are described in RESEARCH DESIGN AND METHODS. The data are expressed as means ± SE; $n = 8$ in KK-A^y/Ta groups and $n = 5$ in the C57BL/6J group. **$P < 0.01$ and ***$P < 0.001$ compared with control KK-A^y/Ta group. N.D., not detected.

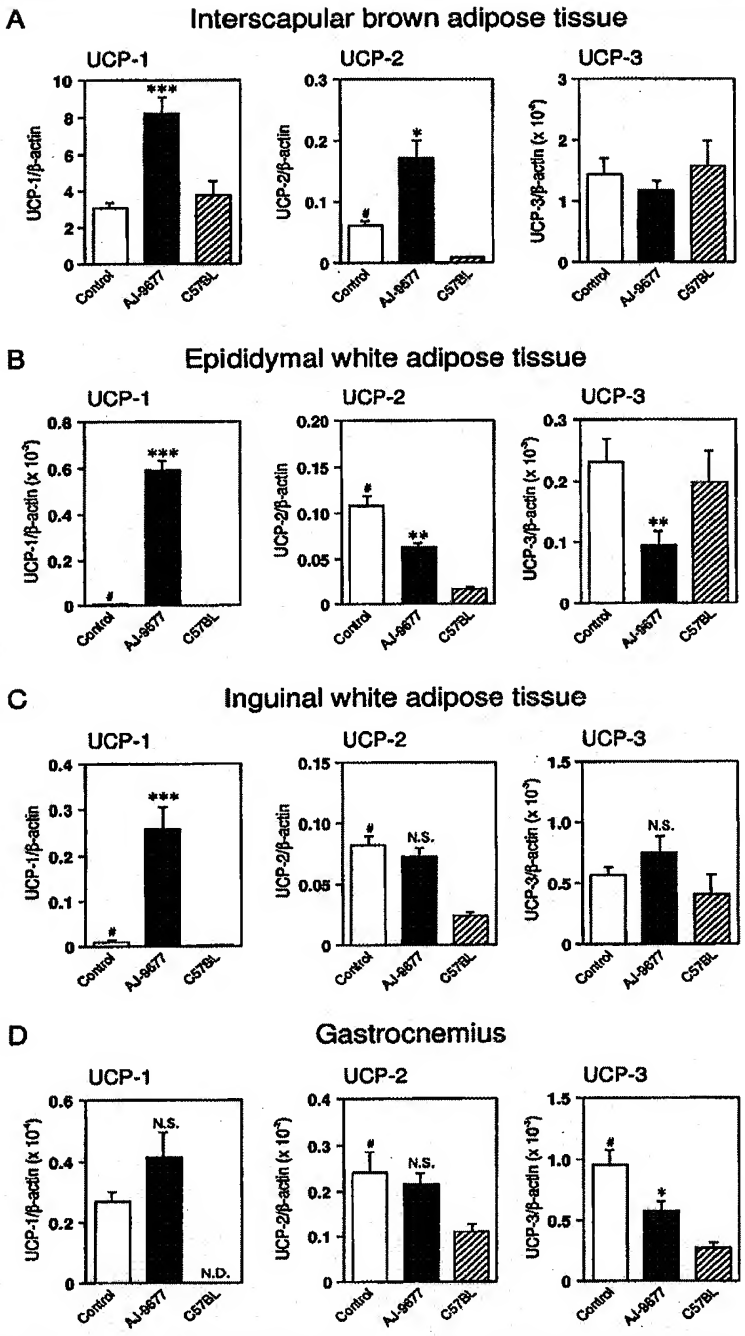

FIG. 5. Expression levels of UCP-1, -2, and -3 mRNA in adipose tissues and the gastrocnemius from control and AJ-9677–treated KK-A^y/Ta diabetic obese mice and C57BL/6J mice. Tissues were removed after a 14-day treatment under well-fed conditions. *A* shows interscapular brown adipose tissues; *B* shows epididymal white adipose tissues; *C* shows inguinal white adipose tissues; and *D* shows the gastrocnemius. The mRNA expression levels were analyzed by the RT-competitive PCR method. The details of the experiments are described in RESEARCH DESIGN AND METHODS. Data are expressed as means ± SE; n = 5–8 in KK-A^y/Ta groups and n = 5 in the C57BL/6J group. *P < 0.05, **P < 0.01, and ***P < 0.001 compared with the control KK-A^y/Ta group. N.S., not significant compared with the control KK-A^y/Ta group. #P < 0.05 compared with the C57BL/6J group.

TABLE 4
Effects of AJ-9677 treatment for 14 days on expression levels of GLUT4 mRNA in epididymal and inguinal white adipose tissues, interscapular brown adipose tissues, and the gastrocnemius in KK-A^y/Ta diabetic obese mice and C57BL/6J mice

	KK-A^y/Ta		
	Control	AJ-9677 (0.1 mg/kg)	C57BL/6J
Epididymal WAT	0.056 ± 0.003	0.207 ± 0.040†	0.059 ± 0.006
Inguinal WAT	0.281 ± 0.013	0.602 ± 0.081*	0.104 ± 0.029
Interscapular BAT	0.636 ± 0.151	1.672 ± 0.152‡	0.786 ± 0.114
Gastrocnemius	0.331 ± 0.056	0.826 ± 0.132†	0.609 ± 0.134

Data are means ± SE; n = 5–8 in each group. All values were normalized by the expression levels of β-actin mRNA. WAT, white adipose tissue; BAT, brown adipose tissue. *P < 0.05, †P < 0.01, and ‡P < 0.001 vs. the control group.

inguinal white adipose tissues (Fig. 5*C*). The expression levels of UCP-1, -2, and -3 mRNA in the gastrocnemius were very low compared with the adipose tissues, and they were not upregulated by AJ-9677 treatment (Fig. 5*D*).

Effect of AJ-9677 treatment on GLUT4 expression. GLUT4 mRNA expression in epididymal white adipose tissues was similar in control KK-A^y/Ta diabetic obese and C57BL/6J mice. AJ-9677 treatment increased GLUT4 mRNA expression approximately fourfold. AJ-9677 treatment also caused a two- to threefold increase in GLUT4 mRNA levels in inguinal white adipose tissues, brown adipose tissues, and the gastrocnemius (Table 4). AJ-9677 treatment also increased GLUT4 protein levels in the crude and plasma membrane of epididymal white adipose tissues four- and sixfold, respectively (Fig. 6).

DISCUSSION

Administration of AJ-9677 for 14 days reduced plasma glucose, insulin, FFA, and triglyceride levels in the diabetic obese mouse model to almost the normal levels seen in C57BL/6J mice. AJ-9677 stimulated lipolysis in adipocytes dose-dependently in vitro. Although the plasma FFA level increased after the first AJ-9677 administration, this effect was not observed after chronic treatment, presumably because plasma FFAs generated by lipolysis may be consumed by thermogenesis. Although we used the dosage of 0.1 $mg^{-1} \cdot kg^{-1} \cdot day^{-1}$, AJ-9677 can reduce these plasma parameters at lower dosages (data not shown). The effective dosage was much lower for AJ-9677 than for other β_3-adrenoceptor agonists reported previously (14,39). White adipose tissues in humans show lower expression levels of β_3-adrenoceptor than in rodents. However, because AJ-9677 is an equally potent agonist against both human and rat β_3-adrenoceptors in the Chinese hamster ovary cell expression system, it may show the same kind of effects, to some extent, in humans as it does in rodents.

Mitochondrial UCPs, which cause respiration without ATP synthesis, are believed to be involved in the expenditure of excess energy. At least three UCP isoforms (UCP-1, -2, and -3) have been cloned. UCP-1 is primarily expressed in brown adipose tissues, and it is slightly expressed in white adipose tissues. In the present study, administration of AJ-9677 increased the expression of UCP-1 threefold in brown adipose tissues and 20- to 80-fold in epididymal and inguinal white adipose tissues. The expression of UCP-2 was increased by 2.5-fold in brown adipose tissues, but it was decreased in epididymal white adipose tissues and unaltered in inguinal white adipose tissues. The expression of UCP-3 was not changed in brown adipose tissues and inguinal white adipose tissues, but it was decreased in epididymal white adipose tissues. Previous reports showed that the β_3-adrenoceptor agonists BRL 35135 and CL 316,243 (40–42) increased the expression of UCP-1 in both brown and white adipose tissues. Our data are consistent with those results. The effect of AJ-9677 on the expression of UCP-2 in brown adipose tissues is different from that of BRL 35135 (40), but consistent with CL 316,243 (41). The effects on UCP-3 expression are inconsistent. Thus, the effects of β_3-adrenoceptor agonists on UCP-2 and UCP-3 expression may depend on the types of β_3-adrenoceptor agonists, the duration of the treatment, and the time of death. Although CL 316,243 increased UCP-1 mRNA in the gastrocnemius (7), AJ-9677 did not increase UCP-1, 2, or 3 mRNA in the tissues. These

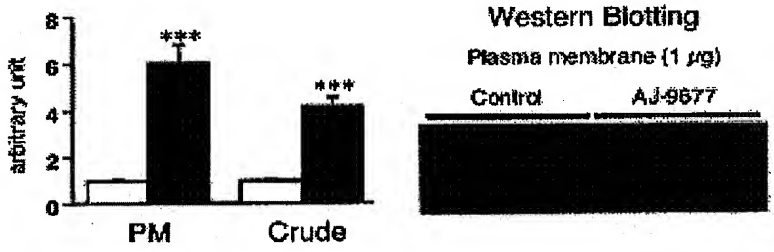

FIG. 6. Protein expression levels of GLUT4 in epididymal white adipose tissues from control and AJ-9677–treated KK-A^y/Ta diabetic obese mice. Tissues were removed after a 14-day treatment under well-fed conditions. Crude and plasma membrane fractions were prepared and analyzed by Western blotting method. The detail was described in RESEARCH DESIGN AND METHODS. Crude, crude membrane; PM, plasma membrane. □, control KK-A^y/Ta mice; ■, AJ-9677–treated KK-A^y/Ta mice. The data are expressed as means ± SE; n = 6 in each group. ***P < 0.001 compared with control KK-A^y/Ta group.

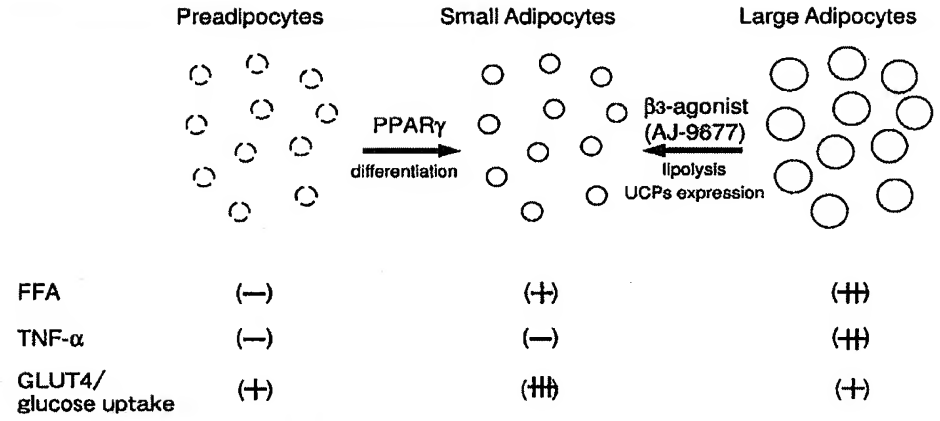

FIG. 7. Proposed mechanism of generation of small adipocytes and amelioration of insulin resistance by β_3-adrenoceptor agonist (AJ-9677). AJ-9677 converts large adipocytes into small adipocytes through increased lipolysis and the induction of uncoupling proteins (e.g., UCP-1) that are associated with the reduction of TNF-α and FFA, which leads to the amelioration of insulin resistance. Thiazolidinediones promote adipocyte differentiation to generate small adipocytes that are also associated with the reduction of TNF-α and FFA, which leads to the amelioration of insulin resistance. Therefore, insulin sensitivity is induced in vivo whether small adipocytes are generated de novo by differentiation via stimulation of PPAR-γ or by conversion from the large adipocytes via β_3-adrenergic receptors. The generation of small adipocytes is the key event in ameliorating insulin resistance.

differences may also depend on the types of β_3-adrenoceptor agonists. The role of UCPs in the muscles may not be very important for the antidiabetic effects of AJ-9677.

The major novel finding of this study is that the β_3-adrenoceptor agonist AJ-9677 reduced the size of white adipocytes, an effect associated with the reduction of mRNA expression and protein secretion of TNF-α and the reduction of plasma FFA levels. The reduction in size of the white adipocytes was confirmed by histological analysis and the triglyceride/DNA ratio. This reduction may be caused by increased lipolysis and energy expenditure mediated by the increased expression of both UCP-1 and UCP-2 after AJ-9677 treatment. We cannot identify the source of UCP-1 overexpressed in white adipose tissues; it is possible that the increased UCP-1 was expressed in the multilocular adipocytes found in the white adipose tissues during AJ-9677 treatment. However, because the absolute expression level of UCP-1 in white adipose tissues was much lower than in brown adipose tissues, white adipose tissues may contribute less to energy expenditure than brown adipose tissues. Thiazolidinediones cause the differentiation of preadipocytes into adipocytes (through the peroxisome proliferator–activated receptor γ [PPAR-γ]) to generate small white adipocytes and, concomitantly, cause the apoptosis of large white adipocytes (23). This reduction of the mean size of adipocytes by thiazolidinediones is associated with the normalization of both increased levels of expression of TNF-α and increased production of FFAs in diabetic obese animal models. Because the increase in the proportion of small adipocytes by thiazolidinediones appears to contribute to the amelioration of insulin resistance via decreased TNF-α expression and decreased FFA production, the reduction in the size of adipocytes by AJ-9677 may contribute to the amelioration of insulin resistance via a similar reduction of TNF-α expression and FFA production. Moreover, the reduction in the size of adipocytes by AJ-9677 may also be associated with decreased levels of leptin expression and secretion in white adipose tissues, which may well reflect the abrogation of the need for compensation for insulin resistance.

TNF-α can cause downregulation of GLUT4 expression (43,44), so decreased TNF-α expression probably contributes to increased GLUT4 expression after AJ-9677 treatment. Moreover, GLUT4 expression on the plasma membrane was preferentially increased compared with the crude membrane, suggesting that AJ-9677 treatment stimulated GLUT4 translocation to the plasma membrane in white adipose tissues. Whether this effect is a direct action of AJ-9677 or secondary to its amelioration of high plasma FFA levels is unclear at present. In either case, the change in the localization of GLUT4 to the plasma membrane, in addition to the increased GLUT4 expression levels, may further contribute to the amelioration of insulin resistance and diabetes.

We would like to propose a novel hypothesis for the relationship between the generation of small adipocytes and the amelioration of insulin resistance, as depicted in Fig. 7. The present study clearly shows that the β_3-adrenoceptor agonist AJ-9677 converted large adipocytes into small adipocytes through increased lipolysis and the induction of UCPs (e.g., UCP-1) that are associated with the reduction of TNF-α and FFA levels and thus the amelioration of insulin resistance. We previously showed that thiazolidinediones promote adipocyte differentiation to generate small adipocytes, which is also associated with reduction of TNF-α and FFA levels, leading to the amelioration of insulin resistance (23). Therefore, insulin sensitivity is induced in vivo whether small adipocytes are generated de novo by differentiation via stimulation of PPAR-γ or by conversion from the large adipocytes via β_3-adrenoceptors. Thus, we would like to propose that the generation of small adipocytes is the key event in the amelioration of insulin resistance.

Hypertrophic obesity resulting from adipocyte hypertrophy, which develops with a high-fat diet and sedentary lifestyle, is closely linked to major health issues (e.g., diabetes, hypertension, hyperlipidemia, and cardiovascular diseases) in Western

countries and in Japan (45). Insulin resistance, which is usually associated with hypertrophic obesity, is believed to be the major mechanism causing these diseases. Thus, the treatment of hypertrophic adipocytes is one of the most important issues in medical science. Thiazolidinediones may not be the ideal agents because the number of adipocytes tends to increase and promote obesity, even though insulin resistance is ameliorated. This study clearly demonstrated that β_3-adrenoceptor agonists (e.g., AJ-9677) appear to convert hypertrophic adipocytes into small adipocytes, thereby ameliorating insulin resistance and obesity simultaneously.

REFERENCES

1. Arch JR, Ainsworth AT, Cawthorne MA, Piercy V, Sennitt MV, Thody VE, Wilson C, Wilson S: Atypical β-adrenoceptor on brown adipocytes as target for anti-obesity drugs. *Nature* 309:163–165, 1984
2. Emorine LJ, Marullo S, Briend-Sutren MM, Patey G, Tate K, Delavier-Klutchko C, Strosberg AD: Molecular characterization of the human β_3-adrenergic receptor. *Science* 245:1118–1121, 1989
3. Granneman JG, Lahners KN, Chaudhry A: Molecular cloning and expression of the rat β_3-adrenergic receptor. *Mol Pharmacol* 40:895–899, 1991
4. Atgie C, D'Allaire F, Bukowiecki LJ: Role of β_1- and β_3-adrenoceptors in the regulation of lipolysis and thermogenesis in rat brown adipocytes. *Am J Physiol* 273:C1136–C1142, 1997
5. Arch JR, Ainsworth AT, Ellis RD, Piercy V, Thody VE, Thurlby PL, Wilson C, Wilson S, Young P: Treatment of obesity with thermogenic β-adrenoceptor agonists: studies on BRL 26830A in rodents. *Int J Obes* 8 (Suppl. 1):1–11, 1984
6. Strosberg AD, Pietri-Rouxel F: Function and regulation of the β_3-adrenoceptor (Review). *Trends Pharmacol Sci* 17:373–381, 1996
7. Nagase I, Yoshida T, Kumamoto K, Umekawa T, Sakane N, Nikami H, Kawada T, Saito M: Expression of uncoupling protein in skeletal muscle and white fat of obese mice treated with thermogenic β_3-adrenergic agonist. *J Clin Invest* 97:2898–2904, 1996
8. Fleury C, Neverova M, Collins S, Raimbault S, Champigny O, Levi-Meyrueis C, Bouillaud F, Seldin MF, Surwit RS, Ricquier D, Warden CH: Uncoupling protein-2: a novel gene linked to obesity and hyperinsulinemia. *Nat Genet* 15:269–272, 1997
9. Gimeno RE, Dembski M, Weng X, Deng N, Shyjan AW, Gimeno CJ, Iris F, Ellis SJ, Woolf EA, Tartaglia LA: Cloning and characterization of an uncoupling protein homolog: a potential molecular mediator of human thermogenesis. *Diabetes* 46:900–906, 1997
10. Boss O, Samec S, Paoloni-Giacobino A, Rossier C, Dulloo A, Seydoux J, Muzzin P, Giacobino JP: Uncoupling protein-3: a new member of the mitochondrial carrier family with tissue-specific expression. *FEBS Lett* 408:39–42, 1997
11. Vidal-Puig A, Solanes G, Grujic D, Flier JS, Lowell BB: UCP3: an uncoupling protein homologue expressed preferentially and abundantly in skeletal muscle and brown adipose tissue. *Biochem Biophys Res Commun* 235:79–82, 1997
12. Millet L, Vidal H, Andreelli F, Larrouy D, Riou JP, Ricquier D, Laville M, Langin D: Increased uncoupling protein-2 and -3 mRNA expression during fasting in obese and lean humans. *J Clin Invest* 100:2665–2670, 1997
13. Boss O, Samec S, Dulloo A, Seydoux J, Muzzin P, Giacobino JP: Tissue-dependent upregulation of rat uncoupling protein-2 expression in response to fasting or cold. *FEBS Lett* 412:111–114, 1997
14. Carroll MJ, Lister CA, Sennitt MV, Stewart-Long N, Cawthorne MA: Improved glycemic control in C57Bl/KsJ (*db/db*) mice after treatment with the thermogenic β-adrenoceptor agonist, BRL 26830. *Diabetes* 34:1198–1204, 1985
15. Cawthorne MA, Carroll MJ, Levy AL, Lister CA, Sennitt MV, Smith SA, Young P: Effects of novel β-adrenoceptor agonists on carbohydrate metabolism: relevance for the treatment of non-insulin-dependent diabetes. *Int J Obes* 8 (Suppl. 1):93–102, 1984
16. Largis EE, Burns MG, Muenkel HA, Dolan JA, Claus TH: Antidiabetic and antiobesity effects of a highly selective β_3-adrenoceptor agonist (CL 316,243). *Drug Dev Res* 32:69–76, 1994
17. Yoshida T, Sakane N, Wakabayashi Y, Umekawa T, Kondo M: Anti-obesity and anti-diabetic effects of CL 316,243, a highly specific β_3-adrenoceptor agonist, in yellow KK mice. *Life Sci* 54:491–498, 1994
18. Hotamisligil GS, Budavari A, Murray D, Spiegelman BM: Reduced tyrosine kinase activity of the insulin receptor in obesity-diabetes: central role of tumor necrosis factor-α. *J Clin Invest* 94:1543–1549, 1994
19. Uysal KT, Wiesbrock SM, Marino MW, Hotamisligil GS: Protection from obesity-induced insulin resistance in mice lacking TNF-α function. *Nature* 389:610–614, 1997
20. Dresner A, Laurent D, Marcucci M, Griffin ME, Dufour S, Cline GW, Slezak LA, Andersen DK, Hundal RS, Rothman DL, Petersen KF, Shulman GI: Effects of free fatty acids on glucose transport and IRS-1-associated phosphatidylinositol 3-kinase activity. *J Clin Invest* 103:253–259, 1999
21. Kamohara S, Burcelin R, Halaas JL, Friedman JM, Charron MJ: Acute stimulation of glucose metabolism in mice by leptin treatment. *Nature* 389:374–377, 1997
22. Wang J, Liu R, Hawkins M, Barzilai N, Rossetti L: A nutrient-sensing pathway regulates leptin gene expression in muscle and fat. *Nature* 393:684–688, 1998
23. Okuno A, Tamemoto H, Tobe K, Ueki K, Mori Y, Iwamoto K, Umesono K, Akanuma Y, Fujiwara T, Horikoshi H, Yazaki Y, Kadowaki T: Troglitazone increases the number of small adipocytes without the change of white adipose tissue mass in obese Zucker rats. *J Clin Invest* 101:1354–1361, 1998
24. Kawashima H, Nomura A, Ohue M, Kato H, Kuwajima J, Furutani Y, Hosoki K, Karasawa T: A novel human β_3-adrenoceptor agonist AD-9677 (Abstract). *Diabetologia* 40 (Suppl. 1):A374, 1997
25. Rodbell, M: Metabolism of isolated fat cells. *J Biol Chem* 239:375–380, 1964
26. Hotamisligil GS, Arner P, Caro JF, Atkinson RL, Spiegelman BM: Increased adipose tissue expression of tumor necrosis factor-α in human obesity and insulin resistance. *J Clin Invest* 95:2409–2415, 1995
27. Sambrook J, Fritsch EF, Maniatis T: *Molecular Cloning: A Laboratory Manual*. 2nd ed. Cold Spring Harbor, NY, Cold Spring Harbor Laboratory, 1989
28. Auboeuf D, Vidal H: The use of the reverse transcription-competitive polymerase chain reaction to investigate the in vivo regulation of gene expression in small tissue samples. *Anal Biochem* 245:141–148, 1997
29. Celi FS, Zenilman ME, Shuldiner AR: A rapid and versatile method to synthesize internal standards for competitive PCR. *Nucleic Acids Res* 21:1047, 1993
30. Kozak LP, Britton JH, Kozak UC, Wells JM: The mitochondrial uncoupling protein gene: correlation of exon structure to transmembrane domains. *J Biol Chem* 263:12274–12277, 1988
32. Zhang Y, Proenca R, Maffei M, Barone M, Leopold L, Friedman JM: Positional cloning of the mouse obese gene and its human homologue. *Nature* 372:425–432, 1994
33. Fransen L, Muller R, Marmenout A, Tavernier J, Van der Heyden J, Kawashima E, Chollet A, Tizard R, Van Heuverswyn H, Van Vliet A Ruysschaert MR, Fiers W: Molecular cloning of mouse tumor necrosis factor cDNA and its eukaryotic expression. *Nucleic Acids Res* 13:4417–4429, 1985
34. Kaestner KH, Christy RJ, Lane MD: Mouse insulin-responsive glucose transporter gene: characterization of the gene and trans-activation by the CCAAT/enhancer binding protein. *Proc Natl Acad Sci U S A* 87:251–255, 1990
35. Tokunaga K, Taniguchi H, Yoda K, Shimizu M, Sakiyama S: Nucleotide sequence of a full-length cDNA for mouse cytoskeletal β-actin mRNA. *Nucleic Acids Res* 14:2829, 1986
36. Simpson IA, Yver DR, Hissin PJ, Wardzala LJ, Karnieli E, Salans LB, Cushman SW: Insulin-stimulated translocation of glucose transporters in the isolated rat adipose cells: characterization of subcellular fractions. *Biochim Biophys Acta* 763:393–407, 1983
37. Kelada AS, Macaulay SL, Proletto J: Cyclic AMP acutely stimulates translocation of the major insulin-regulatable glucose transporter GLUT4. *J Biol Chem* 267:7021–7025, 1992
38. Laemmli UK: Cleavage of structural proteins during the assembly of the head of bacteriophage T4. *Nature* 227:680–685, 1970
39. Arbeeny CM, Meyers DS, Hillyer DE, Bergquist KE: Metabolic alterations associated with the antidiabetic effect of β_3-adrenergic receptor agonists in obese mice. *Am J Physiol* 268:E678–E684, 1995
40. Emilsson V, Summers RJ, Hamilton S, Liu YL, Cawthorne MA: The effects of the β_3-adrenoceptor agonist BRL 35135 on UCP isoform mRNA expression. *Biochem Biophys Res Commun* 252:450–454, 1998
41. Yoshitomi H, Yamazaki K, Abe S, Tanaka I: Differential regulation of mouse uncoupling proteins among brown adipose tissue, white adipose tissue, and skeletal muscle in chronic β_3 adrenergic receptor agonist treatment. *Biochem Biophys Res Commun* 253:85–91, 1998
42. Savontaus E, Rouru J, Boss O, Huupponen R, Koulu M: Differential regulation of uncoupling proteins by chronic treatments with β_3-adrenergic agonist BRL 35135 and metformin in obese *fa/fa* Zucker rats. *Biochem Biophys Res Commun* 246:899–904, 1998
43. Stephens JM, Lee J, Pilch PF: Tumor necrosis factor-α-induced insulin resistance in 3T3-L1 adipocytes is accompanied by a loss of insulin receptor substrate-1 and GLUT4 expression without a loss of insulin receptor-mediated signal transduction. *J Biol Chem* 272:971–976, 1997
44. Long SD, Pekala PH: Regulation of GLUT4 mRNA stability by tumor necrosis factor-α: alterations in both protein binding to the 3′ untranslated region and initiation of translation. *Biochem Biophys Res Commun* 220:949–953, 1996
45. Spiegelman BM, Flier JS: Adipogenesis and obesity: rounding out the big picture (Review). *Cell* 87:377–389, 1996

British Journal of Pharmacology (1999) 127, 949–961
http://www.stockton-press.co.uk/bjp

Characterization of β-adrenoceptor mediated smooth muscle relaxation and the detection of mRNA for β_1-, β_2- and β_3-adrenoceptors in rat ileum

[1,2]S.J. Roberts, [1,2]M. Papaioannou, [1,2]B.A. Evans & *[1,2]R.J. Summers

[1]Department of Pharmacology, University of Melbourne, Parkville, 3052, Victoria, Australia and [2]Department of Pharmacology, Monash University, Clayton, 3168, Victoria, Australia

1 Functional and molecular approaches were used to characterize the β-AR subtypes mediating relaxation of rat ileal smooth muscle.

2 In functional studies, (−)-isoprenaline relaxation was unchanged by CGP20712A (β_1-AR antagonist) or ICI118551 (β_2-AR antagonist) but shifted by propranolol ($pK_B = 6.69$). (±)-Cyanopindolol, CGP12177 and ICID7114 did not cause relaxation but antagonized (−)-isoprenaline relaxation.

3 BRL37344 (β_3-AR agonist) caused biphasic relaxation. The high affinity component was shifted with low affinity by propranolol, (±)-cyanopindolol, tertatolol and alprenolol. CL316243 (β_3-AR agonist) relaxation was unaffected by CGP20712A or ICI118551 but blocked by SR58894A (β_3-AR antagonist; $pA_2 = 7.80$). Enhanced relaxation after exposure to forskolin and pertussis toxin showed that β_3-AR relaxation can be altered by manipulation of components of the adenylate cyclase signalling pathway.

4 The β_1-AR agonist RO363 relaxed the ileum ($pEC_{50} = 6.18$) and was blocked by CGP20712A. Relaxation by the β_2-AR agonist zinterol ($pEC_{50} = 5.71$) was blocked by SR58894A but not by ICI118551.

5 In rat ileum, β_1-, β_2- and β_3-AR mRNA was detected. Comparison of tissues showed that β_3-AR mRNA expression was greatest in WAT > colon = ileum > cerebral cortex > soleus; β_1-AR mRNA was most abundant in cerebral cortex > WAT > ileum = colon > soleus; β_2-AR mRNA was expressed in soleus > WAT > ileum = colon > cerebral cortex.

6 These results show that β_3-ARs are the predominant β-AR subtype mediating rat ileal relaxation while β_1-ARs may produce a small relaxation. The β_2-AR agonist zinterol produces relaxation through β_3-ARs and there was no evidence for the involvement of β_2-ARs in relaxation despite the detection of β_2-AR mRNA.

Keywords: β-adrenoceptors; β_3-adrenoceptors; gastrointestinal smooth muscle; relaxation; rat ileum; messenger RNA

Abbreviations: AR, adrenoceptor; C-R, concentration response; CYP, cyanopindolol; ISO, isoprenaline

Introduction

Although the intestinal β-AR was originally described as a β_1-AR (Lands *et al.*, 1967) atypically low affinities of β-AR antagonists and propranolol-resistant relaxation responses observed in gastrointestinal smooth muscle preparations from several species indicated that other β-AR subtypes were involved in these responses (see Arch & Kaumann, 1993, for review). Atypical β-AR responses that were resistant to blockade by propranolol and selectively stimulated by a novel group of β-AR agonists were also described in adipocytes. The β_3-AR was subsequently cloned and sequenced (Emorine *et al.*, 1989) and found to share many of the pharmacological characteristics of the atypical β-AR. β_3-ARs are highly expressed in adipose tissue and β_3-AR agonists such as BRL 37344, SR 58611A and CL 316,243 are potent stimulants of lipolysis and thermogenesis, cause marked weight loss in obese animals, increase insulin sensitivity and improve glucose tolerance in diabetic animals. Whilst the human β_3-AR is emerging as an exciting target for the development of selective stimulants as potential treatments for obesity and diabetes (Strosberg & Pietri-Rouxel, 1996), these same compounds may also be useful in the treatment of irritable bowel syndrome. β_3-ARs are also highly expressed in regions of the gastrointestinal tract such as colon, ileum and stomach in many species including human (Berkowitz *et al.*, 1995; Evans *et al.*, 1996; Roberts *et al.*, 1997). β_3-AR mediated relaxation in gastrointestinal smooth muscle is resistant to blockade by propranolol and selective β_1- and β_2-AR antagonists such as CGP 20712A and ICI 118551 (for review see Manara *et al.*, 1995).

Earlier studies of gastrointestinal smooth muscle used non-selective β-AR or selective β_1- or β_2-AR agonists to characterize β-AR responses in various animal models. For example, studies using non-selective β-AR or selective β_2-AR agonists in diabetic animal models have shown a marked reduction in β-AR responsiveness in the intestine (Ozturk *et al.*, 1996). Decreased responses to the selective β_2-AR agonist salbutamol are of particular note as the low potency of salbutamol strongly suggests that it is acting through β_3-ARs rather than β_2-ARs. In addition, a recent binding study mapping β-AR subtypes throughout the diabetic rat gastrointestinal tract used a concentration of the radioligand [^{125}I]-CYP (20 pM) so low that it would label only 1.5% of β_3-ARs in each sample (Yu & Ouyang, 1997). The findings from these studies therefore offer limited information on the changes in β-

*Author for correspondence at: Department of Pharmacology, Monash University, Clayton, 3168, Victoria, Australia.
E-mail: roger.summers@med.monash.edu.au

AR density and responsiveness as the tools/compounds used were not appropriate for examination of all three β-AR subtypes. It is necessary to clearly establish the role and contribution of each β-AR subtype to gastrointestinal relaxation and as selective compounds for each subtype are now available, a more comprehensive study is clearly possible. A highly selective β_3-AR agonist, CL 316243, has been developed that has at least 10,000 fold selectivity for the β_3-AR compared with the β_1- and β_2-ARs respectively (Dolan *et al.*, 1994). More recently the first selective β_3-AR antagonists were developed and these new pharmacological tools have enabled a clear demonstration of β_3-AR mediated functional responses in rat colon and rat brown adipose tissue (Manara *et al.*, 1996).

Previous studies of the β_3-AR in rat ileum have been carried out in the presence of β_1- and β_2-AR blockade and the relative contribution of β-AR subtypes has not been examined using agonists and antagonists selective for each of the three β-AR subtypes. Studies of functional responses of rat ileum relaxation (Growcott *et al.*, 1993; Hoey *et al.*, 1996) have shown that stimulation by selective β_3-AR agonists produces a relaxation response in the presence of β_1- and β_2-AR blockade. The aim of this study therefore was to utilize selective β_3-AR compounds as well as selective β_1- and β_2-AR agonists and antagonists to characterize the functional β-AR subtypes present in rat ileum and assess the relative contribution of these subtypes to β-AR mediated relaxation of the rat ileal smooth muscle. We have also measured mRNA levels of the three β-AR subtypes in ileal smooth muscle.

Methods

Tissue preparation and incubation

Male Sprague Dawley rats (250–300 g) were anaesthetized with 80% CO_2/20% O_2 and decapitated. A 12–15 cm segment of the small intestine was removed from 2 cm above the ileocaecal junction and the intraluminal contents flushed out with Krebs Henseleit buffer (composition:- (mM) NaCl 118.4, KCl 4.7, $MgSO_4.7H_2O$ 1.2, KH_2PO_4 1.2, $NaHCO_3$ 25, glucose 11, $CaCl_2$ 2.5) containing ascorbic acid (0.1 mM) and EDTA (0.04 mM). Segments of 1.5–2 cm length were mounted on tissue hooks and suspended in jacketed organ baths containing Krebs Henseleit solution maintained at 37°C and bubbled continuously with 95% O_2/5% CO_2 (pH 7.4) under 5 mN force. Ugo Basile isotonic transducers connected to a MacLab system with an Apple Macintosh IICi Computer were used to measure isotonic changes in the length of the tissues. Tissue strips were equilibrated for 30–45 min in the presence of desipramine (0.5 μM) to block neuronal uptake, hydrocortisone (30 μM) to block extraneuronal uptake of ISO and phentolamine (10 μM) to block β-ARs. Antagonists were added prior to the 30 min equilibration period.

Preliminary experiments

Carbachol concentration response (C-R) curves were performed to determine the concentration producing 70–80% maximum contraction. Carbachol (3 μM) was chosen to precontract longitudinal smooth muscle segments in subsequent experiments (data not shown). The tissue sensitivity to (−)-ISO changed when three successive (−)-ISO C-R curves were performed in individual segments. The first C-R curve ($pEC_{50} = 6.79 \pm 0.02$, $n = 4$) significantly increased the sensitivity ($P < 0.05$) of the tissue to the second C-R curve ($pEC_{50} = 7.14 \pm 0.02$, $n = 4$) and the third C-R curve had a significantly depressed maximum response ($P < 0.05$). By comparison (−)-ISO C-R curves in paired tissues were very consistent so single C-R curves were performed in the absence and presence of antagonists in paired ileum preparations obtained from the same animal.

Concentration response curves in rat ileal smooth muscle

Tissue strips were precontracted submaximally with carbachol (3 μM) for a 15–20 min equilibration period before relaxation by cumulative concentrations of agonists were performed. Agonist curves were constructed using 0.5 log unit increments until a stable state was observed. The time intervals between each concentration ranged from 4–5 min for isoprenaline and zinterol to 20–30 min for BRL 37344 and CL 316,243. At the end of the concentration response (C-R) curve, papaverine (50–100 μM) was added and responses were expressed as a percentage of the maximum papaverine relaxation.

Analysis

The activity of the agonists was expressed as an EC_{50} value obtained by analysis using the non-linear curve fitting program in PRISM (Intuitive Software for Science). When a range of antagonist concentrations was used a Schild plot was constructed (Arunlakshana & Schild, 1959) and the x-intercept of the Schild plot was taken as the pA_2 value. In circumstances where single concentrations of antagonist were used or if the Schild plot was clearly non-linear, pK_B values were calculated according to the method of Furchgott (1972). Statistical significance was determined using Student's *t*-test where $P < 0.05$ was considered to be significant. C-R curves were plotted as means ± s.e.mean of *n* individual experiments. The slope values of regression lines were expressed as slope ± 95% confidence limits (C.L.). All values are expressed as means ± s.e.mean.

Molecular methods

Adult male Sprague Dawley rats (250–300 g) were anaesthetized by 80% CO_2/20% O_2 and killed by cervical dislocation. Epididymal white adipose tissue, cerebral cortex, soleus muscle, ileal and colonic smooth muscle were removed, frozen in liquid N_2 and stored at −70°C. Ileum and colon were carefully dissected free of surrounding adipose tissue, cut open and pinned out, and mucosa removed by scraping with a scalpel. The resulting smooth muscle was washed in Krebs Henseleit solution and blotted dry prior to immersion in liquid N_2.

RNA extractions Frozen tissue was ground to a fine powder in a stainless steel mortar and pestle pre-cooled in liquid nitrogen. Total RNA was extracted by the method of Chomczynski & Sacchi (1987). To avoid any cross-contamination, the homogenizer probe was dismantled and washed thoroughly between each sample. The yield and quality of the RNA were assessed by measuring absorbance at 260 and 280 nm, and by electrophoresis on 1.2% agarose gels. Total RNA from each tissue was treated with DNase to remove any possible contaminating genomic DNA. The reaction mix contained 20 μg RNA, sodium acetate (pH 7.0) (100 mM), $MgSO_4$ (5 mM), dithiothreitol (5 mM), 36 U RNasin (Promega), and 10 U DNase I (Pharmacia) in a total volume of 40 μl. Following digestion at 37°C for 30 min, the solution was diluted to 400 μl with H_2O and extracted with an equal volume

of phenol : chloroform (1 : 1). The RNA was precipitated with 1.0 ml of ethanol and 40 μl of 2 M sodium acetate. The yield and quality of DNase-treated RNA were determined as above.

Reverse transcription/PCR cDNAs were synthesized by reverse transcription of 1.0 μg of each total RNA using oligo (dT)15 as a primer. The RNA in a volume of 7.5 μl was heated to 70°C for 5 min then placed on ice for 2 min prior to the addition of reaction mix containing 1 × RT buffer (supplied by Promega), dNTPs (1 mM), $MgCl_2$ (5 mM), 18 U RNasin (Promega), 20 U AMV reverse transcriptase (Promega), and 50 μg ml^{-1} oligo(dT)15 in a volume of 12.5 μl. Following brief centrifugation, the reactions were incubated at 42°C for 45 min, then at 95°C for 5 min. The completed reverse transcription reactions were stored at −20°C and used for PCR without further treatment.

PCR amplification was done on cDNA equivalent to 100 ng of starting RNA, using oligonucleotide primers specific for rat β_1-AR (forward, 5'-CCGCTGCTACAACGACCCCAAG-3' and reverse, 5'-CGGATCGCCTCTTCGTCTTCTTCAA-3'), β_2-AR (forward, 5'-TGTGTCACAGCCAGCATCGAGACCCTGT-3' and reverse 5'-TTGAAGGCAGAGTTGACATAGCCCAACCAGTT-3'), β_3-AR (set A: forward, 5'-ATCATGAGCCAGTGGTGGCGTGTAG-3' and reverse, 5'-GCGATGAAAACTCCGCTGGGAACTA-3'), β_3-AR (set B, intron spanning forward, 5'-TAGTCCTGGTGTGGATCGTGTCCGC-3' and reverse, 5'-CGCTCACCTTCATAGCCATCAAACC-3'), and β-actin (forward, 5'-ATCCTGCGTCTGGACCTGGCTG-3' and reverse, 5'-CCTGCTTGCTGATCCACATCTGCTG-3') synthesized at the Howard Florey Institute, Melbourne or by Life Technologies, Gaithersburg, MD, U.S.A. Reverse primers for actin were labelled prior to PCR in a reaction mix containing 120 pmol of oligonucleotide, 70 μCi [γ-^{33}P]-ATP, 1 × One-Phor-All Plus buffer (Pharmacia), and 20 U T4 polynucleotide kinase (Pharmacia) in a volume of 40 μl. Following incubation at 37°C for 30 min, reactions were diluted to 100 μl with H_2O and heated at 90°C for 2 min. The labelled primers were separated from unincorporated nucleotide by centrifugation through Chroma-spin 10 columns (Clontech), according to the manufacturer's instructions. PCR mixes contained 1 U of Taq polymerase (Life Technologies), the buffer supplied (Tris-HCl (pH 8.4) (20 mM) and KCl (50 mM)), dNTPs (200 mM), Mg-acetate (2 mM), 2.5 pmol of forward primer, 2.5 pmol of reverse primer and cDNA in a volume of 10 μl. For each set of tissues (e.g. all samples of ileum), a single reaction mix containing all components except the cDNA was prepared for the entire PCR experiment and aliquotted to minimize variation between samples. Each PCR experiment included a negative control consisting of an RT reaction containing no added RNA. PCR was carried out in an FTS-1 capillary thermal sequencer (Corbett Research, Lidcombe, New South Wales, Australia). Following initial heating of samples at 95°C for 2 min, each cycle of amplification consisted of 30 s at 95°C, 30 s at 64°C, and 30 s at 72°C. Following amplification, PCR products were electrophoresed on 1.3% agarose gels and transferred onto Hybond N+ membrane by Southern blotting in 0.4 M NaOH/1 M NaCl. For detection of β-AR products, membranes were exposed to u.v. light for 2 min then pre-hybridized for 4 h at 42°C in a buffer containing 5 × Denharts solution (0.1% (w v^{-1}) ficoll type 400, 0.1% (w v^{-1}) polyvinylpyrrolidone, 0.1% (w v^{-1}) BSA), 5 × SSC, 0.5% SDS, 100 μg ml^{-1} salmon sperm DNA and 0.1 mM ATP, prior to addition of labelled probe and hybridization for 16 h at 42°C. Probes (10 pmol) specific for β_1-AR (5'-AAGAAGATCGACAGCTGCGAGC-3'), β_2-AR (5'-AGCCAGGTGGAGCAGGATGGG-3') and β_3-AR (5'-TGCCAACTCCGCCTTCAACCCGGTC-3') were end-labelled with 15 μCi γ-^{33}P-ATP (2000 Ci $mmol^{-1}$; Bresatec) and T4 polynucleotide kinase (Pharmacia). Filters were washed in 2 × SSC/0.1% SDS, rinsed at room temperature then washed at 30°C for 20–30 min then at 37°C for 5 min. Radioactivity was detected using a Molecular Dynamics SI phosphorimager, and bands were quantitated using the 'Volume Report' function of Image-QuaNT software (Molecular Dynamics).

Drugs and reagents

The authors thank the following companies and individuals for gifts of: ICI D7114 ((S)-4-[2-hydroxy-3-phenoxypropylamino ethoxy]-N-(2-methoxyethyl) phenoxyacetamide), (Imperial Chemical Industries, Wilmslow, Cheshire, England); (+)-alprenolol (Professor B. Jarrott, Monash University, Victoria, Australia); (±)-CGP 20712A (2-hydroxy-5(2-((2-hydroxy-3-(4-((1-methyl-4-trifluoromethyl) 1H-imidazole-2-yl)-phenoxy)-propyl)amino) ethoxy) -benzamide monomethane sulphonate) (Dr G. Anderson, Ciba-Geigy AG Australia); (−)-CYP, (±)-CYP (Sandoz, Basel, Switzerland); BRL 37344 (sodium-4-[-2[-2-hydroxy-2-(-3-chloro-phenyl) ethylamino] propyl] phenoxyacetate) (Dr M.A. Cawthorne, Smith Kline Beecham, Great Burgh, Epsom, U.K.); (−) tertatolol, (+)-tertatolol (Servier, Paris, France); SR 58611A (RS-N-(7-carbethoxymethoxyl 1,2,3,4-tetrahydronophth-2-yl)-2 hydroxy 2-(3-chlorophenyl)-ethanamine), SR58894 (3-(2-allyl-phenoxy)-1-[(1S)-1,2,3,4-tetrahydronaphth-1-ylamino]-(2S)-2-propanol hydrochloride) (Dr Luciano Manara, SANOFI-MIDY S.p.A. Research Centre, Milan, Italy); zinterol hydrochloride (Bristol-Myers Squibb, Noble Park, Australia); CL 316 243 (disodium (R,R)-5-[2-[[2-3-Chlorophenyl)-2-hydroxyethyl]-amino] propyl]-1,3-benzodioxole-2,2-dicarboxylate) (Dr Tim Nash, Wyeth Pharmaceuticals, Sydney, Australia).

Other chemicals were from commercial sources as indicated: (−)-propranolol, (±)-ICI 118551 (erythro-DL-1(7-methylindian-4-yloxy)-3-isopropylaminobutan-2-ol) (Imperial Chemical Industries, Wilmslow, Cheshire, England); (−)-alprenolol, (−)-isoprenaline bitartrate, hydrocortisone, desipramine HCl, carbachol (carbamylcholine chloride), papaverine, forskolin (Sigma Chemical Company, St Louis, MO, U.S.A.); phentolamine HCl (Regitine; Ciba-Geigy AG Australia); (±)-CGP 12177 hydrochloride ((−)-4-)3-t-butylamino-2-hydroxypropoxy) benzimidazol-2-one) (Research Biochemicals Inc., MA, U.S.A.); RO 363 (±)-1-(3,4-dimethoxy-phenethylamino)-3-(3,4-dihydroxyphenoxy)-2-propanol)-oxalate) (Institute of Drug Technology, Boronia, Australia); L(+)-ascorbic acid (Merck, Frankfurt, Germany); EDTA (ethylenediaminetetraacetic acid di-sodium salt (AJAX Chemicals, Melbourne, Australia).

Results

(−)-Isoprenaline mediated relaxation of rat ileal longitudinal smooth muscle

(−)-ISO produced concentration-dependent relaxation of carbachol-precontracted rat ileum longitudinal smooth muscle with a pEC_{50} value of 6.80 ± 0.02 (n = 4). The β_1/β_2-AR antagonist (−)-propranolol (0.1, 1, 10 μM) caused concentration-dependent rightward shifts of the (−)-ISO C-R curve. The corresponding Schild plot was biphasic and the slope of the plot was significantly less than unity (Table 1, Figure 1). Calculation of pK_B values for each propranolol concentration

showed that the higher concentrations (1 and 10 μM) of the drug caused a reduced rightward shift compared to the lower concentration (0.1 μM) indicating the possible involvement of two sites with different affinities for propranolol (Table 1).

Both the selective β_1-AR antagonist CGP 20712A (30, 100, 300 nM) and the selective β_2-AR antagonist ICI 118551 (30, 100, 300 nM) failed to produce significant shifts of the (−)-ISO CR curve (Figure 1). ICI 118551, at a concentration of 30 μM caused a small shift with a pK_B value of 5.06±0.13 (n=4). CGP 20712A did not cause a significant shift in the (−)-ISO C-R curves (pEC_{50} control 6.69±0.04, n=5; pEC_{50} CGP 20712A (300 nM) 6.55±0.06, n=4; $P>0.05$). It was not possible to use CGP 20712A at a concentration equivalent to its affinity at a β_3-AR (1 mM) in the organ bath due to solubility difficulties.

The β_1/β_2-AR antagonist (±)-CYP (30 nM, 0.1, 0.3, 1 μM) caused concentration dependent rightward shifts of the (−)-ISO C-R curve. A Schild plot produced a line with a slope of unity (0.97) and a corresponding pA_2 value of 7.98 (Figure 2). The stereoselectivity of the isomers of alprenolol and tertatolol was examined against (−)-ISO C-R curves (Figure 3). Schild plots for (−)-alprenolol and (−)-tertatolol had slope values which did not differ significantly from unity with pA_2 values of 7.12 and 7.29 respectively (Table 1). The Schild plots for the (+)-stereoisomers of both alprenolol and tertatolol had slope values significantly less than unity and pA_2 values of 5.83 and 5.65 respectively. The stereoselectivity displayed for alprenolol (19.5 fold) and tertatolol (43.7 fold) were somewhat less than expected at β_1- or β_2-AR but in the range expected for a β_3-AR. (Table 1).

Effects of selective β_1-, β_2- and β_3-AR agonists on longitudinal smooth muscle

β_1-AR agonist The selective β_1-AR agonist RO 363 produced a small relaxation of carbachol precontracted rat longitudinal smooth muscle (<20% of papaverine maximum) at a high concentration of 10 μM. The pEC_{50} for this response was 6.18±0.34 (n=4) and this relaxation was abolished by CGP 20712A (100 nM) (Figure 4).

β_2-AR agonist The β_2-AR antagonist, zinterol, caused a concentration dependent relaxation with a pEC_{50} of 5.71±0.16 (n=6) and this relaxation was not affected by ICI 118551 (100 nM; pEC_{50}=5.93±0.16, n=8) or CGP20712A (100 nM; pEC_{50}=5.94, n=2) but was shifted to the right by increasing concentrations of the β_3-AR antagonist SR58894A in the presence of ICI 118551 (100 nM). pK_B values of 7.23±0.02 (0.1 μM, n=4) and 6.95±0.09 (1 μM, n=5) were calculated (Figure 4).

β_3-AR agonists BRL 37344 was a slower acting agonist (each concentration required approximately 15–20 min to achieve equilibrium) and BRL 37344 C-R curves were biphasic. The first phase (pEC_{50} (1)=7.31±0.04, n=4) occurred at lower concentrations than (−)-ISO and caused a response that was approximately 50% of the maximum produced by (−)-ISO (10 μM). This component of the response was shifted to the right by (−)-propranolol (1 μM) (pK_B 6.51). The second phase had an estimated pEC_{50} (2) value of 4.39±0.09, n=4 but failed to reach a maximum within the concentration range used and was not shifted by 1 μM propranolol (Figure 5).

pK_B values for the high affinity component of the BRL 37344 CR curve were determined for single concentrations of antagonists (Table 2). The affinities of the antagonists against BRL 37344 responses were compared with the pK_B values obtained against (−)-ISO responses. This data has been represented as a correlation plot (Figure 5). The regression line has an r value of 0.973 (P=0.0011) and a slope of 0.863 (95% C.L. 0.58–1.14, n=6).

SR 58611A SR 58611A C-R curves were performed using a concentration range of 1×10^{-10} to 3×10^{-5} M. A maximum response was not achieved but the C-R curve appeared monophasic and was not affected by the presence of 1 μM propranolol (Figure 5).

CL 316243 Like BRL 37344 the response to CL 316243 was slow and required 25–30 min to reach a plateau at each concentration. To determine whether this slow response was due to the thickness of the ileal segment, relaxation responses were also examined by inverting the segment, gently scraping off the mucosa with a glass slide, and reinverting the segment to its original orientation. Mucosal removal did not alter the time course of the response or significantly change the potency

Table 1 Affinity values (pA_2) for antagonists against (−)-isoprenaline relaxation of rat ileum. Values are given as pK_B value when single concentrations of antagonists were used or if the Schild plot was clearly non-linear

Antagonist		*pA_2±s.e.mean* (n)	*slope±s.e.mean*	*95% CL*
(−)-tertatolol		7.29±0.17 (28)	1.03±0.09	0.84–1.22
(+)-tertatolol		5.65±0.05 (19)	0.59±0.17	0.24–0.95*
(−)-alprenolol		7.12±0.16 (12)	1.19±0.18	0.78–1.60
(+)-alprenolol		5.83±0.31 (11)	0.73±0.11	0.47–0.98*
CGP 12177		7.65±0.08 (14)	0.77±0.05	0.65–0.89*
(±)-cyanopindolol		7.98±0.07 (14)	0.97±0.06	0.83–1.11
		pK_B±s.e.mean		
Propranolol	0.1 μM	7.50±0.10 (4)		
	1 μM	6.81±0.20 (4)		
	10 μM	6.69±0.07 (4)		
ICI 118551	30 μM	5.06±0.13 (4)		
CGP 20712A	300 nM	no shift (4)		
CGP 12177	0.1 μM	7.55±0.07 (5)		
	1 μM	7.15±0.08 (5)		
	10 μM	7.09±0.06 (4)		
ICI D7114	0.1 μM	7.41±0.03 (4)		
	1 μM	7.62±0.13 (4)		

*Regression line significantly different from unity.

of CL 316243 (pEC_{50} 8.05±0.10 (intact mucosa) 7.85±0.11 (mucosa removed), $P>0.05$, $n=4$), although the maximum relaxation was significantly enhanced in preparations after the mucosa was removed ($P=0.005$) (Figure 6). The CL 316243 CR curve was monophasic and was not shifted by the β_1-AR antagonist CGP 20712A or the β_2-AR antagonist ICI118551 at 100 nM but was shifted to the right by the selective β_3-AR antagonist SR 58894A ($pA_2=7.80\pm0.06$, $n=21$; Figure 6).

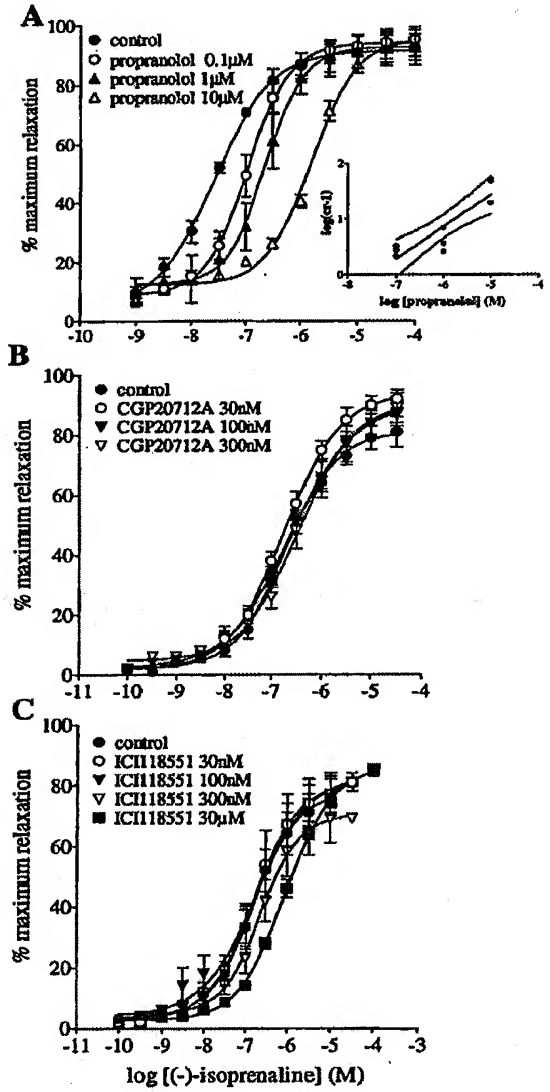

Figure 1 The effect of β_1/β_2 antagonists on the relaxation responses to (−)-isoprenaline in the rat isolated ileum precontracted with carbachol. Graph shows (−)-isoprenaline concentration response curves in the absence and presence of (A) propranolol (B) the β_1-AR antagonist CGP 20712A and (C) the β_2-AR antagonist ICI 118551. Inset (A) shows a Schild plot with a slope significantly less than unity. Note the lack of effect of CGP 20712A and the small rightward shift caused only by a high concentration of ICI 118551. Points show mean±s.e.mean ($n=4$) and are expressed as a percentage of maximum relaxation by papaverine (100 μM).

Effects of putative β_3-adrenoceptor agonists

In the rat ileum neither ICI D7114 or CGP 12177 showed any agonist activity at concentrations up to 10 μM. The Schild plot for CGP 12177 against ISO responses had a slope of 0.77 (95% C.L. 0.65–0.89, $n=12$) and pK_B values are shown in Table 1. ICI D7114 at 0.1 and 1 μM produced rightward shifts of the (−)-ISO C-R curve with pK_B values of 7.41 and 7.62 respectively (Table 1).

Effects of forskolin and pertussis toxin on relaxation of rat ileal longitudinal smooth muscle

Forskolin (0.1 and 1 μM) was added 30 min prior to the commencement of the CR curve. Both concentrations produced a slight relaxation in the basal tone of the tissue – this effect being more pronounced at the higher concentration. Carbachol precontractions were maintained in a similar manner to that observed in the absence of forskolin. A forskolin concentration of 0.1 μM had no effect on ISO and CL 316243 CR curves. At 1 μM, forskolin caused a significant enhancement of the maximum relaxation of both agonists. The ISO response increased by 31% and the CL 316243 response increased by 38% of the maximum relaxation to papaverine. There was no significant change in the pEC_{50} values for CL 316243 or ISO in the presence of forskolin 1 μM (CL 316243 pEC_{50} 7.72±0.20, with forskolin 7.94±0.18 and for ISO pEC_{50} 6.53±0.18, with forskolin 6.93±0.15, $n=4$) (Figure 7). Preincubation of rat ileum for 2 h with 0.5 μg ml^{-1} pertussis toxin also produced a significant increase of 21% in the maximum relaxation of the smooth muscle to CL 316243 (Figure 7).

Detection of β-adrenoceptor mRNA in rat colon and ileum

RT–PCR was used to detect β_1-AR, β_2-AR, β_3-AR and actin mRNA in circular/longitudinal smooth muscle from samples of rat ileum and colon. Determinations were also made with samples of cortex, epididymal white adipose tissue (WAT) and soleus muscle which are known to contain varying levels of the

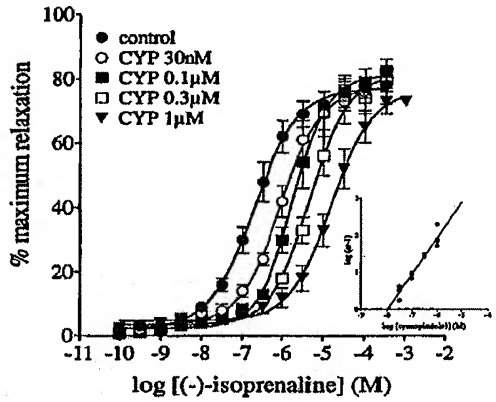

Figure 2 The effect of (±)-cyanopindolol (CYP) on the relaxation responses to (−)-isoprenaline in the rat isolated ileum precontracted with carbachol. Points show mean±s.e.mean and are expressed as a percentage of maximum relaxation by papaverine (100 μM) ($n=4$). Inset shows the Schild plot for (±)-CYP with slope 0.97 and pA_2 value of 7.98.

β-AR subtypes (Figure 8). The PCR products demonstrated the expected sizes of 435 (β_1-AR), 620 (β_2-AR), 473 (β_3-AR), and 559 bp (actin). To ensure that the products were derived exclusively from mRNA and not from contaminating genomic DNA, all RNA samples were treated with DNase, and intron-spanning primers were used to detect actin mRNA. The

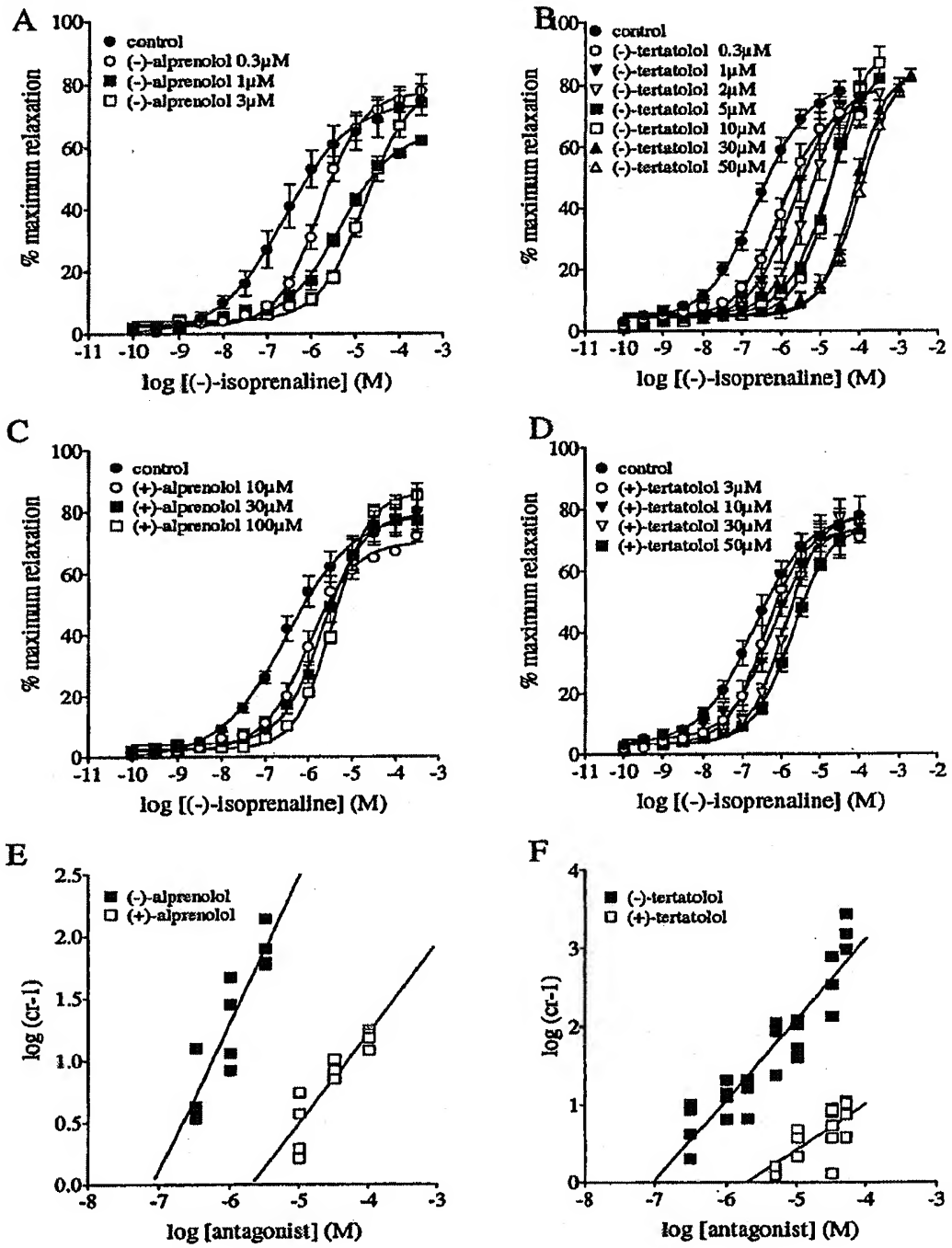

Figure 3 The effect of the stereoisomers of alprenolol (A, C and E) and tertatolol (B, D and F) on the relaxation responses to (−)-isoprenaline in the rat isolated ileum precontracted with carbachol. Shown are (−)-isoprenaline concentration response curves in the absence and presence of (A) (−)-alprenolol (B) (−)-tertatolol (C) (+)-alprenolol and (D) (+)-tertatolol. Points show mean ± s.e.mean ($n = 4-6$) and are expressed as a percentage of maximum relaxation by papaverine (100 μM). Slope values calculated from Schild plots for alprenolol (E) and tertatolol (F) show that the (−)-isomer in each case has a slope value not significantly different from unity while both (+)-isomers had slope values significantly less than unity. Slope values and pA_2 values were calculated and are shown in Table 1.

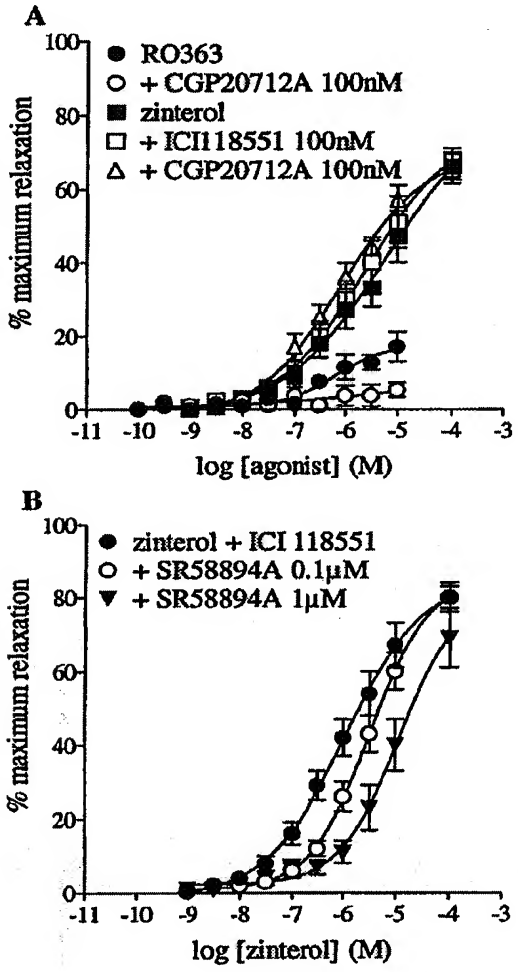

Figure 4 The effect of β_1- and β_2-AR selective agonists on relaxation in rat ileum precontracted with carbachol. Graph (A) shows relaxation with the β_2-AR agonist zinterol in the absence and presence of ICI 118551 and CGP 20712A. Also shown in (A) are the relaxation responses by the β_1-AR agonist RO363 in the absence and presence of CGP 20712A ($n=4$). Graph (B) shows the inhibition of zinterol relaxation by the β_3-AR antagonist SR 58894A in the presence of ICI 118551.

observed actin PCR product corresponded to the expected 559 bp, whereas contaminating DNA would have given a PCR product of 771 bp. Larger bands were not observed in any samples of cDNA used for the subsequent measurement of β-AR mRNA.

To compare the relative levels of β_1-AR, β_2-AR and β_3-AR in ileum, colon, cortex, soleus muscle and WAT the relationship between the log (PCR product) and cycle number was determined for individual samples. Although RT–PCR methods without control templates cannot be used to make direct comparisons between expression of different genes, the amplification of β_1-AR, β_2-AR and β_3-AR cDNA occurred with similar efficiency both in comparison to each other and between tissues as judged by the similar slopes of the product/cycle relationships. All plots were linear up to 28 cycles, and 27 cycles of PCR were used to determine the relative levels of β_1-AR, β_2-AR and β_3-AR mRNA from multiple samples of colon and ileum versus cortex, WAT and soleus muscle. In this experiment intron-spanning primers were used for both actin and β_3-AR, again with no evidence of larger genomic DNA bands. In accord with previous data (Summers *et al.*, 1995; Evans *et al.*, 1996), the greatest expression of β_3-AR mRNA was in WAT > colon = ileum > cerebral cortex > soleus. Levels of β_3-AR mRNA in ileum and colon smooth muscle were not significantly different from each other ($P=0.24$), and amounted to approximately 20% of that in WAT. In contrast β_1-AR mRNA was most abundant in cerebral cortex > WAT > ileum = colon > soleus with the levels in ileum and colon being 7–8% of that in cortex. β_2-AR mRNA was expressed in soleus > WAT > ileum = colon > cerebral cortex. β_2-AR mRNA levels in ileum and colon were approximately 25% of that in soleus muscle.

Discussion

In the present study, the β-AR subtypes mediating smooth muscle relaxation in rat ileum have been examined. The initial characterization of this receptor was performed using the non-selective β-AR agonist (−)-ISO. The effects of (−)-propranolol on (−)-ISO C-R curves suggested the presence of both typical and atypical β-ARs given the reduced shift with progressively higher concentrations. However this was not supported by experiments with the β_1- and β_2-AR selective antagonists CGP 20712A and ICI 118551 which both failed to cause any effect at concentrations up to 300 nM. It would therefore appear that the major component of smooth muscle relaxation was due to activation of a β-AR subtype that was not effectively blocked by propranolol, ICI 118551 or CGP 20712A. The affinity of propranolol ($pK_B=6.69$ at 10 μM) was somewhat higher than previously reported in rat ileum (5.5–5.7) (Growcott *et al.*, 1993) but close to values quoted in rat distal colon (6.57, 6.39) (McLaughlin & MacDonald, 1990). The pK_B values of both propranolol and ICI 118551 (6.69 and 5.06 respectively) in rat ileum corresponded to the affinities of these compounds in rat jejunum (6.1 and 5.5; Van der Vliet *et al.*, 1990), rat colon (6.0, Kaumann & Molenaar, 1996) and also at the rat cloned β_3-AR (5.8 and 5.3; Muzzin *et al.*, 1991).

Evidence for a β_3-AR in rat ileal smooth muscle was strongly supported by concentration-dependent relaxation of the smooth muscle by the β_3-AR agonists CL 316243, BRL 37344 and SR 58611A. The biphasic responses caused by BRL 37344 were consistent with observations made by Growcott *et al.* (1993), as was the slower onset of action by BRL 37344 (also seen for CL 316243 and SR 58611A in the present study) compared to the rapid (−)-ISO response. The pEC_{50} value of 7.31 for the first component of the BRL 37344 C-R curve corresponded well with that at the cloned rat β_3-AR ($pEC_{50}=7.1$, Granneman *et al.*, 1991). This component of the curve was sensitive to high concentrations of β-AR antagonists and a pK_B value of 6.51 for propranolol (1 μM) indicated activity at a β_3-AR. By comparison, the second phase of the BRL 37344 C-R curve was completely resistant to propranolol, cyanopindolol and the stereoisomers of tertatolol and alprenolol and may indicate another mechanism activated by high concentrations of BRL 37344.

The phenylethanolaminotetraline SR 58611A is a potent β_3-AR agonist that was originally described as a colon specific atypical β-AR agonist (see Manara *et al.*, 1995, for review). However SR 58611A was relatively ineffective in the present

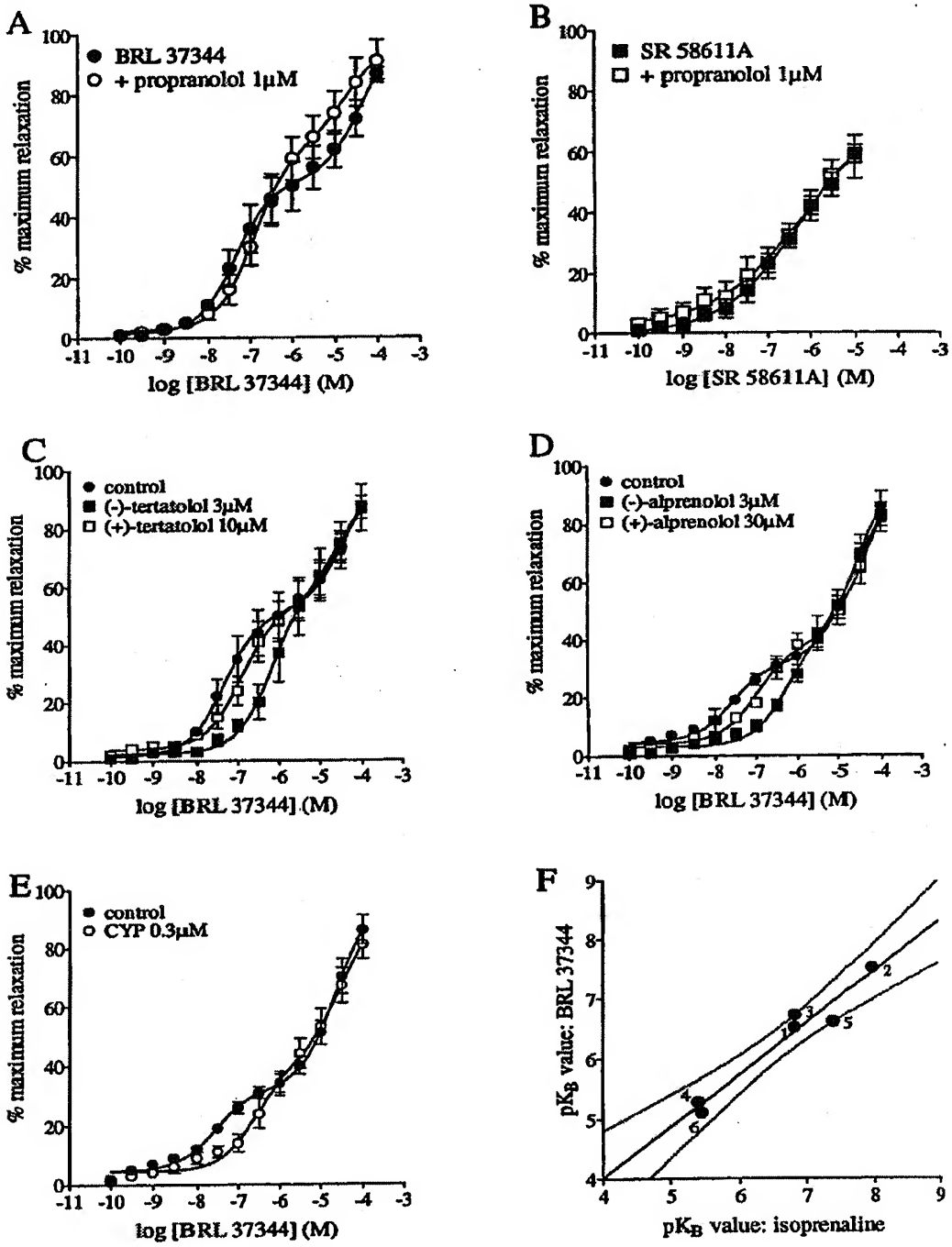

Figure 5 Mean concentration response curves for the relaxation of carbachol precontracted rat ileum by the atypical β-AR agonists (A) BRL 37344 and (B) SR 58611A. Both graphs show control concentration response curves and in the presence of (−)-propranolol (1 μM). Also shown are BRL 37344 concentration response curves in the presence of (C) (−)-tertatolol 3 μM and (+) tertatolol 10 μM; (D) (−)-alprenolol 3 μM and (+)-alprenolol 30 μM and (E) (±)-cyanopindolol 0.3 μM. Points are expressed as a percentage of maximum relaxation by papaverine (100 μM). Points show mean±s.e.mean ($n=4-6$). The pK_B values for all compounds were calculated and are shown in Table 2. Graph (F) shows a correlation plot of pK_B values for a range of compounds obtained against either (−)-isoprenaline concentration-response or BRL 37344 concentration-response curves. The regression line has a correlation coefficient of $r=0.973$, $P=0.0011$ and a slope of 0.863 (95% C.L. 0.58−1.14, $n=6$).

rat ileum preparation and maximum responses could not be obtained within the concentration range available. The reduced activity of SR 58611A in rat ileum compared to rat colon (EC_{50} 3.5 nM, Bianchetti & Manara, 1990) may be due to the hydrolysis of SR 58611A to a more potent acid metabolite by esterases specifically located in the colon giving this compound its preferential action in the colon preparation (Bianchetti & Manara, 1990). Alternatively, SR 58611A may be a partial agonist which is more effective in colon as this tissue has a greater receptor reserve.

In studies of glycerol release from adipocytes (Bloom *et al.*, 1992) and colonic relaxation (Dolan *et al.*, 1994), CL 316243 was described as selective for β_3-AR compared to β_1-(atrial) and β_2-ARs (soleus muscle) and more β_3-AR selective than BRL 37344. In rat ileum, CL 316243 was the most potent β_3-AR agonist and produced a monophasic relaxation of the ileal smooth muscle. This response was not blocked by β_1- and β_2-AR antagonists but was blocked by the β_3-AR antagonist SR58894A with a pA_2 value of 7.8 which corresponds to its published affinity at rat colonic β_3-ARs ($pA_2 = 8.06$, Manara *et al.*, 1996).

Table 2 The affinities of a variety of antagonists against isoprenaline relaxation compared with affinities against relaxation to BRL 37344

Compound	*(−)-isoprenaline* $pK_B \pm$ *s.e.mean* (n)	*BRL 37344* $pK_B \pm$ *s.e.mean* (n)
(−)-propranolol (1 μM)	6.81±0.20 (4)	6.51±0.16 (3)
ICI 188551 (30 μM)	5.06±0.13 (4)	n.d.
CGP 20712A (300 nM)	no shift (4)	n.d.
(−)-tertatolol (3 μM)	6.82±0.15 (4)	6.71±0.10 (5)
(+)-tertatolol (10 μM)	5.39±0.15 (4)	5.28±0.10 (5)
(−)-alprenolol (3 μM)	7.40±0.08 (4)	6.61±0.26 (5)
(+)-alprenolol (30 μM)	5.44±0.04 (4)	5.10±0.07 (5)
(±)-CYP (0.3 μM)	7.96±0.02 (4)	7.50±0.25 (4)

n.d., affinities of these compounds were not determined.

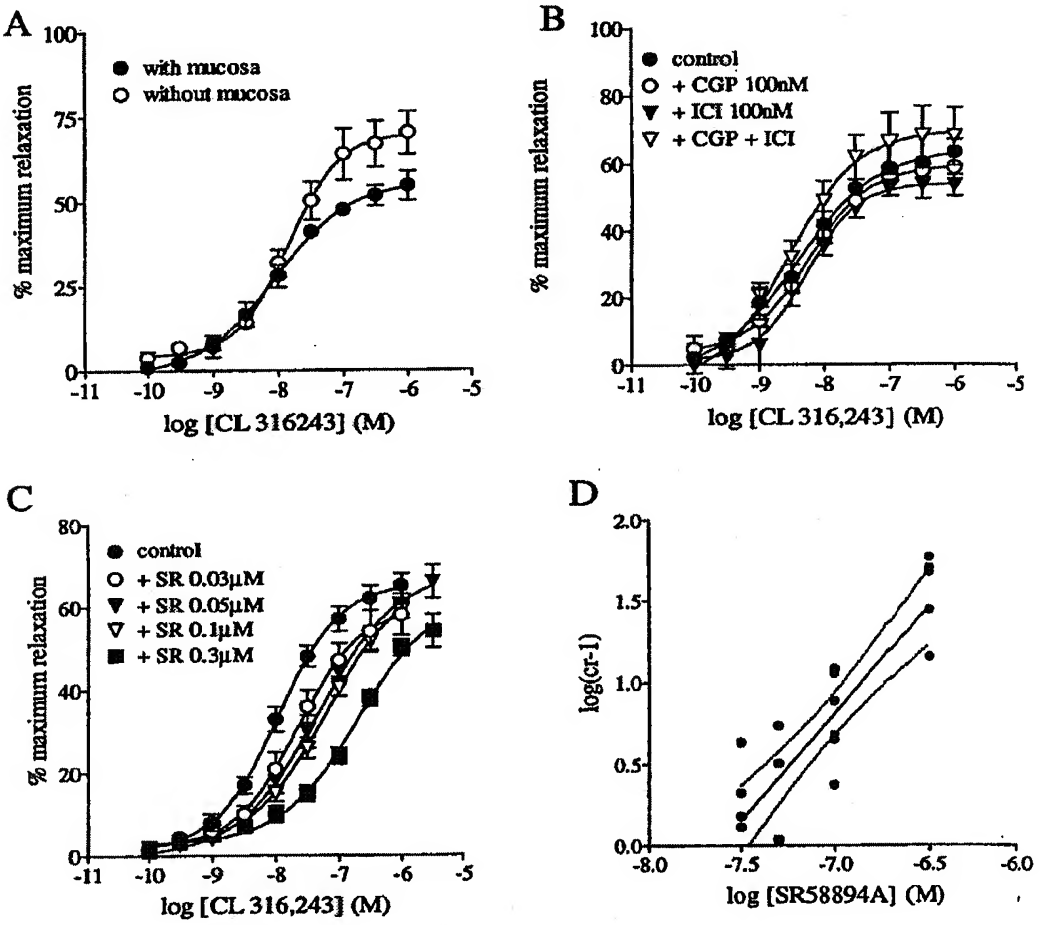

Figure 6 Mean concentration response curves for the relaxation of carbachol precontracted rat ileum by the β_3-AR agonist CL 316243. Graph (A) shows monophasic CL 316243 concentration-response curves in intact preparations and preparations with the mucosa removed. Graph (B) shows a control CL 316243 C-R curve and in the presence of the β_1-AR antagonist CGP 20712A 100 nM, the β_2-AR antagonist ICI 118551 100 nM and both antagonists in combination. Graph (C) shows the concentration dependent rightward shifts of the CL 316243 C-R curve with the β_3-AR antagonist SR 58894A. Graph (D) shows the Schild Plot (slope 95% C.I. 0.94−1.68) for SR 58894A. Points show mean±s.e.mean ($n = 4-6$).

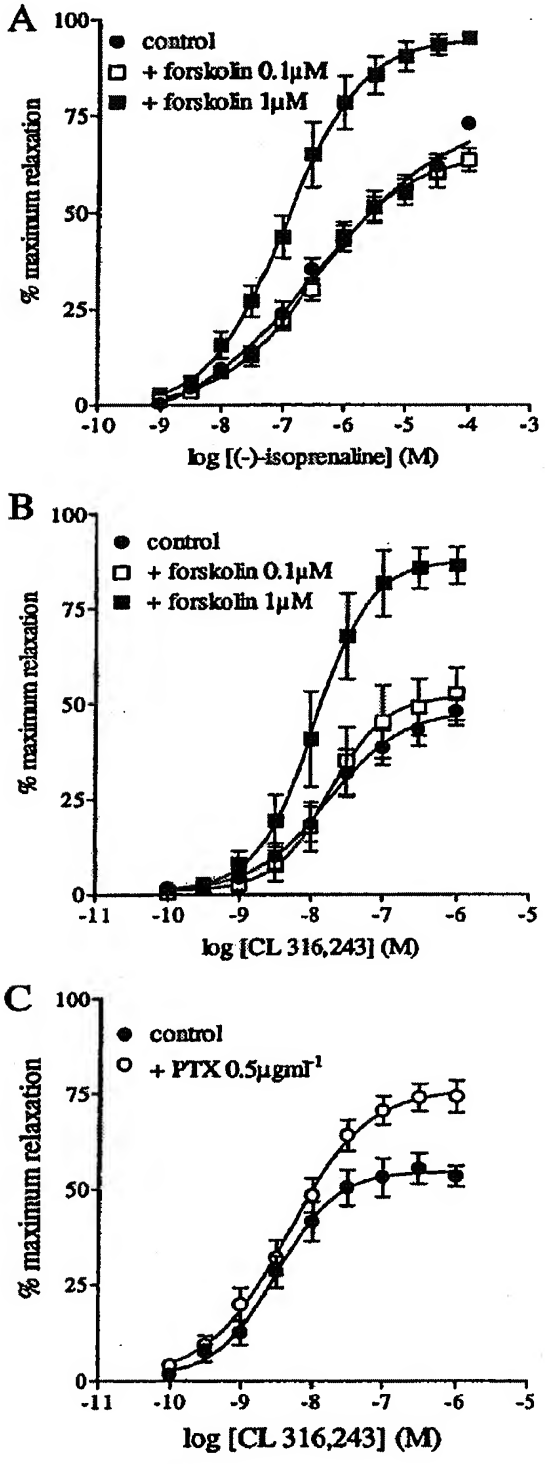

Figure 7 Effects of preincubation of rat ileal strips with forskolin for 45 min at 37°C on concentration-response curves to (A) isoprenaline and (B) CL 316243. Also shown (C) is the effect of preincubation with pertussis toxin (2 h, 37°C, $n=4$) on CL 316243 concentration-response curves.

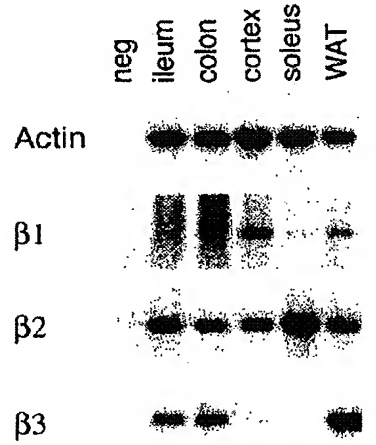

Figure 8 Detection of β_1-AR, β_2-AR, β_3-AR and actin mRNA by RT/PCR. Cycle numbers were 27 for β-ARs and 16 for actin. Sizes of the PCR products were determined from ethidium bromide stained gels by comparison with 100 bp DNA ladder (Pharmacia). The blots were apposed to phosphorimager plates for 7 h prior to scanning.

The affinity of (−)-alprenolol (3 μM) against ISO C-R curves in the present study (pK_B 7.12) was higher than when BRL 37344 was used as the agonist (pK_B 6.61). Other functional studies of β-ARs in gastrointestinal tissues have found affinities of alprenolol ranging from 7.2 in rat jejunum (Van der Vliet *et al.*, 1990) to 6.5 in rat ileum (Growcott *et al.*, 1993) and 6.47 in guinea-pig ileum (Blue *et al.*, 1990). The latter study also demonstrated partial agonist activity of alprenolol in guinea-pig ileum (Blue *et al.*, 1990). Tertatolol has also been described as an effective antagonist at β_3-ARs with a pA_2 value of 6.8 in guinea-pig ileum (Bond & Vanhoutte, 1992) compared to values of 7.29 and 6.71 (pK_B) measured in rat ileum (present study). It is interesting to note that the affinities of both alprenolol and tertatolol in the present study fall closer to values described for atypical β-ARs in other studies when BRL 37344 rather than ISO is used as the agonist. Another interesting observation was a tendency for Schild plots generated for the (+)-isomers to have slope values of less than unity, a feature not shared by the (−)-isomers. The reason for this difference is not known. Low stereoselectivity was observed for isomers of alprenolol competing for (−)-[^{125}I]-CYP binding in rat skeletal muscle (Molenaar *et al.*, 1991; Roberts *et al.*, 1993; Sillence *et al.*, 1993) and brown adipose tissue membranes (Sillence *et al.*, 1993). It is interesting to note that much higher stereoselectivity has been observed for agonists at atypical β-ARs, particularly the isomers of ISO which display 25 fold separation in rat small intestine (Van der Vliet *et al.*, 1990) and 31 fold separation at the cloned human β_3-AR expressed in CHO cells (Emorine *et al.*, 1989).

CYP and CGP 12177 are both β_1/β_2-AR antagonists that have also been described as partial agonists at atypical β-ARs (Mohell & Dicker, 1989; McLaughlin & MacDonald, 1991; McKean & MacDonald, 1994). ICI D7114 was originally described in guinea-pig ileum as having both agonist and antagonist activity, but behaved as an antagonist in rat ileum (Growcott *et al.*, 1993) and colon (MacDonald & Lamont, 1993). All three compounds behaved as antagonists in the present study. (±)-CYP and CGP 12177 produced concentra-

tion dependent rightward shifts of (−)-ISO C-R curves. A single concentration of (±)-CYP (0.3 μM) gave similar pK_B values against both (−)-ISO (7.96) and BRL 37344 (7.50) induced relaxation. This differs from that seen by McLaughlin & MacDonald (1991) in rat gastric fundus where the pK_B value of (±)-CYP was significantly lower against BRL 37344 (6.56) than against (−)-ISO (7.44) induced relaxation. Several other studies have used CYP to identify atypical β-AR populations in gastrointestinal tissues and affinity values quoted include 6.67, 7.12 and 7.07 in rat distal colon (McLaughlin & MacDonald, 1990; McKean & MacDonald, 1994), 6.56 and 7.44 in rat gastric fundus (McLaughlin & MacDonald, 1991) and 7.01 in rat jejunum (MacDonald *et al.*, 1994). One study has reported partial agonist activity of CYP ($pD_2 = 5.3$) and IodoCYP ($pD_2 = 7.0$) in rat ileum preparations (Hoey *et al.*, 1996). The present study confirms reports that ICI D7114 (also known as ZD7114), a reversible competitive antagonist in rat distal colon with a pA_2 value of 7.29 (MacDonald & Lamont, 1993), is also an antagonist in rat ileum (pK_B values 7.41, 7.62). These values are higher than those previously reported in rat ileum (6.3–6.7; Growcott *et al.*, 1993) making ZD7114 a higher affinity β_3-AR antagonist than either alprenolol or tertatolol in our rat ileum preparation. These results are again in contrast to those of Hoey *et al.* (1996) who reported that ICI D7114 was a partial agonist in rat ileum with a pseudo pD_2 value of 6.92.

In previous studies we have characterized (−)-[^{125}I]-CYP binding to β-ARs in rat ileum and atypical (β_3)-AR binding sites were clearly the predominant subtype while β_1- and β_2-ARs were undetectable even using classical binding conditions that favour binding to β_1- and β_2-ARs (Roberts *et al.*, 1995). The marked relaxation observed to the β_2-AR agonist zinterol was therefore unexpected. However this response was not altered by the β_2-AR antagonist, ICI 118551, but was inhibited by the β_3-AR antagonist, SR 58894A. This suggests that zinterol causes relaxation of rat ileal smooth muscle through activation of β_3-ARs. This observation is of particular note with regard to the interpretation of results obtained in diabetic rat models which showed decreased gastrointestinal responses in rat duodenum to the β_2-AR agonist salbutamol (Altan *et al.*, 1987; Yildizoglu-Ari *et al.*, 1988). The low potency of salbutamol in these studies (pD_2 5.9–6.6) compared to its known affinity at β_2-ARs (7.6, from Arch & Kaumann, 1993 review) strongly suggests that these reduced responses may reflect decreases in either β_1- or β_3-AR rather than β_2-AR responsiveness in duodenum in diabetes. It is interesting to note that β_2-AR mRNA was detected in rat ileal smooth muscle at about 25% of the level in soleus muscle a tissue where β_2-AR mediated responses can be readily identified. This may indicate that amplification of the β_2-AR PCR product is particularly efficient, that the mRNA is not translated into functional receptors or that the β_2-AR subserve functions other than smooth muscle relaxation. *In vivo* electromyographic recordings of migrating myoelectric complexes (MMC) in rat duodenum and jejunum have shown that isoprenaline and the β_2-AR agonist ritodrine can disrupt the regular MMC pattern and the irregular spiking can be blocked with ICI 118551 (Thollander *et al.*, 1996). It is therefore possible that although no relaxation response was detected there may be another role for a small population of β_2-ARs which are also undetected in binding studies (Roberts *et al.*, 1995).

The β_1-AR agonist RO363 has a high intrinsic activity compared to ISO in rat colon and guinea-pig ileum (Molenaar *et al.*, 1997) and a study by Hoey *et al.* (1996) found that RO363 caused a relaxation of rat ileum that was 60–70% of the isoprenaline response. In the present study however RO363 caused a relaxation that was less than 20% of the maximum and had a potency ($pEC_{50} = 6.2$) between its potency at β_1- and β_3-ARs in rat colon ($pEC_{50} = 8.5$ and 5.6 respectively, Molenaar *et al.*, 1997). We found that the RO363 relaxation in rat ileum was almost completely blocked by the β_1-AR antagonist CGP 20712A. Although it was not possible to directly compare expression of the β-AR subtypes we found that the level of β_1-AR mRNA in ileum was significantly lower than levels of the same receptor detected in either cortex or white adipose tissue, which both contain functional β_1-ARs (Morin *et al.*, 1992; Arch & Kaumann, 1993). The levels of expression in ileum were comparable to levels found in soleus muscle, a tissue where there is little functional evidence for the presence of β_1-ARs (Roberts *et al.*, 1993).

Finally, we examined the effects of alteration of components of the adenylate cyclase signalling pathway to determine whether β_3-AR mediated relaxation responses were altered. Low concentrations of forskolin, which produced no change in tissue responses by themselves, are known to enhance the responses to compounds acting through adenylate cyclase. In rat ileum, the maximum relaxation of the smooth muscle was significantly enhanced after pretreatment *in vitro* with the adenylate cyclase activator, forskolin. Pertussis toxin pretreatment to ADP ribosylate G_i also enhanced ideal smooth muscle relaxation suggesting that G_i signalling contributes to either the basal or receptor stimulated tone in rat ileum. Granneman and coworkers showed that the adipocyte β_3-AR can couple through both the stimulatory (G_s) protein and the inhibitory (G_i) protein and that abolition of the interaction with G_i using pertussis toxin caused a marked increase in cyclic AMP accumulation in these cells (Chaudry *et al.*, 1994). Whether or not the gastrointestinal β_3-AR also activates both signalling pathways however clearly requires further investigation.

Several anomalies are apparent from these findings. The biphasic nature of the propranolol Schild Plot and the shallow slopes of several antagonists suggests that multiple subtypes are involved in relaxation yet the selective β_1- and β_2-AR antagonists CGP 20712A and ICI 118551 did not shift the ISO C-R curve. However, as the selective β_1-AR agonist RO 363 appears to act through a small population of β_1-ARs it is possible that β_1-ARs play a role in relaxation that is functionally of little significance when β_3-ARs are also being stimulated. The strong signal for β_2-AR mRNA in ileum, colon and white adipose tissue was also interesting as these tissues have been characterized functionally as having predominantly β_1- and/or β_3-ARs (Arch & Kaumann, 1993). Possible explanations may be that in these tissues the β_2-AR mRNA is in blood vessels or nerves or that β_2-AR are mediating a different function from the β_1- and β_3-ARs. Given the absence of β_2-AR binding in rat ileum however (Roberts *et al.*, 1995) it is also possible that the β_2-AR mRNA may not be translated into a functional protein.

The current criteria for classification of the β_3-AR include: (1) stimulation by selective β_3-AR agonists; (2) partial agonist activity of non-conventional β-AR antagonists; (3) low affinity of typical β-AR antagonists; (4) atypically low stereoselectivity indices and (5) blockade by selective β_3-AR antagonists (Strosberg & Pietri-Rouxel, 1996; Kaumann & Molenaar, 1996). The studies presented in this paper show that the responses elicited by ISO and by various β_3-AR agonists in rat ileum smooth muscle are blocked with low affinity by conventional β-AR antagonists, that low stereoselectivity was demonstrated for alprenolol and tertatolol, and that the β_3-AR antagonist, SR 58894A, has high affinity for blocking relaxation to β_3-AR agonists. We also demonstrated the presence of β_3-AR mRNA in rat ileal smooth muscle. The

present characterization of smooth muscle relaxation to β-AR agonists confirms that β_3-ARs are the predominant subtype mediating these responses with little to no evidence for a relaxation role for β_1- or β_2-ARs in rat ileum.

This work was supported by grants from the National Health & Medical Research Council (Australia).

References

ALTAN, V.M., YILDIZOGLU, N. & OZTURK, Y. (1987). Decreased gastro-intestinal responses to certain agonists in streptozotocin- and alloxan-diabetic rats *in vitro*. *Pharmacology*, **34**, 143–148.

ARCH, J.R.S. & KAUMANN, A. (1993). β_3- and Atypical β-adrenoceptors. *Med. Res. Rev.*, **13**, 663–729.

ARUNLAKSHANA, O. & SCHILD, H.O. (1959). Some quantitative uses of drug antagonists. *Br. J. Pharmacol. Chemother.*, **14**, 48–58.

BERKOWITZ, D.E., NARDONE, N.A., SMILEY, R.M., PRICE, D.T., KREUTTER, D.K., FREMEAU, R.T. & SCHWINN, D.A. (1995). Distribution of β_3-adrenoceptor mRNA in human tissues. *Eur. J. Pharmacol.*, **289**, 223–228.

BIANCHETTI, A. & MANARA, L. (1990). *In vitro* inhibition of intestinal motility by phenylethanolaminotetralines, evidence of atypical β-adrenoceptors in rat colon. *Br. J. Pharmacol.*, **100**, 831–839.

BLOOM, J.D., DUTIA, M.D., JOHNSON, B.D., WISSNER, A., BURNS, M.G., LARGIS, E.E., DOLAN, J.A. & CLAUS, T.H. (1992). Disodium (R,R)-5-[2-[[2-(3-Chlorophenyl)-2-hydroxyethyl]-amino]propyl]-1,3-benzodioxole-2,2-dicarboxylate (CL 316,243). A potent β-adrenergic agonist virtually specific for β_3-receptors. A promising antidiabetic and antiobesity agent. *J. Med. Chem.*, **35**, 3081–3084.

BLUE, D.R., BOND, R.A., ADHAM, N., DELMENDO, R., MICHEL, A.D., EGLEN, R.M., WHITING, R.L. & CLARKE, D.E. (1990). Antagonist characterisation of atypical beta adrenoceptors in guinea-pig ileum, blockade by alprenolol and dihydroalprenolol. *J. Pharmacol. Exp. Ther.*, **252**, 1034–1042.

BOND, R.A. & VANHOUTTE, P.M. (1992). Interaction of tertatolol at the 'atypical' or beta$_3$-adrenoceptor in guinea-pig ileum. *Gen. Pharmacol.*, **23**, 171–176.

CHAUDRY, A., MACKENZIE, R.G., GEORGIC, L.M. & GRANNEMAN, J.G. (1994). Differential interaction of β_1- and β_3-adrenergic receptors with G_i in rat adipocytes. *Cell. Sig.*, **6**, 457–465.

CHOMCZYNSKI, P. & SACCHI, N. (1987). Single-step method of RNA isolation by acid guanidium thiocyanate-phenol-chloroform extraction. *Anal. Biochem.*, **162**, 156–159.

DOLAN, J.A., MUENKEL, H.A., BURNS, M.G., PELLEGRINO, S.M., FRASER, C.M., PIETRI, F., STROSBERG, A.D., LARGIS, E.E., DUTIA, M.D., BLOOM, J.D., BASS, A.S., TANIKELLA, T.K., COBUZZI, A., LAI, F.M. & CLAUS, T.H. (1994). Beta-3 Adrenoceptor selectivity of the dioxolane dicarboxylate phenethanolamines. *J. Pharmacol. Exp. Ther.*, **269**, 1000–1006.

EMORINE, L.J., MARULLO, S., BRIEND-SUTTREN, M.-M., PATEY, G., TATE, K., DELAVIER-KLUTCHKO, C. & STROSBERG, A.D. (1989). Molecular characterisation of the human β_3-adrenergic receptor. *Science*, **245**, 1118–1121.

EVANS, B.A., PAPAIOANNOU, M., BONAZZI, V.R. & SUMMERS, R.J. (1996). Expression of β_3-adrenoceptors in rat tissues. *Br. J. Pharmacol.*, **117**, 210–216.

FURCHGOTT, R.F. (1972). The classification of adrenoceptors (adrenergic receptors). An evaluation from the standpoint of receptor theory. In *Handbook of Experiment Pharmacology*, eds. Blaschko, H. & Muscholl, E. pp. 283–335. Berlin: Springer Verlag.

GRANNEMAN, J.G., LAHNERS, K.N. & CHAUDRY, A. (1991). Molecular cloning and expression of the rat β_3-adrenergic receptor. *Mol. Pharmacol.*, **40**, 895–899.

GROWCOTT, J.W., HOLLOWAY, B., GREEN, M. & WILSON, C. (1993). Zeneca ZD 7114 acts as an antagonist at β_3-adrenoceptors in rat isolated ileum. *Br. J. Pharmacol.*, **110**, 1375–1380.

HOEY, A., JACKSON, C., PEGG, G. & SILLENCE, M. (1996). Atypical responses of rat ileum to pindolol, cyanopindolol and iodocyanopindolol. *Br. J. Pharmacol.*, **117**, 712–716.

KAUMANN, A.J. & MOLENAAR, P. (1996). Differences between the third cardiac β-adrenoceptor and the colonic β_3-adrenoceptor in the rat. *Br. J. Pharmacol.*, **118**, 2085–2098.

LANDS, A.M., ARNOLD, A., MCAULIFF, J.P., LUDUENA, F.P. & BROWN, T.G. (1967). Differentiation of receptor systems activated by sympathomimetic amines. *Nature*, **214**, 597–598.

MACDONALD, A., FORBES, I.J., GALLACHER, D., HEEPS, G. & MCLAUGHLIN, D.P. (1994). Adrenoceptors mediating relaxation to catecholamines in rat isolated jejunum. *Br. J. Pharmacol.*, **112**, 576–578.

MACDONALD, A. & LAMONT, M. (1993). Effects of selective antagonism of β-adrenoceptor sub-types on responses to isoprenaline in rat distal colon *in vitro*. *Br. J. Pharmacol.*, **110**, 1551–1555.

MANARA, L., BADONE, D., BARONI, M., BOCCARDI, G., CECCHI, R., CROCI, T., GIUDICE, A., GUZZI, U., LANDI, M. & LE FUR, G. (1996). Functional identification of rat atypical β-adrenoceptors by the first β_3-selective antagonists, aryloxypropanolaminotetralins. *Br. J. Pharmacol.*, **117**, 435–442.

MANARA, L., CROCI, T. & LANDI, M. (1995). β_3-Adrenoceptors and intestinal motility. *Fundam. Clin. Pharmacol.*, **9**, 332–342.

MCKEAN, J. & MACDONALD, A. (1994). Contributions of β-adrenoceptor subtypes to responses to isoprenaline in rat isolated distal colon. *J. Pharm. Pharmacol.*, **47**, 388–391.

MCLAUGHLIN, D.P. & MACDONALD, A. (1990). Evidence for the existence of 'atypical' β-adrenoceptors (β_3-adrenoceptors) mediating relaxation in the rat distal colon *in vitro*. *Br. J. Pharmacol.*, **101**, 569–574.

MCLAUGHLIN, D.P. & MACDONALD, A. (1991). Characterisation of catecholamine-mediated relaxations in rat isolated gastric fundus, evidence for an atypical β-adrenoceptor. *Br. J. Pharmacol.*, **103**, 1351–1356.

MOHELL, N. & DICKER, A. (1989). The β-adrenergic radioligand [^{3}H]CGP-12177, generally classified as an antagonist, is a thermogenic agonist in brown adipose tissue. *Biochem. J.*, **261**, 401–405.

MOLENAAR, P., ROBERTS, S.J., KIM, Y.S., PAK, H.S., SAINZ, R.D. & SUMMERS, R.J. (1991). Localisation and characterisation of two propranolol resistant (−)-[^{125}I]-cyanopindolol binding sites in rat skeletal muscle. *Eur. J. Pharmacol.*, **209**, 257–262.

MOLENAAR, P., SARSERO, D., ARCH, J.R.S., KELLY, J., HENSON, S.M. & KAUMANN, A.J. (1997). Effects of (−)-RO363 at human atrial β-adrenoceptor subtypes, the human cloned β_3-adrenoceptor and rodent intestinal β_3-adrenoceptors. *Br. J. Pharmacol.*, **120**, 165–176.

MORIN, D., ZINI, R., URIEN, S., SAPENA, R. & TILLEMENT, J.P. (1992). Labelling of rat brain beta-adrenoceptors: (^{3}H)CGP-12177 or (^{125}I)iodocyanopindolol? *J. Recep. Res.*, **12**, 369–387.

MUZZIN, P., REVELLI, J.-P., KUHNE, F., GOGAHNE, J.D., MCCOMBIE, W.R., VENTER, J.C., GIACOBINO, J.-P. & FRASER, C. (1991). An adipose tissue specific β-adrenergic receptor. *J. Biol. Chem.*, **266**, 24053–24058.

OZTURK, Y., ALTAN, V.M. & YILDIZOGLU-ARI, N. (1996). Effects of experimental diabetes and insulin on smooth muscle functions. *Pharmacol. Rev.*, **48**, 69–112.

ROBERTS, S.J., MOLENAAR, P. & SUMMERS, R.J. (1993). Characterisation of propranolol-resistant (−)-[^{125}I]-cyanopindolol binding sites in rat soleus muscle. *Br. J. Pharmacol.*, **109**, 344–352.

ROBERTS, S.J., PAPAIOANNOU, M., EVANS, B.A. & SUMMERS, R.J. (1997). Functional and molecular evidence for beta 1-, beta 2- and beta 3-adrenoceptors in human colon. *Br. J. Pharmacol.*, **120**, 1527–1535.

ROBERTS, S.J., RUSSELL, F.D., MOLENAAR, P. & SUMMERS, R.J. (1995). Characterisation and localisation of atypical β-adrenoceptors in rat ileum. *Br. J. Pharmacol.*, **116**, 2549–2556.

SILLENCE, M.N., MOORE, N.G., PEGG, G.G. & LINDSAY, D.B. (1993). Ligand binding properties of putative β_3-adrenoceptors compared in brown adipose tissue and in skeletal muscle membranes. *Br. J. Pharmacol.*, **109**, 1157–1163.

STROSBERG, A.D. & PIETRI-ROUXEL, F. (1996). Function and regulation of the β_3-adrenoceptor. *Trends Pharmacol. Sci.*, **17**, 373–380.

SUMMERS, R.J., PAPAIOANNOU, M., HARRIS, S. & EVANS, B.A. (1995). Expression of β_3-adrenoceptor mRNA in rat brain. *Br. J. Pharmacol.*, **116**, 2547–2548.

THOLLANDER, M., SVENSSON, T. H. & HELLSTROM, P.M. (1996). Beta-adrenoceptors regulate angiotensin activity in the small intestine of rats: stimulation by beta2 and inhibition by beta3 subtypes. *Neurogastroenterol. Motil.*, **8**, 143–151.

VAN DER VLIET, A., RADEMAKER, B. & BAST, A. (1990). A beta adrenoceptor with atypical characteristics is involved in the relaxation of the rat small intestine. *J. Pharmacol. Exp. Ther.*, **255**, 218–226.

YILDIZOGLU-ARI, N., ALTINKURT, O., OZTURK, Y., ALTAN, V.M., PEKINER, C. & KARASU, C. (1988). Decreased gastro-intestinal responses to salbutamol and serotonin on streptozotocin-induced diabetes: Improving effect of insulin *in vivo* and *in vitro*. *Gen. Pharmacol.*, **19**, 665–668.

YU, O. & OUYANG, A. (1997). Distribution of β-adrenoceptor subtypes in gastrointestinal tract of nondiabetic and diabetic BB rats. *Dig. Dis. Sci.*, **42**, 1146–1153.

(Received November 11, 1998
Revised March 4, 1999
Accepted March 19, 1999)

Pergamon

SCIENCE DIRECT®

Bioorganic & Medicinal Chemistry Letters 13 (2003) 1301–1305

BIOORGANIC & MEDICINAL CHEMISTRY LETTERS

Novel and Potent Human and Rat β_3-Adrenergic Receptor Agonists Containing Substituted 3-Indolylalkylamines

Hiroshi Harada,[a,*] Yoshimi Hirokawa,[a] Kenji Suzuki,[a] Yoichi Hiyama,[a] Mayumi Oue,[b] Hitoshi Kawashima,[b] Naoyuki Yoshida,[b] Yasuji Furutani[b] and Shiro Kato[a]

[a]*Chemistry Research Laboratories, Dainippon Pharmaceutical Co., Ltd., Enoki 33-94, Suita 564-0053, Japan*
[b]*Pharmacology & Microbiology Research Laboratories, Dainippon Pharmaceutical Co., Ltd., Enoki 33-94, Suita 564-0053, Japan*

Received 5 December 2002; accepted 16 January 2003

Abstract—A novel series of 2-(3-indolyl)alkylamino-1-(3-chlorophenyl)ethanols was prepared and evaluated for in vitro ability to stimulate cAMP production in Chinese hamster ovary cells expressing cloned human β_3-AR. The optically active **30a** was found to be the most potent and selective human β_3-AR agonist in this series with an EC_{50} value of 0.062 nM. In addition, **30a** selectivity for human β_3-AR was 210-fold and 103-fold that for human β_2-AR and β_1-AR, respectively. Furthermore, **30a** showed potent agonistic activity at rat β_3-AR.

Introduction

β-Adrenergic receptors (β-ARs) have been subclassified as β_1- and β_2-ARs since 1967.[1] A third β-AR, initially referred to as 'atypical'[2] and later called β_3-AR[3,4] has been found in a number of species,[5–7] including man in the early 1980s.[4] The β_3-AR is located on the cell surface of both white and brown adipocytes and its stimulation promotes both lipolysis and energy expenditure.[8]

Since the discovery of β_3-AR, a number of laboratories have been engaged in developing potent and selective β_3-AR agonists for the treatment of obesity and non-insulin dependent (Type-II) diabetes.[9] Early β_3-AR agonists (the 'first generation' of potent and selective rat β_3-AR agonists) such as, BRL 37344,[10] CL 316243,[11] and SR 58611A,[12] having a 3-chlorophenyl moiety in the left-hand side and a carboxylic acid or an ester functionality in the right-hand side as shown in Figure 1, were reported to be effective anti-obesity and anti-diabetic agents in rodents.[13]

However, human clinical trials with these drugs for the treatment of metabolic disorders have been disappointing due to a lack of selectivity and/or potency or poor pharmacokinetics.[14] Because of the structural differences between human and rat β_3-ARs, activity at the rat β_3-AR could not effectively predict that at the human β_3-AR.[15] Thus, a new generation of human β_3-AR agonists with minimal side effects associated with activation of human β_1- and β_2-ARs has long been needed.

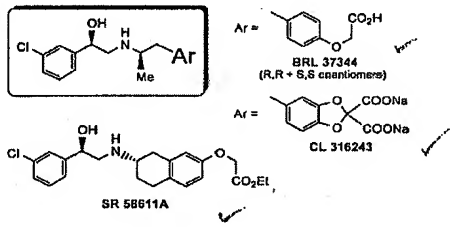

Figure 1.

At the beginning of 1990 and on the basis of results obtained from random screening for rat β_3-AR agonists, we found that a novel 2-[2-(3-indolyl)ethylamino]-1-(3-chlorophenyl)ethanol (**7**) having the 3-chlorophenyl moiety structure known to be required for β_3-AR agonistic activity, potently inhibited rat spontaneous colonic contraction (β_3-AR; $EC_{50} = 22.9 \pm 3.1$ nM) and only slightly relaxed both rat uterus (β_2-AR; $EC_{50} = 577.3 \pm 149.4$ nM) and guinea-pig trachea (β_1-AR; $EC_{50} = > 10{,}000$ nM). In order to improve the selectivity of lead compound **7**, we focused on the introduction of various substituents into the indole nucleus and the

*Corresponding author. Tel.: +81-6-6337-5904; fax: +81-6-6338-7656; e-mail: hiroshi-harada@dainippon-pharm.co.jp

0960-894X/03/$ - see front matter © 2003 Elsevier Science Ltd. All rights reserved.
doi:10.1016/S0960-894X(03)00073-8

side-chain at the 3-position of the indole ring, and performed optical resolution of selected compounds. Additionally, to develop potent and selective human β_3-AR agonists, we examined adenylyl cyclase activity using Chinese hamster ovary (CHO) cell lines expressing human β_1-, β_2-, and β_3-ARs.

Structure–activity relationship (SAR) studies of various 2-(3-indolyl)alkylamino-1-(3-chlorophenyl)ethanols led to the discovery of the optically active **30a**, which is a potent human and rat β_3-AR agonist with low activity for human β_1- and β_2-ARs.

In this paper, we describe the synthesis and SARs of 3-indolylethanolamine derivatives while keeping the 3-chlorophenyl moiety constant as an aryl group.

Chemistry

The requisite intermediate tryptamine derivatives were prepared using procedures previously described in the literatures.[16] In general, the 3-formylindoles obtained by Vilsmeier reaction ($POCl_3$, DMF) of the substituted indoles were treated with nitroalkane in AcOH to produce nitroolefins in good yield. Conjugated nitroolefins were directly reduced by $LiAlH_4$ to give saturated primary amines although the yield was moderate to low (Scheme 1).

Most of the compounds (**7–28** except **24**) listed in Tables 1, 3, and 4 were prepared by coupling reaction of the racemic 3-chlorostyrene oxide **1** or its optical isomer[17] (*R*)-**1** with various tryptamine derivatives in MeOH (Scheme 2).

The optically active **8a–d** listed in Table 2 were synthesized by treatment of the optically active 3-chloromandelic acids[18] (*R*)-**2** and (*S*)-**2** with the optically active α-methyltryptamines[19] (*R*)-**3** and (*S*)-**3** using BOP (benzotriazol-1-yloxytris(dimethylamino)phosphonium hexafluorophosphate) as a coupling reagent followed by reduction of the amide group of **4a–d** with borane (Scheme 3).

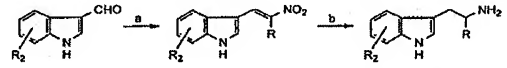

Scheme 1. (a) $MeNO_2$ or $EtNO_2$, AcOH; (b) $LiAlH_4$, THF.

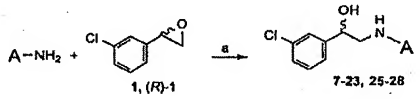

Scheme 2. (a) MeOH.

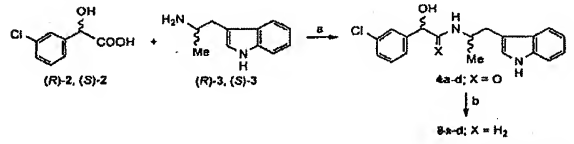

Scheme 3. (a) Benzotriazol-1-yloxytris(dimethylamino)phosphonium hexafluorophosphate (BOP), DMF; (b) BH_3·THF.

The 2-[3-(7-*O*-substituted 3-indolyl)-2-propylamino]-1-(3-chlorophenyl)ethanols **24** and **30** as a mixture of diastereomers and the selected optical isomers **23a,b** and **30a,b** listed in Tables 4 and 5 were synthesized as shown in Scheme 4.

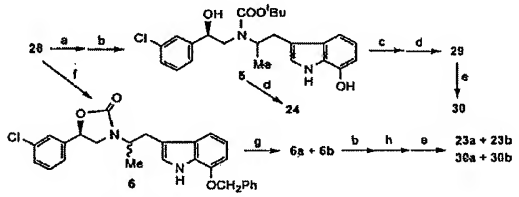

Scheme 4. (a) Boc_2O; (b) Pd/C, H_2, chlorobenzene; (c) $ClCH_2CO_2Me$, K_2CO_3, KI; (d) aqueous HCl; (e) aqueous NaOH; (f) *N,N'*-carbonyldiimidazole; (g) separation by silica gel column chromatography; (h) $ClCH_2CO_2Me$ or MeI.

Protection of the secondary amine functionality of the 7-benzyloxytryptamine **28** with Boc group followed by catalytic hydrogenation in the presence of chlorobenzene to avoid removal of the 3-chlorine atom in the benzene ring produced the 7-hydroxytryptamine **5**. Reaction of **5** with methyl chloroacetate, followed by removal of the Boc protecting group under acidic conditions furnished the 7-methoxycarbonylmethoxytryptamine **29**. Subsequent alkaline hydrolysis of **29** and acid hydrolysis of **5** gave **30** and **24**, respectively.

The optically active **23a,b** and **30a,b** having 7-methoxy- and 7-carboxylmethoxy groups, respectively (Table 5), were synthesized as follows. Protection of the aminoethanol moiety of **28** with a carbonyl group, followed by silica gel column chromatography separation of the resulting diastereomer **6** gave the optical isomers **6a,b** having *R*- and *S*-configuration in the α-methyl group, respectively. A similar method to that described for the

Table 1. Human β_3-AR agonistic activity of 2-(3-indolyl)alkylamino-1-(3-chlorophenyl)ethanols **7–11**[a]

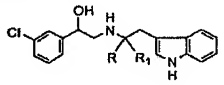

Compd	R	R_1	Human β_3-AR	
			EC_{50} (nM) (IA%)[b]	cAMP accumulation (% at 10^{-7} M)[c]
7[d]	H	H	69 (99)	
8[e]	Me	H	12 (114)	
9[e]	Et	H		20
10[d]	Me	Me	70 (118)	
11[e]	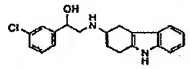			0

[a]β_3-AR agonistic activity was assessed by measuring cAMP accumulation in CHO cells expressing human β_3-AR (150,000 receptors/cell).
[b]The maximal amount of cAMP obtained by (−)-isoproterenol and the amount of cAMP in the absence of agonists were defined as 100 and 0%, respectively, and the relative maximal response of each compound is expressed as intrinsic activity (IA). EC_{50} value is a concentration of the test compound to be required to achieve 50% of cAMP accumulation.
[c]Activity relative to (−)-isoproterenol.
[d]Racemic mixture.
[e]Mixture of four diastereomers.

Table 2. β-AR agonistic activity of compound **8** and its individual diastereomers at cloned human β_1-, β_2-, and β_3-ARs and at the cloned rat β_3-AR[a]

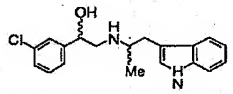

Compd	Configuration of hydroxy center	Configuration of methyl center	EC_{50} (nM) (IA%)[b]			
			Human β_3-AR	Human β_2-AR	Human β_1-AR	Rat β_3-AR
8	Mixture	Mixture	12 (114)	23 (46)	NT[d]	0.97 (107)
8a	*R*	*R*	5.4 (110)	25 (50)	1.9 (65)	0.36 (98)
8b	*R*	*S*	240 (97)	—[c]	9.4 (50)	13 (96)
8c	*S*	*R*	220 (119)	330 (23)	47 (70)	11 (108)
8d	*S*	*S*	3300 (62)	—[c]	140 (47)	33 (108)

[a]β-ARs agonistic activity were assessed by measuring cAMP accumulation in CHO cells expressing various β-ARs. Expression levels[21] of β-ARs were 150,000 receptors/cell, 30,000 receptors/cell, 12,000 receptors/cell and 880,000 receptors/cell for human β_3-, β_2-, β_1-, and rat β_3-ARs.
[b]See footnote b in Table 1.
[c]—, could not be calculated because of low IA.
[d]NT, not tested.

Table 3. Human β_3-AR agonistic activity of substituted indole derivatives **12–22**[a]

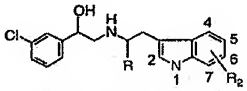

Compd	R	R_2	Human β_3-AR	
			EC_{50} (nM) (IA%)[b]	cAMP accumulation (% at 10^{-7} M)[c]
12[d]	H	1-Me		6
13[d]	H	2-Me		5
14[d]	H	4-Me		20
15[e]	Me	4-Me	96 (165)	
16[d]	H	5-Me		7
17[e]	Me	6-Me	12 (95)	
18[d]	H	7-Me		0
19[e]	Me	6-MeO	22 (102)	
20[e]	Me	7-MeO	1.7 (113)	
21[e]	Me	6-Cl	28 (131)	
22[e]	Me	6-Br	38 (98)	

[a]See footnote a in Table 1.
[b]See footnote b in Table 1.
[c]See footnote c in Table 1.
[d]See footnote d in Table 1.
[e]See footnote e in Table 1.

preparation of **30** from **28** was applied to the preparation of the desired optical isomers **23a,b** and **30a,b**. The absolute configuration of **6b** (*S*-configuration) and **30a** (*R*-configuration) was confirmed by X-ray crystallography, and the ORTEP diagram of **30a** is shown in Figure 2.[20]

Results and Discussion

Activation of β-ARs by the various compounds prepared in this study was assessed by measuring cAMP accumulation in CHO cells expressing cloned human β_1-, β_2-, and β_3-ARs and rat β_3-AR. As shown in Table 1, the lead compound **7** exhibited a relatively modest agonistic activity at the human β_3-AR (EC_{50} = 69 nM).

Table 4. Human β_3-AR agonistic activity of 7-*O*-substituted indole derivatives **23–30**[a]

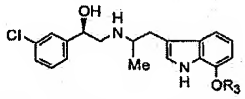

Compd[c]	R_3	Human β_3-AR
		EC_{50} (nM) (IA%)[b]
23	Me	0.67 (114)
24	H	1.7 (128)
25	Et	0.96 (96)
26	Pr	14 (103)
27	*iso*-Pr	2.8 (87)
28	CH_2Ph	11 (114)
29	CH_2CO_2Me	0.92 (102)
30	CH_2CO_2H	0.11 (124)

[a]See footnote a in Table 1.
[b]See footnote b in Table 1.
[c]Mixture of *R,R* and *R,S* diastereomers.

Table 5. β-AR agonistic activity of optically active 7-*O*-substituted indole derivatives **23a,b**, **30a,b**, and reference compounds at cloned human β_1-, β_2-, and β_3-ARs and at the cloned rat β_3-AR[a]

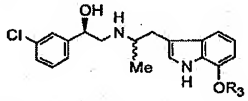

Compd	Configuration of methyl center	R_3	EC_{50} (nM) (IA%)[b]			
			Human β_3-AR	Human β_2-AR	Human β_1-AR	Rat β_3-AR
23a	*R*	Me	0.36 (89)	5.2 (46)	0.13 (118)	0.15 (147)
23b	*S*	Me	120 (51)	—[c]	130 (83)	6.5 (121)
30a (AJ-9677)	*R*	CH_2CO_2H	0.062 (116)	13 (26)	6.4 (26)	0.016 (110)
30b	*S*	CH_2CO_2H	10 (84)	—[c]	14 (107)	1.2 (106)
BRL 37344			21 (95)	290 (31)	1700 (17)	0.095 (109)

[a]See footnote a in Table 2.
[b]See footnote b in Table 2.
[c]See footnote c in Table 2.

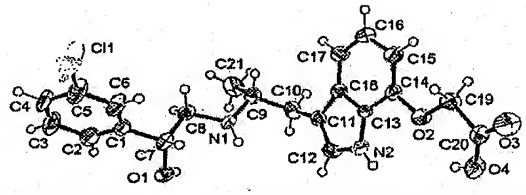

Figure 2. The ORTEP drawing of **30a** with thermal ellipsoids at 50% probabilities.

Introduction of a methyl group (yielding **8**) into the tryptamine side-chain of **7** resulted in good improvement in β_3-AR agonistic activity (EC_{50} = 12 nM, intrinsic activity (IA) value of 114%). However, introduction of an ethyl group (yielding **9**) resulted in low activity at the human β_3-AR. The α,α-dimethyltryptamine **10** had an activity nearly equipotent to that of the parent compound (**7**), and the tetrahydrocarbazole **11** showed significantly poor activity.

From the study on the β-ARs agonistic activity of the four optical isomers of BRL 37344, the (*R,R*)-configuration

had proved to be important for enhancing rat β_3-AR agonistic activity.[22] Thus, the four optical isomers **8a–d** of the selected compound **8** were prepared and their agonistic activity at the human β_1-, β_2-, and β_3-ARs and rat β_3-AR was evaluated. As expected, the optical isomer **8a**, having *R*-configuration in both the hydroxy and α-methyl centers, exhibited a potent agonistic activity at the human and rat β_3-ARs compared with other stereoisomers (**8b–d**). Although **8a** had an agonistic activity at human and rat β_3-ARs 2–3 times more potent than that of the original compound **8**, it was completely nonselective. Other enantiomers (**8b–d**) showed low activity at all β-ARs (Table 2).

Next, we examined the agonistic activity of various substituted tryptamine derivatives. Introduction of a methyl group at 1-, 2-, 4-, 5-, and 7-positions of the indole ring of **7** and **8** resulted in low agonistic activity at the human β_3-AR (compounds **12–16** and **18**, Table 3). The 6-methyl group was well tolerated and **17** displayed comparable agonistic activity to that of its parent **8**. The 6-methoxytryptamine **19** and the tryptamine derivatives **21** and **22** with chlorine and bromine at the 6-position, respectively, were weak human β_3-AR agonists compared with **8**. Fortunately, the 7-methoxyindole counterpart **20** showed much more potent agonistic activity than **8**. From the above SAR studies, the 7-methoxytryptamine **20** was found to exhibit the most preferred agonistic activity at human β_3-AR.

Because the (*R*)-hydroxy isomers of the hydroxy center were more potent than the corresponding (*S*)-hydroxy derivatives, 7-*O*-substituted indole analogues with an (*R*)-hydroxy group were prepared and tested for their agonistic activity at the human β_3-AR. As shown in Table 4, the 7-methoxyindole derivative **23** showed an activity ca. 2.5-fold more potent than that of **20**. Removal of the methyl group on the methoxy substitution gave derivative **24**, which exhibited a decreased agonistic activity at the human β_3-AR. When the methoxy group of **23** was replaced with an ethoxy and methoxycarbonylmethoxy groups, the resultants **25** and **29** exhibited approximately equal agonistic activity at human β_3-AR. A significant loss in activity was observed with the 7-propoxy (**26**), 7-isopropoxy (**27**), and 7-benzyloxy (**28**) derivatives. Replacement of the methoxy group of **23** by a carboxylmethoxy group (yielding **30**) led to a 6-fold improvement in human β_3-AR agonistic activity.

Finally, the 7-methoxy and 7-carboxylmethoxyindole derivatives (**23** and **30**, respectively) with potent agonistic activity at human β_3-AR were selected for diastereomers separation and agonistic activity examination at human β_1-, β_2-, and β_3-ARs and rat β_3-AR. As shown in Table 5, the optical isomers **23a** and **30a** with an (*R*)-α-methyl group were more potent than the corresponding diastereomers **23b** and **30b**. However, **23a** exhibited poor selectivity for human β_3-AR as it potently stimulated both human β_1- and β_2-ARs. On the other hand, the selectivity of **30a** for human β_3-AR was high. The optically active **30a** showed a potent agonistic activity at human and rat β_3-ARs with selectivity for human β_3-AR over 100-fold that for the β_1-AR and 200-fold that for the β_2-AR. Introduction of a carboxylmethoxy group into the indole ring of **30a** led to a much more potent agonistic activity at the human β_3-AR and ca. 6-fold increase in activity at the rat β_3-AR as compared to BRL 37344. The presence of the 7-carboxylmethoxy group and the *R*-configuration for the α-methyl group were therefore found to be necessary for potent agonistic activity and selectivity.

In conclusion, the synthesis and SAR studies of substituted tryptamine derivatives based on human β_3-AR agonistic activity have been discussed. Introduction of a carboxylmethoxy group at the 7-position of the indole ring resulted in the identification of a potent human ($EC_{50} = 0.062$ nM) and rat ($EC_{50} = 0.016$ nM) β_3-ARs full agonist **30a** (AJ-9677). Additionally, this compound (**30a**) showed good selectivity for human β_3-AR as compared to that for human β_1- and β_2-ARs.

References and Notes

1. Lands, A. M.; Arnold, A.; McAuliff, J. P.; Luduena, F. P.; Brown, T. G., Jr. *Nature* **1967**, *214*, 597.
2. Arch, J. R. S. *Proc. Nutrition Soc.* **1989**, *48*, 215.
3. Emorine, L. J.; Marullo, S.; Briend-Sutren, M.-M.; Patey, G.; Tate, K.; Delavier-Klutchko, C.; Strosberg, A. D. *Science* **1989**, *245*, 1118.
4. Tan, S.; Curtis-Prior, P. B. *Int. J. Obesity* **1983**, *7*, 409.
5. Granneman, J. G.; Lahners, K. N.; Chaudhry, A. *Mol. Pharmacol.* **1991**, *40*, 895.
6. Muzzin, P.; Revelli, J.-P.; Kuhne, F.; Gocayne, J. D.; McCombie, W. R.; Venter, J. C.; Giacobino, J.-P.; Fraser, C. M. *J. Biol. Chem.* **1991**, *266*, 24053.
7. Nahmias, C.; Blin, N.; Elalouf, J.-M.; Mattei, M. G.; Strosberg, A. D. *EMBO. J.* **1991**, *10*, 3721.
8. Lafonate, M.; Berlan, M. J. *Lipid Res.* **1993**, *34*, 1057.
9. (a) Weyer, C.; Gautier, J. F.; Danforth, E., Jr. *Diabetes Metab.* **1999**, *25*, 11. (b) Souza, J. C.; Burkey, B. F. *Curr. Pharm. Des.* **2001**, *7*, 1433. (c) Weber, A. E. *Annu. Rep. Med. Chem.* **1998**, *33*, 193.
10. Cantello, B. C. C.; Smith, S. A. *Drugs Future* **1991**, *16*, 797.
11. Bloom, J. D.; Claus, T. H. *Drugs Future* **1994**, *19*, 23.
12. Cecchi, R.; Croci, T.; Boigegrain, R.; Boveri, S.; Baroni, M.; Boccardi, G.; Guimbard, J. P.; Guzzi, U. *Eur. J. Med. Chem.* **1994**, *29*, 259.
13. (a) Arch, J. R. S.; Wilson, S. *Int. J. Obesity* **1996**, *20*, 191. (b) Howe, R. *Drugs Future* **1993**, *18*, 529.
14. (a) Lipworth, B. J. *J. Clin. Pharmacol.* **1996**, *42*, 291. (b) Strosberg, A. A. *Annu. Rev. Pharmacol. Toxicol.* **1997**, *37*, 421.
15. Liggett, S. *Mol. Pharm.* **1992**, *42*, 634.
16. (a) 3-(2-Aminopropyl)indole, 3-(2-aminobutyl)indole: Heinzelman, R. V.; Anthony, W. C.; Lyttle, D. A.; Szmuszkovicz, Z. *J. Org. Chem.* **1960**, *25*, 1548. (b) Bergman, J.; Bäckvall, J.-E.; Lindström, J.-O. *Tetrahedron* **1973**, *29*, 971. 3-(2-Amino-2-methylpropyl)indole: Snyder, H. R.; Katz, L. *J. Am. Chem. Soc.* **1947**, *69*, 3140. 3-Amino-1,2,3,4-tetrahydrocarbazole: Mooradian, A.; Dupont, P. E.; Hlavac, A. G.; Aceto, M. D.; Pearl, J. *J. Med. Chem.* **1977**, *20*, 487.
17. Bloom, J. D.; Dutia, M. D.; Johnson, B. D.; Wissner, A.; Burns, M. G.; Largis, E. E.; Dolan, J. A.; Claus, T. H. *J. Med. Chem.* **1992**, *35*, 3081.
18. Collet, A.; Jacques, J. *Bull. Soc. Chim. Fr.* **1973**, 3330.

19. Repk, D. B.; Ferguson, W. J. *J. Heterocyclic Chem.* **1976**, *13*, 775.
20. Mp 225–226 °C (decomp.) (aqueous NH_3/MeOH). $[\alpha]_D^{29}$ −23.3° (*c* 1.0, 1 mol NaOH). IR (KBr) ν_{max}; 3134, 1609, 1406, 1250, 1057, 783 cm^{-1}. ^1H NMR (dimethylsulfoxide-d_6); 0.93 (3H, d, J=6.0 Hz), 2.5–3.3 (8H, m), 4.55 (2H, s), 4.85 (1H, dd, J=9.8, 2.6 Hz), 6.42 (1H, d, J=7.8 Hz), 6.78 (1H, t, J=7.8 Hz), 6.94 (1H, d, J=2.0 Hz), 6.99 (1H, d, J=7.8 Hz), 7.27–7.33 (3H, m), 7.46 (1H, s), 11.02 (1H, s).
21. Takeda, Y.; Chou, K. B.; Takeda, J.; Sachais, B. S.; Krause, J. E. *Biochem. Biophys. Res. Comm.* **1991**, *179*, 1232.
22. Oriowo, M. A.; Chapman, H.; Kirkham, D. M.; Sennitt, M. V.; Ruffolo, R. R.; Cawthorne, M. A. *J. Pharmacol. Exp. Ther.* **1996**, *277*, 22.

Am J Physiol Heart Circ Physiol 286: H2141–H2150, 2004;
10.1152/ajpheart.00829.2003.

Remodeling of the chronic severely failing ischemic sheep heart after coronary microembolization: functional, energetic, structural, and cellular responses

Yifei Huang,[1] Stephen N. Hunyor,[1] Lele Jiang,[2] Osamu Kawaguchi,[1] Kazuaki Shirota,[1] Yoshihiko Ikeda,[3] Takeshi Yuasa,[1] Gabrielle Gallagher,[1] Biao Zeng,[1] and Xing Zheng[1]

[1]Cardiac Technology Centre, Department of Cardiology, Royal North Shore Hospital, Sydney, New South Wales 2065; [2]Department of Physiology, Institute for Biomedical Research, University of Sydney, New South Wales 2006, Australia; and [3]Department of Pathology, National Cardiovascular Center, Osaka 565-8565, Japan

Submitted 2 September 2003; accepted in final form 8 January 2004

Huang, Yifei, Stephen N. Hunyor, Lele Jiang, Osamu Kawaguchi, Kazuaki Shirota, Yoshihiko Ikeda, Takeshi Yuasa, Gabrielle Gallagher, Biao Zeng, and Xing Zheng. Remodeling of the chronic severely failing ischemic sheep heart after coronary microembolization: functional, energetic, structural, and cellular responses. *Am J Physiol Heart Circ Physiol* 286: H2141–H2150, 2004; 10.1152/ajpheart.00829.2003.—The mandatory use of pharmacotherapy in human heart failure (HF) impedes further study of natural history and remodeling mechanisms. We created a sheep model of chronic, severe, ischemic HF [left ventricular (LV) ejection fraction (LVEF) <35% stable over 4 wk] by selective coronary microembolization under general anesthesia and followed hemodynamic, energetic, neurohumoral, structural, and cellular responses over 6 mo. Thirty-eight sheep were induced into HF (58% success), with 23 sheep followed for 6 mo (21 sheep with sufficient data for analysis) after the LVEF stabilized (median of 3 embolizations). Early doubling of LV end-diastolic pressure persisted, as did increases in LV end-diastolic volume, LV wall stress, and LV wall thinning. Contractile impairment (LV end-systolic elastance, LV preload recruitable stroke work, and dobutamine-responsive contractile reserve) and diastolic dysfunction also remained stable. Cardiac mechanical energy efficiency did not recover. Plasma atrial natriuretic peptide levels remained elevated, but rises in plasma aldosterone and renin activity were transient. Collagen content increased 170%, the type I-to-III phenotype ratio doubled in the LV, but right ventricular collagen remained unaltered. Fas ligand cytokine levels correlated with expression of both caspase-3 and -2, suggesting a link in the apoptotic "death cascade." Caspase-3 activity also bore a close relationship to LV meridional wall stress calculated from echocardiographic and intraventricular pressure measurements. We concluded that the stability of chronic untreated severe ischemic HF depends on the recruitment of myocardial remodeling mechanisms that involve an interaction among hemodynamic load, contractile efficiency/energetics, neurohumoral activation, response of the extracellular matrix, wall stress, and the myocyte apoptotic pathway.

neurohormones; pressure-volume loops; contractile reserve and energy efficiency; collagen and its phenotypes; wall stress and caspases

THE NEED FOR CONTINUING PURSUIT of a suitable animal model of heart failure (HF) is highlighted by the difficulty in studying the underlying basic mechanisms and natural history in the human condition, confounded by pharmacological intervention. Previous emphasis on cardiorenal, hemodynamic, and neurohormonal derangements has shifted toward remodeling and the role played by stretch-activated pathways, cytokine activation, and changes in cardiomyocytes and the extracellular matrix.

HF has previously been induced in several large animal species (e.g., dogs, calves, and pigs) using techniques that damage the myocardium, such as coronary microembolization (40, 42), rapid ventricular pacing (7), coronary artery ligation (29), progressive coronary artery occlusion with Ameroid constrictors (11), or administration of cardiotoxic drugs such as adriamycin. Alternatively, volume loading the heart by creation of an arteriovenous fistula or aortic regurgitation has also been used, as has pressure loading with aortic banding. From the human perspective, the most relevant methods are those that interfere with coronary blood flow to cause infarction or chronic ischemic damage. The principal advantages of the microembolization approach include homogeneity of damage, which is limited to the left ventricle (LV), ability to titrate the response, and potential avoidance of mitral regurgitation. In contrast to the other approaches, the microembolization model has also proven remarkably stable but is subject to the criticism that it lacks associated large coronary artery disease. Coronary ligation or constriction, on the other hand, fails to involve the small vessels that are commonly diseased in humans, especially diabetics.

We established a large animal model of severe HF that bears close resemblance to human ischemic cardiomyopathy (14), the most common cause of HF (9), and studied a cohort of 23 animals for up to 6 mo. The sheep model showed remarkable stability. In a previous small series, we established the practicality of sequential selective coronary artery microembolization (13), examined the microscopic morphometric picture of remodeling (14), and studied cytokines and related links in the apoptotic death cascade and their relationship to wall stress (15).

With the use of a much larger cohort, the present study extends the scope of previous findings (18, 33) and integrates hemodynamic, energetic, neurohumoral, extracellular matrix, wall stress, cytokine, and apoptosis-related responses in terms of remodeling and natural history in chronic, severe, untreated, ischemic HF.

MATERIALS AND METHODS

Sixty-five adult merino sheep of either sex with a body weight of 47 ± 8 kg were used in a study protocol approved by the Institutional Animal Care and Ethics Committee. The animals received humane

Address for reprint requests and other correspondence: S. N. Hunyor, Cardiac Technology Centre, Dept. of Cardiology, Block 4, Level 3, Royal North Shore Hospital, Sydney, New South Wales 2065, Australia (E-mail: stephenh@med.usyd.edu.au).

The costs of publication of this article were defrayed in part by the payment of page charges. The article must therefore be hereby marked "*advertisement*" in accordance with 18 U.S.C. Section 1734 solely to indicate this fact.

care in compliance with the "Principles of Laboratory Animal Care" formulated by the National Society for Medical Research and the *Guide for the Care and Use of Laboratory Animals* (NIH Pub. No. 86-23, Revised 1985).

Study design. The animals were acclimatized for at least 2 wk before being enrolled in experiments that had two major components: selective intracoronary microembolization (ICM) leading to HF and long-term (6 mo) profiling of hemodynamic, energetic, and neurohumoral parameters.

After the final (6 mo) dynamic profiling, the heart was harvested and cellular responses [Fas ligand (FasL)/Fas and caspases] to wall stress as well as extracellular matrix collagen levels and phenotype were assayed (Fig. 1).

Hemodynamic assessment was performed at baseline, when HF was established, and again 3 and 6 mo later and included LV pressure (LVP), LV pressure-volume (P-V) relationship, and cardiac output (CO). LV volume, LV ejection fraction (LVEF), and LV wall thickness were derived echocardiographically. Neurohumoral studies examined plasma atrial natriuretic peptide (ANP), angiotensin II, aldosterone, and plasma renin activity (PRA) on the day of, but before, the hemodynamic studies.

Hearts from 16 sheep, including 11 sheep from the described HF group at 6-mo follow-up and 5 normal controls, were analyzed for collagen content and phenotypic change (Fig. 1). All surgical procedures were performed under anesthesia, which was induced by thiopentone (15–20 mg/kg) and maintained with 1.5–2% isoflurane in 40% oxygen using a respirator (model 8, Bird; Palm Springs, CA). Expired CO_2 was monitored with a POET II monitor (Criticare Systems; Milwaukee, WI) and maintained at 30–35 mmHg. All hemodynamic measurements/recordings were taken after at least 30 min of stable anesthesia and at end expiration. Surgical procedures were performed under sterile conditions.

Staged ICM. Microsphere delivery was guided by preprocedure echocardiography and by the response of the ECG and LV and arterial pressures that were monitored during the entire procedure. A Judkins (5-Fr) catheter was passed via carotid artery cutdown to engage the orifice of either the left anterior descending or left circumflex coronary artery. After the intravenous injection of 25 mg lidocaine, 0.1–0.4 ml of 90-μm polystyrene microspheres (2.54% solid latex, Polysciences; Warrington, PA) diluted in 2 ml of 0.9% saline were injected into the selected artery. The microsphere suspension was subjected to ultrasonic mixing and manual shaking immediately before the injection. In each procedure, the embolization was repeated until significant myocardial compromise was achieved as evidenced by changes in LV end-diastolic pressure (LVEDP), arterial pressure, and ECG S-T. The procedure was repeated every 2 wk, with the end point of microembolization being the achievement of an echocardiographic LVEF <35%, stable for 4 wk.

In a subgroup of sheep (n = 21), after baseline blood sampling, specimens were taken at 2, 6, and 18 h after ICM for measurement of plasma creatine kinase (CK). Postoperatively, pain was managed with intramuscular buprenorphine (Reckitt and Colman Products; London, UK), and heart rate (HR) and respiration were also closely monitored. Other medications such as supplemental potassium, intravenous furosemide, nitroglycerine, and lidocaine were given as necessary.

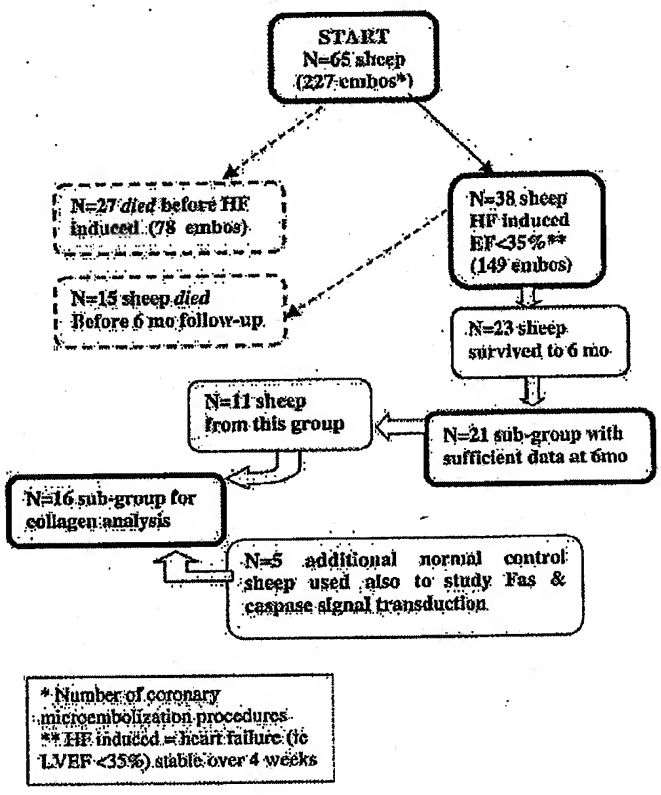

Fig. 1. Sheep numbers (N) at start, with heart failure (HF) at enrollment into study, and at 6-mo follow-up, including breakdown of loss due to death. Also, composition of the subgroups reported and the number of coronary microembolizations (Embos) performed in the principal groups are shown. LVEF, left ventricular (LV) ejection fraction.

LVEF, LV volume, and LV wall thickness measurement. Echocardiography was performed in the right lateral decubitus position using an Ausonics Opus I system (Ausonics; New South Wales, Australia). Standard LV short-axis views at the mitral, midpapillary, and apical levels, together with long-axis views, were recorded on videotape. LV areas measured from the transverse sections and the LV long-axis length were used to calculate LV end-systolic (LVESV) and end-diastolic volumes (LVEDV) using the modified Simpson's rule formula. The inner endocardial margin defined the LV lumen and the LVEF was derived as follows: LVEF = (LV at end diastole − LV at end systole)/LV at end diastole × 100%. LV thickness was measured from the M-mode recording at the midpapillary level. Results from three different cardiac cycles were averaged.

CO and pressure measurement. CO was measured in triplicate with a Swan-Ganz thermodilution catheter positioned in the pulmonary artery using right atrial bolus injections of ice-cold 5% dextrose (model VGS 2, Baxter Healthcare). A Mikro-Millar pressure transducer catheter (Millar Instruments; Houston, TX) was advanced into the ascending aorta and then into the LV via cutdown on the carotid artery to measure arterial and LVP. Pressure signals were amplified (System 6, Triton Technology) and recorded on a Macintosh computer using a MacLab analog-to-digital converter (MacLab/16s, ADInstruments; New South Wales, Australia) at 200 Hz. The maximum rates of LVP increase (LV dP/dt_{max}) and decay (LV dP/dt_{min}) were obtained by numerical on-line differentiation of LVP. The time constant of the isovolumic LV relaxation half-time (τ) was calculated as the time taken for LVP to fall to one-half its level at peak LV dP/dt_{min} (24). LV end-diastolic meridional wall stress (in dyn/cm^2) was calculated as $1{,}333 \cdot P \cdot r/2h(1 + h/2r)$, where P is the LVEDP (in mmHg), r is the internal radius (in cm), and h is the LV wall thickness (in cm). LV wall thickness was taken to be the average of septal and free wall dimensions (19).

Central venous pressure was measured via the atrial port of the Swan-Ganz catheter with a fluid-filled pressure transducer system (Ohmeda). Pulmonary vascular resistance was calculated as mean pulmonary artery pressure × 80/CO (in dyn·s·cm^{-5}).

Myocardial contractility and contractile reserve. A 12-electrode 7-Fr pigtail conductance catheter (CardioDynamics; Leiden, The Netherlands) and a 5-Fr Millar catheter-tipped pressure transducer were positioned in the LV for measurement of LV volume and LVP. A 22-Fr balloon-tipped catheter (CV 1014 Fogarty Occlusion Catheter, Edwards Lab, American Hospital Supply) was placed in the inferior vena cava via jugular vein cutdown for transient (15–20 s) inferior vena cava occlusion to reduce LV preload while the LV P-V relationship was recorded. Data were acquired by a Leycom Sigma-5-DF signal conditioner processor (CardioDynamics) and recorded on an IBM personal computer. LV end-systolic elastance (E_{es}) and preload recruitable stroke work (PRSW) were used as load-independent indexes of LV contractility (1). These indexes were computed by commercial software (CardioDynamics). To study the cardiac contractile reserve, intravenous dobutamine (0.1 mg/ml) was infused at incremental rates of 18, 27, 36, 45, and 54 ml/h. Each infusion rate was continued for 5 min until the HR reached 140 beats/min.

External work (EW), potential energy (PE), and the P-V area (P-V area = EW + PE) were derived, and the ratio of EW/P-V area used to describe the work efficiency of the normal and failing heart (35, 33).

Neurohumoral studies. Venous blood samples were obtained (between 6 and 8 AM and before sheep were feed) from an indwelling central venous catheter previously placed via the jugular vein. The samples were chilled and centrifuged immediately, and the plasma was stored at −70°C. Plasma angiotensin II was measured with a double-antibody RIA modified method using the Buhlmann Laboratories I125 RIA kit (Basel, Switzerland). The sensitivity of the measurement is 0.1 pg/ml with a recovery of 91.0 + 5.1%. Plasma aldosterone was assayed by a Sorin Biomedica RIA kit (Saluggia, Italy) with sensitivity of 15 pg/ml. The α-ANP assay in plasma used a classical RIA (competitive protein binding) in homogenous phase using the double-antibody separation technique specific for α-ANP, with a sensitivity of 7 pg/ml (4).

Myocardial collagen determination. In the 16 sheep (including 5 normal controls) where myocardial collagen content and phenotype were assayed (Fig. 1), the heart was quickly removed and the great vessels and atria were dissected free after death by an intravenous injection of thiopentone and potassium chloride. The right ventricle (RV) and LV were separated, blotted dry, and weighed. Sections of the LV and RV free wall and the interventricular septum just below the papillary muscles were dissected, snap frozen in liquid nitrogen, and stored at −70°C until analysis.

Myocardial collagen content was quantified after hydrolysis of the tissues and incubation with Ehrlich's reagent solution (5), with absorbency of the solution measured at 558 nm. Hydroxyproline content was calculated from a standard curve and expressed as micrograms per milligrams of dry tissue weight. Collagen content was derived as the hydroxyproline level × 7.46.

Interrupted SDS gel electrophoresis (36) was used to assay collagen phenotype after 1 g of heart tissue had been homogenized and pepsin digested (23). The gels were then immersed in a stain solution composed of 1.25% Coomassie brilliant blue for 60 min and then destained. The protein bands α_1 (I) and α_1 (III) were quantitated by scanning at 570 nm. Because most fibrillar collagens have similar cross links, this approach assumes that α-chains alone can be used to characterize collagen type I and III phenotypes and that proportions of β- and γ-chains are similar.

Expression of FasL and caspases-8, -3, and -2. The protein expressions of FasL and caspases were determined by Western blotting as previously described (15, 16). Briefly, protein extracts from the sheep LV were separated by SDS-PAGE. After the proteins were transferred onto a polyvinylidene difluoride membrane, FasL or caspases were probed using primary antibodies from Santa Cruz Biotechnology (Santa Cruz, CA). Positive controls of cell lysates were from Transduction Laboratories (Lexington, KY). The antibody-labeled bands were visualised using the NEN BLAST method (NEN Life Science Products; Boston, MA). Laser scanning densitometry was used to determine volume densities (in arbitrary units) of the bands detected by the corresponding antibody.

Determination of caspase activites. The caspase activity assay was performed as previously described (15) using a fluorescent 7-amino-4-trifluoromethycoumarin (AFC) substrate/inhibitor QuantiPak (Bio-Mol; Plymouth Meeting, PA). With the use of this technique, a linear correlation of $f(x) = 21.9x - 3.1$ was found between the change in fluorescence intensity due to the cleavage of the AFC fluorophore from the substrates by the corresponding caspase activity.

Statistical data analysis. Data are presented as means ± SD unless otherwise stated. Comparison of hemodynamic parameters was performed by the appropriate one-way ANOVA, followed by a post hoc *t*-test. A P value <0.05 was considered statistically significant.

RESULTS

Effect of stepwise coronary microembolization. Myocardial damage due to intracoronary injection of microspheres was evidenced by acute ECG changes and a peak increase in the CK level at 6 h after the procedure (Fig. 2*A*). The baseline LVEF of the 65 sheep was 58.7 ± 6.9%. Of these 65 sheep, 38 sheep were successfully induced into HF with a LVEF decrease of 50% (58.3 ± 7.4% at baseline vs. 29.1 ± 4.4% at HF establishment). The LVEF remained stable when reexamined 3 mo (n = 19 of 38 sheep) and 6 mo (n = 21 of 38 sheep) later (Fig. 2*B*).

Echocardiographic parameters and calculated LV wall stress are detailed in Table 1. LVEDV increased 73% with the induction of HF and remained 55% above baseline, LV end-

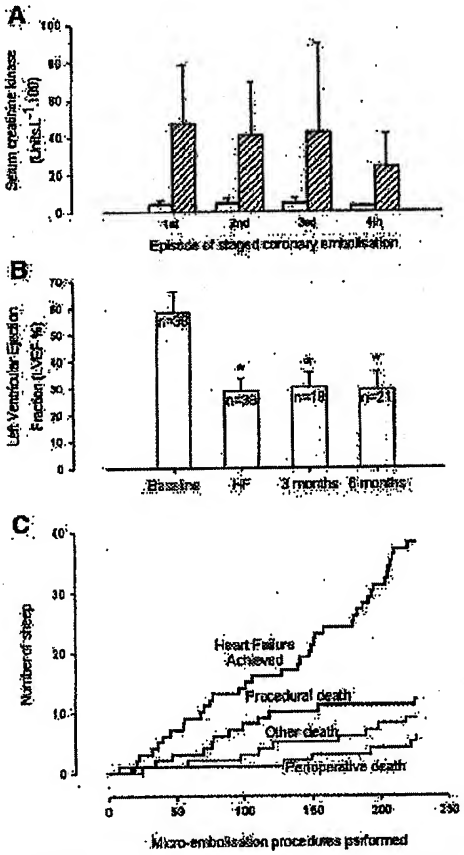

Fig. 2. *A*: serum creatine kinase response to successive intracoronary microembolizations. The "peak" sample was taken 6 h after the injection of microspheres. *B*: change in LVEF after microembolization. HF is considered to be established when there is a decrease of LVEF to <35% persisting for 4 wk after the last microembolization. *C*: success rate of HF induction and causes of early death from microembolization. Note the improved success rate with time and experience, especially in relation to procedural deaths. *n*, No. of animals.

diastolic diameter showed a stable 30% increase, and stable thinning of the LV wall was observed. Accordingly, LV wall stress increased markedly in response to the embolization-induced HF and remained elevated.

Between 1 and 10 embolization procedures (median 3, total of 149 in 38 sheep) were needed to induce HF. Sixty-five procedures involved microsphere injection into the left circumflex coronary artery, 56 procedures into the left anterior descending coronary artery, and 28 procedures into the left main coronary artery, with median doses of 0.4 ml (range 0.1–1 ml), 0.5 ml (range 0.1–1.7 ml), and 0.5 ml (range 0.1–0.9 ml), respectively. The total volume needed to induce HF was a median of 1.6 ml (range 0.5–5.95).

Twenty-seven sheep died before HF could be established (Fig. 1). Their baseline LVEF (59.1 ± 6.6%) did not differ from those who attained HF status. The total volume of the microsphere suspension injected in this group was a median of 0.8 ml (range 0.3–3.7 ml). The causes of death in these animals were as follows: ventricular fibrillation in 10 sheep, severe acute HF in 12 sheep, sudden cardiac death when not monitored in 3 sheep, and lung infection in 2 sheep. The 10 instances of witnessed ventricular fibrillation occurred intraoperatively shortly after microsphere injection, whereas most of the fatal acute HF episodes (8 of 12) occurred postoperatively (>24 h after surgery). The latter subgroup may represent animals with severe HF who died before hemodynamic confirmation of their status. In the other one-third of severe acute HF cases, the condition manifested within 24 h of microembolization, either at the induction of anesthesia or immediately after injection of microspheres. Three sheep died suddenly without a definitive diagnosis of cause of death; these were classified as "sudden cardiac death." Two other sheep died of postoperative pneumonia (4 and 16 days after surgery) resistant to antibiotic treatment.

Fifteen sheep in the HF group died prematurely before the projected 6-mo follow-up (Fig. 1). Ventricular fibrillation (4 intraoperative), acute HF (2 intraoperative and 1 immediate postoperative), high-grade intraoperative atrioventricular conduction block in 2, and postoperative sudden cardiac death in 2 were the causes of mortality. Conditions such as loss of appetite (2 animals), respiratory obstruction (1 animal), and bad general condition (1 animal) were other causes of death.

The success rate of HF induction increased with experience (Fig. 2*C*). Animals dying before HF establishment were noted to have higher LVEDP during the last procedure (18 ± 6 mmHg, $n = 21$) compared with those that achieved HF status (15 ± 6 mmHg, $n = 38$, $P < 0.05$).

Table 1. *Time course of echocardiographic findings in heart failure sheep*

	Baseline	Heart failure		
		Establishment	3 mo	6 mo
LVEDV, ml	82±24 (38)	143±36* (38)	137±30* (18)	127±24* (21)
LVW, cm	0.8 (0.7–0.9) (37)	0.6 (0.5–0.8)* (38)	0.7 (0.6–0.7)* (17)	0.6 (0.6–0.8)* (21)
IVS, cm	0.9±0.2 (37)	0.7±0.1* (38)	0.7±0.2* (17)	0.7±0.2* (21)
LVEDID, cm	4.3±0.6 (37)	5.6±0.6* (38)	5.5±0.6* (17)	5.6±0.5* (21)
LVEDW stress, dyn·cm^{-2}·10^3	14.6±10.6 (35)	56.4±26.8* (38)	55.3±26.9* (17)	55.7±41.4* (21)

Values are means ± SD; nos. in parentheses are nos. of sheep. LVEDV, left ventricular (LV) end-diastolic volume; LVW, LV free wall thickness (data are expressed as medians with nos. in parentheses as percentiles); IVS, interventricular septum thickness; LVEDID, LV end-diastolic internal diameter; LVEDW stress, LV end-diastolic wall stress. Kruskal-Wallis one-way analysis of variance on ranks was used for statistical analysis, followed by Dunn's test. *$P < 0.05$ compared with baseline.

Hemodynamic and neurohumoral changes. With the establishment of HF, LVEDP had doubled from baseline (Table 2). This change was maintained to 6 mo, although a trend for LVEDP to decrease was observed. In HF sheep, the cardiac index was reduced by 16% and stroke volume by 20%, and no improvement occurred during the entire 6-mo period. Myocardial contractile function was compromised in the HF animals (Fig. 3), as shown both by load-independent indexes such as E_{es} (40% decrease) and PRSW (49% decrease) and also by the load-dependent index LV dP/dt_{max} (35% decrease). The compromised contractile function showed no improvement with time. LV diastolic function also deteriorated, as indicated by a 41% increase in τ and a 40% decrease of LV dP/dt_{min}. These changes were maintained over the study period. The HR under anesthesia was no different after the onset of HF. The early decrease of LV systolic pressure at the time of HF establishment was subsequently largely reversed.

After dobutamine infusion, when the HR had reached 140 beats/min, the LV P-V relationship was again established and E_{es} was analyzed. Dobutamine increased E_{es} significantly in both baseline and HF conditions. However, in HF animals, the E_{es} resulting from dobutamine stimulation did not exceed the original unstimulated E_{es} value (Figs. 3 and 4*A*).

PE of the LV increased slightly but not significantly after HF had been established (from 2,434 ± 913 to 3,184 ± 920, 2,976 ± 1,441, and 2,972 ± 746 mmHg·ml at 0, 3, and 6 mo, respectively). The work efficiency (EW/P-V area) of the failing heart was significantly decreased at each of the time points studied (Fig. 4*B*).

Figure 5 shows neurohumoral changes in response to HF and their progress over the next 6 mo. ANP was significantly increased by HF and remained so for the 6-mo observational period. When ANP levels were matched with right atrial pressure over the 6 mo, a significant correlation was observed (Fig. 6). Plasma aldosterone levels, on the other hand, rose sharply but returned to normal by 6 mo. The increase in PRA was even more short lived, showing only a remaining trend toward increase at 3 mo ($P = 0.08$). Plasma angiotensin II was not changed.

Myocardial collagen changes. The total collagen content of the LV in HF animals was increased by 170%, whereas that in the RV remained unchanged (Fig. 7*A*). Analysis of the collagen subtypes showed a twofold increase in the type I-to-type III collagen ratio in HF sheep, again confined to the LV (Fig. 7*B*). An inverse relationship between LV total collagen content and LVEF was established (Fig. 7*C*).

Expression of FasL and expression and activities of caspases-8, -3, and -2. A close relationship was found between myocardial FasL expression, the ligand that couples to Fas, the death receptor, and caspases-3 and -2, which together with other members of this group are held to be responsible for the execution of apoptosis (Fig. 8*A*). A close relationship was also seen between the activities of the upstream protease caspase-8 (a member of the group 2 caspases responsible for the initiation of apoptosis) and caspase-3 (Fig. 8*B*) and between level of caspase-3 expression and LV wall stress (Fig. 8*C*).

DISCUSSION

A chronic ischemic model of HF. Understanding cardiorenal, hemodynamic, and neurohormonal derangements in HF has provided substantial benefits (17, 20), but emphasis has shifted to remodelling and the role played by stretch-activated pathways, cytokine activation, and changes in cardiomyocytes and the extracellular matrix (8, 12, 31). A realistic animal model of chronic HF can provide insights into this complex interplay of factors. Our ovine model uses stepwise selective coronary microembolization and has hallmarks of the most common type of severe HF in humans (14). It results in LV dilatation, deterioration of systolic and diastolic function, changes in fibrillar collagen, and neurohumoral activation. It shows increased wall stress, enhanced cytokine activity, and activation of the caspase pathway with a possible effect on apoptosis. We report on 21 untreated sheep followed for 6 mo with severe HF.

HF is a major cause of morbidity, mortality, and expenditure (30). After the initial pathological insult, there is neurohumoral activation and remodeling of the LV, including changes in interstitial collagen and continued loss of myocytes (20). Therefore, a model that traces this path aids in the understanding of pathophysiology and development of new treatment strategies.

Table 2. *Time course of hemodynamic changes*

		Heart failure		
	Baseline	Establishment	3 mo	6 mo
LVEDP, mmHg	7.2±3.9 (38)	15.4±5.8* (38)	13.2±5.6* (20)	12.6±6.5* (21)
LVESP, mmHg	91.6±15.9 (37)	78.4±12.4* (36)	83.7±13.4 (19)	83.8±12.7 (20)
LV E_{es}, mmHg/ml	2.17±0.77 (13)	1.31±0.28* (13)	1.47±0.4* (12)	1.42±0.38* (13)
LV PRSW, mmHg	74.4±28.8 (13)	38.1±13.3* (15)	47.7±17.3* (13)	47.4±15.8* (13)
LV dP/dt_{max}, mmHg/s	1,278±346 (37)	829±242* (36)	820±177* (19)	830±268* (21)
LV dP/dt_{min}, mmHg/s	1,815±447 (37)	1,062±264* (36)	1,255±281* (19)	1,215±328* (21)
CI, $l \cdot m^{-2} \cdot min^{-1}$	3.23±0.67 (25)	2.63±0.76* (25)	2.7±0.51* (19)	2.70±0.52* (20)
SV, ml	77.5±17 (25)	62.7±15.4* (25)	63.8±14.3* (19)	62.1±13.2* (20)
HR, beats/min	97±12 (25)	94±12 (25)	97±11 (19)	100±17 (20)
τ, ms	27±7 (13)	38±7 (13)*	37±5 (13)*	37±9 (13)*
RAP, mmHg	3±4.6 (19)	6.1±4.1 (21)	6.8±3* (18)	8.1±4.3* (19)
PulVR, $dyn \cdot s \cdot cm^{-5}$	887±279 (17)	980±272 (22)	971±258 (18)	885±174 (18)

Values are means ± SD; nos. in parentheses are nos. of sheep. LVEDP and LVESP, LV end-diastolic and end-systolic pressure; LV E_{es}, LV end-systolic elastance; LV PRSW, LV preload recruitable stroke work; LV dP/dt_{max} and LV dP/dt_{min}, first derivatives of LV pressure rise and decay; CI, cardiac index; SV, stroke volume; HR, heart rate; τ, time constant of LV pressure decay; RAP, right atrial pressure; PulVR, pulmonary vascular resistance. *$P < 0.05$ compared with baseline.

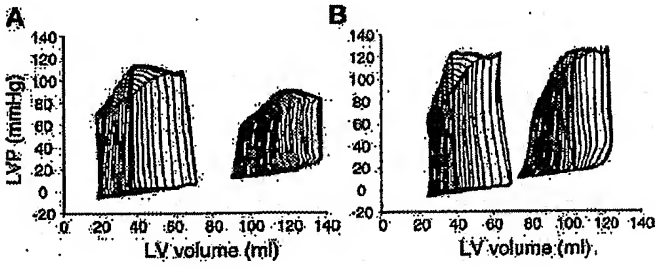

Fig. 3. Representative LV pressure-volume (LVP) loops of a sheep in response to a transient reduction of preload resulting from brief inferior vena cava occlusion. *A*: establishment of HF caused a marked rise in heart volume and end-diastolic pressure and a decrease in EF and end-systolic pressure. LV end-systolic elastance (E_{es}) decreased from 2.1 to 1.3. *B*: dobutamine increased baseline LV E_{es} to 4.3. However, when the failing heart was dobutamine stimulated, its LV E_{es} approached only the baseline nonstimulated level (1.7), indicative of a decrease in the contractile reserve. Note that the data shown here should be seen in the context of data displayed in Fig. 1 and Tables 1 and 2.

The sheep in this study demonstrated a persistent decrease of stroke volume (20%) and the cardiac index (16%) (Table 2), a characteristic not consistently reproduced by coronary ligation or single microembolization. There was also LV dilatation, global impairment of wall movement, and thinning of the LV wall (Table 1). LVEF remained below 30% during the study (Fig. 2*B*). Our previous work suggests that these changes result from myocyte loss due to necrosis, possible myocyte slippage (14, 41), and ongoing apoptosis (15). There was also evidence of myocyte hypertrophy (14) and localization of FasL to the intercalated discs, where adjacent cardiomyocytes transmit mechanical stress. These "compensatory" changes are detrimental, causing increasing myocardial oxygen consumption and reduced energy efficiency (35). Our findings also suggest that increased wall stress may activate the apoptosis signaling

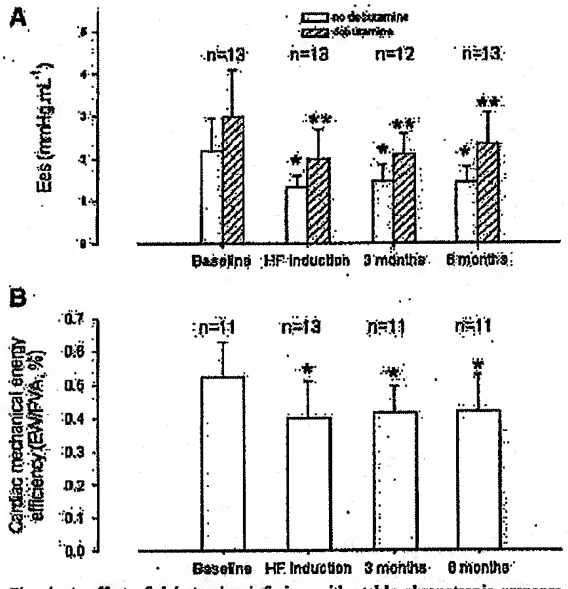

Fig. 4. *A*: effect of dobutamine infusion with stable chronotropic response (heart rate of 140 beats/min) on LV E_{es} in the normal and the microembolized failing heart at various time points. *$P < 0.05$ comparing with and without dobutamine; **$P < 0.05$ compared with dobutamine baseline. *B*: effect of microembolization-induced HF on mechanical energy efficiency over 6 mo. EW, external work; PVA, pressure-volume area. *$P < 0.05$ compared with baseline. *n*, No. of animals.

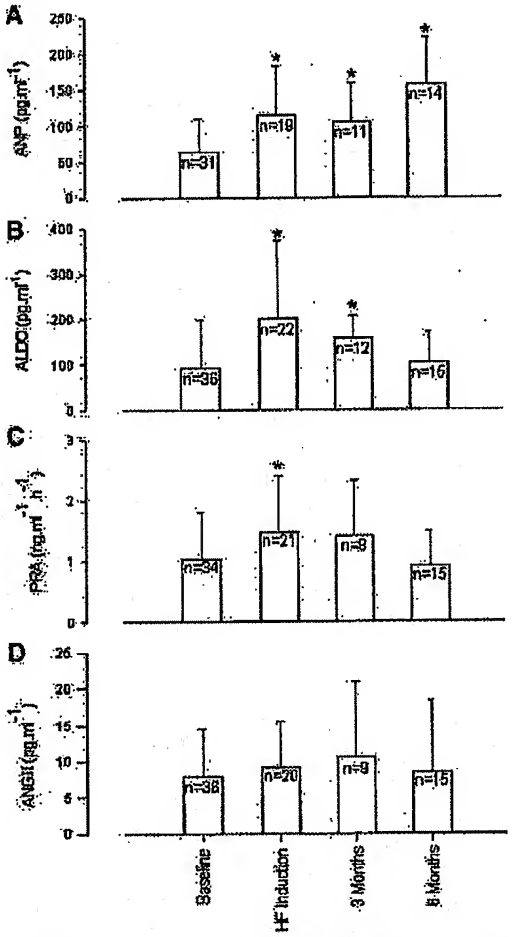

Fig. 5. Plasma neurohumoral changes at various times after the establishment of HF. *A*: atrial natriuretic peptide (ANP); *B*: aldosterone (Aldo); *C*: plasma renin activity (PRA); *D*: ANG II. * $P < 0.05$ compared with baseline. *n*, No. of animals.

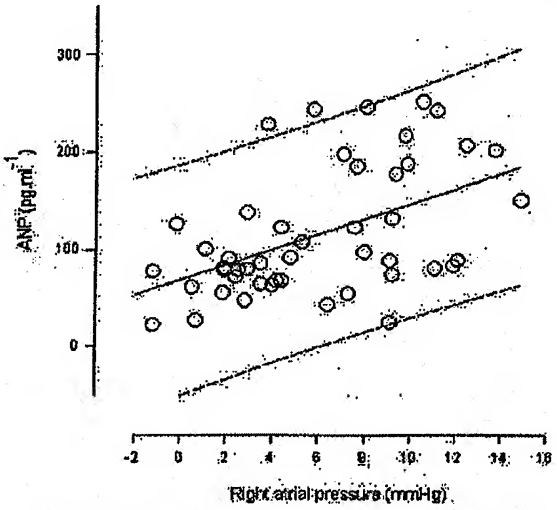

Fig. 6. Relationship between right atrial pressure (RAP) and plasma ANP levels over 6 mo after HF induction (ANP = 68.5 + 7.76 × RAP, $r^2 = 0.504$, $P < 0.01$).

cascade involving the interaction of the FasL/FasL complex with procaspase-8 (15, 37). The lack of deterioration in the majority of our untreated sheep lends support to the heart's potential for myocyte regeneration (2). However, the early deaths suggest that the capacity for remodeling and cellular regeneration may vary.

We measured wall stress rather than myocyte stretch but consider them to be interchangeable with respect to cellular responses. In vivo wall stress may have advantages because it integrates the extracellular matrix with the cytoskeleton via integrins, which are believed to be important stretch mediators (8).

Sheep have advantages over dogs, which have an extensive coronary collateral supply and much faster HRs than humans. Our HF model also contrasts with those involving large myocardial infarcts by producing numerous tiny infarcted and peri-infarct zones leading to relatively homogeneous wall stretch.

ANP peaked after 6 mo, whereas aldosterone and plasma renin activity (but not angiotensin II) showed an early rise before declining. This raises the possibility of varied time courses of response of different stretch-sensitive mediators or, alternatively, variation from the extent and homogeneity of stretch distribution. Alternatively, the stretch response in the architecturally complex myocardium may be directionally sensitive, exerting a favorable influence on gene reprogramming.

This study is the first to effectively characterize LV contractility in large animals with chronic, untreated, severe HF and shows significant impairment of native contractility (LV E_{es} and LV PRSW) and contractile reserve (Table 2). Previously abnormalities of the cardiac force-frequency relationship and response to exogenous β-adrenergic stimulation were demonstrated in patients and experimental animals with HF (27, 42). We achieved a constant HR of 140 beats/min with dobutamine to exclude the Bowditch phenomenon and found increased LV E_{es} in the normal but not failing heart (Fig. 4*A*). This is consistent with a disordered sympathetic drive resulting from reduced cardiomyocyte adenylate cyclase activity (22) and downregulation of adrenergic receptors (3, 10).

Myocardial energy efficiency (EW/P-V area) decreased with chronic HF, indicative of an energy-wasting state (Fig. 4*B*). In contrast, in a canine model of ischemic HF, it did not change (37).

Plasma ANP levels peaked at 6 mo (Fig. 5), indicative of a continued rise in wall stretch (Fig. 6). On the other hand, PRA and aldosterone rose when HF was established and then declined. However, no increase of plasma angiotensin II was observed, in contrast to a recent coronary ligation model of HF (29).

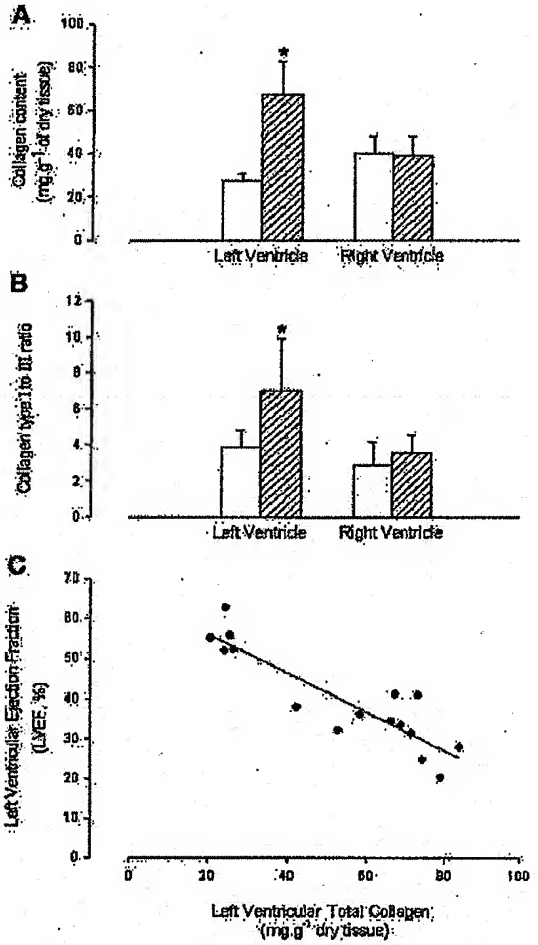

Fig. 7. Changes in myocardial collagen content (*A*) and phenotype ratio (*B*) in normal sheep ($n = 5$; open bars) and 6-mo post-HF sheep ($n = 11$; hatched bars). *$P < 0.05$ compared with normal control. *C*: relationship between LV myocardial collagen content and LVEF. $r^2 = 0.79$, $P < 0.0001$.

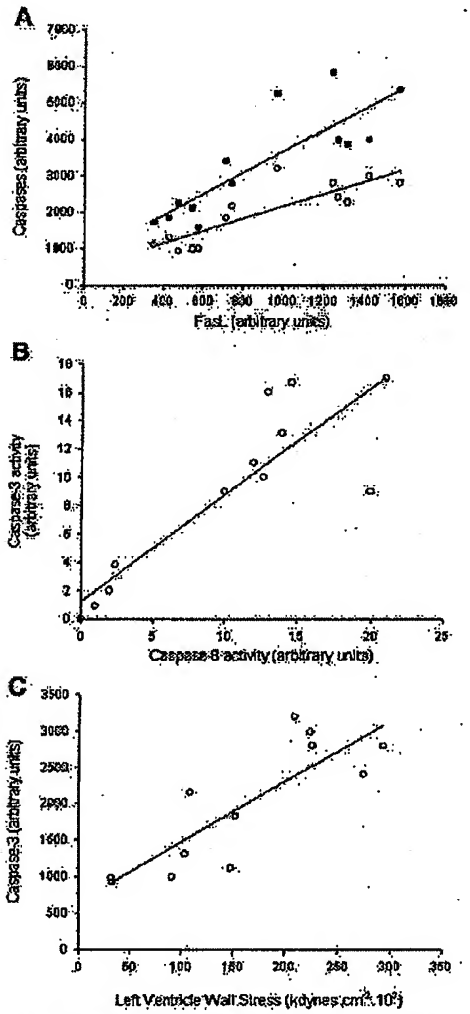

Fig. 8. Interrelationships between expression and activity of different myocardial caspases, LV wall stress, and Fas ligand (FasL) levels. *A*: the levels of protein expression of both caspase-2 (○) and caspase-3 (●) are correlated with the cytokine FasL expression (caspase-2 = 2.9 × FasL + 764, r^2 = 0.84; caspase-3 = 0.93 × FasL − 155, r^2 = 0.77; n = 8 sheep and n = 32 samples). *B*: activity of the upstream caspase-8, initiator of the apoptotic "death cascade," is proportionally related to the activity of the downstream executor caspase-3 (caspase-3 activity = 1.221 + 0.755 × caspase-8, r^2 = 0.78, n = 8 sheep and n = 32 samples). *C*: caspase-3 expression shows a linear correspondence with LV wall stress (caspase-3 = 8.3 × LV wall stress + 650, r^2 = 0.84, n = 7 sheep and n = 28 samples).

Changes in the extracellular matrix (the "myocardial skeleton") are important to the pathophysiological processes that drive the development of HF (25, 28, 39). Matrix metalloproteinases (MMPs) and their tissue inhibitors are differential expressed in the failing hearts of humans and pigs, in a pattern favoring matrix degradation and turnover (34, 39). We previously reported replacement as well as interstitial fibrosis in this model (14) and now confirm that both content and phenotype of myocardial fibrillar collagen remain altered over 6 mo, with a more stiff type I phenotype (Fig. 7). As collagen content increased, both systolic (LVEF) and diastolic (τ and LV dP/dt_{min}) LV function deteriorated.

Neurohumoral activation causes cardiac dilatation and ECM remodeling with increased collagen turnover and breakdown of the normal collagen network (21, 26). Such disruption may result from catecholamine and aldosterone triggered transcription of mRNAs for MMPs. Dispersed interstitial fibrosis can also result from enhanced angiotensin II activity, which is the basis of some of the beneficial effect of HF treatment with angiotensin-converting enzyme (ACE) inhibitors, and β-adrenergic and aldosterone antagonists. Such treatment has demonstrated a protective effect in those with LV dysfunction even before heart failure supervenes (6).

This sheep model has the advantage of a clear ischemic etiology that is common in humans, although there is no occlusion of the principal coronary trunks. The sheep's size makes it suitable for multiple diagnostic and therapeutic strategies, and it has consistent coronary anatomy, with the left coronary artery and coronary sinus responsible for over 90% of LV blood supply and drainage. Also, similar to humans, sheep have few collaterals, rendering the effect of embolization predictable and the study of LV myocardial metabolism more reliable than in dogs. The sheep did not require medication during the 6-mo observation and study, ensuring homogeneity and stability and allowing investigation of basic mechanisms and interventions.

Method of induction and natural history of HF. Despite diverse methods of inducing HF, such as coronary artery ligation, coronary embolization, fast ventricular pacing, and myocardial intoxication (7), only the first two mimic the most common human etiology. However, coronary ligation requires thoracotomy, produces ventricuar dysfunction that is segmental rather than global, and frequently causes mitral regurgitation. Also, the ventricular damage cannot be titrated.

Microsphere injection to induce heart attack in dogs has involved aortic root injection, selective coronary artery delivery, and refinement with repeated injections (32). There are no previous data on microsphere dose needed to induce stable, severe, chronic HF in sheep.

The only previous study of the longer-term hemodynamic and neurohumoral course of experimental severe HF in large animals is that of Sabbah et al. (32), who followed 15 dogs for an average of 3 mo (range 7–19 wk) after coronary embolizations. This corresponds to 2 mo after the establishment of stable HF in our sheep. Our study extends over a threefold longer period and also examines cardiac contractility and energetics. The extensive coronary collateral supply in dogs required greater doses of microspheres (~2 ml during each of the first 3 embolizations and 3–6 ml subsequently) compared with our total of 1.6 ml on average. The myocardial damage in our sheep appears similar (LVEF was 29% at the establishment of HF, corresponding to 26% in dogs 1 mo after the last embolization). However, whereas in sheep the LVEF remained stable over 6 mo, in dogs it continued to decline to 21% over 2 mo, although the fall in the cardiac index was identical. Contrary to expectation, LVEDV in dogs continued to increase on follow-up despite the extensive collateral supply, whereas

our sheep showed a peak increase of LVEDV by 75% at 1 mo, which declined to 55% at 6 mo. This finding may relate to the higher mortality in our sheep (59% of 65 sheep were induced into stable HF, of whom 55%, but only 32% of the original candidates, survived to 6 mo compared with the overall 30% mortality in dogs at 2 mo equivalent follow-up), due to earlier death in the more severely affected animals. One notable difference was the absence of mitral regurgitation in sheep, underscored by the absence of atrial fibrillation, whereas 26% of the dogs had this arrhythmia.

Stepwise coronary embolization causes repeated myocardial infarction and therefore poses a high mortality risk. Our experience shows that ventricular fibrillation and acute LV failure are major causes of mortality, accounting for 37% and 44%, respectively, of the deaths before stable, severe HF could be established. Reduction of intraoperative ventricular fibrillation was achieved by immediate correction of critical hypotension (blood pressure <60 mmHg systolic), administration of prophylactic lidocaine, and use of adequately mixed body temperature microsphere injectate. The quantity of beads injected in any one procedure was based on preoperative echocardiographic LV function and intraoperative arterial pressure and LVEDP. We found that intraoperative LVEDP, with a cutoff of 20 mmHg, was a reliable predictor of postoperative acute HF and the resulting mortality. The success rate of HF induction doubled and intraoperative procedural death declined threefold with the adoption of such precautions (Fig. 2*C*). Death among animals after HF establishment occurred mostly during anesthesia performed for hemodynamic assessment.

Potential shortcomings of this model. It is recognized that damage is confined to the LV myocardium in the sheep HF model described in the present study and that the model does not include disease of large coronary arteries, nor are the animals affected by concomitant disease. It is likely that early deaths occurred in animals with severe myocardial damage, and thus the surviving cohort was self-selected. In an earlier microscopic morphometric study (14), we showed good correlation between microsphere count and replacement fibrosis. Also, the diffuse, small microinfarctions make precise localization and study of the peri-infarct zones virtually impossible. However, the advantages of this model outweigh these shortcomings and allow the methodical pursuit of pathophysiological mechanisms and assessment of various treatment strategies.

In conclusion, the ovine HF model produced by stepped coronary embolization mimics severe HF in humans with respect to etiology, hemodynamics, and neurohumoral activation, histology, changes in the extracellular matrix, and ventricular remodeling. It provides insights into potentially damaging cytokine activation and the resulting cellular mechanisms of injury leading to apoptosis. It integrates knowledge of cellular processes with the hemodynamic and structural changes that express themselves in altered wall stress. The stable nature of the untreated HF is consistent with a delicate balance between apoptotic cardiomyocyte death, perhaps triggered by myocardial wall stress, and myocyte regenerative capacity coupled with other compensatory mechanisms. The model appears suitable for the investigation of HF, including its cellular and molecular basis, and for the development and testing of medical and surgical interventions.

ACKNOWLEDGMENTS

The authors acknowledge the contribution of Dr. Nasser Abdul-Hussein and the technical help of Chris Horam, Dr. Russell Carrington, Marie Pryor, Ray Kearns, Claire Phillips, Julie Hardy, and Gabrial Gomes.

GRANTS

This work was supported by the Australian Government's Cooperative Research Centres (CRC) Scheme (CRC for Cardiac Technology), the National Heart Foundation (Australia), and the North Shore Heart Research Foundation.

REFERENCES

1. **Baan J, van der Velde ET, de Bruin HG, Smeenk GJ, Koops J, van Dijk AD, Temmerman D, and Senden J.** Continuous measurement of left ventricular volume in animals and humans by conductance catheter. *Circulation* 70: 812–823, 1984.
2. **Beltrami AP, Urbanek K, Kajstura J, Yan SM, Finato N, Bussani R, Nadal-Ginard B, Silvestri F, Leri A, Beltrami CA, and Anversa P.** Evidence that human cardiac myocytes divide after myocardial infarction. *N Engl J Med* 344: 1750–1757, 2001.
3. **Bristow MR.** Changes in myocardial and vascular receptors in heart failure. *J Am Coll Cardiol* 22, *Suppl* A: 61A–71A, 1993.
4. **Charles CJ, Espiner EA, Cameron VA, and Richards AM.** Hemodynamic, renal, and endocrine actions of ANF in sheep: effect of 24-h, low-dose infusions. *Am J Physiol Regul Integr Comp Physiol* 258: R1279–R1285, 1990.
5. **Chiariello M, Ambrosio G, Cappelli-Bigazzi M, Perrone-Folardi F, Brigante F, and Sifola C.** A biochemical method for the quantitation of myocardial scarring after experimental coronary artery occlusion. *J Mol Cell Cardiol* 18: 283–290, 1986.
6. **Doughty RN, Whalley GA, Gamble G, MacMahon S, and Sharpe N.** Left ventricular remodeling with Carvedilol in patients with congestive heart failure due to ischemic heart disease. *J Am Coll Cardiol* 29: 1060–1066, 1997.
7. **Einstein R and Abdul-Hussein N.** Animal models of heart failure for pharmacological studies. *Clin Exp Pharmacol Physiol* 22: 864–868, 1995.
8. **Force T, Michael A, Kiloter H, and Haq S.** Stretch-activated pathways and left ventricular remodelling. *J Card Fail* 8, *Suppl*: 8351–8358, 2002.
9. **Gheorghiade M and Bonow RO.** Chronic heart failure in the United States: a manifestation of coronary artery disease. *Circulation* 97: 282–289, 1998.
10. **Gilson N, Bouanani NEH, Corsin A, and Crozatier B.** Left ventricular function and β-adrenoceptors in rabbit failing heart. *Am J Physiol Heart Circ Physiol* 258: H634–H641, 1990.
11. **Hartman JC, Kampine JP, Schmeling WT, and Warltier DC.** Alterations in collateral blood flow produced by isoflurane in a chronically instrumented canine model of multivessel coronary artery disease. *Anesthesiology* 74: 120–133, 1991.
12. **Hu H and Sachs F.** Stretch-activated ion channels in the heart. *J Mol Cell Cardiol* 29: 1511–1523, 1997.
13. **Huang Y, Kawaguchi O, Zeng B, Carrington RAJ, Horam CJ, Yunsa T, Abdul-Hussein N, and Hunyor SN.** A stable ovine congestive heart failure model–a suitable substrate for left ventricular assist device assessment. *ASAIO J* 43: M408–M413, 1997.
14. **Ikeda Y, Yutani C, Huang Y, Masuda K, Yuasa T, Kawaguchi O, and Hunyor SN.** Histological remodeling in an ovine heart failure model resembles human ischemic cardiomyopathy. *Cardiovasc Pathol* 10: 19–27, 2001.
15. **Jiang L, Huang Y, Hunyor S, and dos Remedios C.** Cardiomyocyte apoptosis is associated with increased wall stress in chronic failing left ventricle. *Eur Heart J* 24: 742–751, 2003.
16. **Jiang L, Huang Y, Yuasa T, Hunyor S, and dos Remedios CG.** Elevated DNase activity and caspase expression in association with apoptosis in failing sheep left ventricles. *Electrophoresis* 20: 2046–2052, 1999.
17. **Katz AM.** *Heart Failure: Pathophysiology, Molecular Biology and Clinical Management.* Philadelphia, PA: Lippincott, Williams and Wilkins, 2000, p. 1–32.
18. **Kawaguchi O, Huang YF, Yuasa T, Shirota K, Carrington RAJ, and Hunyor SN.** Cardiomyoplasty reduces myocardial oxygen consumption: implications for direct mechanical assist. *Ann Thorac Surg* 74: 1092–1096, 2002.
19. **Little WC and Braunwald E.** Assessment of cardiac function. In: *Heart Disease: a Textbook of Cardiovascular Medicine* (5th ed.), edited by Braunwald E. Philadelphia, PA: Saunders, 1997, p. 421–444.

20. **Mann DL.** Mechanisms and models in heart failure, a combinatorial approach. *Circulation* 100: 999–1008, 1999.
21. **Mann DL and Spinale FG.** Activation of matrix metalloproteinases in the failing human heart. *Circulation* 98: 1699–1702, 1998.
22. **Matzo KP, Frey MJ, Wilson JR, Liang BT, Manning DR, Lanoce V, and Molinoff PB.** Beta-adrenergic receptor G-protein-adenylate cyclase complex in experimental canine congestive heart failure produced by rapid ventricular pacing. *Circ Res* 69: 1546–1556, 1991.
23. **Medugorac I and Jacob R.** Characterization of left ventricular collagen in the rat. *Cardiovasc Res* 17: 15–21, 1983.
24. **Mirsky I.** Assessment of diastolic function: suggested methods and future considerations. *Circulation* 69: 836–841, 1984.
25. **Mukherjee D and Sen S.** Alteration of collagen phenotypes in ischemic cardiomyopathy. *J Clin Invest* 88: 1141–1146, 1991.
26. **Nagase H.** Activational mechanisms of matrix metalloproteinases. *J Biol Chem* 378: 151–160, 1997.
27. **Opie LH.** Mechanisms of cardiac contraction and relaxation. In: *Heart Disease: a Textbook of Cardiovascular Medicine* (5th ed.), edited by Braunwald E. Philadelphia, PA: Saunders, 1997, p. 360–393.
28. **Pauschinger M, Doerner A, Tannhauser R, Kuhl U, and Schultheiss HP.** Differential myocardial abundance of collagen type I and type III mRNA in dilated cardiomyopathy: effects of myocardial inflammation. *Cardiovasc Res* 37: 123–129, 1998.
29. **Rademaker MT, Cameron VA, Charles CJ, Espiner EA, Nicholls MG, Pemberton CJ, and Richards AM.** Neurohormones in an ovine model of compensated postinfarction left ventricular dysfunction. *Am J Physiol Heart Circ Physiol* 278: H731–H740, 2000.
30. **Reinlib L, Goldman S, and Horan MJ.** Finding tools for fighting heart failure. *Congestive Heart Failure* 3: 34–38, 1997.
31. **Ruwhof C and van der Laarse A.** Mechanical stress-induced cardiac hypertrophy: mechanisms and signal transduction pathways. *Cardiovasc Res* 47: 23–37, 2000.
32. **Sabbah HN, Stein PD, Kono T, Gheorghiade M, Levine TB, Jafri S, Hawkins ET, and Goldstein S.** A canine model of chronic heart failure produced by multiple sequential coronary microembolizations. *Am J Physiol Heart Circ Physiol* 260: H1379–H1384, 1991.
33. **Shirota K, Huang Y, Kawaguchi O, Yuasa T, Carrington RI Brady PW, Ueda Y, and Hunyor SN.** Functional recovery of the native heart after cardiomyoplasty in heart failure sheep: passive and dynamic effects of volume loading. *Ann Thorac Surg* 73: 849–854, 2002.
34. **Spinale FG, Coker ML, Thomas CV, Walker JD, Mukherjee R, and Hebbar L.** Time-dependent changes in matrix metalloproteinase activity and expression during the progression of congestive heart failure: relation to ventricular and myocyte function. *Circ Res* 82: 482–495, 1998.
35. **Suga H.** Ventricular energetics. *Physiol Rev* 70: 247–277, 1990.
36. **Sykes B, Puddle B, Francis M, and Smith R.** The estimation of two collagens from human dermis by interrupted gel electrophoresis. *Biochem Biophys Res Commun* 72: 1472–1480, 1976.
37. **Thornberry NA.** The caspase family of cysteine proteases. *Br Med Bull* 53: 478–490, 1997.
38. **Todaka K, Leibowitz D, Homma S, Fisher PE, Derosa C, Stennett R, Packer M, and Burkhoff D.** Characterizing ventricular mechanics and energetics following repeated coronary microembolization. *Am J Physiol Heart Circ Physiol* 272: H186–H194, 1997.
39. **Tyagi SC.** Proteinases and myocardial extracellular matrix turnover. *Mol Cell Biochem* 168: 1–12, 1997.
40. **Weber KT, Malinin TI, Dennison BH, Faqua JM, Speaker DM, and Hastings FW.** Experimental myocardial ischemia and infarction. *Am J Cardiol* 29: 793–802, 1972.
41. **Weisman HF, Bush DE, Mannisi JA, Weisfeldt ML, and Healy B.** Cellular mechanisms of myocardial infarct expansion. *Circulation* 78: 186–201, 1988.
42. **Wolff MR, de Tombe PP, Harasawa Y, Burkhoff D, Bier S, Hunter WC, Gerstenblith G, and Kass DA.** Alterations in left ventricular mechanics, energetics, and contractile reserve in experimental heart failure. *Circ Res* 70: 516–529, 1992.

or older subjects. These data suggest that vasoconstriction to the kidney occurs during tion of the otolith organs in young but not older humans. Together with our previous .we conclude that otolithic activation elicits a diverse patterning of sympathetic outflow results in heterogeneous vascular responses in humans and that these responses are attenuated in older humans.

rt Failure Remodeling/Mechanisms II

pecialty: Myocardial Ischemia/Function/Metabolism

day

t N Morial Convention Center, Hall I2

cts 959–968

959

sive Serial Quantification of Minimal Aortic Arch Cross-Sectional High-Resolution 3D-MRI After Transverse Aortic Banding in Mice: ternalization is a Major Source for Variability of the Hypertrophic se

ate, Jürgen E Schneider, Karen Hulbert, Michiel ten Hove, Paul J Cassidy, Kieran fan Neubauer; Univ of Oxford, Oxford, United Kingdom

aortic constriction (TAC) is increasingly used as a murine model of left ventricular y and failure, however, there is extensive variability in the hypertrophic response. We d that this may be due to variation in the minimal aortic arch cross-sectional area banding. Forty-three mice underwent TAC with a 7–0 polypropylene suture, of ere identified by echocardiography as resistant to heart failure, with initial left hypertrophy that halted or regressed over time. Seven of these were studied m and were found to have internalized the band resulting in alternative pathways for n a prospective study we followed 12 mice after TAC for 6 weeks. Using a new high D-MRI method we developed to measure CSA *in vivo*, 3/12 mice were found to gnificant increase of aortic CSA after initial successful banding (Table), which was tly confirmed by post mortem dissection. These mice had internalized the band ortic lumen and, by week 6, showed significantly less LV hypertrophy and better ction. Band internalization could be entirely prevented when two banding sutures d side-by-side (n=10). This is the first observation that a significant subset of owing TAC, bypass the stenosis resulting in partial regression of hypertrophy. As it how a particular genetic modification may affect band internalization, we suggest studies using TAC should quantify this phenomenon in each new mouse strain.

rameters

	After Banding				
	Day 2	Day 7	Day 14	Day 28	Day 42
	0.46±0.11	0.51±0.13	0.46±0.14	0.44±0.08	0.48±0.09
	0.31±0.15	0.56±0.14	0.55±0.13	0.87±0.37*	1.11±0.29*
	64±4	80±8	95±13	111±16	146±6
	73±6*	85±13	99±10	108±18	112±6*
	47±6	47±6	44±4	43±6	36±1
	41±5	45±4	49±7	51±7	54±9*

±SD. "Normal" refers to mice with normal band confirmed at post mortem (n=9); while band internalization (n=3). * P<0.05 versus normal band mice at the same time-point.

960

enase-1 is Cardioprotective In the Remodeled, Failing Heart

Ortines, Univ Med Ctrof Louisville and Louisville VAMC, Louisville, KY; Sanjay Med Ctrof Louisville, Louisville, KY; Jianzhu Luo, Univ Med Ctrof Louisville VAMC, Louisville, KY; Gregg Rokosh, Yu-Ting Xuan, Univ Med Ctrof Louisville, umanth D Prabhu; Univ Med Ctrof Louisville and Louisville VAMC, Louisville,

heme oxygenase-1 (HO-1) is an integral component of the cellular stress gh HO-1 induction is acutely cytoprotective, nothing is currently known athophysiologic role of HO-1 in the long-term myocardial remodeling eart failure (HF). We tested the hypothesis the HO-1 upregulation in the failing al adaptation that mitigates pathologic left ventricular (LV) remodeling. Large ced by permanent coronary ligation in wild-type (WT) mice (n = 22) and = 15). Sham operation was also performed in WT control mice (n = 10). uently followed for 4 weeks during the development of post-infarction LV ardiographic and morphometric analysis revealed that compared to WT had significant ($p < 0.05$) LV dilatation (end-diastolic diameter [EDD] 4.2 mm), LV systolic dysfunction (fractional area change[FAC] 33 $\pm$ 9 vs. 53 pertrophy (LV/body weight[BW] ratio 3.83 $\pm$ 0.38 vs. 3.38 $\pm$ 0.04). Western 2-fold increase in HO-1 abundance in WT HF ($p < 0.05$), without change soform HO-2. Immunostaining for protein-malondialdehyde(MDA) adducts 65 subunit of nuclear factor(NF)-kB revealed that immunoreactivity was and 3.7 fold, respectively, in WT HF hearts as compared to WT sham (p < eased oxidative stress and inflammatory activation. In comparison to WT rts demonstrated significant ($p < 0.05$) increases in: 1) LV dilatation (EDD systolic dysfunction, 2) LV hypertrophy (LV/BW ratio 4.34 $\pm$ 0.41, p < ess (2.8-fold greater protein MDA immunoreactivity), and 4) inflammation tivated NF-kB immunoreactivity). HO-1 HF mice also demonstrated a 44% reduction in survival at 4 weeks as compared to WT HF mice. We conclude: HO-1 upregulation in the failing heart serves as a cardioprotective mechanism that counteracts the detrimental process of LV remodeling, and reduces myocardial hypertrophy, oxidative stress, and inflammatory activation. Upregulation of HO-1 may represent an important therapeutic approach in chronic HF.

961

Vagal Nerve Stimulation and Acetylcholine Protect Cardiomyocytes from Acute Ischemia and Hypoxia through Non-Hypoxic Induction of Hypoxia-Inducible Factor-1α

Yoshihiko Kakinuma, Masanori Kuwabara, Yoshinori Doi, Motonori Ando, Takayuki Sato; Kochi Med Sch, Nankoku, Japan

Introduction: It has been reported that the electrical stimulation of the vagal efferent nerve has markedly improved survival of myocardial ischemia in experimental studies. However, a mechanism for the beneficial effect of vagal stimulation remains still unclear. In the present study, we examined the cellular mechanism via hypoxia-inducible factor (HIF)-1α, which is a master transcriptional factor responsible for regulating a line of genes supporting cell survival. **Methods:** To clarify the effect of vagal efferent stimulation on cardiomyocytes, we investigated the effect of the neurotransmitter ACh on HIF-1α induction using rat primary cultured cardiomyocytes and ventricular immortalized cardiomyocytes, H9c2 cells, under the normoxic and hypoxic conditions. We also examined the effect of vagal stimulation on HIF-1α induction in the ischemic rat heart. **Results:** ACh increased the protein level of HIF-1α in cultured cardiomyocytes and H9c2 cells through post-transcriptional regulation. It was identified by actinomycin D, which did not reduce the protein level of HIF-1α. ACh increased the phosphorylation of Akt, which is a kinase responsible for the signal of cell survival, and was inhibited by a PI3K inhibitor, wortmannin as well as a muscarinic receptor antagonist, atropine. Wortmannin also inhibited induction of HIF-1α by ACh. The 12-hour hypoxia-induced decrease in mitochondrial membrane potential was inhibited by ACh, and ACh also inhibited the activation of caspase-3 by hypoxia. It resulted in protection of cardiomyocytes from hypoxia, probably due to dual induction of HIF-1α through ACh and hypoxia. Finally, even in the whole heart it was revealed that induction of HIF-1α was elevated in the myocardial infracted heart with vagal nerve stimulation, and that the stimulation reduced the infarct-area compared to that of the non-stimulated infracted heart (31.5±4.6 % in vagal stimulation vs 40.9±2.5 % in non-stimulation, P<0.05). **Conclusions:** ACh, a neurotransmitter of the cardiac vagal efferent fibers, plays an important role in protecting cardiomyocytes during ischemia and hypoxia via the Akt-HIF-1α pathway with the direct action.

962

β-3 Adrenergic Signaling is Impaired in the *ob/ob* Mouse Model of Obesity

Lili A Barouch, Shakil A Khan, Kwang-Ho Lee, Shubha V Raju, Khalid M Minhas, Alexander C Phan, Dan E Berkowitz; Johns Hopkins Univ Sch of Med, Baltimore, MD

Background: The β3 adrenergic receptor (AR) negatively modulates β-adrenergic signaling in the heart and is dependent on leptin signaling for normal expression levels in adipose tissue. Furthermore, we have shown that the leptin signaling pathway possesses anti-hypertrophic properties in the heart. Accordingly, we tested the hypothesis that β3AR signaling is diminished in leptin-deficient *ob/ob* mice, and that β3AR deficiency leads to cardiac hypertrophy and heart failure. **Methods and Results:** We studied collagenase-digested isolated myocytes (n=1–3 hearts, 6–11 cells each) from WT, $\beta3^{-/-}$, and *ob/ob* mice with the β3-specific agonist BRL37344 (10^{-7}M). BRL produced dose-dependent inhibition of sarcomere shortening (-33±5%, P<0.05) and calcium transients (-17±3%, P<0.05) in WT myocytes. The inhibitory effect of BRL was completely abolished in sarcomere shortening of *ob/ob* myocytes, with a paradoxical increase in the calcium transient (+30±12%, P<0.05), consistent with impaired β3 signaling in *ob/ob*. As a control experiment, we confirmed the absence of BRL response in $\beta3^{-/-}$ myocytes (sarcomere shortening 0±8%; calcium transient +9±4%, P=NS for both). To determine the mechanism of decreased BRL response in *ob/ob*, we performed quantitative PCR, which showed a 1.6-fold downregulation in β3 mRNA expression in *ob/ob* (n=5) compared to control (n=6). Since we had previously observed left ventricular hypertrophy in *ob/ob* mice, we tested the prediction that β3 deficiency would result in age-related hypertrophy by performing echocardiography on young (n=4, 10 months old) and old (n=4, 21 months old) $\beta3^{-/-}$ mice. Old $\beta3^{-/-}$ animals had increased LV wall thickness (0.98±0.04 vs. 0.65±0.03mm, P<0.005) and LV mass (165±17 vs. 63±2mg, P<0.005), increased diastolic diameter (4.1±0.2 vs. 3.3±0.1mm, P<0.05), and decreased fractional shortening (34±3 vs. 46±1%, P<0.01) compared to young $\beta3^{-/-}$. **Conclusion:** These findings demonstrate crosstalk between the leptin and β3 signal transduction pathways in the maintenance of normal cardiac structure and function, and offer new insights into mechanisms for obesity-related LV hypertrophy and heart failure.

963

Genetic Disruption of Angiotensin II Type1a Receptor in Mice Attenuates Volume Overload Cardiomyopathy and Improves Survival in Chronic Aortic Regurgitation

Michio Nakanishi, Ichiro Kishimoto, Masaki Harada, Koichiro Kuwahara, Rika Kawakami, Yasuaki Nakagawa, Keiji Tanimoto, Shinji Yasuno, Satoru Usami, Hideyuki Kinoshita, Kazuwa Nakao; Kyoto Univ Grad Sch of Med, Kyoto, Japan

It is not established whether inhibition of the renin-angiotensin system (RAS) has a beneficial effect on the progression of cardiomyopathy or survival in isolated, chronic, severe aortic regurgitation (AR). To address this question, we produced AR by puncturing the aortic valve with a 1.4-French Millar pressure catheter inserted via the right carotid artery in angiotensin II type1a receptor knockout mice (KO, n=189) and wild-type mice (WT, n=120). Within 2 weeks after induction of AR, more than half of both genotypes died (WT 57.5%, KO 68.3%,

J Physiol 565.3 (2005) pp 815–825

The nitric oxide donor sodium nitroprusside stimulates the Na^+–K^+ pump in isolated rabbit cardiac myocytes

Maged William[1,2,3], Jimmy Vien[1], Elisha Hamilton[3], Alvaro Garcia[1], Henning Bundgaard[1], Ronald J. Clarke[4] and Helge H. Rasmussen[1,3]

[1]*Department of Cardiology, Royal North Shore Hospital, St Leonards, Sydney, NSW 2065, Australia*
[2]*Department of Cardiology, Gosford Hospital, Gosford, NSW 2250, Australia*
[3]*Department of Medicine, University of Sydney, NSW 2006, Australia*
[4]*School of Chemistry, University of Sydney, NSW 2006, Australia*

Nitric oxide (NO) affects the membrane Na^+–K^+ pump in a tissue-dependent manner. Stimulation of intrinsic pump activity, stimulation secondary to NO-induced Na^+ influx into cells or inhibition has been reported. We used the whole-cell patch clamp technique to measure electrogenic Na^+–K^+ pump current (I_p) in rabbit ventricular myocytes. Myocytes were voltage clamped with wide-tipped patch pipettes to achieve optimal perfusion of the intracellular compartment, and I_p was identified as the shift in holding current induced by 100 μM ouabain. The NO donor sodium nitroprusside (SNP) in concentrations of 1, 10, 50 or 100 μM induced a significant increase in I_p when the intracellular compartment was perfused with pipette solutions containing 10 mM Na^+, a concentration near physiological levels. SNP had no effect when the pump was near-maximally activated by 80 mM Na^+ in pipette solutions. Stimulation persisted in the absence of extracellular Na^+, indicating its independence of transmembrane Na^+ influx. The SNP-induced pump stimulation was abolished by inhibition of soluble guanylyl cyclase (sGC) with 1H-[1,2,4]oxadiazole[4,3-a]quinoxalin-1-one, by inhibition of protein kinase G (PKG) with KT-5823 or by inhibition of protein phosphatase with okadaic acid. Inclusion of the non-hydrolysable cGMP analogue 8*p*CPT-cGMP, activated recombinant PKG or the sGC-activator YC-1 in patch pipette filling solutions reproduced the SNP-induced pump stimulation. Pump stimulation induced by YC-1 was dependent on the Na^+ concentration but not the K^+ concentration in pipette filling solutions, suggesting an altered sensitivity of the Na^+–K^+ pump to intracellular Na^+.

(Resubmitted 10 March 2005; accepted 6 April 2005; first published online 7 April 2005)
Corresponding author H. H. Rasmussen: Department of Cardiology, Royal North Shore Hospital, St Leonards, NSW 2065, Australia. Email: helger@med.usyd.edu.au

The simple diatomic molecule nitric oxide (NO) participates in, or modulates, messenger pathways that regulate a variety of cellular functions in all mammalian organs. Its production is mediated by NO synthase (NOS) within endothelial and parenchymal cells. NO may also be supplied exogenously by pharmacological donors frequently used in the treatment of cardiovascular diseases. In cardiac myocytes, NO has a prominent role in the regulation of Ca^{2+} handling. It modifies Ca^{2+} influx via L-type sarcolemmal Ca^{2+} channels, it regulates the sarcoplasmic reticulum (SR) Ca^{2+} release channel and it may inhibit Ca^{2+}-ATPase-mediated SR reuptake of Ca^{2+} (Hare, 2003). Since sarcolemmal Na^+–Ca^{2+} exchange is a key determinant of cardiac myocyte Ca^{2+} content, an effect of NO on the sarcolemmal Na^+–K^+ pump ultimately should affect Ca^{2+} handling because the pump maintains the electrochemical gradient for Na^+. Previous studies in various non-cardiac tissues have reported that NO does regulate the Na^+–K^+ pump. However, results are conflicting.

Na^+–K^+ ATPase activity in isolated membrane fragments, measured with saturating ligand concentrations, was reduced after exposure of opossum kidney cells to the NO donor sodium nitroprusside (SNP; Liang & Knox, 2000). Sodium nitroprusside and other NO donors induced similar inhibition of Na^+–K^+ ATPase activity in permeabilized tissue slices from the renal medulla (McKee *et al.* 1994), choroid plexus (Ellis *et al.* 2000) and ciliary processes (Ellis *et al.* 2001). However, the NO donor spermine NONOate, had no effect on Na^+–K^+ pump activity in the thick ascending limb from rat kidney. Activity was measured at high saturating or physiological

DOI: 10.1113/jphysiol.2005.086447

rate-limiting levels of intracellular Na^+ (Ortiz *et al.* 2001). Varela *et al.* (2004) reported that an inhibitory effect of NO donors on the pump activity in the thick ascending limb is time dependent. SNP induced Na^+–K^+ pump stimulation in rabbit aorta (Gupta *et al.* 1994) and human corpus cavernosum smooth muscle (Gupta *et al.* 1995). Pump stimulation in the aorta was thought to be secondary to Na^+–H^+ exchange-mediated influx of Na^+ and an increase in its intracellular concentration. The mechanism for stimulation in corpus cavernosum smooth muscle was not determined.

Tissue-specific differences in Na^+–K^+ pump regulation, differences in methodology used to study the Na^+–K^+ pump and variable delivery of NO and its bioactive derivatives by the donor compounds may have contributed to the conflicting results between studies. We have used the whole-cell patch clamp technique to examine the effect of NO on the sarcolemmal Na^+–K^+ pump in isolated rabbit ventricular myocytes. Provided wide-tipped patch pipettes are used, the technique allows control of the ligands of the Na^+–K^+ pump at intra- and extracellular sites and control of membrane voltage. It also allows the intracellular delivery of membrane-impermeable drugs and compounds dissolved in patch pipette solutions, including compounds of large molecular size. Electrogenic Na^+–K^+ pump current (I_p), arising from the $3Na^+$:$2K^+$ exchange ratio, can be identified as the shift in holding current induced by blocking the pump with ouabain. We show that SNP induces an increase in I_p. To further characterize the mechanism, we examine the dependence of Na^+–K^+ pump stimulation on intracellular Na^+ and K^+. To avoid non-specific effects of pharmacological NO donors in these studies, we used the synthetic benzyl indazole derivative YC-1 (Russwurm & Koesling, 2002) to selectively activate soluble guanylyl cyclase (sGC), a downstream target molecule for NO.

Methods

Cells

Single ventricular myocytes isolated from male New Zealand White rabbits were used. The rabbits, weighing 2.8–3.5 kg, were anaesthetized with 50 mg kg^{-1} ketamine and 20 mg kg^{-1} xylazine hydrochloride given intramuscularly. The heart was excised when deep anaesthesia was assured as indicated by the absence of a corneal reflex and response to deep pressure between the metatarsal bones. Details of techniques used to isolate ventricular myocytes have been previously described (Hool *et al.* 1995). The institutional review committee for animal research had approved experimental protocols. The myocytes were used on the day of isolation only. They were stored at room temperature in Krebs–Henseleit buffer solution until used for patch-clamp studies.

Solutions

Myocytes were suspended in a tissue bath mounted on an inverted microscope for experimentation. While we established the whole-cell configuration, the bath was perfused with modified Tyrode solution, which contained (mM): NaCl, 140; KCl, 5.6; $CaCl_2$, 2.16; $MgCl_2$, 1; glucose, 10; NaH_2PO_4, 1; sodium glutamate, 9; and Hepes, 10. It was titrated to a pH of 7.40 ± 0.01 at 35°C with NaOH. For measurement of I_p, we switched to a superfusate that usually was identical except that it was nominally Ca^{2+} free and contained 0.2 mM $CdCl_2$ and 2 mM $BaCl_2$. In some experiments we modified this solution by replacing Na^+-containing compounds with *N*-methyl-D-glucamine chloride (NMG-Cl; Hansen *et al.* 2000). The K^+ concentration in the superfusate was 5.6 mM in all experiments unless otherwise indicated.

For most experiments, wide-tipped patch pipettes (4–5 μm diameter) were filled with solutions containing (mM): Hepes, 5; MgATP, 2; EGTA, 5; potassium glutamate, 0–140; and sodium glutamate, 10. Osmotic balance was maintained with 150–10 mM tetramethylammonium chloride (TMA-Cl). We eliminated Na^+-containing compounds in pipette solutions in some experiments (replaced with TMA-Cl) while we increased the Na^+ concentration to 80 mM in others (osmotic balance was maintained by adjusting the concentration of TMA-Cl). The dependence of I_p on the intracellular Na^+ concentration in the absence of intracellular K^+ was examined using pipette solutions that included 0–80 mM sodium glutamate. The osmotic balance was maintained with TMA-Cl. All pipette solutions were titrated to a pH of 7.05 ± 0.01 at 35°C with 1 mM TMA-OH.

Wide-tipped patch pipettes were used to optimize control of the concentration of the intracellular ligands for the Na^+–K^+ pump. The patch pipettes had initial resistances of 0.8–1.1 MΩ when filling solutions included K^+ at the concentration of 70 mM used in most experiments. Results were independent of series resistance in the whole-cell configuration only if levels were ≤ 2.8 MΩ; the levels in accepted experiments ranged from 1.6 to 2.8 MΩ. Since K^+ has a higher conductivity than the other ions in pipette solutions (Hille, 1992) the series resistance was higher when we used K^+-free pipette filling solutions. Control of the concentration of intracellular pump ligands, as indicated by independence of the measured pump currents of the series resistance, was achieved at levels ≤ 4.0 MΩ.

I_p was identified at a holding potential of −40 mV as the difference between stable plateaus of holding current before and after Na^+–K^+ pump blockade with 100 μM ouabain. Na^+–K^+ pump inhibition is saturated when rabbit ventricular myocytes are exposed to ouabain at this concentration (Drewnowska & Baumgarten, 1991; Hool *et al.* 1995). A stable current plateau was identified when

no drift could be identified on the digital display of the voltage clamp amplifier for at least 50 s. The plateaus were defined by the means of 10 samples acquired with an electronic cursor at ~5 s intervals. Recordings were obtained using the continuous single-electrode mode of Axoclamp 2A or 2B amplifiers supported by AxoTape and pCLAMP software (Axon Instruments, Foster City, CA, USA). We report I_p normalized for membrane capacitance and hence cell size.

We used ouabain to inhibit the pump in this study because alternative, faster acting, cardiac steroids are less potent and would have to be used at a higher concentration to assure complete Na^+–K^+ pump inhibition. Any compound at a high concentration may have effects on non-pump membrane currents. We did not attempt to achieve wash-off of ouabain because, even when short-acting cardiac steroids are used, their effects on inotropy and intracellular Na^+ in cardiac tissue remain for > 30 min (Lee *et al.* 1980; Boyett *et al.* 1986). In agreement with this, Na^+–K^+ pump currents of ventricular myocytes (Mogul *et al.* 1990) do not return to control levels within a time frame that assures drift-free recordings.

Chemicals and reagents

TMA-Cl and NMG-Cl were purum grade and were obtained from Fluka Chemicals (Switzerland). All other chemicals used in Tyrode solutions were analytical grade and were obtained from BDH (Australia). Ouabain, SNP and bovine Cu,Zn superoxide dismutase were obtained from Sigma-Aldrich (St Louis, MO, USA) and YC-1, 1H-[1,2,4]Oxadiazole[4,3-a]quinoxalin-1-one (ODQ), KT-5823, okadaic acid, methyl okadaic acid, 8-*p*CPT-cGMP and recombinant bovine cGMP-activated protein kinase (PKG) were supplied by Calbiochem (La Jolla, CA, USA).

Statistical analysis

Results are expressed as means ± S.E.M. Student's *t* test for unpaired data is used for statistical comparisons. We used Dunnett's test when the same control group was used for more than one comparison and a Mann–Whitney rank sum test for unequal sample sizes when data could not be assumed to be normally distributed. $P < 0.05$ is regarded as significant in all comparisons.

Results

Effect of sodium nitroprusside on pump current

To examine whether the NO donor SNP has an effect on the Na^+–K^+ pump we measured I_p of control myocytes and of myocytes exposed to 50 μM SNP. Patch pipette solutions contained 10 mM Na^+, a concentration near physiological intracellular levels in rabbit ventricular myocytes (Hool *et al.* 1995). The concentration of K^+ in pipette solutions was 70 mM. The superfusate included 150 mM Na^+. We maintained control myocytes as well as myocytes exposed to SNP in the whole-cell configuration for 10–12 min before exposing them to ouabain. Figure 1*A* shows traces of holding currents recorded from a control myocyte and a myocyte exposed to SNP. Ouabain induced a larger shift in holding current of the myocyte exposed to SNP than of the control myocyte.

Additional experiments were performed to examine whether SNP induces an increase in I_p due to an increase in transsarcolemmal Na^+ influx. Such influx could cause secondary stimulation of the pump due to an increase in the intracellular Na^+ concentration. In one set of experiments we patch clamped myocytes using pipette filling solutions that were nominally Na^+ free. The superfusate contained Na^+. Figure 1*B* shows traces of holding currents of a control myocyte and of a myocyte exposed to SNP. Ouabain-induced shifts in holding currents were barely detectable for either myocyte. Similar results were obtained for two additional myocytes exposed to SNP. If SNP enhances transsarcolemmal Na^+ influx it does not cause an increase in the intracellular Na^+ concentration that can be detected as an increase in I_p.

To obtain independent support for the conclusion that the SNP-induced increase in Na^+–K^+ pump activity is not due to enhanced Na^+ influx we used patch pipette solutions that contained 10 mM Na^+ and a superfusate that was Na^+ free. This eliminates any possible SNP-induced Na^+ influx. Figure 1*C* shows holding currents of a control myocyte and of a myocyte exposed to SNP. Ouabain induced a

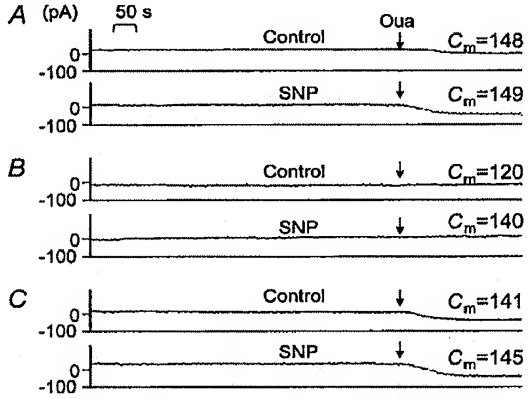

Figure 1. Sodium dependence of ouabain-induced shifts in holding currents
Patch pipette filling solutions and superfusates included 10 and 150 mM Na^+ for experiments shown in *A*, 0 and 150 mM for *B* and 10 and 0 mM for experiments shown in *C*. The traces show holding currents before and after exposure to ouabain (Oua). The membrane capacitance, C_m (in pF) is indicated to facilitate comparisons.

larger shift in the holding current of the myocyte exposed to SNP than of the control myocyte. The mean levels of I_p in experiments performed using Na^+-containing patch pipettes and superfusates that contained Na^+ or were Na^+ free are summarized in Fig. 2. Mean I_p recorded using control, SNP-free superfusates appeared higher in the presence than in the absence of extracellular Na^+. We attribute this to an allosteric effect of extracellular Na^+ which accelerates conversion of the enzyme from the low-affinity E_2 state to the high-Na^+-affinity E_1 state and enhances the apparent affinity for Na^+ at cytosolic Na^+–K^+ pump sites (Buhagiar *et al.* 2004). However, a statistically significant increase in I_p with exposure to SNP persisted in the absence of extracellular Na^+.

To examine the relationship between the concentration of SNP and I_p we exposed myocytes to SNP in concentrations ranging from 1 to 1000 μM. Patch pipettes and superfusates contained 10 mM Na^+ and 70 mM K^+. The superfusate contained 150 mM Na^+. Results are shown in Fig. 3. SNP at concentrations of 1, 10, 50 and 100 μM induced a statistically significant increase in I_p. However, there was no significant stimulation relative to control myocytes when the concentration was increased further to 1000 μM, i.e. there was not a simple concentration-dependent effect of SNP. Since SNP at high concentrations has oxidant effects *in vitro* that can be prevented by superoxide dismutase (Jaworski *et al.* 2001) we included 200 μM cytosolic Cu,Zn superoxide dismutase (SOD) in pipette filling solutions and exposed myocytes 1000 μM SNP. Mean I_p has been included in Fig. 3. Superoxide dismutase restored SNP-induced stimulation of I_p.

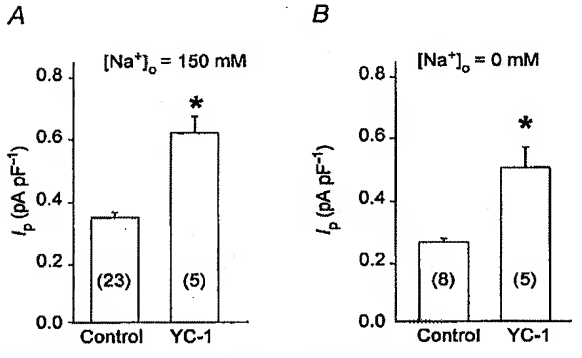

Figure 2. Effect of SNP on Na^+ –K^+ pump current
The Na^+ concentration in patch pipette filling solutions was 10 mM in all experiments. Mean (± S.E.M.) I_p values recorded in a superfusate that included 150 mM Na^+ (*A*) or was Na^+ free (*B*) are shown. The extracellular Na^+ concentration ($[Na^+]_o$) is indicated in the figure. The number of experiments is indicated in parentheses. *$P < 0.05$.

Intracellular messengers linking NO to Na^+–K^+ pump stimulation

Soluble guanylyl cyclase is the classical target molecule mediating cellular effects of NO. However, since some effects of NO are independent of sGC, we measured I_p while blocking sGC and its downstream messengers. Patch pipettes contained 10 mM Na^+ and 70 mM K^+. The superfusate contained 150 mM Na^+ and we used SNP at a concentration of 50 μM. We included 10 μM of the NO-competitive antagonist ODQ in patch pipette solutions to block access of NO to sGC and so block stimulation of cGMP synthesis. Figure 4 shows that ODQ abolished the SNP-induced pump stimulation.

The inhibition of the SNP-induced pump stimulation by ODQ implicates protein kinase G (PKG) in the downstream messenger pathways that mediate the stimulation. However, since cGMP can directly activate effector proteins independent of phosphorylation (Dimmeler *et al.* 1999), we examined the effect of inhibiting PKG by including 0.5 μM KT-5823 in patch pipette solutions. KT-5823 abolished the SNP-induced pump stimulation, implicating a role for PKG in the stimulation. If the pump stimulation is due to PKG directly phosphorylating Na^+–K^+ pump molecules, inhibition of phosphatase-mediated dephosphorylation might enhance the effect of SNP. To examine this we included 0.1 μM okadaic acid in patch pipette solutions. Figure 4 shows that phosphatase inhibition abolished, rather than enhanced, the SNP-induced pump stimulation.

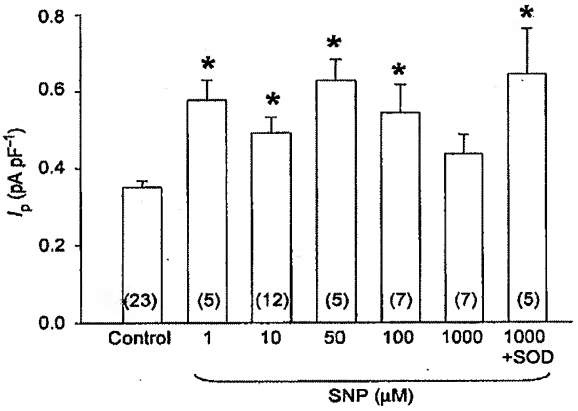

Figure 3. Dependence of Na^+ –K^+ pump current on the concentration of SNP
The Na^+ concentration in patch pipette filling solutions was 10 mM. The superfusate contained 150 mM Na^+ and 5.6 mM K^+. Superoxide dismutase (SOD) was included in the patch pipette solution as indicated. Mean (± S.E.M.) I_p values at different concentrations of SNP are indicated. The numbers of experiments are indicated in parenthesis. Asterisk indicates a statistically significant SNP-induced increase in I_p.

Figure 3 shows that there is not a simple concentration-dependent effect of the NO donor SNP on I_p. To examine the effect of activating messengers downstream from the NO-activated sGC we activated PKG by including a cGMP analogue in patch pipette solutions. We used the non-hydrolysable analogue 8-*p*CPT-cGMP to prevent its rapid intracellular breakdown. Figure 5 shows that 8-*p*CPT-cGMP induced a concentration-dependent increase in I_p. Since 8-*p*CPT-cGMP in high concentrations might activate protein kinase A (PKA), we examined the effect of adding 0.5 μM of H-89 (N-[2-(p-bromocinnamylamino)ethyl]-5-isoquinolinesulfonamide dihydrochloride) to pipette solutions containing 1 mM 8-*p*CPT-cGMP. The mean I_p recorded in such experiments is included in Fig. 5. The 8-*p*CPT-cGMP-induced increase in I_p persisted after PKA blockade.

To avoid non-specific effects of high concentrations of 8-*p*CPT-cGMP we also examined the effect of including 400 U ml^{-1} recombinant bovine PKG in the patch pipette solution (White *et al.* 2000). To activate PKG we included 20 μM 8-*p*CPT-cGMP in the solution. Figure 5 shows that 20 μM 8-*p*CPT-cGMP in patch pipette solutions had no effect on I_p in the absence of recombinant PKG. However, the combination of 20 μM 8-*p*CPT-cGMP and recombinant PKG in pipette solutions induced a large increase in I_p.

Activation of sGC with YC-1

Figure 5 shows that there is a clear concentration-dependent effect of an analogue of the product of sGC, cGMP, while Fig. 3 shows that the relationship between the NO donor SNP and I_p is much less predictable. In addition, activation of sGC by exposure to SNP causes a smaller increase in I_p than activation of messenger pathways downstream from sGC. This suggests that there are non-specific effects of SNP. To avoid this while still inducing activation *via* the classical target molecule for NO, sGC, we included 1 μM YC-1 in patch pipette solutions. The solutions included 10 mM Na^+ and 70 mM K^+. Superfusates included 5.6 mM K^+ and they contained 150 mM Na^+ or they were Na^+ free. Figure 6*A* shows that ouabain induced a shift in holding current in the presence or absence of extracellular Na^+. All experiments using the same protocols are summarized in Fig. 6*B*. YC-1 induced a large, statistically significant increase in I_p that was independent of the presence or absence of extracellular Na^+.

The Na^+–K^+ pump stimulation induced by YC-1 might be due to an increase in maximal turnover of the pump or due to an increase in its sensitivity to intracellular Na^+. An increase in maximal turnover should be reflected by

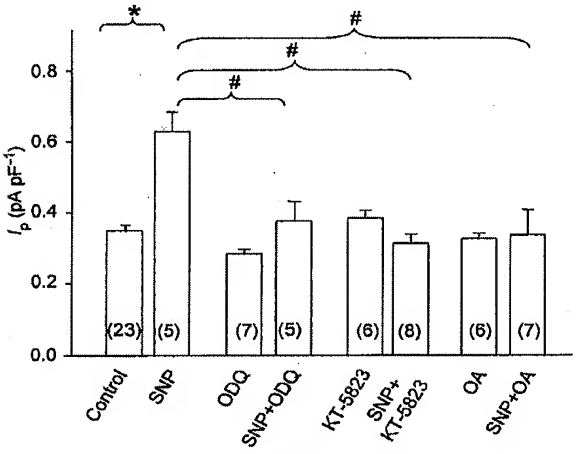

Figure 4. Intracellular messenger pathways linking SNP to Na^+–K^+ pump stimulation
Myocytes were superfused with control solutions or solutions containing SNP. Patch pipettes contained control solutions or solutions containing inhibitors of soluble guanylyl cyclase (ODQ), protein kinase G (KT-5823) or protein phosphatase (okadaic acid, OA). Numbers in parentheses indicate the number of myocytes studied with each set of conditions. * Significant difference between mean (± S.E.M.) I_p values of myocytes exposed or not exposed to SNP; # significant difference between I_p of myocytes exposed to SNP and patch clamped using control pipette filling solutions and solutions containing ODQ, KT-5823 or OA. Results of experiments using an SNP-free superfusate and ODQ, KT-5823 or OA in pipette solutions are also shown.

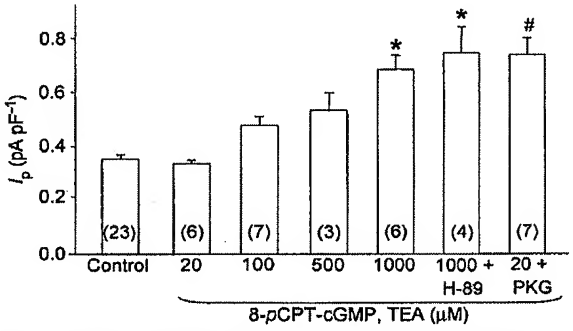

Figure 5. Effect of 8-*p*CPT-cGMP, TEA and recombinant PKG on Na^+–K^+ pump current
Myocytes were exposed to control superfusates, and the compounds indicated in the figure were included in patch pipette solutions. Numbers in parentheses indicate the number of myocytes for each set of experimental conditions. Asterisk indicates a significant difference ($P < 0.05$) between I_p values of myocytes patch clamped using control patch pipette filling solutions and solutions containing 8-*p*CPT-cGMP, TEA. The protein kinase A inhibitor H-89 did not prevent the activation of I_p induced by the highest concentration of 8-*p*CPT-cGMP,TEA. # Significant difference ($P < 0.05$) between I_p values of myocytes patch clamped using filling solutions containing 20 μM 8-*p*CPT-cGMP, TEA with or without recombinant bovine protein kinase G (PKG).

an increase in I_p recorded when intracellular pump sites are nearly saturated by a high concentration of Na^+. We patch clamped myocytes using 80 mM Na^+ and 70 mM K^+ in pipette solutions. The superfusate included 150 and 5.6 mM K^+. Figure 6*C* shows examples of ouabain-induced shifts in holding currents of a control myocyte and a myocyte exposed to YC-1. The ouabain-induced shifts in currents were much larger than those recorded using 10 mM Na^+ in pipette solutions (Fig. 6*A*) and they were similar for a myocyte exposed or not exposed to YC-1. All experiments performed using 80 mM Na^+ in the pipette solution are summarized in Fig. 6*D*. There was no significant difference between the mean I_p of control myocytes and that of myocytes exposed to YC-1, suggesting that YC-1 does not stimulate maximal pump turnover.

To ascertain that YC-1 activates the same messenger pathways as those implicated for SNP-induced Na^+–K^+ pump stimulation we examined the effects of ODQ, KT-5823 or okadaic acid in patch pipette solutions. The pipette solutions included 10 mM Na^+ and 70 mM K^+. Figure 7 shows that ODQ, KT-5823 and okadaic acid abolished the YC-1-induced Na^+–K^+ pump stimulation, i.e. the pattern of inhibition by blockers of implicated messenger pathways was identical to that shown for SNP in Fig. 4.

Dependence of Na^+–K^+ pump stimulation on intracellular Na^+ and K^+

The dependence of pump stimulation on a non-saturating concentration of intracellular Na^+ suggests that YC-1 causes a change in the sensitivity of the pump to intracellular Na^+. Since Na^+ binds at two sites on the cytosolic side of the pump in competition with K^+ and at a third site selective for Na^+, we examined the dependence of pump stimulation induced by YC-1 on the intracellular K^+ concentration. We voltage clamped myocytes

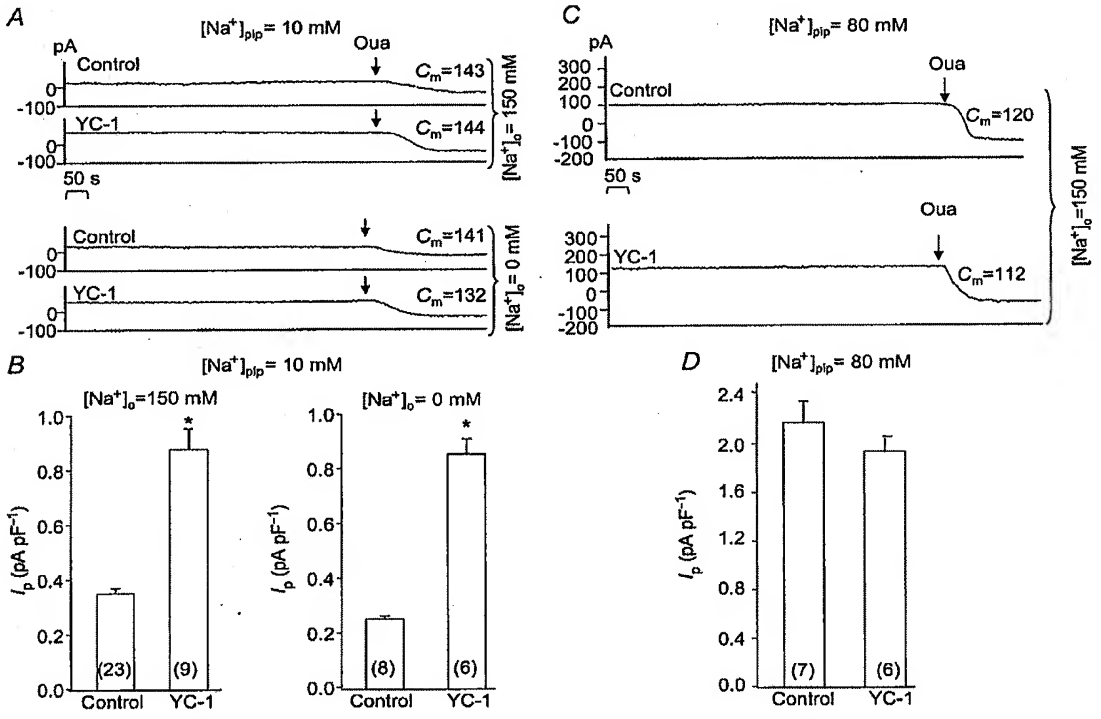

Figure 6. Effect of activation of soluble guanylyl cyclase with YC-1 on Na^+–K^+ pump current
Inclusion of 1 μM YC-1 in pipette solutions is indicated in the figure. *A* shows shifts in holding current induced by ouabain (Oua) recorded using Na^+ at a concentration ($[Na^+]_{pip}$) of 10 mM Na^+ in patch pipette solutions. The Na^+ concentration in superfusates ($[Na^+]_o$) was 150 mM (upper traces) or 0 mM (lower traces). *B* summarizes mean (± S.E.M.) I_p values recorded in Na^+-containing and Na^+-free superfusates. *C* shows ouabain-induced shifts in holding current recorded using 80 mM Na^+ in patch pipette solutions, recorded in Na^+-containing superfusates. *D* summarizes mean I_p values recorded using 80 mM Na^+ in pipette solutions. C_m indicates membrane capacitance in pF. $^*P < 0.05$.

using patch pipettes containing 10 mM Na^+ and K^+ at a concentration ($[K]_{pip}$) ranging from 0 to 140 mM. Superfusates included 150 mM Na^+ and 5.6 mM K^+. Figure 8 shows a summary of I_p of control myocytes and of myocytes patch clamped using 1 μM YC-1 in pipette filling solutions. As expected, there was a $[K]_{pip}$-dependent decrease in I_p. YC-1 induced a significant increase in I_p in the presence or absence of K^+ in patch pipette filling solutions.

Since YC-1 induces Na^+–K^+ pump stimulation at a non-saturating concentration of intracellular Na^+ only and since stimulation can occur in the nominal absence of intracellular K^+, we examined whether YC-1 alters the sensitivity of the pump to intracellular Na^+ in the absence of intracellular K^+. We patch clamped myocytes using pipette solutions that were K^+ free and included Na^+ at concentrations ranging from 0 to 80 mM. To eliminate binding of K^+ at extracellular sites as a rate-limiting step at high pipette Na^+ concentration we used a K^+ concentration of 15 mM in the superfusate in these experiments. The Na^+ concentration in the superfusate was 150 mM. Figure 9*A* shows the ouabain-induced shift in holding current of a control myocyte patch clamped using a pipette solution that contained 80 mM Na^+. The ouabain-induced shift in current appeared much larger than the shift recorded using K^+-containing pipette filling solutions with the same Na^+ concentration (Fig. 6). Figure 9*B* summarizes experiments performed using different Na^+ concentrations in pipette solutions.

For the purpose of assigning a value to the intracellular Na^+ concentration that induces half-maximal pump activation we fitted the Hill equation to the data. We derived values of 24.0 mM for control myocytes and 14.1 mM for myocytes perfused with pipette solutions containing YC-1. Since I_p is not a direct measure of Na^+ binding, the fit is without mechanistic implications and is therefore not shown. Mean I_p is similar for control myocytes and for myocytes exposed to YC-1 when $[Na^+]_{pip}$ is 0 or 80 mM. However, YC-1 seemed to induce an increase in I_p when $[Na]_{pip}$ was at the rate-limiting concentrations of 5, 10 or 20 mM. A Mann–Whitney test indicated that YC-1 induces a significant increase in I_p when data obtained at these three Na^+ concentrations are considered in combination.

Discussion

Previous studies have reported inhibition (McKee *et al.* 1994; Liang & Knox, 2000; Ellis *et al.* 2000, 2001; Varela *et al.* 2004), the absence of any effect (Ortiz *et al.* 2001) and stimulation (Gupta *et al.* 1994, 1995) of the membrane Na^+–K^+ pump when various tissues were exposed to NO donor compounds. Stimulation was secondary to

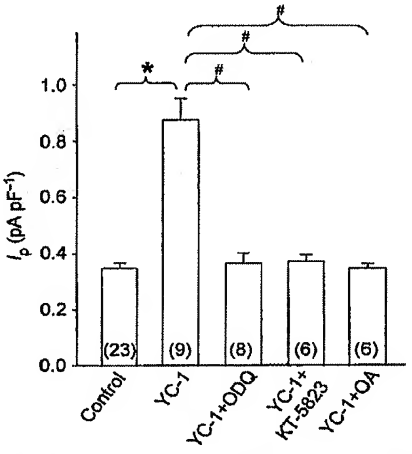

Figure 7. Intracellular messenger pathways linking YC-1 to Na^+–K^+ pump stimulation
Patch pipettes contained control solutions or solutions that contained YC-1 and inhibitors of soluble guanylyl cyclase (ODQ), protein kinase G (KT-5823) or protein phosphatase (okadaic acid, OA) as indicated. The Na^+ concentrations in pipette solutions and superfusates were 10 and 150 mM, respectively. Numbers in parentheses indicate the number of myocytes studied with each set of conditions. * Significant difference ($^*P < 0.05$) between mean (± S.E.M.) I_p values of myocytes perfused or not perfused with pipette solutions containing YC-1; # significant difference ($^*P < 0.05$) between mean I_p values of myocytes perfused with pipette solutions containing YC-1 alone and solutions containing both YC-1 and ODQ, KT-5823 or OA. Results of control experiments using ODQ, KT-5823 or OA alone are shown in Fig. 4.

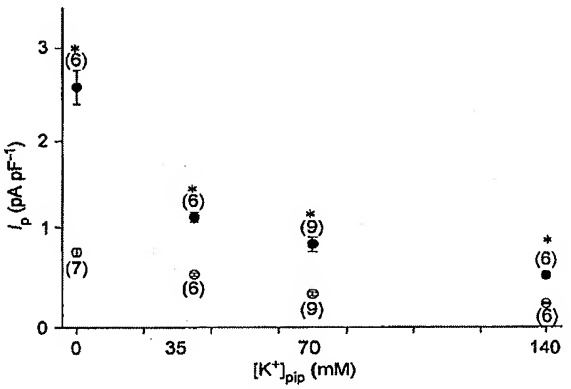

Figure 8. Dependence of Na^+ –K^+ pump stimulation induced by YC-1 on intracellular K^+
I_p was measured in myocytes voltage clamped using control pipette filling solutions (○) or solutions containing YC-1 (●). The pipette filling solutions contained Na^+ at a concentration of 10 mM and K^+ at a concentration ($[K^+]_{pip}$) ranging from 0 to 140 mM. The numbers of experiments for each set of conditions are indicated in parentheses. Mean (± S.E.M.) I_p values for myocytes perfused with pipette solutions containing YC-1 were significantly ($^*P < 0.05$) higher than for myocytes perfused with control solutions at all levels of $[K]_{pip}$.

enhanced Na^+ influx rather than due to a direct effect on the Na^+–K^+ pump in vascular smooth muscle (Gupta *et al.* 1994). In our study, SNP stimulated intrinsic pump activity, independent of enhanced transsarcolemmal Na^+ influx. The discrepancy between our results and previous studies may be organ dependent (Therien & Blostein, 2000). However, use of pharmacological NO donor compounds may also have contributed to inconsistent results. The pathways leading to formation of NO from the compounds and derivative side reactions are exquisitely sensitive to the local oxygen tension, and the amount of bio-active intermediate and end products that form during metabolism and degradation may exceed the amount of NO (Ignarro *et al.* 2002). The net response may arise from a balance between, at times opposing, effects of compounds generated. NO and its derivatives can directly inhibit isolated Na^+–K^+ ATPase, in part via effects on membrane fluidity (Muriel & Sandoval, 2000), and the derivative peroxynitrite inhibits Na^+–K^+ ATPase activity in renal cells exposed to NO donors. The inhibition is abolished when the peroxynitrite precursor, superoxide, is eliminated with SOD (Varela *et al.* 2004). In our study, SNP induced Na^+–K^+ pump stimulation at all but the highest concentration used, and stimulation at the high SNP concentration was restored by SOD.

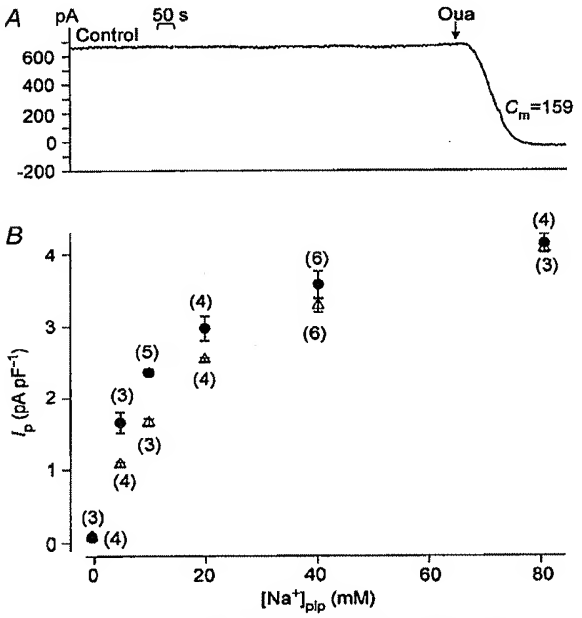

Figure 9. Dependence of Na^+ –K^+ pump stimulation induced by YC-1 on intracellular Na^+

I_p was measured in myocytes voltage clamped using control pipette filling solutions (△) or solutions containing YC-1 (●). The pipette filling solutions contained Na^+ at concentrations ranging from 0 to 80 mM. They were nominally K^+ free. The numbers of experiments for each set of conditions are indicated in parentheses. Mean (± S.E.M.) I_p values for myocytes perfused with pipette solutions containing YC-1 were significantly higher than for myocytes perfused with control solutions when the pipette Na^+ concentration was at rate-limiting levels.

Activation and inhibition of messengers implicated in NO-mediated pathways

While SNP consistently induced Na^+–K^+ pump stimulation, there was not a simple concentration -dependent increase in I_p and there was considerable variability of I_p with exposure to SNP (Fig. 3). To avoid ambiguities of pharmacological NO donors we used YC-1 in patch pipette solutions to selectively activate sGC, a downstream target molecule for NO. Since a scaffold protein directs sGC to a membrane association in close proximity to nitric oxide synthase (Russwurm & Koesling, 2002), YC-1 activates sGC at sites of endogenous NO synthesis (Russwurm *et al.* 2002). Such activation may better reflect physiological signalling than exposure of cells to SNP because effects of YC-1 should be largely restricted to the microdomains of synthesis and breakdown of NO. YC-1 reproduced the SNP-induced stimulation of I_p. This, in combination with the effect of selective inhibition of sGC with ODQ (Russwurm *et al.* 2002) in pipette solutions (see Figs 4 and 7), strongly implicates sGC in Na^+–K^+ pump stimulation. The effect of cGMP synthetized on activation of sGC is usually mediated by PKG. However, it may also be due to a cGMP-mediated increase in cAMP and activation of PKA, it may be due to activation of PKA by cGMP in high concentrations or due to a direct effect of cGMP on effector proteins (White, 1999). The persistence of pump stimulation when H-89 is included in patch pipette solutions rules out involvement of PKA.

Since KT-5823 has imperfect selectivity for PKG we included recombinant PKG in the pipette solution and activated it with 20 μM 8-*p*CPT-cGMP. PKG reproduced effects of SNP and YC-1. Of note, 20 μM 8-*p*CPT-cGMP in the absence of PKG in pipette solutions had no effect on I_p. While a difference in sensitivity to activation of endogenous and recombinant PKG may account for this, PKG endogenous to the myocyte may have been exposed to 8-*p*CPT-cGMP in a concentration lower than 20 μM because 8-*p*CPT-cGMP is highly membrane permeable. Rate-limiting diffusion through the patch pipette tip can result in an intracellular concentration in voltage clamped cardiac myocytes of membrane-permeable compounds that is lower than the concentration in pipette solutions (Mathias *et al.* 1990).

Taken together, the data indicate that PKG mediates Na^+–K^+ pump stimulation induced by SNP and YC-1. There are few established molecular targets for PKG (Moreno *et al.* 2001). Phosphorylation of the pump molecule or of the closely associated FXYD1 protein

implicated in pump regulation (Cornelius *et al.* 2001) is unlikely because FXYD1 is not reported to be phosphorylated by PKG and the pump itself is not easily phosphorylated by PKG (Fotis *et al.* 1999). In addition, if Na^+–K^+ pump stimulation were mediated by phosphorylation of the pump molecule or the FXYD1 protein, inhibition of protein phosphatases with okadaic acid should enhance rather than abolish stimulation. Protein phosphatases are often implicated in PKG-mediated signalling (White, 1999; Moreno *et al.* 2001), and phosphatase-mediated dephosphorylation of FXYD1 has been reported (Neumann *et al.* 1999). PKG can mediate phosphorylation of a regulatory protein for protein phosphatase 1 in smooth muscle myocytes. However, the phosphorylation inhibits rather than activates phosphatase activity (Tokui *et al.* 1996) and cannot account for our results. The available information cannot identify the okadaic acid-sensitive step in our study.

Effect of NO on functional properties of the Na^+–K^+ pump

Interpretation of the YC-1- and SNP-induced change in the sensitivity of the Na^+–K^+ pump to intracellular Na^+ depends on the assumption that Na^+ concentrations in the cytosol and pipette solutions are similar. Concentration gradients could exist between the pipette solution and the intracellular bulk phase (Mathias *et al.* 1990) or between the bulk phase and a diffusion-restricted subsarcolemmal space (Despa & Bers, 2003; Silverman *et al.* 2003). Transsarcolemmal influx should maintain intracellular Na^+ at a level high enough to support an easily detectable Na^+–K^+ pump current when Na^+-free pipette solutions are used, unless the intracellular concentration largely reflects the concentration in the patch pipettes (Mathias *et al.* 1990; Silverman *et al.* 2003). Nakao & Gadsby (1989) used wide-tipped patch pipettes to optimize control of intracellular Na^+. When I_p was recorded in Na^+-containing superfusates with Na^+-free patch pipettes it was ~3.5% of the I_p recorded with pipettes containing 50 mM Na^+. This fraction was reduced to ~0.8% when superfusates were Na^+ free to eliminate transsarcolemmal Na^+ influx. The I_p we recorded with Na^+-free patch pipettes was ~0.3% of the I_p expected when pipettes contained 50 mM Na^+ (extrapolated from Fig. 9*B*). This low level was achieved in Na^+-containing superfusates, and suggests that a diffusion-restricted subsarcolemmal space does not give rise to substantial Na^+ concentration gradients. In support of this we have reported that a ouabain-sensitive current is easily detectable when the Na^+ concentration in pipette solutions is as low as 0.1 mM (Hansen *et al.* 2002). We conclude that the Na^+ concentration at cytosolic pump sites approximates that in pipette solutions in our experiments.

Na^+–K^+ pump regulation can depend on intracellular K^+ (Buhagiar *et al.* 1999, 2004), which is consistent with an effect on the backward $E_1 + 2K^+ \rightarrow E_2(K^+)_2$ reaction (Buhagiar *et al.* 2004) where E_1 is the unphosphorylated conformation of the enzyme with a high affinity for cytoplasmic NA^+ ions and E_2 is the alternative unphosphorylated conformation which is stabilised by cytoplasmic K^+ ions. However, such a mechanism cannot account for the pump stimulation in this study because stimulation could be demonstrated in the absence of intracellular K^+ (Figs 8 and 9). A change in the apparent Na^+ affinity might account for pump stimulation. A change in the affinity could be due to a change in intrinsic Na^+ binding to the E_1 conformation of pump molecules or due to an apparent change in affinity from a change in the rate of reactions determining availability of the E_1 conformation (Apell & Karlish, 2001). Mechanistic details cannot be determined from this study.

The relative increase in I_p induced by YC-1 was larger at 5.6 than at 15 mM extracellular K^+ (Figs 8 and 9). The higher concentration must stimulate the pump. Any additional stimulation may then be less evident if subsequent steps, independent of K^+, become rate limiting. Effects of binding of K^+ to the E_2 conformation should be small because binding is nearly saturated at 5.6 mM. Nor can an increase in the rate of the K^+-stimulated dephosphorylation reaction account for stimulation because the reaction is not rate limiting (Kane *et al.* 1998; Kong & Clarke, 2004). However, allosteric binding of K^+ stimulates rate-limiting (Kong & Clarke, 2004) deocclusion of K^+ and the $E_2 \rightarrow E_1$ conformational transition (Forbush, 1987). We considered the stimulation this may mediate. We modified a mathematical model of the Na^+–K^+ pump cycle (Kong & Clarke, 2004) to take into account allosteric effects of extracellular K^+ (see Appendix for details). Simulations indicated that one might expect a 28% increase in pump rate when extracellular K^+ is increased from 5.6 to 15 mM. A quantitative interpretation of the simulations is not justified because most parameters in the model were derived from presteady-state kinetic measurements on purified Na^+–K^+ ATPase from kidney while our experimental data were obtained in intact cardiac cells. However, the simulations are consistent with the qualitative conclusion that the difference in extracellular K^+ concentration may affect the relative size of pump stimulation induced by YC-1. This highlights how details of experimental conditions may affect analysis of Na^+–K^+ pump regulation.

Appendix

To examine allosteric effects of K^+ we simulated steady-state Na^+–K^+ pump activity under the experimental conditions used here (extracellular Na^+ concentration 150 or 140 mM, extracellular

K^+ concentration 5.6 or 15 mM, intracellular Na^+ concentration 10 mM, intracellular K^+ concentration 0 mM and intracellular ATP concentration 2 mM). We modified eqn (5) of a previously published model (Kong & Clarke, 2004) by changing the dissociation constants for the activation of enzyme dephosphorylation by the two transported K^+ ions, K^o_{K1} and K^o_{K2}. They were estimated at 2.8 and 4.3 mM (Gray *et al.* 1997). In addition, the equation for the observed rate constant for the $E_2 \rightarrow E_1$ transition, k_1^{obs}, was modified to include an allosteric effect of external K^+. The new equation was:

$$k_1^{obs} = \{k_1^a + k_1^b[Na^+]_o/K_N^o + k_1^c[ATP]/K_A + k_1^d[Na^+]_o[ATP]/(K_N^o K_A) + k_1^e[K^+]_o/K_K^o + k_1^f[K^+]_o[Na^+]_o/(K_N^o K_K^o) + k_1^g[K^+]_o[ATP]/(K_K^o K_A) + k_1^h[K^+]_o[Na^+]_o[ATP]/(K_K^o K_N^o K_A)\}/\{(1 + [Na^+]_o/K_N^o)(1 + [ATP]/K_A)(1 + [K^+]_o/K_K^o)\}$$

We refer to Table 1 of Kong & Clarke (2004) for the values and meanings of the parameters already included in the model.

We made the assumption that the binding of Na^+ and K^+ to the allosteric sites is non-competitive and that the effects of the two ions are simply additive. K_K^o represents the dissociation constant of the external allosteric K^+ ions from the E_2 conformation of the enzyme, irrespective of whether Na^+ and/or ATP are simultaneously bound to allosteric sites. It has been set to the same value as K_N^o, the dissociation constant for allosteric external Na^+ ions, i.e. 31 mM, in accord with the results of Forbush (1987) that the affinity of the enzyme for various allosteric ions is not substantially different. k_1^e, k_1^f, k_1^g and k_1^h represent rate constants for the $E_2 \rightarrow E_1$ transition (with up to two K^+ ions initially bound to E_2 at transport sites) when the allosteric sites are saturated by K^+ alone (k_1^e), by K^+ and Na^+ (k_1^f), by K^+ and ATP (k_1^g) and by K^+, Na^+ and ATP (k_1^h). In the absence of ATP, Na^+ and K^+ have similar effects in accelerating the $E_2 \rightarrow E_1$ transition (Forbush, 1987). Thus, the values of k_1^e and k_1^f have been chosen to be equal to k_1^b, the rate constant for the transition at which only allosteric external Na^+ ions are bound, i.e. 0.8 s^{-1}.

External K^+ causes approximately 16% greater acceleration of the $E_2 \rightarrow E_1$ transition than external Na^+ in the presence of ATP (Forbush, 1987). Accordingly, since k_1^d, the rate constant for the transition when the enzyme is saturated by allosteric Na^+ and ATP, has been determined to have a value of approximately 70 s^{-1} (Lüpfert *et al.* 2001), the value of k_1^g was taken as 81 s^{-1}. When the allosteric sites are saturated by ATP, Na^+ and K^+, no experimental data are presently available on the value of the rate constant, i.e. k_1^h. For the purpose of the simulation we assumed the effects of Na^+ and K^+ are additive, i.e. $k_1^h = k_1^d + k_1^g = 151$ s^{-1}.

The simulations were carried out using the commercially available program Berkeley Madonna 7.0 via the variable step size Rosenbrock integration method for stiff systems of differential equations. The simulations yield the time course of the concentration of each enzyme intermediate, as well as the concentration of inorganic phosphate, from which the turnover number of the enzyme can be calculated. The simulations show that the turnover number of the enzyme is predicted to be 28 s^{-1} in the presence of 5.6 mM external K^+ and 36 s^{-1} in the presence of 15 mM external K^+.

References

Apell HJ & Karlish SJ (2001). Functional properties of Na,K-ATPase, and their structural implications, as detected with biophysical techniques. *J Membr Biol* **180**, 1–9.

Boyett MR, Hart G & Levi AJ (1986). Dissociation between force and intracellular sodium activity with strophanthidin in isolated sheep Purkinje fibres. *J Physiol* **381**, 311–331.

Buhagiar KA, Hansen PS, Gray DF, Mihailidou AS & Rasmussen HH (1999). Angiotensin regulates the selectivity of the Na^+-K^+ pump for intracellular Na^+. *Am J Physiol* **277**, C461–C468.

Buhagiar KA, Hansen PS, Kong BY, Clarke RJ, Fernandes C & Rasmussen HH (2004). Dietary cholesterol alters Na^+/K^+ selectivity at intracellular Na^+/K^+ pump sites in cardiac myocytes. *Am J Physiol* **286**, C398–C405.

Cornelius F, Mahmmoud YA & Christensen HR (2001). Modulation of Na,K-ATPase by associated small transmembrane regulatory proteins and by lipids. *J Bioenerg Biomembr* **33**, 415–423.

Despa S & Bers DM (2003). Na/K pump current and [Na](i) in rabbit ventricular myocytes: local [Na](i) depletion and Na buffering. *Biophys J* **84**, 4157–4166.

Dimmeler S, Fleming I, Fisslthaler B, Hermann C, Busse R & Zeiher AM (1999). Activation of nitric oxide synthase in endothelial cells by Akt-dependent phosphorylation. *Nature* **399**, 601–605.

Drewnowska K & Baumgarten CM (1991). Regulation of cellular Volume in rabbit ventricular myocytes: bumetanide, chlorothiazide, and ouabain. *Am J Physiol* **260**, C122–C131.

Ellis DZ, Nathanson JA, Rabe J & Sweadner KJ (2001). Carbachol and nitric oxide inhibition of Na,K-ATPase activity in bovine ciliary processes. *Invest Ophthalmol Vis Sci* **42**, 2625–2631.

Ellis DZ, Nathanson JA & Sweadner KJ (2000). Carbachol inhibits Na^+-K^+-ATPase activity in choroid plexus via stimulation of the NO/cGMP pathway. *Am J Physiol* **279**, C1685–C1693.

Forbush B III (1987). Rapid release of ^{42}K or ^{86}Rb from two distinct transport sites on the Na,K-pump in the presence of P_i or vanadate. *J Biol Chem* **262**, 11116–11127.

Fotis H, Tatjanenko LV & Vasilets LA (1999). Phosphorylation of the alpha-subunits of the Na^+/K^+-ATPase from mammalian kidneys and Xenopus oocytes by cGMP-dependent protein kinase results in stimulation of ATPase activity. *Eur J Biochem* **260**, 904–910.

Gray DF, Hansen PS, Doohan MM, Hool LC & Rasmussen HH (1997). Dietary cholesterol affects Na^+-K^+ pump function in rabbit cardiac myocytes. *Am J Physiol* **272**, H1680–H1689.

Gupta S, McArthur C, Grady C & Ruderman NB (1994). Role of endothelium-derived nitric oxide in stimulation of Na^+-K^+-ATPase activity by endothelin in rabbit aorta. *Am J Physiol* **266**, H577–H582.

Gupta S, Moreland RB, Munarriz R, Daley J, Goldstein I & Saenz De Tejada I (1995). Possible role of Na^+-K^+-ATPase in the regulation of human corpus cavernosum smooth muscle contractility by nitric oxide. *Br J Pharmacol* **116**, 2201–2206.

Hansen PS, Buhagiar KA, Gray DF & Rasmussen HH (2000). Voltage-dependent stimulation of the Na^+-K^+ pump by insulin in rabbit cardiac myocytes. *Am J Physiol* **278**, C546–C553.

Hansen PS, Buhagiar KA, Kong BY, Clarke RJ, Gray DF & Rasmussen HH (2002). Dependence of Na^+-K^+ pump current-voltage relationship on intracellular Na^+, K^+, and Cs^+ in rabbit cardiac myocytes. *Am J Physiol* **283**, C1511–C1521.

Hare JM (2003). Nitric oxide and excitation-contraction coupling. *J Mol Cell Cardiol* **35**, 719–729.

Hille B (1992). *Ionic Channels of Excitable Membranes*. Sinauer Associates Inc., Sunderland, MA, USA.

Hool LC, Whalley DW, Doohan MM & Rasmussen HH (1995). Angiotensin-converting enzyme inhibition, intracellular Na^+, and Na^+-K^+ pumping in cardiac myocytes. *Am J Physiol* **268**, C366–C375.

Ignarro LJ, Napoli C & Loscalzo J (2002). Nitric oxide donors and cardiovascular agents modulating the bioactivity of nitric oxide: an overview. *Circ Res* **90**, 21–28.

Jaworski K, Kinard F, Goldstein D, Holvoet P, Trouet A, Schneider YJ & Remacle C (2001). *S*-nitrosothiols do not induce oxidative stress, contrary to other nitric oxide donors, in cultures of vascular endothelial or smooth muscle cells. *Eur J Pharmacol* **425**, 11–19.

Kane DJ, Grell E, Bamberg E & Clarke RJ (1998). Dephosphorylation kinetics of pig kidney Na^+,K^+-ATPase. *Biochemistry* **37**, 4581–4591.

Kong BY & Clarke RJ (2004). Identification of potential regulatory sites of the Na^+,K^+-ATPase by kinetic analysis. *Biochemistry* **43**, 2241–2250.

Lee CO, Kang DH, Sokol JH & Lee KS (1980). Relation between intracellular Na ion activity and tension of sheep cardiac Purkinje fibers exposed to dihydro-ouabain. *Biophys J* **29**, 315–330.

Liang M & Knox FG (2000). Production and functional roles of nitric oxide in the proximal tubule. *Am J Physiol* **278**, R1117–R1124.

Lüpfert C, Grell E, Pintschovius V, Apell HJ, Cornelius F & Clarke RJ (2001). Rate limitation of the Na^+,K^+-ATPase pump cycle. *Biophys J* **81**, 2069–2081.

McKee M, Scavone C & Nathanson JA (1994). Nitric oxide, cGMP, and hormone regulation of active sodium transport. *Proc Natl Acad Sci U S A* **91**, 12056–12060.

Mathias RT, Cohen IS & Oliva C (1990). Limitations of the whole cell patch clamp technique in the control of intracellular concentrations. *Biophys J* **58**, 759–770.

Mogul DJ, Singer DH & Ten Eick RE (1990). Dependence of Na-K pump current on internal Na^+ in mammalian cardiac myocytes. *Am J Physiol* **259**, H488–H496.

Moreno H, Vega-Saenz De Miera E, Nadal MS, Amarillo Y & Rudy B (2001). Modulation of Kv3 potassium channels expressed in CHO cells by a nitric oxide-activated phosphatase. *J Physiol* **530**, 345–358.

Muriel P & Sandoval G (2000). Nitric oxide and peroxynitrite anion modulate liver plasma membrane fluidity and Na^+/K^+-ATPase activity. *Nitric Oxide* **4**, 333–342.

Nakao M & Gadsby DC (1989). [Na] and [K] dependence of the Na/K pump current-voltage relationship in guinea pig ventricular myocytes. *J General Physiol* **94**, 539–565.

Neumann J, Maas R, Boknik P, Jones LR, Zimmermann N & Scholz H (1999). Pharmacological characterization of protein phosphatase activities in preparations from failing human hearts. *J Pharmacol Exp Ther* **289**, 188–193.

Ortiz PA, Hong NJ & Garvin JL (2001). NO decreases thick ascending limb chloride absorption by reducing Na^+-K^+-$2Cl^-$ cotransporter activity. *Am J Physiol* **281**, F819–F825.

Russwurm M & Koesling D (2002). Isoforms of NO-sensitive guanylyl cyclase. *Mol Cell Biochem* **230**, 159–164.

Russwurm M, Mergia E, Mullershausen F & Koesling D (2002). Inhibition of deactivation of NO-sensitive guanylyl cyclase accounts for the sensitizing effect of YC-1. *J Biol Chem* **277**, 24883–24888.

Silverman BZ, Warley A, Miller JI, James AF & Shattock MJ (2003). Is there a transient rise in sub-sarcolemmal Na and activation of Na/K pump current following activation of I(Na) in ventricular myocardium? *Cardiovasc Res* **57**, 1025–1034.

Therien AG & Blostein R (2000). Mechanisms of sodium pump regulation. *Am J Physiol* **279**, C541–C566.

Tokui T, Brozovich F, Ando S & Ikebe M (1996). Enhancement of smooth muscle contraction with protein phosphatase 1 inhibitor: activation of inhibitor 1 by cGMP-dependent protein kinase. *Biochem Biophys Res Commun* **220**, 777–783.

Varela M, Herrera M & Garvin JL (2004). Inhibition of Na-K-ATPase in thick ascending limbs by NO depends on O_2^- and is diminished by a high-salt diet. *Am J Physiol* **287**, F224–F230.

White RE (1999). Cyclic GMP and ion channel regulation. *Adv Second Messenger Phosphoprotein Res* **33**, 251–277.

White RE, Kryman JP, El-Mowafy AM, Han G & Carrier GO (2000). cAMP-dependent vasodilators cross-activate the cGMP-dependent protein kinase to stimulate BK(Ca) channel activity in coronary artery smooth muscle cells. *Circ Res* **86**, 897–905.

Acknowledgements

This work was supported by grants from the North Shore Heart Research Foundation and the National Medical Research Council. M.W. was a recipient of Postgraduate Scholarship from the North Shore Heart Research Foundation. R.J.C. acknowledges support from the Australian Research Council.

Conclusion

In this study, we conducted administration of 30 mg and 60 mg of nadolol once per day for 7 consecutive days and administration of 30 mg (per dose) twice per day for 1 day, in 20 healthy volunteers and patients, examined and considered plasma concentration, chest X-rays, electrocardiogram, blood pressure, hematology and blood biochemistry and urine during this period, and obtained the following results.

1) Plasma concentration of nadolol reached a peak 2 to 4 hours after administration, and subsequently exhibited biphasic elimination. The elimination half-life of the β phase was 14 to 19 hours, and it was speculated based on this elimination half-life that a steady state would be reached through repeated dosing after 4 to 5 days.

2) Assuming that the plasma concentration of nadolol follows a two-compartment model, we were able to estimate the plasma concentration after repeated dosing based on the measured values from the first day of dosing.

3) Based on $AUC_{0-\infty}$ for the first day and the steady state AUC_{0-24} for the 7^{th} day, it was confirmed that repeated dosing with nadolol does not have an accumulation effect in the body.

4) Compared to administration of 30 mg once per day, administration of 60 mg of nadolol once per day or 30 mg twice per day lead to greater changes in cardiovascular dynamics, such as pulse rate, blood pressure and double product, with a significant difference as compared to the value before administration being observed at nearly all measurement points.

5) Based on the long half-life of plasma concentration, the significant decrease in double product, etc., as described above, it was concluded that nadolol is a clinically useful drug for angina pectoris, with one dose per day being sufficient.

6) No side effects were found during the study period either in terms of subjective symptoms or clinical laboratory tests.

TRANSPERFECT

I, Molly Stone, Director, hereby certify that the following is, a true and accurate translation following our ISO 9001:2008 quality assurance process of the conclusion only of Niitani H. et al., Studies of plasma level and hemodynamics of Nadolol, a new β adrenergic blocking agent
(June 1984, Vol. 12, No. 6),

Molly Stone

Director

Date: September 23, 2011